



Formulation Development and evaluation of a Nanofibrous Gel Containing Ketoconazole and Clotrimazole.

DIPTI S. PATIL^{1*}, VIKRAM VEER², AMIT KASABE³, TANMAYI KALAMKAR¹,
MAYURI GAVHANE¹

¹Research Scholar Department of Pharmaceutical Quality Assurance, PDEA's Shankarrao Ursal College of Pharmaceutical Sciences and Research Centre, Pune, Maharashtra, India.

²Assistant Professor of Department of Pharmaceutical Quality Assurance, PDEA's Shankarrao Ursal College of Pharmaceutical Sciences and Research Centre, Pune, Maharashtra, India.

³Assistant Professor of Department of Pharmaceutical Quality Assurance, PDEA's Shankarrao Ursal College of Pharmaceutical Sciences and Research Centre, Pune, Maharashtra, India.

For Correspondence-DIPTI S. PATIL*

waghdipti02@gmail.com

Abstract---

Topical drug administration is a localized method of delivering drugs to specific areas of the body via topical channels such as ophthalmic, rectal, vaginal, and cutaneous. The major route of topical medication delivery is through the skin, which is one of the most easily accessible organs on the human body for topical drug administration. The present investigation involves formulation of topical Nanofibrous gel using Ketoconazole and Clotrimazole. For the treatment of fungal Infection, Topical Ketoconazole and Clotrimazole is used to treat Fungal Infection. Ketoconazole and Clotrimazole belongs to the antifungal family of drugs. It works by reducing fungal infection. Topical Nanofibrous gel of Ketoconazole and Clotrimazole was prepared by using High molecular weight water soluble polymer Hydroxy propyl methyl cellulose such as K35 grade and other excipients including carbopol, methyl paraben, Glycerin and purified water were reported in the formation of Nanofibrous gel. In the present investigation combination of Ketoconazole and Clotrimazole Nanofibrous gel. The formulated gel was evaluated for pH, viscosity, Spreadability, extrudability, conductivity, particle size, zeta potential, in vitro drug diffusion studies. Among the formulated gel batch 3 has met all the specifications and was found to be optimized. Efficient delivery of drug to skin application was found to be highly beneficial in localizing the drug to desired site in the skin and reduced side effects associated with conventional treatment.

Keywords -ketoconazole, clotrimazole, fungal , topical

Introduction

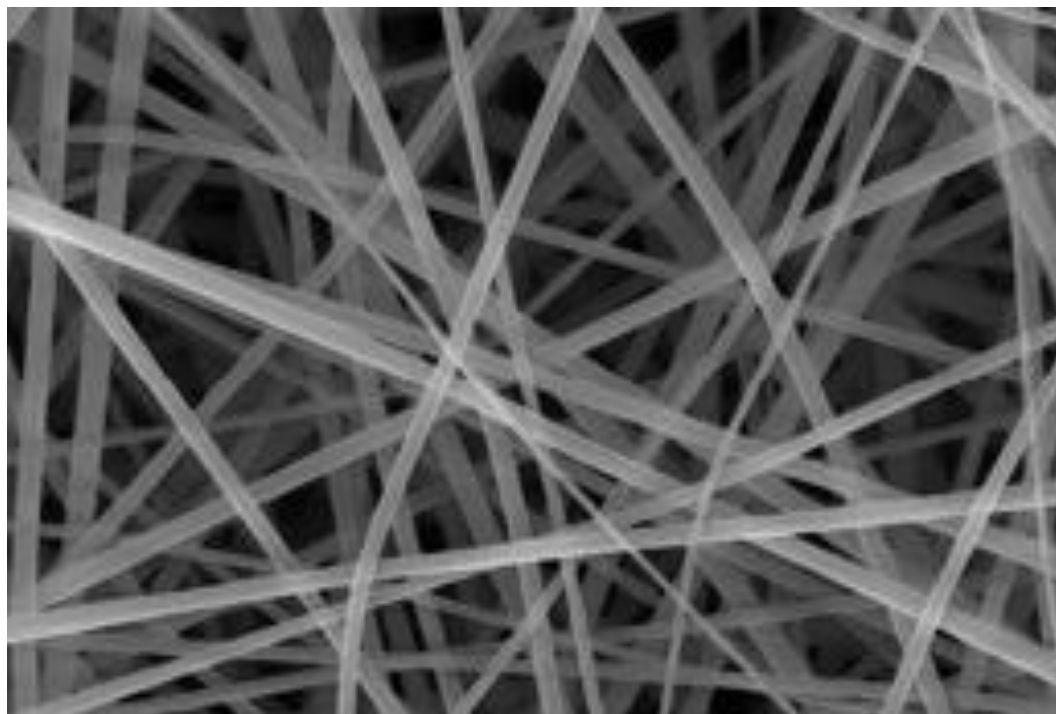
- Nanofibers are **fibers with diameters in the nanometer range** (typically, between 1 nm and 1 μm).
- Nanofibers can be generated from different polymers and hence have different physical properties and application potentials.
- There exist many different methods to make nanofibers, including drawing, electrospinning, self-assembly, template synthesis, and thermal-induced phase separation.
- Electrospinning is the most commonly used method to generate nanofibers because of the straightforward setup, the ability to mass-produce continuous nanofibers from various polymers, and the capability to generate ultrathin fibers with controllable diameters, compositions, and orientations.

Electrospinning method for Both the Solutions

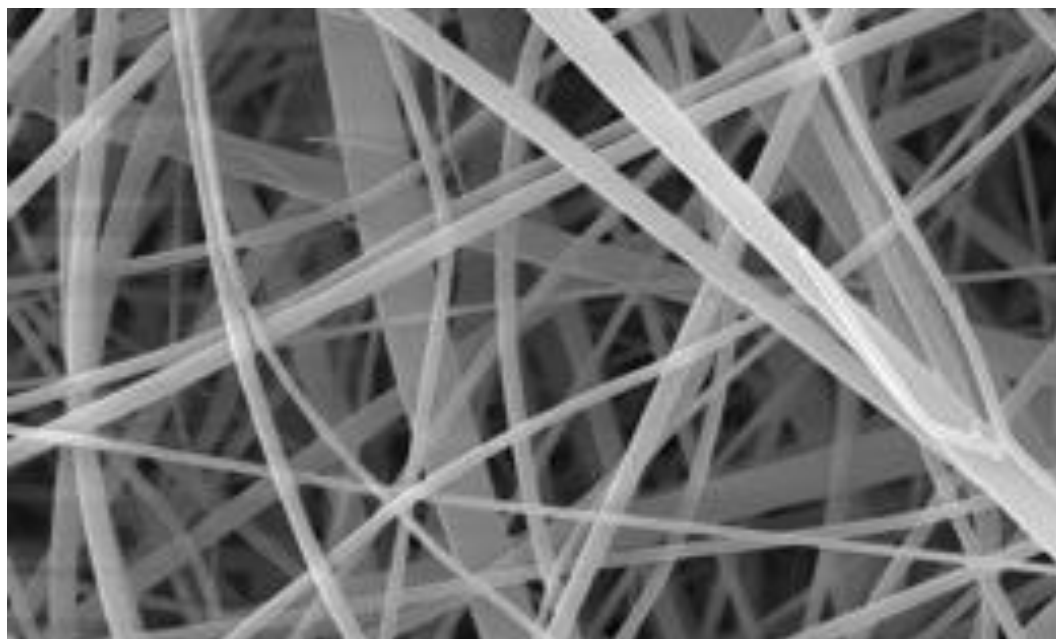
All spinning solutions were prepared at room temperature under stirring for 24 h to ensure their homogeneity. Electrospinning was conducted using a γ -High Voltage Research DC power supply generator with a maximum voltage of 50 kV. The electrospinning solutions were fed through the tip of the needle by syringe pump with a stable flow rate (0.5 mL/h). Meanwhile, high voltage (15 kV) was applied to the needle and the nanofibers were concurrently collected on the grounded and steady metal plate which was placed at 15 cm from the needle and covered with Al foil. Temperature and relative humidity were $20\pm 2^\circ\text{C}$ and $60\pm 5\%$, respectively.

5 μM

Sample 1



Sample 2



Sample 3

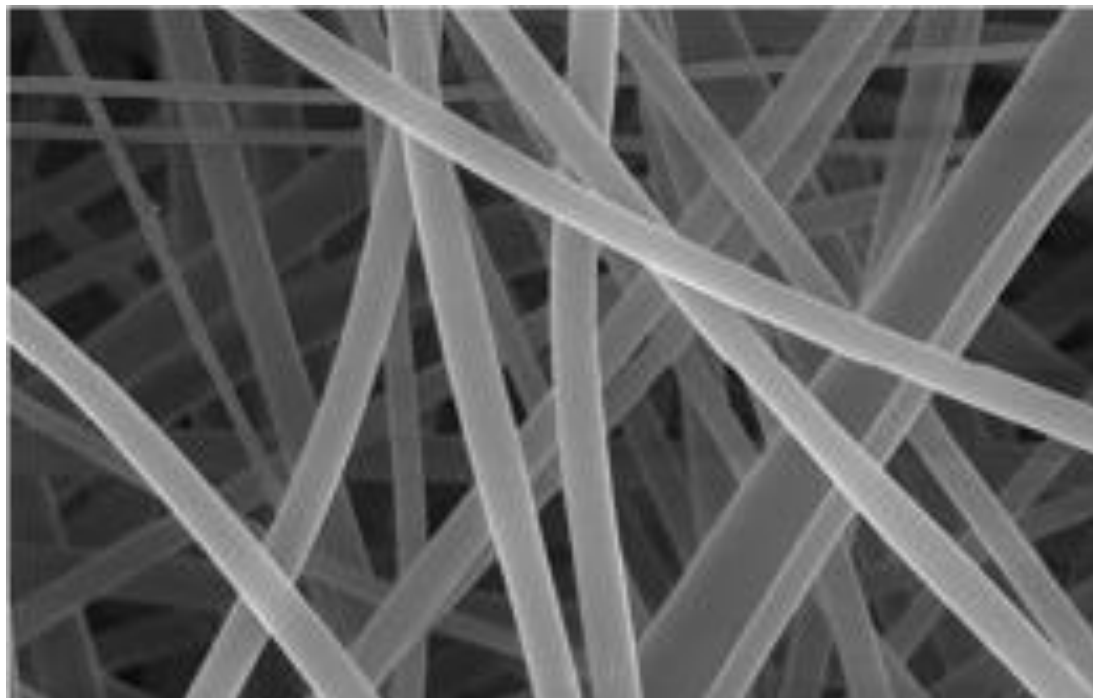


Table 1 . The effect of electrospinning parameters on the size of the nanofibers.

Effect of flow rate		Effect of distance		Effect of Volt	
Flow rate (mL h ⁻¹)	Size (nm)	Distance (cm)	Size (nm)	Voltage (kV)	Size (nm)
0.3	415±102	5	458±108	10	412±115
0.5	201±112	10	315±156	20	358±123
0.7	517±251	15	158±253	30	195±147
0.9	602±62	20	641±45	50	174±125

ELECTROSPINNING

As illustrated, the basic setup for electrospinning is rather simple, making it accessible to almost every laboratory.^{1,2} The major components include a high-voltage power supply, a syringe pump, a spinneret (usually, a hypodermic needle with blunt tip), and a conductive collector. The power supply can be either direct current (DC) or alternating current (AC). During electrospinning, the liquid is extruded from the spinneret to produce a pendant droplet as a result of surface tension. Upon electrification, the electrostatic repulsion among the surface charges that feature the same sign deforms the droplet into a Taylor cone, from which a charged jet is ejected. The jet initially extends in a straight line and then undergoes vigorous whipping motions because of bending instabilities. As the jet is stretched into finer diameters, it solidifies quickly, leading to the deposition of solid fiber(s) on the grounded collector. In general, the electrospinning process can be divided into four consecutive steps: (i) charging of the liquid droplet and formation of Taylor cone or cone-shaped jet; (ii) extension of the charged jet along a straight line; (iii) thinning of the jet in the presence of an electric field and growth of electrical bending instability (also known as whipping instability); and (iv) solidification and collection of the jet as solid fiber(s) on a grounded collector.,^{2,3,4} A more detailed discussion of these four

Materials and Methods

Ketoconazole was purchased from Yarrow chem Products (Pune, India). Clotrimazole was purchased from Yarrow chem Products. Methyl paraben was purchased from Research-lab Fine Chem Industries (Mumbai, India). HPMC K35 was purchased from Ashland Inc. Netherland. All the chemicals were of analytical grade. Polyvinyl Alcohol (PVA) was purchased from Research-lab Fine Chem Industries (Mumbai, India). Poly Lactic co Glycolic Acid (PLGA) was purchased from Research-lab Fine Chem Industries (Mumbai, India).

Methods ^{5,6}

Identification of pure drug

Identification of pure drug was carried out by Fourier Transform Infra-red Spectrophotometry (Shimadzu 8400s) scanned in the range of 400-200nm.

Drug-excipient compatibility study

Studies of drug-excipient compatibility are important to ascertain drug and excipients are compatible with each other. DSC graph and IR spectra are used to study drug-excipient compatibility.

FTIR study

FTIR (Shimadzu 8400s)spectrophotometer were used in the range of 400-4000 cm^{-1} using potassium bromide discs (Mixing ratio1:1) The samples were hermetically sealed in aluminium pans and heated at a constant rate of $10^{\circ}\text{C}/\text{min}$ over a temperature range of 40 to 300°C .

FTIR spectroscopy The FTIR spectrums of pure Ketoconazole as well Clotrimazole and physical mixtures of drugs and polymers were studied separately as per the excipients used in the formulation. It was observed that there were no major shifts in the main peaks of either drug. This indicates that there were no compatibility problems with the drug with the polymers and excipients used in the formulation. Ketoconazole had peaks at 1643 ($\text{C}=\text{CO}$ stretching), 817 ($\text{C}-\text{Cl}$ stretching), 1512($\text{C}=\text{C}$ stretching), 2841($\text{C}-\text{H}$ stretching), and 1041($\text{C}-\text{O}$ stretching), while Clotrimazole showed characteristic peak values at 756 ($\text{C}-\text{Cl}$ stretching); 2940 ($\text{C}-\text{H}$ stretching); 1535 ($\text{C}=\text{C}$ stretching) and 1620 ($\text{C}=\text{N}$ stretching). These peak values were in accordance with previously reported spectra of Clotrimazole(Fig. 2)

Fig.1 FTIR of Ketoconazole

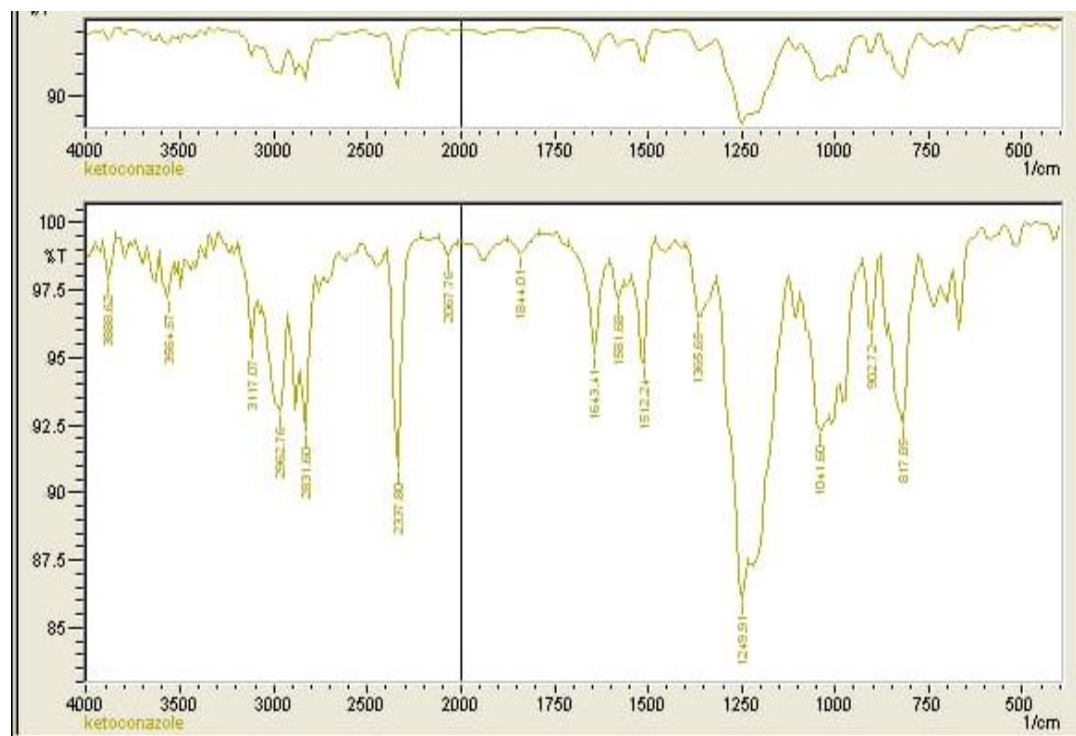
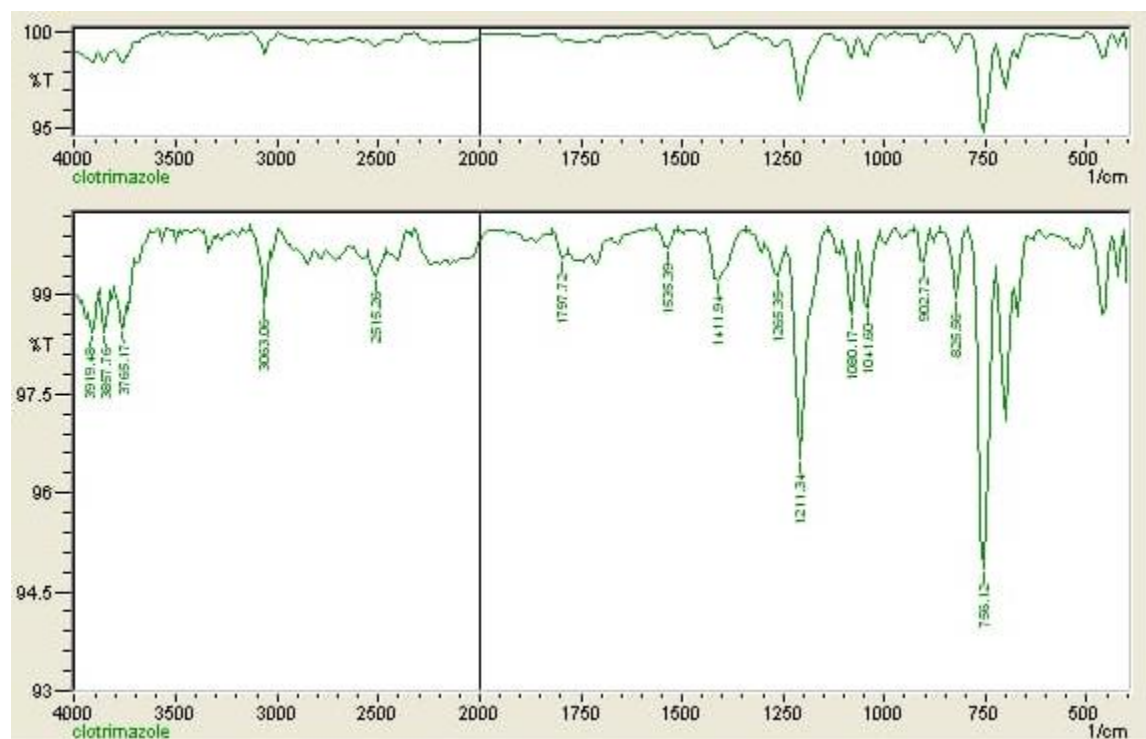


Fig.2 FTIR of Clotrimazole**UV spectroscopy**

The linearity of the responses of both drugs was verified at 2–10 µg/ml concentrations. The calibration curve was obtained by plotting the absorbance versus the concentration data and was treated by linear regression analysis. The equation of the linearity curve for Ketoconazole obtained was $y = 0.1995x + 0.533$. The linearity curve was found to be linear in the a for mentioned concentrations (the correlation coefficient (r^2) of determination was 0.9994) (Fig.1). Similarly, the equation of the linearity curve for Clotrimazole obtained was $y = 0.132x + 0.0515$. The linearity curve was found to be linear for mentioned concentrations. (the correlation coefficient (r^2) of determination was 0.995) (Fig.2)

Fig 3. Calibration Curve of Ketoconazole

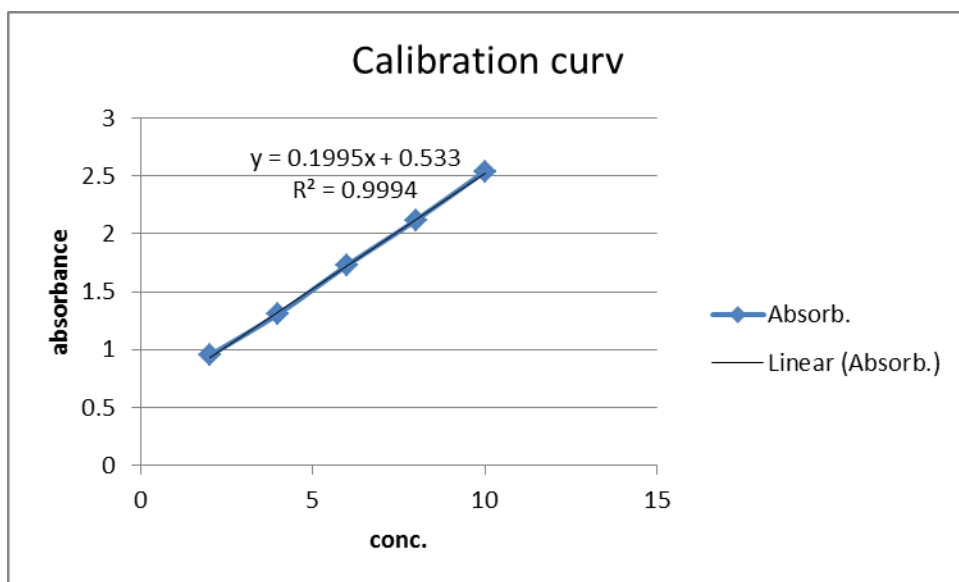
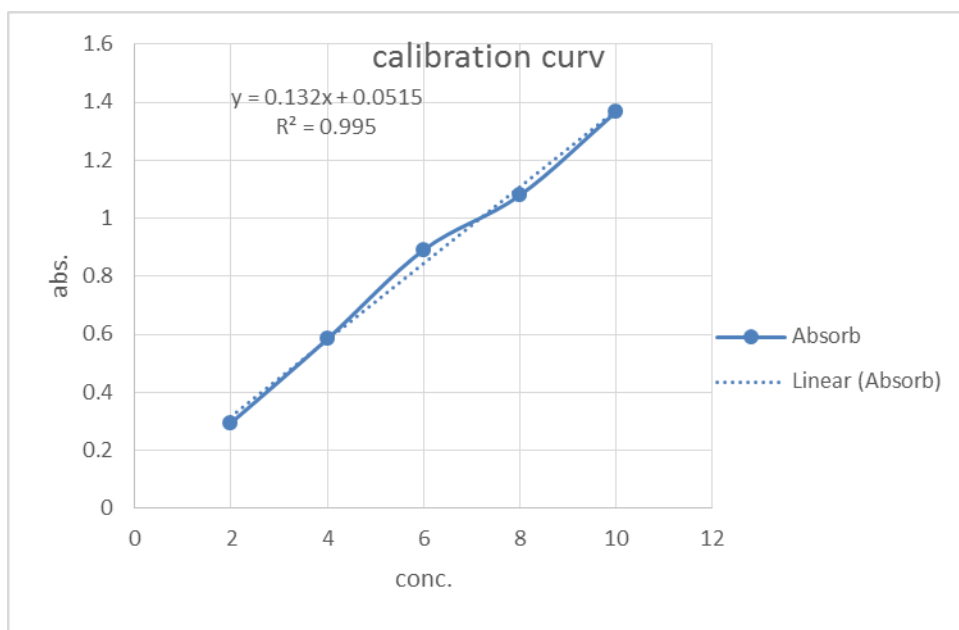


Fig 4. Calibration Curve of Clotrimazole



Preparation of Gel

To obtain O/W gel formulation HPMC K35 polymer was solubilized in purified water with constant trituration. In polymer dispersion Carbopol was added slowly with continuous stirring along with Ketoconazole, Clotrimazole and methyl paraben and was mixed well by continuous trituration. Finally gel was made by adjusting the pH of the mixture to 7.0 and resulted in desired gel consistency good homogeneity and spreadability.

Table 2- Composition of gel (KC1-KC3)

Ketoconazole	10mg	10mg	10mg
Clotrimazole	10mg	10mg	10mg
Methyl Paraben	0.025	0.025	0.025
HPMC K35	200mg	220mg	240mg
Carbopol	0.025	0.025	0.025
Glycerin	Q.S	Q.S	Q.S
Purified water	Q.S	Q.S	Q.S

Evaluation of Gel

1. Appearance - Patient compliance is aided by the use of colour. The prepared gels were examined visually for clarity, colour, and particle presence.

2. pH^{7,8} :- A digital pH metre (Model EQ-610) was used to determine the pH of the gel. In distilled water, 1 gm gel was swirled until a homogeneous suspension was obtained. The volume of the solution was increased to 100 mL, and the pH was determined. The pH of each formulation was done in triplicate and average value are determine.

3. Viscosity^{9,10}:- The gel's viscosity was determined using a (LV) Brookfield viscometer. The spindle no. 96 is utilised since the system is nonNewtonian. The viscosity was tested for 2 minutes.

4. Conductivity¹¹:- A direct reading digital conductivity meter (Systronics model no. 304) and dipping type conductivity cell.

5. Zeta Potential¹²:- The charge on the surface of particles is characterized by the HORIBA Scientific SZ-100 by measuring the zeta potential of a gel. The sample is injected into a

disposable cell and a measurement of the particle electrophoretic mobility results in the calculated zeta potential.

6. Particle size¹³:- Horiba sz-100 windows [z type] were used to investigate the particle size (PS) of the gel. Particle size and zeta potential were measured in triplicates after dilution with distilled water, and the average values \pm SD were recorded.

7. Spreadability^{14,15}:- Excess sample was sandwiched between the two glass slides, and a 100 g weight was used to compress the sample to a uniform thickness for 5 minutes. The pan was filled with weight (250 g). The time it took to separate the two slides in seconds was used as a measure of spreadability.

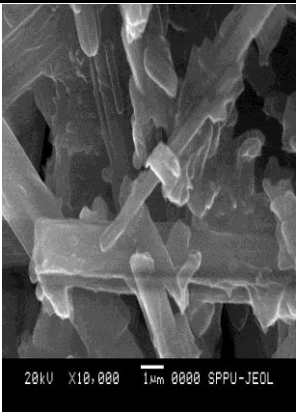
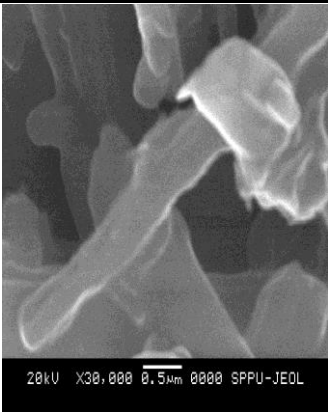
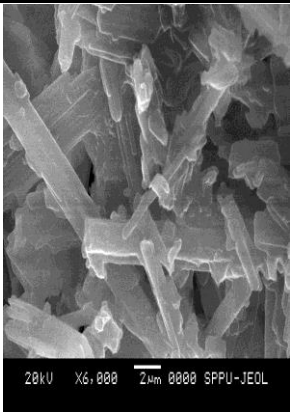
8. Extrudability^{16,17}:- Measure the force required to extrude the material from tube. Extrudability was based upon the quantity in percentage of gel and gel extruded from lacquered aluminium collapsible tube on application of weight in grams required to extrude at least 0.5 cm ribbon of gel in 10 seconds. +++ excellent ++ very good + average

9. Scanning electron microscopy¹⁸:- Scanning electron microscopy (SEM) provides high-resolution imaging that may be used to evaluate diverse materials for surface cracks, defects, contaminants, or corrosion. When a focused stream of secondary electrons interacts with atoms in the sample, multiple signals are produced that include information about the surface topography and sample composition using the Nova NanoSEM NPEP, all pictures were scanned at 10000x with a 5 m dimension scale 303.

10. Content uniformity¹⁹:- Drug content of gel was determine by dissolving accurately weighed 1gm of gel in methanol. After suitable dilution absorbance was recorded by using UV- visible spectrophotometer (UV – 1800 Shimadzu, Japan) at 290 and 225nm. Drug content was determined using slope of standard curve.

11. Diffusion studies^{20,21}:- The study was performed using Franz diffusion cells with dialysis membrane with the use of the instrument Jasco V-630 model no V-630. Here the microemulsion based gel equivalent to 10mg of Ketoconazole was placed on the donor compartment and the receptor compartment was filled with mixture of phosphate buffer solution (pH 7.4) and 30% methanol, maintained at 37 ± 10 °C for in vitro diffusion studies, artificial dialysis membrane was soaked in the same buffer solution for 24hrs before mounting on the diffusion cells. Receptor liquid was withdrawn after each hours and sink condition was maintained by replacing liquid kept at same temperature. Ketoconazole concentration was assayed using UV spectrophotometer. Using the photometric mode for noting absorbance of UV/VIS bandwidth was taken at wavelength of Clotrimazole was taken at wavelength of 263nm and diffusion study of gel was performed.

Particulars	KC	KC	KC
Appearance	Off-white to yellow gel with suspended particles	Off-white to yellow gel with suspended particles	Off-white to yellow gel with suspended particles
Fill volume (gm)	10	10	10
pH	6.8-7.2	6.8-7.2	6.8-7.2
Conductivity 1)200ms 2)20ms 3)2ms 4)200μs 5)20μs	1)0 2)00.7 3)0.67 4)1 5)1	1)0 2)00.6 3)0.69 4)1 5)1.0	1)0 2)00.1 3)0.12 4)148 5)1
Zeta potential (mV)	-20.7mV	-22.3mV	-23.7mV
Particle size (nm)	333.1nm	339.1nm	244.3nm
Spredability (gm.cm/sec)	3.2±0.0156	4.1±0.0264	3.9±0.057
Extrudibility	++	+++	++

Scanning electron microscopy			
Uniformity of content(%)1) Ketoconazole	94.6	96.1	98.4
Clotrimazole	93.5	95.4	97.3

In vitro Diffusion studies

Table 3- Data of In-vitro drug release studies of gel of Ketoconazole (%)

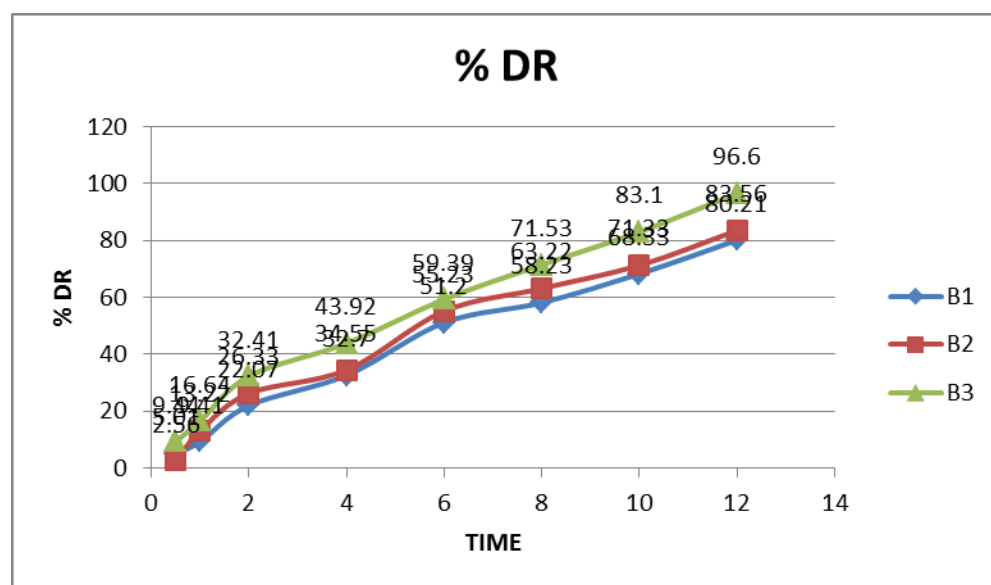
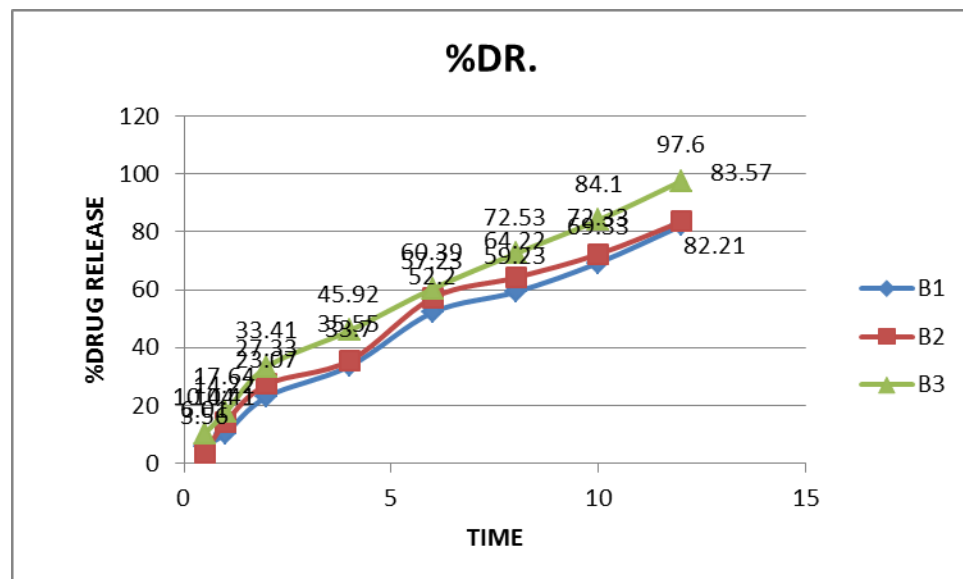


Table 4- Data of In-vitro drug release studies of gel of Clotrimazole(%)**Viscosity results KC1 (Spindle number-96)**

RPM	Surface(cP)	Middle(cP)	Bottom(cP)
20	8766	9281	9563
30	6844	7656	7594
50	4331	4931	5006
60	3000	4375	4578

Viscosity results KC2 (Spindle number-96)

RPM	Surface(cP)	Middle(cP)	Bottom(cP)
20	7313	9094	9188
30	5063	6781	7375
50	3938	4294	5139
60	2313	2531	3038

Viscosity results KC3 (Spindle number-96)

RPM	Surface(cP)	Middle(cP)	Bottom(cP)
20	7453	9328	9757
30	7969	7344	7438
50	5044	5100	5456
60	6047	6422	7422

Conclusion

- It can be concluded that from the experimental study carried out that the formulation of a Nanofibrous gel containing Ketoconazole and Clotrimazole drug yields a formulation with spherical and smooth surface, nano in size range. The prepared Nanofibrous was smooth without any lumps, particle and aggregates. So, all the formulations are homogenous. Based on all the factors the nanofibrous gel drug delivery system B3 shows good drug content compared to other. The particle size of the nanofibrous gel formulation is optimum and it is less than 1000 nm. So, it concluded that the particles are in tiny and nano in size range. All nanofibrous gel formulations shows pH in the range of 5.5 to 7. Based on the Spreadability diameter study it shown the nanofibrous gel is having good Spreadability. Nanofibrous gel formulations shown viscosity range from 5000-50000 cps. It concluded that they are stable in nature. Formulation Batch-3 shows highest percentage of drug release compare to other formulations. In-vitro diffusion studies show Batch-3 formulation shows controlled release pattern of drug from the formulation. Zeta potential of batch B-3 shows -22.3mV. High zeta potential values shows there will be no particles coming together and no flocculation. Hence it is conclude that formulation Batch-3 is an optimized batch containing optimum HPMC and Carbopol.

Acknowledgement

For the completion of the research work the authors would like to show sincere gratitude to PDEA'S Shankarrao Ursal College of Pharmaceutical Sciences & Research center, Kharadi, Pune to provide with a lot of support and help whenever needed.

References

1. (41) Li D; Xia Y Electrospinning of Nanofibers: Reinventing the Wheel? *Adv. Mater* 2004, 16, 1151–1170.
2. (42) Xue J; Xie J; Liu W; Xia Y Electrospun Nanofibers: New Concepts, Materials, and Applications. *Acc. Chem. Res* 2017, 50, 1976–1
3. (43) Sun B; Long YZ; Zhang HD; Li MM; Duvail JL; Jiang XY; Yin HL Advances in Three-Dimensional Nanofibrous Macrostructures via Electrospinning. *Prog. Polym. Sci* 2014, 39, 862–890.

4. (44) Liao Y; Loh CH; Tian M; Wang R; Fane AG Progress in Electrospun Polymeric Nanofibrous Membranes for Water Treatment: Fabrication, Modification and Applications. *Prog. Polym. Sci* 2018, 77, 69–94.
5. 14. Nappinnai M., Pakalapati S, Arimilli R. Rofecoxib gels-preparation and evaluation. *Indian Drugs*. 2006; 43(65):13-51
6. 15. Cartensen JT, Rhodes CT (2005) Preformulation. In: Cartensen JT, Rhodes CT (eds.). *Drug Stability principles and practices* (3rd edn)., Marcel Dekker Inc., New York, USA
7. 16. Murthy TGEK, Kishore VS. Formulation and evaluation of transdermal gels of diltiazem hydrochloride. *Indian J. Pharm. Educ. Res.* 2008; 42(3): 272-276.
8. 17. Rupal J, Kaushal J, Setty MC, Dipti P. Preparation and evaluation of topical gel Valdecoxib. *Inter J. Pharm. Sci. Research*. 2010; 2(1):51-54.
9. 18. Kauri LP, Garg R, Gupta GD. Development and evaluation of topical gel of minoxidil from different polymer bases in application of alopecia. *Int. J. Pharmacy Pharm. Sci.* 2010; 2(3): 43-47
10. 19. <https://www.brookfieldengineering.com>
11. Kumar Nrendra (2014), Study Of extraction, Isolation and Physico-Chemical Properties of Psidium Gaujava, *International Journal Of Research Science and Management*, ISSN: 2349- 5197
12. Hiemenz, *Principles of Colloid and Surface Chemistry*, Marcel Decker, 1977
13. Chowhan ZT. Role of binders in moisture-induced hardness increase in compressed tablets and its effect on in vitro disintegration and dissolution. *J. Pharm. Sci.* 1980; 69; 1-4.
14. Rupal J, Kaushal J, Setty MC, Dipti P. Preparation and evaluation of topical gel Valdecoxib. *Inter J. Pharm. Sci. Research*. 2010; 2(1):51-54
24. Gupta A, Mishra AK, Singh AK, Gupta V, Bansal P. Formulation and evaluation of topical gel of diclofenac sodium using different polymers. *Drug Invent. Today*. 2010; 2: 250-253.
15. Ahmed M, Gendy E, Alaa A. In vitro Release Studies of Flurbiprofen from Different Topical Formulations. *Drug Dev. Ind. Pharm.* 2002; 28(7):823-831.
16. Goyal S, Sharma P, Ramchandani U, Shrivastava SK. et al. Formulation development and characterization of aceclofenac gel containing linseed oil and ginger oleoresin. *Int. J. Pharm. Biol. Arch.* 2011; 3(3):1087-1094.
17. Karthik. T.V.K., Martinez, V., Agrawal. V., Porous silicon ZnO/SnO₂ structures for CO₂ detection, *Journal of alloys and Compounds*, 731, 2008, 853-863
18. Michaels A.S, Chandrasekaran S. K, Shaw J.E. Drug permeation through human skin: Theory and invitro experimental measurement. *AIChE J.* 2004; 21(5) 16 Williams AC, Barry BW. Penetration enhancers. *Adv drug deliv rev.* 2004; 56(5):603-618.
19. Belgamwar V, Patel H, Joshi A, Agrawal A, Surana S. Design and development of nasal mucoadhesive microspheres containing tramadol HCl for CNS targeting. *Drug Delivery, Informa Healthcare*, 2011; 18(5):353-360.

20. Patel, J., Ketkar, S., Patil, S., Fearnley, J., Mahadik, K. R., & Paradkar, A. R. (2015). Potentiating antimicrobial efficacy of propolis through niosomal-based system for administration. *Integrative medicine research*, 4(2), 94-101
 21. Vollrath F; Knight DP Liquid Crystalline Spinning of Spider Silk. *Nature* 2001, 410, 541–548.
 22. Heim M; Keerl D; Scheibel T Spider Silk: From Soluble Protein to Extraordinary Fiber. *Angew. Chem., Int. Ed* 2009, 48, 3584–3596
 23. Andersson M; Jia Q; Abella A; Lee X-Y; Landreh M; Purhonen P; Hebert H; Tenje M; Robinson CV; Meng Q; et al. Biomimetic Spinning of Artificial Spider Silk from a Chimeric Minispidroin. *Nat. Chem. Biol* 2017, 13, 262–
 24. Woodings C, Ed. *Regenerated Cellulose Fibres*; Woodhead: Cambridge, U.K., 2001; Chapter 5.
 25. Carothers WH *Alkylene Ester of Polybasic Acids* U.S. Pat. 2,012,267, 1935.
 26. Carothers WH *Linear Condensation Polymers* U.S. Pat. 2,071,250, 1937.
 27. McIntyre JE *Synthetic Fibres: Nylon, Polyester, Acrylic, Polyolefin*; Woodhead: Cambridge, U.K., 2005; Chapter 1.
 28. Gupta V, Kothari V, Eds. *Manufactured Fibre Technology*; Chapman & Hall: London, 1997; Chapter 1.
 29. Luo C; Stoyanov SD; Stride E; Pelan E; Edirisinghe M Electrospinning Versus Fibre Production Methods: From Specifics to Technological Convergence. *Chem. Soc. Rev* 2012, 41, 4708–4735
 30. Boys CV On the Production, Properties, and Some Suggested Uses of the Finest Threads. *Proc. Phys. Soc. London* 1887, 9, 82013
-



Formulation Development and Evaluation of a Topical Nanogel Containing Kojic acid

Borase Pallavi S.^{1*}, Dr. Barge Vijaya², Dr. Kasabe Amit³,

Gaikwad Rajratna¹, Avhad Pratiksha¹, Deshmane Kamlesh¹

¹Research Scholar, Department of Pharmaceutical Quality Assurance, PDEAs Shankarrao Ursal College of Pharmaceutical Sciences and Research Centre, Pune, Maharashtra, India.

²Vice Principal, Professor Department of Pharmaceutical Quality Assurance, PDEA'S Shankarrao Ursal College of Pharmaceutical Sciences & Research centre, Kharadi, Pune, Maharashtra, India.

³Assistant Professor, Department of Pharmaceutical Quality Assurance, PDEA'S Shankarrao Ursal College of Pharmaceutical Sciences & Research centre, Kharadi, Pune, Maharashtra, India.

For Correspondence: Borase Pallavi S.

pallaviborse41296@gmail.com

ABSTRACT- Topical drug administration is a localized method of delivering drugs to specific areas of the body via topical channels. The major route of topical medication delivery is through the skin, which is one of the most easily accessible organs on the human body for topical drug administration. The present investigation involves formulation of topical nanogel using Kojic acid for the treatment of hyperpigmentation, Kojic acid is an effective and well tolerated drug having melanin neutralising activity (Tyrosinase inhibitor). Topical nanogel of Kojic acid was prepared by using High molecular weight water soluble polymer Hydroxy propyl methyl cellulose such as K35M grade and other excipients including methyl paraben, Carbopol 940, glycerine and purified water were reported in the formation of nanogel. In the present investigation nanogel the formulated nanogel was evaluated for pH, viscosity, Spreadability, extrudability, conductivity, particle size, zeta potential, in vitro drug diffusion studies. Among the formulated nanogel batch 4 has met all the specifications and was formed to be optimized Efficient delivery of drug to skin application was found to be highly beneficial in localizing the drug to desired site in the skin.

KEYWORDS- Nanogel, Kojic acid, Particle size, Zeta potential, Drug Release.

INTRODUCTION

Nanogels are defined as nanoscale particles that, either physically or chemically, create crosslinked polymers. In order to transport polynucleotides, cross-linked bifunctional networks of a polyion and a non-ionic polymer were first developed [1]. Although soluble in water, nanogels differ from linear macromolecules with comparable molecular weights in their properties. These structures along with their larger equivalents [2]. Structures along with their larger equivalents [2]. Nanogels are typical formulations that typically range in size from 1000 nm, and their three-dimensional structure can be maintained by altering volume proportion and solvent quality. Nanogels have revolutionized the field of gene therapy because they have made it possible to deliver genes within cellular organelles for gene silencing therapy [3]. Nanogels are composed of ionic or non-ionic polymer chains that are hydrophilic or amphiphilic and

grow into nanoscale structures. Despite its use as a drug delivery system, nanogel has been studied for longer periods in the production of other substances like quantum dots, dyes, and other diagnostic agents [4]. The development of nano-sized microgels and hydrogels as a result of specific delivery system anticipation has been made possible by the wide range of polymer systems and the simple modification of their physico-chemical properties [5]. Transdermal delivery of drug is promising but challenging system is available for local as well as systemic effect of drug. The entry of drug through the stratum corneum may follow the intercellular, transcellular or appendageal route. The intercellular route is the more common pathway of the drug permeation through the skin [6].

Melanocytes create the biological pigment called skin melanin. Skin colour is primarily determined by melanin, which shields human skin from ultraviolet (UV) solar radiation's harmful effects. Hyperpigmentation is the term used to describe melanin over synthesis [7]. For most people, especially women, hyperpigmentation treatment is usually difficult and disappointing [8]. Kojic acid (KA) is a popular hydrophilic tyrosinase inhibitor with natural whitening properties that is used to treat hyperpigmentation. By chelating copper atoms, Kojic Acid inhibits the tyrosinase enzyme and prevents the synthesis of dopachrome. It synthesized several fungi species, including *Aspergillus* and *Penicillium* [9]. Despite KA and its derivatives distinctive qualities, the cosmetic industries hardly ever use them. Due to its hydrophilic nature and the two hydroxyl functional groups that make up its chemical structure, Kojic Acid is a hydrophilic component. Its skin absorption is inadequate [10].

The present study was conducted to design and evaluate Kojic Acid nanogel which provides prolonged release, increase the residence time of drug on the skin thereby enhance bioavailability.

MATERIALS AND METHOD

Kojic Acid was purchased from Arti pharmaceuticals, Mumbai. Carbopol 940 Research-lab Fine Chem Industries, Mumbai. HPMC K35M was obtained as a gift sample from Ashlands, Netherlands. Co., Methylparaben and Glycerine was purchased from Research-lab Fine Chem. Industries, Mumbai [11].

METHOD

Preparation of Kojic Acid Nanogel [12]

Preparation of 2% drug solution of KA- weigh 2 gm of drug Kojic acid dissolve in 100ml of distilled water.

2% of prepared kojic acid measure 2ml of solution mix with given quantity of HPMC K35m, mix well then add glycerine. (Organic phase). Weigh carbopol940 accurately, add 10ml distilled water (aqueous phase). Stir aq. phase on magnetic stirrer add organic phase dropwise. Add methylparaben (preservative). Batch B1, B2, B3, B4 was prepared at highest rpm 8000 with variation in composition.

Evaluation Parameters

Appearance: The prepared nanogel bases were inspected visually for clarity, colour and presence of any particles.

Homogeneity

All developed nanogels were tested for homogeneity by visual inspection after the gels have been set in the container. They were tested for their appearance and presence of any aggregates [12].

Measurement of particle size of formulation

Horiba sz-100 windows [z type] were used to investigate the particle size (PS) of the gel. Particle size and zeta potential were measured in triplicates after dilution with distilled water, and the average values \pm SD were recorded [13].

pH measurement

The pH measurement was carried out by using calibrated digital type pH meter by dipping the glass electrode and the reference electrode completely into gel system so as to cover the electrodes.

Conductivity

A direct reading digital conductivity meter (Systronics model no. 304) and dipping type conductivity cell [14].

Drug content

For the estimation of the drug in nanogel, kojic acid was extracted from 1 gm of nanogel formulation with 50 ml of distilled water. From this, 2 ml was pipette out and made up to 10 ml. The absorbance of the sample was determined spectrophotometrically at 268 nm. The concentration of Kojic acid was estimated from the calibration curve [12, 24].

In vitro drug Release studies

The drug release from the formulation was determined by using the apparatus known as Franz Diffusion Cell, which consist of a cylindrical glass tube which was opened at both the ends. 1 gm of nanogel equivalent to 4 mg of Kojic acid was spread uniformly on the surface of cellophane membrane (previously soaked in medium for 24 hrs) and was fixed to the one end of tube. The whole assembly was fixed in such a way that the lower end of tube containing gel was just touches (1-2 mm deep) the surface of diffusion medium i.e., 100 ml of pH 7.4 phosphate buffer contained in 100 ml beaker. The assembly was placed on thermostatic hot plate with magnetic stirrer and maintained at temperature $37^{\circ}\pm 2^{\circ}$ the contents were stirred using magnetic bar at 100 rpm for a period of 24 hrs, 5 ml of samples were withdrawn at different time intervals. This 5 ml was diluted up to 10 ml of fresh phosphate buffer (pH 7.4) and sample were analyse at 268 nm in UV-Visible spectrometer for KA. [12, 25-26].

Skin irritation test

Test for irritation was performed on human volunteers. For each gel, four volunteers were selected and 1.0 g of formulated gel was applied on an area of 2 square inch to the back of hand. The volunteers were observed for lesions or irritation [12].

Spreadability

Spreadability is determined by apparatus suggested by Mutimer. It consists of wooden block, which is provided by a pulley at one end. By this method, Spreadability is measured on the basis of “Slip” and “Drag”. A ground glass slide is fixed on this block. A sample of 0.1 g of nanogel under study is placed on this ground slide. The gel is fixed on the beach formula was pressed between two slides and a 1 kg weight is placed on the top of two slides and left for about 5 min to expel air and to provide a uniform film of the nanogel between two slides. Excess of the nanogel is scrapped from edges. The top plate is then subjected to pull the weight. With help of string attaches to the hook and the time required by top slide to cover the distance is noted. A shorter interval indicates better spreadability, spreadability was calculated by using the formula,

$$S=M.L/T,$$

Where,

S= spreadability, L=Length of glass slide, M=weight tied to upper slide, T=Time taken to separate the slides [13, 15].

Extrudability

Measure the force required to extrude the material from tube. Extrudability was based upon the quantity in percentage of gel and gel extruded from lacquered aluminum collapsible tube on application of weight in grams required to extrude at least 0.5 cm ribbon of gel in 10 seconds [16, 17]

+++ excellent ++ very good + average

Scanning electron microscopy

Scanning electron microscopy (SEM) provides high-resolution imaging that may be used to evaluate diverse materials for surface cracks, defects, contaminants, or corrosion. When a focused stream of secondary electrons interacts with atoms in the sample, multiple signals are produced that include information about the surface topography and sample composition using the Nova NanoSEM NPEP, all pictures were scanned at 10000x with a 5 m dimension scale 303 [18].

Zeta Potential

Zeta Potential of the prepared Nanosuspension was determined using Light Scattering method. The charge on the surface of particles is characterized by the HORIBA Scientific SZ-100 by measuring the zeta potential of a gel. The sample is injected into a disposable cell and a measurement of the particle electrophoretic mobility results in the calculated zeta potential [19-22].

Particle size

Horiba sz-100 windows [z type] were used to investigate the particle size (PS) of the gel. Particle size and zeta potential were measured in triplicates after dilution with distilled water, and the average values \pm SD were recorded [13, 23].

Content uniformity

Identification of pure drug

Identification of pure drug was carried out by Fourier Transform Infra-red Spectrophotometry (Shimadzu 8400s) scanned in the range of 200-400 nm.

Drug-excipient compatibility study

Studies of drug-excipient compatibility are important to ascertain drug and excipients are compatible with each other. IR spectra are used to study drug-excipient compatibility.

FTIR study

FTIR (Shimadzu 8400s) spectrophotometer were used in the range of 400-4000 cm^{-1} using potassium bromide discs (Mixing ratio 1:1) The samples were hermetically sealed in aluminium pans and heated at a constant rate of 10°C/ min over a temperature range of 40 to 300°C.

FTIR spectroscopy

The FTIR spectrums of pure Kojic acid and physical mixtures of drugs and polymers were studied separately as per the excipients used in the formulation. It was observed that there were no major shifts in the main peaks of either drug. This indicates that there were no compatibility problems with the drug with the polymers and excipients used in the formulation. Kojic acid had peaks at 1715 (C=O stretching), 3549 (O-H str.), 1620 (C-O), 2839 (C-H).

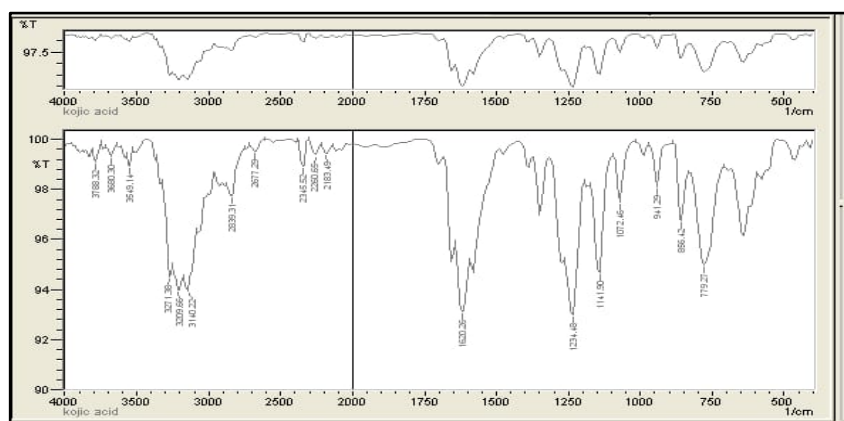
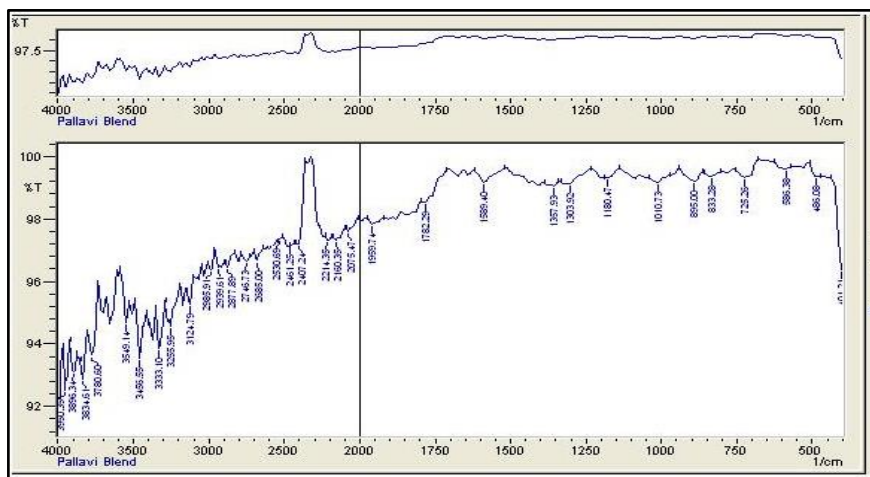


Figure 1: FTIR Studied of Kojic acid



UV spectroscopy:

The linearity of the response of kojic acid was verified at 2–10 µg/ml concentrations. The calibration curve was obtained by plotting the absorbance versus the concentration data and was treated by linear regression analysis. The equation of the linearity curve for kojic acid was $y = 0.0646x + 0.0036$. The linearity curve was found to be linear in the a for mentioned concentrations (the correlation coefficient (r^2) of determination was 0.9978)

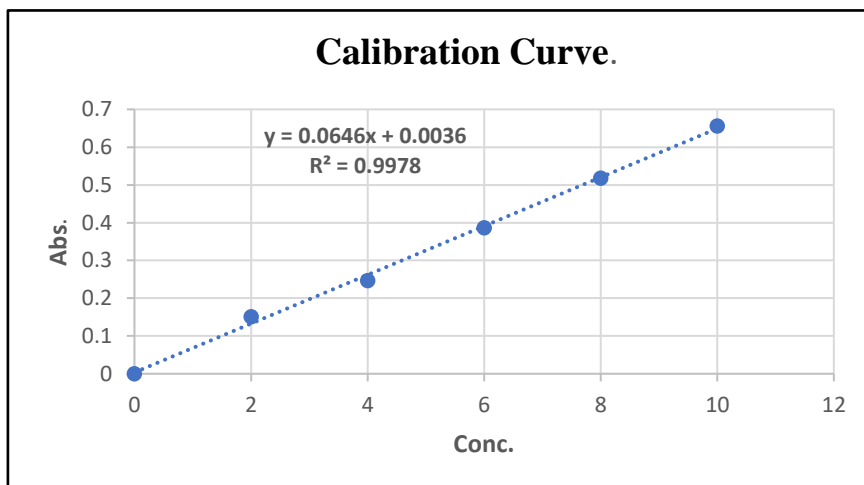


Fig 3: Calibration curve of Kojic acid

Composition of Nanogel: -

Table 1- Composition of nanogel (B1-B4)

Evaluation of prepared nanogel:

Appearance

Appearance of the prepared Nanogel was inspected visually and all the batches were white to Clear, and free from any particulate matters.

Particle Size Determination

Particle size of the prepared Nanogel was determined using Dynamic Light Scattering (DLS) method. Particle size determination results for all the prepared batches kojic acid nano are presented in the Table 3 and all the Graph obtained are reported in the Figure 4-7.

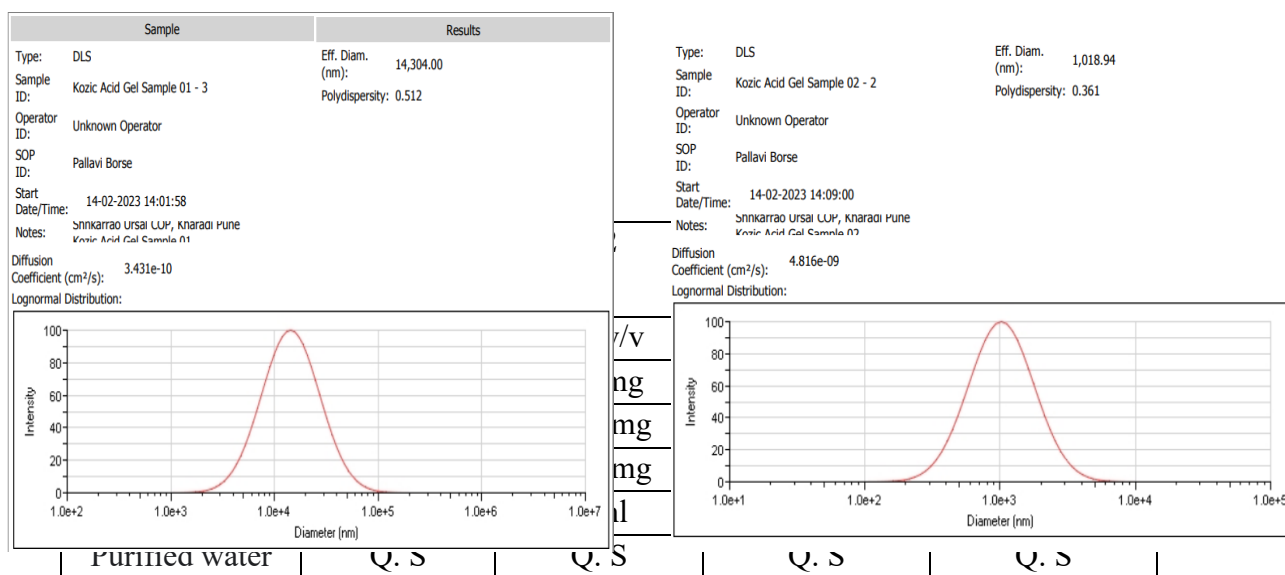


Fig 4D: Particle size of formulation B4

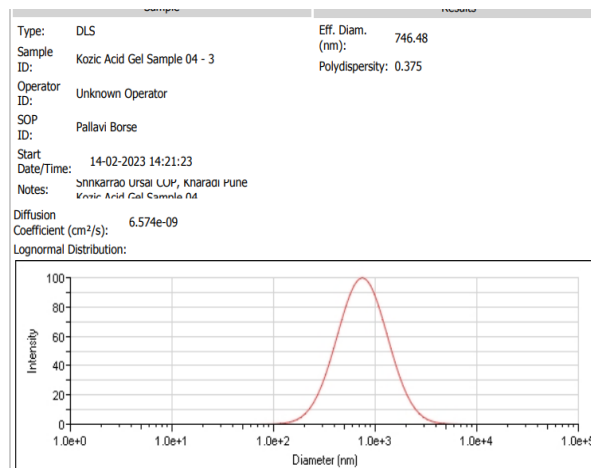
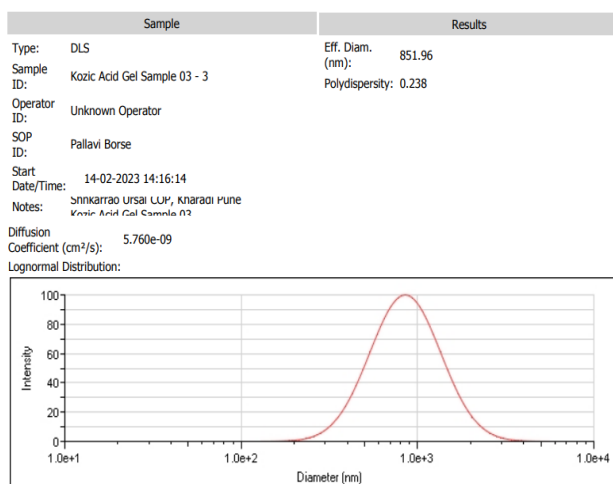


Fig 4C: Particle size of formulation B3

Particle size of batch 4 shows optimum size 746.48nm compare to other 3 batches. Batch4 is having optimum conc. of HPMC K35M and Carbopol 940.

Zeta Potential analysis

From the Graphical representation in following figures, it was observed that when the Nanogel was prepared using maximum conc. Of HPMC polymer compared to other batches is more stable.

Zeta Potential (Mean) : 0.4 mV
Electrophoretic Mobility Mean : 0.000003 cm²/Vs

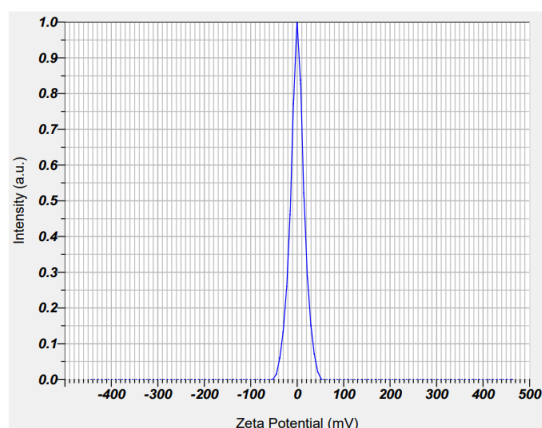


Fig 5A. zeta potential of formulation B1

Zeta Potential (Mean) : -16.3 mV
Electrophoretic Mobility Mean : -0.000126 cm²/Vs

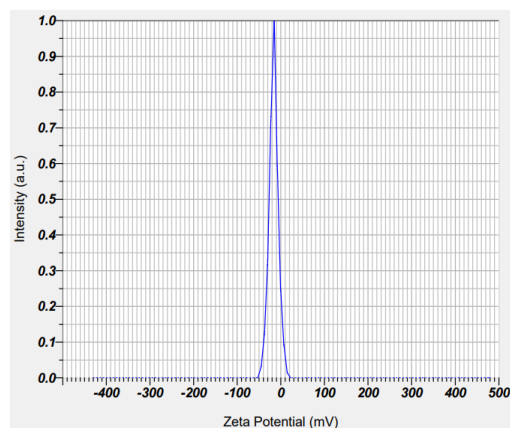


Fig 5B. zeta potential of formulation B2

Zeta Potential (Mean) : -22.2 mV
Electrophoretic Mobility Mean : -0.000171 cm²/Vs

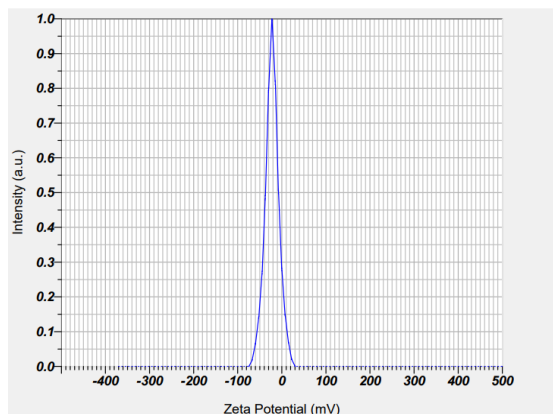


Fig 5C. zeta potential of formulation B3

Zeta Potential (Mean) : -67.1 mV
Electrophoretic Mobility Mean : -0.000519 cm²/Vs

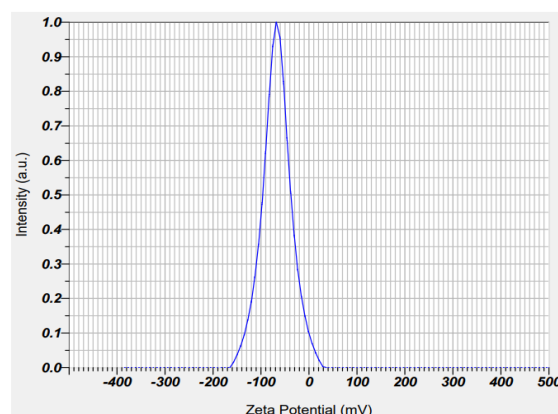


Fig 5D. zeta potential of formulation B4

To stabilize the Nanogel the Zeta Potential must be more than ± 20 mV and it was observed from the above figure that batch 4 shows -67.1 mV. From the Graphical representation the prepared Nanogel of B4 is more stable.

***In-vitro* Diffusion studies:**

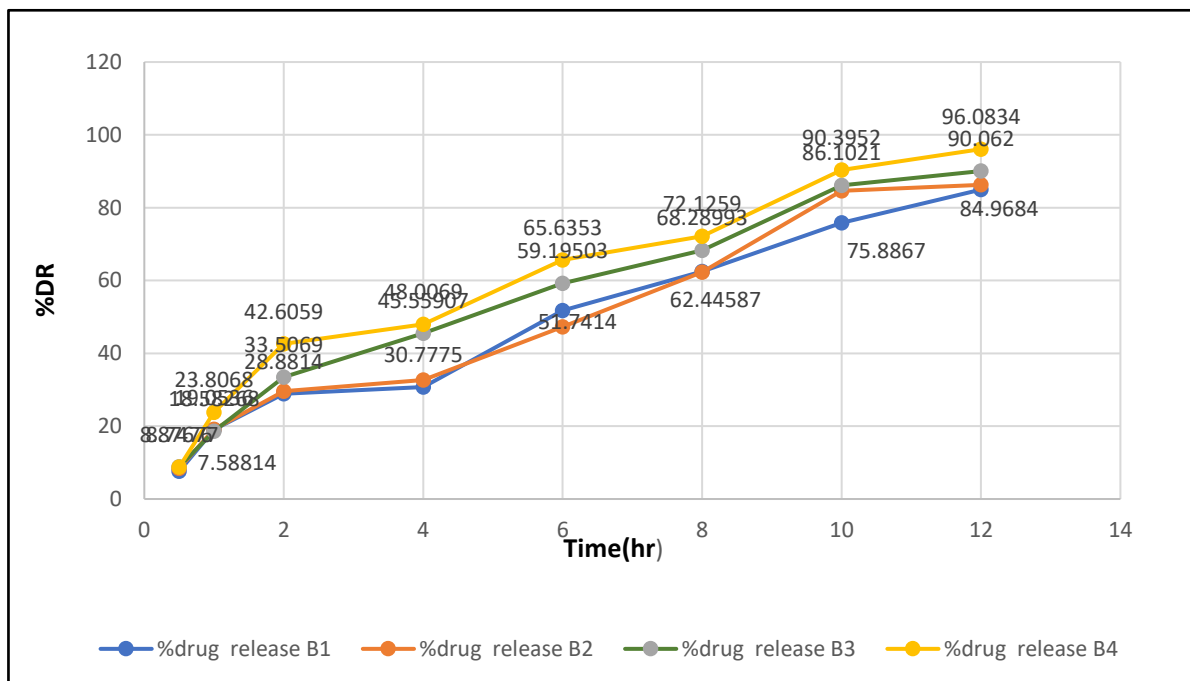


Fig 6: In-vitro drug release profile of nanogel of Kojic acid

From the above graph and % drug released readings batch 1 has 84.96% of drug release, batch 2 shows 86.27% drug release, batch 3 shows 90.06% drug release, batch 4 shows 96.83% drug

release in 12 hours. Formulation batch 4 shows maximum %drug release. Batch 4 have optimum concentration of polymer. Hence batch 4 consider optimise batch among 4 batches.

Viscosity study: (Spindle number-96)

Table 2: Viscosity results of B1

RPM	Surface (cP)	Middle (cP)	Bottom (cP)
10	27000	27560	28970
20	17530	19310	20480
30	14690	15250	16220
40	10200	10800	10930
50	9328	9469	1547

Table 4: Viscosity results of B3

RPM	Surface (cP)	Middle (cP)	Bottom (cP)
10	22220	23110	24000
20	13550	13730	13880
30	10840	11090	11410
40	7388	7575	8231
50	6516	6531	6875

Particulars	Batch1	Batch2	Batch3	Batch4
Appearance	Whitish to colourless	Whitish to colourless	Whitish to colourless	Whitish to colourless
Fill volume (gm)	10gm	10gm	10gm	10gm
pH	5-7.5	5-7.5	5-7.5	5-7.5
Extrudability	++ (very good)	++ (very good)	+++ (excellent)	+++ (excellent)

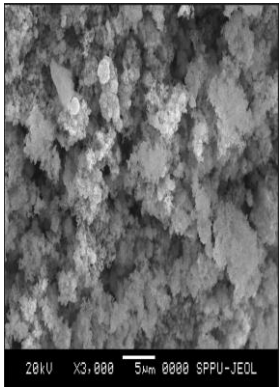
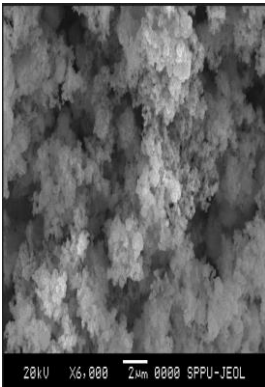
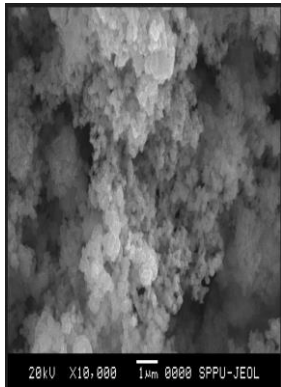
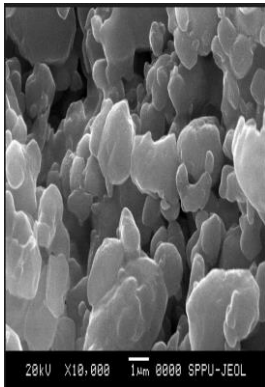
Table 3: Viscosity results of B2

RPM	Surface (cP)	Middle (cP)	Bottom (cP)
10	21940	21840	25590
20	15230	15940	14160
30	10650	10560	11120
40	7969	7406	7631
50	6688	6531	6625

Table 5: Viscosity results of B4

RPM	Surface (cP)	Middle (cP)	Bottom (cP)
10	45000	50440	51000
20	30050	30560	31220
30	23380	23970	24560
40	15960	16560	16610
50	14200	14500	14690

Table 6: Evaluation For all formulated batches (B1-B4)

Conductivity				
1)200ms	0	0	0	0
2)20ms	0	0.2	0.0	0.1
3)2ms	0.03	0.05	0.03	0.12
4)200 μ s	27	057	021	123
5)20 μ s	1.0	1.0	1.0	1.0
Zeta potential (mV)	0.4mV	-16.3mV	-22.2mV	-67.4mV
Particle size (nm)	1754.20nm	1018.9nm	851nm	746nm
Spreadability (gm.cm/sec)	4.1 \pm 0.0264	4.6 \pm 0.0284	3.9 \pm 0.057	3.2 \pm 0.0156
Scanning electron microscopy				
Content Uniformity (%)	94.6%	96.1%	98.4%	98.7%

Conclusion:

It can be concluded from the experimental study carried out that the formulation of a Nanogel containing Kojic acid drug yields a formulation with a spherical and smooth surface, nano in the size range. The prepared nanogel was smooth without any lumps, particles and aggregates. So, all the formulations are homogenous. Based on all the factors the nanogel drug delivery system Batch-4 shows good drug content compared to others. The particle size of the nanogel formulation is optimum and it is less than 1000 nm. So, it concluded that the particles are in the tiny and nano in the size range. All nanogel formulations show pH in the range of 5.5 to 7. Based on the Spreadability diameter study it shows the nanogel is having good Spreadability. Nanogel formulations show a viscosity range from 5000-50000 cps. It concluded that they are stable in nature. Formulation Batch-4 showed the highest percentage of drug release compared to other formulations. In-vitro diffusion studies show Batch-4 formulation shows a controlled release pattern of drug from the formulation. The Zeta potential of batch Batch-4 showed -67.3mV. High zeta potential values show there will be no particles come together and no

flocculation. Hence it can be concluded from the experimental study carried out, that the formulation Batch-4 is an optimized batch with optimum HPMC K35M and Carbopol940.

ACKNOWLEDGEMENT

For the completion of the research work the authors would like to show sincere gratitude to PDEA'S Shankarrao Ursal College of Pharmaceutical Sciences & Research centre, Kharadi, Pune to provide with a lot of support and help whenever needed.

CONFLICT OF INTEREST

All authors declared no conflicts of interest.

References

- [1] Sultana F, Manirujjaman M, Imran-Ul-Haque MA, Sharmin S. An overview of nanogel drug delivery system. *Journal of Applied Pharmaceutical Science*. Sep 2013; 3(8): 95- 105.
- [2] Patel HA, Patel JK. Nanogel as a controlled drug delivery system. *Int. J. Pharm. Sci. Rev. Res.* 2010; 4(2): 37-41.
- [3] Dorwal D. Nanogels as novel and versatile pharmaceuticals. *Int J Pharm Sci.* 2012; 4(3): 67-74.
- [4] Adhikari B, Cherukuri S, Reddy CS, Haranath C, Bhatta HP, Naidu Inturi R. Recent advances in nanogels drug delivery systems. *World Journal of Pharmacy and Pharmaceutical Sciences.* 2016; 5(9): 505-30.
- [5] Prasad K, Vijay G, Jayakumari NK, Dhananjaya A, Valliyil L. Nanogel as a smart vehicle for local drug delivery in dentistry. *American Journal of Pharmacy and Health Research.* 2015; 3(1): 19-30.
- [6] Dinda SC. *Advances in Pharmaceutical Techonology. School of Pharmaceutical Education and Research.* 2011;69-82.
- [7] Kang M, Park S-H, Oh SW, et al. Anti-melanogenic effects of resorcinol are mediated by suppression of cAMP signaling and activation of p38 MAPK signaling. *Biosci Biotechnol Biochem.* 2018; 82(7):1188–1196.
- [8] Nicolaidou E, Katsambas AD. Pigmentation disorders: hyperpigmentation and hypopigmentation. *Clin Dermatol.* 2014;32(1): 66–72.
- [9] Saeedi M, Eslamifar M, Khezri K. Kojic acid applications in cosmetic and pharmaceutical preparations. *Biomed Pharmacother.* 2019; 110:582–593.
- [10] Khezri K, Saeedi M, Morteza-Semnani K, et al. An emerging technology in lipid research for targeting hydrophilic drugs to the skin in the treatment of hyperpigmentation disorders: kojic acid solid lipid nanoparticles. *Artif Cells Nanomed Biotechnol.* 2020; 48(1):841–853.

- [11] Yogesh Pounikar*, Pushpendra Jain, Navneet Khurana, L. K. Omray, S. Patil Formulation and Characterization of Aloe Vera Cosmetic Herbal Hydrogel, International Journal of Pharmacy and Pharmaceutical Sciences Vol 4, Suppl. 4, 2012: 85-86.
- [12] Swati Talele, Preetam Nikam¹, Braja Ghosh, Chaitali Deore, Ashwini Jaybhavne, Anil Jadhav², A Research Article on Nanogel as Topical Promising Drug Delivery for Diclofenac sodium, Indian Journal of Pharmaceutical Education and Research | Vol 51 | Issue 4S: Oct-Dec (Suppl.), 2017.
- [13] Chowhan ZT. Role of binders in moisture-induced hardness increase in compressed tablets and its effect on in vitro disintegration and dissolution. J. Pharm. Sci. 1980; 69; 1-4.
- [14] Kumar Nrendra (2014), Study Of extraction, Isolation and Physico-Chemical Properties of Psidium Gaujava, International Journal of Research Science and Management, ISSN: 2349-5197.
- [15] Gupta A, Mishra AK, Singh AK, Gupta V, Bansal P. Formulation and evaluation of topical gel of diclofenac sodium using different polymers. Drug Invent. Today. 2010; 2: 250-253.
- [16]. Ahmed M, Gendy E, Alaa A. In vitro Release Studies of Flurbiprofen from Different Topical Formulations. Drug Dev. Ind. Pharm. 2002; 28(7):823-831.
- [17]. Goyal S, Sharma P, Ramchandani U, Shrivastava SK. et al. Formulation development and characterization of aceclofenac gel containing linseed oil and ginger oleoresin. Int. J. Pharm. Biol. Arch. 2011; 3(3):1087-1094.
- [18] Karthik. T.V.K., Martinez, V., Agrawal. V., Porous silicon ZnO/SnO₂ structures for CO₂ detection, Journal of alloys and Compounds, 731, 2008, 853-863
- [19] Hiemenz, Principles of Colloid and Surface Chemistry, Marcel Decker, 1977
- [20] <https://www.brookhaveninstruments.com/>
- [21] <https://www.brookhaveninstruments.com/product/srel-solvent-resistant-electrode/>
- [22] [https://www.brookhaveninstruments.com/wp-content/uploads/2021/02/guide-to-choosing-zeta](https://www.brookhaveninstruments.com/wp-content/uploads/2021/02/guide-to-choosing-zeta-potential-analyzer-brookhaven-instruments-new.p) potential-analyzer-brookhaven-instruments-new.p
- [23] <https://www.brookhaveninstruments.com/>
- [24] Michaels A.S, Chandrasekaran S. K, Shaw J.E. Drug permeation through human skin: Theory and invitro experimental measurement. AIChE J. 2004;21(5) 16 Williams AC, Barry BW. Penetration enhancers. Adv drug deliv rev.2004;56(5):603-618.
- [25] Belgamwar V, Patel H, Joshi A, Agrawal A, Surana S. Design and development of nasal mucoadhesive microspheres containing tramadol HCl for CNS targeting. Drug Delivery, Informa Healthcare, 2011;18(5):353-360.
- [26] Patel, J., Ketkar, S., Patil, S., Fearnley, J., Mahadik, K. R., & Paradkar, A. R. (2015). Potentiating antimicrobial efficacy of propolis through niosomal-based system for administration. Integrative medicine research, 4(2), 94-10.



Analytical Method Development and Validation of Allopurinol in Bulk and it's Dosage Form by Using RP-HPLC

**Ms. Komal Kendre, Dr. Ashok Bhosale, Mr. Vikram Veer, Dr. Amit Kasabe,
Ms. Pranali Pinjari, Almisba Shaikh**

Research Scholar, PDEA's Shankarrao Ursal College of Pharmaceutical Sciences and
Research Centre, Kharadi, Pune

Principal, PDEA's Shankarrao Ursal College of Pharmaceutical Sciences

and Research Centre, Kharadi, Pune

Assitant Professor , PDEA's Shankarrao Ursal College of Pharmaceutical Sciences
and Research Centre, Kharadi, Pune

Assitant Professor , PDEA's Shankarrao Ursal College of Pharmaceutical

Sciences and Research Centre, Kharadi, Pune

Research Scholar, PDEA's Shankarrao Ursal College of Pharmaceutical Sciences
and Research Centre, Kharadi, Pune

Research Scholar, PDEA's Shankarrao Ursal College of Pharmaceutical
Sciences and Research Centre, Kharadi, Pune

ABSTRACT

Development of a simple, accurate, time-tested, high-performance liquid chromatography method for determination of Allopurinol in bulk and Pharmaceutical Formulation. HPLC system used was JASCO system equipped with model PU 4180 RHPLC pump, Rheodyne sample injection port (20 μ l), JASCO UV-4075 UV-VIS detector. Separation was carried out on HiQSil C18 (250 mm \times 4.6 mm, 5 μ m) column using mixture of acetonitrile and ammonium acetate buffer (20 mM) in the ratio of 55:45, v/v as mobile phase at flow rate of 1.0 mL/min. Samples were injected using Rheodyne injector with 20 μ L loop, Detection was carried out at 254nm. The retention time was found to be 3.05 min. The HPLC linear regression analysis results for calibration plots demonstrated a good relationship with ($r^2 = 0.9992$). The method has been validated for its accuracy, Recovery, Robustness and documented. The LOD and LOQ were found to be 1.52 & 2.55 μ g/m/ respectively for API and 1.78 & 2.78 μ g/ml respectively for tablet. The proposed HPLC method has been proven to be effective for the determination of Allopurinol in Bulk as well as pharmaceutical dosage forms.

KEYWORDS : RP-HPLC, Allopurinol, API, TABLET

INTRODUCTION

Allopurinol is a structural isomer of hypoxanthine and a purine analog. (a purine that occurs naturally in the body) and is a xanthine oxidase inhibitor. That means it stops xanthine oxidase enzyme to function properly. Xanthine oxidase. Converts oxypurines (hypoxanthine and xanthine) to uric acid. It is prevalent in many organs like the kidneys, blood plasma, the liver, the stomach, the heart, and the brain. Xanthine oxidase turns hypoxanthine into xanthine, which is then converted into uric acid¹⁻⁴. Foods that have been broken down and excreted by cells produce uric acid, which is then excreted to the kidneys. Xanthine oxidase production was up but at a decreased level. The can be raised by hypoxanthine, xanthine, or by having less efficient kidneys the blood's level of uric acid⁵⁻⁶. Blood uric acid levels are too high. causes the gout-related pain and swelling when it accumulates around joints. Increases in uric acid are also linked to organ damage and failure. Allopurinol used in the treatment of medical conditions associated with high uric acid levels, such as gout and cancer prevention lysis syndrome Allopurinol is effective for treating both primary hyperuricemia of gout and secondary hyperuricemia related to haematological disorders or antineoplastic therapy. Its molecular weight is 136.11. It is chemically named as 1,5-dihydropyrazolo[3,4-d]pyrimidine-4-one.⁷⁻¹²

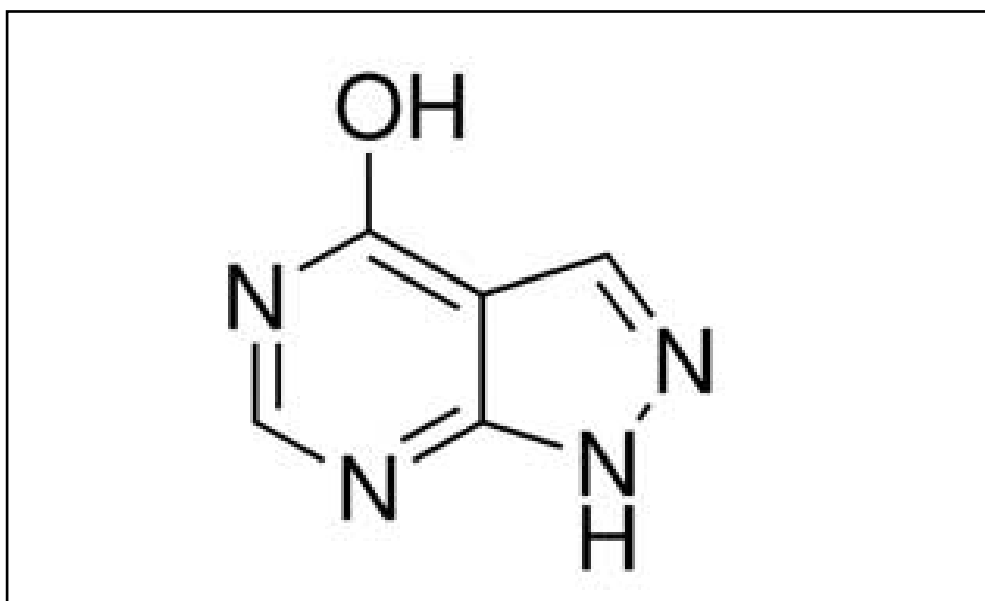


Figure 1: Structure of Allopurinol

Analytical method development

Allopurinol API and Tablet

Determination of Lambda maximum

Preparation of stock solution of Allopurinol API and Tablet

Allopurinol API and Tablet (100 mg) in a 100mL volumetric flask and 25 mL of ACN to it and it was vortexed (Eltek) for 2 minutes. This was the main stock accounting for concentrations of 1000 µg/mL. A diluted solution was used to scan in UV-Spectrophotometer in the range of 200-400nm, taking ACN as blank.

The lambda maximum for Allopurinol API was found to be 254nm.

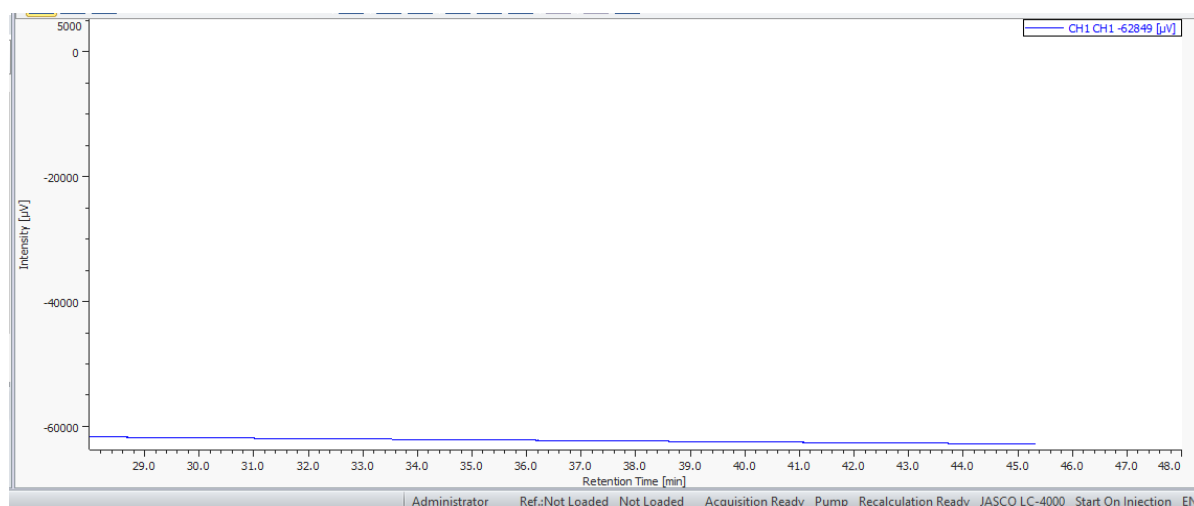


Figure 2: HPLC chromatogram of blank.

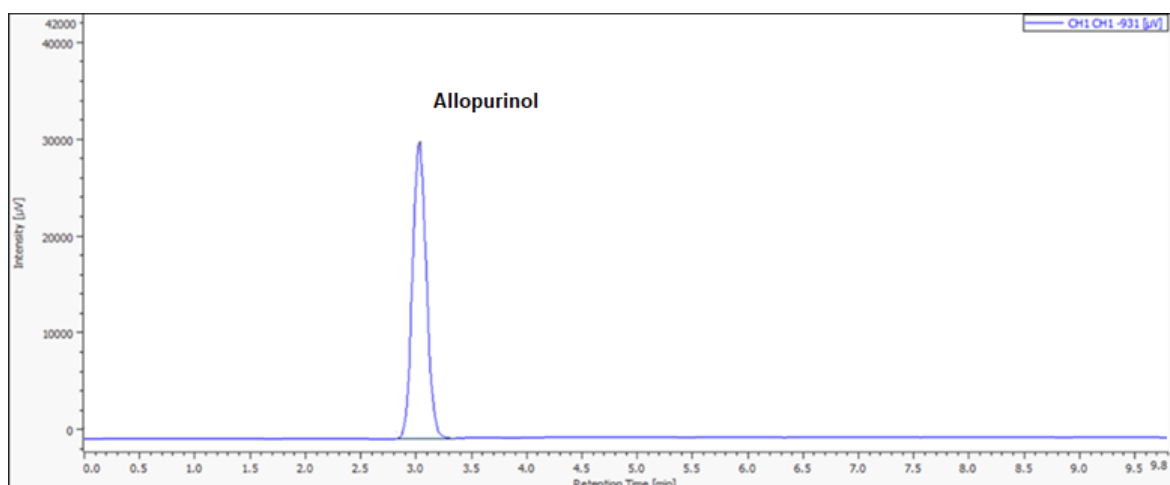


Figure 3 : HPLC chromatogram of standard Allopurinol API

The retention time was found to be 3.05 min with distinct peak.

MATERIALS AND METHODS

Materials

Allopurinol API and Tablet was procured from Solanki enterprises (Pune, India) Chemicals utilized for method development are of HPLC grade includes ACN, Ammonium acetate buffer (20 mM) were purchased from Merck (India) Ltd.

Preparation of mobile phase

The preparation of mobile phase was done by mixing mixture of acetonitrile and ammonium acetate buffer (20 mM) in the ratio of 55:45, v/v. Removal of gases was carried out in ultrasonic water bath for 15 minutes. Filtered the solution through 0.45 μ filter.

Diluent preparation

Mobile phase used as diluents.

Preparation of standard stock solution

100mg of Allopurinol API standard was transferred into 100ml volumetric flask, dissolved & make up to volume with mobile phase. Further dilution was done by transferring 1 ml of the above solution into a 10ml volumetric flask and make up to volume with mobile phase and performed the subsequent dilutions.

Preparation of test solution

100mg equivalent of Allopurinol API and Tablet was transferred into 100ml volumetric flask, dissolved & make up to volume with mobile phase. Further dilution was done by transferring 1 ml of the above solution into a 10ml volumetric flask and make up to volume with mobile phase and performed the subsequent dilutions.

Selection of analytical wavelength

It is the characteristic of a compound which helps to provide the electronic structure of the compound or analyte. The structural analysis of Allopurinol API and Tablet was carried out under UV ranging from 200-400nm using the standard solution.

Method Validation¹³⁻²²

Linearity

The linearity of the developed method was studied over the concentration ranges between 10-60µg/ml. The aliquots of 10, 20, 30, 40, 50 and 60µg/ml were prepared by diluting standard stock solution of 1, 2, 3, 4, 5 and 6 ml with mobile phase. The obtained concentrations were injected into the chromatographic system. Calibration curve of Allopurinol API was constructed by plotting peak area versus used concentration of Allopurinol API. To assure the concentration range studied is linear the regression equation and correlation coefficient were evaluated.

Accuracy

Accuracy was carried out by % recovery studies at three different concentration levels. To the pre-analysed sample solution of Allopurinol API and Tablet, a known amount of standard drug powder of Allopurinol API and Tablet was added to 80, 100, 120% level.

Precision method

By studying the changes in the inter-day and intra-day determined the precision of the method. In the intra-day studies, six repeated injections of standard solution were made and % RSD were calculated. In the inter-day variation studies, six repeated injections of standard solution were made for six consecutive days and %RSD were calculated.

Limit of Detection and Limit of Quantitation

Based on the standard deviation of response of the calibration curve the LOD and LOQ of the drug was determined separately.

Robustness

Robustness of the method was tested by small but deliberate variations of flow rate, mobile phase composition and wavelength.

RESULTS AND DISCUSSION

Selection of wavelength maxima

The solution of Allopurinol API was scanned between ranges 200- 400nm. UV spectra of the drug show maximum absorbance at 254nm.

Method development

The proposed chromatographic method was found to be suitable for effective separation of Allopurinol API and Tablet with good resolution, peak shape given in the figure. The mobile phase composed of mixture of acetonitrile and ammonium acetate buffer (20 mM) in the ratio of 55:45 v/v, at a flow rate of 1.0 ml/min was selected as it gave well resolved peaks of standard Allopurinol API and Tablet. The optimum wavelength 254nm selected for detection and quantitation.

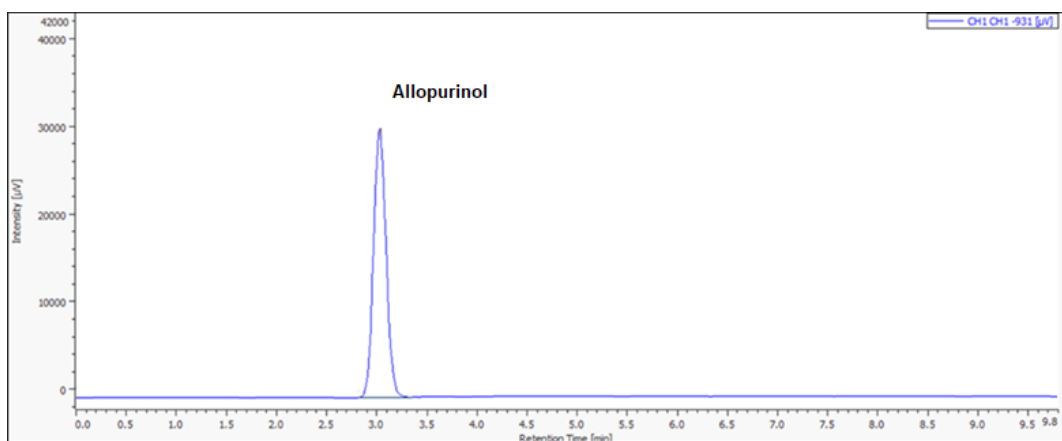


Figure 4 : HPLC Chromatogram with resolved peak of Allopurinol pure drug

Figure 5 : HPLC Chromatogram with resolved peak of Allopurinol Tablet

Sr. No.	Parameter	Conditions used for analysis
1	Column	HiQSil C18 (250 mm × 4.6 mm, 5 μm)
2	Mobile phase	Acetonitrile and ammonium acetate buffer (20 mM)) in the ratio of 55:45, v/v
3	Flow rate	1.0 mL/min

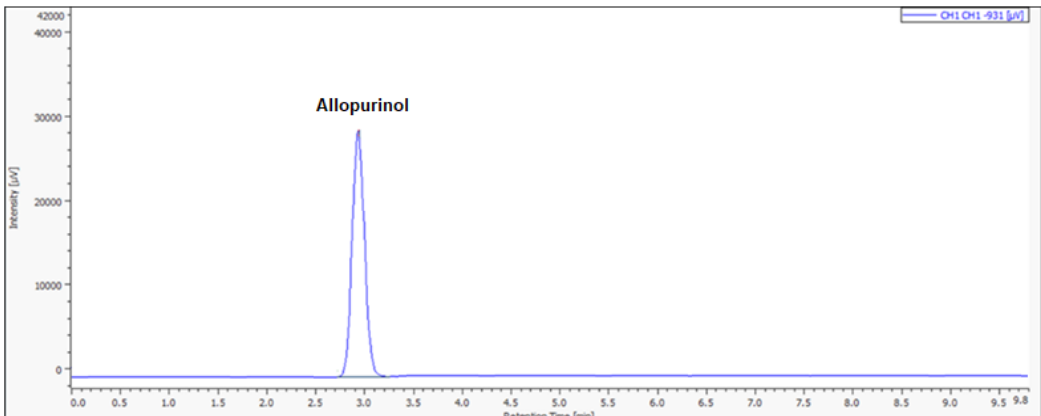


Table no. 1 : Optimized Chromatographic Conditions

Method validation

Linearity

The calibration curves were found be linear for the concentration range of 10-60ppm. The standard working curve equation for drug was found to be $y = 9304x + 9301.1$ with correlation coefficient value $r^2 = 0.9992$. The results of linearity are given in Table and Figure.

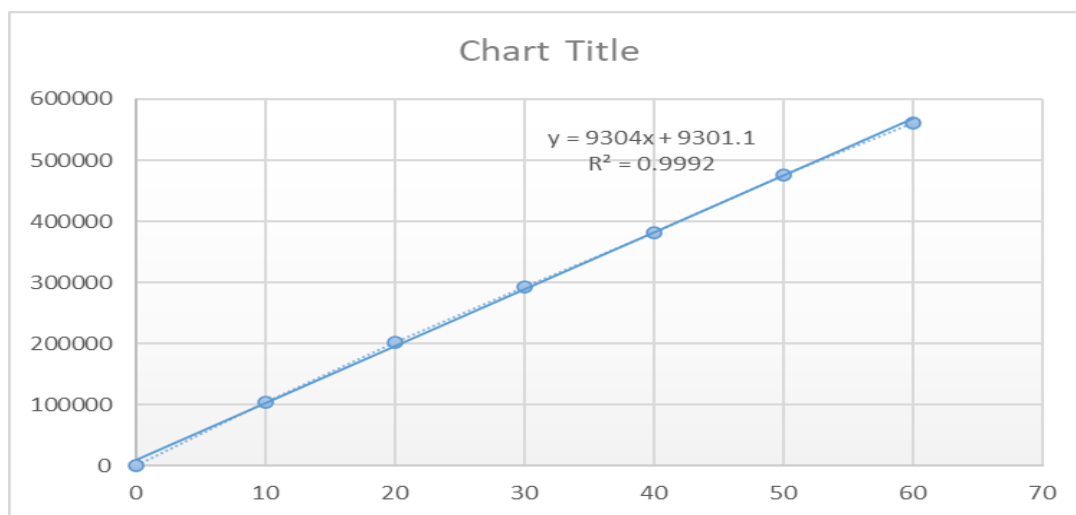


Figure 6 : Linearity curve of standard Allopurinol API

Concentration µg/mL	Area
10	104562
20	202775
30	293123
40	381478
50	475489
60	561521

Table- 2: Linearity data of Allopurinol API

Recovery studies

The mean % recovery at 80, 100, 120 % of the test concentration along with its statistical validation for drug Allopurinol API and Tablet given in Table. The % recovery at 80, 100, and 120 % is given below. It was confirmed that the developed method was accurate as the percent recovery was in the range of 100%.

Level (%)	Drug Conc (mg)	Amount recovered (mg)	% Recovery
80%	8	8.1	101.2
100%	10	10.04	100.4
120%	12	11.8	98.33

Table-3: Recovery data of Allopurinol API

Level(%)	Drug conc (mg)	Amount recovered (mg)	% Recovery
80%	8	8.2	102.5
100%	10	10.15	101.5
120%	12	12.11	100.9

Table-4: Recovery data of Allopurinol Tablet

Precision

The repeatability of sample application and measurement of peak area were expressed in terms of % RSD and was found to be less than 2.0%. The % RSD of intra-day precision is given below. The results of precision studies are shown in Table.

Conc µg/mL	Area	AVG	%RSD
10	125462	125502.333	0.04507605
	125567		
	125478		
20	184256	186077	0.88351421
	187452		
	186523		
30	245458	245865.333	0.18445195
	245784		
	246354		

Table- 5: Precision study (intra- day) of Allopurinol API

Conc µg/mL	Area	AVG	%RSD
10	125364	125402.333	0.05225673
	125478		
	125365		
20	185421	185590.667	0.50013497
	186592		
	184759		
30	245632	246450	0.49230598
	247844		
	245874		

Table- 6: Precision study (intra- day) of Allopurinol Tablet

Conc µg/mL	Area	AVG	%RSD
10	125463	125620	0.17112147
	125865		
	125532		
20	184526	184970.667	0.31570784
	184754		
	185632		
30	245156	246298.667	0.56289403
	245899		
	247841		

Table- 7: Precision study (inter-day) of Allopurinol API

Conc µg/mL	Area	AVG	%RSD
10	125478	125298	0.27907057
	125521		
	124895		
20	184756	182949	0.14237934
	178452		
	185639		
30	235878	235436.667	0.24467624
	235647		
	234785		

Table- 8: Precision study (inter-day) of Allopurinol Tablet

Limit of Detection (LOD) and Limit of Quantification (LOQ)

This data showed that the sensitivity of method to determine the drug Allopurinol API and Tablet. The Minimum concentration level at which the analyte can be reliable detected (LOD) & quantified (LOQ) were found to be 1.52 & 2.55 µg/m/ respectively for API and 1.78 & 2.78 µg/m/ respectively for tablet.

Robustness

Robustness of method was measured by multiple injections of a homogenous sample containing Allopurinol API and Tablet by changing flow rate 0.9 mL/min and 1.1 mL/min, mobile phase composition ammonium acetate buffer (20 mM) in the ratio of 54:46 and 56:44 v/v, wavelength i.e., 253nm and 255nm. The method was found to be robust in the range of deliberate changes made.

Flow rate mL/min	Conc µg/mL	Area	AVG	%RSD
0.9	20	187454	185874.667	0.76517091
0.9		185475		
0.9		184695		
1.1	20	185478	185684.667	0.31866782
1.1		186352		
1.1		185224		

Table-9: Robustness study with change in flow rate of Allopurinol API

Flow rate mL/min	Conc µg/mL	Area	AVG	%RSD
0.9	20	184755	187388.333	1.31858649
0.9		189656		

0.9		187754		
1.1	20	186320	185837.667	0.22813348
1.1		185524		
1.1		185669		

Table-10: Robustness study with change in flow rate of Allopurinol Tablet

Mobile phase (ACN: 01% OPA)	Conc µg/mL	Area	AVG	%RSD
54:46	20	187474	186234.667	0.57698876
54:46		185667		
54:46		185563		
56:44	20	180254	183800.333	1.6711687
56:44		185524		
56:44		185623		

Table-11: Robustness study with change in concentration of mobile phase of Allopurinol API

Mobile phase (ACN: 01% OPA)	Conc µg/mL	Area	AVG	%RSD
54:46	20	180263	182761.333	1.25197629
54:46		184755		
54:46		183266		
56:44	20	185996	185438.333	0.34110935

56:44		184751		
56:44		185568		

Table-12: Robustness study with change in concentration of mobile phase of Allopurinol Tablet

Wavelength nm	Conc µg/mL	Area	AVG	%RSD
253	20	187549	186221.667	0.62014868
253		185447		
253		185669		
255	20	182563	184521.333	0.9192206
255		185475		
255		185526		

Table-13: Robustness study with change in Wavelength of Allopurinol API.

Wavelength nm	Conc µg/mL	Area	AVG	%RSD
253	20	180254	180461	1.22701005
253		175466		
253		185663		
255	20	182052	182648.333	1.49886542
255		180258		
255		185635		

Table-14: Robustness study with change in Wavelength of Allopurinol tablet

CONCLUSION

A HPLC method developed has been validated as per ICH guidelines in terms of accuracy, precision, linearity, robustness, limit of detection and limit of quantitation, for the determination of Allopurinol API and Allopurinol tablet. A good linear relationship was observed in concentration ranges of 10 and 60 µg/ml. The correlation coefficients was 0.9992. The inter day and intraday precision results were good enough to say that the method developed is precise and reproducible. Accuracy studies revealed that mean recoveries after spiking experiments were between 100.6 and 101 %, an indicative of accurate method. Accordingly it can be concluded that the developed method is accurate, precise, linear, and robust.

ACKNOWLEDGEMENTS

The author wishes to express gratitude to the Solanki Enterprises for providing sample of Allopurinol API and Aster Lab for permission and facilities to carry out the research work.

REFERENCES

1. Ammar AA, Samy AM, Marzouk MA, Ahmed MK. Formulation, characterization and biopharmaceutical evaluation of Allopurinol tablets. *International Journal of Biopharmaceutics* 2011; 2(2):63-71.
2. Derek K, Da-peng wang TL. Formulation development of Allopurinol suppositories and injectables. *Drug development and Industrial pharmacy* 1999; 25(11):1205-1208.
3. Clark's analysis of drugs and poisons in pharmaceutical body fluids and post mortem materials. 3rdEdn. London: Pharmaceutical press;2004, 601-603
4. Analytical procedures and methods validation (2000): Chemistry, manufacturing, and controls federal register (Notices). PP. 776-7
5. Cameron, J.S; Moro, F and Simmonds, H.A. (1993) "Gout, uric acid and purine metabolism in paediatric nephrology".7(1):105-118
6. Dalbeth, N and Stamp, L (2007). Allopurinol Dosing in Renal Impairment: Walking the Tightrope between Adequate Urate Lowering and Adverse Events 20 (5): 391–5.

7. International Conference on Harmonization (ICH) of Technical Requirements for the Registration of Pharmaceuticals for Human use, Validation of analytical procedures (1996): definition and terminology, Geneva 2005; 3-10.
8. Lindholm J, Development and Validation of HPLC Method for Analytical and Preparative Purpose, Acta Universities Upsaliensis Uppsala, 2004; 13-14.
9. Analytical procedures and methods validation (2000): Chemistry, manufacturing, and controls federal register (Notices). PP. 776-7
10. Pacher, P; Nivorozhkin, A and Szabo, C. (2006). "Therapeutic affected of xanthine oxidase inhibitors: Renaissance half century the discovery of allopurinol". 58(1):87-114
11. World Health Organization (2007) "Quality assurance of pharmaceutical". p (5)
12. Kasture A V, Mahadil K.R, Wadodhkar S G, More A H, Pharmaceutical Analysis vol-2 instrumental method, Nirali Prakashan page no.6-9, 60-65.
13. Willard H H, Merritt L L, Dean J A, Settle F A, Instrumental method of analysis, New Delhi, CBS publishers and distributors pg no:513-538.
14. McMurry J (2011). Organic chemistry: with biological applications (2nd ed.). Belmont, CA: Brooks/Cole. pp. 395.
15. Hostettmann K, Marston A, Hostettmann M (1998). Preparative Chromatography Techniques Applications in Natural Product Isolation (Second ed.). Berlin, Heidelberg: Springer Berlin Heidelberg. p. 50.
16. Gerberding SJ, Byers CH. Preparative ion-exchange chromatography of proteins from dairy whey. J Chromatogr A. 1998;808:141-51. [PubMed]
17. Donald PL, Lampman GM, Kritz GS, Engel RG. Introduction to organic laboratory techniques. 4th ed. Thomson Brooks/Cole; 2006. pp. 797-817.
18. Harwood LM, Moody CJ. Experimental organic chemistry : Principles and Practice. Oxford :Blacwell Science; 1989:180-5.
19. Das M, Dasgupta D. Pseudo-affinity column chromatography based rapid purification procedure for T7 RNA polymerase. Prep Biochem Biotechnol. 1998;28:339-48.

20. Karlsson E, Ryden L, Brewer J Protein purification. Principles, High Resolution Methods, and Applications. Ion exchange chromatography. 2nd ed. New York: Wiley; 1998; 456
21. Amercham Biosciences. Ion Exchange chromatohgraphy, Principles and methods, Amercham Pharmacia. Biotech SE. 2002;751
22. Walls D, Loughran ST. Protein chromatography: Methods and protocols, methods in molecular biology. 2011;681



Analytical Method Development And Validation Of Econazole Nitrate by using RP-HPLC

Ms. Pranali Pinjari, Mr. Krunal Kanase, Dr. Vijaya Barge, , Dr. Amit Kasabe, Ms. Komal Kendre, Almisba Shaikh

Research Scholar, PDEA's Shankarrao Ursal College of Pharmaceutical

Sciences and Research Centre, Kharadi, Pune

Assitant Professor, PDEA's Shankarrao Ursal College of Pharmaceutical

Sciences and Research Centre, Kharadi, Pune

Vice Principal & Professor, PDEA's Shankarrao Ursal College of Pharmaceutical Sciences and Research Centre, Kharadi, PAssitant Professor , PDEA's Shankarrao Ursal College of Pharmaceutical

Sciences and Research Centre, Kharadi, Pune

Research Scholar, PDEA's Shankarrao Ursal College of Pharmaceutical

Sciences and Research Centre, Kharadi, Pune

Research Scholar, PDEA's Shankarrao Ursal College of Pharmaceutical

Sciences and Research Centre, Kharadi, Pune

Abstract

A simple and accurate method was developed for the determination and validation of the Econazole Nitrate. HPLC system used was JASCO system equipped with model PU 4180 RHPLC pump, Rheodyne sample injection port (20 μ l), JASCO UV-4075 UV-VIS detector and ChromNAV CFR chromatography software (version 2.0). Separation was carried out on HiQSil C18 (250 mm \times 4.6 mm, 5 μ m) column using Acetonitrile:Methanol (85:15v/v) as mobile phase at flow rate of 1.2 mL/min. Samples were injected using Rheodyne injector with 20 μ L loop, Detection was carried out at 225nm.

The HPLC linear regression analysis results for calibration plots demonstrated a good relationship with ($R^2 = 0.9994$). The method has been validated for its accuracy, Recovery, Robustness and documented. The LOD and LOQ were found to be 1.12 & 2.59 μ g/m/ respectively.

Keywords- Econazole nitrate, Method Development, Validation,

Introduction

Econazole Nitrate is an imidazole derivative and broad-spectrum antimycotic agent with fungistatic properties. Econazole nitrate inhibits biosynthesis of ergosterol, thereby damaging the fungal cell wall membrane and altering its permeability which leads to a loss of essential intracellular components. Additionally, Econazole Nitrate inhibits the biosynthesis of

triglycerides and phospholipids as well as oxidative and peroxidative enzyme activity, which may aid in cell necrosis and death. It is also active against some gram-positive bacteria. The treatment of different dermatomycoses uses this antifungal agent.

Econazole nitrate is an antifungal drug containing imidazole ring which interacts with 14 demethylase a cytochrome P-40 enzyme which converts to lanosterol to ergosterol. Econazole inhibits the ergosterol synthesis which is the essential component of fungal cell membrane, as a result of increased cellular permeability, fungal cells die because cellular components leak out of the cells. Econazole Nitrate is incompletely absorbed after being administered orally due to its low solubility. Additionally, it can be used topically to treat skin infections like tinea and cutaneous candidiasis.

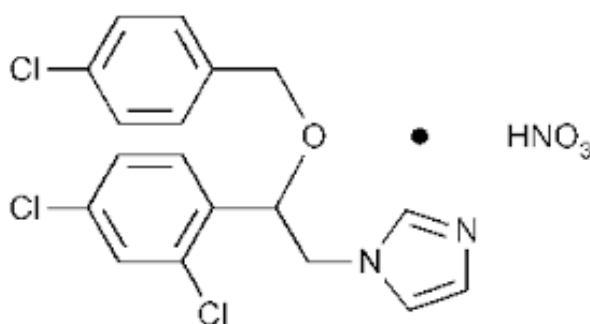


Figure. Structure of Econazole Nitrate

Analytical method development

Determination of Lambda maximum

Preparation of stock solution of Econazole nitrate

Econazole nitrate (100 mg) in a 100mL volumetric flask and 100 mL of methanol to it and it was vortexed (Eltek) for 2 minutes. This was the main stock accounting for concentrations of 1000 µg/mL. A diluted solution was used to scan in UV-Spectrophotometer in the range of 200-400nm, taking methanol as blank.

The lambda maximum for Econazole Nitrate was found to be 225nm.

Instrumentation and Chromatographic Conditions

HPLC system used was JASCO system equipped with model PU 4180 RHPLC pump, Rheodyne sample injection port (20 μ l), JASCO UV-4075 UV-VIS detector and ChromNAV CFR chromatography software (version 2.0). Separation was carried out on HiQSil C18 (250 mm \times 4.6 mm, 5 μ m) column using Acetonitrile: Methanol (85:15v/v) as mobile phase at flow rate of 1.2 mL/min. Samples were injected using Rheodyne injector with 20 μ L loop, Detection was carried out at 225nm. All weighing were done on Shimadzu balance (Model AY-120)

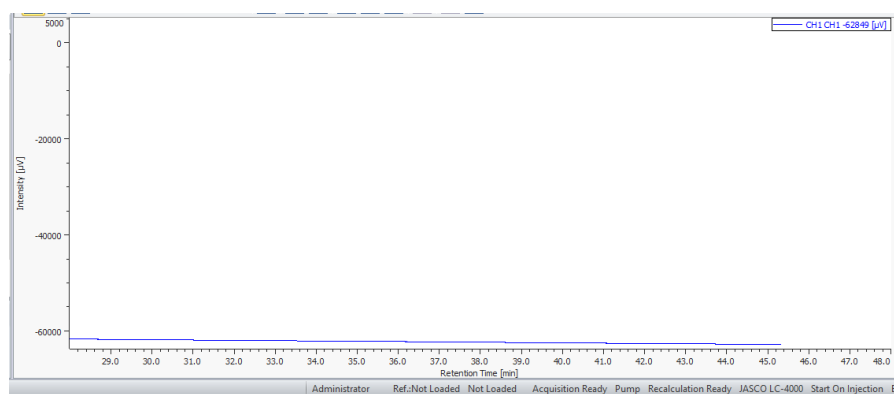


Figure 1: HPLC chromatogram of blank.

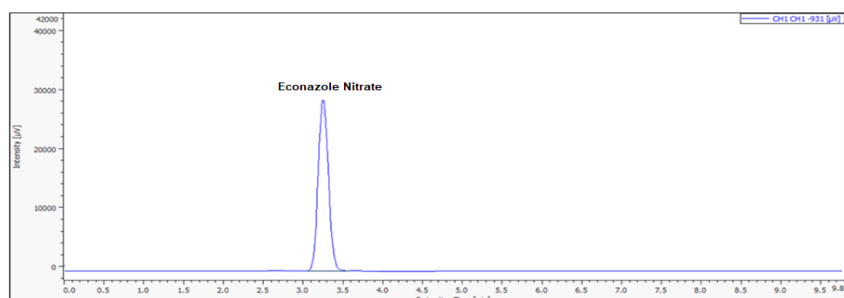


Figure 2: HPLC chromatogram of standard Econazole nitrate.

The retention time was found to be 3.32 with distinct peak.

MATERIALS AND METHODS

Material

Econazole nitrate standard is procured from Solanki Suppliers (Pune, India). Chemicals utilized for method development are of HPLC grade includes Methanol, water were purchased from Merck (India) Ltd.

Preparation of mobile phase

The preparation of mobile phase was done by mixing methanol with ACN in the ratio of 85:15 v/v. Filtered the solution through 0.45 μ filter.

Diluent preparation

Mobile phase used as diluents.

Preparation of standard stock solution

100mg of Econazole nitrate standard was transferred into 100ml volumetric flask, dissolved & make up to volume with mobile phase. Further dilution was done by transferring 1 ml of the above solution into a 10ml volumetric flask and make up to volume with mobile phase and performed the subsequent dilutions.

Preparation of test solution

100mg equivalent of Econazole nitrate API standard was transferred into 100ml volumetric flask, dissolved & make up to volume with mobile phase. Further dilution was done by transferring 1 ml of the above solution into a 10ml volumetric flask and make up to volume with mobile phase and performed the subsequent dilutions.

Selection of analytical wavelength

It is the characteristic of a compound which helps to provide the electronic structure of the compound or analyte. The structural analysis of Econazole nitrate was carried out under UV ranging from 200-400nm using the standard solution.

Method Validation

Linearity:

The linearity of the developed method was studied over the concentration ranges between 10-30 μ g/ml. The aliquots of 5, 10, 15, 20, 25 and 30 μ g/ml were prepared by diluting standard stock solution of 0.1, 0.2, 0.3, 0.4, 0.5 and 0.6 ml with mobile phase. The obtained concentrations were injected into the chromatographic system. Calibration curve of

Econazole nitrate was constructed by plotting peak area versus used concentration of Econazole nitrate. To assure the concentration range studied is linear the regression equation and correlation coefficient were evaluated.

Accuracy

Accuracy was carried out by % recovery studies at three different concentration levels. To the pre-analysed sample solution of Econazole nitrate, a known amount of standard drug powder of Econazole nitrate was added to 80, 100, 120% level.

Precision method

By studying the changes in the inter-day and intra-day determined the precision of the method. In the intra-day studies, six repeated injections of standard solution was made and % RSD were calculated. In the inter-day variation studies, six repeated injections of standard solution were made for six consecutive days and %RSD were calculated.

Limit of Detection and Limit of Quantitation

Based on the standard deviation of response of the calibration curve the LOD and LOQ of the drug was determined separately.

Robustness

Robustness of the method was tested by small but deliberate variations of flow rate, mobile phase composition and wavelength.

RESULTS AND DISCUSSION

Selection of wavelength maxima

The solution of Econazole nitrate was scanned between ranges 200- 400nm. UV spectra of the drug show maximum absorbance at 225nm.

Method development

The proposed chromatographic method was found to be suitable for effective separation of Econazole nitrate with good resolution, peak shape given in the figure. The mobile phase composed of Acetonitrile: Methanol in ratio of 85:15 % v/v, at a flow rate of 1.2 ml/min was selected as it gave well resolved peaks of standard Econazole nitrate. The optimum wavelength 225nm selected for detection and quantitation.

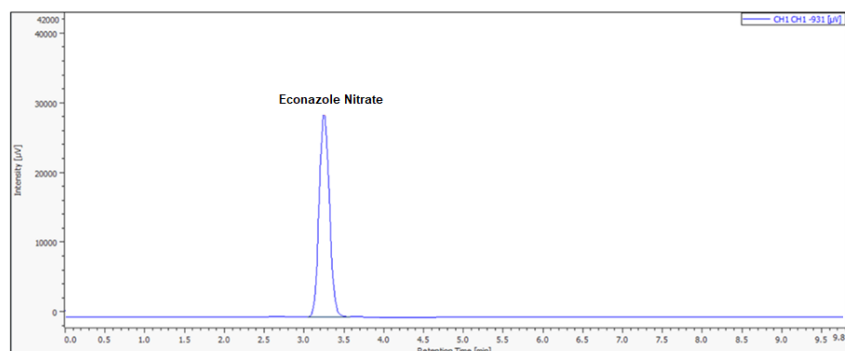


Figure 3: HPLC Chromatogram with resolved peak of Econazole nitrate

Method validation

Linearity

The calibration curves were found be linear for the concentration range of 5-30ppm. The standard working curve equation for drug was found to be $y = 2768.4x + 670.53$ with correlation coefficient value $R^2 = 0.9994$. The results of linearity are given in Table and Figure.

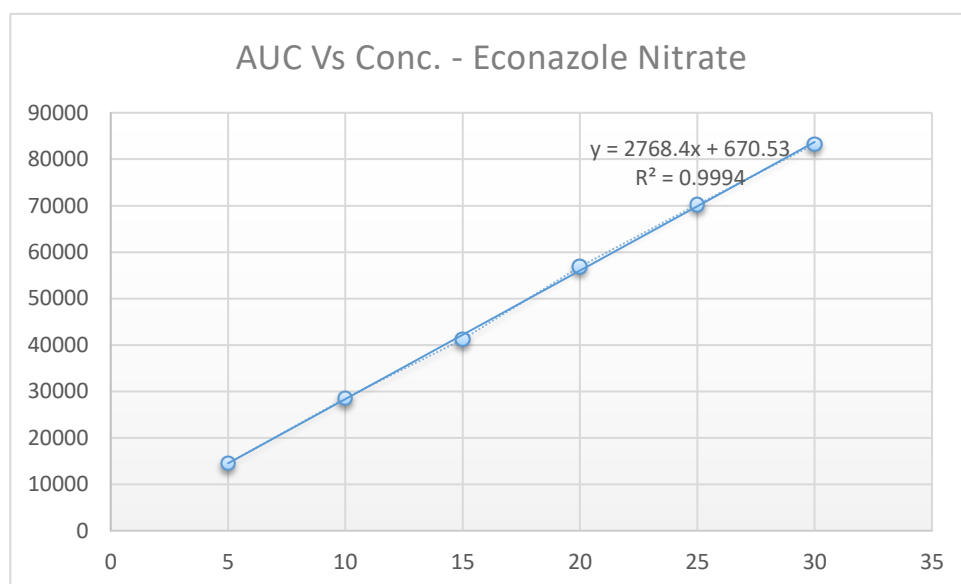


Figure 4: Linearity curve of standard Econazole nitrate

Table 1: Linearity data of Econazole nitrate

Concentration µg/mL	Area
5	14512
10	28567
15	41215
20	56897
25	70254
30	83256

Recovery studies

The mean % recovery at 80, 100, 120 % of the test concentration along with its statistical validation for drug Econazole nitrate given in Table. The % recovery at 80, 100, and 120 % was found to be 101.25, 99.8, and 101.25. It was confirmed that the developed method was accurate as the percent recovery was in the range of 100%.

Table 2: Recovery data of Econazole nitrate

Level (%)	Drug Conc (mg)	Amt recovered (mg)	% Recovery
80%	8	8.1	101.25
100%	10	9.98	99.8
120%	12	12.15	101.25

Precision

The repeatability of sample application and measurement of peak area were expressed in terms of % RSD and was found to be less than 2.0%. The % RSD of intra-day precision was found to be 0.009, 0.006 and 0.004 % RSD of interday precision was found to be 0.011, 0.009 and 0.004. The results of precision studies are shown in Table.

Table 3: Precision study (intra- day) of Econazole nitrate

Conc µg/mL	Area	AVG	%RSD
10	28745	28624.6667	0.48911778
	28658		
	28471		
15	42156	42370.3333	0.50863294
	42587		
	42368		
20	56874	56624.3333	0.94181701
	56987		
	56012		

Conc, Concentration; AVG, average; RSD, Relative standard deviation

Table 4: Precision study (inter-day) of Econazole nitrate

Conc µg/mL	Area	AVG	%RSD
10	28456	28608	0.50714043
	28623		
	28745		
15	41545	41711.6667	1.87815881
	41025		
	42565		
20	56897	56486	0.63400044
	56241		
	56320		

Conc, Concentration; AVG, average; RSD, Relative standard deviation

Limit of Detection (LOD) and Limit of Quantification (LOQ)

This data showed that the sensitivity of method to determine the drug Econazole nitrate. The Minimum concentration level at which the analyte can be reliable detected (LOD) & quantified (LOQ) were found to be 1.12 & 2.59 µg/m/ respectively.

Robustness

Robustness of method was measured by multiple injections of a homogenous sample containing Econazole nitrate by changing flow rate 1.0 mL/min and 1.4 mL/min, mobile phase composition ACN: Methanol ratio 84:16 and 86:14, wavelength i.e., 224nm and 226nm. The method was found to be robust in the range of deliberate changes made.

Table 5: Robustness study with change in flow rate of Econazole nitrate

Flow rate mL/min	Conc µg/mL	Area	AVG	%RSD
1.0	20	55421	55836.67	1.565403
1.0		55248		
1.0		56841		
1.4	20	55789	55411.67	0.590198
1.4		55210		
1.4		55236		

Conc, Concentration; AVG, average; RSD, Relative standard deviation

Table 6: Robustness study with change in concentration of mobile phase of Econazole nitrate

Mobile phase (Methanol: 01% OPA)	Conc µg/mL	Area	AVG	%RSD
84:16	20	56321	56542.67	0.545612
84:16		56895		
84:16		56412		
86:14	20	56321	56367	0.171372
86:14		56478		
86:14		56302		

Conc, Concentration; AVG, average; RSD, Relative standard deviation

Table 7: Robustness study with change in Wavelength of Econazole nitrate.

Wavelength nm	Conc µg/mL	Area	AVG	%RSD
224	20	56320	56334	0.251217

224		56482		
224		56200		
226	20	56874	56376	0.786936
226		56231		
226		56023		

CONCLUSION

A HPLC method developed has been validated as per ICH guidelines in terms of accuracy, precision, linearity, robustness, limit of detection and limit of quantitation, for the determination of Econazole Nitrate API. A good linear relationship was observed in concentration ranges of 5 and 30 μ g/ml. The correlation coefficient was 0.9994. The inter day and intraday precision results were good enough to say that the method developed is precise and reproducible. Accuracy studies revealed that mean recovery after spiking experiments was 100.7%, an indicative of accurate method. Accordingly, it can be concluded that the developed method is accurate, precise, linear, and robust.

ACKNOWLEDGEMENTS

The authors are thankful to Solanki Enterprises for providing sample of Econazole nitrate and Aster Lab for permission and facilities to perform the research work.

REFERENCES

1. Gajra B, Pandya, Singh S and Rabari: Mucoadhesive hydrogel films of econazole nitrate formulation and optimization using factorial design. *Journal of Drug Delivery* 2014: 1-14.
2. Gupta PC, Kapoor A and Pandey P: Designing and characterization of econazole nitrate nanostructured lipid carriers gel for topical delivery. *European Journal of Pharmaceutical and Medical Research* 2018; 5(6): 559-67.
3. Shaikh NM and Kulkarni KB: Formulation and evaluation of nanoemulsion for topical application. *Journal of Drug Delivery and Therapeutics* 2019; 9(4): 370-75
4. Patel H C, Parmar G, Seth A K, Patel J D and Patel S R, "Formulation and evaluation of o/w nanoemulsion of ketoconazole", *International Journal of Pharmaceutical Sciences*, 2013, 4(4): 338-351.
5. A.R. Martin, in: J.N. Delgado, W.A. Remers (Eds.), *Wilson and Davold's Textbook of Organic Medicinal and Pharmaceutical Chemistry*, Lippincot Williams & Wilkins, England, 1998, pp. 173–221.
6. Harry GB, et.al. *Analytical Profiles of Drug Substances and Excipients*. New York: Academic Press. 1994, 23:126-149.
7. Gordana P, Mira C, Katarina V, Sote V, Danica A. Comparison of HPTLC and HPLC for Determination of Econazole Nitrate in Topical Dosage Forms. *JPC*. 2004, 17:109.
8. Stephen E, Wolverton. *Comprehensive Dermatologic Drug Therapy*. Elsevier Inc. 2007.
9. A. Zahoor, S. Sharma, G.K. Khuller, *FEMS Microbiol. Lett.* 258 (2006) 200.
10. A. Zahoor, S. Sharma, G.K. Khuller, *FEMS Microbiol. Lett.* 261 (2006) 181.

11. International Conference on Harmonization (ICH) of technical requirements for the registration of pharmaceuticals for human use, validation of analytical procedures (1996): methodology, adopted, Geneva.
12. International Conference on Harmonization (ICH) of Technical Requirements for the Registration of Pharmaceuticals for Human use, Validation of analytical procedures (1996): definition and terminology, Geneva.
13. Bahia Abbas MOUSA et.al Stability Indicating Methods for the Determination of some Anti-fungal Agents Using Densitometric and RP-HPLC Methods.
14. Angel Arturo Gaona-Galdos et.al Simultaneous determination of econazole nitrate, main impurities and preservatives in cream formulation by high performance liquid chromatography.
15. Christinat R, Zulliger HW, Stability indicating HPLC-method for the determination of econazole nitrate in creams and lotion formulations.
16. INDIAN PHARMACOPOEIA 2014 Published By The Indian Pharmacopoeia Commission, Ghaziabad, Volume II, Pg: 1643-1645.
17. BRITISH PHARMACOPOEIA 2016 Published By Health Ministers Of The United Kingdom, Volume I, Pg: 784-785.
18. ICH Q2A, Validation of Analytical Procedures (1995): Definitions and Terminology, Geneva.
19. ICH Q2B, Validation of Analytical Procedures (1996): Methodology, adopted, Geneva.
20. United States Pharmacopeia, 31st ed. The United States Pharmacopoeial Convention, Rockville, 2008, pp. 683–687.
21. E. McEvoy, S. Donegan, J. Power, K. Altria, J. Pharm. Biomed. Anal. 44 (2007) 137.
22. International Conference on Harmonization (ICH) of Technical Requirements for Registration of Pharmaceuticals for Human Use, Topic Q2 (R1): Validation of Analytical Procedures: Text and Methodology, Geneva, 2005.



Formulation Development and Evaluation for Nanofibrous Tablet of Glibenclamide

Kalamkar Tanmayi^{1*}, Veer Vikram², Dr. Kasabe Amit³,

Patil Dipti¹, Gavhane Mayuri¹

¹Research Scholar, Department of Pharmaceutical Quality Assurance, PDEAs Shankarrao Ursal College of Pharmaceutical Sciences and Research Centre, Pune, Maharashtra, India.

²Assistant Professor, Department of Pharmaceutical Quality Assurance, PDEA'S Shankarrao Ursal College of Pharmaceutical Sciences & Research Centre, Kharadi, Pune, Maharashtra, India.

³Assistant Professor, Department of Pharmaceutical Quality Assurance, PDEA'S Shankarrao Ursal College of Pharmaceutical Sciences & Research Centre, Kharadi, Pune, Maharashtra, India.

For Correspondence –Kalamkar Tanmayi Dattatray

kalamkartanu@gmail.com

ABSTRACT - Poor solubility, erratic bioavailability and delivery challenges associated with Glibenclamide, which is commonly used in type 2 diabetes mellitus (T2DM) treatment, are overcome by exploring electrospun nanofibers technology. Employing electrospinning method with polyvinyl alcohol (PVA) combination with poly(D,L-lactide-co-glycolic acid) (PLGA), nanofibers were fabricated. Different concentrations of PLGA at 0.02%, 0.03% and 0.05% w/v were added to PVA to achieve a modified drug release profile to meet the typical physiological needs of T2DM, such as a faster drug release at meals followed by prolonged release to maintain constant plasma glucose level, which is highly desirable in T2DM management. Fabricated Glibenclamide-nanofibers were characterized by Scanning electron microscopy (SEM) and Fourier transform infrared (FTIR) spectroscopy. Fabricated nanofibers compressed with other excipients in a tablet and used for oral administration. Formulated tablets were evaluated for hardness, friability, thickness, drug content and in-vitro study. F3 batch was selected as optimize batch from the similarity factor, cumulative drug release and drug content study.

KEYWORDS – Nanofibers, Electrospinning, Glibenclamide, Fabrication

INTRODUCTION - **Nanofibers** are fibers with diameters in the nanometer range (typically, between 1 nm and 1 μ m). Nanofibers can be generated from different Polymers and hence have different physical properties and application potentials. Examples of natural polymers include collagen, cellulose, silk fibroin, keratin, gelatin and polysaccharides such as chitosan and alginate. Examples of synthetic polymers include poly (lactic acid) (PLA), polycaprolactone (PCL), polyurethane (PU), poly(lactic-co-glycolic acid) (PLGA), poly (3-hydroxybutyrate-co-3-hydroxyvalerate)

(PHBV), and poly(ethylene-co-vinyl acetate) (PEVA). Polymer chains are connected via covalent bonds. The diameters of nanofibers depend on the type of polymer used and the method of production. All polymer nanofibers are unique for their large surface area-to-volume ratio, high porosity, appreciable mechanical strength, and flexibility in functionalization compared to their microfiber counterparts. ^[1]

Diabetes mellitus Type 2 is a long term metabolic disorder that is characterized by high blood sugar, insulin resistance and relative lack of insulin. It primarily occurs due to obesity. Symptoms of high blood sugar include frequent urination, increased thirst and increased hunger ^[2]. Type 2 diabetes is a progressive condition in which the body becomes resistant to the normal effects of insulin and/or gradually loses the capacity to produce enough insulin in the pancreas. We do not know what causes type 2 diabetes. Type 2 diabetes is associated with modifiable lifestyle risk factors. Type 2 diabetes also has strong genetic and family related risk factors. Type 2 diabetes is diagnosed when the pancreas does not produce enough insulin (reduced insulin production) and/or the insulin does not work effectively and/or the cells of the body do not respond to insulin effectively known as insulin resistance. ^[3] Over 90% cases of diabetes are type 2. ^[4,5] Glibenclamide, also known as glyburide, is an antidiabetic drug belonging to the class of sulfonylureas. Therapy with Glibenclamide is usually initiated with 2.5mg given once daily. The maximal recommended daily dose is 20mg. Glibenclamide is 200 times more potent than tolbutamide in evoking pancreatic secretion of insulin. It differs from other oral hypoglycemic drugs where in tolerance to this action apparently does not occur. It also upregulates insulin receptors in the periphery, which seems to be the primary action. It has a special status in the treatment of non-insulin-dependent diabetes mellitus because it is effective in many cases which are resistant to all other oral hypoglycemic drugs. It differs from other oral hypoglycemic drugs i.e. more effective during eating than during fasting ^[6].

The present study was conducted to design and evaluate Glibenclamide nanofibrous tablet for increasing Half life of Glibenclamide by formulating nanofibrous tablet which will be prolonging the duration of action as antidiabetic medicine.

MATERIALS AND METHODS :

MATERIAL : Glibenclamide was obtained as a sample product from Yarrow chemical products, Mumbai. PLGA and PVA was obtained from Solanki Enterprises, Pune. HPMC K4M and cross-linked PVP was obtained from Ashland Netherlands. Co., Magnesium Stearate, Microcrystalline cellulose, Talc was obtained from Research Lab Fine chem. Industries, Mumbai.

METHOD :

Preparation of Spinning Solution for Glibenclamide Nanofibers

Polymer PVA was dissolved in distilled water to form 10% (w/v) PVA solution. The polymeric PVA mixture was then stirred for 4 h at a temperature of 80 °C followed by cooling at room temperature. Then, Glibenclamide, 0.1% w/v and PLGA in different concentration 0.02%, 0.03%, 0.05%, were pre-dissolved in 1 mL of acetone and added in to PVA polymer solution. The mixture was then stirred for at least 20 min at room temperature to form homogenous solution before performing the electrospinning

process. The design of different batches of formulations and their compositions used in the preparation of the spinning solution for Glibenclamide loaded PVA/PLGA electrospun nanofibers.^[7]

Electrospinning method for Solutions

All spinning solutions were prepared at room temperature under stirring for 24 h to ensure their homogeneity. Electrospinning was conducted using a γ -High Voltage Research DC power supply generator with a maximum voltage of 50 kV. The electrospinning solutions were fed through the tip of the needle by syringe pump with a stable flow rate (0.5 mL/h). Meanwhile, high voltage (15 kV) was applied to the needle and the nanofibers were concurrently collected on the grounded and steady metal plate which was placed at 15 cm from the needle and covered with Al foil. Temperature and relative humidity were $20\pm 2^\circ\text{C}$ and $60\pm 5\%$, respectively.

Characterization of Glibenclamide Nanofibers :

Scanning Electron Microscopy :

The morphology of Glibenclamide + PVA + PLGA Nanofibers formulation were observed using a tabletop scanning electron microscope (Hitachi TM3000) with 20 kV. The metal carriers of copper stubs with double-sided conductive tape were used to fix the electrospun nanofibers samples. Before an examination, a thin layer of gold was coated on the sample using an ion sputtering device. The diameter of fibers from the SEM image was measured using ImageJ software. Different parts of each nanofiber sample was selected for measurement and the average fiber diameter was calculated. ^[8]

Preparation of Nanofibrous tablet of Glibenclamide by Direct Compression Method

Nanofibrous tablet of Glibenclamide are prepared by direct compression method. The corresponding amount of nanofibers and excipients were accurately weighed and mixed properly and the matrix is formed. The tablet blends for different batches (F1-F3) are prepared according to table and further studied for Pre-compression properties.

Table 1: Formulation of Nanofibrous tablet of Glibenclamide

Sr. No.	Ingredients	Formulation Codes		
		F1(mg)	F2(mg)	F3(mg)
01	Glibenclamide Nanofibers	10	10	10
02	HPMC K4M	10	20	30

03	Cross-linked PVP	50	50	50
04	Microcrystalline Cellulose	164	154	144
05	Magnesium Stearate	8	8	8
05	Talc	8	8	8
Total		250	250	250

PRECOMPRESSION EVALUATION OF BLEND OF SUSTAINED RELEASE TABLET OF GLIBENCLAMIDE [9,10,11,12,13,14,15,16] :

Angle of Repose

This is the maximum angle possible between the height of pile of blend powder and horizontal plane. The frictional forces in the loose powder can be measured by angle of repose. The tangent of angle of repose is equal to the coefficient friction (Θ) between the particles. Hence the rougher and more irregular the surface of particles the greater will be angle of repose.

$$\Theta = \tan^{-1} (r/h)$$

Where, H = height of the pile

Table 2 : Standards for Angle of Repose

Angle of Repose	Flowability
<20	Excellent
20-30	Good
30-34	Passable
>40	Very Poor

Bulk density:

Apparent bulk density (BD) was determined by pouring blend into a graduated cylinder. Weighted quantity of the powder mass (M) was poured into measuring cylinder, then the powder was levelled carefully, and the unsettled apparent volume V_o was noted to the nearest graduated unit. The bulk density was calculated in gm/ml by the formula:
The bulk density was calculated using the formula

$$\text{Bulk Density} = M/V_o$$

Tapped density:

After determination of the bulk density, the cylinder was tapped mechanically by mounting on a holder in a mechanical tapped density tester that provided a fixed drop of 14 ± 2 mm at a nominal rate of 300 drops per minute. The cylinder was tapped for 500 times initially and the tapped volume V_t was measured to the nearest graduated unit. The tapping was repeated for an additional 750 times and the tapped volume was measured. Final tapped volume was measured and tapped density was calculated by the formula:

$$\text{Tapped Density} = M/V_t.$$

Compressibility Index and Hausner's Ratio:

The Compressibility Index and Hausner's Ratio are measures of the propensity of a powder to be compressed. As such, they are measures of the relative importance of inter-particulate interactions. In a free-flowing powder, such interactions are generally less significant, and the bulk and tapped densities will be closer in value. For poorer flowing materials, there are frequently greater inter-particle interactions, and a greater difference between the bulk and tapped densities will be observed. These differences are reflected in the compressibility index or Carr's index (CI) and the Hausner's ratio (HR) which is calculated using the following formulas

Compressibility Index

The simplest way for measurement of free flow of powder is compressibility, a indication of the ease with which a material can be induced to flow is given by compressibility index (CI) which is calculated as follows

$$\text{Carr's Index} = [(\text{Tapped density} - \text{Bulk density}) / \text{Tapped density}] \times 100$$

Table 3: Standards for Compressibility Index

Carr's Index	Properties
5-15	Excellent
12-16	Good
18-21	Fair to Passable
23-35	Poor
35-38	Very Poor
>40	Very Very Poor

Hausner's ratio

Hausner's ratio is an indirect index of ease of powder flow. It is calculated by the following formula:

$$\text{Hausner's ratio (Hr)} = [\text{Tapped Density (}\rho_{\text{tap}}\text{)}/\text{Bulk Density (}\rho_{\text{b}}\text{)}]$$

Table 4: Standards for Hausner's Ratio

Hausner's ratio	Flow
1.2-1.3	Excellent
1.3-1.4	Good
1.4-1.5	Fair
1.5-1.6	Poor

MANUFACTURING OF NANOFIBROUS TABLET OF GLIBENCLAMIDE BY DIRECT COMPRESSION METHOD

Accurate quantity of Glibenclamide nanofibers and all ingredients were weighed according to formula powders except talc and magnesium stearate was blended homogeneously in mortar and pestle for 15 minutes. Prepared powder blend was passed through sieve no. 60. Finally, Talc and Magnesium stearate passed from sieve no. 30 added and was further mixed for 10 minutes.

Accurately weighed 250 mg homogeneously mixed powder blend was fed manually and compressed with constant compression force and hardness on 16 stations tablet compression machine with 9 mm, breakthrough, and flat faced punches.

Total three formulations were prepared.

EVALUATION OF NANOFIBROUS TABLET OF GLIBENCLAMIDE^{9,11,13}

The prepared tablet batches (F1-F3) are subjected to post compression evaluation and evaluation parameters like appearance, weight variation, thickness, hardness, friability, content uniformity, disintegration time, dissolution time was performed and the results are shown in **table 10**.

Appearance:

The tablets were visually observed for capping, chipping and lamination.

Weight Variation:

When a tablet is designed to contain a certain quantity of medication in a specific amount of tablet formula, the weight of the tablet is frequently tested to confirm that the correct amount of drug is included in the tablet. In actuality, ten tablets were consumed and weighed on a digital weighing balance individually. The averageweight of the tablets was determined, and the weight of each tablet was compared to the average. If no more than two tablets are outside the % restriction and no tablet varies by more than twice the percentage limit, the tablet passes the test.

Table 5: Specifications of % weight variation allowed in tablets

Average Weight of Tablet	% Deviation Allowed
80 mg or less	10
More than 80 mg but less than 250 mg	7.5
250 or more	5

Thickness:

The uniformity of tablet size is dependent on the thickness of the tablet. Vernier caliper was used to determine thickness. randomly selected three pills from each formulation were tested to determine it.

Hardness:

The “force necessary to shatter a tablet in diametric compression test” is the definition of hardness. As a result, tablet crushing strength is also known as hardness. The resistance before use is determined by the hardness of the material. For each formulation the hardness of 6 tablets was determined using a Pfizer hardness tester. In the hardness tester, tablet was held along its oblong axis in between the two jaws of the tester and the

load necessary to crush it was measured. Then force was applied until the tablet fractured. The value at this point was noted in kg/cm².

Friability:

This test is used to determine if tablets can survive abrasion while being packed, handled, or transported. Friability is a sign of inadequate tablet ingredient cohesiveness. Friability of the tablets was determined using Roche Friabilator. A total of ten pills are weighed and placed in the Friabilator, which is made up of a circular plastic chamber separated into two or three compartments. The chamber rotates at 25 revolutions per minute for 4 minutes, dropping the tablets 15 cm away and completing 100 rotations. The pills are then weighed for the second time. The weight difference is observed and given as a percentage difference. It's best if it's less than 1%.

$$\% \text{ Friability} = (W1 - W2) / W1 \times 100$$

Where,

W1 = Weight of tablet before test

W2 = Weight of tablet after test

Content uniformity

The Glibenclamide content was estimated as follows :

20 tablets were finely powdered and weight equivalent to 10 mg of Glibenclamide was dissolved in 100 ml of 0.1N HCL and assayed against 0.1 N HCL for drug content using UV-Visible spectrophotometer at 229 nm.

Disintegration test:

Six tablets were placed in each six tubes of the basket and the apparatus operated containing water maintained at 37°C as the disintegration fluid. The Disintegration time was recorded.

In-vitro Dissolution studies

Dissolution profiles of Glibenclamide tablets were determined using the USP Type II Dissolution test apparatus (paddle) (Electrolab, Mumbai, India). set with a paddle speed of 50 rpm & at temperature 37° C ± 0.5°C. The dissolution media used were 900 mL of 0.1N HCl for first 2 h followed by pH 6.8 phosphate buffer solutions for 12 h. 5 ml samples were removed at specified intervals up to 1h and filtered through Whatmann filter paper. An equal volume of fresh medium, prewarmed at 37°C was replaced into the dissolution medium after each sampling to maintain the constant volume throughout

the test. Samples were analyzed by UV spectrophotometer at 274 nm. Drug dissolved at specified time periods was plotted as cumulative percent release versus time (h) curve.

Stability Study

The prepared sustained release tablet of Glibenclamide were placed in plastic tubes containing desiccant and stored at ambient conditions, such as room temperature at $40^{\circ}\text{C} \pm 2^{\circ}\text{C}$ / 75 % RH \pm 5% for period of 90 days. Each tablet is weighed and wrapped in aluminum foil and packed in black PVC bottle and put at above specified condition in a heating humidity chamber for 3 months and evaluated for their physical appearance, hardness, disintegrate time, dissolution testing and drug content at specified intervals of time.

RESULTS AND DISCUSSION

Spectrophotometric Analysis of Glibenclamide UV Spectrophotometric Analysis Determination of λ max of Glibenclamide in 0.1 N HCL

In UV spectroscopy study, the maximum wavelength (λ max) of Glibenclamide in 0.1N HCL was found to be 229 nm. The reported λ max value of Glibenclamide in 0.1N HCL was also 230 nm, so the values similar with the reported value indicates that the given sample of Glibenclamide was in pure form.

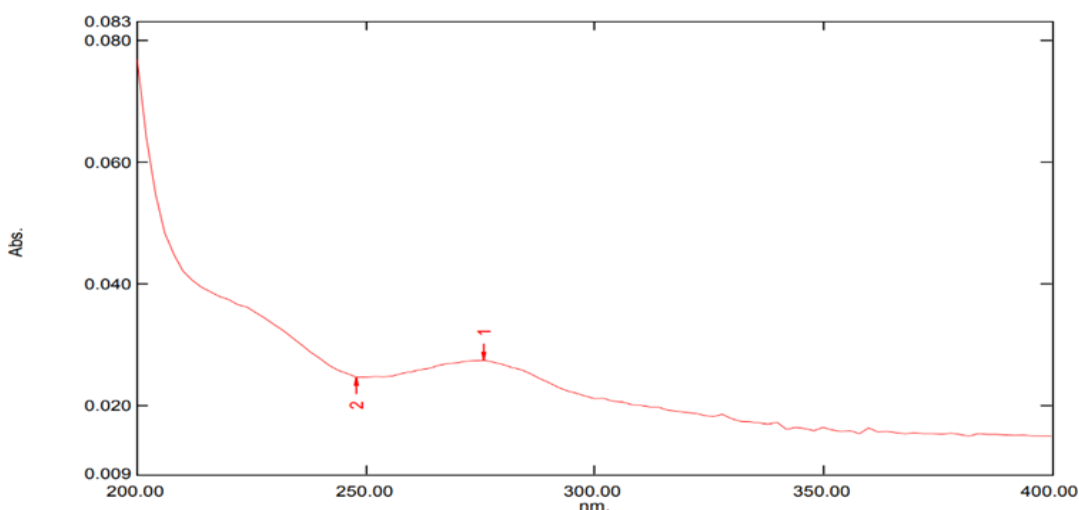


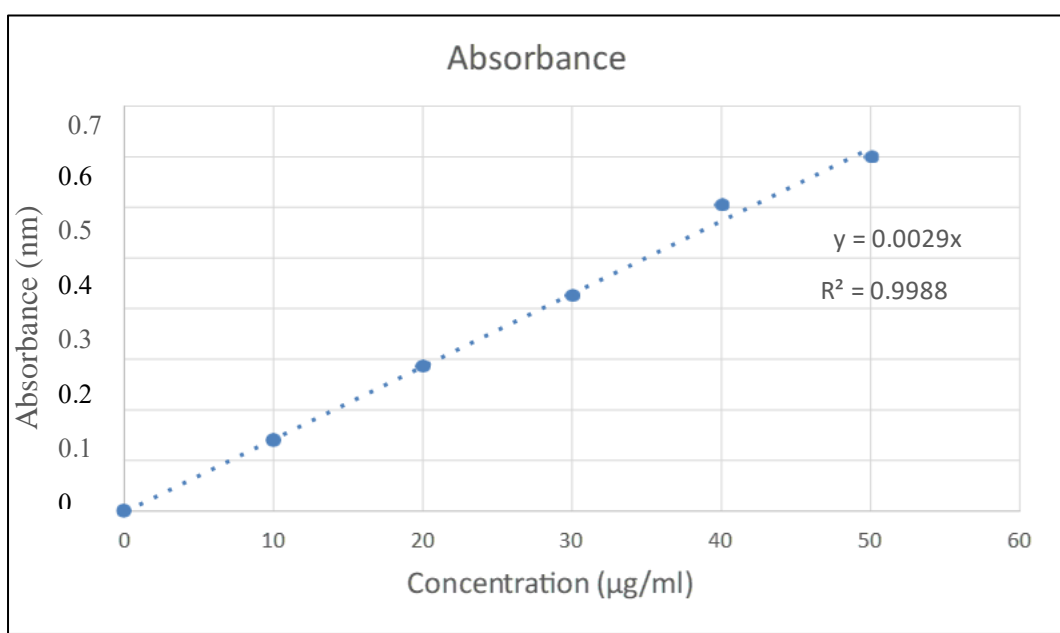
Figure 1: UV Spectrum of Glibenclamide in 0.1 N HCl at 229 nm

Preparation of Standard Calibration Curve of Glibenclamide in 0.1N HCl

The Standard curve of Glibenclamide was determined by plotting absorbance Vs concentration at 229 nm. It was found that there was linear relationship between concentration and absorbance with R^2 value 0.9988. Which reveals that, the drug Glibenclamide obeys the Beers lamberts law.

Table 6: UV Absorbance of Glibenclamide in 0.1 N HCl at 229 nm

Sr. No.	Concentration (µg/ml)	Absorbance
1	0	0
2	10	0.028
3	20	0.057
4	30	0.087
5	40	0.121
6	50	0.14

**Figure 2: Standard Calibration Curve Graph of Glibenclamide in 0.1N HCL****Determination of λ max of Glibenclamide in 6.8 Phosphate Buffer**

In UV spectroscopy study, the maximum wavelength (λ max) of Glibenclamide in 6.8 Phosphate Buffer was found to be 229 nm. The reported λ max value of Glibenclamide in 6.8 Phosphate Buffer was also 230 nm, so the values similar with the reported value indicates that the given sample of Glibenclamide was in pure form.

Sr. no.	Concentration (µg/ml)	Absorbance
1	0	0
2	10	0.12
3	20	0.215
4	30	0.315
5	40	0.4
6	50	0.48
7	60	0.6

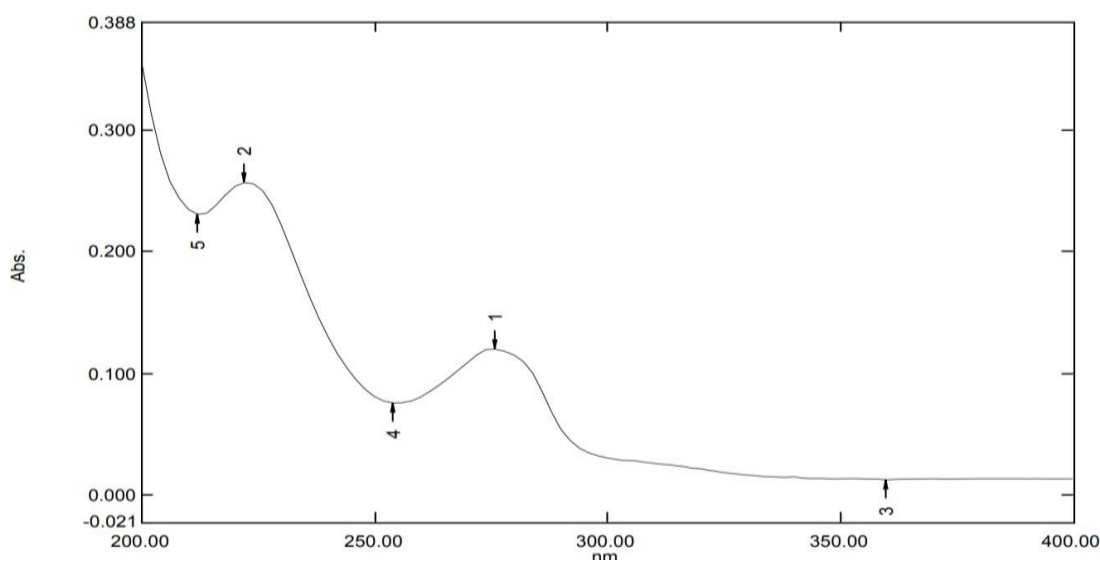
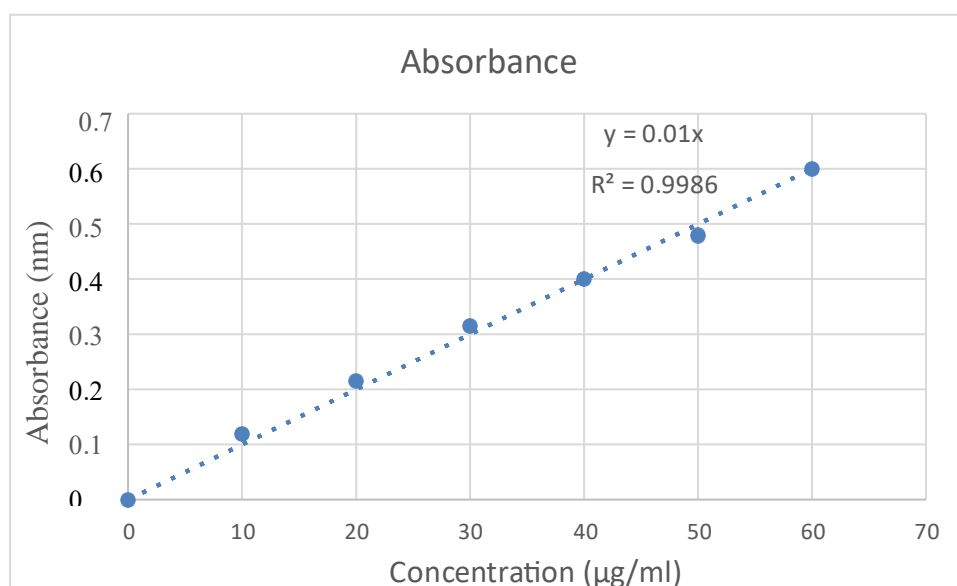


Figure 3: UV Spectrum of Glibenclamide in 6.8 Phosphate Buffer at 229 nm

Preparation of Standard Calibration Curve of Glibenclamide in 6.8 Phosphate Buffer:

The Standard curve of Glibenclamide was determined by plotting absorbance Vs concentration at 229 nm. It was found that there was linear relationship between concentration and absorbance with R² value 0.9986. Which reveals that, the drug Glibenclamide obeys the Beers lamberts law.

Table 7: UV Absorbance of Glibenclamide in 6.8 Phosphate Buffer at 229 nm**Figure 4: Standard Calibration Curve Graph of Glibenclamide in 6.8 Phosphate Buffer**
Drug-Excipient Compatibility Study**Fourier Transform Infra-red Spectroscopy (FTIR) Interpretation of Glibenclamide**

The FTIR spectrums of pure Glibenclamide and physical mixtures of drugs and polymers were studied separately as per the excipients used in the formulation. It was observed that there were no major shifts in the main peaks of either drug. This indicates that there were no compatibility problems with the drug with the polymers and excipients used in the formulation. Glibenclamide had peaks at 1658 (C=O amide), 2890 (C=H), 3471 (NH stretch), 1033 (S=O), 1072 (C-O-C).

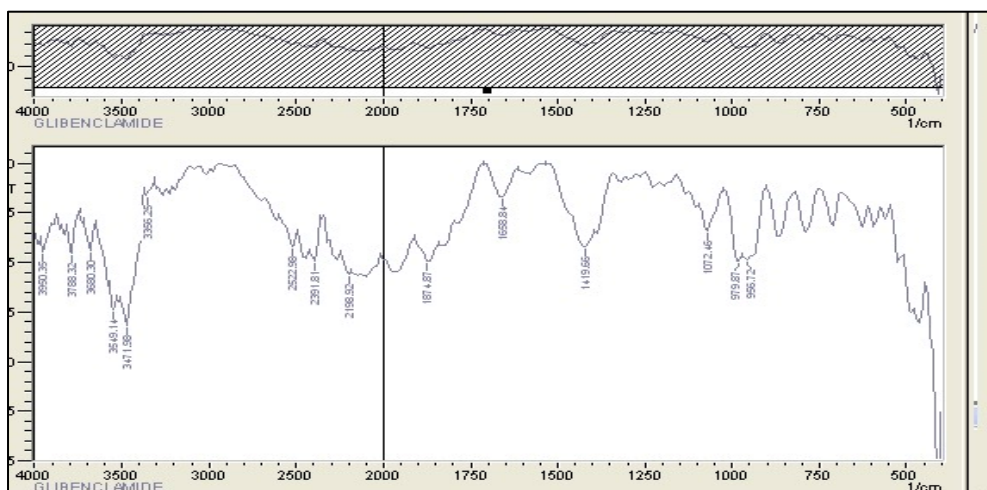


Figure 5: FTIR Spectrum of Glibenclamide

Fourier Transform Infra-red Spectroscopy (FTIR) Interpretation of FTIR of Glibenclamide Nanofibers + HPMC (K4M) + Cross-linked PVP + Microcrystalline Cellulose + Magnesium Stearate + Talc

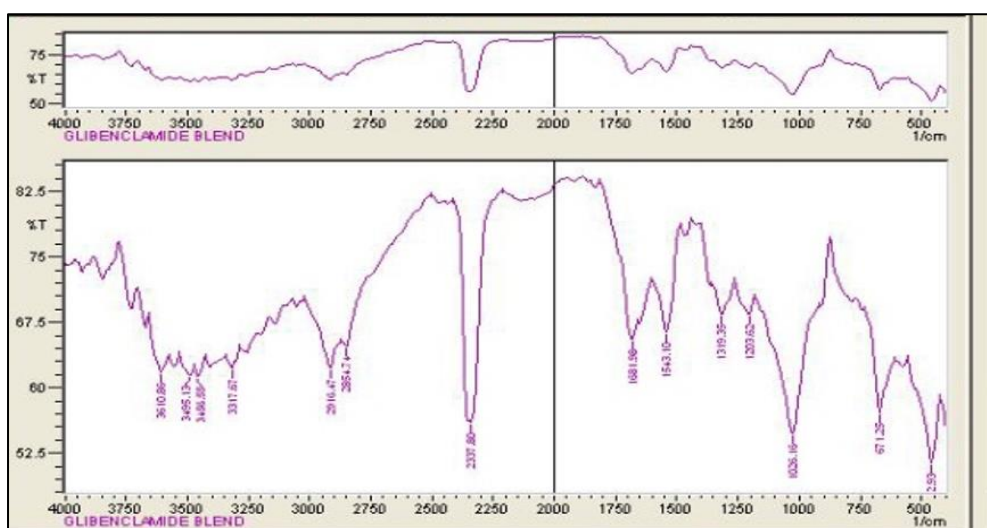


Figure 6 : FTIR Spectrum of Glibenclamide Nanofibers + HPMC (K4M) + Cross-linked PVP + Microcrystalline Cellulose + Magnesium Stearate + Talc

Characterization of Glibenclamide Nanofibers

Scanning Electron Microscopy :

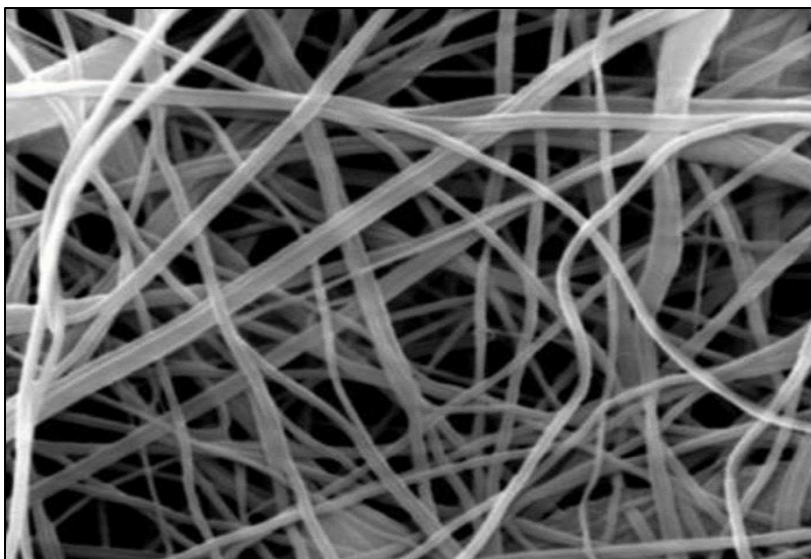


Figure 7: SEM image of batch first Nanofibers

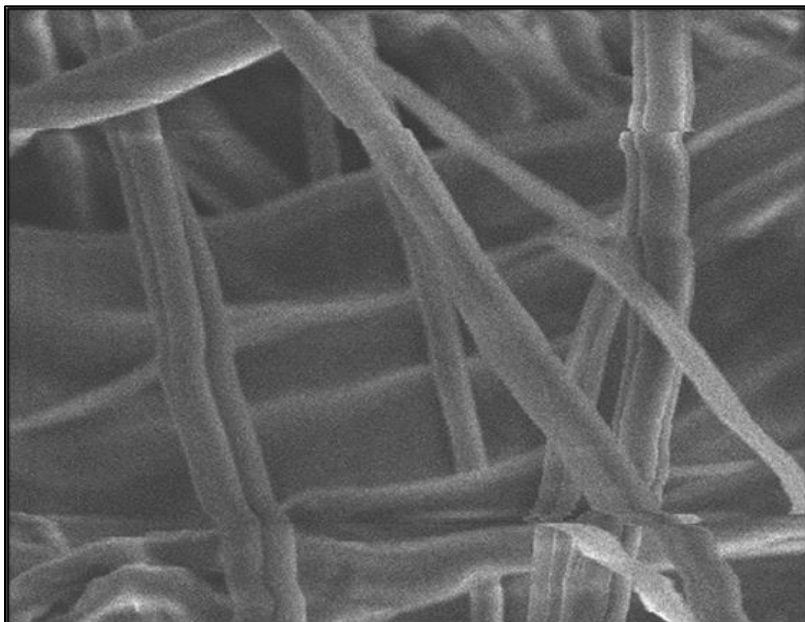


Figure 8: SEM image of batch second Nanofibers

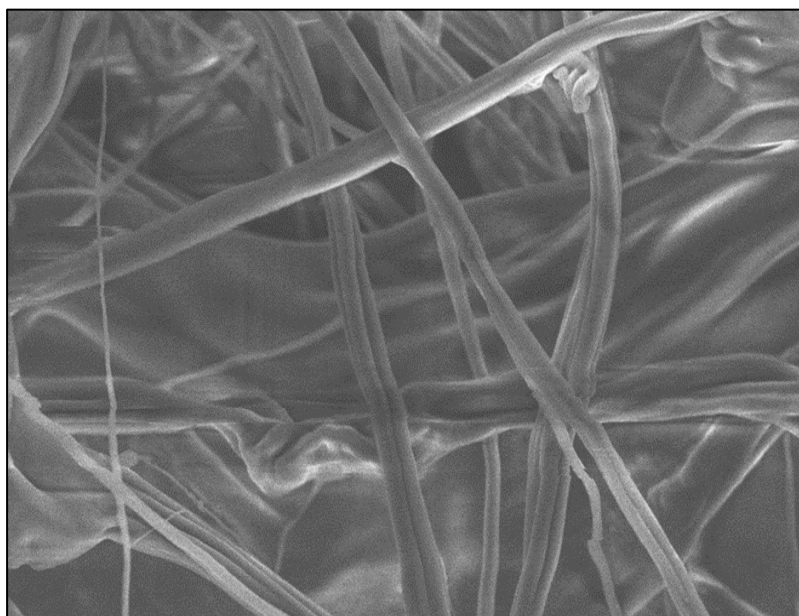


Figure 9: SEM image of batch second Nanofibers

Table 8 :The effect of electrospinning parameters on the size of the nanofibers

Effect of flow rate		Effect of distance		Effect of Volt	
Flow rate (mL h ⁻¹)	Size (nm)	Distance (cm)	Size (nm)	Voltage (kV)	Size (nm)
0.3	213±	5	125±108	10	547±115
0.5	174±	10	653±156	20	326±123
0.7	452±	15	221±253	30	452±147
0.9	369±	20	198±45	50	251±125

PRECOMPRESSION EVALUATION OF BLEND OF NANOFIBROUS TABLET OF GLIBENCLAMIDE:

Sustained release tablets of Glibenclamide were prepared by direct compression method using polymer HPMC-Calcium phosphate complex. A total of five formulations were designed. The flow properties of the powder mixture are important for the uniformity of mass of the tablets; the flow of the powder mixture was analysed before compression to tablets. Low Hausner's ratio (≤ 1.18), compressibility index (≤ 15.68) and angle of repose (≤ 29.39) values indicated fairly good flowability of the powder mixture **Table 9**.

Table 9: Precompression Evaluation of tablet for sustained release tablets

Formulations	Angle of repose (θ°)	Bulk Density (gm/cm^3)	Tapped Density (gm/cm^3)	Hausner's Ratio (HR)	Carr's Compressibility index (%)
F1	27.68 \pm 0.5	0.37 \pm 0.20	0.41 \pm 0.32	1.10 \pm 0.10	9.75 \pm 0.71
F2	28.21 \pm 0.9	0.38 \pm 0.02	0.45 \pm 0.02	1.18 \pm 0.11	15.55 \pm 0.5
F3	28.41 \pm 0.3	0.36 \pm 0.35	0.42 \pm 0.62	1.16 \pm 0.21	14.29 \pm 0.80

Results are mean of three dimensions*

EVALUATION OF SUSTAINED RELEASE TABLET OF GLIBENCLAMIDE:

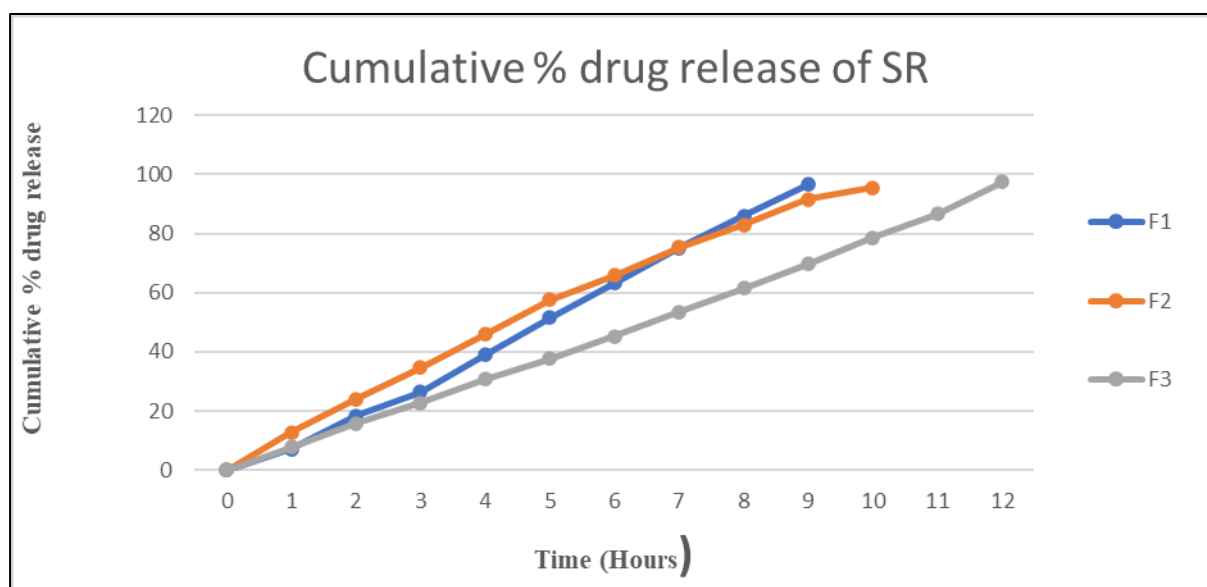
As the tablet powder mixture was free flowing, tablets produced were of uniform weight with acceptable weight variation in the range from 298 mg to 301 mg due to uniform die fill. Hardness ($5.7 \pm 0.5 - 6.1 \pm 0.3 \text{ kg/cm}^2$) and friability loss ($0.71 \pm 0.04 - 0.82 \pm 0.03 \%$) indicated that tablets had good mechanical resistance. Drug content was found to be high ($\geq 98.75 \%$) in all the tablet formulations **Table 10**.

Table 10: Evaluation of Sustained Release Tablet of Glibenclamide

Formulations	Weight variation (mg)	Thickness (mm)	Hardness (Kg/cm ²)	Friability (%)	Drug Content (%)
F1	248±0.50	3.45±0.25	5.7± 0.5	0.73±0.04	98.75±0.45
F2	251±0.58	3.55±0.10	5.9± 0.2	0.76±0.07	98.23±0.04
F3	249±0.20	3.48±0.17	6.0± 0.3	0.82±0.03	99.67±0.37

***In vitro* % Drug Release of Drug from Tablet**

All the three tablet batches Nanofibrous tablet of Glibenclamide were subjected for the *in vitro* dissolution studies using tablet dissolution test apparatus (USP type II). The dissolution media used were 900 mL of 0.1 N HCl for first 2 h followed by pH 6.8 phosphate buffer solutions for 12 h.

**Figure 10 : Cumulative % drug release of Nanofibrous tablet****STABILITY STUDY**

The formulation F3 was selected for stability studies on the basis of their high cumulative % drug release time was studied. The stability studies were carried out at $40^{\circ}\text{C}\pm 2^{\circ}\text{C}/75\% \pm 5\%$ relative humidity for the selected formulation up to two months. For every 1-month time interval the tablets were analysed for drug hardness, content uniformity, % drug release up to two months.

CONCLUSION

The purpose of this study was to fabricate drug-loaded fibers and establish a proof of concept for the electrospun method of making electrostatic fiber as a functional specialized carrier system for oral delivery of Glibenclamide in type 2 diabetes mellitus (T2DM). The drug delivery challenges associated with oral Glibenclamide delivery are poor solubility, low dissolution rate, variable gastrointestinal absorption and erratic bioavailability. In this research, Glibenclamide loaded PVA/PLGA electrostatic fibers were successfully fabricated to improve the drug delivery challenges with enhanced drug dissolution and modified drug release profile employing the electrospinning method. The formulation composed of with Drug :PVA : PLGA in 0.1:10:0.05% w/v ratio produced optimized and desired Glibenclamide nanofibers. Formulated nanofibers were evaluated for Scanning Electron Microscopy (SEM) study. Then formulation of Glibenclamide loaded nanofibers was compressed into an tablet for oral administration. Formulated tablets were evaluated for hardness, friability, thickness, drug content and in-vitro study. F3 batch was selected as optimize batch from the similarity factor, cumulative drug release and drug content study.

ACKNOWLEDGEMENT

For the completion of the research work the authors would like to show sincere gratitude to PDEA'S Shankarrao Ursal College of Pharmaceutical Sciences & Research Center, Kharadi, Pune to provide a lot of support and help whenever needed.

CONFLICT OF INTEREST

All authors declared no conflicts of interest

REFERENCES-

1. <http://en.m.wikipedia.org/wiki/.Nanofiber>
2. https://en.wikipedia.org/wiki/diabetes_mellitus
3. <https://www.diabetesaustralia.com.au/type-2-diabetes>
4. Tripathi K.D, Essential's of Pharmacology 7th edition, Page. No.258.
5. Anitha P., Ramkanth S., Salem T.S., Umasankari S., Reddy B.P. and Chetty M., Pak. J. Pharm. Sci., 2011; 24(2): 155-163.
6. Marikanti Rajkumar et.al. *J.Chem.Pharm.Res.*,2010,2(4):291-303
7. Ghafoor, B.; Aleem, A.; Najabat Ali, M.; Mir, M. Review of the fabrication techniques and applications of polymeric electrospun nanofibers for drug delivery systems. *J. Drug Deliv. Sci. Technol.* 2018, 48, 82–87, doi:10.1016/j.jddst.2018.09.005.
8. Baishya, H. Application of Mathematical Models in Drug Release Kinetics of Carbidopa and Levodopa ER Tablets. *J. Dev. Drugs* 2017, 6, 1–8, doi:10.4172/2329-6631.1000171.
9. Lieberman H.A., Lachman L., The Theory and Practice of Industrial Pharmacy, Indian Edition, CBS Publishers, and Distributors Pvt. Ltd., 2009, 293, 457, 479-501.
10. Lieberman HA, Lachman L, Schwartz JB. Pharmaceutical dosage forms: Tablets, Ed 3, New York, Marcel Dekker, 1990.225-228.
11. <https://go.drugbank.com/drugs/DB01016>
12. Michael E Aulton. *Pharmaceutics, The Science of Dosage form Design*. 2nd Edition. 2005.335-346.
13. Leon Lachman, Herbart liebeman. *The theory and practice of industrial pharmacy*. Indian Edition CBS publishers.2009.331-334.
14. Cooper J, Gunn C. Powder flow and compaction. In: Carter SJ, eds. "Tutorial Pharmacy". New Delhi, India: CBS Publishers and Distributors; 1986: 211-233.
15. 5. Shah D, Shah Y, Rampradhan M. *Drug Dev.Ind. Pharm.* 1997; 23(6): 567-574.
16. 6. Wells J., *Pharmaceutical Preformulation: The Physicochemical Properties Of Drug Substances* In: Aulton ME, "Pharmaceutics: The Science of Dosage Form Design". International eds: Churchill Livingstone; second Eds.2002; 133-134.
17. *Indian Pharmacopoeia*, Controller Of Publications, Govt. Of India, New Delhi, Fourth Edition, 1996; Vol-II: 736.



FORMULATION DEVELOPMENT, EVALUATION AND MTT ASSAY OF HERBAL VITAMIN C POWDER.

Mangesh Rode ^{a*}, Vivek Ingale ^a, Vijaya Barge ^a, Amit Kasabe ^a,

Gajanan Bhagwat ^b, Pravin Kamble ^b

^a *Department of Pharmaceutical Quality Assurance, PDEA's Shankarrao Ursal College of
Pharmaceutical Sciences and Research Centre, Kharadi, Pune-411014.*

^b *R&D Center, Healing Hands & Herbs Pvt. Ltd., 101, Mangalmurti Complex, CTS No. 990, Shukrawar
Peth, Tilak Road, Pune - 411002. Maharashtra, India.*

***Correspondence to: Mangesh Rode**

rodemangesh706@gmail.com

Abstract: The present work was aimed at formulation development, evaluation and MTT assay of Herbal Vitamin C Powder. The formulation was prepared by mixing Acerola Extract, Rosehip Extract, Moringa Extract, Amla Powder, Bilberry Extract, Glycine, L- lysine, L- proline, Elaichi Powder, Rock salt, Spirulina Powder and excipients such as Lemon flavor. Initially, the pre-formulation evaluation of each separate ingredient was done by evaluating its Organoleptic characters, Bulk density, Tap density, Hausner Ratio, Moisture Content, pH, and Solid-state stability study. The formulation was prepared after the pre-formulation study was completed and then evaluated for powder characters and MTT assay. Powder evaluation was performed using various physiochemical and microbiological parameters and the cytotoxicity of the formulation was performed by an MTT assay on Human embryonic kidney cells (HEK). From the above study, we can conclude that the stable polyherbal formulation of Vitamin C was prepared and evaluated and did not exhibit cytotoxicity at the daily dose limit.

Keywords: Vitamin C, MTT assay, Cell viability assay, Human embryonic kidney cells

Introduction:

The new single chemical entity is responsible for the medicine's significant therapeutic activity in modern pharmacology and drug development. Still, Ayurveda formulations are founded on different standards: using a single herb and multiple herbs, known as polyherbal formulation. Polypharmacy or polyherbalism refers to the impact of combining several medicinal plants to increase the efficacy of a preparation.¹ Historically, the classic text of Ayurveda, "Sarangdhar Samhita," has emphasized the concept of polyherbalism.² Although the bioactive components of individual herbs in many formulations have been well-known, they generally exist in small proportion. They are mostly not sufficient enough to attain the desired therapeutic efficacy. Scientific studies have discovered that when mixed, these herbs of varied effectiveness may yield better results concerning the single or sum of their single effect. This occurrence gives rise to positive herb interaction known as synergism which confers some benefits of the polyherbal formulation. It is evident that with a single multi-constituent formulation, better therapeutic outcomes can be attained.¹ The term "nutraceuticals" can be explained as the food items as a whole or a part which possesses some nutritional value along with medicinal properties.³ These findings have triggered a series of studies in the nutraceuticals field.⁴ There is a controversy over a specific definition and set of regulations to define nutraceutical compounds.⁵ However, nutraceutical compounds are health-enhancing products that improve the mental and physical activities of the body. They are commercialized to minimize the risk factors of various diseases. Nutraceutical products are simply a hybrid between drug and food. On the other hand, this terminology is a broader term that includes minerals, vitamins, amino acids, botanicals, or herbs. Therefore, both dietary supplements and fortified foods can be classified as nutraceuticals. The terminology of nutraceutical was defined by the foundation for innovation in medicine in (New York, USA) in 1989. Defelice's definition in 1995 was: "A food or parts of food that provide

medical or health benefits, including the prevention and/or treatment of disease.⁵ Nutraceuticals term originated from two terminologies: “nutrition” and “pharmaceutical”.⁶

Vitamin C (ascorbate) is an essential water-soluble micronutrient in humans and is obtained through the diet, primarily from fruits and vegetables.⁷ Vitamin C is necessary for the development and maintenance of connective tissues. It plays a vital role in bone formation, wound healing, and the care of healthy gums. It helps synthesize and metabolize tyrosine, folic acid and tryptophan and hydroxylation of glycine, proline, and lysine carnitine.⁸ It is a cofactor for collagen synthesis and a primary antioxidant and is rapidly consumed post-wounding. Vitamin C could promote wound healing by altering the inflammatory, proliferative and remodelling phases. Vitamin C protects the immune system, reduces the severity of allergic reactions, and helps to fight off infections.⁹ Humans cannot synthesize ascorbic acid due to the lack of gulonolactone oxidase enzyme. Hence, ascorbic acid has to be supplemented mainly through fruits and vegetables. It is present in oranges, lemons, grapefruit, watermelon, papaya, strawberries, mango, pineapple, raspberries and cherries. It is also found in green leafy vegetables, tomatoes, broccoli, green and red peppers, cauliflower and cabbage.¹⁰ Vitamin C is a cofactor in the hydroxylation of proline and lysine residues in procollagen, which is vital for the strength and stability of collagen fibers. In addition, ascorbic acid enhances neutrophil function and acts as an antioxidant.⁵ Systemic administration of vitamin C plays a vital role in gingival fibroblast proliferation and functions.⁶ According to ICMR guidelines, adults' daily allowance (RDA) for ascorbic acid ranges between 70–90 mg daily.⁷ The polyherbal formulation comprises Acerola (*Malpighia emarginata* DC.), known as Barbados cherry or West Indian cherry, which belongs to the Malpighiaceae family. The fruit is known to be one of the world's rich natural sources of ascorbic acid. Apart from containing an exorbitant amount of ascorbic acid, the fruit

also contains several phytonutrients like carotenoids, phenolics, flavonoids, and anthocyanins and possesses numerous bio-functional properties.⁸ The rosehip is a repository of flavonoids, pectin, vitamins A, B complex, C and E, also minerals like Ca, Fe, Se and Mn. Trace amounts of Mg, K, S and Si have also been discovered.⁹ Moringa leaves are an essential source of several nutrients. One hundred grams of dried leaves contain 27.1 g protein, 16.3 mg vitamin A, 17.3 mg vitamin C, 2.0 g calcium, 1.3 g potassium, and 28.2 mg iron, in addition to 19.2 g dietary fiber and several other nutrients.¹⁰ Along with the active vitamin C ingredients glycine, L-proline and L-lysine were added, which metabolize by the vitamin C easily and get maximum benefits.¹¹ Also, some taste improvements agents such as Elaichi and Rock salt were added to the formulation. The supplementation of spirulina as a potent alternative source of iron and folic acid. Ascorbic acid facilitates iron absorption by forming a chelate with ferric iron at an acid pH that remains soluble at the alkaline pH of the duodenum.¹²

In the present study, the biological effects of vitamin C on cells were investigated in vitro by using the MTT assay. 3-(4,5-dimethylthiazol-2-yl)-2,5-diphenyltetrazolium bromide test was used to explore the cell viability in the MTT assay. The MTT colorimetric assay was conducted in a 96-well plate format. The cells may require preincubation in the wells before adding the test drug. The preincubation times may vary from 0-24 hrs. according to the cell line properties. Cells are usually exposed to the drug for 24-96 hrs. depending on the drug activity. MTT solution is then added to the treated cells, where the yellow MTT is reduced to purple formazan by various mitochondrial and cytosolic enzymes that are operational in viable cells. The MTT molecule is not reduced by dead cells, red blood cells (metabolically inactive cells), spleen cells (resting cells) and Stimulated lymphocytes (activated cells). After 3-4 hrs. of incubation with MTT, the formazan absorbance at 550 nm is directly proportional to the number of cells in a range of 200-

50,000 cells per well, and thus very small amounts of cells can be detected. The absorbance indicates the number of viable cells remaining after treatment with the drug and is compared to the absorbance of control cells not exposed to the drug.¹³.

Material and methods:

Materials:

Methanol, sulfuric acid, acetic acid, toluene, ethyl acetate, formic acid (Merck made), alpha naphthol, ferric chloride, potassium permanganate, indigo carmine (Loba Chemie made) and polysorbate 80, etc. which are of AR grade and procured from Vijay chemicals, Pune. For microbiological evaluation, chemicals like Soyabean casein digest medium, Gram Negative broth, Rappaport Vassiliadis Salmonella Enrichment Broth, Soyabean casein digest agar, Xylose lysine deoxycholate agar, Bismuth sulphate agar, Cetrimide agar, MacConkey broth & agar, sabouraud dextrose broth & agar (HIMEDIA made) which are of LR grade and procured from Vijay chemicals, Pune. MTT reagent (3-(4,5-dimethylthiazol-2-yl)-2,5-diphenyltetrazolium bromide), DMEM media (Gibco), and Fetal bovine serum (Gibco) were procured from genexindia Bioscience.

Instruments:

1. Weighing Balance (Master)
2. Hot Air Oven (Bio-Techniques India)
3. pH Meter (Global)
4. Muffle Furnace (Bio-Techniques India)
5. Mechanical Shaker (Bio-Techniques India)
6. Laminar airflow (Bio-Techniques India)
7. Bacteriological Incubator (Bio-Techniques India)
8. CO₂ incubator
9. Automated microplate reader

Methods:

Pre-formulation studies were done by performing color, odor, taste, bulk density, tap density, Hausner ratio, carr index, angle of repose and solid-state stability. Organoleptic Properties of the formulation like color, odor, taste and powder characteristics like bulk density, tap density, Hausner ratio, carr index and angle of repose, were determined. Physiochemical stability was checked by performing loss on drying, pH, total ash, acid insoluble ash value, water-soluble extractive value, alcohol-soluble extractive value and also the presence of phytochemical constituents like tannin, phenols, flavonoids and carbohydrates was checked.

The microbial evaluation was done by performing the total aerobic bacterial count, total aerobic fungal count and specific pathogen test for Escherichia Coli, Staphylococcus Aureus, Salmonella Species and Pseudomonas aeruginosa. The nutritional values were also estimated and the MTT assay was performed to assess the cytotoxicity of the formulation.

A. Pre-formulation Study

Pre-formulation is a phase of the research and development process in which a new medicinal molecule's physical, chemical, and mechanical properties are studied individually and in combination with excipients to generate a stable, safe, and effective bioavailable dosage form.

1. Organoleptic Properties:

Color: Observation was done on bright background with light using drug powder. It was carefully observed by the naked eye.

Odor: Before smelling coffee, beans were used to remove all previous odors. Powders took in between the thumb and 1st finger and smelled it.

Taste: Powders are taken, tasted on the tongue, and examined for the type of taste.

2. Powder characteristics:

Bulk Density:

5 gm of the powdered drug was weighed in the digital balanced weighing machine. These powders were added to the dried 25 ml graduated cylinder. The volume of the cylinder was noted.¹⁵

$$\text{Bulk Density} = M / V$$

Where, M = mass of powder

V = Volume of powder

Determination of tap density:

5 gm of the powdered drug was weighed in the digital balanced weighing machine. These powders were added to the dried 25 ml graduated cylinder. After measuring the initial volume of a cylinder, it was mechanically tapped using a tap density apparatus of BIO TECHNICS INDIA, BTI-08. The final volume was noted.¹⁵

$$\text{Tapped density} = M / V_t$$

Where, M = Mass of powder

V_t = Minimum volume occupied after tapping

Hausner Ratio:

Hausner ratio (HR) indicates the powder's flow characteristics and flowability. The ratio between the bulk densities of compacted and loosely poured powder is called Hausner.¹⁶

$$\text{Hausner Ratio} = \rho_{\text{tapped}} / \rho_{\text{bulk}}$$

Where, ρ = Density

Carr Index:

Carr index gives an idea indirectly about the flow behavior of a powder. Carr index (Ci) is determined using Hr values as given in Eq. ¹⁶

$$\text{Hr} = 100 - (100 / \text{Ci})$$

Angle of repose:

In the fixed funnel method, the granular materials are poured from a funnel at a certain height onto a selected base with known roughness properties. The funnel is either fixed or raised slowly while the conical shape of the material heap is forming to minimize the effect of the falling particles. The pouring of the material is stopped when the heap reaches a predetermined height or width. Then, the angle of repose is measured by the inverse tangent (arctan) rule, at which the average radius of the formed conical shape and the maximum height of the heaped material is measured. Then the angle of repose is determined as the arctan of the maximum height.¹⁷

The following formula can calculate the angle of repose:

$$\tan \theta = h/r$$

So,

$$\theta = \tan^{-1} h/r$$

Where,

θ = Angle of repose

h = height of pile of powder(cm)

r = radius (cm)

Moisture Content:

In the dried petri dish 1.5 gm weighed powder was taken and placed in an oven at 105– 110⁰c. After drying and cooling in a desiccator, it was weighed in a digital balanced weighing machine. After drying, the weight was reported and the drying loss was measured.¹⁷

pH:

In a digital balanced weighing machine, 1 gm of powder was weighed and mixed with 20 ml of distilled water. pH of this solution was calculated using a digital pH meter.¹⁷

Solid State stability study:

Solid-state reactions are much slower and more difficult to interpret than solution-state reactions, due to a reduced no. of molecular contacts between drug and excipient molecules and to the occurrence of multiple-phase reactions.

A small mixture of drug and excipient was prepared. The mixture was then placed in the vial. A rubber closure was placed on the vial and the stopper was dipped in the melted Carnauba wax to seal. Then the vials are kept for 1-3 weeks for specified storage conditions. The sample was physically observed for the following.¹⁷

- 1) Caking
- 2) Liquefaction
- 3) Discoloration

4) Odor

5) Gel formation

B. Formulation Evaluation:

1. Organoleptic Properties:

Color: Observation was done on bright background with light using drug powder. The naked eye carefully observed it.

Odor: Before smelling coffee, beans were used to remove all previous odors. Both Powders took in between the thumb and 1st finger and smelled it.

Taste: Both Powders took and tasted on the tongue and examined for the type of taste.¹⁴

2. Powder characteristics:

Bulk Density:

5 gm of the powdered drug was weighed in the digital balanced weighing machine. These powders were added to the dried 25 ml graduated cylinder. The volume of the cylinder was noted.¹⁵

$$\text{Bulk Density} = M / V$$

Where, M = mass of powder

V = Volume of powder

Determination of tap density:

5 gm of the powdered drug was weighed in the digital balanced weighing machine. These powders were added to the dried 25 ml graduated cylinder. After measuring the initial volume of a cylinder, it was mechanically tapped using a tap density apparatus of BIO TECHNICS INDIA, BTI-08. The final volume was noted.¹⁵

$$\text{Tapped density} = M / V_t$$

Where, M = Mass of powder

V_t = Minimum volume occupied after tapping

Hausner Ratio:

Hausner ratio (HR) indicates the powder's flow characteristics and flowability. The ratio between the bulk densities of compacted and loosely poured powder is called Hausner.¹⁶

$$\text{Hausner Ratio} = \rho_{\text{tapped}} / \rho_{\text{bulk}}$$

Where, ρ = Density

Carr Index:

Carr index gives an idea indirectly about the flow behavior of a powder. Carr index (Ci) is determined using Hr values as given in Eq. ¹⁶

$$Hr = 100 - (100 / Hr)$$

Angle of repose:

In the fixed funnel method, the granular materials are poured from a funnel at a certain height onto a selected base with known roughness properties. The funnel is either fixed or raised slowly while the conical shape of the material heap is forming to minimize the effect of the falling particles. The pouring of the material is stopped when the heap reaches a predetermined height or width. Then, the angle of repose is measured by the inverse tangent (arctan) rule, at which the average radius of the formed conical shape and the maximum height of the heaped material is measured. Then the angle of repose is determined as the arctan of the maximum height.¹⁷

The following formula can calculate the angle of repose:

$$\begin{aligned} \tan \theta &= h/r \\ \text{So,} \quad \theta &= \tan^{-1} h/r \end{aligned}$$

Where,

θ = Angle of repose

h = height of the pile of powder (cm)

r = radius (cm)

3. Physiochemical parameters:

Determination of loss on drying:

In a dried petri dish, 1.5 gm weighed vitamin C powder was taken and placed in an oven at 105– 1100 c. After drying and cooling in a desiccator, it was weighed in a digital balanced weighing machine. After drying, the weight was reported, and the drying loss was measured.¹⁸

Determination of pH:

In a digital balanced weighing machine, 1 gm of vitamin C powder was weighed and mixed with 20 ml of distilled water. pH of this solution was calculated using a digital pH meter.¹⁹

Determination of total ash:

2 gm of vitamin C powder was weighed in a digital balanced weighing machine and was taken as a sample into the silica crucible. It was gradually heated with a burner using a 2 cm high flame and supporting the dish about 7 cm above the flame until vapors almost stopped being produced. The dish was lowered, and the heat increased until all the carbon had burned away. After cooling it in a desiccator, it is placed in a balanced weighing machine. Total ash content was calculated and expressed as % w/w of air-dried material.²⁰

Acid insoluble ash value:

After assessing the total ash, it was poured into a 250 ml beaker with no ash loss, and 100 ml of diluted hydrochloric acid was added to it. Using a water bath, this solution was boiled for 5 minutes, followed by filtration of the solution and collecting the insoluble matter on an ashless filter paper (Whatman no.41). This filtrate was washed with hot water till getting the neutral filtrate. Transferred the insoluble matter-containing filter paper to the initial crucible and dried it on a hot plate at 600⁰c using a muffle furnace for ignition (until it became white ash). Allowed this residue to cool in suitable desiccators for about 30 minutes and weigh without delay. Repeated the process until a constant weight was obtained. Calculated this acid-insoluble ash concerning the air-dried drug.²⁰

Determination of water-soluble extractive value:

A digital balanced weighing machine measured 5 gm of air-dried vitamin C powder. These powders were mixed with 100 ml of distilled water in a glass stoppered conical flask. It was set aside for 24 hours with frequent shaking. Rapidly filter it after 24 hrs. A pipette is used to transfer 25 ml of filtrate into a tarred flat bottom evaporating dish, which is then put over boiling water to evaporate it to dryness. Again, evaporated dish dried at 105⁰ c in the oven. The weight of this residue was measured after cooling, and the percentage of water-soluble extractive was determined and expressed as % w/w with reference to air dried sample.^{20,21}

Determination of alcohol soluble extractive value:

A digital balanced weighing machine measured 5 gm of air-dried vitamin C powder. These powders were mixed with 100 ml of ethanol in a glass stoppered conical flask. It was set aside for 24 hours with frequent shaking. Rapidly filter it after 24 hrs. A pipette is used to transfer 25 ml of filtrate into a tarred flat bottom evaporating dish, which is then put over boiling water to evaporate it to dryness. Again, evaporated dish dried at 105⁰ c in the oven. The weight of this residue was measured after cooling, and the percentage of alcohol-soluble extractive was determined and expressed as % w/w with reference to air dried sample.^{20,21}

Determination of phytochemical constituents:

Test for the presence of tannin and phenol:

- A test tube was filled with 2 ml of vitamin C powder aqueous extract and a few drops of 5 % FeCl₃ solution. Deep blue-black color was observed at the end.
- A test tube was filled with 2 ml of vitamin C powder aqueous extract. It was treated with a few drops of acetic acid solution. The red color persists at the end.

- A test tube was filled with 2 ml of vitamin C powder aqueous extract and a few drops of dilute potassium permanganate solution. Discoloration of the solution was observed at the end. This test was performed for the 1st, 2nd, 3rd and 6th months and was found present each month.²²

Test for the presence of Flavonoids:

- Shinoda test: We took 2 ml of vitamin C powder aqueous drug extract and mixed it with 5 ml of 95% ethanol. Then it was mixed with a few drops of concentrated HCl and 0.5 gm of magnesium. The pink color was observed.
- Adding an increasing amount of sodium hydroxide to the residue shows yellow coloration, which decolorizes after adding acid.²²

Test for the presence of carbohydrates:

- Fehling's Test: Take 2 ml of the sample solution in a clean test tube. Add 2 ml of Fehling's solution A and Fehling's solution B. Keep the solution in a boiling water bath for about 10 minutes. If a red precipitate is formed, then the presence of carbohydrates is confirmed.
- Molisch's Test: Take 2 ml of the sample solution in a clean test tube. Add 2-3 drops of Molisch reagent slowly. Now add concentrated sulfuric acid along the sides of the test tube. The acid layer forms a layer at the bottom. Note the junction of the two layers. If there is a formation of the violet ring, then the presence of carbohydrates is confirmed.²²

Determination of total tannin:

For blank: 300 ml distilled water and 25 ml, indigo carmine solution was transferred to a 500 ml conical flask and thoroughly mixed. This solution was titrated against 0.02 M KMnO_4 solution until stable golden-yellow color developed and the burette reading was noted.

For sample: Air-dried vitamin C powder was weighed 0.05 gm in the digital balanced weighing machine. This sample was poured into a 500 ml conical flask, and 50 ml of distilled water was added until the sample was fully dissolved. 250 ml sterile water was carefully added to this solution and thoroughly mixed. 25 ml of indigo carmine solution was added to it and mixed well. Carefully titrated this solution against 0.02 M KMnO_4 until stable golden-yellow color persisted. The burette reading was noted. The percentage of total tannin was calculated using the following factor. 1 ml of 0.02 M KMnO_4 is equivalent to 0.00415 gm of tannin.²³

4. Microbiological parameters

Determination of total aerobic bacterial count:

Before starting microbial analysis LAF (Laminar Air Flow) and UV (Ultra Violet) lights were switched on for about 30 minutes. Before starting microbial analysis under LAF, UV lights were switched off and daylight was switched on. 10 gm of air-dried vitamin C powder were dissolved and suspended in 90 ml sterile soybean casein digest medium with 4% polysorbate 80 (Tween -80). 1 ml of the solution was pipette out from the above solution using a micropipette and poured into each of the two sterile petri plates. Micropipette tips were discarded in a beaker containing disinfectant in use. Hands were wiped with 70% IPA immediately. 15-20 ml of sterile molten soybean casein digest agar (40-45⁰c) was poured into the two plates for the total aerobic bacterial count. Plates were swirling slowly to give them uniform dispersion of sample by taking

care that media did not touch the plate lid. Negative control was prepared by pouring 15-20 ml of each used media in a separate empty sterile petri plate and allowing it to solidify at the end of the analysis. Soybean casein digest agar plates were inverted and incubated at 30- 35⁰c for 120 hours.²⁴

Determination of total aerobic fungal count:

Before starting microbial analysis LAF (Laminar Air Flow) and UV (Ultra Violet) lights were switched on for about 30 minutes. Before starting microbial analysis under LAF, UV lights were switched off, and daylight was switched on. 10 gm of air-dried vitamin C powder were dissolved and suspended in 90 ml sterile soybean casein digest medium with 4% polysorbate 80 (Tween -80). 1 ml of the solution was pipette out from the above solution using a micropipette and poured into each of the two sterile petri plates. Micropipette tips were discarded in a beaker containing disinfectant in use. Hands were wiped with 70% IPA immediately. 15-20 ml of sterile molten sabouraud dextrose agar (40-45⁰c) was poured into the two plates for the total aerobic fungal count. Plates were swirling slowly to give them uniform dispersion of sample by taking care that media did not touch the plate lid. Negative control was prepared by pouring 15-20 ml of each used media in a separate empty sterile petri plate and allowing it to solidify at the end of the analysis. Sabouraud dextrose agar plates were inverted and incubated at 20-25⁰ c for 120 hours.²⁴

Determination of specified microorganisms:

Test for Escherichia coli:

100 ml of Soyabean Casein Digest Broth was prepared and autoclaved for 15-20 minutes at 121⁰ c and 15 psi pressure. 10 gm of air-dried vitamin C powder were dissolved and suspended in a sterile 90 ml Soyabean casein digest medium with 4% polysorbate 80 (Tween80). (Solution

A). 100 ml MacConkey's broth was prepared and autoclaved for 15-20 minutes at 121⁰ c and 15 psi pressure and then add 1 ml of solution A was added. The above solution was incubated at 43-45⁰ c for about 24 hours. Then 100 ml of MacConkey's agar was prepared and sterilized by autoclaving. After sterilization, the agar solution was cooled and poured into the sterile petri dish. Wait until it solidifies. Incubated broth solution was removed and inoculated into solidified agar using an inoculation loop under the laminar airflow. These agar plates were incubated at 37⁰ c for about five days. Growth of E- coli was compared with the standard. ²⁴

Test for pseudomonas aeruginosa:

100 ml of Soyabean Casein Digest Broth was prepared and autoclaved for 15-20 minutes at 121⁰ c and 15 psi pressure. 10 gm of air-dried vitamin C powder were dissolved and suspended in a sterile 90 ml Soyabean casein digest medium with 4% polysorbate 80 (Tween80). (Solution A). The above solution was incubated at 43-45⁰c for about 24 hours. 100 ml Cetrimide agar was then prepared and sterilized by autoclaving. Wait until it solidifies. Incubated broth solution was removed and inoculated into solidified agar using an inoculation loop under the laminar airflow. These agar plates were incubated at 37⁰c for about five days. The growth of Pseudomonas aeruginosa was compared with the standard.²⁴

Test for Salmonella species:

100 ml of Soyabean Casein Digest Broth was prepared and autoclaved for 15-20 minutes at 121⁰ c and 15 psi pressure. 10 gm of air-dried vitamin C powder were dissolved and suspended in a sterile 90 ml Soyabean casein digest medium with 4% polysorbate 80 (Tween80). (Solution A). The above solution was incubated at 43-45⁰c for about 24 hours. 100 ml Rappaport Vassiliadis Salmonella Enrichment Broth was prepared, and 1 ml solution A was added. Again,

the above solution was incubated at 30-35⁰ c for 24 hrs. 100 ml of Bismuth sulfate agar was prepared and sterilized by autoclaving. Incubated broth solution was removed and inoculated into solidified agar using an inoculation loop under the laminar airflow. These agar plates were incubated at 37⁰ c for about five days. The growth of salmonella species was compared with the standard.²⁴

Test for shigella boydii:

100 ml of Soyabean Casein Digest Broth was prepared and autoclaved for 15-20 minutes at 121⁰ c and 15 psi pressure. 10 gm of air-dried vitamin C powder were dissolved and suspended in a sterile 90 ml Soyabean casein digest medium with 4% polysorbate 80 (Tween80). (Solution A). The above solution was incubated at 43-45⁰ c for about 24 hours. 100 ml of GN broth was prepared, 1 ml of solution A was added, and it was incubated at 30-35⁰c for 24 hours. 100 ml of Xylose Lysine Deoxycholate agar was then prepared and sterilized by autoclaving. Incubated broth solution was removed and inoculated into solidified agar using an inoculation loop under the laminar airflow. These agar plates were incubated at 37⁰ c for about five days. The growth of shigella boydii was compared with the standard.²⁴

5. Estimation of Nutritional Value: We tested vitamin C powder's nutritional value from the TUV lab in Pune. All (**Table 3**)

6. Cell viability assay/ MTT assay:

Human embryonic kidney (HEK293) cells were obtained from the National Centre for Cell Science (Pune). HEK293 cells were cultured in DMEM. The culture media were supplemented with 10% Fetal Bovine Serum, grown in a humidified incubator with 5% CO₂.

Cell viability was assessed by MTT assay. Briefly, HEK293 cells (1×10^4) were seeded into 96-well microplates (flat-bottom), treated with vitamin C powder at 25-1100 $\mu\text{g/ml}$ concentrations, and incubated for 24 h. After 24 h. MTT (0.5 mg/ml) solution was added to each well and incubated for 24 hr. at 37°C . MTT solution was carefully aspirated and isopropanol was added to dissolve formazan crystals, and the optical density of formazan solutions was recorded at 570 nm using an automated microplate reader (EPOCH2; Bio Tek Instruments, Highland Park, VT, USA). All experiments were done in biological triplicates.

Result and discussion:**Result:****Table 1: Table: Organoleptic Properties of Raw Material**

Parameters	Acerola Extract	Rosehip Extract	Moringa Extract	Amla Powder	Bilberry Extract
Colour	Light Red	Light Brown	Brown	Light Brown	Brown
Odour	Characteristics	Characteristics	Characteristics	Characteristics	Characteristics
Taste	Characteristics	Characteristics	Characteristics	Slightly bitter and sour	Characteristics

Table 2: Powder Characterization of Raw Material

Parameters	Acerola Extract	Rosehip Extract	Moringa Extract	Amla Powder	Bilberry Extract
Bulk Density	0.62	0.64	0.63	0.64	0.62
Tapped Density	0.70	0.71	0.70	0.72	0.70
Hausner Ratio	1.12	1.11	1.11	1.12	1.12
Carr Index	11.50	9.90	9.90	11.50	11.50
Angle of repose	40.06	37.23	39.35	40.03	39

Table 3: Solid-State Stability Study Parameters

Sr. No.	Test Parameters	Observations
1.	Caking	Absent
2.	Liquefaction	Absent
3.	Discoloration	Absent
4.	Odor	Absent
5.	Gel formation	Absent

Table 4: Powder characterization of Vitamin C powder formulation

Sr. No.	Test parameter	Result
1.	Color	Light Brown
2.	Odor	Characteristics
3.	Taste	Bitter

Table 5: Powder characterization of Vitamin C powder formulation

Sr. No.	Test parameter	Result
1.	Bulk density(gm/ml)	0.63 ± 0.02
2.	Tapped density(gm/ml)	0.70 ± 0.02
3.	Hausner Ratio	1.11 ± 0.01
4.	Carr Index	10.86 ± 0.02
5.	Angle of repose	$39.39^\circ \pm 0.20$

Table 6: Physicochemical characteristics of Vitamin C powder formulation

Sr. No.	Test parameter	Result
1	Loss on Drying	8 %
2	Ph	3.87
3	Total Ash	5.73
4	Acid Insoluble Ash	0.43 %
5	Water soluble extractive value	67 %
6	Alcohol soluble extractive value	25 %
7	Determination of Phytochemical constituents	
	a) Tannin	Present
	b) Flavonoid	Present
	c) Phenol	Present
	d) Carbohydrates	Present
8	Essay	
	a) Determination of Total Tannin	21.24 %

Table 7: Microbiological parameters of Vitamin C powder formulation

Sr. No.	Test parameter	Result
1	Total Aerobic Bacterial Count	12 cfu /gm
2	Total Aerobic Fungal Count	7 cfu /gm
3	Specific Pathogens	
	a) Escherichia Coli	Absent
	b) Staphylococcus Aureus	Absent
	c) Salmonella Species	Absent
	d) Pseudomonas Aeruginosa	Absent

Figure 1: Total aerobic bacterial count in SCDA medium

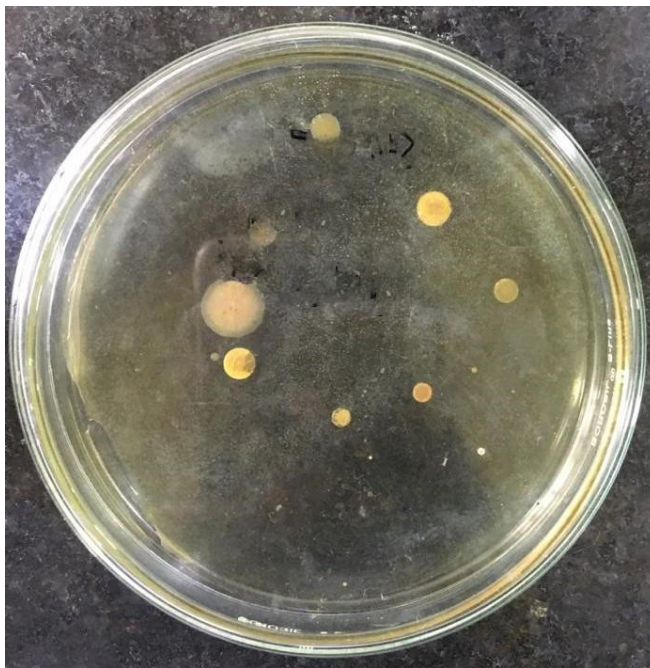


Figure 2: Total aerobic fungal count in SDA medium



Figure 3: Specific Pathogen test of *Escherichia coli* in MacConkey agar

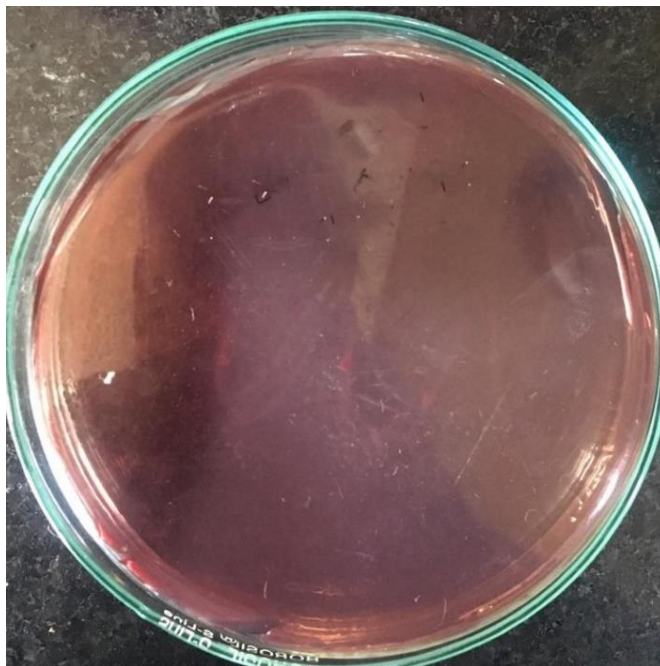


Figure 4: Specific Pathogen test of *Pseudomonas aeruginosa* in cetrimide agar



Figure 5: Specific Pathogen test of salmonella species in Bismuth sulphate agar

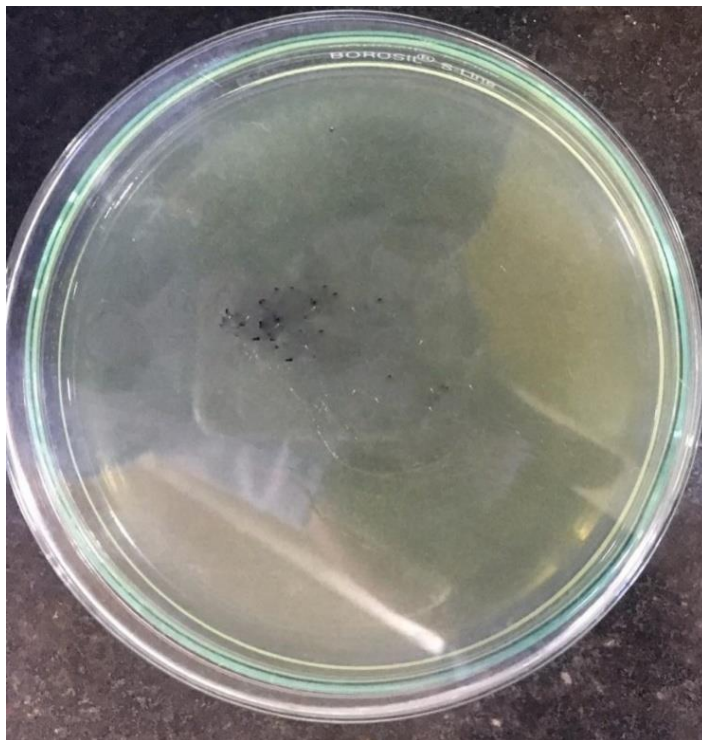


Figure 6: Specific Pathogen test of shigella boydii in Xylose Lysine Deoxycholate agar



Table 8: Estimation of Nutritional Value of Vitamin C powder formulation: -

Nutritional Facts			
NUTRIENTS	APPROX PER		% RDA*
	100 g	6g	
Energy (Kcal)	383	22.98	1.03 % [#]
Total Protein (g)	7.15	0.43	0.94 %
Carbohydrate (g)	79.27	4.76	**
Total Sugar (g)	16.85	1.01	**
Added Sugar (g)	0.00	0.00	**
Dietary Fibre (g)	17.59	1.06	**
Total Fat (g)	0.27	0.02	0.06% [#]
Cholesterol (mg)	0.00	0.00	**
Vitamin C (mg)	1050.64	63.04	96.98 %*
Potassium (mg)	693.22	41.59	1.19 %*
Sodium (mg)	1270.14	76.21	3.81 %*
Zinc (mg)	0.67	0.04	0.40 % [#]

* %RDA values established as per ICMR Guidelines-2020.

** %RDA values not established.

%RDA values established as per ICMR Guidelines-2010

Cell viability assay/ MTT assay:

The cell viability of the vitamin C was determined by MTT assay (Fig 7). The IC₅₀ (Inhibitory concentration) value for the MTT assay is 850 mcg/ml, meaning that 50% of cells die at this concentration. It demonstrates that we can give the maximum daily dose of 850 mcg/ml.

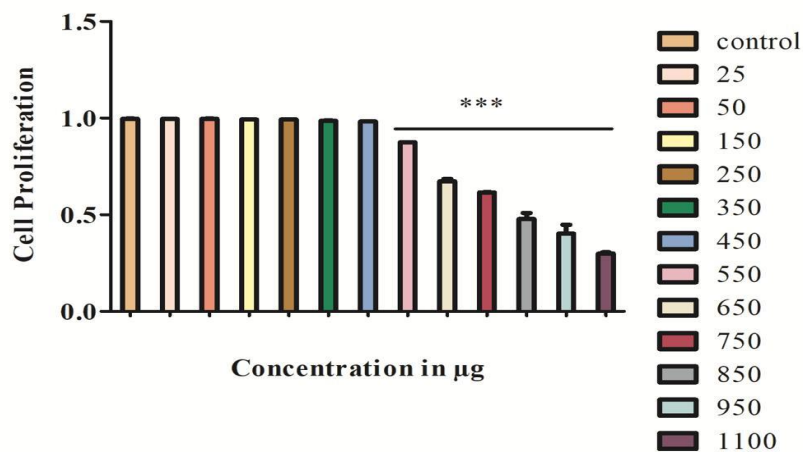


Fig 7. Cell viability for HEK293.

Discussion:

The physical characteristics of the powder were evaluated. The color of the powder was light brown with characteristics of odor and bitter taste. The powder characterization of powder is illustrated in (Table 1). The mean values of bulk density, tapped density, Hausner's ratio, Carr Index, compressibility index, and angle of repose were 0.633 ± 0.02 , 0.70 ± 0.02 , 1.11 ± 0.01 , 10.86 ± 0.02 , 10.25 ± 0.22 and $39.39^\circ \pm 0.20$ respectively. The mean weight loss percentage on drying of vitamin C powder is 8 %. (Table 2) The pH of vitamin C powder was found to be 3.87. A high ash value indicates contamination, substitution, adulteration, or carelessness in preparing the drug or drug combinations for marketing. The total ash value of vitamin C powder was found to be 5.73% w/w. The acid-insoluble ash value of vitamin C powder was $0.43\% \pm 0.01$. The water-soluble and alcohol-soluble extractive values of vitamin C powder were 67% and 25%, respectively. (Table 2) Phytochemical constituents' tannins, flavonoids, phenols, and carbohydrates were present on qualitative estimation tests. The overall tannin percentage was found to be 21.24%. The total aerobic bacterial and fungi count below the permitted range, while specific pathogens were reported to be absent during the study.

The percentage of the recommended daily allowance (%RDA) for nutritional parameters such as energy (Kcal), total protein (g), carbohydrate (g), added sugar (g), dietary fiber (g), total fat (g), cholesterol (mg), potassium (mg), sodium (mg) and zinc (mg) in vitamin C powder formulations is not exceeded, according to ICMR guidelines. Also, it fulfills the daily Vitamin C (Table 3) requirement of adults.

The in vitro cellular cytotoxicity test of vitamin C powder showed no significant cytotoxicity against the HEK293cell line.

Conclusion:

In the present study, a stable vitamin C powder formulation was prepared and evaluated physiochemically and microbiologically. Also, the MTT assay proved that it does not indicate cytotoxicity at the daily dose limit and fulfills adults' daily Vitamin C requirement.

References:

1. Parasuraman S, Thing G.S, Dhanaraj S.A. Polyherbal formulation: Concept of Ayurveda. *Phcog. Rev.* 2014; 8: 73-80.
2. Srivastava S, Lal V.K, Pant K.K. Polyherbal formulations based on Indian medicinal plants as antidiabetic phytotherapeutics. *Phytopharmacology.* 2013; 2: 1–15.
3. Ruchi S. Role of nutraceuticals in health care: A review. *Int J Green Pharm.* 2017;11(3)
4. Nada H, Heba E, Ahmed A, Mohamed E, Ivan E, and Mohamed N. Nutraceuticals' Novel Formulations: The Good, the Bad, the Unknown and Patents Involved. *Recent Patents on Drug Delivery & Formulation.* 2019; 13(2): 105–156.
5. Nasri H., Baradaran A., Shirzad H., Rafieian-Kopaei M. New concepts in nutraceuticals as an alternative for pharmaceuticals. *Int. J. Prev. Med.* 2014;5(12):1487–1499.
6. Andlauer W., Fürst P. Nutraceuticals: A piece of history, present status and outlook. *Food Res. Int.* 2002;35(2-3):171–176.
7. Carr A, Vissers M. Synthetic or Food-Derived Vitamin C—Are They Equally Bioavailable?. *Nutrients*, 2013; 5(11): 4284–4304.
8. Chambial S, Dwivedi S, Shukla K, John P, Sharma P. Vitamin C in Disease Prevention and Cure: An Overview. *Indian Journal of Clinical Biochemistry*, 2013; 28(4): 314–328.
9. Mohammed M, Fisher B, Kraskauskas D, Ward S, Wayne J, Brophy D et al. Vitamin C promotes wound healing through novel pleiotropic mechanisms. *International Wound Journal*, 2016; 13(4): 572–584.
10. K. Akhilender Naidu. Vitamin C in human health and disease is still a mystery? An overview. *Nutrition Journal*, 2003; 2: 7.

11. Chow O, Barbul A. Immunonutrition: Role in Wound Healing and Tissue Regeneration. *Advances in Wound Care*. 2014; 3(1): 46–53.
12. Lynch S, Cook J. Interaction of vitamin c and iron. *Annals of the New York Academy of Sciences*. 1980; 32–44.
13. Ganot N, MekerS,Reytman L, Tzuberly A, Tshuva E. Anticancer Metal Complexes: Synthesis and Cytotoxicity Evaluation by the MTT Assay. *Journal Of Visualized Experiments*. 2013; (81): 1-6.
14. Anonymous, Indian Pharmacopoeia. Govt. of India Ministry of Health and Family Welfare, Published by Indian Pharmacopoeia Commission, I, II, &III (2010) 153,187- 202,300, 576, 1130, 2479-2481, 2544-2546.
15. Lavekar GS, Padhi E, Pant P. Laboratory guide for the analysis of Ayurveda and Siddha formulations. New Delhi: Central Council for Research in Ayurveda and Siddha; 2010, p. 88.
16. Meghwal M, Goswami T. Flow characterization of ambiently and cryogenically ground black pepper (*piper nigrum*) powder as a function of varying moisture content. *Journal of food process engineering*, 40(1); e12304.
17. Beakawi H, H. M., Baghabra A., Omar S. A review on the angle of repose of granular materials. *Powder Technology*. 2018; 397–417.
18. Lachman L, Lieberman HA, Kanig JL; The theory and practice of industrial pharmacy, 3rd edition. Varghese Publishing House, New Delhi, 1987:293-639.
19. General guidelines for drug development of Ayurvedic formulations. Vol. 1. New Delhi: Central Council for Research in Ayurvedic sciences, Ministry of AYUSH; 2018; 23-26.
20. Lavekar GS, Padhi E, Pant P. Laboratory guide for the analysis of Ayurveda and Siddha formulations. New Delhi: Central Council for Research in Ayurveda and Siddha; 2010,27.

21. General guidelines for drug development of Ayurvedic formulations. Vol. 1. New Delhi: Central Council for Research in Ayurvedic sciences, Ministry of AYUSH; 2018; 23-26.
22. Patra Karthik, Pareta Surendra Kumar, Singh Brijesh & Jayaram Kumar, Comparative Standardization of a polyherbal Ayurvedic formulation Talishadi churna, Indian Journal of Traditional Knowledge. (2011); 10(4): 608-611.
23. Kokate CK, Purohit AP, Gokhale SB, Textbook of pharmacognosy, career publication. (2009);43(3): 1.107-1.110, 3.64 3.67, 3.80-3.82.
24. Atanassova M, Christova-bagadassarian V. Determination of tannins content by titrimetric method for comparison of different plant species. Journal of the University Chemical Technology and metallurgy. 2009; 44, 4: 413-415.



Formulation Development and Evaluation for Mouth Dissolving Tablet Containing Bromelain

Deshmane Kamlesh ^{1*}, Dr. Barge Vijaya ², Dr. Kasabe Amit ³, Avhad Pratiksha ¹, Borase Pallavi ¹, Gaikwad Rajratna ¹, Pawar Ajay ⁴

¹*Research Scholar, Department of Pharmaceutical Quality Assurance, PDEA's Shankarrao Ursal College of Pharmaceutical Sciences and Research Centre, Pune, Maharashtra, India.*

²*Vice Principal, Department of Pharmaceutical Quality Assurance, PDEA's Shankarrao Ursal College of Pharmaceutical Sciences & Research Centre, Kharadi, Pune, Maharashtra, India.*

³*Associate Professor, Department of Pharmaceutical Quality Assurance, PDEA'S Shankarrao Ursal College of Pharmaceutical Sciences & Research Centre, Kharadi, Pune, Maharashtra, India.*

⁴*Research Scholar, Department of Pharmaceutics, PDEA's Shankarrao Ursal College of Pharmaceutical Sciences and Research Centre, Pune, Maharashtra, India.*

For Correspondence- Deshmane Kamlesh Ravindra

Kamleshdeshmane2299@gmail.com

ABSTRACT:

Bromelain is a proteolytic enzyme that is used as an anti-inflammatory drug. Administration of Bromelain through the oral route is a challenge in children, who have difficulty swallowing tablets. In the present study, six batches of Bromelain Mouth Dissolving tablets (MDT) dosage form at the dose of 100 mg were formulated and evaluated. Results showed that the thickness, weight variation, friability, hardness, and content uniformity of all six formulations were within acceptable limits. But in the in-vitro dissolution study formulation 3 demonstrated better cumulative drug release than other formulations. Hence the study concludes that Bromelain mouth dissolving tablets formulated using crospovidone (Formulation 3) showed better characteristics of mouth dissolving tablets.

KEYWORDS: Bromelain, Mouth dissolving tablets, Drug-Excipient Compatibility, Crospovidone.

INTRODUCTION:

Many patients, particularly old find it difficult in swallowing tablets, capsules, and fluids and subsequently do not comply with prescriptions, which results in a high frequency of resistance. Situated research has resulted in bringing out many secure, safe new drug delivery system. Among the several dosage forms developed to improve the difficulty of administration, the Mouth Dissolving Tablet (MDT) is the most favoured commercial product. [1] The oral cavity is an appealing site for the administration of drugs because of the simplicity of administration. Several dosage forms like Tablets, Capsules, and Liquid preparations are administered by oral route. During the most recent decade, Mouth Dissolving Tablet (MDT) advances that make tablets disintegrate in the mouth without chewing and additional water intake have drawn a lot of consideration. The MDTs are also known as fast liquefying, rapid dispersing, rapid dissolve, rapid melt, as well as speedy disintegrating tablets. [2-4] MDTs can be prepared by various conventional methods like direct compression, wet granulation, molding, spray drying, freeze-drying, and sublimation. Firstly, MDTs disintegrate and then dissolve quickly in the saliva without any need for solvents, releasing the drug. A few drugs are absorbed from the mouth, pharynx, and oesophagus as the saliva goes down into the stomach. In many cases, the bioavailability of these drugs is significantly more than those observed from conventional tablet dosage forms. [5,6]

Bromelain is a proteolytic enzyme with anti-inflammatory activity. It is found in pineapple juice and in the pineapple stem. Anti-inflammatory activity by activation of plasmin production from plasminogen and reduction of kinin via inhibition of the conversion of kininogen to kinin. Bromelain has low oral bio-availability because of high first pass metabolism rate. Hence, the formulation in orodispersible form of Bromelain upgrades the bioavailability, decreases side effects, low dosing, patient compliance, and rapid onset of action with great steadiness. In the present work, Orodispersible tablets of Bromelain were prepared by direct compression method using sodium starch glycollate, and croscopolvidone as the superdisintegrants. The aim of the study was to evaluate the effect of the superdisintegrants on the wetting time, disintegration time, and drug release profile of the orodispersible tablets. The present investigation deals with the improvement of an effective and stable MDT of Bromelain having a sufficient hardness, low disintegration time, and pleasant taste.

MATERIAL AND METHODS:

Materials:

Bromelain was obtained from Arti Pharma, Mumbai, India. Crospovidone and sodium starch glycolate were obtained from Research Lab Fine Chemical Industries Pvt. Ltd. Mumbai. Microcrystalline cellulose and mannitol were also obtained from Research Lab Fine Chemical Industries Pvt. Ltd. Mumbai. All other chemicals of analytical grade were purchased from commercial sources.

Methods:

Preparation of Mouth Dissolving Tablets by Direct Compression Method:

Mouth dissolving tablets of Bromelain were prepared by direct compression. All the ingredients (except granular directly compressible excipients) were passed through # 60-mesh separately. The ingredients were then weighed and mixed in geometrical order and compressed into tablets of 250 mg using 6 mm round concave punches on an 8-station rotary tablet machine (Table 1).

Table 1: Formulation Table of Bromelain Mouth Dissolving Tablet

Formulations	F1	F2	F3	F4	F5	F6
Ingredient	Unit Formula (mg per tablet)					
Bromelain	100	100	100	100	100	100
Crosspovidone	5	10	15	-	-	-
Sodium starch glycolate	-	-	-	5	10	15
Mannitol	50	50	50	50	50	50
Menthol	10	10	10	10	10	10
Avicel PH 102	81	76	71	81	76	71
Sodium stearate	2	2	2	2	2	2
Talc	2	2	2	2	2	2
Total	250	250	250	250	250	250

Evaluation of Bromelain Mouth Dissolving Tablet:

Evaluation of pre-compression parameters of powder:

Preformulation study:**Angle of repose (Θ) [7]**

The angle of repose was determined by using the funnel method. The accurately weighed blend was taken in a funnel. The height of the funnel was adjusted in such a way that the tip of funnel just touched the apex of the heap and the drug-excipient blend was allowed to flow through the funnel freely to the surface. The diameter of the powder cone was measured and angle of repose calculated using the following equation.

$$\tan \theta = h/r$$

Different ranges of flowability in terms of angle of repose (Table II) are given below (Bikshapathi et al., 2011).

Table 2: Relationship Between Angle of Repose and Flowability

Flow property	Angle of repose
Excellent	25-30
Good	31-35
Fair (aid not needed)	36-40
Passable (may hang up)	41-45
Poor (must agitate, vibrate)	46-55
Very Poor	56-65
Very Very Poor	>66

Bulk Density [8]

Bulk density was determined by pouring presieved drug excipient blend into a 100 ml graduated cylinder. The sample occupied volume and its weight has been recorded It is expressed in g/mL and calculated by using following formula:

$$\rho_b = M / V_p$$

Where,

ρ_b = Bulk density

M = Weight of sample in grams

V_p = Final volumes of Powder in cm³

Tapped Density [9]

It was carried out by pouring powder blend in 100ml graduated cylinder. The cylinder was tapped mechanically by Tap density apparatus until a constant volume was obtained. Volume occupied by the sample after tapping were recorded and tapped density was calculated by using following formula:

$$\rho_t = M / V_T$$

Where,

ρ_t = Tap density

M = Weight of sample in grams

V_T = final tap volume of powder in cm³

Hausner's ratio [10]

Hausner's ratio is the ratio of tapped density to bulk density. The lower the value of Hausner's ratio the better the flow property. The ratio is calculated by the following formula

$$\text{Hausner's ratio} = \frac{\text{Tapped density}}{\text{Bulk density}}$$

Lower Hausner's ratios (<1.25) indicate better flow properties than higher ratios (>1.25) (Sayeed et al., 2011).

Carr's Index (Compressibility Index) [10]

It is also one of the simple methods to evaluate flow property of a powder by comparing the bulk density and tapped density. The percentage compressibility of a powder is a direct measure of the potential powder arch or bridge strength and stability. The grading of compressibility of powder according to carr's index is shown in table no.3. It can be calculated by following formula:

$$\text{Carr's Index} = \frac{\text{Tapped density} - \text{Bulk density}}{\text{Tapped density}} \times 100$$

Table 3: Relationship Between Carr's Index and Flowability

Carr's Index	Flow property
5-10	Excellent
12-16	Good
18-21	Fair to possible
23-35	Poor
33-38	Very poor
>40	Extremely poor

Drug-excipient compatibility study

Studies of drug-excipient compatibility are important to as certain drug and excipients are compatible with each other. IR spectra are used to study drug-excipient compatibility.

FTIR study [11]

The study was carried out to determine the molecular structure, serving as an identification test to ascertain the purity of the molecule. IR spectroscopy was obtained by a FTIR spectrophotometer (H400-84100, Shimadzu, Japan) using KBr pellets. The scanning range used was 4400 to 400 cm⁻¹ at a scan period of 1min. Spectra of pure drug and the blend are shown in Figures 1 and 2. There is no change in the shape of the peak or shift of the peak, hence the drug and excipients are compatible (Prameela et al., 2010).

Evaluation of Post-Compression Parameters of Tablets:**Weight variation test [12]**

Weight variation was calculated as per method described in Indian pharmacopeia (I.P.2007). Twenty tablets were weighted individually by using Electronic balance (Shimatzu) and the average weight is calculated. The tablets meet the test if no more than 2 tablets are outside the percentage limit and no tablet differs by more than 2 times the percentage limit. The limit of weight variation in tablet are listed in Table 4.

Table 4: Limits for Weight Variation in Tablet as Per I.P. 2007

Average weight of tablet (mg)	Percentage deviation allowed
80 mg or less	± 10
More than 80 mg but less than 250 mg	±7.5
or more	±5

Hardness test [13]

Hardness indicates the ability of a tablet to withstand mechanical shocks while handling. The hardness of the tablets was determined using Digital hardness tester. It is expressed in Kg/cm². Digital hardness tester was used to measure hardness of the tablet. In which the tablet was placed in the tester and pressure needed to break the tablet was measured.

Thickness [14]

The thickness of the tablets was determined using a Vernier Caliper. Ten tablets from formulation batch were used and average values were calculated.

Friability [15]

Friability is the measure of tablet strength. It was carried out by using Roch friability apparatus, in which the accurately weighed 20 tablets was allowed to rolling and free fall at 25 rpm, after 100 revolutions weight of tablet was again measured and % friability was calculated by following formula

$$\% \text{ Friability} = \frac{\text{Initial weight of tablet} - \text{Final weight of tablet}}{\text{Initial weight of tablet}} \times 100$$

Disintegration time [16]

The disintegration time of tablet was determined by using Disintegration test apparatus. Tablets were placed in disintegration test assembly and disc was placed on tablets in each glass tube of assembly. The assembly was dipped in a vessel containing 900 ml phosphate buffer 6.8 pH. The time for disappearance of tablet residue above mesh was noted as disintegration time.

Wetting time [17]

About 6-8 ml of phosphate buffer 6.8 pH was taken in 10 mL of measuring cylinder. Tablet was placed in the cylinder and complete dispersion of tablet in the cylinder was recorded as the disintegration time. Wetting time in that the tissue paper has been folded twice and placed in petri dish above that tablet is placed. A small quantity of amaranth red color was put on the upper surface of the tablet and 10 ml distilled water was added. The time required to get the tablet completely wet and indicate red color was measured.

Uniformity of drug content [18]

This method is performed as per Indian Pharmacopoeia. Two tablets were crushed and added to 30 ml of 0.1M NaOH in 100 ml volumetric flask sonicated to disintegrate, then diluted by acetonitrile, then this solution was filtered and diluted the filtrate with a mixture of seven volumes acetonitrile and three volumes of 0.1M NaOH. Absorbance was measured by UV spectroscopy at 280 nm and drug content was calculated.

In-vitro Dissolution study [16]

The dissolution study of selected Bromelain formulations was conducted by using USP dissolution apparatus Type – II (Electrolab Mumbai) by taking 900 ml phosphate buffer pH 6.8 as dissolution medium which maintained at $37 \pm 0.5^{\circ}\text{C}$. At every 5 min interval upto 30 min 1 ml samples was withdrawn and the same volume was replaced to maintain the sink condition. The samples were analyzed using UV spectroscopy at wavelength maxima 280 nm. The % drug release was calculated and is reported in Table 10.11 and drug release profile of selected formulations tablets are depicted in Figure 12.

RESULTS AND DISCUSSION:

Spectroscopic Analysis:

UV spectroscopy:

Determination of λ_{max} of Bromelain in Water:

In UV spectroscopy study, the maximum wavelength (λ_{max}) of Bromelain in water was found to be 279.40 nm. The reported λ_{max} value of Bromelain in water was also 279.40 nm respectively, so the values similar with the reported values indicates that the given sample of Bromelain was in pure form.

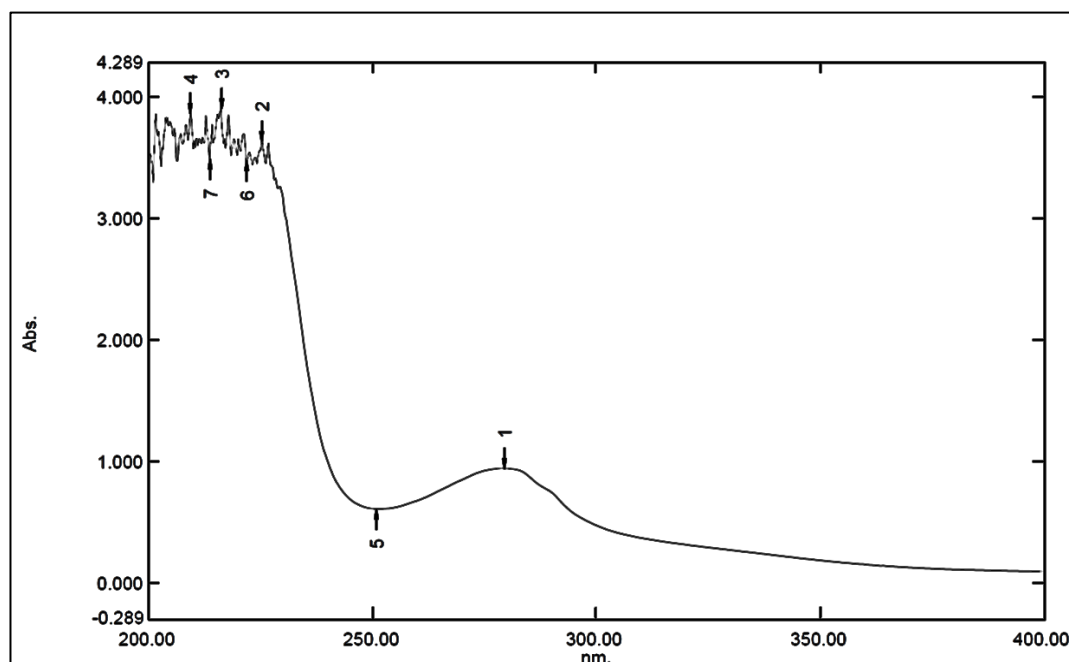


Figure 1: UV spectra of Bromelain in water at 279.40 nm

Calibration Curve of Bromelain in Water:

The linearity of the response of Bromelain was verified at 2–10 $\mu\text{g/ml}$ concentrations. The calibration curve was obtained by plotting the absorbance versus the concentration data and was treated by linear regression analysis. The equation of the linearity curve for Bromelain was $y = 0.0127x + 0.0033$. The linearity curve was found to be linear in the a for mentioned concentrations (the correlation coefficient (r^2) of determination was 0.9922) (Figure 2).

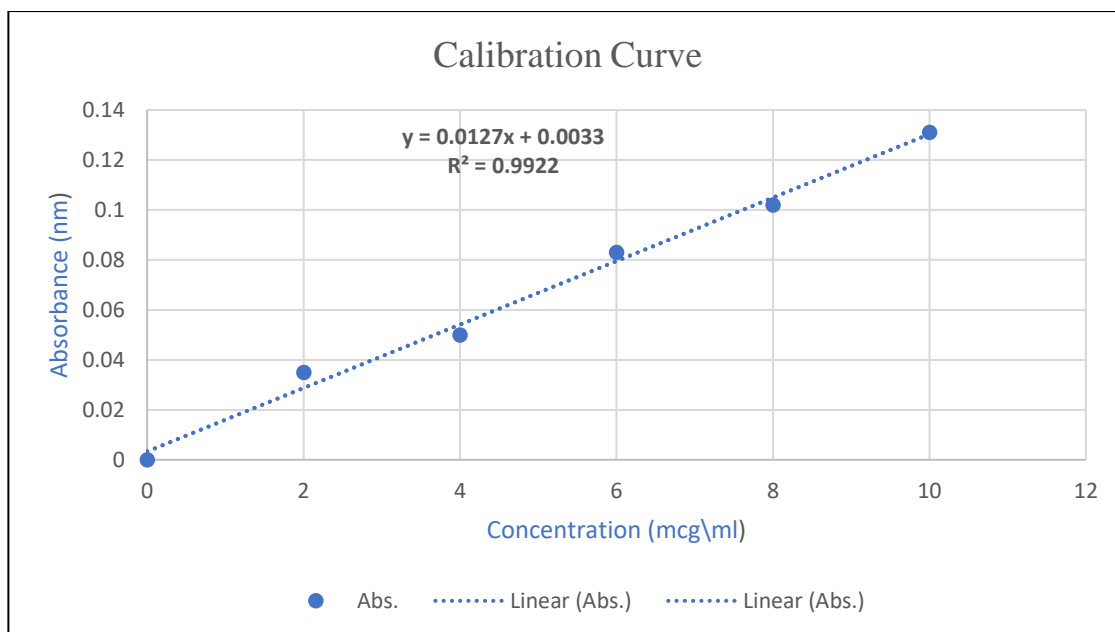


Figure 2: Calibration Curve of Bromelain in Water

FTIR spectroscopy:

The FTIR spectrums of pure Bromelain and physical mixtures of drugs and polymers were studied separately as per the excipients used in the formulation. It was observed that there were no major shifts in the main peaks of either drug. This indicates that there were no compatibility problems with the drug with the polymers and excipients used in the formulation. Bromelain had peaks at 3433 (-OH elongation), 1643 (CO elongation), 3487 (NH stretch), 1384 (C-N stretch), 2862 (C-H).

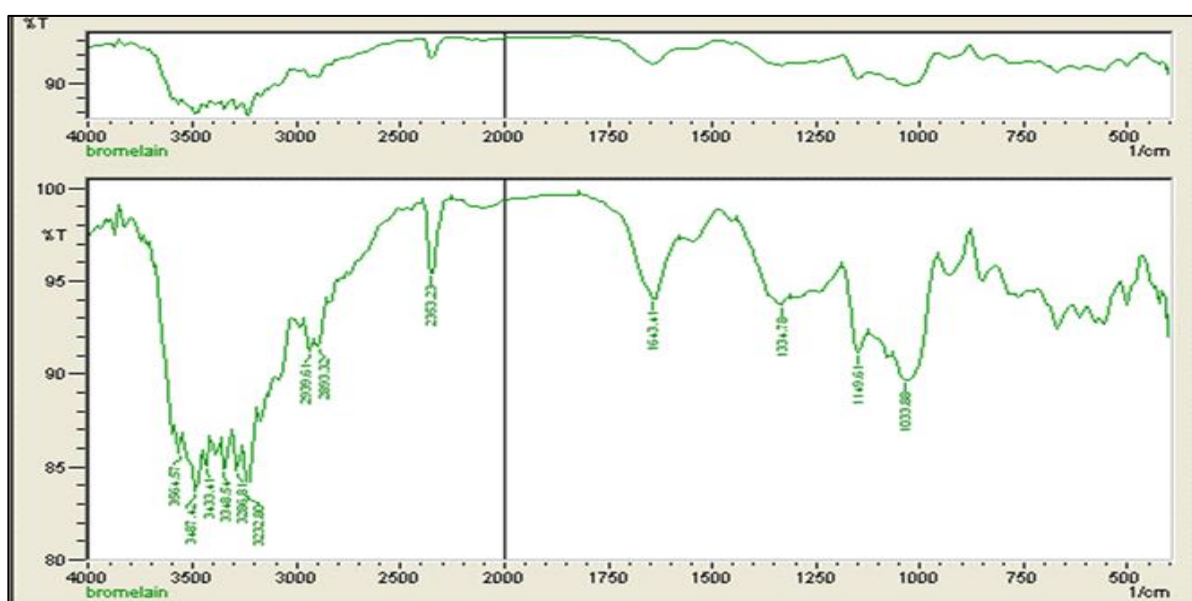


Figure 3: FTIR Studies of Bromelain

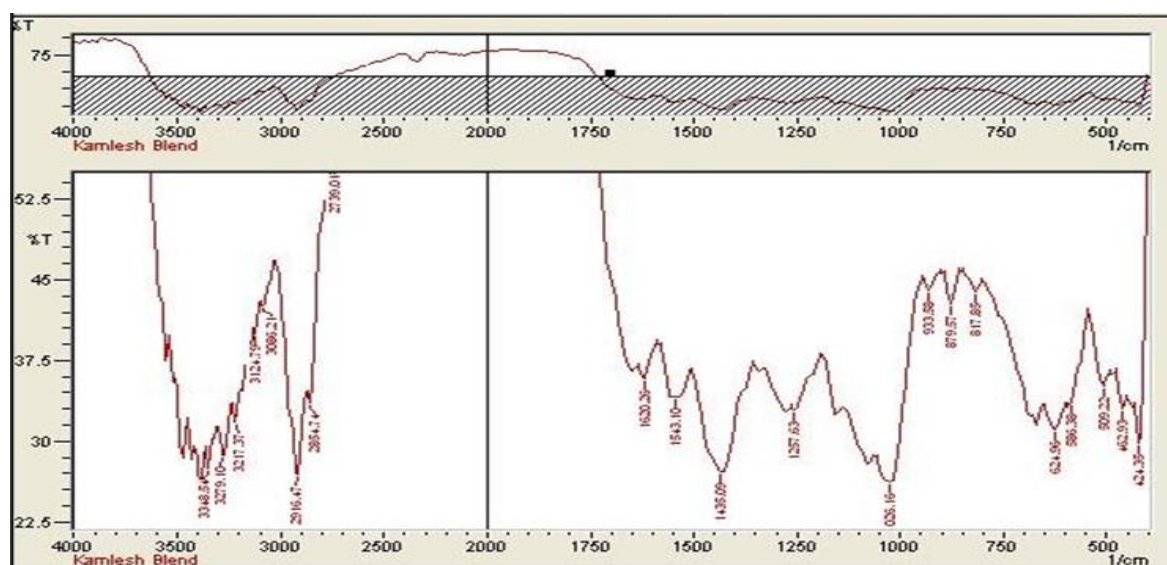


Figure 4: FTIR Studies of Bromelain Tablet Blend

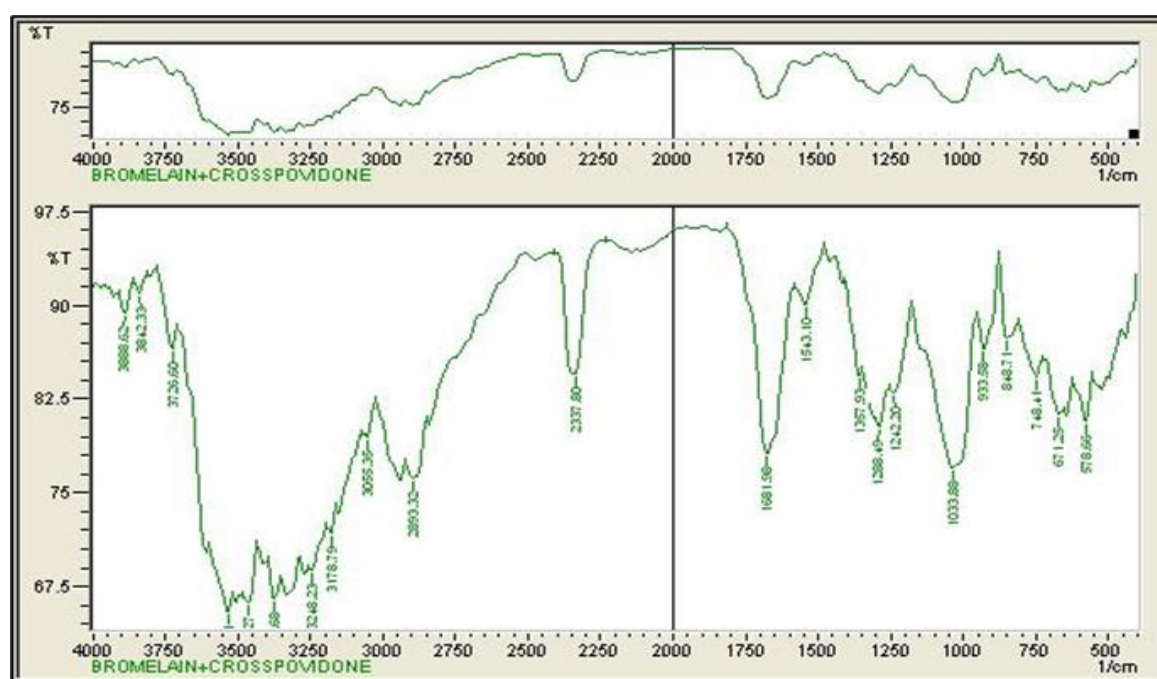


Figure 5: FTIR Studies of Bromelain + Crospovidone

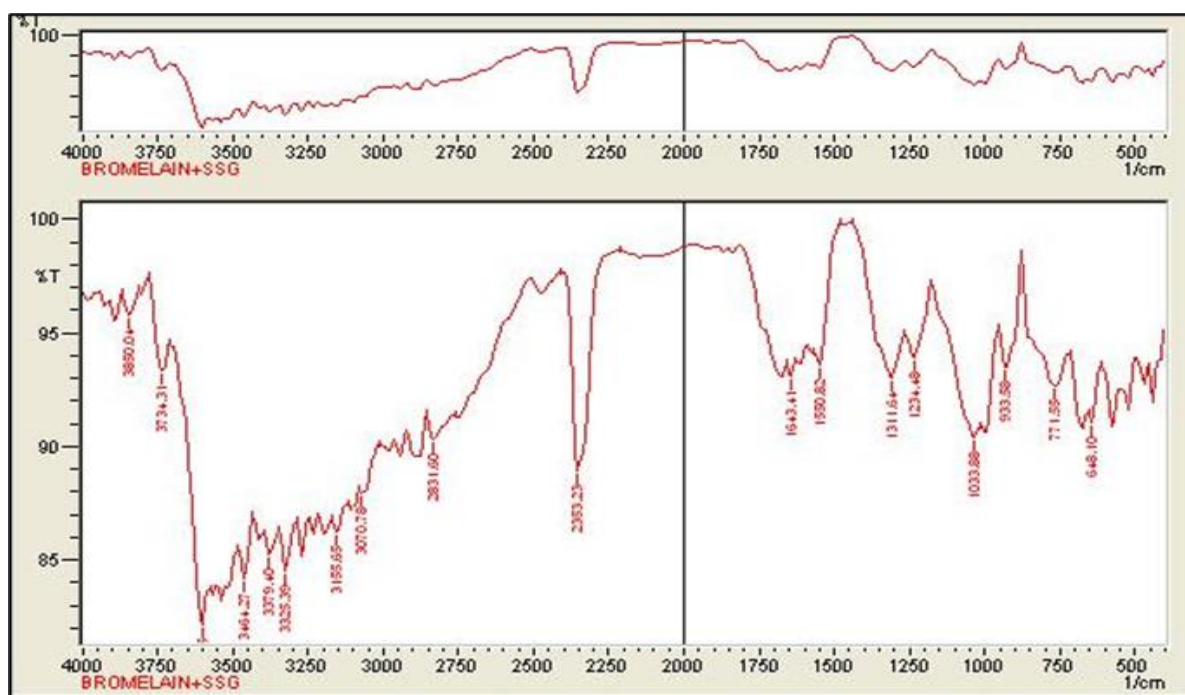


Figure 6: FTIR Studies of Bromelain + SSG

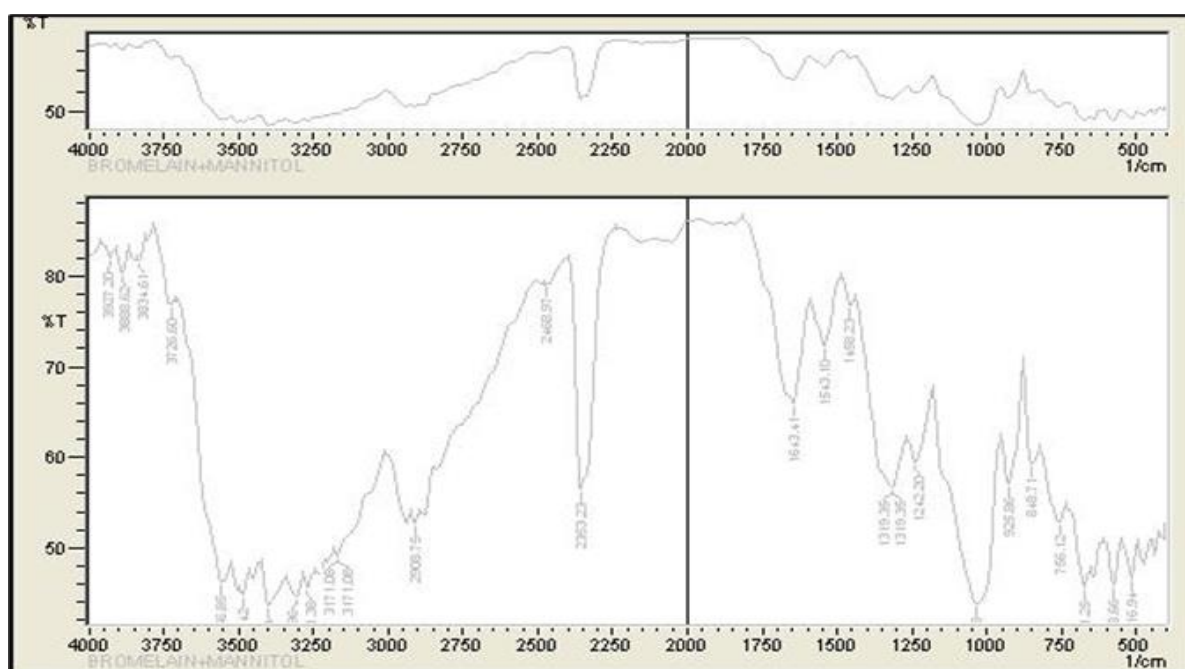


Figure 7: FTIR Studies of Bromelain + Mannitol

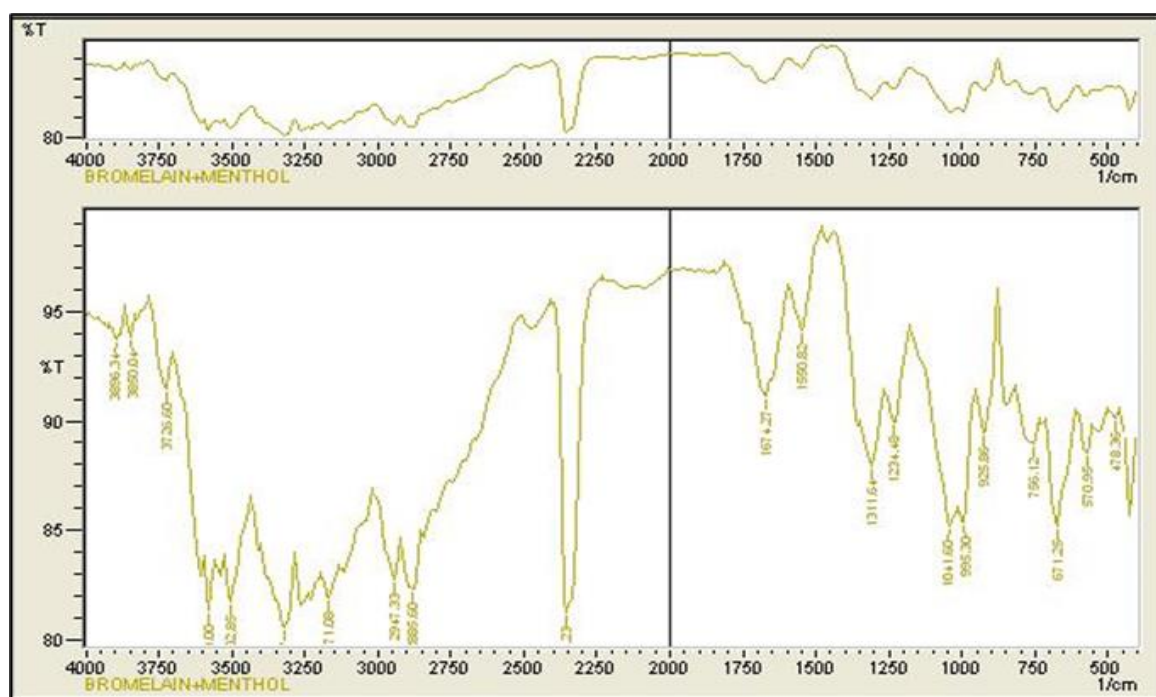


Figure 8: FTIR Studies of Bromelain + Menthol

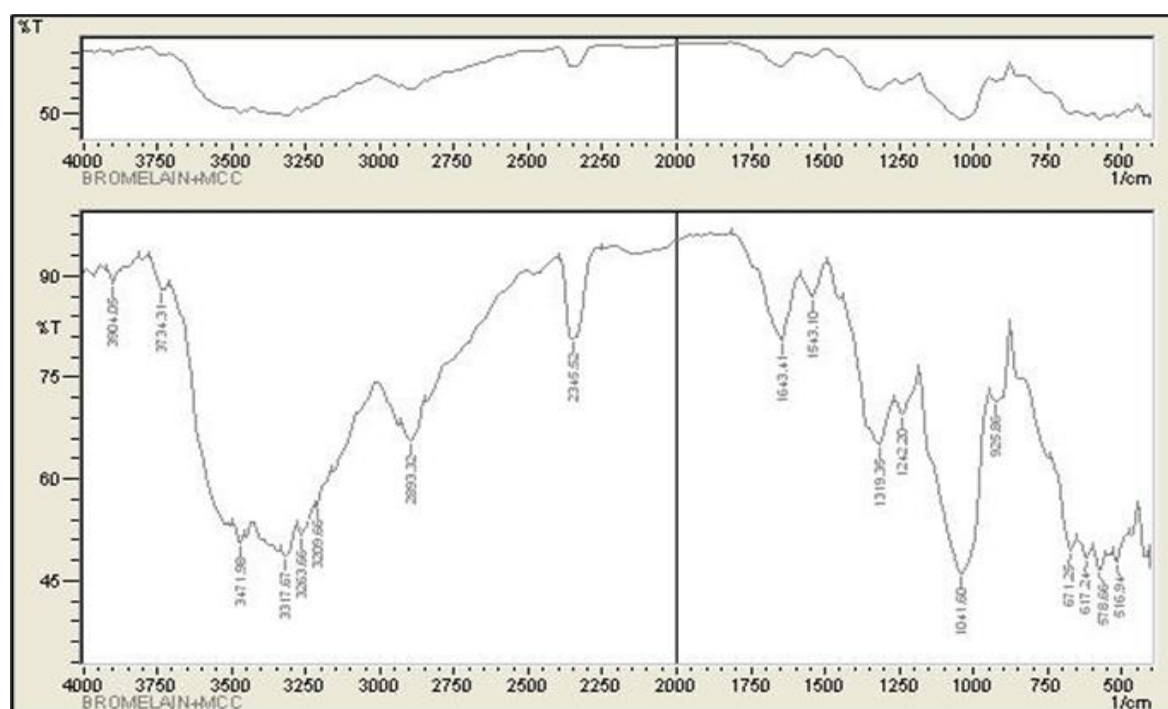


Figure 9: FTIR Studies of Bromelain + MCC

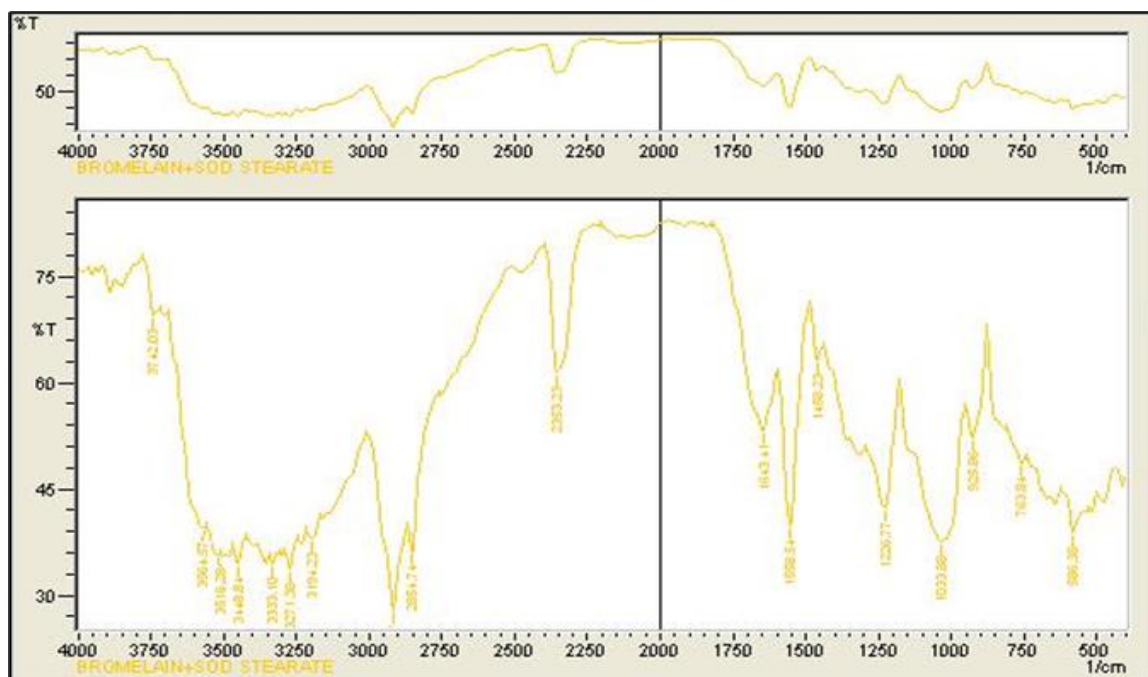


Figure 10: FTIR Studies of Bromelain + Sodium Stearate

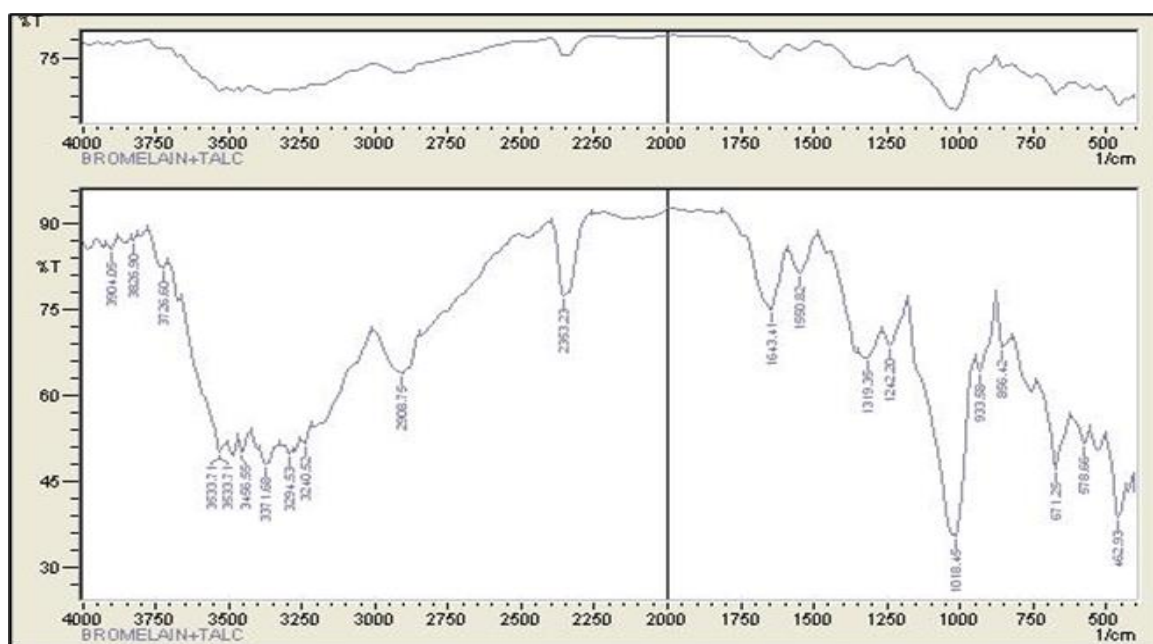


Figure 11: FTIR Studies of Bromelain + Talc

Evaluations:

Mouth dissolving tablets of Bromelain were prepared by a method employing croscopidone and sodium starch glycolate as super-disintegrants at different ratios. A total of six formulations were designed. The flow properties of the powder mixture are important for the uniformity of mass of the tablets; the flow of the powder mixture was analysed before compression to tablets.

Low Hausner's ratio (≤ 1.18), compressibility index (≤ 14.81) and angle of repose (≤ 29.04) values indicated fairly good flowability of the powder mixture (Table 5).

Table 5: Evaluation of Tablet Blend of Mouth Dissolving Tablet of Bromelain.

Batches	Angle of Repose (θ)	Bulk Density (gm/cm^3)	Tapped Density (gm/cm^3)	Housner's Ratio (H_R)	Carr's Compressibility Index
F1	21.78 \pm 1.88	0.45 \pm 0.12	0.50 \pm 0.23	1.18 \pm 0.10	10.00 \pm 0.20
F2	20.67 \pm 0.95	0.43 \pm 0.16	0.49 \pm 0.09	1.13 \pm 0.21	12.24 \pm 0.33
F3	23.59 \pm 0.47	0.43 \pm 0.17	0.48 \pm 0.26	1.11 \pm 0.20	10.41 \pm 0.10
F4	28.42 \pm 1.27	0.41 \pm 0.10	0.47 \pm 0.20	1.14 \pm 0.32	12.76 \pm 0.63
F5	23.78 \pm 1.45	0.45 \pm 0.90	0.52 \pm 0.21	1.15 \pm 0.28	13.46 \pm 0.39
F6	29.04 \pm 1.14	0.47 \pm 0.12	0.54 \pm 0.21	1.14 \pm 0.18	14.81 \pm 0.91

As the tablet powder mixture was free flowing, tablets produced were of uniform weight with acceptable weight variation in the range from 251 mg to 254 mg due to uniform die fill. Hardness (3.2 ± 0.05 - 3.4 ± 0.1 kg/cm^2) and friability loss (0.8 ± 0.090 - 0.9 ± 0.117 %) indicated that tablets had good mechanical resistance. Drug content was found to be high (≥ 98.25 %) in all the tablet formulations (Tables 6).

Table 6: Evaluation of Mouth Dissolving Tablets of Bromelain

Batches	Thickness (mm)	Hardness (Kg/cm^2)	Friability (%)	Drug Content (%)	Weight Variation (mg)	Disintegration time (sec)
F1	4.04 \pm 0.10	3.26 \pm 0.05	0.8 \pm 0.05	98.50 \pm 0.11	252 \pm 0.93	49 \pm 3.28
F2	4.35 \pm 0.17	3.36 \pm 0.11	0.8 \pm 0.15	98.75 \pm 0.01	251 \pm 0.32	44 \pm 1.41
F3	4.27 \pm 0.25	3.26 \pm 0.15	0.9 \pm 0.1	98.75 \pm 0.13	251 \pm 0.70	41 \pm 1.41
F4	4.35 \pm 0.10	3.36 \pm 0.15	0.9 \pm 0.13	98.25 \pm 0.06	252 \pm 0.93	50 \pm 1.89
F5	4.01 \pm 0.17	3.33 \pm 0.25	0.8 \pm 0.07	98.70 \pm 0.23	251 \pm 0.17	48 \pm 1.41
F6	4.20 \pm 0.10	3.43 \pm 0.10	0.8 \pm 0.09	98.75 \pm 0.14	254 \pm 0.51	45 \pm 1.91

The most important parameter that needs to be optimized in the development of mouth dissolving tablets is the disintegration time of tablets. In the present study. The faster disintegration of crospovidone tablets may be attributed to its rapid capillary activity and pronounced hydration with low capacity for gel formation. Thus, these results suggest that disintegration times can be reduced by using a wicking type disintegrant (crospovidone). Thus, disintegration times of tablets with crospovidone were found to be less than those with sodium starch glycolate. IR shows the drug interaction study, indicating that the drug is compatible with all the excipients (Figures 3 to 11).

In vitro, drug release studies were carried out in phosphate buffer pH 6.8 and the dissolution profile is depicted in Table 7 and Figures 12. The drug release from the optimized batch (F3) was 97.67 % at 30 min.

Table 7: In vitro Cumulative % Drug Release from Tablets

Time (In Min)	Cumulative % Drug Release					
	F1	F2	F3	F4	F5	F6
0 min	0	0	0	0	0	0
05 min	30.88±0.97	32.47±1.76	33.34±1.06	30.75±1.46	32.89±1.92	34.55±2.11
10 min	46.76±1.55	41.13±1.23	51.34±1.88	49.98±1.65	42.18±1.54	44.8±0.94
15 min	54.35±1.89	55.04±0.76	61.37±1.46	53.24±2.45	58.6±1.98	61.35±1.56
20 min	75.52±2.63	75.14±1.89	84.21±1.23	75.14±1.33	72.55±1.17	72.55±2.35
25 min	83.29±1.44	83.09±1.27	91.06±0.89	83.29±1.39	81.69±1.43	81.25±1.34
30 min	95.17±1.93	96.59±1.09	97.67±1.98	94.47±1.47	95.88±2.78	96.95±1.89

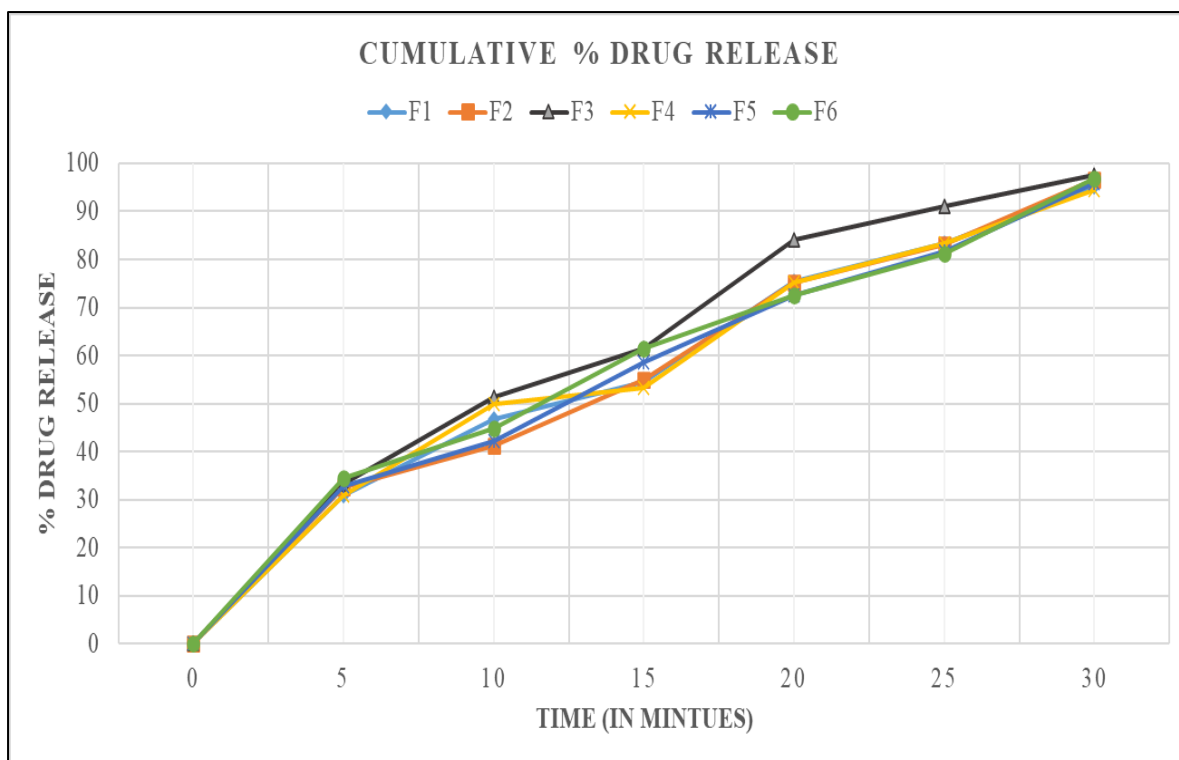


Figure 12: Cumulative % Drug Release

CONCLUSION:

In the present work, mouth dissolving tablets of Bromelain were prepared by direct compression method using superdisintegrants such as sodium starch glycolate and croscopovidone. All the tablets of Bromelain were subjected to tests for weight variation, hardness, friability, drug polymer interaction, drug content uniformity, water absorption ratio, wetting time, and in vitro drug release.

Based on the above studies, the following conclusions can be drawn:

Tablets prepared by direct compression methods were found to be good and free from chipping and capping.

- The low values of the standard deviation of average weight of the prepared tablets indicated weight uniformity within the batches prepared.
- The hardness of the prepared tablets was found to be in the range of 3.2 ± 0.05 - 3.4 ± 0.1 kg/cm². The friability values of the prepared tablets were found to be less than 1%.
- IR spectroscopic indicated that the drug is compatible with all the excipients.

- The in vitro disintegration time of Bromelain MDT prepared by the direct compression method was found to be in the range of 41 sec. to 50 sec. fulfilling the official requirements.
- Based on the in vitro disintegration time, formulation F3 (crospovidone) was found to be promising and showed a disintegration time of 41 sec, facilitating faster dispersion in the mouth.
- The drug content of tablets was uniform across all batches, ranging from 98.25 ± 0.06 - 98.75 ± 0.14 %w/w
- The drug release from the optimized batch (F3) was about 97.67 % at 30 min.

ACKNOWLEDGEMENT

For the completion of the research work the authors would like to show sincere gratitude to PDEA'S Shankarrao Ursal College of Pharmaceutical Sciences & Research centre, Kharadi, Pune to provide a lot of support and help whenever needed.

CONFLICT OF INTEREST

All authors declared no conflicts of interest.

REFERENCES:

1. Modasiya MK, Lala LL, Prajapati BG, Patel VM, Shah DA. Vol. 1 No. 2. Design and characterization of Fast Dissolving Tablets of Piroxicam, Indian J. Pharm.Tech. Res; 2009. p. 353.
2. Sahoo S, Mishra B, Biswal PK, Panda Omprakash, Mahapatra K Santosh, Jana K Goutam. Vol. 2. Fast Dissolving Tablet: As A Potential Drug Delivery System. Drug Inv. Today; 2010.
3. Kaur et al., Vol. 3. Mouth dissolving tablets: A novel approach to drug delivery, International Journal of Current Pharmaceutical Research; 2011.p. 1-7.
4. Nayak UK., Patra SK., Rout PK., Patro BK. and Nayak BS. Development and optimization of promethazine theoclate Mouth dissolving tablets; The Indian pharmacist; 2008.p. 65- 68.
5. Seager H. Vol. 50. Drug-delivery Products and the Zydis Fast-dissolving Dosage Form. J Pharm Pharmacol; 1998.p. 375-382.
6. Bradoo R, Shahani S, Poojary S, Deewan B, Sudarshan S. Vol. 4 No. 10. Fast Dissolving Drug Delivery Systems. JAMA India; 2001.p. 27-31.

7. Bikshapathi, D.; Saikrishna, k.; Kumar, u. fast dissolving tablets: an update. *int. res. j. pharm.*, v.2, n.3, p.45-53, 2011.
8. Shah, v.; Patel, s.; Rakesh, k. formulation and evaluation of mouth dissolving tablets of metoclopramide hydrochloride by direct compression technique. *int. j. drug disc. herbal res.*, v.1, n.2, p.100-103, 2011.
9. Suresh, s.; Senthil, a.; Manikandan, c. formulation and evaluation of mouth dissolving tablets of amlodipine besylate. *int. res.j. pharm.*, v.2, n.9, p.161-165, 2011.
10. Sayeed, a.; Mohiuddin, m. mouth dissolving tablets an overview. *int. res. pharm. biomed. sci.*, v.2, n.3, p.959- 970, 2011.
11. Prameela, a.; Archana, p.; Siva Teja, p.; Vikas m. formulation and evaluation of Orodispersible metformin tablets: a comparative study on hisapghula husk and crospovidone as superdisintegrants. *int. j. appl. pharm.*, v.2, n.3, p.15-21, 2010.
12. Chandira, r.; Venkataeswarlu, b. formulation and evaluation of mouth dissolving tablets of the etoricoxib. *pak. j. pharm. sci.*, v.23, n.2, p.178-181, 2010.
13. Puttewar, t.; Kshirsagar, m.; Chandewar, a.; Chikhale, r. formulation and evaluation of Orodispersible tablet of test masked doxylamine succinate using ion exchange resin. *j. king saud univ. sci.*, v.22, p.229-240, 2010.
14. Parmar, r.; Baria, a.; tank, h.; Faldu, s. formulation and evaluation of domperidone fast dissolving tablets. *int. j. pharm. tech. res.*, v.1, n.3, p.483-487, 2009.
15. Mehta, m.; Deepak, p.; Gupta, g. fast dissolving tablets of sertraline hydrochloride. *int. j. chem. tech. res.*, v.1, n.4, p.925-930, 2009.
16. chacko, a.; jose, s.; babu n. Design and development of Orodispersible tablets of promethazine theoclate using coprocessed superdisintegrants and subliming materials. *Int. J. Innov. Pharm. Res.*, v.1, n.2, p.53-56, 2010.
17. Margret, R.; Venkataeswarlu, B.; Kumudhavalli M. Formulation and evaluation of mouth dissolving tablets of the etoricoxib. *Pak. J. Pharm. Sci.*, v.23, n.2, p.178-181, 2010.
18. Bagul, u.; Gujar, k.; Patel, n.; Aphale, s. formulation and evaluation of sublimed fast melt tablets of levocetirizine dihydrochloride. *int. j. pharm. sci.*, v.2, n.2, p.76-80, 2010.
19. Satpute MM, Tour NS. Formulation and in vitro evaluation of fast dissolving tablets of metoprolol tartrate. *Brazilian Journal of pharmaceutical sciences*. 2013; 49:783-92.
20. Rana R, Devi N, Kumar V, Thakur R, Singla S, Goyal S. The formulation and evaluation of mouth dissolving tablet Levocetirizine by using synthetic Superdisintegrants. *Himalayan Journal of Health Sciences*. 2020 Mar 22:1-1.

Formulation and Development of Oral Dental Films of Doxycycline Loaded Chitosan Films for efficient Treatment of Periodontitis

Jaydeep Dusane^{1*} and Ashok Bhosale²

¹Seth Govind Raghunath Sable College of Pharmacy, Saswad, Pune (Maharashtra), India.

²Shankarrao Ursal College of Pharmacy, Kharadi, Pune (Maharashtra), India.

(Corresponding author: Jaydeep Dusane*)

(Received: 03 January 2023; Revised: 19 February 2023; Accepted: 26 February 2023; Published: 01 March 2023)

(Published by Research Trend)

ABSTRACT: The present study demonstrates the development of intrapocket dental films of Doxycycline for efficient treatment of periodontitis. The films were developed by solvent casting method using chitosan, TPP, and PEG 400 as polymer, crosslinking agent, and plasticizer respectively. The developed films were characterised by physicochemical properties including drug release, tensile strength, and bactericidal activity against *E. coli* and *Staphylococcus aureus*. One of the major challenges was achieving uniform drug distribution in the chitosan matrix. Doxycycline has poor solubility in water and acidic pH, which are the conditions required for chitosan gelation. To get uniform drug distribution proper mixing of the drug was carried out in polymeric dispersion. All physical parameters of the films were found to be acceptable for dental application. It was observed that the drug release occurred in a sustained manner. The optimised film formulation was found to be stable over 2 months at accelerated conditions. This newly developed film could be used as a potential alternative drug delivery system for periodontitis conditions.

Keywords: Doxycycline, chitosan, TPP, PEG 400, bactericidal.

INTRODUCTION

Periodontitis is an inflammatory disorder of the gum that destructs the alveolar bone, forms periodontal pockets, and causes degeneration of periodontal ligaments that results in the disruption or destruction of the support required for the teeth. Periodontal pockets are formed when the gingiva detaches from the tooth, creating the perfect favourable condition for anaerobic bacterial growth (Joshi *et al.*, 2016). All around the world, dental diseases are acknowledged as serious public health issues. According to the WHO, 10 to 15 % of people worldwide have severe periodontitis. In India, severe periodontitis affects between 19-32 % of people (Fisher *et al.*, 2018). Severe periodontal disease ranked as the 11th most common disease in the world, following the Global Burden of Disease Study (James *et al.*, 2018). According to reports, the incidence of periodontal disease varies between 20-50 % worldwide (Sanz *et al.*, 2010). It is one of the leading causes of tooth loss, which can impair quality of life, mastication, aesthetics, and self-confidence.

Systemic antibiotics have shown some potential for the treatment of periodontitis; however, they are only advised in the case of resistant or quickly developing periodontitis (Genco, 1981). Minimum concentration of antibiotics at the application site, rapid decline in antibiotic concentration, and rapid development of microbial resistance are just a few of the drawbacks associated with multiple systemic doses of antibiotics (Gates *et al.*, 1994). Intrapocket delivery of active ingredients has sparked attention considering these obvious drawbacks (Greenstein, 2006). A periodontal

pocket is an accessible natural reservoir for the implantation of a drug delivery system. Additionally, gingival crevicular fluid (GCF) acts as a leaching medium for a drug's release from the dosage form and for its distribution throughout the pocket. Together with the fact that periodontal diseases are limited to the pocket's natural environment, these features make the periodontal pocket a perfect area for therapy employing local delivery systems. Intra-pocket drug delivery systems are highly desirable because they may have fewer adverse side effects, are more effective, and have more patient compliance (Jain *et al.*, 2008).

Drugs are distributed throughout the polymer in intrapocket oral dental films, which are matrix-type delivery devices. Drug release occurs via diffusion, matrix dissolution, or matrix erosion. This dosage form is beneficial physically for usage within the pocket. Depending on the size of the pocket to be treated, it is simple to adjust the form and size of the films. It may be quickly put into the pocket's base while causing the patient the least amount of discomfort possible (Junmahasathien *et al.*, 2018). It has been demonstrated that this novel treatment strategy is more efficient than conventional drug delivery systems. Based on the physicochemical characteristics of the utilized polymers, the best forming method is selected. By mixing different co-polymers, the drug release can be prolonged for a long period (Joshi *et al.*, 2016).

The manufacturing of the films involved the use of several natural and synthetic polymers. Chitosan is a natural polymer have the significant benefit of not interfering with the regeneration of periodontal tissue. Chitin, a key component of arthropod shells, is

converted into the hydrophilic biopolymer chitosan by an alkaline deacetylation process. Chitosan is advantageous because of its nontoxicity, biocompatibility, bioadhesive, and biodegradability (Rodrigues *et al.*, 2012). Chitosan was investigated for its antibacterial properties against *P. gingivalis* by Ikinci *et al.* (2002) and co-workers. They discovered that chitosan films have antimicrobial action, which was enhanced by increasing the molecular weight of the chitosan and combining it with chlorhexidine (Ikinci *et al.*, 2002; Prashanth *et al.*, 2022).

Doxycycline (DOX) is a tetracycline antibiotic used to treat bacterial infections. Due to its low minimum inhibitory concentration, DOX is the most widely used broad-spectrum antibiotic and is effective against most periodontal infections (Chaturvedi *et al.*, 2013). DOX is a bacteriostatic drug that suppresses bacterial protein synthesis and is well-recognized for its antibacterial properties (Mahmoud and Samy 2016). Collagenase inhibition, anti-inflammatory effects, and bone resorption inhibition are among the other qualities. It can, however, attach to the solid tissue walls of pockets to create a drug reservoir (Rajeshwari *et al.*, 2019). Dinte *et al.* (2023) developed mucoadhesive buccal films of DOX for the efficient treatment of periodontitis. The developed film served as a potential supportive treatment for periodontitis by providing sustained release of the antibiotic after local application (Dinte *et al.*, 2023). Swain *et al.* (2023) developed site-specific and local action dental films loaded with DOX for the treatment of periodontitis. Based on the study it was conducted that the use of DOX-loaded dental films made of HPMC E15 and Eudragit RS 100 was effective in the local treatment of periodontitis. Moreover, the combination of HPMC E15 and Eudragit RS 100 can be utilized in the development of dental films for other drugs, as it has shown promising results in terms of mucoadhesion, drug release, and stability (Swain *et al.*, 2023). Ghavami *et al.* (2020) studied the antibacterial activity of polymeric local drug delivery system against pathogens associated with periodontitis. In this research work, they developed polymeric films of the DOX and metronidazole. DOX-loaded polymeric films were more effective on multispecies bacteria, inhibiting both planktonic and biofilm growth at relatively low concentrations (Ghavami *et al.*, 2020). Chuenbarn *et al.* (2022) also developed DOX-loaded Eudragit RSPO in situ forming microparticles for the treatment of periodontitis. The obtained microparticles were spherical with a porous structure. Moreover, the formulation exhibited effectiveness against periodontal pathogens, which was appropriate for development into

local drug delivery to treat periodontitis (Chuenbarn *et al.*, 2022). Considering all these latest research studies it has been observed that very limited work was performed with DOX-loaded chitosan films with the DOE approach. Chitosan itself has antibacterial activity and that could show a synergistic effect when coupled with DOX. Considering all these current research gaps as well as potential benefits and characteristics DOX was used in the present investigation to develop oral dental films for the efficient treatment of periodontitis.

MATERIALS AND METHODS

Materials: Doxycycline (DOX) was purchased from Cipla Ltd. Mumbai, India, and Chitosan (CS) was obtained from the Indian Sea Food Company (Kochin, India). Polyethylene glycol 400 (PEG 400), Tripolyphosphate (TPP) was purchased from Sigma Aldrich, India.

Methods:

Statistical Design of experiments (DOE): 2³ full factorial design approach was utilised in the development of DOX-loaded intrapocket films. The concentration of Chitosan (A, mg), TPP (B, mg), and PEG 400 (C, ml) were considered as independent variables which were varied at two levels (-1 and +1) while tensile strength (Y1) and *in vitro* drug release at 12th day (DR) (Y2) were considered dependent variables. Variables and three levels are presented in Table 1. The statistical experimental data were analyzed using the Design-Expert® Software.

Development of DOX-loaded chitosan (CS) films: DOX-loaded CS films were developed by using the solvent-casting evaporation method (Khajuria *et al.*, 2018). The chitosan was used as a gelling polymer, as well as a film former, TPP as a crosslinking agent, and PEG 400, was used as a plasticizer. The formula composition in coded form is presented in Table 2. The CS was dissolved in acetic acid (3% v/v; 10 ml) under continuous magnetic stirring till a clear and transparent clear solution was obtained. PEG 400 was added slowly under stirring to the chitosan solution and mixed properly for 15-20 minutes. DOX (100 mg) was added to CS-PEG 400 solution and vortex for 10 minutes for even distribution in polymeric dispersion. This viscous dispersion containing DOX was kept aside for 2 hours for the complete removal of air bubbles. TPP already dissolved in distilled water was added dropwise to the viscous dispersion under continuous stirring to form crosslinking between CS and TPP. This dispersion was again stirred for 3-4 hours and kept aside to remove the air bubbles.

Table 1: Variables and levels.

Variable	(-1) Low level	(+1) High level
Independent		
A= Chitosan	15 (mg)	30 (mg)
B= TPP	3 (mg)	6 (mg)
C= PEG 400	2.5 (ml)	5 (ml)
Dependent		
Y1= Tensile strength		
Y2 = % DR at 12 th day		

Table 2: Formulation batches of films.

Batch	Factor		
	A	B	C
F1	+1	+1	+1
F2	+1	-1	+1
F3	+1	-1	-1
F4	-1	+1	+1
F5	-1	+1	-1
F6	+1	+1	-1
F7	-1	-1	+1
F8	-1	-1	-1

The drug-polymer dispersion was cast in a petri dish and dried at 35-40°C for 24 h in a vacuum oven. The films were removed carefully and observed for any physical damage or imperfections and further used for characterization.

Characterization of DOX-loaded CS films:

Thickness: The patch thickness (n=3) was determined using a vernier caliper and the average thickness of the patches was calculated (Ozdogan *et al.*, 2018).

Uniformity of weight of the films: Randomly selected three patches were weighed on analytical balance individually. The average weight of the patches was calculated with standard deviation (Ozdogan *et al.*, 2018).

Folding endurance: The films were folded manually at the same point till it breaks down. The value for folding endurance was determined by how many folds the film could withstand without tearing. The test was performed in triplicate and the average value was determined (Ozdogan *et al.*, 2018).

Drug Content Uniformity: Films with 5 cm² dimensions were randomly obtained from different places. The films were dissolved separately in 3% v/v acetic acid. The samples were filtered and analyzed at 273 λ_{max} using UV spectroscopy and drug content was calculated (Ozdogan *et al.*, 2018).

Moisture content:

The formulations were weighed accurately and stored in desiccators with anhydrous calcium chloride. The films were removed and weighed after 3 days. The following formula was used to calculate moisture content (Ozdogan *et al.*, 2018).

$$\text{Moisture Content (\%)} = \frac{\text{Initial Weight} - \text{Final Weight}}{\text{Initial Weight}} \times 100$$

Tensile strength: Using a tensile strength tester with a 5 g load cell, the tensile strength of the film was assessed. Films having a 5 cm² surface area and no physical damage were held between two clamps. The top clamp was pushed during the measurement at a speed of 0.5 mm/s, and the force applied when the film broke was recorded. The outcomes from the film samples that ruptured between the clamps were recorded (Ozdogan *et al.*, 2018).

IR spectroscopy: IR spectra were obtained for DOX, CS, and optimized film by the KBr pellet method. The IR spectra were compared and possible drug excipient interaction was determined (Nyavanandi *et al.*, 2023).

Differential Scanning Calorimetry (DSC) Studies: A small amount of sample was accurately balanced in an aluminum pan and heated from 40 °C to 400 °C, with a

heating rate of 10 °C/min. DSC thermograms of pure drug, optimised formulations were recorded using DSC (Narala *et al.*, 2022).

In vitro drug release study: DOX release study was performed in pH 6.8 phosphate buffer (release media) which was simulated with gingival fluid. The test was performed under static conditions because, after the application of film in pockets, it will remain immobilized. Six films with a 5 cm² area were placed separately in test tubes already filled with 1 ml of release media. The entire setup was kept at 37± 0.5 °C. The sampling of 1 ml was done at a predetermined time interval and replaced with fresh buffer to maintain sink condition. Using a UV/VIS spectrophotometer, the drug's concentration was found at 273 nm. The operation was carried out for 12 days in a row (Nakahara *et al.*, 2003).

Zone of inhibition study using cup plate method:

The suspension of the microorganisms (*Staphylococcus aureus* ATCC29737) was prepared in the medium at a temperature between 40 °C and 50 °C. This inoculated medium was poured into previously sterilized Petri plates to give approximately 3 to 4 mm depth with uniform thickness. These plates were stored properly to ensure that no growth or death of the microorganisms occurred till the agar layer gets solidified. The test and standard antibiotic solution were applied in the cavities at the same volume and concentration. The plates were kept for incubation for 18 hours at 35-37 °C. At the end of the experiment, the zone of inhibitions was measured and compared (Khan *et al.*, 2021).

In-Vitro Kill Kinetics Study: The test was performed on (*Staphylococcus aureus* ATCC29737 and *E. coli*). Pure DOX, DOX-loaded films, and positive control were added to the broth cultures of 10⁶ CFU/mL. A kill kinetics study was performed at twice the concentration of MIC (2MIC) of the antimicrobial agent. Viable counts were performed at 0, 1, 2, 4, 6, 8, and 24, 168 h after the addition of pure DOX, DOX-loaded film, and a positive control following serial dilution in saline solution. The bacterial count was determined at 24 hours and the graph was plotted as a viable count against time (Naik *et al.*, 2019).

Stability study. The optimized formulations were kept for stability studies after wrapping them with aluminum foil and butter paper at 40 ± 2°C, 75% ± 6% relative humidity for 2 months. At the end of the stability studies, the samples were analysed and compared with the initial results (Khagga *et al.*, 2019).

RESULTS AND DISCUSSION

Physicochemical properties of the developed films.

The developed DOX-loaded films were characterized for various physicochemical properties to check whether the formulation satisfies the requirement of the dental pocket. Table 3 describes various parameters of the DOX-loaded film.

Thickness: The thickness is one of the important parameters to be considered for the formulations to be applied in dental pockets. The thickness of the films was found between 0.288 mm (F7) to 0.300 mm (F3). The variation in film thickness was due to the polymer concentration used in formulations. The films with higher thickness would be difficult to apply in dental pockets. F7 formulation showed very lesser thickness and that can be ideally placed at the site of application. The minimum thickness observed in the F7 formulation was attributed to the lower chitosan concentration used.

Weight uniformity: The weight variation in the films was found due to the different chitosan and PEG 400 used in the formulations. The weight of the films was found between 8.38 ± 0.15 mg (F7) to 10.02 ± 0.09 mg (F1). The weight variation showed that the weights of the film from various film sections were quite similar.

Folding endurance: The higher folding endurance is quite desirable for dental films which indicates that the film will remain intact and integrated into the periodontal pocket. The folding endurance is indirectly correlated to the strength of the films. F7 formulation showed the highest folding endurance of 314.4 ± 0.17 indicating excellent strength and can maintain integrity in the periodontal pocket. The higher folding endurance was found to be dependent on the perfect concentration of CS and PEG 400. The CS played an excellent role as films former and PEG 400 provided the desired plasticity to the film and avoided brittleness (Vieira *et al.*, 2011).

Drug content: The uniformity in the drug content (94.25 ± 0.77 to $98.50 \pm 0.55\%$) was observed between all the formulated batches of the films. This observation indicated that the drug was evenly distributed in the polymeric dispersion. The uniformity in drug content is quite desirable for any dosage form. The highest drug content was found in the F7 formulation indicating minimum loss during the film manufacturing process.

Moisture content: Moisture content is a very crucial parameter for films. Higher moisture content in the film will promote bacterial growth during its storage at room temperature. The films with lower moisture content are considered ideal formulations for avoiding any bacterial growth (Loke *et al.*, 2000). It has been observed that the moisture content was associated in a linear relationship with the concentration of PEG 400. A similar observation was noted by Swain *et al.* in their research work (Swain *et al.*, 2023). The F7 formulation showed minimum moisture content of $2.5 \pm 0.08\%$ due to the minimum PEG 400 concentration.

IR spectroscopy: FTIR spectra of pure DOX showed characteristic peaks at 3481 cm^{-1} corresponding to the (O-H) group, 3250 cm^{-1} corresponding to the (N-H) group, 2997 cm^{-1} corresponding to the (C-H) group,

1650 cm^{-1} corresponding to (C=O) group and at 1498 cm^{-1} corresponding to (CO-NH) group. Similar IR peaks were also observed in one of the studies (Swain *et al.*, 2023). All these characteristic peaks of DOX are also present in the final formulation which indicates the absence of any physical as well as chemical incompatibility between DOX and other excipients. The comparative IR spectra of DOX, chitosan and DOX-loaded films are presented in Fig. 1.

DSC analysis: The DSC analysis of the pure DOX showed an endothermic peak at $206.09\text{ }^{\circ}\text{C}$ corresponding to its melting point while DOX-loaded films showed an endothermic peak at $205.73\text{ }^{\circ}\text{C}$ (Fig. 2). From the DSC thermograms, it was observed that the DOX did not interact with other excipients present in films indicating good compatibility.

Statistical analysis of Tensile strength (Y2): The intrapocket DOX-loaded films were developed using CS as film former, TPP as a crosslinking agent, and PEG 400 as a plasticiser. The tensile strength of the film is also one of the important parameters that need to be considered during the development of the films and hence is considered the dependent variable in this study. The results of the tensile strength of all the formulations are presented in Table 4 along with the coded levels of the dependent variables.

The tensile strength of the developed films ranged between 0.722 ± 0.11 (F1) to 2.785 ± 0.11 (F7) Kg/cm^2 . The F7 formulation showed the highest tensile strength in comparison to the rest of the formulations. It has been observed that the tensile strength is directly related to the chitosan concentration used in the formulation. The batch (F7) with the highest concentration of Chitosan, PEG 400, and crosslinking agent TPP showed the highest tensile strength. Chitosan concentration had a very tremendous impact on the tensile strength of the films. Higher polymer concentration might have increased the viscosity of the dispersion leading to the improvement in the tensile strength. In addition to it, TPP being used as the crosslinking agent contributed to tensile strength. A perfect crosslinking happened between Chitosan and TPP that gave additional strength to the formulation (Yanat and Schroen 2021). PEG 400 was used as a plasticizer to provide plasticity, and flexibility as well as to prevent the breakage of the films. Also, it prevented the brittleness of the film. PEG 400 also had a positive impact on the tensile strength like chitosan and TPP concentration. Higher levels of DBT increased physical strength, which increased the resistance to breaking the film. The effect of independent variables on tensile strength is presented in Fig. 3.

The polynomial equation for tensile strength (Y1) can be presented below

$$Y1 = +42.15 + 4.11A + 13.23B + 0.39C \quad (1)$$

In the above equation, Y1 is tensile strength, A is Chitosan concentration, B is TPP concentration and C is PEG 400 concentration. The effect of all these independent variables is statistically significant with $p < 0.05$. The model was also found to be statistically significant with F value of 0.0025. The 2FI model was suggested for Y1 as shown in Table 5. The correlation

coefficient (R^2) was found to be 0.9890 for Y1 indicating a good fit model of 2FI.

The model for Y1 was found to be statistically significant based on the p -value of 0.0012. The effect of independent variables was also found to be statistically significant based on the p -value shown in Table 6.

Statistical analysis of drug release on the 12th day (Y2): The *in vitro* DOX release was performed in phosphate buffer pH 6.8 for 12 days to check for the sustained release behaviour of the films. At the end of 12 days, the drug release was found to be in the range of 72.51 (F7) to 99.55 % (F8). The comparative drug release profile of all the formulations is presented in Fig. 4.

The concentration of the Chitosan played a very significant role in the retardation of DOX release from the films. The effect of Chitosan was found to be concentration-dependent. The films with a higher concentration of Chitosan showed retarded drug release from the formulation. Similarly, the TPP has also shown a positive effect on the retardation of the drug release from the formulations. It has also been observed that an increase in plasticizer PEG 400 concentration in formulations also helped in the retardation of drug release. Chitosan being hydrophilic, sustained-release polymer, along with TPP, formed a great complex and sustained the drug release efficiently (Fig. 5).

The polynomial equation for DR (Y2) can be presented below

$$Y2 = +92.12 + 3.14A + 2.21B + 1.12C \quad (2)$$

In the above equation, Y2 is tensile strength, A is Chitosan concentration, B is TPP concentration and C is PEG 400 concentration. The effect of all these independent variables is statistically significant with $p < 0.05$. The model was also found to be statistically significant with F value of 0.023. The 2FI model was suggested for Y2 as shown in Table 5. The correlation coefficient (R^2) was found to be 0.9798 for Y2 indicating a good fit model of 2FI. The model for Y2 was found to be statistically significant based on the p -value of 0.0395. The effect of independent variables was also found to be statistically significant based on the p -value shown in Table 6.

Zone of inhibition (ZOI) study. The ZOI study of different concentrations of pure DOX and films manufactured with concentrations were studied against *Staphylococcus Aureus*. It has been observed that DOX-loaded chitosan films showed greater zone of inhibition in comparison to the pure DOX. The comparative graphical representation of the ZOI is presented in Fig. 6. The actual antibacterial effect in the form of ZOI of pure DOX and DOX-loaded films is presented in Fig. 7. Chitosan itself has some sort of antibacterial activity (Eldin *et al.*, 2008) and hence the films manufactured from Chitosan displayed greater potency against *Staphylococcus Aureus*. In one of the studies DOX loaded films showed MIC of 4, 0.25, and 4 $\mu\text{g/mL}$, against *A. actinomycetemcomitans*, *P. gingivalis* and *P. intermedia* respectively (Ghavami *et al.*, 2020). The results of this study are comparable with our study showing excellent antibacterial activity.

Time-Kill Kinetics on *Staphylococcus aureus* and *E. Coli*: A kill kinetic study was performed on *Staphylococcus Aureus* and *E. Coli* using optimised film formulation (F7). The film was found to be successful in killing *Staphylococcus Aureus* and *E. Coli* because there was a reduction in the colony count treated with chitosan film and pure drug when compared to the control, and the results were repeatable (Fig. 8). The fundamental idea behind the Time-Kill Kinetic study is to determine the rate at which a microorganism is killed by a dosage form as a function of survival data collected at enough exposure time points to enable the construction of a graph that models the population's decline over time until it reaches extinction (Levin and Udekwu 2010). The study confirmed the bactericidal activity against the selected microbial strength proving efficiency in periodontitis disease.

Stability studies. The optimised formulation was kept for stability studies at $40^\circ\text{C} \pm 2^\circ\text{C}/75\% \pm 5\% \text{ RH}$ for 2 months. The physicochemical parameters tested after 2 months did not show any significant change in storage. The comparative parameters are presented in Table 7. The results demonstrated excellent stability of the developed films.

Table 3: Physicochemical properties of the DOX-loaded dental films.

Batch	Thickness (mm)	Weight Uniformity (mg)	Folding endurance	Drug content (%)	Moisture content (%)
F1	0.298	10.02 \pm 0.09	250.1 \pm 0.22	95.11 \pm 0.45	3.9 \pm 0.11
F2	0.297	8.40 \pm 0.11	248.3 \pm 0.17	96.17 \pm 0.65	4.1 \pm 0.14
F3	0.300	8.59 \pm 0.13	262.5 \pm 0.27	97.24 \pm 0.70	3.8 \pm 0.12
F4	0.298	9.12 \pm 0.21	259.4 \pm 0.35	95.87 \pm 0.52	3.9 \pm 0.17
F5	0.296	9.17 \pm 0.05	265.8 \pm 0.42	96.18 \pm 0.64	4.0 \pm 0.10
F6	0.299	9.59 \pm 0.17	287.1 \pm 0.12	95.24 \pm 0.11	3.9 \pm 0.10
F7	0.288	8.38 \pm 0.15	314.4 \pm 0.17	98.50 \pm 0.55	2.5 \pm 0.08
F8	0.921	9.87 \pm 0.12	272.1 \pm 0.21	94.25 \pm 0.77	4.1 \pm 0.07

Table 4: DOX loaded films with coded form and their responses.

Batch	Factor			Response	
	A	B	C	Y1 (kg/cm ²)	Y2 (%)
F1	+1	-1	+1	0.722±0.11	87.24
F2	-1	-1	+1	0.883±0.12	96.51
F3	+1	-1	-1	0.983±0.16	89.12
F4	-1	+1	+1	1.114±0.24	90.21
F5	-1	+1	-1	0.945±0.09	94.67
F6	+1	+1	-1	0.834±0.10	82.51
F7	+1	+1	+1	2.785±0.11	72.51
F8	-1	-1	-1	0.612±0.10	99.55

Table 5: Statistical analysis of responses Y1 and Y2.

Model	R ²	Adjusted R ²	Predicted R ²	Std. Dev	Press	Remarks
Response Y1						
Linear	0.7825	0.7942	0.6312	6.15	412.25
2FI	0.9890	0.9521	0.8215	4.44	575.51	Suggested
Quadratic	0.9122	0.8951	0.7642	0.39	450.11
Cubic	0.8745	0.8559	0.6517	0.35	397.14
Response Y2						
Linear	0.5213	0.5535	0.2914	4.24	102.11
2FI	0.9798	0.8212	0.5314	1.25	189.14	Suggested
Quadratic	0.8956	0.8632	0.8771	5.89	135.51
Cubic	0.9235	0.8911	0.8799	7.13	155.45
<i>Regression equations of the fitted models</i>						
$Y1 = +42.15 + 4.11A + 13.23B + 0.39C$						
$Y2 = +92.12 + 3.14A + 2.21B + 1.12C$						

Table 6: ANOVA of models for Y1 and Y2.

Source	DF	Sum of squares	Mean Square	F Value	P value
Model for Y1					
	3	2215	405.12	18.22	0.0012
A	1	72.15	81.21	1.00	0.0123
B	1	1850.22	1897.21	71.75	0.0221
C	1	1.5	1.89	0.015	0.0011
Model for Y2					
	4	271.89	67.97	10.85	0.0395
A	1	19.59	19.59	3.13	0.0351
B	1	216.53	216.53	34.56	0.0098
C	1	18.24	18.24	2.91	0.02865

Table 7: Comparative physicochemical parameters of film stored at 2 M (40 °C ± 2 °C/75% ± 5 %).

Sr. No.	Parameter	Initial	2 M (40 °C ± 2 °C/75% ± 5 %)
1.	Thickness (mm)	0.288	0.298
2.	Weight Uniformity (mg)	8.38 ±0.15	9.01 ±0.20
3.	Folding endurance	314.4 ±0.17	302.1 ±0.11
4.	Moisture content (%)	2.5±0.08	2.9±0.12
5.	Drug content (%)	98.50 ±0.55	98.90 ±0.95
6.	Drug release (%) at 12 days	72.51	75.12

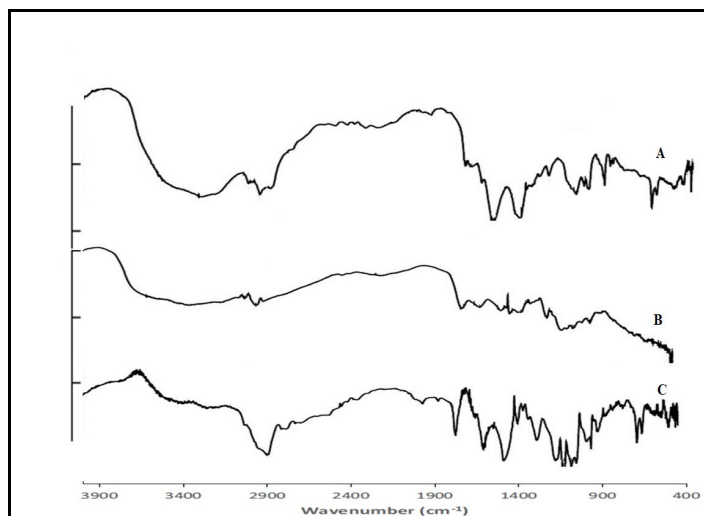


Fig. 1. FTIR spectra of (A): Pure DOX; (B): Chitosan; (C): DOX loaded films.

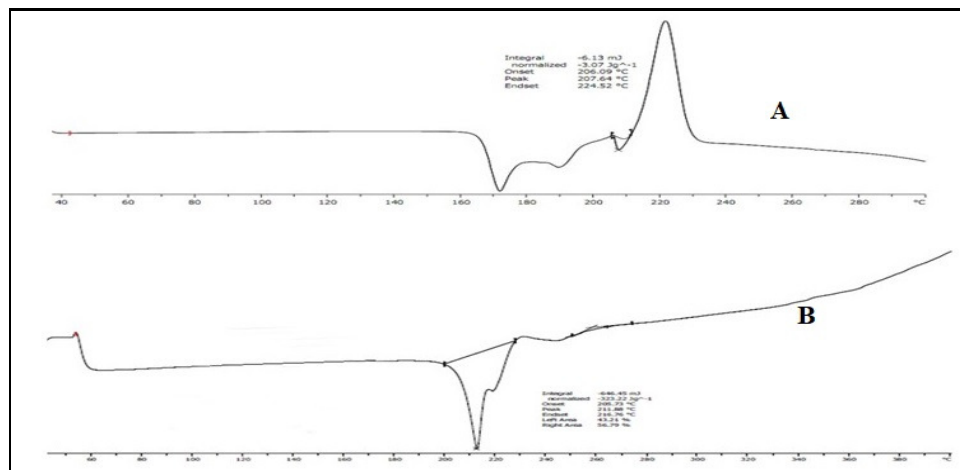


Fig. 2. DSC analysis of (A): Pure DOX and (B): Dox loaded films.

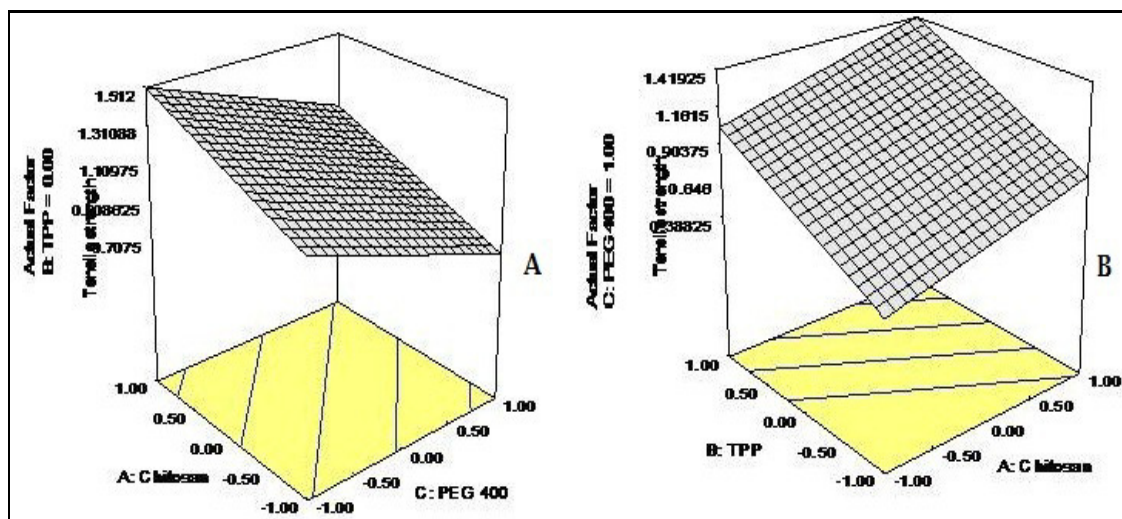


Fig. 3. 3D surface responses of chitosan, TPP and PEG 400 on tensile strength.

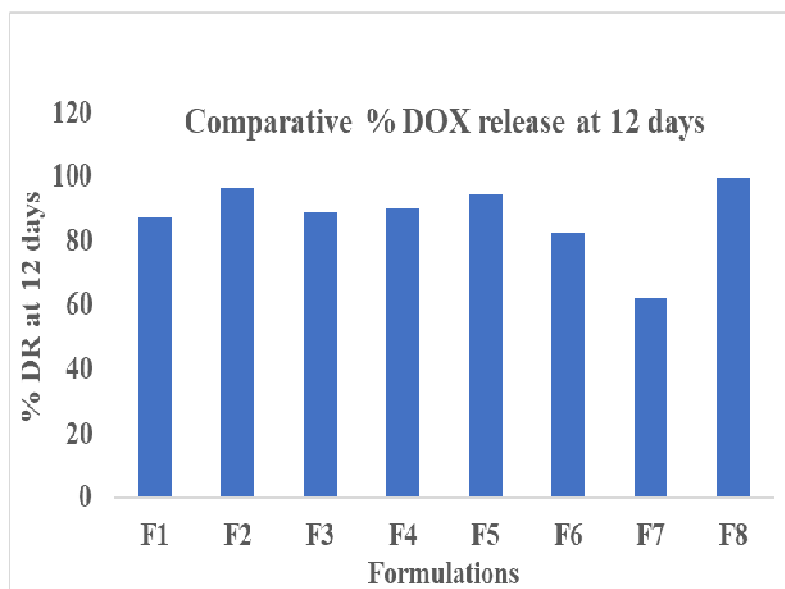


Fig. 4. Comparative % DOX release at 12 days in phosphate buffer pH 6.8.

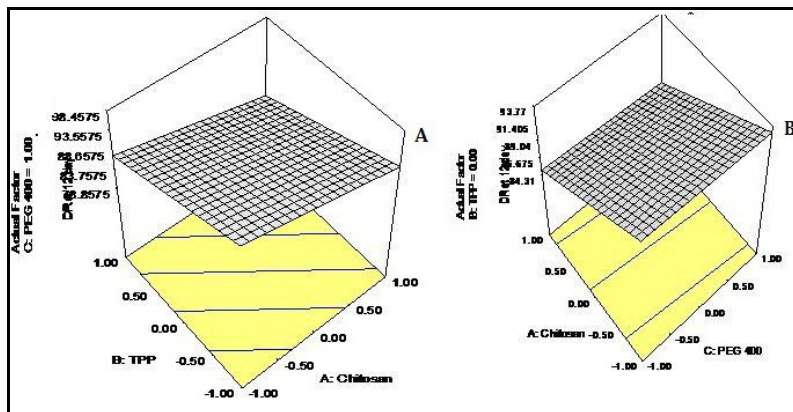


Fig. 5. 3D surface responses of chitosan, TPP and PEG 400 on % DR.

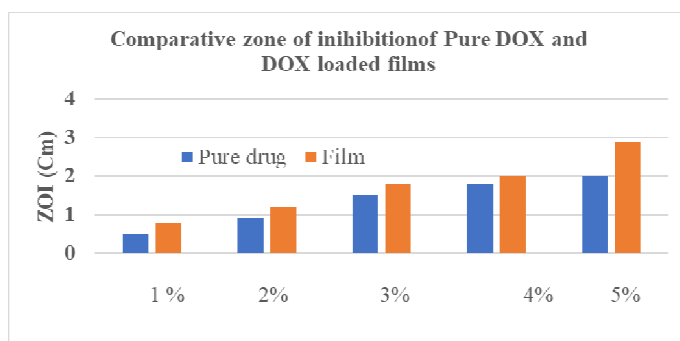


Fig. 6. Comparative ZOI of pure DOX and DOX loaded chitosan films.

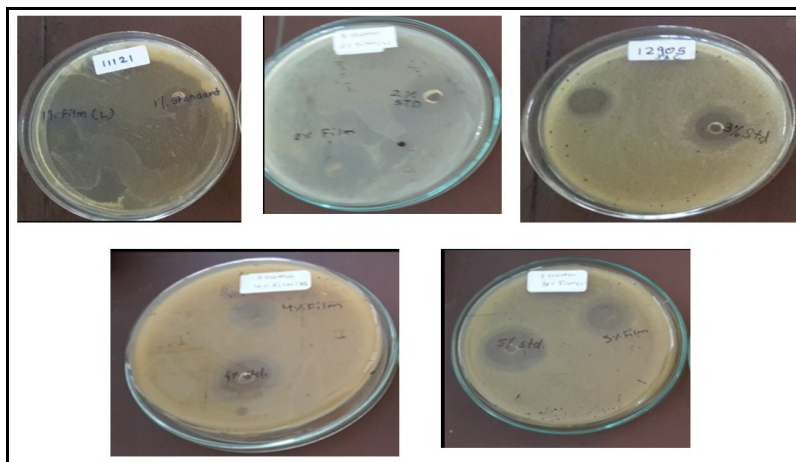


Fig. 7. Zone of inhibition of study of 1 to 5% film against *Staphylococcus aureus*.

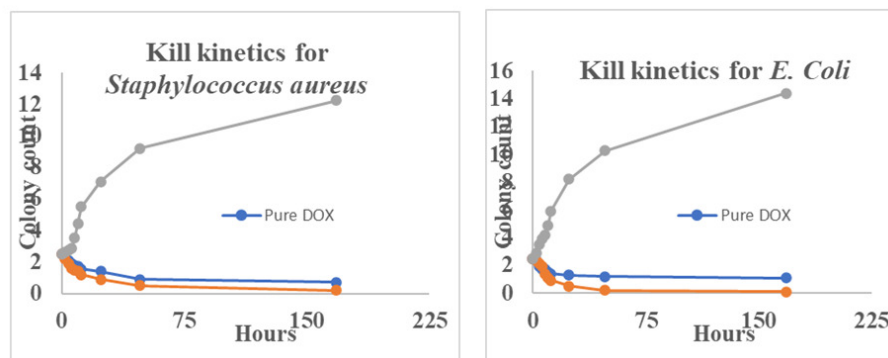


Fig. 8. Kill kinetics study against *Staphylococcus Aureus* and *E. coli*.

CONCLUSIONS

The aforementioned results justify the use of Doxycycline in films developed with chitosan, TPP, and PEG 400 as polymer, crosslinking agent, and plasticizer respectively. The films' physicochemical characteristics were deemed to be acceptable. It was discovered that the drug release occurred in a sustained manner. The DOX-loaded films demonstrated good bactericidal efficacy against *E. coli* and *Staphylococcus aureus*. The drug did not interact chemically with the excipients while being stored at accelerated stability conditions. This newly developed film could be used for future medication delivery applications in periodontitis conditions.

FUTURE SCOPE

The developed Doxycycline dental films can be evaluated preclinically in a suitable animal model to establish their safety. Furthermore, scale-up batches can also be planned to check the process feasibility.

Acknowledgement. Jaydeep Dusane and Ashok Bhosale wish to acknowledge the Seth Govind Raghunath Sable College of Pharmacy, Saswad, Pune, Maharashtra, India for providing the research facility.

Conflict of Interest. None.

REFERENCES

- Chaturvedi, T. P., Srivastava, R., Srivastava, A. K., Gupta, V. and Verma, P. K. (2013). Doxycycline poly ϵ -caprolactone nanofibers in patients with chronic periodontitis—a clinical evaluation. *Journal of Clinical and Diagnostic Research*, 7(10), 2339-2348.
- Chuenbarn, T., Chantadee, T. and Phaechamud, T. (2022). Doxycycline hyclate-loaded Eudragit® RS PO in situ-forming microparticles for periodontitis treatment. *Journal of Drug Delivery Science and Technology*, 71, 103294.
- Dinte, E., Muntean, D. M., Andrei, V., Boca, B. A., Dutescu, C. M., Barbu-Tudoran, L., Borodi, G., Andrei, S., Gal, A. F., Rus, V. and Gherman, L. M. (2023). In Vitro and In Vivo Characterisation of a Mucoadhesive Buccal Film Loaded with Doxycycline Hyclate for Topical Application in Periodontitis. *Pharmaceutics*, 15(2), 580.
- Eldin, M. M., Soliman, E. A., Hashem, A. I. and Tamer, T. M. (2008). Antibacterial activity of chitosan chemically modified with a new technique. *Trends in Biomaterials and Artificial Organs*, 22(3), 125-137.
- Fisher, J., Selikowitz, H. S., Mathur, M. and Varenne B. (2018). Strengthening oral health for universal health coverage. *The Lancet*, 392(10151), 899-901.
- Ghavami-Lahiji, M., Shafiei, F., Pourhajibagher, M., Najafi, F. and Bahador, A. (2020). The Antibacterial Activity of a New Polymeric Local Drug Delivery System against an In-vitro Multispecies Pathogens Associated with Periodontitis. *Journal of Dentomaxillofacial Radiology, Pathology and Surgery*, 9(4):1-10.
- Gates, K. A., Grad, H., Birek, P. and Lee, P. I. (1994). A new bioerodible polymer insert for the controlled release of metronidazole. *Pharmaceutical research*, 11(11), 1605-1609.
- Genco, R. J. (1981). Antibiotics in the treatment of human periodontal diseases. *Journal of Periodontology*, 52(9), 545-558.
- Greenstein, G. (2006). Local drug delivery in the treatment of periodontal diseases: assessing the clinical significance of the results. *Journal of periodontology*, 77(4), 565-578.
- Ikinci, G., Şenel, S., Akıncıbay, H., Kaş, S., Erciş, S., Wilson, C. G. and Hıncal A. A. (2002). Effect of chitosan on a periodontal pathogen *Porphyromonas gingivalis*. *International journal of pharmacaceutics*, 235(1-2), 121-127.
- Jain, N., Jain, G. K., Javed, S., Iqbal, Z., Talegaonkar, S., Ahmad, F. J. and Khar, R. K. (2008). Recent approaches for the treatment of periodontitis. *Drug discovery today*, 13(21-22), 932-943.
- James, S. L., Abate, D., Abate, K. H., Abay, S. M., Abbafati, C., Abbasi, N., Abbastabar, H., Abd-Allah, F., Abdela, J., Abdelalim, A. and Abdollahpour, I. (2018). Global, regional, and national incidence, prevalence, and years lived with disability for 354 diseases and injuries for 195 countries and territories, 1990–2017: a systematic analysis for the Global Burden of Disease Study 2017. *The Lancet*, 392(10159), 1789-1858.
- Joshi, D., Garg, T., Goyal, A. K. and Rath, G. (2016). Advanced drug delivery approaches against periodontitis. *Drug delivery*, 23(2), 363-377.
- Junmahasathien, T., Panraksa, P., Protiarn, P., Hormdee, D., Noisombut, R., Kantrong, N. and Jantrawut, P. (2018). Preparation and evaluation of metronidazole-loaded pectin films for potentially targeting a microbial infection associated with periodontal disease. *Polymers*, 10(9), 1021-1032.
- Khagga, B., Kaitha, M. V., Dammu, R. and Mogili, S. (2019). ICH guidelines– “Q” series (quality guidelines)-A review. *GSC Biological and Pharmaceutical Sciences*, 6(3), 089-106.
- Khajuria, D. K., Patil, O. N., Karasik, D., & Razdan, R. (2018). Development and evaluation of novel biodegradable chitosan based metformin intrapocket dental film for the management of periodontitis and alveolar bone loss in a rat model. *Archives of oral biology*, 85, 120-129.
- Khan, S., Kale, M., Siddiqui, F. and Nema, N. (2021). Novel pyrimidine-benzimidazole hybrids with antibacterial and antifungal properties and potential inhibition of SARS-CoV-2 main protease and spike glycoprotein. *Digital Chinese Medicine*, 4(2), 102-119.
- Levin, B. R. and Udekwu, K. I. (2010). Population dynamics of antibiotic treatment: a mathematical model and hypotheses for time-kill and continuous-culture experiments. *Antimicrobial agents and chemotherapy*, 54(8), 3414-3426.
- Loke, W. K., Lau, S. K., Yong, L. L., Khor, E., and Sum, C. K. (2000). Wound dressing with sustained antimicrobial capability. *Journal of Biomedical Materials Research: An Official Journal of The Society for Biomaterials, The Japanese Society for Biomaterials. The Australian Society for Biomaterials and the Korean Society for Biomaterials*, 53(1), 8-17.
- Mahmoud, M. and Samy, W. (2016). Enhanced periodontal regeneration by novel single application sustained release nano-structured doxycycline films. *Current Drug Delivery*, 13(6), 899-908.
- Naik, S., Raikar, P. and Ahmed, M. G. (2019). Formulation and evaluation of chitosan films containing sparfloxacin for the treatment of periodontitis. *Journal of Drug Delivery and Therapeutics*, 9(1), 38-45.
- Nakahara, T., Nakamura, T., Kobayashi, E., Inoue, M., Shigeno, K., Tabata, Y., Eto, K. and Shimizu, Y. (2003). Novel approach to regeneration of periodontal tissues based on in situ tissue engineering: effects of controlled release of basic fibroblast growth factor

- from a sandwich membrane. *Tissue engineering*, 9(1), 153-162.
- Narala, S., Nyavanandi, D., Mandati, P., Youssef, A. A., Alzahrani, A., Kolimi, P., Zhang, F. and Repka, M. (2022). Preparation and in vitro evaluation of hot-melt extruded pectin-based pellets containing ketoprofen for colon targeting. *International Journal of Pharmaceutics*: X, 5, 100156.
- Nyavanandi, D., Narala, S., Mandati, P., Alzahrani, A., Kolimi, P., Almotairy, A. and Repka, M. A. (2023). Twin Screw Melt Granulation: Alternative Approach for Improving Solubility and Permeability of a Non-steroidal Anti-inflammatory Drug Ibuprofen. *AAPS Pharm Sci Tech.*, 24(1), 47.
- Ozdogan, A.I., Akca, G. and Şenel, S. (2018). Development and in vitro evaluation of chitosan-based system for local delivery of atorvastatin for treatment of periodontitis. *European Journal of Pharmaceutical Sciences*, 1, 124, 208-216.
- Prashanth, R., Kiran Kumar, A., Rajkumar, M. and Aparna, K. (2022). Studies on Postharvest Quality and Shelf Life of Pink Fleshed Dragon Fruit (*Hylocereus* spp.) Coated with Chitosan and Stored at Ambient Temperature. *Biological Forum – An International Journal*, 14(3), 340-347.
- Rajeshwari, H. R., Dhamecha, D., Jagwani, S., Rao, M., Jadhav, K., Shaikh, S., Puzhankara, L. and Jalalpure, S. (2010). Local drug delivery systems in the management of periodontitis: A scientific review. *Journal of Controlled Release*, 10, 307:393-409.
- Rodrigues, S., Dionísio, M., Remunan, L. C. and Grenha, A. (2012). Biocompatibility of chitosan carriers with application in drug delivery. *Journal of functional biomaterials*, 3(3), 615-641.
- Swain, R. P., Unnisa, M. S., Swain, M. R., Bhattacharjee, A., Karna, N., Dash, S. K. and Padhan, A. (2023). Formulation And In Vitro Evaluation of Site-Specific Local Action Dental Films Of Doxycycline Hyclate For Treatment of Periodontitis. *Journal of Pharmaceutical Negative Results*, 1, 347-360.
- Sanz, M., D'Aiuto, F., Deanfield, J. and Fernandez-Avilés, F. (2010). European workshop in periodontal health and cardiovascular disease—scientific evidence on the association between periodontal and cardiovascular diseases: a review of the literature. *European heart journal supplements*, 12(suppl B): B3-B12.
- Vieira, M. G., da Silva, M.A., dos Santos, L. O. and Beppu, M. M. (2011). Natural-based plasticizers and biopolymer films: A review. *European polymer journal*, 47(3), 254-263.
- Yanat, M. and Schroen, K. (2021). Preparation methods and applications of chitosan nanoparticles; with an outlook toward reinforcement of biodegradable packaging. *Reactive and Functional Polymers*, 1, 161, 104849-104857.

How to cite this article: Jaydeep Dusane and Ashok Bhosale (2023). Formulation and Development of Oral Dental Films of Doxycycline Loaded Chitosan Films for efficient Treatment of Periodontitis. *Biological Forum – An International Journal*, 15(3): 06-15.



Development and Evaluation of Solid Self-Microemulsifying Drug Delivery System for Solubility Enhancement of Valsartan.

Aditi R. Beldar^{1*}, Sujit S. Kakade², Prashant H. Khade², Ashok V. Bhosale³

Riya R. Bhondve¹, Harshal M. Shinde¹, Ruchita A. Bhalerao¹

¹Research Scholar, Department of Pharmaceutics, PDEAs Shankarrao Ursal College of Pharmaceutical Sciences and Research Centre, Pune, Maharashtra, India.

² Assistant Professor, Department of Pharmaceutics, PDEAs Shankarrao Ursal College of Pharmaceutical Sciences and Research Centre, Pune, Maharashtra, India.

³ Principal, Department of Pharmaceutics, PDEAs Shankarrao Ursal College of Pharmaceutical Sciences and Research Centre, Pune, Maharashtra, India.

Correspondence – Aditi R. Beldar

aditibeldar@gmail.com

ABSTRACT:

Valsartan is orally active, and specific angiotensin II antagonist acting on the AT1 receptor subtype (angiotensin receptor blocker). It is a lipophilic in nature and is feebly aqueous soluble drug with absolute bioavailability of 25%. The goal of the present study was to develop Solid self-micro emulsifying Drug Delivery System (S-SMEDDS) of valsartan to improve its oral bioavailability. The formulations were explored on the basis of solubility, FTIR study and excipient compatibility, emulsification efficiency, particle size and zeta potential. Solubility of valsartan was determined in various vehicles and maximum solubility was found in Castor oil as (oil), Tween 60 as (surfactant) and Kollisolv PG as (co-surfactant). These elements were used to design pseudo-ternary phase diagrams to identify the micro emulsion zone. Solid-SMEDDS were prepared by adsorption technique using Aerosil 200 (1% w/w) and were evaluated for micromeritic properties, scanning electron microscopy, X-ray diffraction, FTIR study and Drug content. The designed Solid-SMEDDS were further evaluated for stability study. Solid-SMEDDS may be considered as a better solid dosage form as solidified formulations are more ideal than liquid ones in terms of its stability. These results suggest the potential use of SMEDDS and solid-SMEDDS to improve the dissolution and hence oral bioavailability of poorly water-soluble drugs like valsartan through oral route.

KEYWORDS: Valsartan, Bioavailability, Lipophilicity, Microemulsion, L-SMEDDS, S-SMEDDS.

1. INTRODUCTION:

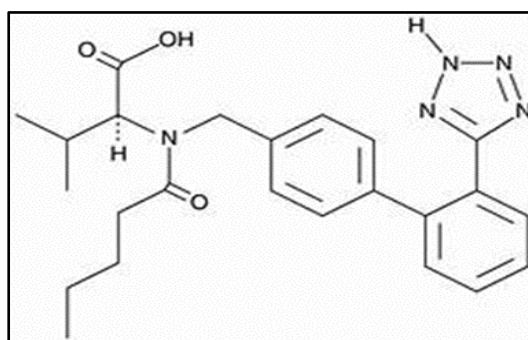
Self-microemulsifying drug delivery system (SMEDDS) are the newly emerging techniques for the enhancement of lipophilic drug delivery. Primary challenge of any oral formulation design program is to maintain drug solubility within G.I tract and particularly maximizing drug solubility within primary absorption site of the gut.¹ For lipophilic drug compounds which exhibit dissolution rate limited absorption self microemulsifying drug delivery systems (SMEDDS) can offer great step-up in rate and extent of absorption, leading to reproducible blood time profiles of BCS class II drugs in particular.²

According to Lipinski's rule of five for oral absorption trends, it predicts that poor permeation or poor absorption is more likely when there are more than 5 H-bond donors, more than 10 H-bond acceptors, with molecular weight >500 and log P>5. ³

SMEDDS are isotropic mixtures of oils, surfactants and co-surfactants, which form oil-in-water micro emulsion in aqueous media under gentle agitation. The finely divided oily droplets, with a droplet size less than 50 nm, provide a large surface area for drug release and absorption. The oily phase allows the drug to be present in its solubilised state, thereby avoiding the slow and rate-limiting dissolution process of a hydrophobic drug. ⁴ It can be prepared either in liquid form or encapsulated in hard or soft gelatine capsule. Nevertheless, it has some drawbacks also such as instability, leakage, precipitation of drug, and ageing of shells of the capsules. ⁵ to solve these above obstructions, the researchers have successfully developed solid SMEDDS using solid carriers and demonstrated their usefulness in dissolution and bioavailability. Recently the spray drying method for solidification of SMEF has been reported using different adsorbent materials for enhancement of solubility and bioavailability. ⁶

Valsartan is a potent, orally active nonpeptide tetrazole derivative and selectively inhibits Angiotensin II Receptor type 1 which causes reduction in blood pressure and is used in treatment of hypertension. ⁷ It is a lipophilic drug and possesses moderate onset of action than other drugs of the same category. It is soluble in the neutral pH range. Valsartan is 3-methyl-2-[pentanoyl-[[4-[2-(2H-tetrazol-5-yl)phenyl]phenyl]methyl]amino]-butanoic acid (Structure 1) with empirical formula C₂₄H₂₉N₅O₃. Its molecular weight is 435.519g/mol. ⁸ Valsartan is a white coloured powder that is freely soluble in ethanol, methanol, and sparingly soluble in water. The partition coefficient of Valsartan is 0.033 (log P=1.499), suggesting that the compound is hydrophilic at physiological pH. The compound is stable under storage in dry conditions. Valsartan has bioavailability of about 25% due to its acidic nature. Being acidic in nature it is poorly soluble in the acidic environment of GIT and is absorbed from the upper part of GIT that is acidic in nature and where its solubility is low. ⁹

Fig.1: Molecular Structure of Valsartan.



The main aim of the study was to develop valsartan SMEDDS to improve upon the solubility of the valsartan which will have some bearing on the bioavailability. The SMEDDS consists of an isotropic mixture of drug, lipid, surfactant, and typically a co-surfactant or co-solvent. When exposed to the fluids of the gastrointestinal (GI) tract, these precursor solutions spontaneously emulsify to form highly dispersed microemulsions. These dispersions commonly have been shown to enhance the oral bioavailability of lipophilic drugs. The ease of dispersion and the very small particle size of the resultant colloidal microemulsion have

historically been viewed as the principal reasons for their utility in the delivery of lipophilic drugs.¹⁰

2. MATERIALS AND METHODS:

2.1 MATERIALS:

Valsartan was purchased from Dhamtec Pharma Ltd. Navi Mumbai. Tween 60, Etocas, Isopropyl myristate was a kind gift from Croda India Company Pvt. Ltd, Navi Mumbai, Maharashtra. Kollisolv PG was kind gift from BASF India, Ltd. Navi Mumbai. Acrysol EL-135 and Acrysol K-150 was a kind gift received from Corel Pharma Chem Pvt. Ltd. Ahmedabad, Gujarat. All other chemicals used were of analytical reagent grade.

2.2 METHODS:

2.2.1 Solubility of the oil phase, surfactant and co-surfactant:

The solubility study was performed to select the suitable oil (O), surfactant (S), and co-surfactant (Co-S) that possesses high solubilizing capacity for valsartan. Selection of the oil phase was based upon the maximum solubility of the drug. Different oils like Oleic acid, Etocas, long-chain triglycerides (Soyabean, Sunflower, Castor oil, and Coconut Oil) and Isopropyl Myristate. Surfactants like Tween 20, Tween 40, Tween60, Tween80, Span 20, Acrysol EL-135, and Acrysol K-150. Co-surfactants like Kollisolv PG, Polyethylene Glycol 200 and Polyethylene Glycol 400 were selected and their solubility was determined by shaking flask method.¹¹ The excess amount of drug was placed in 5.0 mL screw cap glass bottle having 2.0 mL of each oil, surfactant, and co-surfactant. The mixture vials were then kept at 25 ± 1.0 °C in an isothermal shaker for 72 hr. to reach equilibrium. The equilibrated samples were removed from shaker and centrifuged at 3000 rpm for 20 min. The supernatant was taken and filtered through a 0.45 μ m membrane filter. The concentration of Valsartan was determined in oils and water using UV Spectrophotometer at wavelength of 248 nm.¹² The data is shown in the Table 3.1, 3.2, 3.3 and Figure 3.1, 3.2 and 3.3.

2.3 Drug-Excipients Compatibility:

The Drug – Excipients Compatibility Studies were performed in order to confirm the drug-excipients compatibility. The study mainly include FT-IR study. Mixture of Drug+ Oil, Drug + Surfactant, and Drug + Co-Surfactant.¹³

2.4 Construction of Pseudo-ternary phase diagram:

On the basis of the solubility study of drug, oil, surfactants, co-surfactants and aqueous phase were used for construction of phase diagram. Oil, surfactant, and co-surfactant are grouped in four different combinations for phase studies. Surfactant and co-surfactant (Smix) in each group were mixed in different weight ratio (1:1, 1:2, 2:1, 3:1).¹⁵ These Smix ratios are chosen in increasing concentration of surfactant with respect to co-surfactant and in increasing concentration of co surfactant with respect to surfactant for detail study of the phase diagram for formulation of micro emulsion. For each phase diagram, oil, and specific Smix ratio are mixed thoroughly in different weight ratio from 1:9 to 9:1 (1:9, 2:8, 3:7, 4:6, 5:5, 6:4, 7:3, 8:2, 9:1) in different glass vials.¹⁶ Different combination of oils and Smix were made so those maximum ratios were covered for the study to delineate the boundaries of phase precisely formed in the phase diagrams. Pseudo-ternary phase diagram was developed using aqueous

titration method. Slow titration with aqueous phase is done to each weight ratio of oil and Smix and visual observation is carried out for transparent and easily flow able o/w micro emulsion. The physical state of the micro emulsion was marked on a pseudo-three-component phase diagram with one axis Data of aqueous phase, the other Data of oil and the third Data of a mixture of surfactant and co-surfactant at fixed weight ratios (Smix ratio).¹⁷ Each of these ratios was mixed with increasing percentage of oil, i.e., 10%, 20%, 30%, 40% up to 90% of oil to get phase diagram. To determine the effect of drug addition in SMEDDS, phase diagrams were also constructed in presence of drug. In order to prepare SMEDDS, selection of microemulsion region from phase diagram was based on the fact that solution remains clear even on infinite dilution.¹⁸

2.5 Selection of Formulation from Pseudo ternary Phase Diagram:

From each phase diagram, constructed, different formulations were selected from micro-emulsion. Selected formulations were subjected to different thermodynamic stability and Dispersibility tests.¹⁹

2.5.1 Thermodynamic stability studies:²⁰

It was determined by carrying heating cooling cycle, centrifugation test and freeze thaw cycle.

a. Heating cooling cycle:

Six cycles between refrigerator temperatures 4°C and 45°C with storage at each temperature for not <48 hr. was studied. If SMEDDS stable at these temperatures was subjected to centrifugation test.

b. Centrifugation test:

Passed SMEDDS were centrifuged at 3500 rpm for 30 min using digital centrifuge (Remi motors Ltd). If SMEDDS did not show any phase separation was taken for freeze-thaw stress test.

c. Freeze-thaw cycle :

Three freeze-thaw cycles between -21°C and +25°C with storage at each temperature for not < 48 h was done for SMEDDS.

2.5.2 Dispersibility Studies:²¹

The dispersibility test of SMEDDS was carried out to assess to compatibility to disperse into emulsion and the size of resulting globules to categorize them as SMEDDS. It was carried by using a standard USP Paddle type dissolution test apparatus, formulation was added to 500 ml of water at 37±0.5°C and the paddle was rotated at 50 rpm. On titration with water the SMEDDS formulation forms a mixture which was of different type. Depending upon which the in vitro performance of formulation can be assessed.

Grade	Dispersibility and Appearance
A	Rapidly forming (Within 1 min) microemulsion having a clear or bluish appearance
B	Rapidly forming, slightly clear emulsion having a bluish white appearance
C	Fine milky emulsion that formed within 2 min

D	Dull, greyish white emulsion having slightly oily appearance that is slow to emulsify (longer than 2min)
---	--

Those formulations that passed the thermodynamic stability and also Dispersibility test in Grade A, and Grade B was selected for further studies.²²

2.6 Preparation of SMEDDS:

A series of microemulsions of SMEDDS were prepared with varying ratios of oil, surfactant, and co-surfactant. Formulations 1, 2, and 3 were prepared using Castor oil as oil, Tween 60 as surfactant, and Kollisolv PG as co-surfactant. In all the formulations, the level of Valsartan was kept constant (i.e. 20mg). The amount of SMEDDS should be such that it should solubilize the drug (single dose) completely.²³ The Valsartan (20 mg) was added in the mixture. Then the components were mixed by gentle stirring and mixing, and heated at 37°C. The mixture was stored at room temperature until used. So, prepared SMEDDS was the concentrate of oil, surfactant, co-surfactant and drug. The composition of formulations is given in Table 1, 2 and 3.²⁴

Table No. 2.1: Composition of Formulation 1

Formulation 1 (1:1)	Valsartan (mg)	Castor Oil (w/w)	Tween 60 (w/w)	Kollisolv PG (w/w)
M1	20	40	30	30
M2	20	30	35	35
M3	20	20	40	40
M4	20	10	45	45

Table No. 2.2: Composition of Formulation 2

Formulation 2 (2:1)	Valsartan (mg)	Castor Oil (w/w)	Tween 60 (w/w)	Kollisolv PG (w/w)
M1	20	40	40	20
M2	20	30	46.10	23.30
M3	20	20	53.3	26.7
M4	20	10	60	30

2.7 Physicochemical characterization of self-microemulsifying drug delivery system:

a) Appearance:

The prepared microemulsion was inspected visually for clarity, colour and presence of any particulate matter.

b) FT-IR Study

In this study FTIR instrument was used. FTIR spectra for the drug and the excipients of the optimized formulations were obtained.²⁵

c) Drug content:

Self-microemulsifying drug delivery system containing valsartan 10 mg was added in 10 mL methanol and mixed well with shaking and was sonicated for 10-15 min. Further was centrifuged and supernatant was further diluted with suitable quantity of fresh methanol and drug content was determined using UV-spectrophotometer at λ_{max} 248 nm.²⁶

d) Robustness to dilution:

Robustness to dilution was studied by diluting SMEDDS to 50, 100 and 1000 times with water, 0.1 N HCl and phosphate buffer pH 6.8. The diluted SMEDDS were stored for 12 h and observed for any signs of phase separation or drug precipitation.²⁷

e) Self-Emulsification Time:

The emulsification time of SMEDDS was determined according to USP 22, dissolution apparatus each formulation added drop wise to 500ml purified water at 37°C. Gentle agitation was provided by a standard stainless steel dissolution paddle rotating at 50 rpm. Emulsification time was assessed visually.²⁸

f) Viscosity:

The viscosities were measured to determine rheological properties of formulations. Brookfield viscometer at 30°C used to serve this purpose.²⁹

g) Refractive index :

Refractive indices of the prepared micro emulsions were determined at 25°C by Abbe's refractometer by placing one drop of micro emulsion on the slide.³⁰

h) % Transmittance:

The percent transmittance of various formulations was measured at 248 nm using UV spectrophotometer keeping water as a blank.³¹

i) Cloud Point Measurement:

The formulated SMEDDS was diluted with 50ml water in a beaker which was placed on a water bath with gradually increasing temperature until the diluted formulation turned cloudy. It mainly insists about the stability of microemulsion at the temperature of body.³²

j) Particle Size Determination:

Particle size of the prepared microemulsion was determined using Dynamic Light Scattering (DLS) method. For DLS particle sizing, the sample needs to be crystal clear to very slightly hazy. If the solution is white or too hazy, it should be diluted further before attempting a DLS size measurement. When the solution is ready for analysis and transfer it in the cuvette, care should be taken to avoid bubbles which are formed on the walls of the cuvette. Slowly tilting or tapping the cuvette on a hard surface may help also. Once the solution was homogenous and ready for DLS measurement, the cuvette containing the solution was placed in the instrument. The instrument was run and solution was analysed for particle size.³³

k) Zeta Potential:

Zeta Potential of the prepared microemulsion was determined using Light Scattering method. For Zeta Potential determination, the sample needs to be crystal clear. When the solution is ready for analysis and transfer it in the cuvette, care should be taken to avoid bubbles which are formed on the walls of the cuvette. Slowly tilting or tapping the cuvette on a hard surface may also help to remove the bubble formed. Then the electrode was dipped inside the cuvette containing sample solution. Care should be taken to avoid bubbles in between the electrodes.

The cuvette containing the solution was placed in the instrument. The instrument was run and solution was analysed for Zeta Potential.³³

l) Polydispersity Index (PI) :

Polydispersity Index (PI) of the prepared microemulsion was determined using Dynamic Light Scattering (DLS) method. For DLS method, the sample needs to be crystal clear to very slightly hazy. If the solution is white or too hazy, it should be diluted further before attempting a DLS size measurement. When the solution was ready for analysis and transfer it in the cuvette, care should be taken to avoid bubbles which are formed on the walls of the cuvette. Slowly tilting or tapping the cuvette on a hard surface may also help to remove the bubbles formed. Once the solution was homogenous and ready for DLS measurement, the cuvette containing the solution was placed in the instrument. The instrument was run and solution was analysed for Polydispersity Index.³³

m) *in vitro* Dissolution Studies:

In vitro dissolution study was performed by using USP Dissolution Apparatus II. The dissolution vessel was fitted with 900 mL dissolution media 0.1 N HCl and 6.8 buffer and kept at $37 \pm 0.5^\circ\text{C}$ with a rotating speed of 50 rpm. The aliquot of 5.0 mL was withdrawn at 5, 15, 30, and 60 min and filtered through 0.45 μm Whatman membrane filter. The volume withdrawn was replaced each time by fresh dissolution media.³⁴

2.8 Preparation of Solid SMEDD:

The optimized liquid self microemulsifying formulation was transformed into free flowing granules using Aerosil 200 colloidal porous carriers as adsorbent. The L-SMEDDS and Aerosil 200 were taken in ratio 1:1 w/w to optimize the drug loading on colloidal silica. The mixture was further dried to obtain the free flowing powder.

2.9 Evaluation of Solid SMEDDS Formulations:

1. Micromeritics Properties:

Prepared solid-SMEDDS was evaluated for micromeritics properties such as angle of repose, bulk and tapped density, compressibility index and Hausner ratio (HR).³⁵

2. Scanning electron microscopy:

Scanning electron microscopy (SEM) for Valsartan and prepared solid-SMEDDS was taken using scanning electron microscope (Philips, XL-30) at accelerating voltage at 3-5 kV to study surface topography.³⁶

3. *in vitro* release studies :

Dissolution study was carried out using USP Type II apparatus (Paddle method) at 50 rpm, and at $37^\circ\text{C} \pm 0.5^\circ\text{C}$. The dissolution medium was 0.1 N HCl and 6.8 pH Phosphate Buffer and. Prepared solid-SMEDDS with equivalent amount of drug 20 mg were placed in 900 ml of dissolution medium respectively. A sample of 5 ml were withdrawn at regular time interval of 5, 15, 30, and 60, and filtered using 0.45 μm filter. An equal volume of respective dissolution medium was added to maintain sink conditions. Drug content from sample was analysed using UV-spectrophotometer at 248 nm.³⁷

4. X-ray diffraction study:

The X-ray diffraction (X-RD) of Valsartan were obtained using X-RD instrument Bruker AXS, D8 Advance with Ni-filtered Cu radiation, at a voltage of 45 kV and current of 40 mA. The scanning speed was 2°/min between 50 and 500. ³⁸

5. Drug content:

S-SMEDDS equivalent to 20mg was diluted in suitable quantity of methanol. The sample was mixed thoroughly to dissolve drug in methanol by stirring. Drug content in the solvent extract is filtered through 0.45 µm membrane filter. Drug content analysed by suitable analytical method against the standard solvent solution of drug. ³⁹

6. Fourier transform-infrared spectroscopy :

In this study FTIR instrument was used. FTIR Spectra was determined of Solid SMEDD.

2.10 Stability Study:

Stability studies for solid-SMEDDS were studied at different temperature conditions according to ICH guidelines at room temperature i.e. 25°C ± 2°C/60% ± 5% relative humidity (RH). The samples were withdrawn at different time intervals as 0, 30, 60, 90 days. Formulation was evaluated for Appearance, equivalent to 20 mg of the drug was dissolved in methanol, diluted approximately and estimated for the drug content spectrophotometrically at 248 nm using methanol as blank. Effect of storage conditions on drug release was also studied. ⁴¹

3. RESULT AND DISCUSSIONS:

3.1. Screening of Excipients:

3.1.1 Solubility Study:

Table 3.1: Data for solubility of Valsartan in various oil phase

Sr No	Oil Phase	Solubility (mg/ml)
1	Oleic Acid	11.38
2	Castor oil	12.35
3	Isopropyl myristate	11.33
4	Soyabean Oil	5.15
5	Coconut Oil	3.79
6	Etocas	11.71
7	Sunflower Oil	3.98

SMEDDS of Valsartan, it should possess good solubility in the oil, surfactants and co-surfactants of system. The solubility of Valsartan in various oils, surfactants and co-surfactants was investigated. Valsartan had significantly higher solubility in castor oil (12.35 mg/ml) than, Sunflower oil, Coconut oil, soyabean oil, etocas, isopropyl myristate, oleic acid. Among surfactants and co-surfactants, tween 60 (12.38 mg/ml) and Kollisolv PG (12.378mg/ml)

respectively showed highest solubilities .Therefore, castor oil was screened as oil phase , Tween 60 as surfactant and Kollisolv PG as co-surfactant based on solubility studies. Table 3.1, 3.2, 3.2 respectively and it is represented graphically in Figure 3.1, 3.2, 3.3.

Table 3.2: Data for solubility of Valsartan in various surfactants

Sr No	Surfactants	Solubility (mg/ml)
1	Cremophor RH 40	10.13
2	Tween 20	10.92
3	Tween 60	12.38
4	Tween 80	11.22
5	Span 20	11.88
6	Acrysol K-150	9.934
7	Acrysol EL-135	9.625

solubility of Valsartan in various co-surfactants

Sr. No.	Co-Surfactants	Solubility (mg/ml)
1.	Kollisolv PG	12.37
2	Polyethylene Glycol 200	9.52
3	Polyethylene Glycol 400	10.08

Figure 3.1: Solubility of Valsartan in Various Oil Phases

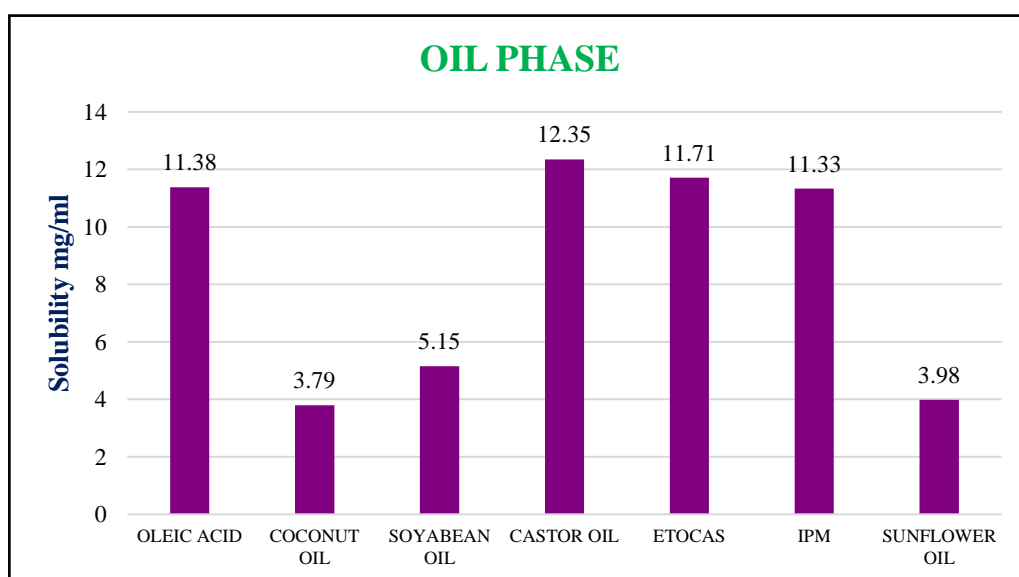


Figure 3.2: Data for solubility of Valsartan in various surfactant

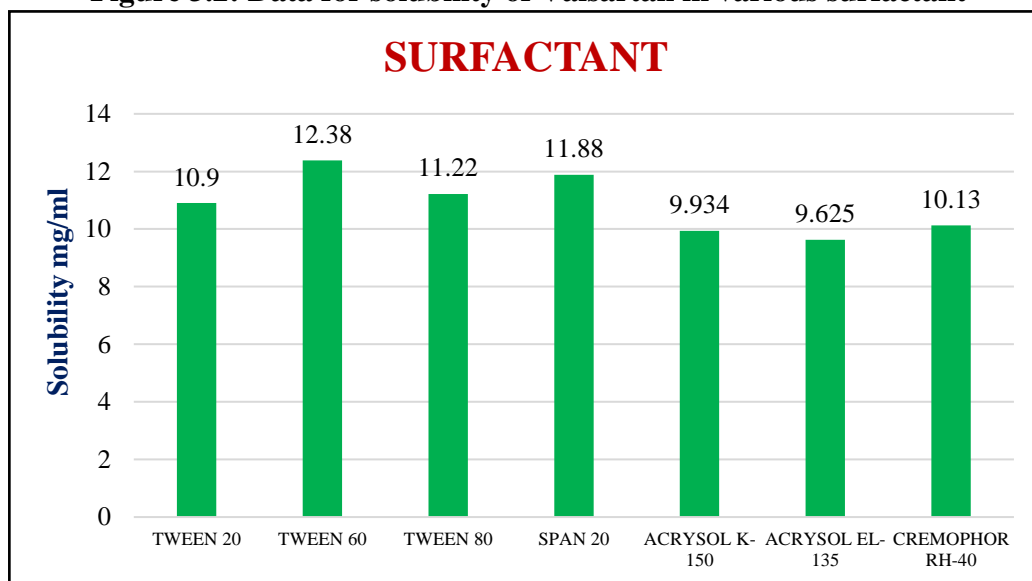
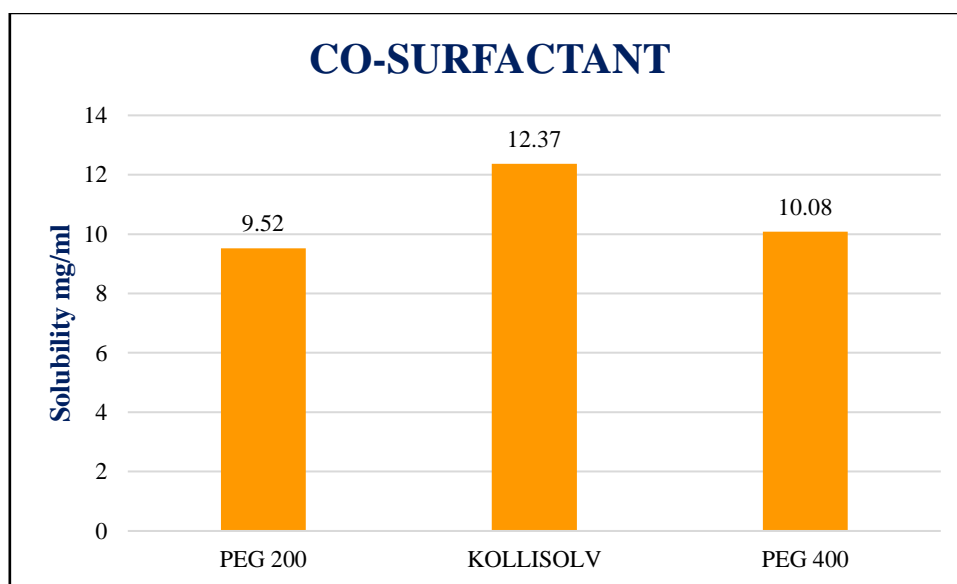


Figure 3.3: Data for solubility of Valsartan in various co-surfactants



Based on the results of Solubility screening, one distinct system was selected which was: Castor Oil as oily phase, Tween 60 as surfactant, Kollisol PG as co-surfactant for further studies.

3.2 Drug – Excipients Compatibility Study:

The scanning range was 400 to 4000 cm^{-1} and resolution was 1cm^{-1} . The major peaks in recorded spectra were compared with standard spectra given in figure below. So it can be concluded that the spectra of pure drug valsartan and the combination of drug with additives,

that all the characteristic peaks of valsartan were present in the combination spectrum, thus indicating compatibility of the drug and additives.

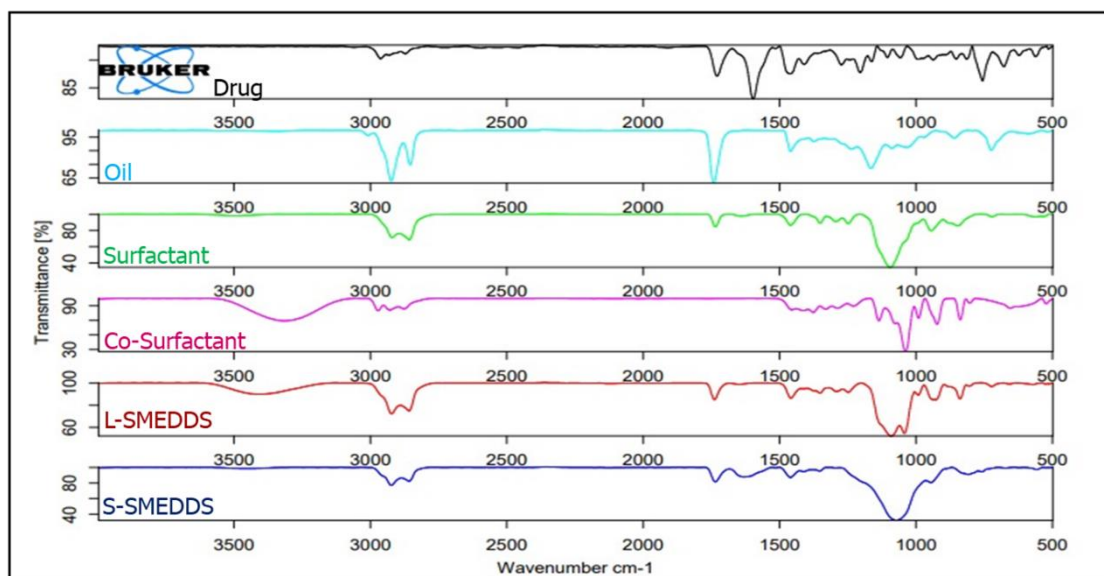
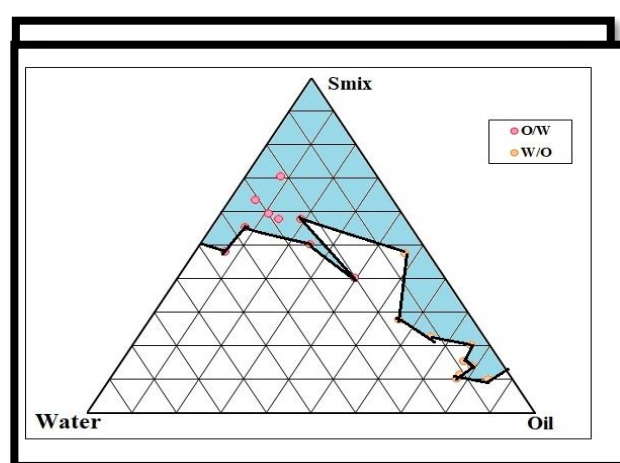
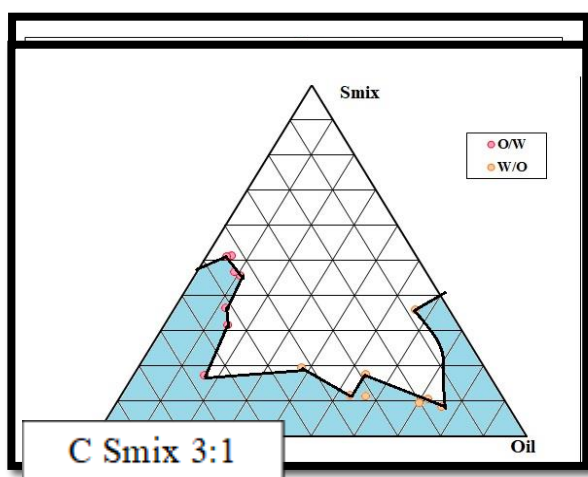


Figure 3.4: FT-IR Spectra of Overlay for compatibility study.

3.3 Construction of Pseudo ternary phase diagram:

The consideration for screening formulation of SMEDDS usually involves: the formulation composition should be simple, safe, and compatible; it should possess good solubility; a large efficient self-microemulsification region which should be found in the pseudo-ternary phase diagram, and have efficient droplet size after forming microemulsion. Thus, pseudo-ternary phase diagrams were constructed to identify the self-microemulsifying regions with maximum drug loading and to optimize the concentration of oil, surfactant and co-surfactant in the SMEDDS formulations and to obtain transparent and stable O/W micro-emulsions. The shaded areas in the pseudo-ternary phase-diagrams shown in fig 3.9 represented the existence field of stable, clear and transparent O/W microemulsions containing Castor oil as oil and with the Tween 60: Kollisolv PG fixed mixing ratio, respectively. For any selected composition of



surfactant and co-surfactant ratio from self-microemulsifying region of ternary phase diagram (shaded) the addition of great volumes of continuous phase allowed the clear system.

Figure 3.5: Phase diagram of Castor oil (oil), Smix (Tween 60 and Kollisolv PG) were water system having different Smix ratio.

3.4 Selection of Formulation from Pseudo ternary Phase Diagram:

After the construction of Pseudo ternary phase diagram 1:1, 2:1 and 3:1 Smix ratios, maximum area was selected and also which indicate that the area covers the maximum number of formulation. The phase diagram of selected formulation is shown in Fig 3.9. The Smix ratios 1:2 and 3:1 was discarded due to smaller microemulsion region and excess of surfactant concentration which cause GIT irritation. Hence it was discarded. Ratio 1:1 and 2:1 were taken for further studies.

3.4.1 Thermodynamic stability studies:

Microemulsions are thermodynamically stable systems and are formed at a particular concentration of oil, surfactant and water, with no phase separation, creaming or cracking. It is the thermostability which differentiates microemulsion from emulsions that have kinetic stability and will eventually phase separate. Thus, the selected formulations were subjected to different thermodynamic stability testing by using heating cooling cycle, centrifugation and freeze thaw cycle stress tests. Those formulations, which passed thermodynamic stability tests, were taken for dispersibility test. (Table 3.8, and 3.9). Thus it was concluded that the efficiency of surfactant and co-surfactant mixture was unaffected after exposing to extreme conditions.

3.4.2 Dispersibility test:

When infinite dilution is done to microemulsion formulation, there is every possibility of phase separation, leading to precipitation of a poorly soluble drug as microemulsions are formed at a particular concentration of oil, surfactant and water. For oral microemulsions the process of dilution by the GI fluids will result in the gradual desorption of surfactant located at the globule interface. The process is thermodynamically driven by the requirement of the surfactant to maintain an aqueous phase concentration equivalent to its CMC. In the present study, we used distilled water as a dispersion medium because it is well reported that there is no significant difference in the microemulsions prepared using non-ionic surfactants, dispersed in either water or simulated gastric or intestinal fluid. Formulations in Group I (Table 3.8) and Group II (Table 3.9) that passed dispersibility test in Grade A, B and C were taken for further study, as Grade A and B formulations will remain as microemulsions when dispersed in GIT. Formulation falling in Grade C could be recommended for self microemulsifying drug delivery formulation.

So from the study, total four formulations were selected for further study two from each group i.e. M3 and M4 from Group I and M3 and M4 from Group II.

Table 3.4 - Data for Thermodynamic stability test and Dispersibility test of different formulations selected from Group I

Group I Smix 1:1	Observations based on the preparation, thermodynamic stability studies and dispersibility tests				Inference
Formulation	Heating Cooling	Centrifugation Test	Freeze Thaw	Dispersibility	
M1	X	X	X	D	Rejected
M2	✓	X	X	C	Rejected
M3	✓	✓	✓	A	Selected
M4	✓	✓	✓	A	Selected

Table 3.5 - Data for Thermodynamic stability test and Dispersibility test of different formulations selected from Group II

Group II Smix 2:1	Observations based on the preparation, thermodynamic stability studies and dispersibility tests				Inference
Formulation	Heating Cooling	Centrifugation Test	Freeze Thaw	Dispersibility	
M1	✓	X	X	B	Rejected
M2	✓	✓	X	C	Rejected
M3	✓	✓	✓	A	Selected
M4	✓	✓	✓	B	Selected

3.5. Preparation of Liquid SMEDDS Formulations:

Formulations selected in section 3.8 and 3.9 were prepared as per the composition reported in Table 2.1 and 2.2 and found to be thermodynamically stable.

3.6. Evaluation of Liquid SMEDDS Formulations:

a. Appearance:

Appearance of the prepared microemulsion was inspected visually and all the batches of Valsartan were Clear, Colourless, and free from any particulate matters.

b. FTIR Spectra:

The scanning range was 400 to 4000 cm^{-1} and resolution was 1cm^{-1} . So it can be concluded that the spectra of pure drug valsartan and the Liquid SMEDDS spectrum, that all the characteristic peaks of valsartan were present in the Liquid SMEDDS spectrum.

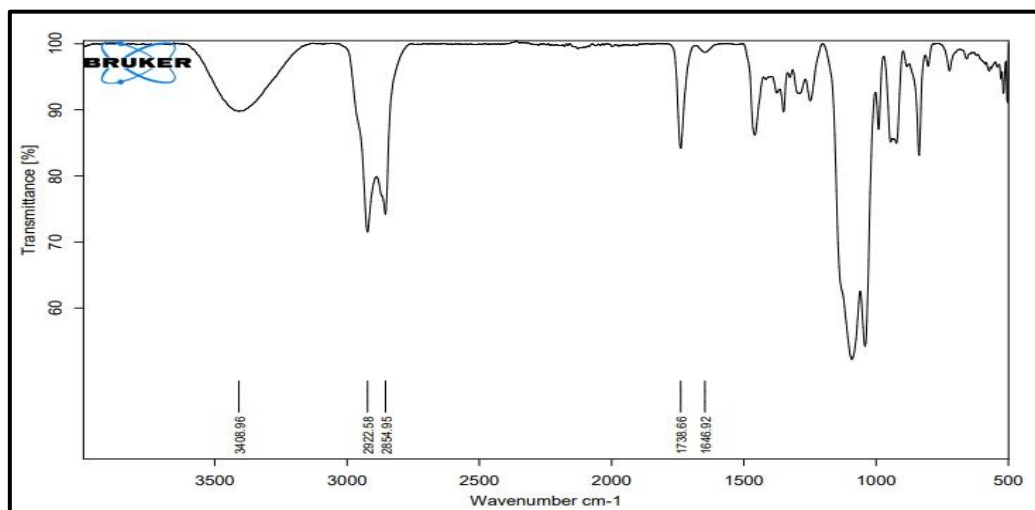


Fig 3.6: FTIR Spectra of Optimized Liquid SMEEDS

c. Drug content:

The drug content at 250 nm was found to be in the range of in the selected batch of Group I formulation M3 and M4 as well as Group II formulations M3 and M4. The data is shown in the table no. 3.6

Formulation Code	Group I	Group II
M3	91.01±0.01	97.77±0.16
M4	94.08±0.22	97.48±0.08

Table 3.6: Drug Content of Selected formulation.

d. Robustness to dilution:

After diluting SMEDDS to 50, 100 and 1000 times with water, 0.1 N HCl and buffer pH 6.8 and storing for 12 h, it was observed that there was no sign of phase separation or drug precipitation in formulations.

Formulation	Drug Precipitation or Phase Separation		
	Water	0.1 N HCl	6.8 pH buffer
Group I			
M3	-	-	-
M4	-	-	-
Group II			
M3	-	-	-
M4	-	-	-

Table 3.7: Data of the Robustness to dilution.

e. Self-Emulsification Time:

The emulsification time of liquid SMEDDS are presented in Table 3. Among the tested formulations, formulations of Group I's M4 and Group II's both formulation M3 and M4 showed shortest emulsification time than Group I's M3.

Formulation Code	Group I	Group II
M3	Within 2 min	Within 1 min
M4	Within 1 min	Within 1 min

Table 3.8: Data of self-emulsification time.

f. Viscosity:

All
of Group I

Formulation Code	Group I	Group II
M3	13.20±1.3 cps	18.00±1.2 cps
M4	14.40±1.2 cps	19.20±1.6 cps

formulations
and Group II

were found to have rather low viscosities, ranging from to cps. The viscosity of the micro emulsion increased with increasing concentration of the surfactant.

Table 3.9: Data of Viscosity of Group I and Group II.

g. Refractive Index (RI):

The refractive index was carried out by Abbe refractometer was found to be in the range of 1.45 to 1.49 of Group I to Group II formulations along with the plain formulation which is closely related to the RI of water.

Formulation Code	Group I	Group II
M3	1.4971	1.4591
M4	1.4886	1.4692

Table 3.10: Data of Refractive Index of Group I and Group II.

h. % Transmittance:

Formulation Code	Group I	Group II
M3	93.28±0.04	98.40±0.01

The percent transmission was found to be in the range of 98.23 % to 99.37 % for formulations of Group I and Group II along with the plain formulation which confirms good transparent nature of formulations.

Table 3.11: Data of % Transmittance of Group I and Group II.

i) Cloud Point Measurement:

Cloud point of prepared SMEDDS formulations Group I and Group II was found to be higher than 70°C, which indicates that micro emulsion will be stable at physiological

Formulation	Particle Size (nm)	Zeta Potential
Group I		
M3	219	88°C-40.78
M4	217	-41.95
Group II		
M3	191	-45.60
M4	215	-43.60

temperature without risk of phase separation.

Table3.12: Data of Cloud Point of Group I and Group II.

j) Particle Size Determination:

Particle Size Determination Particle size of the prepared Valsartan microemulsion was determined using Dynamic Light Scattering (DLS) method. Particle size determination results for all the prepared batches of Valsartan microemulsion are presented in the Table 3.13 and all the Graph obtained are reported in the Figure 3.7

Table 3.13: Data of Particle Size and Zeta Potential values of Group I and Group II

k) Zeta Potential:

Zeta Potential of the prepared Valsartan microemulsion was determined using Light Scattering method. Zeta Potential results for all the prepared batches of Valsartan microemulsion are presented in the Table 3.13 and all the Graph obtained are reported in the Figure 3.8

I) Polydispersity Index (PI):

Polydispersity Index (PI) of the prepared microemulsion was determined using Dynamic Light Scattering (DLS) method. Result of Polydispersity Index (PI) is reported in the Table 3.14 and Figure 3.7

Formulation Code	Polydispersity Index
Group I	
M3	0.244
M4	0.285
Group II	
M3	0.264
M4	0.276

Table 3.14: Polydispersity Index of Group I & Group II

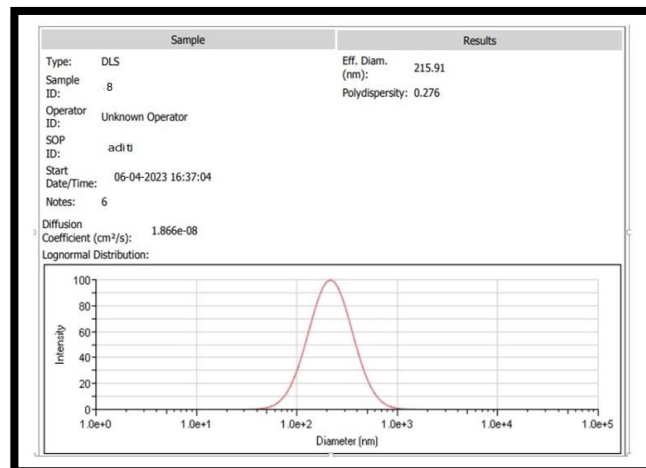
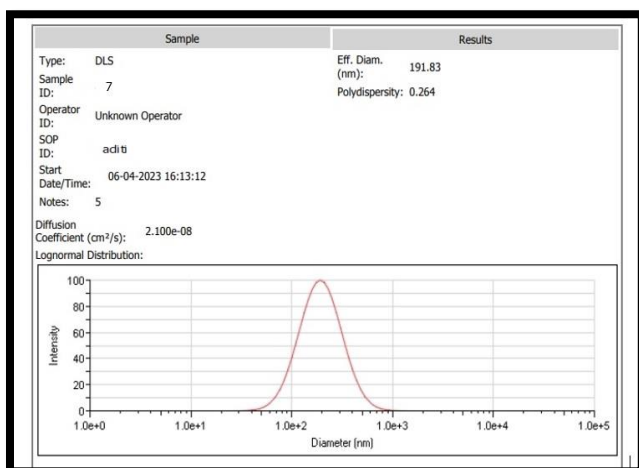
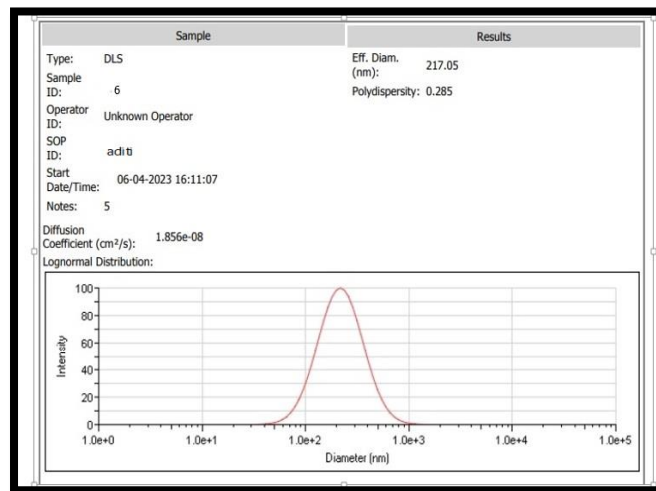
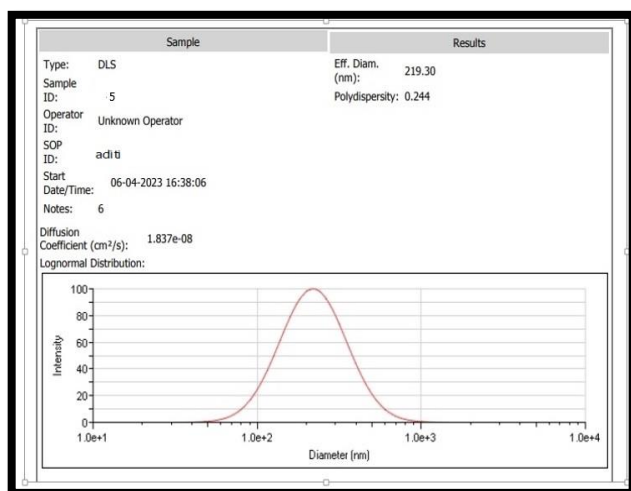


Figure 3.7: Particle Size Analysis of all the Formulation.

Where, Sample 5 and Sample 6 indicate Group I M3 and M4 respectively whereas Sample 7 and Sample 8 indicate Group II M3 and M4 respectively.

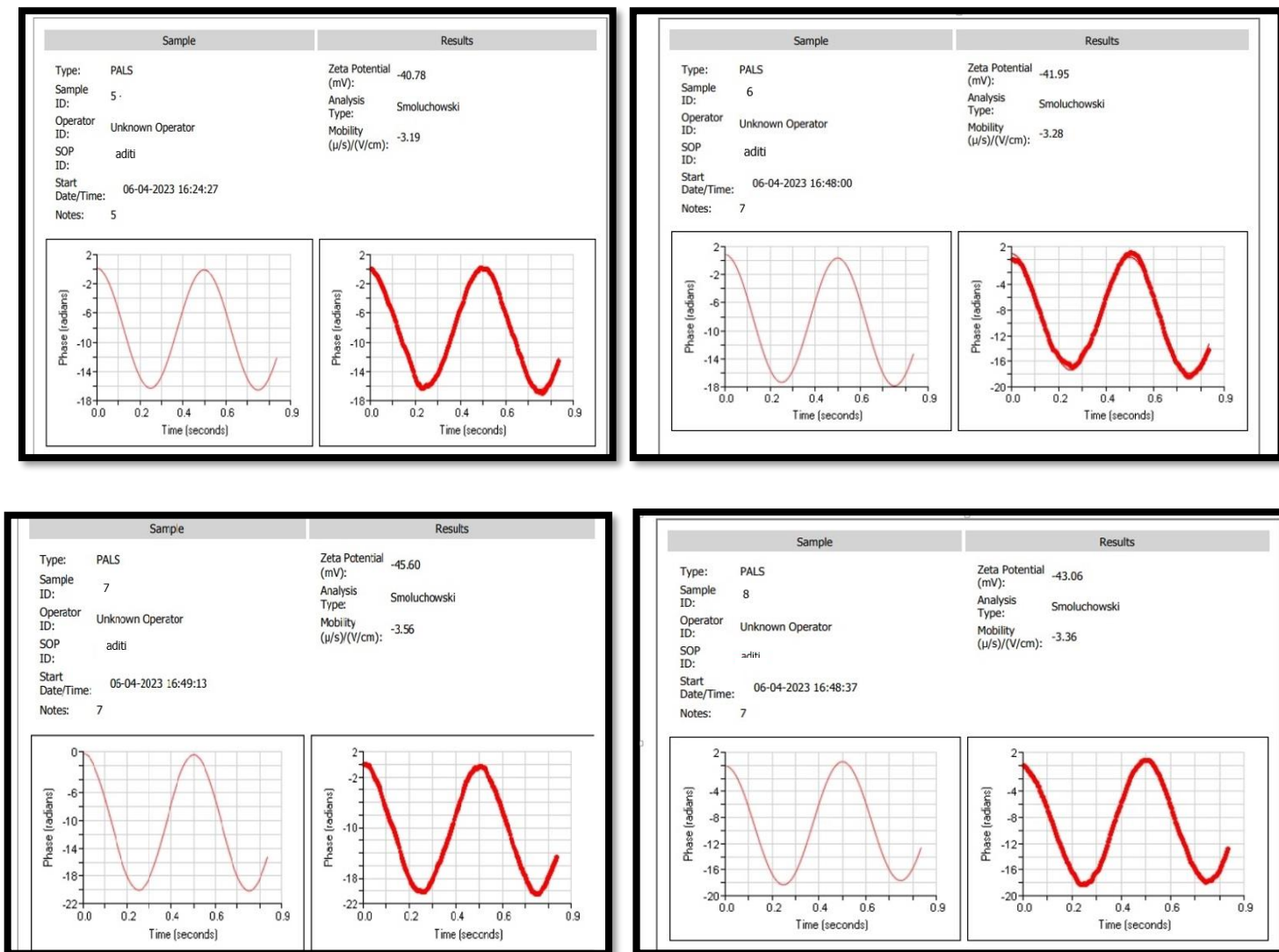


Figure3.8: Data of Zeta Potential of Group I & Group II

Where, Sample 5 and Sample 6 indicate Group I M3 and M4 respectively whereas Sample 7 and Sample 8 indicate Group II M3 and M4 respectively.

m) *in-vitro* drug release:

The *in-vitro* drug release study for the batches for Valsartan drug and microemulsion was carried out using paddle method (USP apparatus II). Data for *in-vitro* drug release study is presented in the following Table and the graphical representation of Percentage Drug Release vs. Time graph is shown in the Figure and. The release study was carried out in both 0.1N HCl and 6.8 pH phosphate buffer. The data showed that release of valsartan was faster in phosphate

buffer of pH 6.8 than other media. The pH-dependent solubility of drug can be responsible for higher release.

➤ *in-vitro* drug release in 0.1 N HCl :

Time (min)	% Drug Release		
	Valsartan	SMEDDS(1:1)	SMEDDS(2:1)
0	0	0	0
5	15.1±1.2	17.53±0.89	22.71±0.94
15	20.25±1.04	22.19±2.5	24.69±0.32
30	23.7±1.05	24.12±0.75	26.56±0.26
45	25.96±1.1	28.99±0.23	29.65±0.51
60	29.93±1.02	30.91±1.2	31.89±0.47
75	31.85±1.02	32.90±0.68	33.89±1.3
90	32.79±1.05	34.93±1.01	36.14±2.2
105	34.16±1.01	36.64±1.06	39.61±1.2
120	35.6±1.02	37.57±1.22	41.37±0.79

Table 3.15: Dissolution data for Liquid SMEDDS in 0.1N HCl

➤ *in-vitro* drug release in 6.8 pH Phosphate Buffer:

Formulation	Percent Drug Release				
	0 min	5 min	15 min	30 min	60 min
Valsartan	0	26.26±1.02	28.37±1.28	32.06±1.17	42.39±2.1
M4(Group I)	0	76.34±1.4	78.75±1.02	81.56±1.08	83.79±2.0
M3 (Group II)	0	84.48±1.2	86.26±1.09	90.23±1.10	92.33±2.1

Table 3.16: Dissolution data for Liquid SMEDDS in 6.8 pH buffer

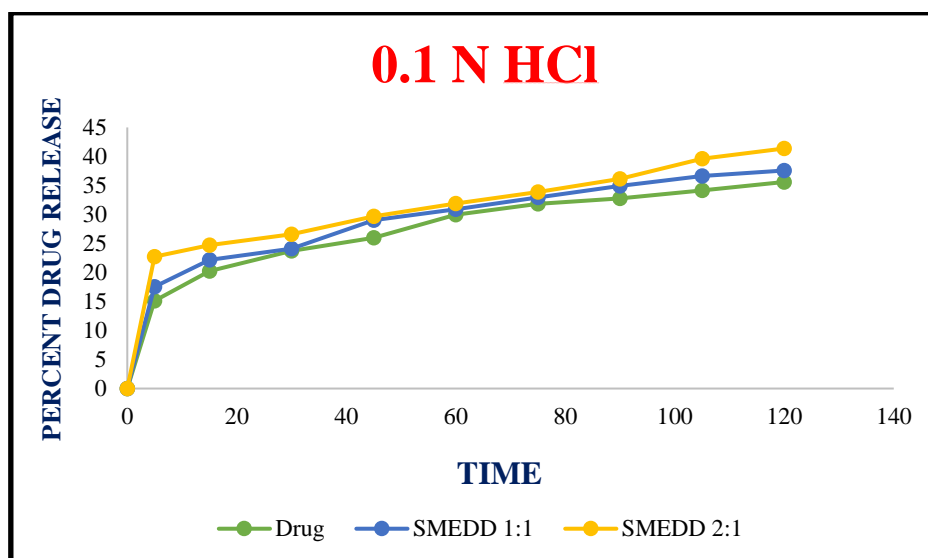


Figure 3.9: In- vitro drug release profile of Liquid SMEDDS and Valsartan (API), M4 (Group I), M3 (Group II) in 0.1N HCl.

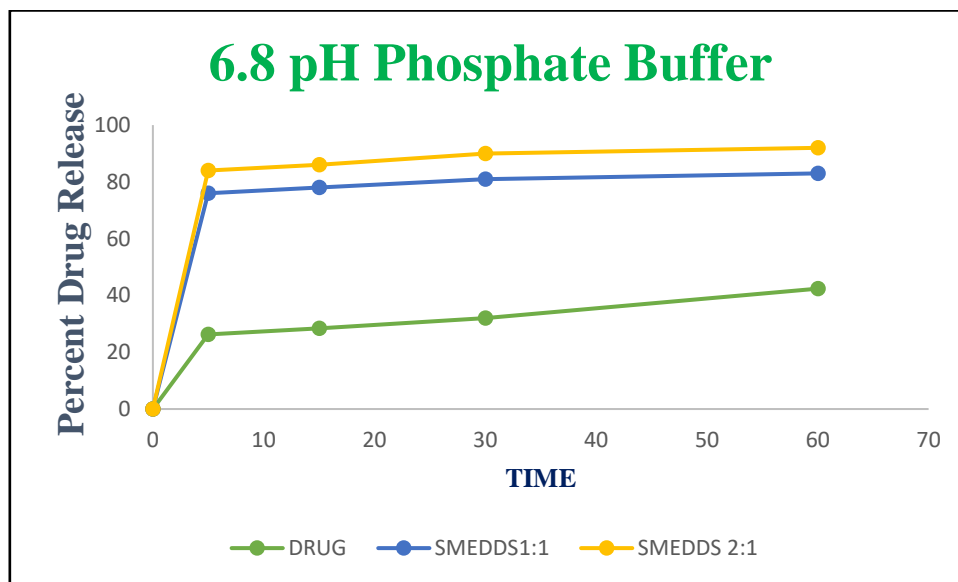


Figure3.10: - In- vitro drug release profile of Liquid SMEDDS and Valsartan (API), M4 (Group I), M3 (Group II) in 6.8 pH phosphate buffer.

3.7. Preparation of Solid SMEDDS:

Solid SMEDDS were prepared as per the composition reported

3.8. Evaluation of Solid SMEDDS Formulations:

1. Micromeritics properties:

The formulation indicated angle of repose < 30 which showed that they had excellent flow properties. Bulk density and tapped density was evaluated to study Carr's index and Hausner's Ratio. Results indicated in the table 3.17.

Formulation Code	Angle of repose	Bulk density	Tapped density	Carr's index	Hausner's ratio
S1	25.64°	0.47m/ml	0.54gm/ml	12.96%	1.12

Table 3.17 : Micromeritic properties of Solid SMEDD.

2. Scanning electron microscopy:

Solid-SMEDDS appeared as smooth surfaced particles, indicating that the liquid SMEDDS is adsorbed onto the Aerosil 200 with a lesser amount of aggregation which showed effective particle size reduction of SOLID SMEDDS as compared to the drug. It is indicated in figure 3.11.

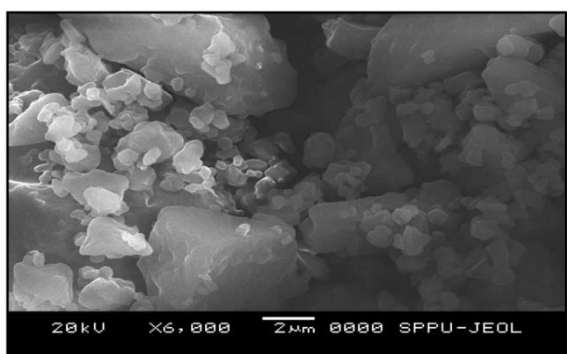


Fig 1: SEM of Valsartan

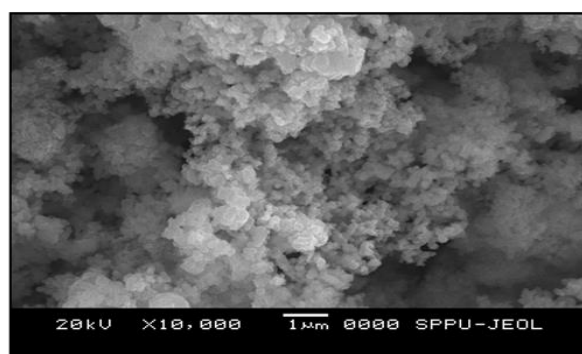


Fig 2: SEM of Solid SMEDDS

Figure 3.11: Scanning Electron Microscopy of Valsartan and Solid SMEDDS.

3. *in-vitro* release studies:

The release study of SOLID SMEDDS was carried out in both 0.1N HCl and 6.8 pH phosphate buffer. The data showed that release of valsartan was faster in phosphate buffer of pH 6.8 than other media. Data for *in-vitro* drug release study is presented in the following Table 3.18 and 3.19 and the graphical representation of Percentage Drug Release vs. Time graph is shown in the Figure 3.12 and 3.13.

➤ *in-vitro* drug release 0.1 N HCl:

Time (min)	% Drug Release of Solid SMEDD
0	0
5	20.505±0.76
15	23.225±1.02
30	25.948±1.05
45	29.409±1.1
60	30.668±1.02
75	32.664±1.03
90	34.661±1.02
105	36.661±0.49
120	39.644±1.03

Table 3.18: Dissolution data for Solid SMEDDS in 0.1N HCl.

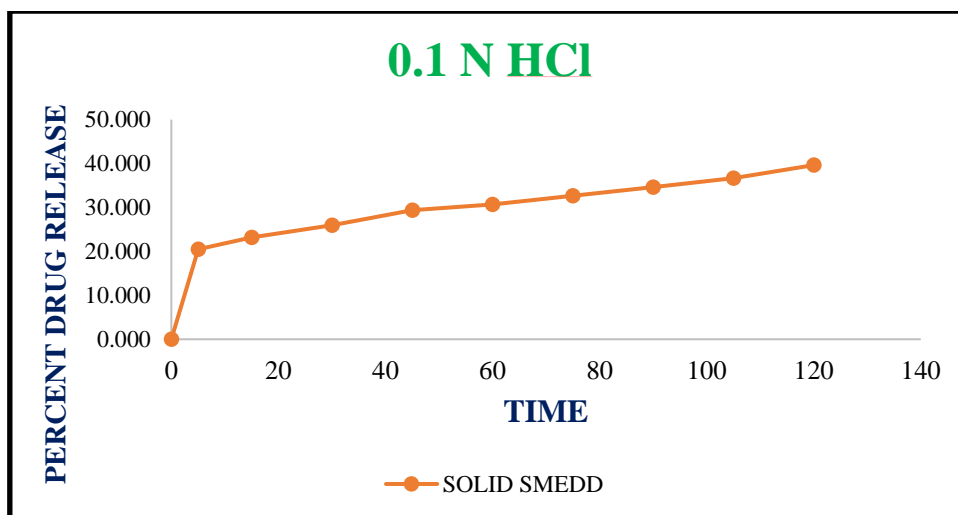


Figure 3.12: - In- vitro drug release profile of Solid SMEDDS in 0.1N HCl.

➤ in-vitro drug release 6.8 pH phosphate buffer:

Formulation	Percent Drug Release				
S1	0 min	5 min	15 min	30 min	60 min
	0	83.82 ±1.02	85.99 ±1.05	88.99 ±2.1	91.58 ±1.02

Table 3.19: Dissolution data for Solid SMEDDS in 6.8 pH phosphate buffer

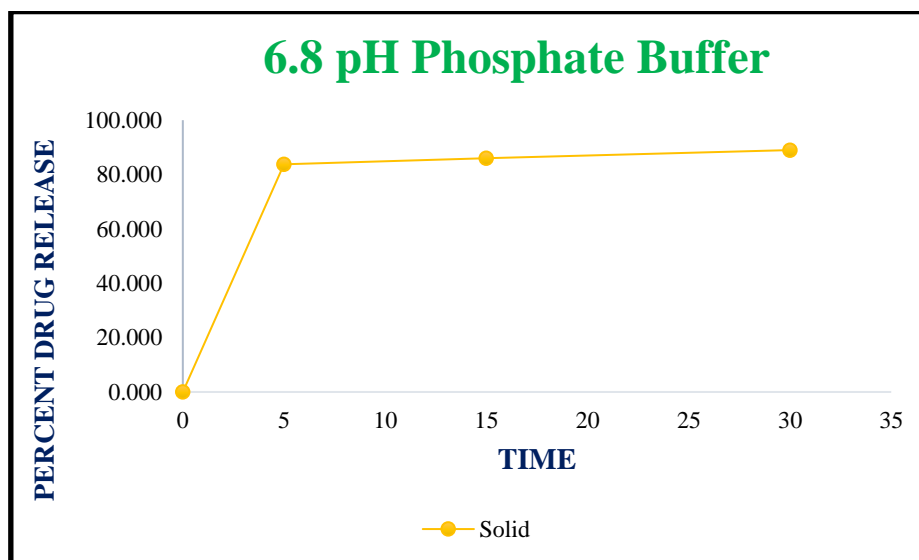


Figure 3.13: In- vitro drug release profile of Solid SMEDDS in 6.8 pH phosphate buffer.

4. X-ray diffraction study:

The diffraction pattern of valsartan revealed several sharp high-intensity peaks at diffraction angles 2θ suggesting that the drug existed as crystalline material. There were few

characteristic peaks of valsartan with a considerable reduction in the peak intensity. This diminished peak suggests conversion of the drug into an amorphous form. This marked reduction in peak intensities provides may increase dissolution rates of Solid-SMEDDS preparation. It is indicated in figure 3.14.

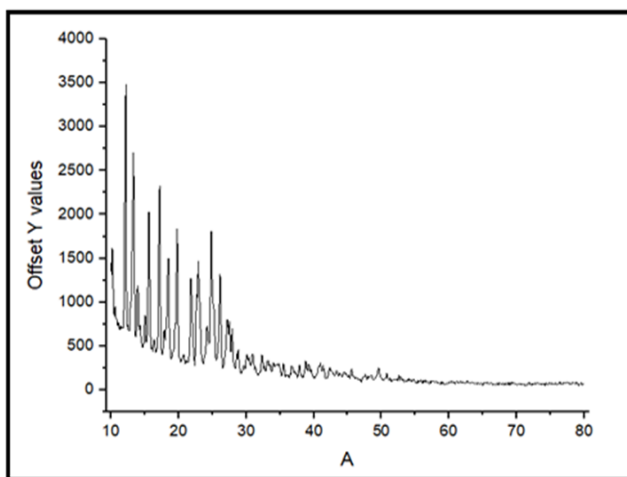


Fig: X-ray Diffraction of Valsartan

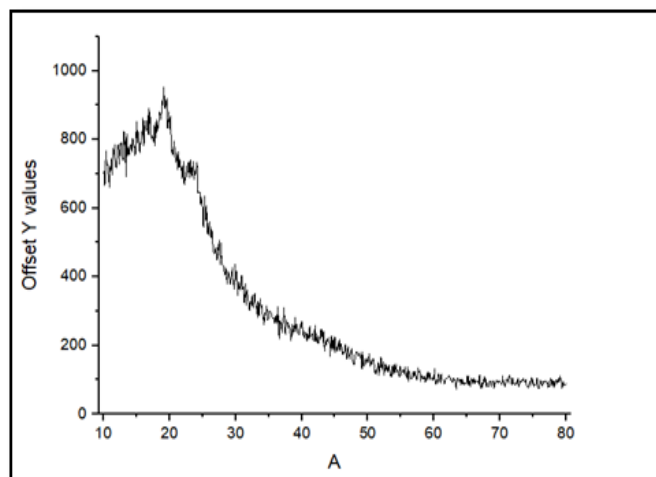


Fig: X-ray Diffraction of Solid SMEDDS

Figure 3.14: X ray diffraction of Valsartan and Solid SMEDDS

5. Drug Content:

The drug content of Solid SMEDDS formulation was found at 248 nm. The data is shown in the Table no 3.20

Formulation Code	Drug Content
S1	97.73±1.05

Table 3.20: Drug Content of Solid SMEDDS formulation.

6. FTIR Spectra:

The scanning range was 400 to 4000 cm^{-1} and resolution was 1cm^{-1} . So it can be concluded that the spectra of pure drug valsartan and the Solid SMEDDS spectrum, that all the characteristic peaks of valsartan were present in the Solid SMEDDS spectrum.

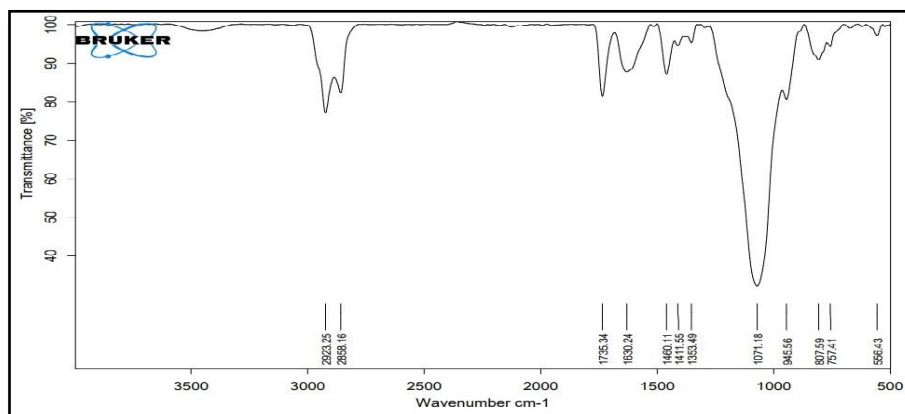


Figure3.15: FT-IR Spectra of Solid SMEDDS.

7. Stability study:

The results of stability studies depicted that the solid-SMEDDS formulation remained clear even after a period of 3 months at temperature $25^{\circ}\text{C} \pm 2^{\circ}\text{C}$ & $60\% \pm 5\%$. All the formulations were found to be consistent with respect to their drug content and appeared clear on reconstitution.

Temperature & Humidity	Month	Appearance	Drug Content
$25 \pm 2^{\circ} \& 60\% \pm 5\%$	0	Clear	97.73 ± 1.5
$25 \pm 2^{\circ} \& 60\% \pm 5\%$	1	Clear	97.56 ± 1.2
$25 \pm 2^{\circ} \& 60\% \pm 5\%$	2	Clear	97.49 ± 2.5
$25 \pm 2^{\circ} \& 60\% \pm 5\%$	3	Clear	97.37 ± 2.1

Table 3.21: Stability Study of S-SMEDDS

CONCLUSION:

In the present study, Valsartan an antihypertensive drug who has low aqueous solubility was formulated in the form of Self-Microemulsifying Drug Delivery System (SMEDDS) to increase its solubility which will result in enhancement in Dissolution Rate and Bioavailability of the drug. Firstly the solubility was checked in various oil, surfactant and co-surfactant. Liquid SMEDDS were formulated from which the optimized micro emulsion formulation M3 containing Castor oil as oil, Tween 60 as surfactant, and Kollisolv PG as co-surfactant and distilled water was a transparent, clear and low viscosity system, with particle size 191 nm. The optimized formulation was converted into solid by adsorption on a Solid Carrier (Aerosil 200). The *in-vitro* release of drug was checked in both the medium 0.1N HCl and 6.8 pH Phosphate buffer. It was found out that valsartan has more solubility in the 6.8 pH phosphate buffer. Optimized SMEDDS showed good in vitro release which is increased more than 90%. Solid-SMEDDS were preferred over SMEDDS in terms of stable dosage form. It can be concluded that valsartan solid-SMEDDS offer more predictable and more extensive drug release/absorption than the corresponding conventional formulations. The results from the study showed the utility of solid-SMEDDS to enhance solubility and bioavailability of sparingly soluble compounds like valsartan, which can be helpful to reduce dose and related side effects of the drug. The present research work successfully illustrates the prospective advantage of Solid-SMEDDS for the delivery of poor aqueous soluble compounds.

ACKNOWLEDGEMENT:

The authors would like to acknowledge PDEA's Shankarrao Ursal College of Pharmaceutical Sciences and Research Centre, Pune, Maharashtra, India for offering all vital help to accomplish this work efficaciously.

REFERENCE:

1. Johanna Mercke Odeberg, Peter Kaufmann, Karl-Gunnar Kroon *et al.* Lipid drug delivery and rational formulation design for lipophilic drugs with low oral bioavailability, applied to cyclosporine. *Int.J.Pharm.* 20; 2003:375-382.
2. Sandeep Kalepu, Mohanvarma Manthina, Veerabhadraswamy Padavala. Oral lipid –based drug delivery systems – an overview. *Acta Pharmaceutica Sinica B.* 3(6);2013: 361-372
3. Date AA, Nagarsenkar MS. “Design and evaluation of self-nanoemulsifying drug delivery system(SNEDDS) for cefpodoxime proxetil”. *Int. J. Pharm.* 329;2007:166-172.
4. Aditi R. Beldar, Sujit S. Kakade, Ashok V. Bhosale, Self-Micro-emulsifying Drug Delivery System: A Promising Technique to Enhance the Solubility of Lipophilic Drugs" Published in *International Journal of Trend in Scientific Research and Development (ijtsrd)*, ISSN: 2456-6470, Volume-7 | Issue-3, June 2023, pp.133-144
5. Bhondve Riya R, Kakade Sujit S, Bhosale Ashok V "A Review on Solid Self Micro-emulsifying Drug Delivery System: A Method for Enhancement of Oral Bioavailability" Published in *International Journal of Trend in Scientific Research and Development (ijtsrd)*, ISSN: 2456- 6470, Volume-7 | Issue-3, June 2023, pp.145-155.
6. S. Nazzari and M. A. Khan, “Controlled release of a self-emulsifying formulation from a tablet dosage form: stability assessment and optimization of some processing parameters,” *International Journal of Pharmaceutics*, vol. 315, no. 1-2, pp. 110– 121, 2006.
7. P. Balakrishnan, B.-J. Lee, D. H. Oh *et al.*, “Enhanced oral bioavailability of Coenzyme Q10 by self-emulsifying drug delivery systems,” *International Journal of Pharmaceutics*, vol. 374, no. 1-2, pp. 66–72, 2009.
8. Flesch G., Muller Ph., Lloyd P. Absolute bioavailability and pharmacokinetics of valsartan, an angiotensin II receptor antagonist in man. *Eur J Clin Pharmacol* 1997; 52: 115-120.
9. Saydam, Takka. Bioavailability File: Valsartan. *FABAD J Pharm Sci* 2007; 32:185-196.
10. Demiralay EC., Cubuka B., Ozkan SA., Alsancak G. Combined effect of polarity and pH on the chromatographic behavior of some angiotensin II receptor antagonists and optimization of their determination in pharmaceutical dosage forms. *J Pharm Biomed Anal* 2010; 53: 475-482.
11. Jayaraj AA, Keirns JJ. Lipid-based delivery systems for improving the bioavailability and lymphatic transport of a poorly water soluble LTB₄ inhibitor. *J Pharm Sci.*1998;87: 164–9.
12. Shailesh T. Prajapati Harsh A, Joshi Chhaganbhai N. Patel. (2013)., Preparation and Characterization of Self-Micro emulsifying Drug Delivery System of Olmesartan medoxomil for Bioavailability Improvement., *Journal of Pharmaceutics*. 2013; 2: 01-09.
13. Sheikh S, Shakeel F, Talegaonkar S, Ahmad FJ, Khar RK and Ali M(2007). Development and bioavailability assessment of ramipril nanoemulsion formulation. *Eur J Pharm Biopharm*, 66, 227–243.

14. Kang BK, Lee JS, ChonSK, Jeong SY, Yuk SH, Khang G, Lee HB, Cho SH.(2004) Development of selfmicroemulsifying drug delivery systems (SMEDDS) for oral bioavailability enhancement of simvastatin in beagle dogs. *International Journal of Pharmaceutics*, 274: 65-73.
15. Atef E, Belmonte AA. Formulation and in-vitro and in-vivo characterization of a Phenytoin self-emulsifying drug delivery system. *Eur J Pharm Sci* 2008; 35:257-263.
16. Hosmer J, Reed R, Bentley MV, Nornoo A, Lopes LB. Microemulsions containing medium-chain glycerides as transdermal delivery systems for hydrophilic and hydrophobic drugs. *Aaps Pharmscitech*. 2009 Jun;10:589-96.
17. More HN, Hazare AA. *Practical Pharmaceutics (Physical pharmacy)*. 1st ed. Kolhapur: Manas Prakashan; 2004. p. 86-105.
18. Gupta A.K, Mishra D.K and Mahajan S.C. Preparation and in-vitro evaluation of self-emulsifying drug delivery system of antihypertensive drug, Valsartan. 2011;2 (3): 633-639.
19. Singh SK, Vuddanda PR, Singh S, Srivastava AK. A comparison between use of spray and freeze drying techniques for preparation of solid self-microemulsifying formulation of valsartan and in vitro and in vivo evaluation. *BioMed research international*. 2013 Jan 1;2013.
20. Shahu SG, Wadetwar RN, Dixit GR. Development of microemulsion for solubility enhancement of poorly water soluble drug valsartan. *Int. J. Pharm. Sci. Rev. Res*. 2013;22(2):246-51.
21. Patel KB, Patel B. Enhancement of oral bioavailability of valsartan by using solid self-emulsifying drug delivery system. *International Journal of Universal Pharmacy and BioSciences*. 2014; 3(3):141-56.
22. Mahajan HD, Shaikh T., Bhaviskar D. Design and development of self-emulsifying drug delivery system. *IJPS* 2011; 3 163-166.
23. Khoo SM, Humberstone AJ, Porter CJH, Edwards GA., Charman WN.(1998) Formulation design and bioavailability assessment of lipidic self-emulsifying formulations of halofantrine. *International Journal of Pharmaceutics*, 167, 155-164.
24. Srinivas C, Sagar SV, Enhancing the Bioavailability of Simvastatin Using Micro emulsion Drug Delivery System, *Asian Journal of Pharmaceutical and Clinical Research*, 5, 2012, 134-139.
25. Shweta Gupta, Sandip Chavhan, Kruthika K Sawanth. Self nanoemusifying drug delivery systems for adefovir-dipivoxil: Design, characterization, in vitro and ex vivo evaluation. *Colloids and Surfaces A: Physiochem Eng Aspects*. 392; 2011:145-155.
26. K. Khedekar, and S. Mittal, "Self-emulsifying drug delivery system: A review, " *International Journal of Pharmaceutical Science and Research*, vol. 4, no. 12, pp. 4494-4497, 2013.
27. Ghosh PK, Majithiya RJ, Umrethia ML, Murthy RSR, Design and Development of Microemulsion Drug Delivery System of Acyclovir for Improvement of Oral Bioavailability, *American Association of Pharmaceutical Scientists*, 7, 2006, E1- E6

28. Madhav S, Gupta D, A Review On Micro emulsion Based System, International Journal of Pharmaceutical Sciences and Research, 2, 2011, 1888-1899.
29. Shin DJ, Chae BR, Goo YT, Yoon HY, Kim CH, Sohn SI, Oh D, Lee A, Song SH, Choi YW. Improved dissolution and Oral bioavailability of valsartan using a solidified Supersaturable self-microemulsifying drug delivery system containing Gelucire® 44/14. Pharmaceutics. 2019 Jan 31;11(2):58.
30. Prashant H. Khade , Gururaj Shahabade , Sachin V.Kotwal , Priyanka D. Borude , Jyoti B.Darkunde, Harshal M.Shinde, Self-Emulsifying Drug Delivery System (SEDDS) for Enhancement of Solubility and Photostability of Amlodipine Besilate, doi: [10.31838/ecb/2023.12.si4.168](https://doi.org/10.31838/ecb/2023.12.si4.168)
31. Dixit AR, Rajput SJ, Patel SG. Preparation and bioavailability assessment of SMEDDS containing valsartan. AAPS pharmscitech. 2010 Mar;11:314-21.
32. Ponnaganti H, Abbulu K. Enhanced dissolution of repaglinide: SMEDDS formulation and in-vitro evaluation. Research Journal of Pharmacy and Technology. 2014;7(11):1246-52.
33. Harshal M. Shinde , Prashant H. Khade , Ashok V. Bhosale, Aditi R. Beldar , Riya R. Bhondve , Rajratna D. Gaikwad, Preparation, Evaluation and Optimization of Nanosuspension of Poorly Water-Soluble Rosuvastatin Calcium, doi: [10.48047/ecb/2023.12.si6.177](https://doi.org/10.48047/ecb/2023.12.si6.177)
34. Jaiswal P, Aggarwal G, Harikumar SL, Singh K. Development of self-microemulsifying drug delivery system and solid-self-microemulsifying drug delivery system of R. International journal of pharmaceutical investigation. 2014 Oct;4(4):195.
35. Taha E I, Saidam S A, Samy A M, Khan M A. Preparation and in-vitro characterization of a eutectic based semisolid self nanoemulsified drug delivery system of all trans-retinol acetate. Int J Pharm 2004; 285: 247-263.
36. Rai S, Yasir M. Cinnarizine loaded lipid based system: preparation, optimization and in-vitro evaluation. IOSR Journal of Pharmacy. 2012 Sep;2(5):47-56.
37. Bhagwat DA, Souza JI. Formulation and evaluation of solid self micro emulsifying drug delivery system using aerosil 200 as solid carrier. International current pharmaceutical journal. 2012 Nov 1;1(12):414-9.
38. Bhattacharya S, Prajapati BG. Formulation approach of self-emulsifying drug delivery system. Int J Pharm Formula 2015;6(1):1-6.
39. Anand S. Formulation & development of Self-Micro Emulsifying Drug Delivery System (SMEDDS) for oral bioavailability enhancement of a low soluble anti-diabetic drug: gliclazide.
40. Albekery MA, Alharbi KT, Alarifi S, Ahmad D, Omer ME, Massadeh S, Yassin AE. Optimization of a nanostructured lipid carriers system for enhancing the biopharmaceutical properties of valsartan. Digest journal of Nanomaterials and Biostructures. 2017 Apr 1;12(2):381-9.
41. Poudel BK, Marasini N, Tran TH, Choi HG, Yong CS, Kim JO. Formulation, characterization and optimization of valsartan self-microemulsifying drug delivery system

using statistical design of experiment. Chemical and pharmaceutical bulletin. 2012 Nov 1;60(11):1409-18.



Preparation, Evaluation and Optimization of Nanosuspension of Poorly Water-Soluble Rosuvastatin Calcium

Harshal M. Shinde ^{1*}, Prashant H. Khade ², Ashok V. Bhosale ³,
Aditi R. Beldar ¹, Riya R. Bhondve ¹, Rajratna D. Gaikwad ⁴

¹ Research Scholar, Department of Pharmaceutics, PDEAs Shankarrao Ursal College of Pharmaceutical Sciences and Research Centre, Pune, Maharashtra, India.

² Assistant Professor, Department of Pharmaceutics, PDEAs Shankarrao Ursal College of Pharmaceutical Sciences and Research Centre, Pune, Maharashtra, India.

³ Principal, Department of Pharmaceutics, PDEAs Shankarrao Ursal College of Pharmaceutical Sciences and Research Centre, Pune, Maharashtra, India.

⁴ Research Scholar, Department of Pharmaceutical of Analysis, PDEAs Shankarrao Ursal College of Pharmaceutical Sciences and Research Centre, Pune, Maharashtra, India.

For Correspondence -

Harshal M. Shinde

Research Scholar,

Department of Pharmaceutics,

PDEAs Shankarrao Ursal College of Pharmaceutical Sciences and Research Centre, Pune – 411014,

Maharashtra, India

E-mail Id: shindeharshal006@gmail.com

ABSTRACT - Rosuvastatin calcium, an antihyperlipidemic agent with poor water solubility which comes under BCS Class II with 20% bioavailability, was chosen for the study. The present study focuses on Preparation, Evaluation and Optimization of Nanosuspension of Poorly Water-Soluble Rosuvastatin Calcium. Rosuvastatin Calcium Nanosuspension was prepared used Solvent-Anti-Solvent Precipitation method. Experimental Design was obtained using Design Expert Software. 10 Batches of Rosuvastatin Calcium Nanosuspension was prepared. Interaction between Independent factor and dependent factor was studied. Optimization was carried out and Batch B9 was selected as the Optimized Batch. Batch B9 was Prepared using 1:10 Ratio of Solvent-Anti-Solvent, 6 % Concentration of Stabilizer was used and it was sonicated for 10 minutes. The Results of the Formulation B9 was also satisfying. The Particle Size of the Optimized batch was found to be 351.64 nm, Zeta Potential was -20.21 mV and % Drug Release was 88.52 % in 60 minutes. Stability studies of B9 was carried out and no significant growth in Particle Size was found which indicates Good Stability. Comparison of *in-vitro* % Drug Release of Pure Drug and Optimized Batch of Rosuvastatin Calcium Nanosuspension was carried. Optimized Batch B9 showed 88.52% Drug Release in 60 min while Pure Drug Showed 26.29% drug Release in 60 min.

KEYWORDS – Nanosuspension; Solubility; Particle Size; Zeta Potential; Drug Release.

1. INTRODUCTION –

During development of new formulation, the parameters of the drug which are considered are aqueous solubility, stability, temperature, humidity, compatibility with solvent and excipient. The most important parameter is aqueous solubility (1). In 1995 to 2022, many drugs have been discovered and approved from which 46% of new drug belongs to class IV according to the BCS classification and only 9% of drug belongs to Class I of BCS classification. Drugs which belong to Class IV are poorly soluble in aqueous medium as well as in non – aqueous medium and have low permeability (2). As most of the drugs have low solubility, low bioavailability and low dissolution rate has been observed and the effectiveness of the drug is also affected (3).

As poorly soluble drug have major problem like poor bioavailability, lack of dose response proportional, suboptimal dosing, etc. When formulating such drugs, harsh excipient for solubility enhancement are used but they are not orally accepted. For minimizing this problem and to improve drugs property various

approaches have been made. In Last few decades, the main goal in drug development is to improve the bioavailability of the drug. There are many conventional techniques which were used to enhance the effectiveness of the drug³. Conventional methods includes Micronization, Solubilization using co-solvent, Salt formation technique, Precipitation technique, Oil solution, Solid dispersion, Emulsion, Milling technique, Complexation, Supercritical processing, etc.(1,2). The most common technique is Micronization (particle size reduction). Micronization is a technique where surface area of the drug particles is increased by particle size reduction. In which particle size ranges between 2 μm to 5 μm , but Dissolution rate and Absorption rate in the GI tract is not increase to excepted rate. The common disadvantage of Size reduction techniques is deterioration of the drug particles and their properties. Due to which electrostatic charge is enhanced and development of suspicious formulation may take place. Conventional methods also have other disadvantages too which are broad particle size distribution, contamination of formulation, crystal structure variation, uncontrolled particle morphology and many more. To tackle or to minimize the disadvantages of conventional technique use of advanced technique like Nanotechnology is being carried out from last few years (3).

Nano technique/technology is used to solve the problem which is arise due to poor solubility of the drug. Nano is a Greek word which means 'Small'. By the use of Nanotechnology, we can formulate drugs which belongs to Class II and Class IV which have major problems of solubility in both aqueous and non-aqueous medium. Nanotechnology is safe, simple and mostly importantly the advantages are more in compare to conventional methods (4). Nanosuspension is the formulation which contains submicron colloidal Nano sized drug particle which are stabilized by use of suitable surfactants. They are also defined as biphasic liquid dosage form in which pure drug are suspended or dispersed in aqueous medium intended for oral, topical or parental administration. Particle size distribution in Nanosuspension is less than 1micron and the average particle size is 1 μm . Furthermore, in Nanosuspension, the pure drug is maintained in its crystalline form with particle size less than 1 μm . Due to decrease in drug particle size, surface area increases which leads to enhancement in the dissolution rate and bioavailability (5). Nanotechnology also helps us to administer poorly soluble drug intravenously as the particle size is less, due to which there are minimum chances of blockage of blood capillaries (2). Most important advantage of Nanosuspension is it prevent Oswald ripening as there is absence of particles with large amount of difference in their sizes. In Oswald repining, there is movement of molecules from high concentration region (around small particle) to low concentration region (around large particle). When smaller particles in Nanosuspension moves towards larger particles super saturation occurs and due to aggregation of smaller particles and larger particles, large crystals (micro particles) formation takes place. Stability is an essential parameter which is considered in any type of biphasic liquid dosage form. The stability of Nanosuspension is high in comparison to Micro-Suspension due to uniform particle size. Nanosuspension also can be incorporated in the solid matrix by preforming lyophilization and spray drying techniques (5).

The attempt of this study was to prepare Nanosuspension of Poorly Water Soluble Rosuvastatin Calcium by Solvent-Antisolvent Precipitation technique which may enhance the Solubility and Dissolution Rate of the Drug and to find out suitable Ratio of Solvent: Anti-solvent, Concentration of Stabilizer and Sonication Time to prepare Nanosuspension of Rosuvastatin Calcium with Smaller Particle Size, perfect Zeta potential and faster Percentage Drug Release.

2. MATERIAL AND METHOD

2.1. MATERIALS –

Rosuvastatin calcium, an Antihyperlipidemic agent was received as gift sample from Lupin Limited, Pune. All other excipients and reagents such as Dimethyl Sulfoxide (DMSO) was used as an Organic Solvent, Polyvinylpyrrolidone (PVP K30) used as a Stabilizers and Distilled water used as an Anti-solvent all of these were obtained from COSMO CHEM, Pune.

2.2. METHOD OF PREPARATION OF NANOSUSPENSION OF ROSUVASTATIN CALCIUM

Nanosuspension was prepared using Anti-Solvent precipitation technique. 15 mg of API Rosuvastatin calcium was dissolved in 1 mL of Dimethyl Sulfoxide (DMSO) which results in formulation of drug Solution (Organic Phase). For Preparation of Stabiliser Solution (Aqueous Phase), Polyvinylpyrrolidone (PVP K30) of definite amount was dissolved in specific amount of distilled water. Rapid mixing of aqueous phase and organic phase was carried out. This mixture was then stirrer using magnetic stirrer at 1000 rpm for 5 minutes. After

Stirrer is completed, then the suspension was sonicated for sufficient period of time to obtain Nanosuspension (6-32).

2.3. EXPERIMENTAL DESIGN USING FACTORIAL DESIGN

The Experimental Design for formulating Nanosuspension of Rosuvastatin Calcium was done using Factorial design method. The three Level Factorial design was generated using Design expert stat ease software (Version 13.0). It is more advantageous because it required fewer experimental than a full factorial design. In this design, effect of independent factor on Dependant factor (Response) was studied. Ratio of Solvent: Anti-solvent (X1), Concentration of stabilizer (X2), and Sonication Time(X3) were selected as the three independent factor for study. Each factor was evenly set at low, medium, and high levels as shown in the Table 1. Particle Size (Y1), Zeta Potential (Y2), and % Drug Release (Y3) were selected as the Dependent Factors (Response) (33-44).

Table 1 – Independent Factors with their Level

Independent Factor	Unit	Variable Level		Actual Value
Ratio of S:AS (X1)	Ratio (mL)	Low	-1	1:10
		Medium	0	-
		High	+1	1:50
Concentration of stabilizer (X2)	% (w/v)	Low	-1	2
		Medium	0	6
		High	+1	10
Sonication Time (X3)	Minutes	Low	-1	8
		Medium	0	10
		High	+1	12

2.4. EVALUATION OF PREPARED ROSUVASTATIN CALCIUM NANOSUSPENSION

1. Appearance

The prepared Nanosuspension was inspected visually for clarity, colour and presence of any particulate matter.

2. Particle Size Determination

Particle size of the prepared Nanosuspension was determined using Dynamic Light Scattering (DLS) method. For DLS particle sizing, the sample needs to be crystal clear to very slightly hazy. If the solution is white or too hazy, it should be diluted further before attempting a DLS size measurement. When the solution is ready for analysis and transfer it in the cuvette, care should be taken to avoid bubbles which are formed on the walls of the cuvette. Slowly tilting or tapping the cuvette on a hard surface may help also. Once the solution was homogenous and ready for DLS measurement, the cuvette containing the solution was placed in the instrument. The instrument was run and solution was analysed for particle size (45-47).

3. Zeta Potential

Zeta Potential of the prepared Nanosuspension was determined using Light Scattering method. For Zeta Potential determination, the sample needs to be crystal clear. When the solution is ready for analysis and transfer it in the cuvette, care should be taken to avoid bubbles which are formed on the walls of the cuvette. Slowly tilting or tapping the cuvette on a hard surface may also help to remove the bubble formed. Then the electrode was dipped inside the cuvette containing sample solution. Care should be taken to avoid bubbles in between the electrodes. The cuvette containing the solution was placed in the instrument. The instrument was run and solution was analysed for Zeta Potential (45, 48-49).

4. Polydispersity Index (PI)

Polydispersity Index (PI) of the prepared Nanosuspension was determined using Dynamic Light Scattering (DLS) method. For DLS method, the sample needs to be crystal clear to very slightly hazy. If the solution is white or too hazy, it should be diluted further before attempting a DLS size measurement. When the

solution was ready for analysis and transfer it in the cuvette, care should be taken to avoid bubbles which are formed on the walls of the cuvette. Slowly tilting or tapping the cuvette on a hard surface may also help to remove the bubbles formed. Once the solution was homogenous and ready for DLS measurement, the cuvette containing the solution was placed in the instrument. The instrument was run and solution was analysed for Polydispersity Index (PI) (45-47).

5. Drug Content

About 1 ml of Rosuvastatin calcium Nanosuspension was taken and then it was diluted upto 10ml with 0.1N HCL. Sample prepared was analysed using UV spectroscopy. Absorbance was observed at 240 nm and drug content was calculated (25).

6. *in-vitro* Drug Release Studies

The *in-vitro* drug release study was carried out using paddle method (USP apparatus II). 900ml of 0.1N HCL was used as the dissolution medium. Temperature was set at $35^{\circ}\text{C} \pm 0.5^{\circ}\text{C}$. The Paddle was rotated at 50 rpm. The sample containing an equivalent 10 mg of Rosuvastatin Calcium was transfer to the Dissolution Medium. 10 ml of Sample was removed for the dissolution medium at 0, 10, 20, 30, 40, 50, 60 min of dissolution time. Sample removed at specific interval of time was analyzed using UV spectroscopy. Absorbance was observed at 240nm and Percentage Drug Release was calculated (32).

2.5. OPTIMIZATION OF ROSUVASTATIN CALCIUM NANOSUSPENSION

Optimization of the formulations was studied by Regular Level Factorial design. Ratio of Solvent: Anti-solvent (X1), Concentration of stabilizer (X2), and Sonication Time (X3) were selected as independent variables and the dependent variables were Particle Size (Y1), Zeta Potential (Y2), and % Drug Release (Y3). The data obtained were treated using Design expert stat ease software and analyzed statistically using Model Graph technique. Various graphs obtained from the Model Graph technique which indicates Interaction Between each independent Factor and dependent Factor (Response) were studied (33-44).

2.6. STABILITY STUDY

The Optimized Batch of Rosuvastatin Calcium Nanosuspension was selected for the stability Study. The Optimize Batch of Rosuvastatin Calcium Nanosuspension was kept at $2-4^{\circ}\text{C}$ in Refrigerator and at Room Temperature Physical Stability of the Nanosuspension was after 5 Months. Rosuvastatin Calcium Nanosuspension was inspected visually for clarity, any kind of colour change. The Nanosuspension was also evaluated for change in Particle size (25-30).

2.7. Comparison of *in-vitro* % Drug Release of Pure Drug and Optimized Batch of Rosuvastatin Calcium Nanosuspension

Comparison of *in-vitro* % Drug Release of Pure Drug and Optimized Batch of Rosuvastatin Calcium Nanosuspension was carried out using paddle method (USP apparatus II). 900ml of 0.1N HCL was used as the dissolution medium. Temperature was set at $35^{\circ}\text{C} \pm 0.5^{\circ}\text{C}$. The Paddle was rotated at 50 rpm. The sample containing an equivalent 10 mg of Rosuvastatin Calcium was transfer to the Dissolution Medium. 10 ml of Sample was removed for the dissolution medium at 0, 10, 20, 30, 40, 50, 60 min of dissolution time. Sample removed at specific interval of time was analyzed using UV spectroscopy. Absorbance was observed at 240nm and Percentage Drug Release was calculated (32).

3. RESULTS AND DISCUSSIONS

3.1 EXPERIMENTAL DESIGN USING FACTORIAL DESIGN

The Three level Factorial design was run using Design Expert Software and Experimental design Layout was obtained as shown in the Table 2, where X1 is the Solvent: Anti-Solvent Ratio (ml), X2 is the Concentration of Stabilizer (% w/v) and X3 is the Sonication time (min).

Table 2 - Experimental Design Layout

Batch Code	Independent Factor					
	Variable Level			Actual Value		
	X1	X2	X3	X1	X2	X3
B1	+1	0	0	1:50	6	10
B2	+1	+1	+1	1:50	10	12

B3	-1	-1	-1	1:10	2	8
B4	+1	+1	-1	1:50	10	8
B5	-1	+1	-1	1:10	10	8
B6	-1	-1	+1	1:10	2	12
B7	+1	-1	-1	1:50	2	8
B8	-1	+1	+1	1:10	10	12
B9	-1	0	0	1:10	6	10
B10	+1	-1	+1	1:50	2	12

Table 2 – Formulation Table

Ingredients	Rosuvastatin Calcium (in mg)	DMSO (in mL)	PVP K30 (in % w/v)	Distilled Water (in mL)
B1	15	1	6	50
B2	15	1	10	50
B3	15	1	2	10
B4	15	1	10	50
B5	15	1	10	10
B6	15	1	2	10
B7	15	1	2	50
B8	15	1	10	10
B9	15	1	6	10
B10	15	1	2	50

3.2. EVALUATION OF PREPARED ROSUVASTATIN CALCIUM NANOSUSPENSION

1. Appearance –

Appearance of the prepared Nanosuspension was inspected visually and all the batches of Rosuvastatin Calcium Nanosuspension were Clear, Colourless, and free from any particulate matters.

2. Particle Size Determination

Particle size of the prepared Rosuvastatin Calcium Nanosuspension was determined using Dynamic Light Scattering (DLS) method. Particle size determination results for all the prepared batches of Rosuvastatin Calcium Nanosuspension are presented in the Table 3 and all the Graph obtained are reported in the Figure 1.

3. Zeta Potential

Zeta Potential of the prepared Rosuvastatin Calcium Nanosuspension was determined using Light Scattering method. Zeta Potential results for all the prepared batches of Rosuvastatin Calcium Nanosuspension are presented in the Table 3 and all the Graph obtained are reported in the Figure 2.

Table 3 – Particle Size Analysis and Zeta Potential of Each Batch of Rosuvastatin Calcium Nanosuspension

Batch No	Particle size (nm)	Zeta Potential (mV)
B1	327.83 nm	-7.57 mV
B2	568.29 nm	-20.29 mV
B3	263.29 nm	-4.45 mV
B4	381.13 nm	-10.81 mV
B5	427.16 nm	-22.13 mV
B6	343.79 nm	-25.06 mV
B7	658.90 nm	-11.19 mV
B8	384.87 nm	-14.64 mV
B9	351.64 nm	-20.21 mV
B10	397.60 nm	-10.77 mV

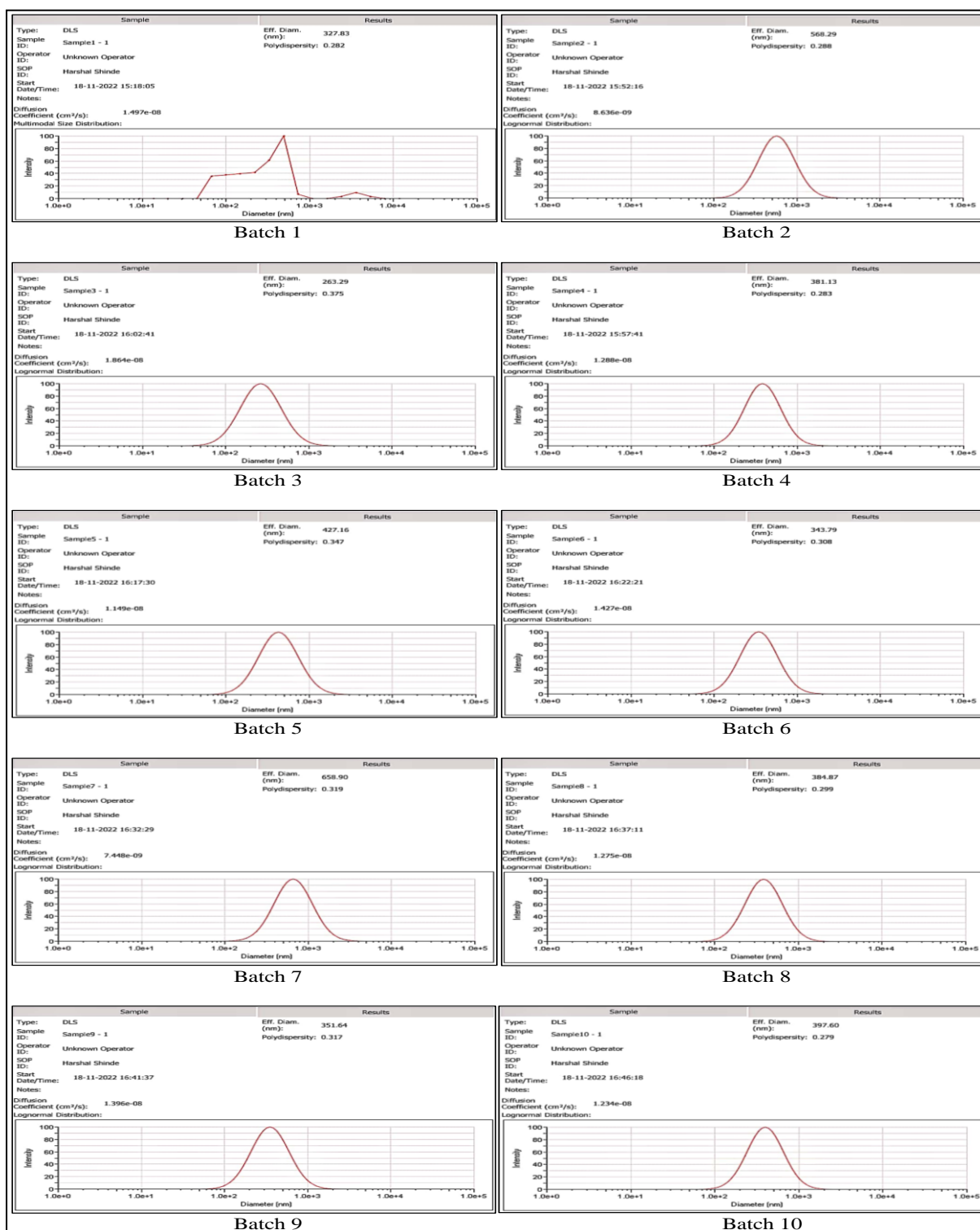


Figure 1 – Particle Size Analysis of all the Batches

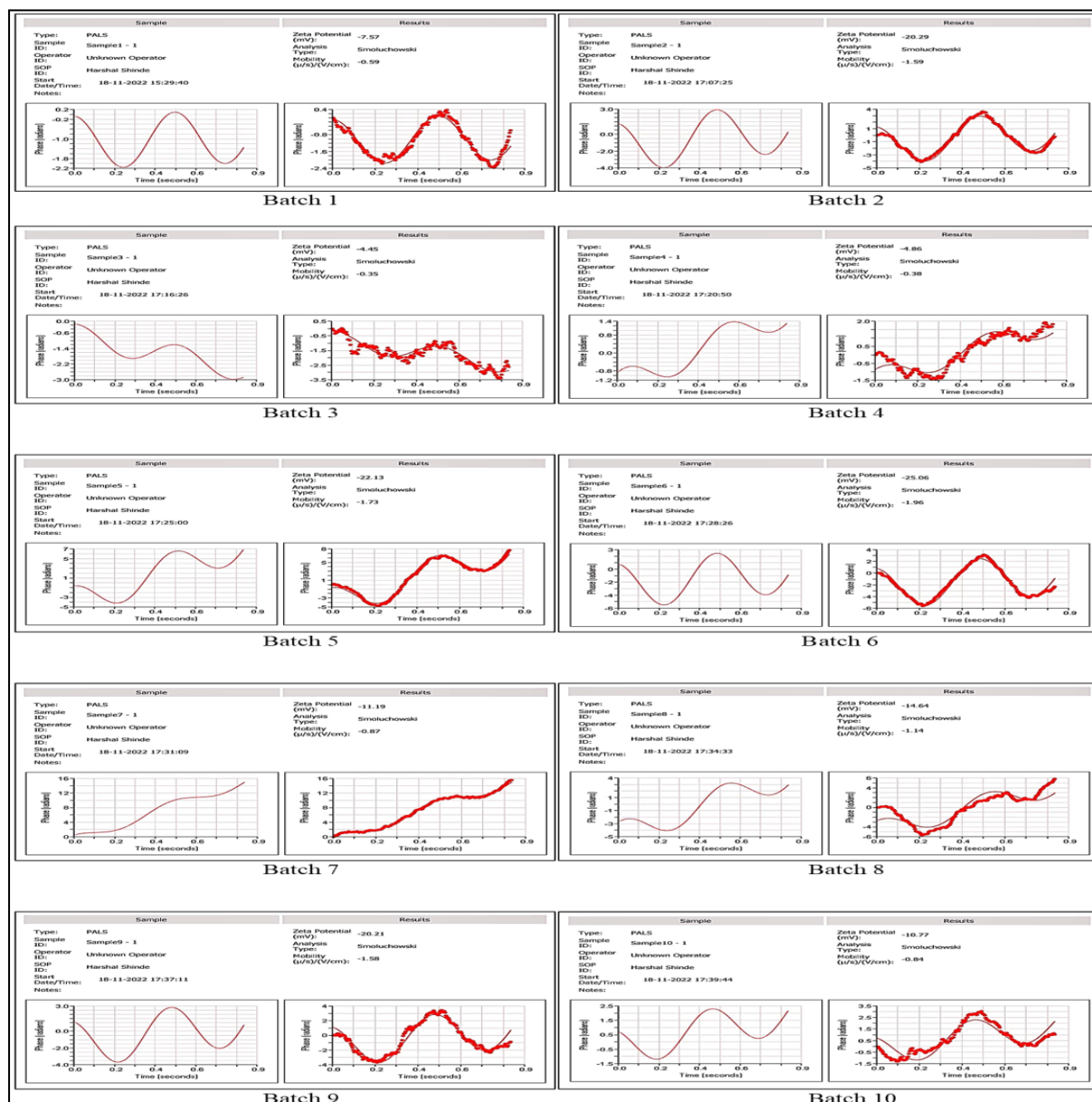


Figure 2 –Zeta Potential of all the Batches

4. Polydispersity Index (PI)

Polydispersity Index (PI) of the prepared Nanosuspension was determined using Dynamic Light Scattering (DLS) method. Result of Polydispersity Index (PI) is reported in the Table 4.

5. Drug Content

All the Batches of the Rosuvastatin Calcium Nanosuspension was evaluated for the Drug Content. Results of Drug Content are reported in the Table 4 and represented graphically in Figure 3.

Table 4 – Drug Content and Polydispersity Index of Each Batch of Nanosuspension

Batch No	Polydispersity Index	Drug Content (mg/ml)
B1	0.282	0.31
B2	0.288	0.26
B3	0.375	1.43
B4	0.283	0.46
B5	0.347	1.94
B6	0.308	1.73
B7	0.319	0.51

B8	0.299	1.11
B9	0.317	1.59
B10	0.279	0.39

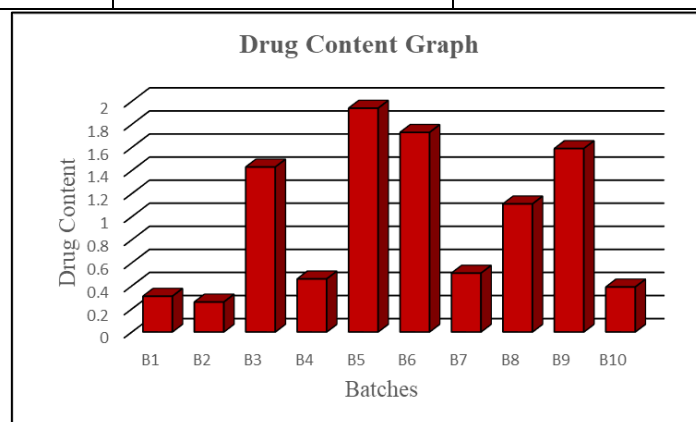


Figure 3 – Drug Content of each Batch

6. *in-vitro* drug release study

The *in-vitro* drug release study for all the batches for Rosuvastatin calcium Nanosuspension was carried out using paddle method (USP apparatus II). Data for *in-vitro* drug release study is presented in the following Table 5 and the graphical representation of Percentage Drug Release vs. Time graph is shown in the Figure 4.

Table 5 – Percentage Drug Release of Each Batch of Nanosuspension

Batch No	Percentage Drug Release (%)						
	0 min	10 min	20 min	30 min	40 min	50 min	60 min
B1	0	0.27	36.34	42.83	51.64	83.31	88.05
B2	0	4.91	24.43	26.69	27.34	41.16	54.06
B3	0	21.31	23.17	66.3	95.20	98.92	98.92
B4	0	11.76	29.38	41.60	71.45	82.51	84.50
B5	0	4.55	13.97	33.60	40.82	49.75	54.62
B6	0	6.89	20.13	46.86	63.69	74.19	86.26
B7	0	13.92	20.39	24.94	30.08	34.56	47.55
B8	0	5.99	24.81	36.62	50.19	69.93	79.23
B9	0	10.68	14.58	44.49	68.06	87.02	88.52
B10	0	11.94	27.40	32.21	51.85	55.85	65.29

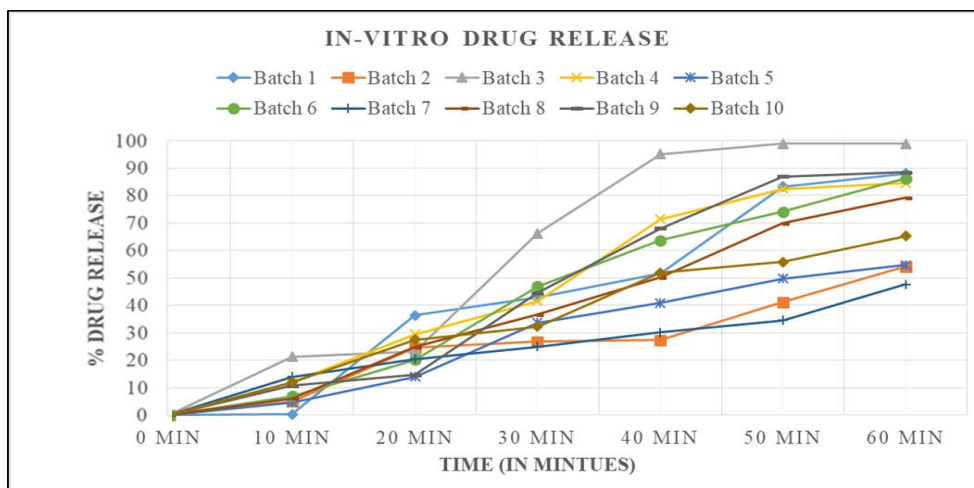


Figure 4 - Percentage Drug Release vs. Time Graph

3.3. OPTIMIZATION OF NANOSUSPENSION

Optimization of the formulations was studied by Regular Level Factorial design. The data obtained were treated using Design expert stat ease software and analysed statistically using Model Graph technique. Various graphs obtained from the Model Graph technique which indicates Interaction Between each independent Factor and dependent Factor (Response) were Studied. Graphical Optimization Technique was studied to select the Optimize Batch of Rosuvastatin Calcium Nanosuspension

Table 6 – Experimental Design and Data obtained of Particle Size, Zeta Potential and % drug Release

Batch No	Ratio of S:AS (ml)	Conc. of Stabilizer (% w/v)	Sonication Time (min)	Particle size (nm)	Zeta Potential (mV)	% Drug Release (%)
B1	1:50	6	10	327.83 nm	-7.57 mV	88.05 %
B2	1:50	10	12	568.29 nm	-20.29 mV	54.06 %
B3	1:10	2	8	263.29 nm	-4.45 mV	98.92 %
B4	1:50	10	8	381.13 nm	-10.81 mV	84.50 %
B5	1:10	10	8	427.16 nm	-22.13 mV	54.62 %
B6	1:10	2	12	343.79 nm	-25.06 mV	86.26 %
B7	1:50	2	8	658.90 nm	-11.19 mV	47.55 %
B8	1:10	10	12	384.87 nm	-14.64 mV	79.23 %
B9	1:10	6	10	351.64 nm	-20.21 mV	88.52 %
B10	1:50	2	12	397.60 nm	-10.77 mV	65.29 %

1. Analyses of Particle Size

The Graphs Obtained from Model Graph technique were studied.

From the Graphical representation in Figure 5, it was observed that as the Ratio of Solvent: Anti-solvent was kept 1:50 the Particle Size was found to be smaller in compare to the Formulation containing Ratio of Solvent: Anti-solvent as 1:10. But the Difference between Particle size of Formulation containing 1:10 and 1:50 was not so large we can say that Interaction between Ratio of S: AS (X1) and Particle Size (Y1) is minimum.

From the Graphical representation in Figure 5, it was observed that as the Concentration of Stabilizer Decreases the Particle Size also Decreases and vice versa. Three different concentration of Stabilizer were used for formulating Nanosuspension which is 2%, 6% and 10%. It was observed that when 2% of Stabilizer was used for formulating Nanosuspension the Particle Size was found to be the small. Therefore, it is concluded that Interaction between Concentration of Stabilizer (X2) and Particle Size (Y1) are directly proportional to each other.

From the Graphical representation in Figure 5, it is observed that Particle Size Decreases as Sonication Time goes on Increasing. Three different Sonication Time were used to prepare Nanosuspension and it was found that when Nanosuspension was sonicated for 12 minutes, Particle Size was found to be smaller in compared to Nanosuspension which was sonicated for 8 minutes. Therefore, it was concluded that Interaction between Sonication Time (X3) and Particle Size (Y1) is inversely proportional to each other and to Formulate Nanosuspension with smaller Particle Size, Sonication Time should be more as possible.

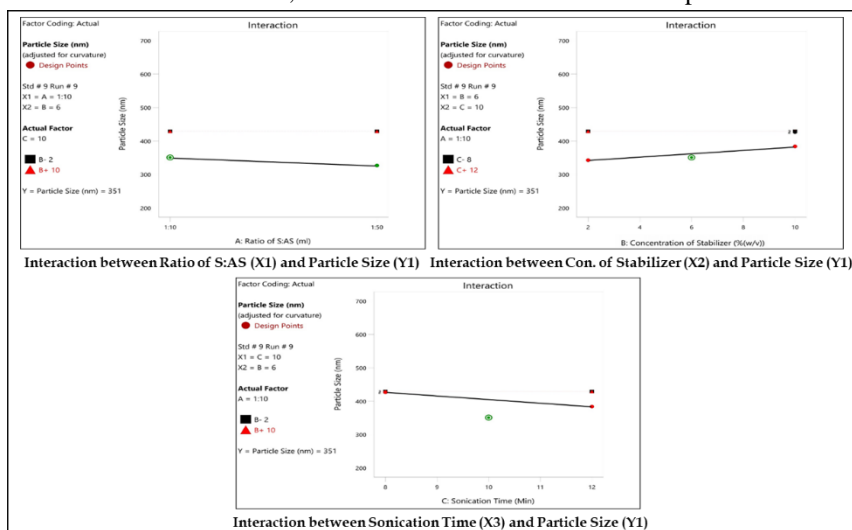


Figure 5 - Analyses of Particle Size (Y1)

2. Analyses of Zeta Potential

From the Graphical representation in Figure 6, it was observed that when the Nanosuspension was prepared using Ratio of Solvent: Anti-solvent as 1:10 then the prepared Nanosuspension is more stable in compared to Nanosuspension prepared using Ratio of Solvent: Anti-solvent as 1:50. To stabilize the Nanosuspension the Zeta Potential must be more that ± 20 mV and it was observed from the Figure 5 that keeping the Ratio of Solvent: Anti-solvent 1:10, the Zeta Potential move close toward -20 mV. Therefore, it was concluded that at low Ratio of Solvent: Anti-solvent (1:10) the prepared Nanosuspension is more stable and as the Ratio of Solvent: Anti-solvent increases the stability of Nanosuspension decreases.

From the Graphical representation in Figure 6, it was observed that when the Nanosuspension was prepared using 2% Concentration of Stabilizer than the prepared Nanosuspension is more stable than that of Nanosuspension prepared using 6% and 10% Concentration of Stabilizer. To stabilize the Nanosuspension the Zeta Potential must be more that ± 20 mV. From Figure 5, we can say that at 2% Concentration of Stabilizer Zeta Potential was found to be more than -20 mV. Therefore, it was concluded that to prepare stable Nanosuspension Concentration of the Stabilizer should be low (2%) in case of Rosuvastatin Calcium Nanosuspension.

From the Graphical representation in Figure 6, it was observed that as the Sonication Time is less than the Nanosuspension formed is more stable. When the Nanosuspension is sonicated for 8 minutes or for at least for 10 minutes, the Zeta Potential is found to be more than or close to -20 mV which is sufficient for the Nanosuspension to be stable.

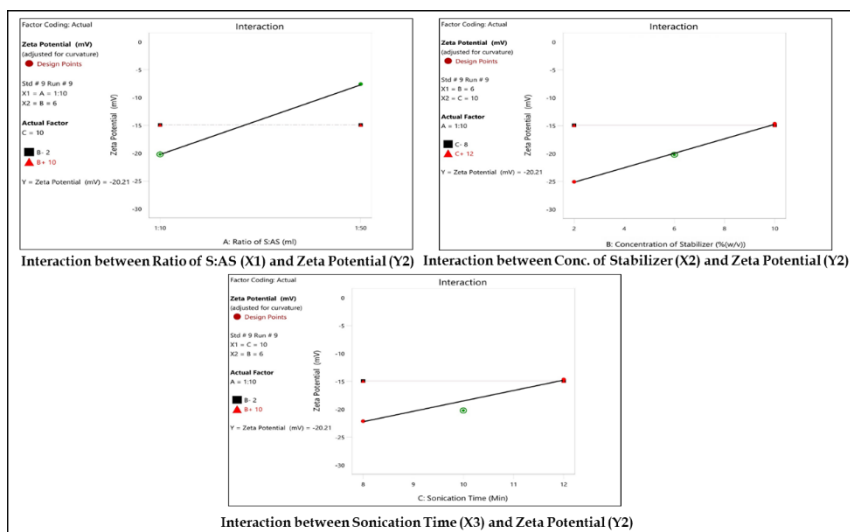


Figure 6 - Analyses of Zeta Potential (Y2)

3. Analysis of Percentage Drug Release

From the Graphical representation in Figure 7, it was observed that whether the Nanosuspension is prepared using Ratio of Solvent: Anti-Solvent as 1:10 or 1:50 the Percentage Drug Release is more than 80%. Formulation prepared using 1:10 Ratio of Solvent: Anti-Solvent, % Drug Release was found to be 88.52% and formulation prepared using 1:50 Ratio of Solvent: Anti-Solvent, % Drug Release was found to be 88.05 %. Therefore, to conclude any relation between Solvent: Anti-Solvent and Percentage Drug Release is difficult as there was no significant data observed.

From the Graphical representation in Figure 7, it was observed that as Concentration of Stabilizer Decrease the % Drug Release Increase. As Concentration of Stabilizer was 2% and 6% the formulation shows higher % Drug Release in compared to formulation containing 10% of concentration of Stabilizer. It was concluded that to achieve higher % Drug Release the Concentration of Stabilizer should be low as possible in the case of Rosuvastatin Calcium Nanosuspension.

From the Graphical representation in Figure 7, it was observed that as sonication Time increases the % Drug Release also Increases. These may due to Decrease in Particle Size with Increase i.e. at higher Sonication Time Particle Size is smaller and due to which there is Increase in % drug Release. Therefore, it was concluded that to Interaction between Sonication Time (X3) and % Drug Release (Y3) is directly proportional to each other and to achieve higher % Drug Release the sonication Time should be higher.

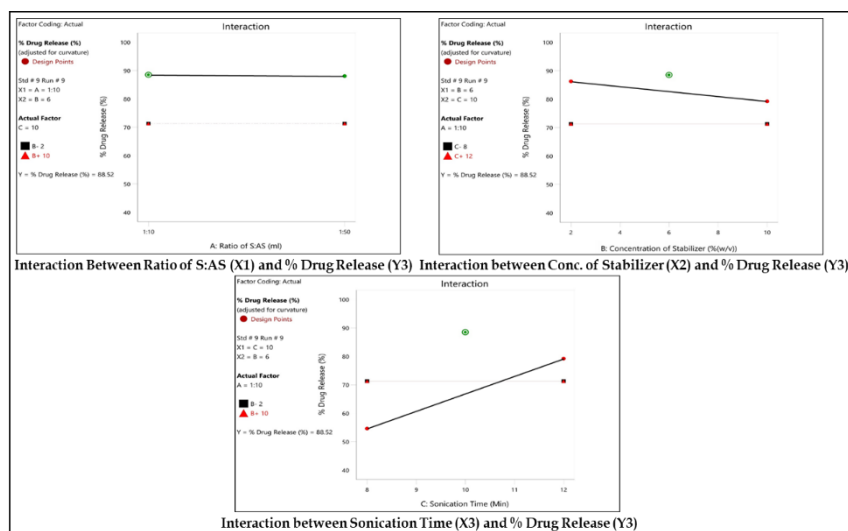


Figure 7 - Analyses of % Drug Release (Y3)

4. Optimization Analysis

The optimization module searches for a combination of factor levels that simultaneously satisfy the criteria and finds the best formulation. Graphical optimization was used for the Optimization Analysis. Graphical optimization uses the models to show the volume where acceptable response outcomes can be found. Data obtained from the Contour Plot and Overlay Plot shown in Figure 8 was studied and it showed that Formulation B9 lies in the Region where all the Criteria was satisfied and Formulation B9 was selected as the Optimized batch. Formulation B9 was prepared using 1:10 Ratio of Solvent: Anti-Solvent, 6% of Concentration of Stabilizer and it was sonicated for 10 minutes. The Results of the Formulation B9 was also satisfying and result is reported in the Table 7.

Table 7 – Results of Optimized Batch B9

Evaluations	Results of Batch B9
Particle Size (nm)	351.64 nm
Zeta Potential (mV)	- 20.21 mV
% Drug Release (%)	88.52 %

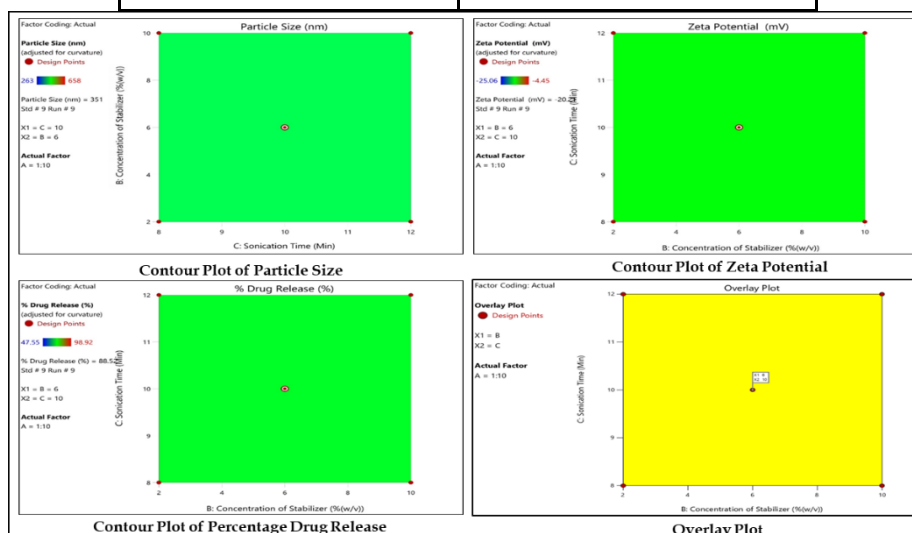


Figure 8 – Contour Plot and Overlay Plot

3.4. STABILITY STUDY

The Optimize Batch of Rosuvastatin Calcium Nanosuspension was selected for the stability Study. The Optimize Batch of Rosuvastatin Calcium Nanosuspension was kept at 2-4 °C in Refrigerator and at Room Temperature Physical Stability of the Nanosuspension was after 5 Months. The Result of Stability Study is present in the following Table 8 and Figure 9 shows graph of Particle Size of Optimized Batch after 5 Months. It was found that Formulation kept at 4 °C was stable in compared to Formulation kept in Room Temperature as no significant growth in Particle Size was found in the Optimized batch.

Table 8 - Stability Study of Optimized Batch

Batch No.	Initial Particle Size	Storage Condition (Temperature in °C)	Particle Size After 5 Months
Batch 9 (Optimized Batch)	351.64 nm	4 °C	354.12 nm
		Room Temperature	372.94 nm

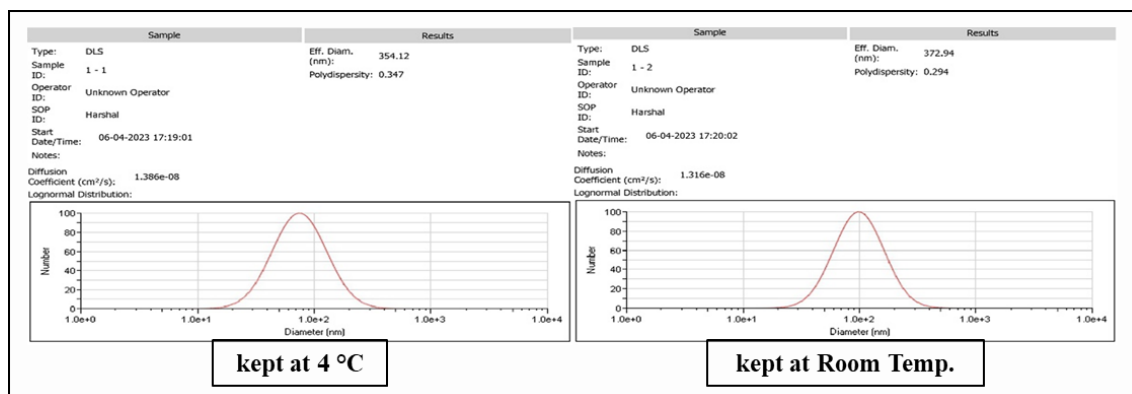


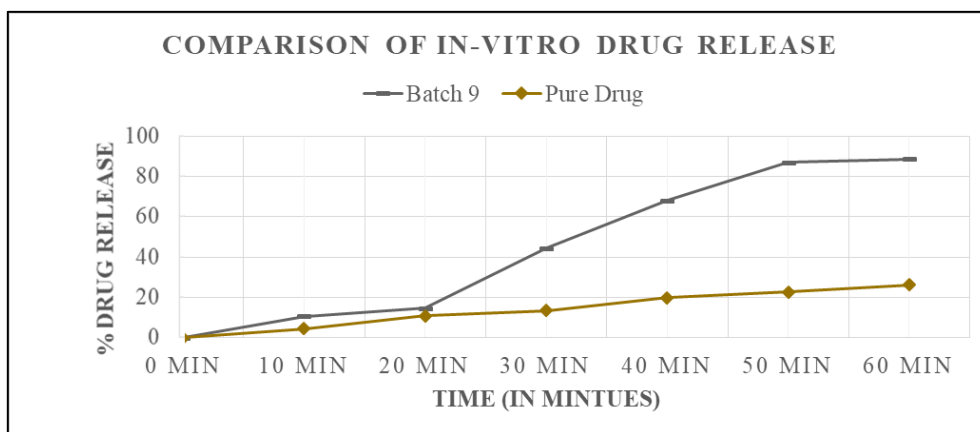
Figure 9 – Stability Study of Batch 9 (Optimized Batch) Using Particle Size Analysis

3.5. Comparison of *in-vitro* % Drug Release of Pure Drug and Optimized Batch of Rosuvastatin Calcium Nanosuspension

Comparison of *in-vitro* % Drug Release of Pure Drug and Optimized Batch of Rosuvastatin Calcium Nanosuspension was carried. Optimized Batch B9 showed 88.52% Drug Release in 60 min while Pure Drug Showed 26.29% drug Release in 60 min. Table 9 shows the Data Obtained in *in-vitro* Drug Release and Data is represented graphical in Figure 10.

Table 9 – Comparison of *in-vitro* Drug Release of Pure Drug and Optimized Batch of Rosuvastatin Calcium Nanosuspension

Time (in min)	Percentage Drug Release (%)	
	Batch B9	Pure Drug
0 min	0	0
10 min	10.68	4.37
20 min	14.58	10.79
30 min	44.49	13.49
40 min	68.09	19.84
50 min	87.02	22.57
60 min	88.52	26.29

Figure 10- Comparison of *in-vitro* Drug Release of Pure Drug and Optimized Batch of Rosuvastatin Calcium Nanosuspension

CONCLUSION

In the present study, Rosuvastatin calcium, an antihyperlipidemic agent was successfully prepared in the form of Nanosuspension. Rosuvastatin Calcium Nanosuspension was prepared used Solvent-Anti-Solvent Precipitation method. Experimental Design was obtained using Design Expert Software. Ratio of Solvent: Anti-

solvent (X1), Concentration of stabilizer (X2), and Sonication Time (X3) were selected as the 3 independent factor and Particle Size (Y1), Zeta Potential (Y2), and % Drug Release (Y3) were selected as the Dependent Factors.

10 Batches of Rosuvastatin Calcium Nanosuspension was prepared. Interaction between Independent factor and dependent factor was studied. Optimization was carried out using Graphical Method and Batch B9 was selected as the Optimized Batch. Batch B9 was Prepared using 1:10 Ratio of Solvent-Anti-Solvent, 6 % (w/v) Concentration of Stabilizer was used and it was sonicated for 10 minutes. The Results of the Formulation B9 were was also satisfying. The Particle Size of the Optimized batch was found to be 351.64 nm with Zeta Potential of -20.21 mV and Percentage Drug Release was 88.52% in 60 minutes. Stability study was carried at 4 °C and at room temperature for 5 Months. It was found that Formulation kept at 4 °C was stable in compared to Formulation kept in Room Temperature as no significant growth in Particle Size was found in the Optimized batch. Comparison of *in-vitro* % Drug Release of Pure Drug and Optimized Batch of Rosuvastatin Calcium Nanosuspension was also carried out. Optimized Batch B9 showed 88.52% Drug Release in 60 min while Pure Drug Showed 26.29% drug Release in 60 min.

ACKNOWLEDGEMENT

The authors are very much thankful to PDEAs Shankarrao Ursal College of Pharmaceutical Sciences and Research Centre, Pune, Maharashtra, India, all teaching and non-teaching staff for providing the necessary support to complete this Research work successfully.

CONFLICT OF INTEREST

All authors declared no conflicts of interest.

REFERENCES

1. Lakshmi P, Kumar GA. Nanosuspension technology: A review. *Int J Pharm Sci.* 2010 Aug; 2(4):35-40.
2. Arunkumar N, et al. Nanosuspension technology and its applications in drug delivery. *Asian Journal of Pharmaceutics (AJP).* 2009; 3(3); 168-173. <https://doi.org/10.22377/ajp.v3i3.261>.
3. Chakravorty R. Nanosuspension as an emerging Nanotechnology and Techniques for its Development. *Research Journal of Pharmacy and Technology.* 2022 Jan 25; 15(1):489-93. DOI: 10.52711/0974-360X.2022.00079.
4. Kulkarni RR, et al. A novel approach towards nanosuspension. *Asian Journal of Pharmaceutical Research.* 2015; 5(4):186-94. DOI: 10.5958/2231-5691.2015.00029.5.
5. Chingunpituk J. Nanosuspension technology for drug delivery. *Walailak Journal of Science and Technology (WJST).* 2007; 4(2):139-53.
6. Zhou Y, et al. Comparative studies on amphotericin B nanosuspensions prepared by a high pressure homogenization method and an antisolvent precipitation method. *Colloids and Surfaces B: Biointerfaces.* 2018 Dec 1; 172:372-9. <https://doi.org/10.1016/j.colsurfb.2018.08.016>.
7. Shariare MH, et al. The impact of process parameters on carrier free paracetamol nanosuspension prepared using different stabilizers by antisolvent precipitation method. *Journal of Drug Delivery Science and Technology.* 2018 Feb 1; 43:122-8. <https://doi.org/10.1016/j.jddst.2017.10.001>.
8. Kommavarapu P, et al. Preparation and characterization of efavirenz nanosuspension with the application of enhanced solubility and dissolution rate. *HIV & AIDS Review.* 2016 Jan 1; 15(4):170-6. <https://doi.org/10.1016/j.hivar.2016.11.007>.
9. Cerdeira AM, et al. Miconazole nanosuspensions: influence of formulation variables on particle size reduction and physical stability. *International journal of pharmaceutics.* 2010 Aug 30; 396(1-2):210-8. <https://doi.org/10.1016/j.ijpharm.2010.06.020>.
10. Cerdeira AM, et al. Formulation and drying of miconazole and itraconazole nanosuspensions. *International journal of pharmaceutics.* 2013 Feb 25; 443(1-2):209-20. <https://doi.org/10.1016/j.ijpharm.2012.11.044>.
11. He S, et al. Preparation and in vitro–in vivo evaluation of teniposide nanosuspensions. *International journal of pharmaceutics.* 2015 Jan 15; 478(1):131-7. <https://doi.org/10.1016/j.ijpharm.2014.11.020>.

12. Baek IH, et al. Dissolution and oral absorption of pranlukast nanosuspensions stabilized by hydroxypropylmethyl cellulose. *International journal of biological macromolecules*. 2014 Jun 1; 67:53-7. <https://doi.org/10.1016/j.ijbiomac.2014.03.006>.
13. Xu Y, et al. Enhanced dissolution and oral bioavailability of aripiprazole nanosuspensions prepared by nanoprecipitation/homogenization based on acid–base neutralization. *International journal of pharmaceutics*. 2012 Nov 15; 438(1-2):287-95. <https://doi.org/10.1016/j.ijpharm.2012.09.020>.
14. Mendes Cerdeira AM. Production and stabilization of nanosuspensions of poorly soluble drug substances (Doctoral dissertation, ETH Zurich). <https://doi.org/10.3929/ethz-a-007613986>.
15. Ibrahim MA, et al. Formulation and evaluation of docetaxel nanosuspensions: In-vitro evaluation and cytotoxicity. *Saudi pharmaceutical journal*. 2019 Jan 1; 27(1):49-55. <https://doi.org/10.1016/j.jsps.2018.07.018>.
16. John R, et al. Innovative Betulin Nanosuspension exhibits enhanced anticancer activity in a Triple Negative Breast Cancer Cell line and Zebrafish angiogenesis model. *International Journal of Pharmaceutics*. 2021 May 1; 600:120511. <https://doi.org/10.1016/j.ijpharm.2021.120511>.
17. Al-Heibshy FN, et al. Physicochemical characterization and pharmacokinetic evaluation of rosuvastatin calcium incorporated solid lipid nanoparticles. *International journal of pharmaceutics*. 2020 Mar 30; 578:119106. DOI: 10.1016/j.ijpharm.2020.119106.
18. Al-Shdefat R, et al. Preparation and evaluation of spray dried rosuvastatin calcium-PVP microparticles for the improvement of serum lipid profile. *Journal of Drug Delivery Science and Technology*. 2020 Feb 1; 55:101342. <https://doi.org/10.1016/j.jddst.2019.101342>.
19. Vemuri VD, Lankalapalli S. Amino acid based Rosuvastatin cocrystals: Towards the improvement of physicochemical parameters. *Journal of Crystal Growth*. Volume 570, 15 September 2021, 126241. <https://doi.org/10.1016/j.jcrysgro.2021.126241>.
20. Ahmed TA, et al. Rosuvastatin lyophilized tablets loaded with flexible chitosomes for improved drug bioavailability, anti-hyperlipidemic and anti-oxidant activity. *International Journal of Pharmaceutics*. 2020 Aug 19; 588:119791. <https://doi.org/10.1016/j.ijpharm.2020.119791>.
21. Thamer AK, Abood AN. Preparation and In vitro Characterization of Aceclofenac Nanosuspension (ACNS) for Enhancement of Percutaneous Absorption using Hydrogel Dosage Form. *Iraqi Journal of Pharmaceutical*. 2021 Dec 9; 30(2):86-98. <https://doi.org/10.31351/vol30iss2pp86-98>.
22. Wong CR. Multistage nanoparticle delivery system for deep penetration into solid tumor and electrically controlled catalytic nanowire growth (Doctoral dissertation, Massachusetts Institute of Technology). 2011 Feb 8; 108(6): 2426-2431. doi: 10.1073/pnas.1018382108
23. Jawahar N, et al. Studies on physico-chemical and pharmacokinetic properties of olanzapine through nanosuspension. *Journal of pharmaceutical sciences and research*. 2013 Oct 1; 5(10):196.
24. Bose S, et al. Comparative in vitro evaluation of glimepiride containing nanosuspension drug delivery system developed by different techniques. *Journal of Molecular Structure*. 2021 May 5; 1231:129927. <https://doi.org/10.1016/j.molstruc.2021.129927>.
25. Manishaanjane AS, Khan A. Formulation and evaluation of nano-suspension of valsartan. *Int J Curr Pharm Res*. 2018; 10:68-74. <https://doi.org/10.22159/ijcpr.2018v10i2.25874>.
26. Huang T, et al. Preparation of high drug-loading celastrol nanosuspensions and their anti-breast cancer activities in vitro and in vivo. *Scientific Reports*. 2020 Jun 1; 10(1):8851. DOI:10.1038/s41598-020-65773-9.
27. Sahu BP, Das MK. Nanosuspension for enhancement of oral bioavailability of felodipine. *Applied nanoscience*. 2014 Feb; 4:189-97. DOI:10.1007/s13204-012-0188-3.
28. Das S, et al. Design of Eudragit RL 100 nanoparticles by nanoprecipitation method for ocular drug delivery. *Nanomedicine: Nanotechnology, Biology and Medicine*. 2010 Apr 1; 6(2):318-23. <https://doi.org/10.1016/j.nano.2009.09.002>.
29. Mandal B, et al. Sulfacetamide loaded Eudragit RL100 nanosuspension with potential for ocular delivery. *J Pharm Pharm Sci*. 2010 Jan 1; 13(4):510-23. PMID: 21486528.

30. Rahim H, et al. Fabrication and characterization of glimepiride nanosuspension by ultrasonication-assisted precipitation for improvement of oral bioavailability and in vitro α -glucosidase inhibition. *International Journal of Nanomedicine*. 2019 Aug 6:6287-96. DOI: 10.2147/IJN.S210548.
31. M. Santhosh Raja, K. Venkataramana. Formulation and Evaluation of Stabilized Eprosartan Nanosuspension. *Int J App Pharm*, Vol 12, Issue 6, 2020, 83-87. DOI:10.22159/ijap.2020v12i6.39123.
32. Alshora DH, et al. Rosuvastatin calcium nanoparticles: improving bioavailability by formulation and stabilization codesign. *PLoS One*. 2018 Jul 9; 13(7):e0200218. <https://doi.org/10.1371/journal.pone.0200218>.
33. <https://www.statease.com/>
34. https://cdnm.statease.com/pubs/handbk_for_exp_sv.pdf
35. Mahesh KV, et al. A comparative study of top-down and bottom-up approaches for the preparation of nanosuspensions of glipizide. *Powder technology*. 2014 Apr 1; 256:436-49. <https://doi.org/10.1016/j.powtec.2014.02.011>.
36. Yadav D, Kumar N. Nanonization of curcumin by antisolvent precipitation: process development, characterization, freeze drying and stability performance. *International journal of pharmaceutics*. 2014 Dec 30; 477(1-2):564-77. <https://doi.org/10.1016/j.ijpharm.2014.10.070>.
37. Kakran M, et al. Preparation of nanoparticles of poorly water-soluble antioxidant curcumin by antisolvent precipitation methods. *Journal of Nanoparticle Research*. 2012 Mar; 14:1-1. <https://doi.org/10.1007/s11051-012-0757-0>.
38. Patel AA, et al. Nanosuspension for oral delivery of tadalafil: Pharmacodynamic and pharmacokinetic studies. *Journal of Drug Delivery Science and Technology*. 2021 Feb 1; 61:102203. DOI:10.1016/j.jddst.2020.102203.
39. Shariare MH, et al. In vitro dissolution and bioavailability study of furosemide nanosuspension prepared using design of experiment (DoE). *Saudi pharmaceutical journal*. 2019 Jan 1; 27(1):96-105. <https://doi.org/10.1016/j.jsps.2018.09.002>.
40. Patel HM, et al. Formulation and development of nanosuspension as an alternative approach for solubility and dissolution enhancement of aceclofenac. *Int J Adv Pharm*. 2018; 7(5):33-47. <https://doi.org/10.7439/ijap>.
41. Sharannavar B, Sawant S. Formulation and Evaluation of Nanosuspension of Rosuvastatin for Solubility Enhancement by Quality by Design Approach. *Int J Pharm Sci Res*. 2021 Jan 11; 12(11):5949-58. DOI: 10.13040/IJPSR.0975-8232.12(11).
42. Shah M, et al. Oral solid compritol 888 ATO nanosuspension of simvastatin: optimization and biodistribution studies. *Drug development and industrial pharmacy*. 2011 May 1; 37(5):526-37. <https://doi.org/10.3109/03639045.2010.527983>.
43. Dhoranwala KA, et al. Formulation optimization of rosuvastatin calcium-loaded solid lipid nanoparticles by 32 Full-factorial design. *NanoWorld journal*. 2015 Dec 30; 1(2). DOI:10.17756/nwj.2015-015.
44. Babu VS, et al. Formulation and Optimization of Rosuvastatin Nanoparticles By Using of Lyophilization Technique, *WJPPS*, Vol 8, Issue 4, March 2019, 1202-1217. DOI: 10.20959/wjpps20194-13487.
45. <https://www.brookhaveninstruments.com/>
46. <https://www.brookhaveninstruments.com/applications/particle-sizing/>
47. <https://www.brookhaveninstruments.com/wp-content/uploads/2021/02/guide-determination-of-particle-size-brookhaven-instruments-new.pdf>
48. <https://www.brookhaveninstruments.com/product/srel-solvent-resistant-electrode/>
49. <https://www.brookhaveninstruments.com/wp-content/uploads/2021/02/guide-to-choosing-zeta-potential-analyzer-brookhaven-instruments-new.pdf>



FORMULATION, EVALUATION AND OPTIMIZATION OF B –CYCLODEXTRIN BASED NANOSPONGES OF CLARITHROMYCIN

Dr. Prashant H. Khade¹, Amol Talware², Sujit S. Kakde¹, Dr. Sachin V. Kotwal³,
Priyanka D. Borude⁴, Harshal M. Shinde⁵

¹Assistant Professor, PDEAs Shankarrao Ursal College of Pharmaceutical Sciences and Research Centre, Pune, Maharashtra, India.

²Sector Manager, Croda India Company Pvt. Ltd, Mumbai, Maharashtra, India.

³Principal, PDEAs Shankarrao Ursal College of Pharmacy (Diploma), Pune, Maharashtra, India.

⁴Lecturer, PDEAs Shankarrao Ursal College of Pharmacy (Diploma), Pune, Maharashtra, India.

⁵Research Scholar, PDEAs Shankarrao Ursal College of Pharmaceutical Sciences and Research Centre, Pune, Maharashtra, India.

For Correspondence -

Prashant H. Khade,

Assistant Professor, Department of Pharmaceutics,

PDEAs Shankarrao Ursal College of Pharmaceutical Sciences and Research Centre,
Pune, Maharashtra, India.

E-mail Id: phkhade@gmail.com

ABSTRACT

The aim of present study was to develop an optimized gastric floating controlled drug delivery system of Clarithromycin (CLA). The Clarithromycin is poorly water soluble drug and gastric irritant. To overcome these problems attempt was made in present study to form inclusion complex of Clarithromycin with Nanosponges. β -Cyclodextrin (CD) based Nanosponges (NS) are novel class of cross-linked derivatives of Cyclodextrin. The Nanosponges were synthesized by carbonylation of β -Cyclodextrin to exploit its porous structure for drug entrapment. A better alternative to β -CD is it's Nanosponges due to low solubility & toxicity of β -CD. The final Nanosponges structure contains both lipophilic cavities of CD and carbonate bridges leading to a network of more hydrophilic channels. NS are solid, insoluble in water, crystalline in nature and thermally stable compounds. They have been used to increase the solubility of poorly water soluble actives, to avoid gastric irritation and control the release of drug. Present study aimed at formulating complex of CLA with NS by solid dispersion technique and absence of interaction of CLA with NS was confirmed by XRPD, DSC and FTIR studies. The result of XRPD results showed that the crystallinity of CLA was decreased after loading into NS. The 3² full factorial experimental designs were applied for tablet formulation. The *in vitro* dissolution studies indicated a slow and prolonged release of drug over the period of 12 h. Histopathological study revealed non irritancy of drug-NS complex to gastric mucosa (of rat). Hence drug-NS complex found to be suitable for designing into unit dosage forms. The release study of drug from tablet as well as capsule as unit dosage forms indicated controlled release of a drug when compared with marketed preparation.

Keywords: Nanosponges, β -Cyclodextrin, Clarithromycin, Solubility, Controlled drug delivery System.

1. INTRODUCTION

The objective of any drug delivery system is to provide therapeutic amount of drug to targeted site in body to achieve the desired therapeutic effect (1). For curing of disease, it is necessary to achieve and maintain the concentration of administered drug within the therapeutically effective range for this drug dosage must be taken several times which results in fluctuating drug levels in plasma. This drawback of conventional dosage form can be overcome by formulation of controlled release dosage forms which provides drug release in an

4999

amount sufficient to maintain the therapeutic drug level over extended period of time, with release profiles controlled by the special technological construction and design of the system (2). The primary objectives of controlled drug delivery are to ensure safety and enhancement of efficacy of drug with improved patient compliance. So the use of these dosage forms is increasing in treatment of acute and chronic diseases as they maintain the concentration of drug in plasma above minimum effective concentration and below the minimum toxic level for extended period of time. Thus, controlled drug delivery results in optimum drug therapy with reduced frequency of dosing and side effects (3).

Effectiveness can also be enhanced by Gastro retentive systems. These are hydro dynamically balanced systems. In these systems dosage form have the specific gravity less than gastric juice, so they float in stomach and retain the drug over for extended period of time. Thus, total residence time in stomach is increased. Also these systems are relatively large in size and passing from pyloric opening is prohibited. This system is useful for drugs which are absorbed in stomach and also for local action of drug (4). Floating Drug Delivery is one of the method to enhance Gastric retention. The drug is released progressively from the swollen matrix, as in the case of conventional hydrophilic matrices (5, 6).

Another most effective method to deliver the insoluble drug at the targeted site is to preparation of Complexation with Nanosponges. A complex is a species of definite substrate-to-ligand stoichiometry that can exist both in solution and in solid state. The distinction between substrate and ligand is arbitrary, and is made solely for experimental convenience. Based on the type of chemical bonding, complexes can be classified into coordination and molecular complexes. The first form coordinate bond then present weak intermolecular force between substrate and ligand. Generally, pharmaceutical systems belong to the second group, being small molecule small molecule complexes, and/or inclusion complexes in which one molecule (host) possess a cavity into which it can admit a guest molecule (7). Nanosponges are prepared from β -Cyclodextrin as nanoporous materials for possible use as carriers for drug delivery. The structure of β -Cyclodextrin-based Nanosponges was principally investigated analyses. Sizes, morphology and toxicity were also examined. The capacity of the Nanosponges to incorporate molecules within their structure was evaluated using drugs with different structures and solubility. The Nanosponges were found capable of carrying both lipophilic and hydrophilic drugs and of improving the solubility of poorly water-soluble molecules (8). Nanosponges are a new class of material made of microscopic particles with cavities a few nanometers wide, characterized by the capacity to encapsulate a large variety of substances that can be transported through aqueous media. The efficacy of some pharmaceuticals adsorbed in the Nanosponges showed an activity 3–4 times higher and exhibited no detrimental side effects. Cyclodextrin based Nanosponges (of dexamethasone, flurbiprofen and Doxorubicin hydrochloride) demonstrated the ability to include either lipophilic or hydrophilic drugs and to release them slowly into physiological media. Thus Nanosponges can be used as a vessel for pharmaceutical principles to improve the aqueous solubility of lipophilic drugs, to protect degradable molecules and to formulate drug delivery systems for various administration routes beside the oral one. Beta Cyclodextrin (β CDs) have been the most widely used of all the Cyclodextrin (9, 10).

2. MATERIALS AND METHODS

2.1 Materials - Clarithromycin was gifted by Cipla pvt Ltd, Kurkumbh, India. Hydroxypropyl Methyl Cellulose K100 was also received as Gift Sample from Colorcon, Goa. Beta – Cyclodextrin was obtained from Gangwal Chemicals, Mumbai. TLC Plate and Diphenyl Carbonate was purchased from S.K. Enterprises. Dimethyl Sulfoxide, Dichloromethane, Acetone, Methanol, Benzene, Chloroform, Hexane, and acetonitrile was purchased from Research lab, Mumbai and all the solvent used were of Analytical Grade.

2.2 Synthesis of Nanosponges

2.2.1 Reaction

The reaction is a nucleophilic substitution where Cyclodextrin is reacted with Carbonyl compound of formula X-CO-X wherein X is Imidazolyl or -OR group in which R is C₁-C₄ alkyl (11). The reaction can be represented by the following scheme:



Where X is the carbonyl compound and n is the integer which can range within 3 to 6 depending upon the conditions used in the reaction which is shown in Figure 3.1.

2.2.2 Procedure

A round-bottomed flask equipped with a reflux condenser with thermometer. Weighed accurate quantities of beta CD and Diphenyl Carbonate (DPC) with DMSO as a solvent. The ratio was varied with 1:2, 1:4, and 1:8 equimolar mixture of beta CD: diphenyl carbonate. The reaction time was 12 h with conventional heating continuously with temperature maintain to 90⁰-100⁰C. The reaction mixture then added to cold water and product obtained was filtered and washed with water to remove excess amount of the beta CD. The product was Soxhlet extracted by ethanol to remove either impurities or unreacted diphenyl carbonate (11).

2.3 Optimization of Synthesized Product (Nanosponges)

The synthesized product was optimized to cross linker used in 1:2, 1:4, 1:8 (β- CD: Diphenyl Carbonate). The optimization for percentage yield is shown in Table 3.1.

2.4 Characterization of Synthesized Product (Nanosponges) (12, 13, 14)

1) Thin Layer Chromatography (TLC)

The TLC was used to evaluate the change in the R_f value of starting and product. Both samples dissolve into appropriate solvent and used for TLC. Chloroform is used as a mobile solvent. The TLC is observed under U.V. chamber. The photograph of TLC was shown in Figure 3.2 and R_f value are shown in Table 3.2.

2) FTIR Spectra

FTIR spectrophotometer was used for recording IR Spectrum of various samples by mixing the sample with dry potassium bromide and the sample was examined at transmission mode over a range 4000-400 cm⁻¹ for studying principle peaks using FTIR spectrophotometer (FTIR-8400, Shimadzu). The FTIR Spectrum of product obtained in synthesis and beta-Cd are shown in Table 3.3 and in Figure 3.3.

3) Differential Scanning Calorimetric analysis (DSC)

Thermogram of the NS was taken on a Mettler Toledo India Pvt. Ltd, Switzerland. (STAR^o SW 9.20). An empty aluminium pan was used as a reference. DSC measurements were performed at a heating rate of 10⁰C/min from 30⁰ to 400⁰C using aluminium sealed pan. During the measurement, the Sample was purged with nitrogen gas. DSC thermograms of Nanosponges are shown in Figure 3.4.

4) Powder X-ray diffraction (PXRD)

The PXRD spectra of samples were recorded using high power powder x-ray diffractometer (Ru-200B, Pune, India) with Cu as target filter having a voltage/current of 40 KV/40 mA at a scan speed of 4^o/min. The samples were analyzed at 2θ angle range of 5^o to 50^o. Step time was 0.5 seconds and time of acquisition was 1 h. The results are reported in Figure 3.5.

5) Nuclear Magnetic Resonance Spectroscopy

The C¹³ NMR of β- CD and NS were recorded in DMSO using as a solvent in NMR Varian-Mercury 30 MHz spectrometer and chemical shifts are given in Parts per million, downfield from tetramethylsilane (TMS) as an internal standard. C¹³ NMR of Nanosponges and beta- CD are shown in Figure 3.6 and Figure 3.7.

2.5 Phase solubility study

Phase solubility equilibrium plots were obtained for binary systems at 25 ⁰C in 0.1 N HCl. The studies were performed as per the procedure of Higuchi and Connors. Studies for binary system were carried out by adding excess amount of the drug to 10 ml of 0.1 N HCl containing increasing amounts of Nanosponges (0–2% w/v). The so formed series of suspensions were equilibrated on a mechanical shaker for 48 h. The equilibrated suspensions were then filtered through a membrane filter (0.45 lm) and absorbances observed by UV-spectrophotometer (13). The phase solubility diagram was constructed by plotting the dissolved clarithromycin concentration against the respective concentration of Nanosponges. The binding constant K_a was calculated from phase solubility diagram using its slope and intercept values (15). The phase solubility graph is shown in Figure 3.8. The stability constant was calculated by using equation 8.1.

$$K_{(a) 1:1} = \frac{\text{Slope}}{S_o (1 - \text{Slope})} M^{-1} \dots\dots\dots (2.1)$$

Where, S_o is intrinsic solubility of drug

M is molar concentration

Ka is apparent stability constant

Slope is calculated from regression equation

2.6 Preparation of binary systems

1) Drug incorporation (13)

Clarithromycin was dissolved in dichloromethane to form a solution. To this solution Nanosponges were added and triturated until the solvent evaporates. The drug and Nanosponges were added in a ratio of 1:1 by weight. The obtained solid dispersion was dried in an oven over night (at 50 °C at atmospheric pressure) to remove any traces of dichloromethane. The obtained powder was sieved through 60 mesh and used for further work.

2) Preparation of Physical mixture

Equimolar physical mixtures were prepared 1:1 by weight homogenously blending exactly weighed amounts of drug and Nanosponges mixture is obtained.

2.7 Characteristics of Complex

1) FT-IR spectroscopy study (16)

FT-IR spectra of selected inclusion complex, Nanosponges and drug were recorded on Jasco FT-IR spectrophotometer using KBr discs. The instrument was operated under dry air purge and the scans were collected at scanning speed 2 mm/sec with resolution of 4 cm⁻¹ over the region 4000-400 cm⁻¹. The scans were evaluated for presence of principle peaks of drug, shifting and masking of drug peaks due to Nanosponges and appearance of new peaks due to complexation. The FT-IR spectra of pure Clarithromycin, pure Nanosponges, physical mixture, and inclusion complex are shown in Figure 3.9.

2) Differential Scanning Colorimetry (DSC) (17)

The DSC study was carried out for pure Clarithromycin, pure Nanosponges, beta-CD, complex of Nanosponges and drug. The DSC patterns were recorded on a Mettler Toledo India Pvt. Ltd, Switzerland (STAR[®] SW 9.20). Each sample (2-4mg) was heated in crimped aluminum pans at a scanning rate of 10°C/min in an atmosphere of nitrogen using the range of 30-400°C. The temperature calibrations were performed periodically using indium as a standard. The DSC curves are shown in Figure 3.10.

3) Powder X-Ray Diffraction Study

The PXRD spectra of samples were recorded using high power powder x-ray diffractometer (Ru-200B, Pune, India) with Cu as target filter having a voltage/current of 40 KV/40 mA at a scan speed of 4°/min. The samples were analyzed at 2θ angle range of 5° to 50°. Step time was 0.5 seconds and time of acquisition was 1 h which is shown in Figure 3.11.

4) Scanning Electron Microscopy

The morphology of the surfaces of the drug loaded Nanosponges and Complex was examined by scanning electron microscopy (SEM). The dried sample was observed under different magnifications with an analytical scanning electron microscope (JEOL-JSM 6360A-Japan). SEM Images of Nanosponges and Complex is shown in the Figure 3.12 and 3.13 respectively.

2.8 Gastric Irritation Test on Rats

As Clarithromycin supposed to cause irritation to gastric mucosa. To determine whether the complex of Clarithromycin and Nanosponges causes gastric irritation or it prevents gastric irritation test was done as follows. Rats weighing about (200-250 g) are selected. They are divided into 3 groups each group contain three rats. One group is treated with control, second group is treated with standard Clarithromycin and another is treated with test i.e. complex. 75 mg of complex is given to test group by oral suspension for 15 days and to standard group is also given 37.5 mg of drug for 15 days. On 16th day all animals are fasted and their stomach is removed and examined for irritation after that histopathology was done (18). The photographs of the stomach tissue of all three groups were shown in Figure 3.14 and the histology reports were shown in Table 3.4.

2.9 Preparation of Preliminary Batches for selection of Polymer

2.9.1 Preparation of Granules

Granules required for controlled release tablet (CRT) formulations were prepared by Wet granulation technique. All the ingredients as given in Table 2.1 were weighed accurately and passed through sieve 30 mesh.

Isopropyl alcohol used as a granulating agent. Required quantity of complex, polymer and diluents were mixed thoroughly in a glass mortar. Sufficient quantity of granulating agent was sprinkled over the powder mixture to obtain enough cohesiveness. This cohesive mass was then sieved through 16 mesh to obtain granules. The granules were then dried at 60°C for 30 min. in hot air oven. Magnesium stearate and talc were finally added as glidant and lubricant mixed well with granules for 5 minutes (19).The prepared dried granules ready for compression was then evaluated for various granule properties as discussed below.

Table 2.1: Data for Composition of Preliminary Batches

Batches		H1	H2	H3	P1	P2	P3	P4	P5
Complex		200	200	200	200	200	200	200	200
HPMC	K4M	100	-	-	-	-	-	-	-
	K15M	-	100	-	-	-	-	-	-
	K100M	-	-	100	30	40	50	60	70
Lactose		50	50	50	120	110	100	90	80
Magnesium Stearate		5	5	5	5	5	5	5	5
Talc		5	5	5	5	5	5	5	5
NaHCO ₃		60	60	60	60	60	60	60	60
Citric Acid		15	15	15	15	15	15	15	15
Total		435	435	435	435	435	435	435	435

*All quantities in mg / tablet

2.9.2 Preparation of Control Release Tablet (CRT)

Different control release tablet (CRT) formulations were prepared by procedure reported in preparation of granules (section 2.9.1) using wet granulation technique. All the batches of tablets were prepared using rotary punch tablet compression machine (Karnavati Rimek minipress II) using 12 mm size punch. Prepared tablets were evaluated for various tablet properties.

2.9.3 Evaluation of CRT (Preliminary Batches)

1) *In vitro* dissolution study for Preliminary batches

In vitro dissolution study was performed using USP Dissolution Testing Apparatus II (Disso TDT 08L, Electrolab). The dissolution test was performed using 900 ml of 0.1 N HCL, at 37 ± 0.5°C and paddle speed was rotated at 50 rpm. A sample (5 ml) of the solution was withdrawn from the dissolution apparatus after every 1hr. for next 12 hrs, and the samples were replaced with fresh dissolution medium equilibrated at the same temperature to maintain the volume. The samples were filtered through Whatman filter paper no. 41. The samples collected were diluted taking dilution factor as 10 i.e. 1ml sample diluted with 2ml of sodium carbonate(20%), 3ml of FCR(2:1 diluted with water) and then 4ml of 0.1N HCL. Samples were then analyzed by UV spectrophotometer at 760 nm using UV spectrophotometer Jasco V-630. The % drug release data is reported in sec 2.9.4, Table 3.6. The graphical presentation of % drug released verses time interval is shown in Figure 3.15 and 3.16. Dissolution tests were performed in duplicate (20).

2.10 Factorial Design Batches (Experimental design) (8, 21,22)

A 3² factorial design was implemented for optimization of oral controlled release tablet. According to the model it contains two independent variables at three levels +1, 0 and -1 (Table 2.2). The translation of coded levels in actual units is enumerated in Table 2.3. According to the model total nine formulations are possible. The composition of different formulations is shown in Table 2.4.

A. Dependent variables

Y1 - Time taken for 50% drug release (%)

Y2 - Time taken for 85% drug release (%)

Y3 - Floating lag time (Seconds)

B. Independent variables:

X1 - HPMC K100M (%)

X2 - Citric Acid

Table 2.2: Factorial Design for Preparation of Batches.

Batch Code	Variable levels in Coded form	
	X ₁	X ₂
F1	+1	+1
F2	+1	0
F3	+1	-1
F4	0	+1
F5	0	0
F6	0	-1
F7	-1	+1
F8	-1	0
F9	-1	-1

Table 2.3: Translation of coded values in actual unit.

Independent Variable levels	Low (-1)	Medium (0)	High (+1)
X ₁ = Concentration of HPMC K100 M (%)	20	30	40
X ₂ = Concentration of Citric Acid (%)	5	7.5	10

Table 2.4: Combination batches by using HPMC K100M & Citric Acid in various concentrations according to 3² factorial designs.

Batch code	F1	F2	F3	F4	F5	F6	F7	F8	F9
Complex	500	500	500	500	500	500	500	500	500
HPMC K100M	100	100	100	150	150	150	200	200	200
Citric Acid	25	37.5	50	25	37.5	50	25	37.5	50
PVP K-30	60	60	60	60	60	60	60	60	60
Mg. Stearate	5	5	5	5	5	5	5	5	5
NaHCO ₃	80	80	80	80	80	80	80	80	80
Lactose	30	17.5	5	30	17.5	5	30	17.5	5
Total	800	800	800	850	850	850	900	900	900

*All quantities in mg/tablet

2.11 Preparation of Factorial Design Batches

2.11.1 Preparation of Granules

Preparation of Granules was done by Wet Granulation Technique using composition mention in Table 2.4. Procedure is mention in the section 2.9.1 was used (19).

2.11.2 Evaluation of Granules

The granule properties include bulk density; tap density, Hausner ratio, and Carr's index were determined using Tap density tester (TD 1025, Lab India).

1) Angle of Repose

Angle of repose has been defined as the maximum angle possible between the surface of pile of powder and horizontal plane. The angle of repose for the granules of each formulation was determined by the funnel method. The granules mass was allowed to flow out of the funnel orifice on a plane paper kept on the horizontal surface. This forms a pile of angle of granules on the paper. The angle of repose was calculated with the help of values of the base radius 'R' and pile height 'H' (23,24).

$$\tan \Theta = h / r \dots\dots\dots (2.2)$$

Where, Θ = angle of repose

h = height of the cone

r = Radius of the cone

Table 2.5: Relationship between angle of repose (Θ) and Flowability

Angle of Repose (Θ)	Flowability
< 20	Excellent
20 – 30	Good
30 – 34	Passable
> 40	Very Poor

2) Bulk Density

The bulk density was obtained by dividing the mass of a powder by the bulk volume in cm³ (23,24). It was calculated by using equation given below:

$$\rho_b = M / V_0 \dots\dots\dots (2.3)$$

Where, ρ_b = bulk density

M = weight of sample in grams

V_0 = Apparent unstirred volume

3) Tapped Density

The tapped density was obtained by dividing the mass of a powder by the tapped volume in cm³ (23,24).It was calculated by using equation given below:

$$\rho_t = M / V_f \dots\dots\dots (2.4)$$

Where, ρ_t = Tap density

M = weight of sample in grams

V_f = final Tap volume

4) Carr's Index

The Carr's index is determined from the tapped density and poured density (bulk density) as per the formula (Eq. (2.4)) given below (23,24).

$$\text{Carr's index (\%)} = \frac{\text{Tapped density} - \text{bulk density}}{\text{Tapped density}} \times 100 \dots\dots\dots (2.5)$$

Table 2.6: Relationship between % compressibility and flowability

% Compressibility	Flowability
5 – 15	Excellent
12 – 16	Good
18 – 21	Fair to Passable
23 – 35	Poor
33 – 38	Very Poor
> 40	Extremely Poor

5) Hausner ratio

Hausner ratio is determined from the ratio of tapped density to poured density using formula given below (23,24).

$$\text{Hausner ratio} = \frac{\text{Tapped density}}{\text{Poured density}} \dots\dots\dots (2.6)$$

The Angle of repose, Bulk density, Tap density, Carr's index and Hausner ratio are reported in sec 3.9.2, Table 3.6.

2.11.3 Preparation of Control Release Tablet (CRT)

Different control release tablet (CRT) formulations were prepared by wet granulation technique. All the batches of tablets were prepared using rotary punch tablet compression machine (Karnavati Rimek minipress II) using 12 mm size punch. Prepared tablets were evaluated for various tablet properties.

2.11.4 Evaluation of Control Release Tablet (CRT)

1) Weight Variation Test

I. P. procedure for uniformity of weight was followed. Twenty tablets were randomly selected from each batch and individually weighed. By using Electronic balance (Shimatzu). The average weight and standard deviation of twenty tablets were calculated .The average weight of tablet and its allowed percent deviation were shown in Table 2.7. Result for Weight Variation test is reported in section 3.9.4, Table 3.7 (25,26).

Table 2.7: Allowable limit for weight variation

Average weight of tablet (X mg)	Percentage deviation
$X \leq 80 \text{ mg}$	10 %
$80 < X < 250 \text{ mg}$	7.5 %
$X \geq 250 \text{ mg}$	5 %

2) Tablet hardness

The resistance of tablet to shipping or breakage, under conditions of storage, transportation and handling before usage depend on its hardness. The hardness of tablet of each formulation was measured by Pfizer hardness tester. The hardness was measured in terms of kg/cm². For each batch three tablets were tested. The average hardness and standard deviation is reported in section 3.9.4, Table 3.7 (25,26).

3) Friability

Friability is the measure of tablet strength. Roche friabilator (FT1020, Labindia) was used for testing the friability. Twenty tablets were weighed accurately and placed in the tumbling apparatus that revolves at 25 rpm dropping the tablets through a distance of six inches with each revolution. After 100 revolutions, the tablets were weighed and the % friability was calculated measured using the formula (Eq. (8.7)). The friability of different formulations is reported section 3.9.4, Table 3.7 (25,26).

$$\text{Friability} = \frac{\text{Initial weight of tablets} - \text{Final weight of tablets}}{\text{Initial weight of tablets}} \times 100 \dots\dots (2.7)$$

4) Thickness

Thickness of tablet is important for uniformity of tablet size. Thickness was measured using Vernier Calliper. It was determined by checking ten tablets from each formulation. Results for thickness are reported in section 3.9.4, Table 3.7 (25,26).

5) Drug Content

Five tablets were weighed individually, crushed to fine powder and about 100 mg of drug was dissolved in 0.1N HCl, the solution was filtered through 0.45μ membrane filter. The absorbance was measured at 760 nm after suitable dilution using F. C. Phenol reagent as a colour forming agent. Results for drug content section 3.9.4, Table 3.7 (25,26).

6) In vitro dissolution study for Factorial batches

In vitro dissolution study was performed using USP Dissolution Testing Apparatus II (Disso TDT 08L, Electrolab). The dissolution test was performed using 900 ml of 0.1 N HCL, at $37 \pm 0.5^{\circ}\text{C}$ and paddle speed was rotated at 100 rpm. A sample (5 ml) of the solution was withdrawn from the dissolution apparatus after every 1hr. for next 12 hrs, and the samples were replaced with fresh dissolution medium equilibrated at the same temperature to maintain the volume. The samples were filtered through Whatman filter paper no. 41. The samples collected were diluted taking dilution factor as 10 i.e. 1ml sample diluted with 2ml of sodium carbonate(20%), 3ml of FCR(2:1 diluted with water) and then 4ml of 0.1N HCL. Samples were then analyzed at 760 nm using UV spectrophotometer (Jasco V-630). The % drug release was calculated using disso software (PCP V3) and is reported in section 3.9.4, Table 3.8 and 3.9. The graphical presentation of % drug released verses time interval is shown in Figure 3.17, 3.18, and 3.19. The FLT for all factorial batches is shown in Figure 3.20. Dissolution tests were performed in triplicate (25,26).

2.12 Curve fitting

Release data were fitted to various mathematical models for describing the release mechanism from controlled release zero-order (Eq.2.8) [Lee, 1984] and Hixon Crowell.

$$M_t/M_{\infty} = k_k P t^n \dots\dots\dots (2.8)$$

Where, M_t/M_{∞} = fraction of drug released at time 't';

$k_k P$ = release rate constant;

n = the release exponent.

$$M_t = M_0 + k_0 \dots\dots\dots (2.9)$$

Where, M_t = the amount of drug released at time 't';

M_0 = the concentration of drug in the solution at $t=0$;

k_0 = the zero-order release constant.

$$M_t = k_H t^{1/2} \dots\dots\dots (2.10)$$

Where, M_t = the amount of drug release at time ' \sqrt{t} ';

k_H = the Higuchi release constant.

All curve fitting, simulation and plotting was carried out by using PCP disso software. The parameters for both zero order and Hixon Crowell models were shown in Table 3.11 (27,28,29).

2.13 Optimization of Factorial Design Batches

2.13.1 Regression analysis

The effect of formulation variables on the response variables were statistically evaluated by applying one way ANOVA at $P < 0.05$ level using a commercially available software package Design-Expert® version 7.1.6 (Stat-Ease Inc.) (8,22). To describe the response surface curvature, the design was evaluated by quadratic model, which bears the form of equation (Eq. 2.11).

$$Y = b_0 + b_1X_1 + b_2X_2 + b_3X_1X_2 + b_4X_1^2 + b_5X_2^2 \dots\dots\dots (2.11)$$

Where, Y is the response variable,

b_0 the constant,

$b_1, b_2 \dots b_5$ the regression coefficient,

X_1 and X_2 stand for the main effect,

X_1X_2 are the interaction terms, show how response changes when

Two factors are simultaneously changed.

1) Regression analysis for response Y_1

The effect of formulation variables on the response variables were statistically evaluated by applying one way ANOVA at $P < 0.05$ level using a commercially available software package Design-Expert® version 7.1.6 (Stat-Ease Inc.) (8, 22).

2) Regression analysis for response Y_2

The effect of formulation variables on the response variables were statistically evaluated by applying one way ANOVA at $P < 0.05$ level using a commercially available software package Design-Expert® version 7.1.6 (Stat-Ease Inc.) (8, 22).

3) Regression analysis for response Y_3

The effect of formulation variables on the response variables were statistically evaluated by applying one way ANOVA at $P < 0.05$ level using a commercially available software package Design-Expert® version 7.1.6 (Stat-Ease Inc.) (8, 22).

4) ANOVA, Pure Error and Lack of Fit

The results for ANOVA, pure error and lack of fit were discussed in section 3.11.1.

2.14 Studies on Final Formulation

1) Water uptake studies

The rate of test medium uptake by the polymer was determined by equilibrium weight gain method similar to Fantasies and Vlachos (2000). The study was carried out in the USP dissolution apparatus II. The FCRT Tablet was accurately weighed, placed in dissolution baskets, and immersed in 0.1 N HCl solution maintained at $37 \pm 0.5^\circ\text{C}$ in the dissolution vessel. At regular intervals, the pre-weighed basket-matrix system was withdrawn from the dissolution vessel, lightly blotted with a tissue paper to remove excess test liquid and re-weighed. The percent water uptake, i.e., degree of swelling due to absorbed test liquid, was estimated at each time point using formula given below:

$$\% \text{ Water uptake} = \frac{(W_t - W_i)}{W_i} \times 100 \dots\dots\dots (2.12).$$

Where, W_t is the weight of the swollen matrix at time, t , W_i is the initial weight of the tablet. The % swelling or water uptake data is reported in section 3.12 in Table 3.13 (26).

2) Comparison of In vitro release study of marketed formulation with capsule fills with complex and formulated tablet

The in vitro profile of optimized formulation and complex were compared with marketed SR tablet (Biaxin-500). *In vitro* dissolution study was performed using USP Dissolution Testing Apparatus II (Disso TDT 08L, Electrolab). The dissolution test was performed using 900 ml of 0.1 N HCL, at $37 \pm 0.5^\circ\text{C}$ and paddle speed was rotated at 100 rpm. A sample (5 ml) of the solution was withdrawn from the dissolution apparatus after every 1hr. for next 12 hrs, and the samples were replaced with fresh dissolution medium equilibrated at the same temperature to maintain the volume. The samples were filtered through Whatman filter paper no. 41. The samples collected were diluted taking dilution factor as 10 i.e. 1ml sample diluted with 2ml of sodium carbonate(20%), 3ml of FCR(2:1 diluted with water) and then 4ml of 0.1N HCL. Samples were then analysed at 760 nm using UV spectrophotometer (Jasco V-630). The % drug release was calculated using disso software (PCP V3) and is reported in section 3.12 (Table 3.14). The graphical presentation of % drug released verses time interval is shown in Figure 3.27 (25,26).

3) Optimization

A numerical optimization technique by the desirability approach was used to generate the optimum settings for formulation. The process was optimized for dependent variables Y_1 - Y_3 . The optimized formula arrived by targeting the Y_2 at 650 minute, Y_1 was kept at range 360-400 min., Y_3 also kept at range 16-62 sec. Results were discussed in section 3.12 (30)

3. RESULTS AND DISCUSSIONS

3.1 Synthesis of Nanosponges

3.1.1 Reaction

Nanosponges was synthesized and purified by ethanol in Soxhlet apparatus. The carbonylation of β -CD and DPC occurred and characterised by various techniques. The reaction is represented in Figure 3.1.

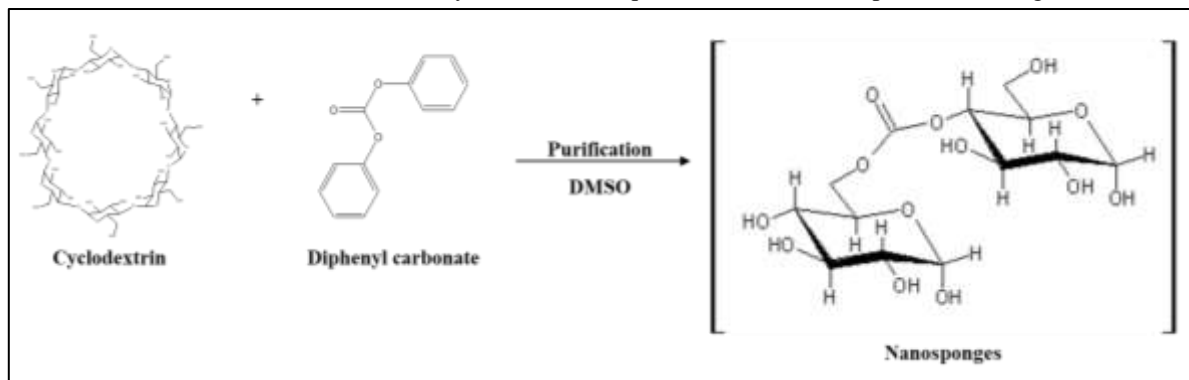


Figure 3.1: Nucleophilic reactions of beta-CD and Diphenyl Carbonate.

3.1.2 Preparation of Nanosponges

Preparation of Nanosponges was carried out according to the procedure mention in the section 2.2.2.

3.2 Optimization of Synthesized Product (Nanosponges)

Reaction was optimised to various concentrations of cross linker. This reaction was optimised in terms of percentage yield. The obtained yield was 55%, 69% and 70% by keeping β -CD: DPC in the ratio 1:2, 1:4 and 1:8. The reactions were carried out batch 1, 2 & 3 for these proportions respectively. The yield obtained in batch 2 and 3 were almost same so combination used in the batch number 2 was finally selected for Nanosponges synthesis.

Table 3.1: Optimization of Synthetic procedure

Batches	BCD:DPC ratio	Energy type	Yield %
1	1:2	Conventional Heating	55
2	1:4	Conventional Heating	69
3	1:8	Conventional Heating	70

3.3 Characterization of Synthesized Product (Nanosponges)

Table 3.2: Characteristics of Nanosponges

Parameters	Characteristics
Colour, State	White, Solid
TLC	Chloroform; $R_f = 0.23$
IR (KBr) cm^{-1}	1775 / cm^{-1} (C=O group)
DSC	Degradation occurs after 300 $^{\circ}\text{C}$

1) Thin Layer Chromatography (TLC)

TLC showed clear separation between starting material and product. As there was complete consumption of starting material β -CD absence of spot in product the formation of product was confirmed.

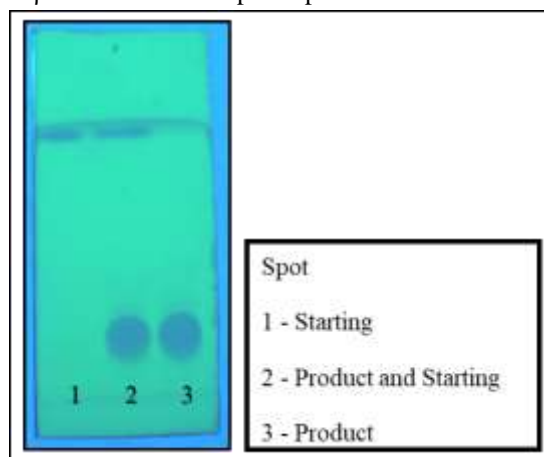


Figure 3.2: TLC Photograph

2) FTIR Spectra

The FTIR spectra of Nanosponges and β -CD were portrayed in Figure 3.3. FTIR spectra of β -CD was characterized by 2925 cm^{-1} (C-H asym./sym. stretch), peak at 1646 cm^{-1} (C=C stretching), 1415 (C-H bend) cm^{-1} and a band with distinct peaks in the region between 1200 and 1000 cm^{-1} . The FTIR spectra of Nanosponges exhibited distinct peaks at 2926 cm^{-1} (C-H asym. /sym. stretch), 1638 cm^{-1} (C=C stretching), 1775 cm^{-1} (Aryl Carbonate), 1026 cm^{-1} (Primary alcohol, C-O stretch), 1413 cm^{-1} (C-H bend) confirming the earlier report. The appearance of peak at 1775 cm^{-1} clearly indicated the carbonylation of β -CD which is shown in Table 3.3. The peak at 1775 / cm^{-1} confirmed presence of the carbonyl group in the structure of Nanosponges.

Table 3.3: IR peak of β -CD and NS

Group	Beta-CD	Nanosponges
C-H asym./sym. stretch	2925	2926
C=C stretching	1646	1638
Aryl Carbonate	absent	1775
Primary alcohol, C-O stretch	1027	1026
C-H bend	1415	1413

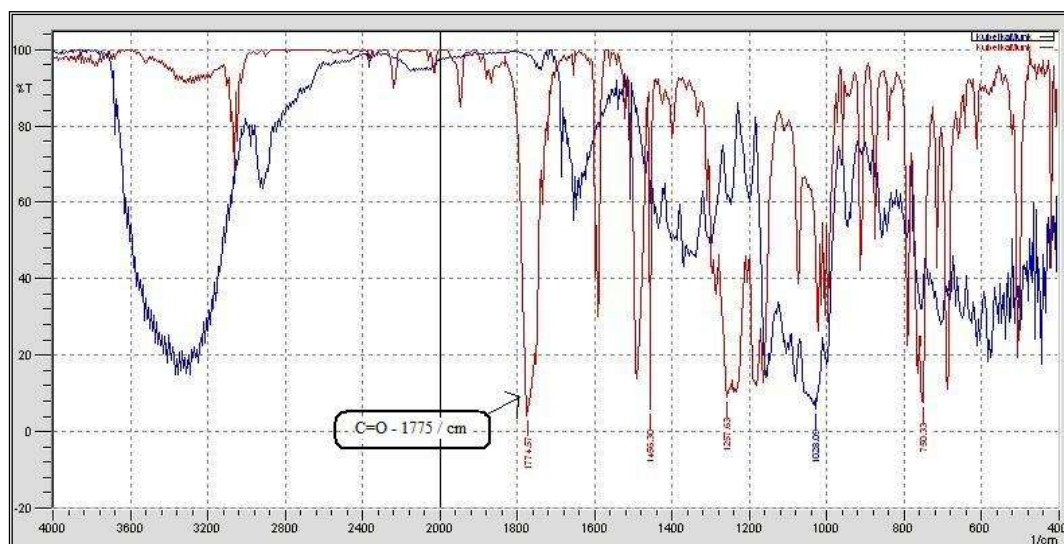


Figure 3.3: FTIR spectra of Nanosponges and Beta-CD

3) DSC Graph

Thermal degradation of Nanosponges is reported after 300°C. The absence of endotherm below 300°C in the present study it was confirmed that the Nanosponges was synthesized. The graph of β -CD and Nanosponges are shown in Figure 3.4.

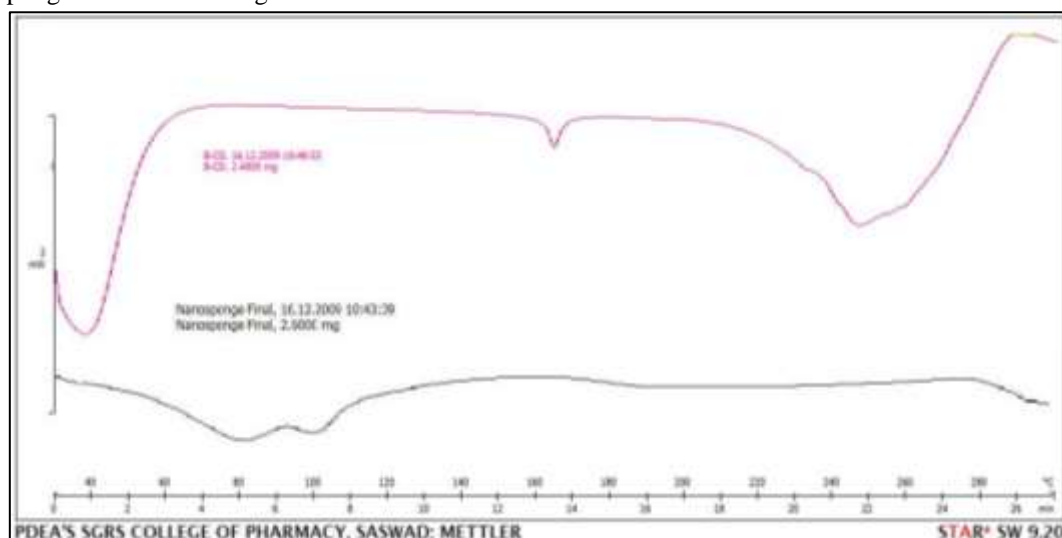


Figure 3.4: DSC graph of Nanosponges and Beta-CD.

4) X-Ray Powder Diffraction (XRPD) Analysis

Formation of Nanosponges was confirmed by XRPD spectra. As shown in Figure 3.5, the number of peaks reduced in Nanosponges as compared to β -CD with peak broadening. This clearly indicated formation of poorly crystalline Nanosponges.

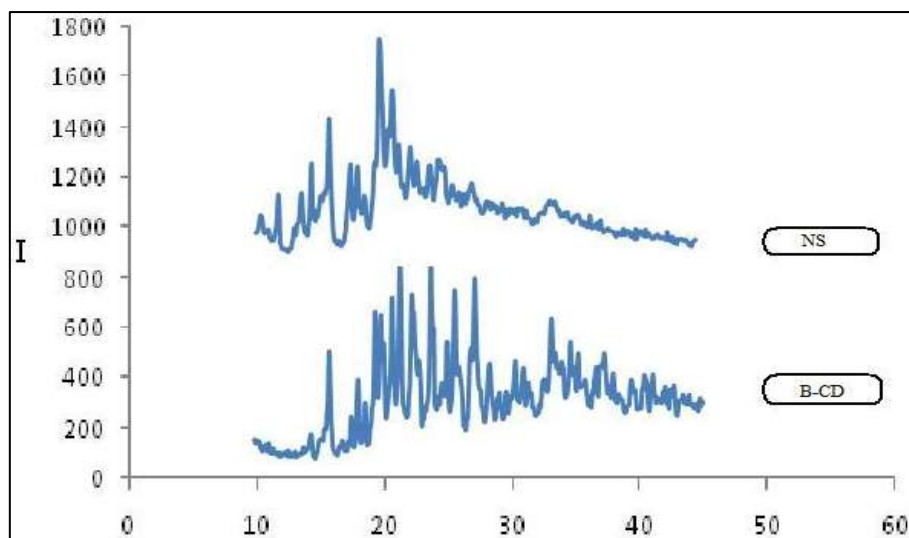


Figure 3.5: PXRD of Nanosponges and Beta-CD

5) NMR

The C^{13} NMR of Nanosponges and β -CD were shown in Figure 3.6 and 3.7 respectively. NMR of NS shows various peaks at different δ - values. The carbonyl bridge between two β -CD showed the peak at 155.5 δ value which confirmed the Nanosponges was synthesized.

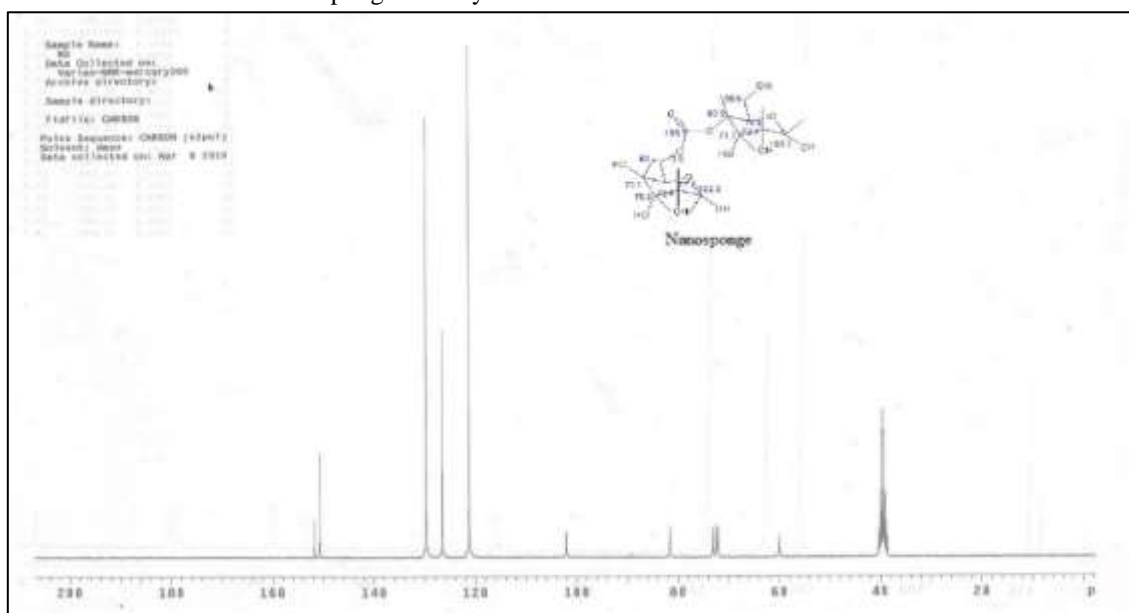


Figure 3.6: NMR of Nanosponges

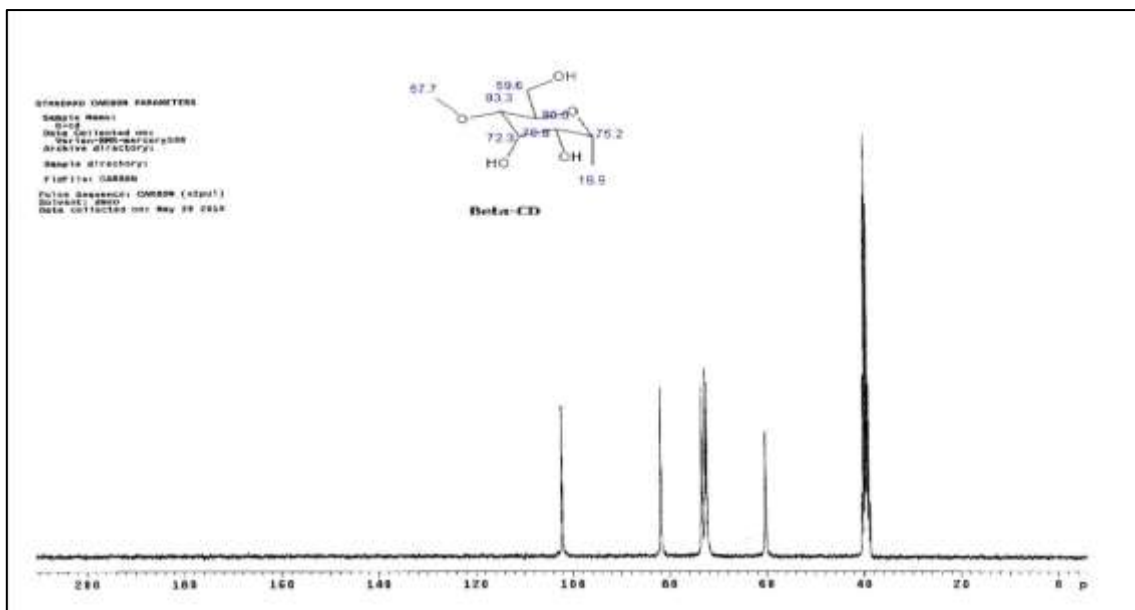


Figure 3.7: NMR of Beta-CD

3.4 Phase solubility studies

The phase solubility studies conducted at 25°C indicated that, solubility of Clarithromycin increased linearly ($R^2=0.961$) as a function of Nanosponges concentration, as shown in Figure 3.8. As apparent solubility of Clarithromycin increased linearly with Nanosponges concentration over the entire concentration range studied; the phase solubility diagram was classified as A_L type. The slope and intercept of the curve were found to be 0.0003047 and 28.21×10^{-8} M, respectively. The stability constant computed from the slope and intercept of the phase solubility diagram was found to be 1080.12 M^{-1} . The value of stability constant obtained indicated a labile association of Clarithromycin and Nanosponges. The solubility of clarithromycin was significantly increased with Nanosponges.

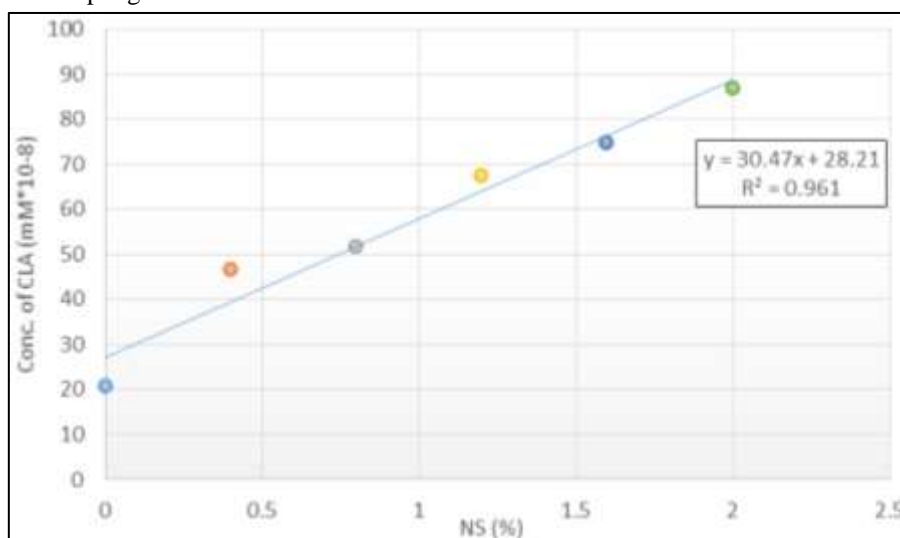


Figure 3.8: Phase solubility study of drug and Nanosponges in 0.1 N HCL

3.5 Preparation of binary systems

Drug Incorporation and Preparation of Physical Mixture was done using the procedure mention in the section 2.6.

3.6 Characteristics of Complex

1) FT-IR spectroscopy study

The FTIR spectra of Nanosponges, Clarithromycin and complex were portrayed in Figure 3.9. The FTIR studies showed that there are weak interactions between NS and CLA that were evident from broadenings and disappearance of the drug peak in case of complexes.

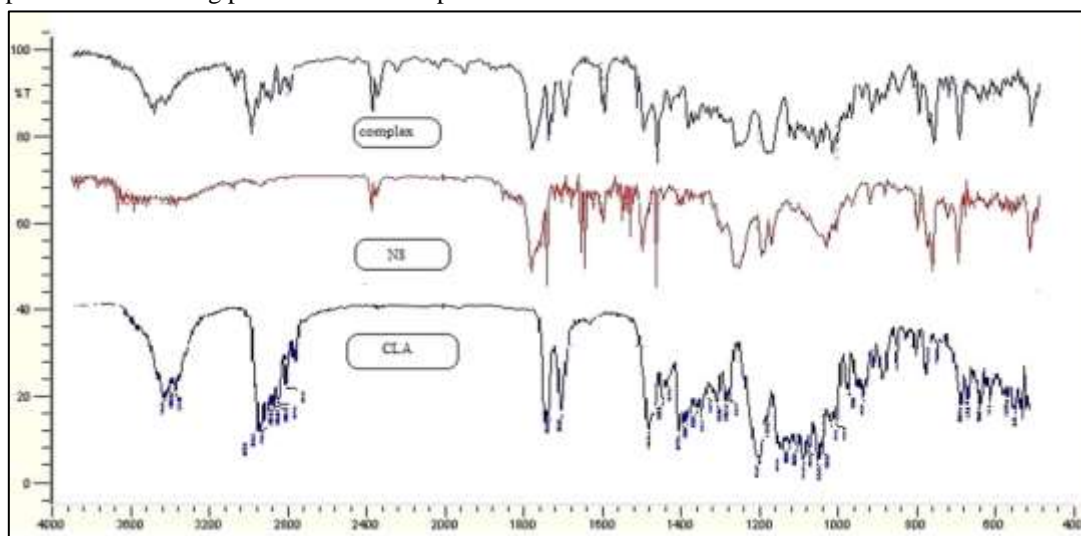


Figure 3.9: FTIR spectra of Nanosponges, Clarithromycin and complex

2) DSC study

The thermal analysis graphs of pure Clarithromycin, complex and Nanosponges are shown in Figure 3.10. Area of enthalpies of the drug progressively decreased in following order Plain drug, Nanosponges, drug Nanosponges PM, and drug Nanosponges solid dispersions.

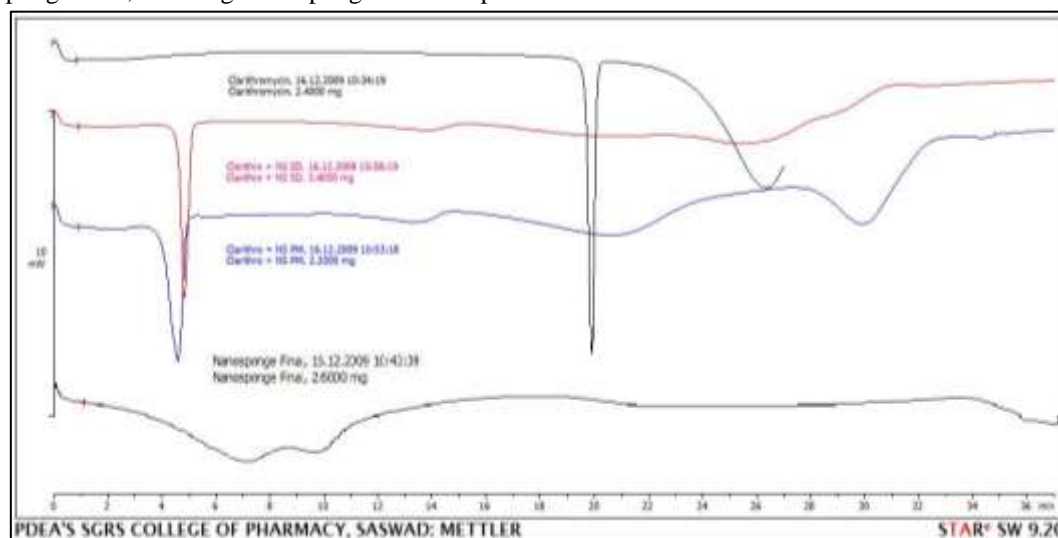


Figure 3.10: DSC graph of pure CLA, complex and Nanosponges

These could be due to change in the state of the drug from crystalline to amorphous. Thus the energy required to melt the drug is reduced i.e. enthalpy reduced. DSC thermograms of the complexes did not show the melting peak corresponding to drug fusion. This indicates that the drug is no longer crystalline and confirms its interaction with NS structure. On the contrary, the binary P.M. presented the melting peak of the drug indicating that CLA maintained its original crystallinity in the P.M. due to a lack of interaction.

3) PXRD Study

The complexation between Clarithromycin and Nanosponges was also confirmed by PXRD. As shown in the PXRD pattern of drug loaded Nanosponges (Figure 3.11), number of peaks of Clarithromycin were reduced. Also, no perfect coincidence was found in PXRD patterns of CLA and CLA- NS complex indicating

the formation of a new ordered phase which might be responsible for increase in the solubility of CLA. Thus it can be predicted that the solubility of CLA is due to its molecular dispersion i.e. complexation with Nanosponges.

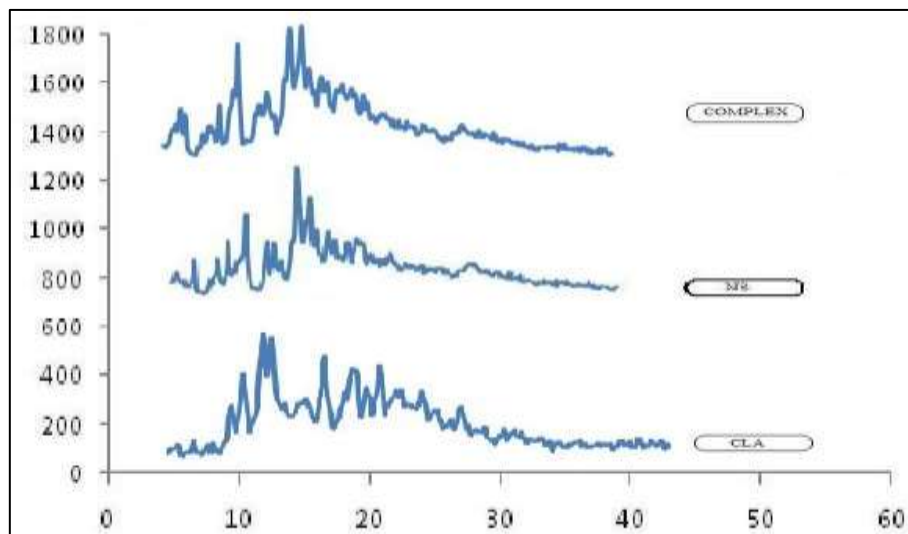


Figure 3.11: PXRD of CLA, NS and Complex

4) Scanning Electron Microscopy

SEM images of NS and complex were shown in Figure 3.12 and 3.13. These images revealed striking difference between the microstructure of plain NS and complex of NS and CLA. Plain NS exhibited highly porous structure while complex was compacted. The SEM of complex confirmed drug loading in the NS as the surface is smooth as compared to porous surface of plain NS.

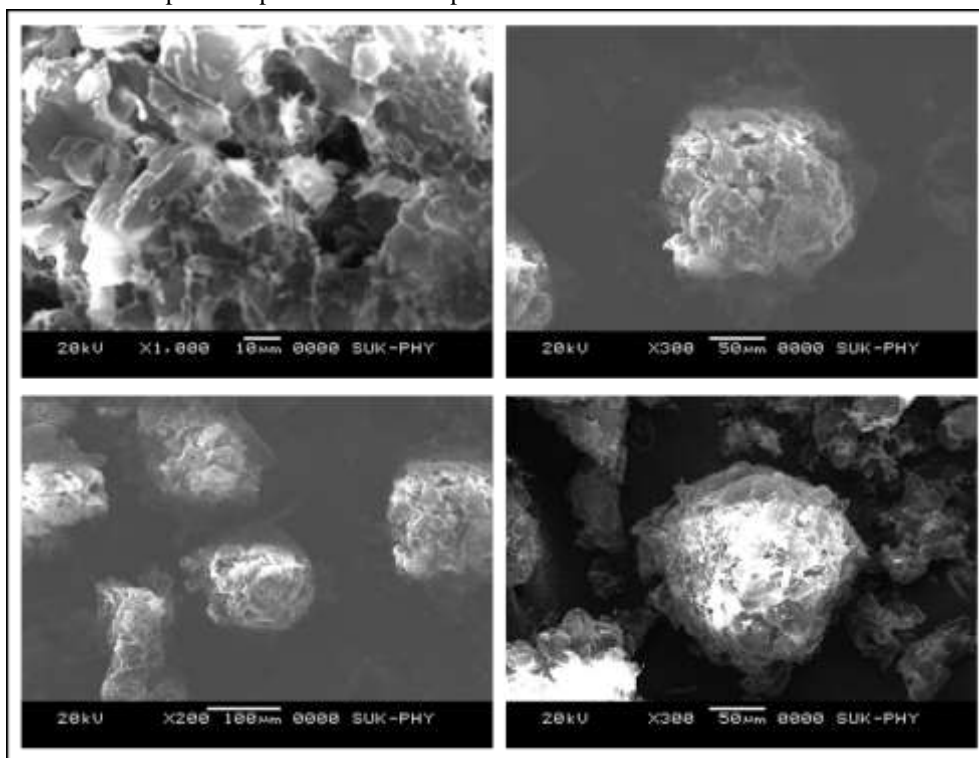


Figure 3.12: SEM Images of NS

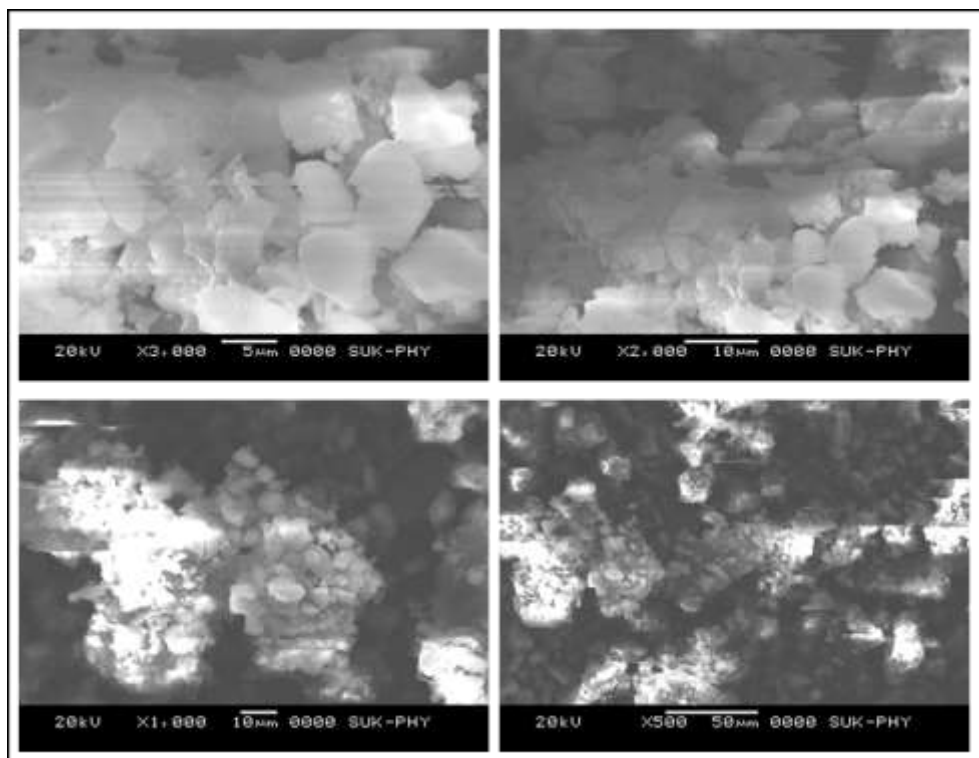


Figure 3.13: SEM Images of Complex

3.7 Gastric Irritation Test

Histopathological examination - Rats treated with Plain drug showed marked mucosal damage. Lesion formation was found to be 75% in these cases whereas in rats which received complex showed reduced gastric lesions as compared with plain drug photographs are shown in Figure 3.14. The results are shown in Table 3.4. From the results it was concluded that severity of ulceration was lowered in test groups than standard group.

Table 3.4: Histopathological report of stomach tissues

Group	Control (A)	Standard(B)	Test (C)
Congestion	00	++	+
Necrosis	00	+++	+
Cellular infiltration	00	++	+
Edema	00	++	+
Ulceration	00	+++	+
Hemorrhages	00	+++	+
Note: 0 indicates no abnormality detected, + indicates pathological changes up to less than 25 %, ++ indicates Pathological changes up to less than 50 % , +++ indicates Pathological changes up to less 75 %, ++++ indicates Pathological changes up to more than 75 %			

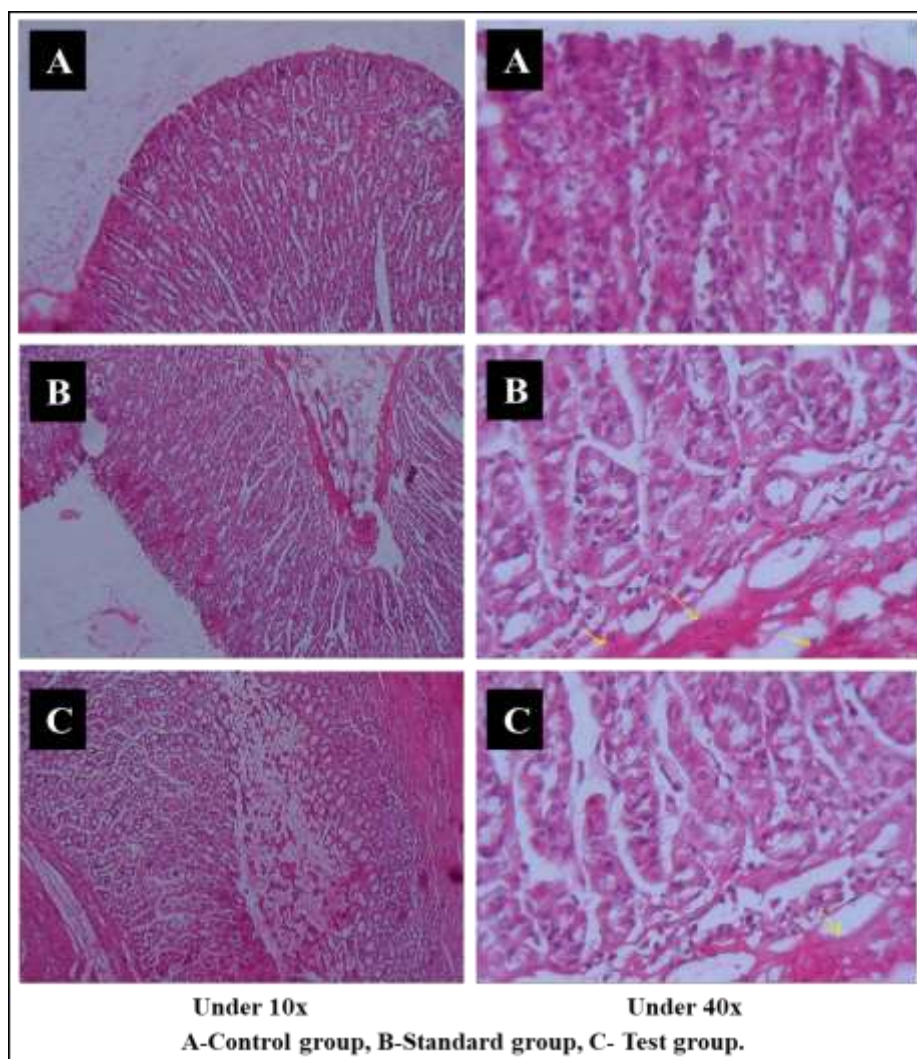


Figure 3.14: Photographs of stomach Tissue

3.8 Preparation of Preliminary Batches for selection of Polymer

3.8.1 Preparation of Granules

Granules were prepared according to the Procedure mentioned in the section 2.9.1.

3.8.2 Preparation of Control Release Tablet (CRT)

Control release tablet of clarithromycin was prepared according to the procedure mentioned in the section 2.9.2.

3.8.3 Evaluation of CRT (Preliminary Batches)

1) *In vitro* dissolution study for Preliminary batches

In vitro dissolution study was performed using USP Dissolution Testing procedure and the result are mention in the Table 3.5. Figure 3.15 shows % Drug Release of Clarithromycin from batches H1-H3. H1 contains HPMC K4M 100 mg alone and released 50% of the drug in 3 hrs. H2 contains HPMC K15M 100 mg alone and released 50% of the drug in 5 hrs. H3 contains HPMC K100M 100 mg alone and released 50% of the drug in 9 hrs which was attributed to its high viscosity as compared to K4M & K15M (Table 3.5). Hence HPMC K100M was used in further studies of preliminary formulations. From the discussion data for batches H1-H3 it was concluded that HPMC K100M showed highest release retarding property.

Table 3.5: *In vitro* dissolution study of preliminary batches in 0.1N HCL

Time (h)	Drug Release %							
	H1	H2	H3	P1	P2	P3	P4	P5
0	0.000	0.000	0.00	0.00	0.00	0.00	0.00	0.00
1	21.76	13.46	01.32	23.12	16.64	08.97	07.54	05.06

2	44.54	23.12	11.65	32.63	22.87	16.86	14.63	18.47
3	57.89	39.54	19.87	43.78	39.56	23.83	21.36	27.90
4	65.43	42.45	24.75	51.75	45.21	35.19	33.69	33.17
5	78.63	58.37	31.21	63.71	53.87	41.09	42.14	35.68
6	89.12	67.84	37.43	72.05	63.97	50.59	47.96	44.01
7	95.27	75.28	41.65	79.24	73.56	59.93	52.41	53.14
8	99.12	82.45	49.08	87.41	81.43	68.48	61.37	58.45
9	99.13	85.63	55.60	94.83	89.54	78.12	68.57	61.45
10	99.19	89.91	57.98	98.67	94.67	82.63	79.63	62.98
11	99.20	92.59	59.12	99.32	99.67	96.94	89.31	75.32
12	99.20	97.61	61.78	99.32	99.68	99.72	95.78	79.92

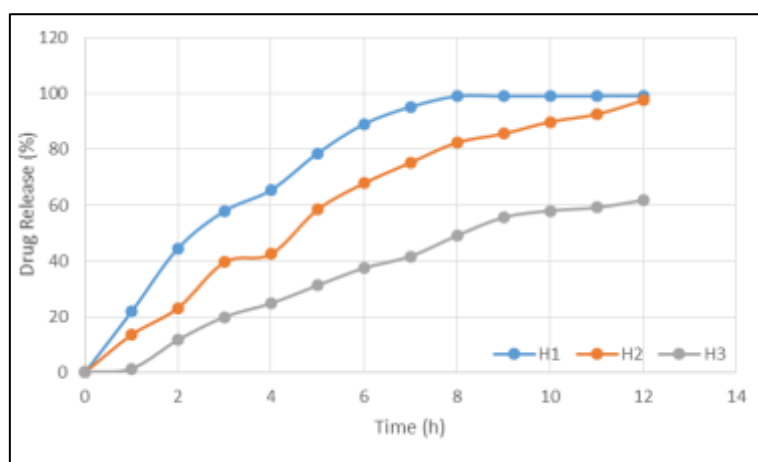


Figure 3.15: % Cumulative Drug release from preliminary Batches H1-H3 in 0.1N HCL

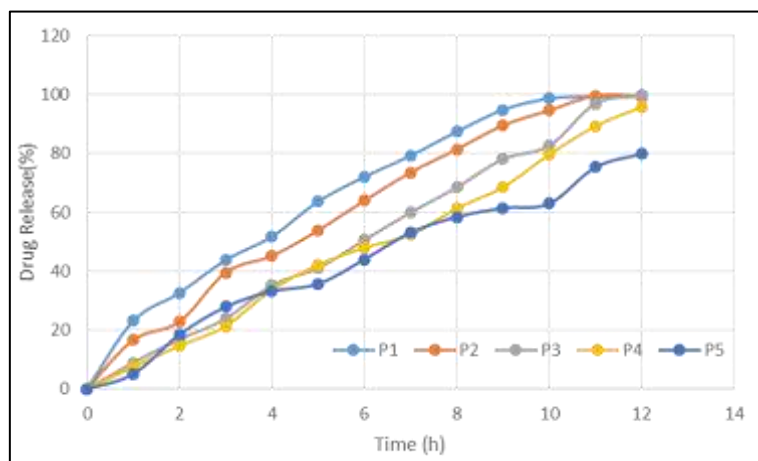


Figure 3.16: % Cumulative Drug release from preliminary Batches P1-P5 in 0.1N HCL

Figure 3.16 shows, Clarithromycin release from batches P1, P2, P3, P4 and P5 contained HPMC K100M alone in increasing concentration from 30, 40, 50, 60 and 70mg /tablet respectively. Preliminary Batches P1, P2, P3, P4 and P5 released its 50% drug content in 230 min., 282min., 355min., 409min. and 407min respectively. As the concentration of HPMC K100M increased the release rate decreased. From the results it was clear that optimized release was from batch P3 and P4 containing 50mg & 60 mg of HPMC K100M per tablet (25% w/w & 30% w/w per tablet). To evaluate the effect of concentration of HPMC K100M and citric acid on in vitro dissolution pattern of drug a statistical model of 3^2 full factorial designs was applied. Hence for further study 20, 30 and 40 % of the HPMC and Citric acid used in 5, 7.5 and 10% used in 3^2 Factorial design.

3.9 Preparation of Factorial Design Batches

3.9.1 Preparation of Granules

Preparation of Granules was done by Wet Granulation Technique using composition mention in Table 2.4.

3.9.2 Evaluation of Granules

The dried granules were evaluated for Angle of repose, Bulk Density, Tapped Density, Carr's index and Hausner's Ratio and the data is shown in Table 3.6.

Table 3.6: Data for Granules properties prepared for Factorial Design Batches

Batch	Angle of Repose	Tapped Density (g/ml)	Bulk Density (g/ml)	Carr's Index %	Hausner ratio
F1	32.80±0.11	0.878±0.05	0.754±0.07	15.09±0.06	0.858±0.05
F2	30.06±0.08	0.899±0.09	0.781±0.09	15.10±0.05	0.86±0.07
F3	31.33±0.16	0.930±0.11	0.784±0.09	15.68±0.09	0.843±0.05
F4	32.97±0.12	0.836±0.08	0.735±0.12	14.52±0.06	0.879±0.09
F5	30.68±0.09	0.891±0.09	0.764±0.14	16.62±0.13	0.857±0.06
F6	32.16±0.11	0.902±0.08	0.782±0.08	15.34±0.08	0.866±0.09
F7	31.83±0.12	0.883±0.13	0.767±0.09	15.12±0.11	0.868±0.07
F8	31.62±0.09	0.895±0.09	0.781±0.12	14.59±0.05	0.872±0.05
F9	30.85±0.13	0.910±0.11	0.792±0.15	14.89±0.05	0.8703±0.07

3.9.3 Preparation of Control Release Tablet (CRT)

Different control release tablet (CRT) formulations were prepared by wet granulation technique. All the batches of tablets were prepared using rotary punch tablet compression machine (Karnavati Rimek minipress II) using 12 mm size punch. Prepared tablets were evaluated for various tablet properties.

3.9.4 Evaluation of compressed tablets:

The Tablets from each batch of factorial design were evaluated for Uniformity in Average weight, Thickness, Hardness, Friability, Drug content and result are reported in Table 3.7.

1) Weight Variation Test

The results indicated was no weight variation as per I.P limit. The average weight of the tablet was found to be in range.

2) Tablet Hardness

The hardness of the tablets was found in the range of 5.2 to 5.8 kg/cm². The results indicated that the tablets having enough hardness and sufficient strength.

3) Friability

Percentage weight loss was measured and found to be less than 1%. As all the batches were within the pharmacopoeial limit (F< 1%).

4) Thickness

Size of tablets was found to be 12 mm in diameter and thickness of tablet was found to range from 3.8 to 4.9 mm.

5) Drug Content

All the formulations complied with the uniformity of drug content test for tablets. The drug content in all the batches of Clarithromycin floating tablets was in the range of 95 to 105%. This ensured good uniformity of the drug content in the tablets

Table 3.7: Data for Tablet properties from Factorial Batches.

Formulation	Average Weight in mg (n=5)	Hardness in Kg/cm ² (n=2)	Thickness in mm (n=2)	Friability in %	Drug Content in % (n=3)
F1	800.03 ±0.64	5.5 ± 0.3	3.9 ± 0.07	0.28	103.03 ±0.31
F2	800.14 ±0.91	5.2 ± 0.6	3.8 ± 0.05	0.32	97.86 ±0.70

F3	800.06 ±1.02	5.5 ± 0.2	3.9 ± 0.11	0.23	96.27 ±1.02
F4	850.52 ±0.83	5.8 ± 0.2	4.5 ± 0.08	0.22	99.61 ±0.73
F5	850.05 ±0.61	5.5 ± 0.4	4.4 ± 0.27	0.33	98.83 ±0.41
F6	850.12 ±0.90	5.8 ± 0.3	4.4 ± 0.13	0.31	104.83 ±1.13
F7	900.05 ±1.24	5.2 ± 0.2	4.9 ± 0.15	0.29	99.94 ±0.42
F8	900.79 ±1.61	5.5 ± 0.2	4.8 ± 0.09	0.33	102.02 ±1.1
F9	900.02 ±1.02	5.8 ± 0.4	4.9 ± 0.07	0.28	99.57 ±0.7

6) In-Vitro Drug release for Factorial batches F1-F9

The matrix tablets displayed a controlled drug release that depended on the total polymer level and citric acid level as well as presence of the drug either in the free or the complexes form. The actual values of % cumulative Drug release of factorial batches F1- F9 are reported in Table 3.8 and Drug release profile of factorial batches F1- F9 are shown in Figure 3.17, 3.18 and 3.19. The values of the release at of T₅₀, T₈₅ and floating lag time are shown in Table 3.9. At lower concentration of polymer % release was more. As concentration of polymer increases the release rate was retarded. The drug release at the end of 12h from the matrix tablets containing Clarithromycin was found to range from 68.15 ± 1.56 to 98.90 ± 1.09 %.

Table 3.8: Dissolution data for Factorial Batches F1-F9 in 0.1N HCL

Time (h)	% Drug Release (n=3)								
	F1	F2	F3	F4	F5	F6	F7	F8	F9
0	0	0	0	0	0	0	0	0	0
1	15.73±1.47	18.68±1.21	21.12±0.52	8.93±1.25	9.85±2.09	11.25±0.37	4.32±1.23	3.95±1.05	4.06±2.09
2	22.15±1.21	29.48±1.93	31.24±1.45	17.84±1.82	11.52±1.27	18.03±1.29	12.49±1.82	16.74±1.25	17.47±2.64
3	34.12±2.67	41.34±1.37	43.49±1.96	23.71±1.57	29.45±1.23	26.87±1.42	17.89±1.62	23.51±2.34	26.9±2.09
4	43.47±1.82	54.93±2.35	57.85±2.31	31.24±2.09	33.81±1.85	37.09±1.65	27.84±1.07	29.21±1.21	32.17±1.84
5	55.42±0.89	58.71±1.83	62.37±1.21	39.71±2.26	42.9±1.07	41.87±1.97	34.16±2.48	30.42±2.14	35.68±1.96
6	61.53±2.41	67.43±1.02	71.81±2.94	43.88±2.67	49.85±1.63	51.74±1.21	38.12±2.09	35.2±1.34	44.03±1.41
7	69.85±1.79	73.84±2.19	79.8±1.57	52.79±1.21	54.61±1.83	56.41±1.32	48.02±2.15	39.41±1.82	52.14±1.82
8	77.6±1.25	79.3±1.07	87.92±1.89	61.82±1.05	63.89±2.09	66.83±1.82	54.56±1.54	48.19±1.52	59.45±1.09
9	85.87±2.09	87.85±2.26	89.8±1.62	69.84±0.59	71.33±1.78	78.41±2.58	62.14±1.71	51.54±1.45	62.64±1.07
10	91.93±1.19	92.73±2.09	94.37±1.97	78.73±0.54	79.84±1.27	81.3±1.67	63.48±1.21	57.58±2.09	63.78±1.48
11	97.3±2.36	97.8±1.27	98.3±1.58	84.67±1.93	87.02±1.82	89.56±2.09	67.73±2.69	63.58±1.26	74.62±1.21
12	98.41±1.63	98.81±2.51	98.9±1.09	94.79±1.37	95.82±2.48	95.87±2.50	68.15±1.56	72.8±1.17	79.5±1.86

The Factorial batches F1, F2 & F3 which had lower total polymer level, were found to release 98.41 ± 1.63 %, 98.81±2.51% and 98.9±1.09 of the drug by the end of 12 h respectively which is shown in Figure 3.17. The Factorial batches F4, F5 & F6 which had medium level of polymer exhibited better drug release as they released 94.79 ± 1.37% ,95.82 ± 2.48 % & 95.87 ± 2.50 % respectively of the drug at the end of 12 h of dissolution , which is shown in Figure 3.18.

The Factorial batches F7, F8 & F9 which had higher polymer level, exhibited an impeded drug release as they released 68.15 ± 1.56 %, 72.8 ± 1.17 % & 79.5 ± 1.86 % respectively of the drug at the end of 12 h of dissolution which is shown in Figure 3.19. An increase in the polymer i.e. HPMC K100M concentration caused the increase in viscosity of diffusion layer and also the formation of gel layer serve as longer diffusional path for drug this might had decreased the effective diffusion coefficient of drug and therefore there was reduction in drug release rate.

Formulation F4, F5 & F6 containing medium polymer level exhibit better drug release in 12 h. So by considering release profile from all factorial batches batch F5 which containing 30% of HPMC K100M and 7.5% citric acid. Formulation F4 & F6 also release nearly same but medium level concentration of citric acid containing F5 was selected. These formulations contain drug in the complexes form exhibited a controlled and complete drug release during the dissolution period due to improved drug solubility.

The 3^2 factorial designs, preliminary trials were carried out to obtain the optimized concentration of polymer. The second variable citric acid was chosen because of its significant effect on the FLT and the drug release profile. All the nine batches showed variable release profile. The polymer concentration being constant and an increase in the concentration of citric acid the dissolution profile was improved significantly. The 3^2 full factorial design was selected to study the effect of independent variables HPMC K100M (X1) and Citric Acid (X2) on dependent variables t50%, t85% and floating lag time (Figure 3.20).

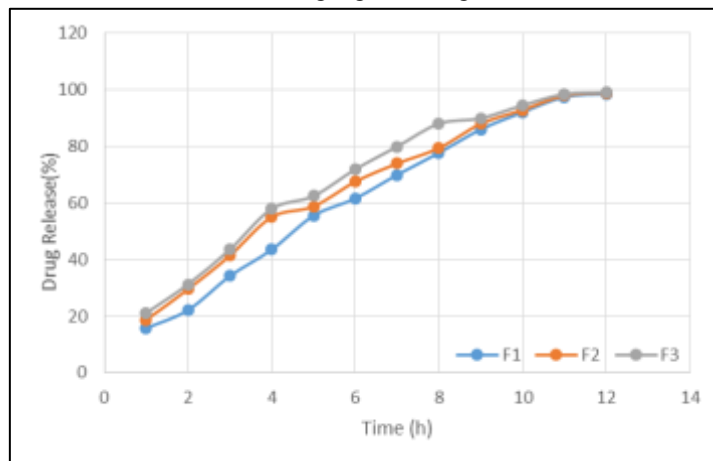


Figure 3.17: % Cumulative Drug release from factorial batches F1-F3

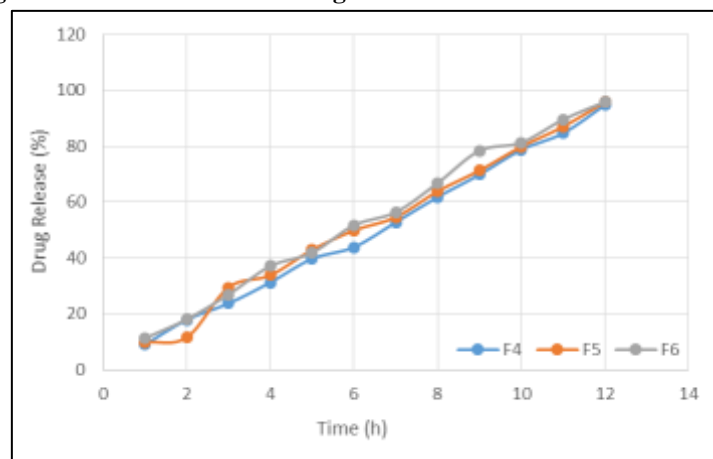


Figure 3.18: % Cumulative Drug release from factorial batches F4-F6

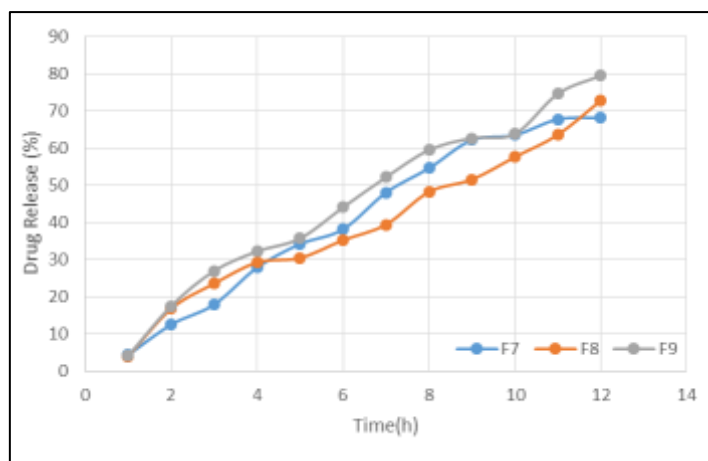


Figure 3.19: % Cumulative Drug release from factorial batches F7-F9

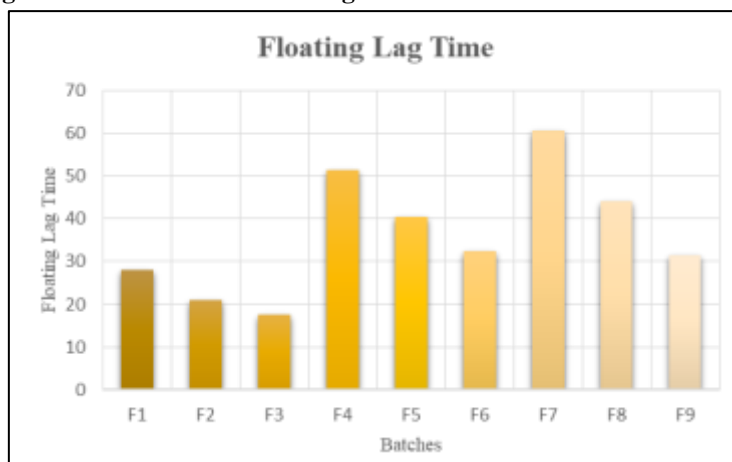


Figure 3.20: Floating Lag Time of Factorial Batches

Table 3.9: Data for Response parameter of Tablet

Batch Code	Clarithromycin release at 12 h (%)	T _{50%} (minutes)	T _{85%} (minutes)	Floating Lag Time (seconds)	Tablet Integrity
F1	98.41±1.63	281.4±1.04	539.5±1.23	28±1	+
F2	98.81±2.51	223.42±1.21	518.41±0.57	21±1	+
F3	98.9±1.09	208.14±1.43	403.83±1.09	17.66±1.52	+
F4	94.79±1.37	394.9±1.62	671.47±1.32	51.33±1.52	+
F5	95.82±2.48	381.2±0.79	648.13±1.54	40.33±2.08	+
F6	95.87±2.5	365.4±1.97	613.40±1.93	32.33±1.53	+
F7	68.15±1.56	444.0±1.34	1008.8±1.46	60.66±1.52	+
F8	72.8±1.17	414.6±1.51	889.5±1.75	44±1	+
F9	79.5±1.86	391.7±1.47	859.9±1.39	31.33±1.52	+
*The values represent the average of three determinations (n=3) + = Good Integrity for 12 h, - =No Integrity.					

3.10 Curve fitting (Release mechanism)

The response Parameter and curve-fitting data of matrix tablet prepared as per 3² Factorial designs are summarized in Table 3.9 and 3.10 respectively, indicated that the possible mechanism of drug release. As most of the batches produced yielded quality adjustment with the Hixon Crowell (average R²=0.9832). However, the best fit model was found to be the Zero order (average R²=0.9942) suggesting that the mechanism of drug release was

combination of diffusion and erosion. Different values for diffusion exponent n in equation represent different drug release mechanisms. When the n value is around 0.45, the Fickian diffusion phenomenon dominates, and when n ranges between 0.45 and 0.89 it is anomalous or non-Fickian release that is, the drug release proceeded by diffusion as well as erosion of the polymer. When the n value exceeds 0.89, the release can be characterized by case II and super case II, which illustrate a zero-order release. The values of the diffusion exponent, as shown in Table 3.10 were found to range from 0.77- 1.0239. Formulations F1, F2 and F3 showed non Fickian type drug release as values of 'n' that is diffusional exponent is lies between 0.45 to 0.89 remaining formulations (F4 – F9) shows Class 2 drug release as the value of 'n' is greater than 0.89. The hydrophilic matrix tablets exhibited $R^2 = (0.9942)$ when analyzed using the Zero-order equation, suggesting that the drug release from most of the batches followed zero-order kinetics.

Table 3.10: Data for study of release mechanism by curve fitting analysis.

Batch code	Zero order			Hixon Crowell		
	K	R ²	n	K	R ²	n
F1	0.64±0.017	0.9946±0.003	0.77±0.01	0.62± 0.033	0.9858±0.005	0.65±0.02
F2	0.65±0.023	0.9933±0.004	0.78±0.01	0.60 ±0.034	0.9887±0.006	0.68±0.02
F3	0.64±0.013	0.9907±0.002	0.78±0.02	0.64±0.024	0.9953±0.004	0.69±0.01
F4	0.15±0.017	0.9983±0.005	0.97±0.03	0.12± 0.017	0.9610±0.008	0.94±0.03
F5	0.16±0.021	0.9971±0.006	0.97±0.02	0.26± 0.021	0.9768±0.007	0.91±0.02
F6	0.14±0.025	0.9964±0.004	0.96±0.02	0.13± 0.034	0.9648±0.003	0.93±0.01
F7	0.11±0.014	0.9940±0.05	1.02±0.03	0.59± 0.016	0.9843±0.008	1.09±0.03
F8	0.10±0.016	0.9910±0.004	1.01±0.02	0.37± 0.021	0.9900±0.007	1.03±0.02
F9	0.11±0.015	0.9927±0.002	1.07±0.02	0.54± 0.021	0.9776±0.005	1.02±0.01

3.11 Optimization of Factorial Design Batches

3.11.1 Regression analysis

1) Effect of formulation variables on T_{50%} Clarithromycin release

The Quadratic model for T_{50%} (Y₁) was found to be significant with an F value 361.54 (P<0.0001). In this case X₁, X₂, X₂² was found to be significant and the model describes the T_{50%} release. The factorial equation for T_{50%} (Y₁) can be written as:

$$T_{50\%} = + 375.40 - 25.50 A + 88.78 B + 6.06 A B + 7.58 A^2 - 52.61B^2 \dots\dots (3.1)$$

As the concentration of HPMC K100M increased it causes an increase in viscosity of swollen gel matrix, which contributes more hindrance for drug diffusion and thus decreases the release rate whereas Citric acid increase the solubilization increase the release rate. The combined effect of X₁ & X₂ shown in response surface plot Figure 3.22 While the increasing amount of HPMC K100M causes the decreases in the drug release, due to formation of high viscous gel matrix. HPMC K100M is swellable polymer which causes a gel layer. The Figure 3.21 shows a graph of observed verses predicted values. The HPMC K100M (X₁) have negative effect on Y₁ & Citric acid (X₂) have positive effect on Y₁, means if we increasing the concentration of X₁ T_{50%} decreases & increase in X₂ the T_{50%} increases due to increased solubilization of drug.

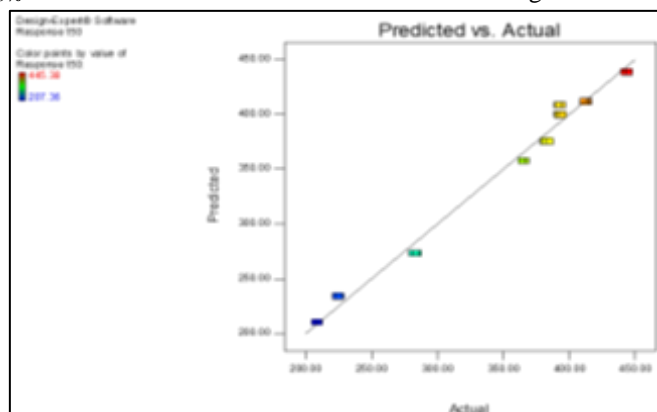


Figure 3.21: Correlation between actual and predicted values for T_{50%} (Y₁)

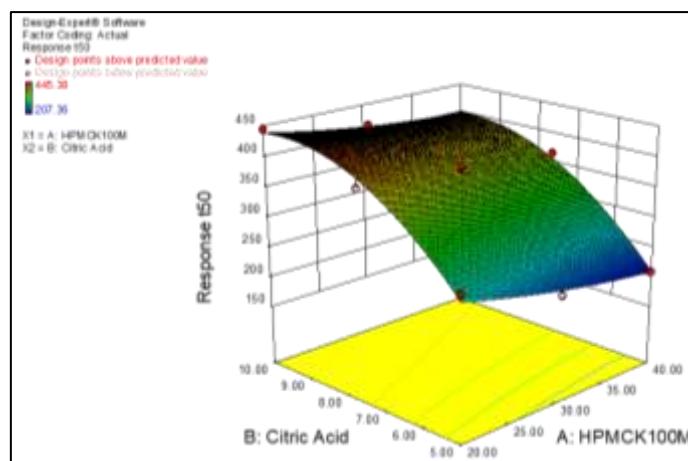


Figure 3.22: Response surface plot showing effect of formulation variables on $T_{50\%}$ (Y_1)

2) Effect of formulation variables on $T_{85\%}$ (Y_2)

The Quadratic model terms for response Y_2 ($T_{85\%}$) were found to be significant with F value of 229.56 ($p < 0.0001$). In this case all the factors except X_1 , X_2 and X_1^2 were found to be significant and the factorial equation for response Y_2 ($T_{85\%}$) can be written as:

$$T_{85} = +645.90 - 56.81 A + 214.75 B - 3.64 A B - 1.16 A^2 + 56.47 B^2 \dots \dots \dots (3.2)$$

As the amount of X_1 increases the corresponding $T_{85\%}$ (time required to release 85% of the drug) also increases. The Figure 3.24 shows the response surface plot. It indicates at all the high levels of X_1 the $T_{85\%}$ value is high. As discussed above this behavior is due to increase in amount of HPMC K100M forms a high viscous gel matrix and thus decreases the drug release and hence $T_{85\%}$ value increases. Whereas X_2 increases the release rate also increases. The Figure 3.23 shows the graph of predicted versus actual data. The HPMC K100M (X_1) has positive effect on $T_{85\%}$ Y_2 and Citric acid (X_2) has negative effect on Y_2 means if we increasing the concentration of X_1 then Y_2 of the drug also increases due to increased viscosity and gel strength and increase in X_2 then decrease in Y_2 means decrease in time require for release.

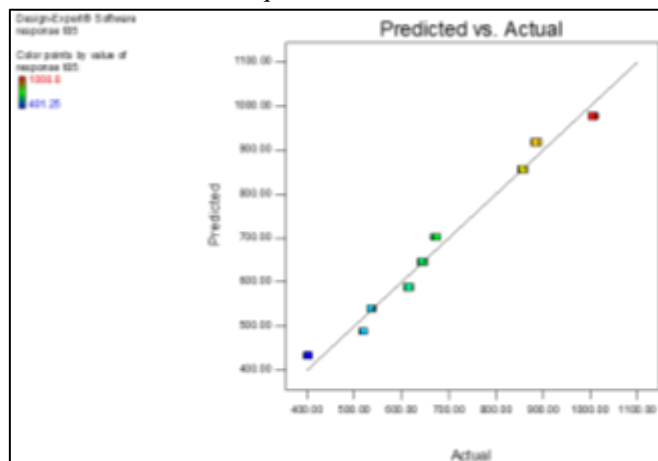


Figure 3.23: Correlation between actual and predicted values for $T_{85\%}$ (Y_2)

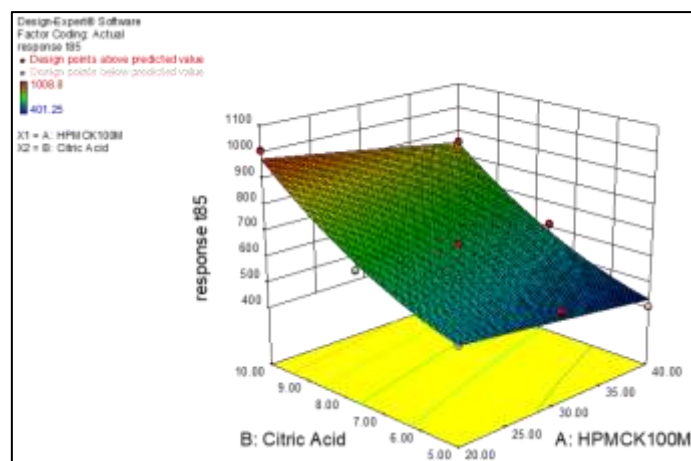


Figure 3.24: Response surface plot showing effect of formulation variables on $T_{85\%}$ (Y_2)

3) Effect of formulation variables on Floating Lag Time (FLT, Y_3)

The Quadratic model terms for response Y_3 (FLT) were found to be significant with F value of 229.56 ($p < 0.0001$). In this case all the factors except X_1^2 were found to be significant and the factorial equation for response Y_3 (FLT) can be written as:

$$FLT = +40.15 - 9.78 A + 11.56 B - 4.75 A B + 1.78 A^2 - 7.56 B^2 \dots \dots \dots (3.3)$$

As the amount of X_1 increases the corresponding FLT (time required to float the tablet) also increases. The Figure 3.26 shows the response surface plot. It indicates at all the high levels of X_1 the FLT value is high. On the contrary X_2 increases the FLT decreases respectively. The Figure 3.25 shows the graph of predicted versus actual data. The HPMC K100M (X_1) has negative effect on Y_3 and Citric acid (X_2) has positive effect on Y_3 means if we increasing the concentration of X_1 then Y_3 of the drug also increases due to increased viscosity and gel strength and increase in X_2 then decrease in Y_3 means decrease in time required for float.

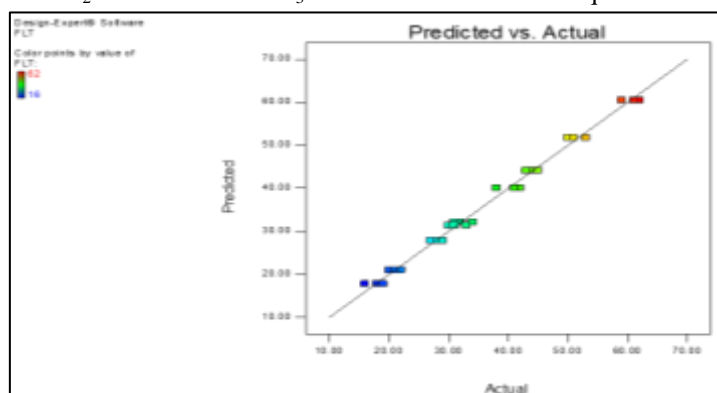


Figure 3.25: Correlation between actual and predicted values for FLT (Y_3)

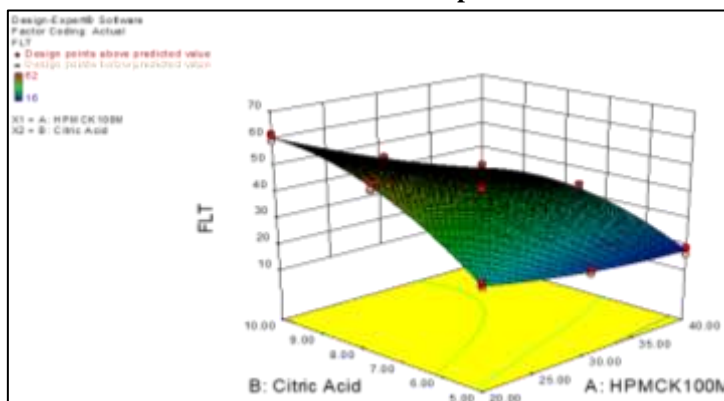


Figure 3.26: Response surface plot showing effect of formulation variables on FLT (Y_3)

4) ANOVA, Pure error, Lack of fit

The results of ANOVA for dependent variables from 3^2 factorial designs shown in Table 3.11 demonstrate that the model was significant for all response variables. Regression analysis was carried out to obtain the regression coefficient shown in Table 3.11 and effects as follows; all factors other than X_1 , X_2 and X_1^2 found significant for response Y_1 and Y_2 whereas for response Y_3 except X_1^2 all other factors found significant. The above results conveyed us that the amount of HPMC K100M & Citric acid plays important role in formulation of Oral Controlled Release matrix tablets of Clarithromycin. The data of pure error and lack of fit are summarized in Table 3.12. The residuals are the difference in the observed and predicted value. Since computed F values were respectively less than critical F values, denotes non-significance of lack of fit.

Table 3.11: Data of ANOVA study for dependent variables from 3^2 factorial designs

Source	d.f.	Sum square	Mean square	F value	Probability
Response (Y_1) = $T_{50\%}$ (h)					
X_1	1	11705.52	11705.52	127.77	< 0.0001*
X_2	1	1.419E+005	1.419E+005	1500.03	< 0.0001*
X_1X_2	1	440.08	440.08	4.65	0.0427
X_1^2	1	345.14	345.14	3.65	0.0698
X_2^2	1	16607.22	16607.22	175.60	< 0.0001*
Response (Y_2) = $T_{85\%}$ (h)					
X_1	1	58084.82	58084.82	73.47	< 0.0001*
X_2	1	8.301E+005	8.301E+005	1049.91	< 0.0001*
X_1X_2	1	158.92	158.92	0.20	0.6585
X_1^2	1	8.13	8.13	0.010	0.9202
X_2^2	1	19130.53	19130.53	24.20	< 0.0001*
Response (Y_3) = FLT(Sec)					
X_1	1	1720.89	1720.89	927.73	< 0.0001*
X_2	1	2403.56	2403.56	1295.76	< 0.0001*
X_1X_2	1	270.75	270.75	145.96	< 0.0001*
X_1^2	1	18.96	18.96	10.22	0.0043
X_2^2	1	342.52	342.52	184.65	< 0.0001*

* -Indicates significant

Table 3.12: Data of ANOVA study for results in analysing lack of fit and pure error

For T_{50}						
Source	Sum of Squares	Degrees of Freedom	Mean Square	F Value	P Value	Model Significant/ Non-significant Relative to Noise
Model	1.710E+05	5	34191.91	361.54	0.0001	Significant
Residual	1986.02	21	94.57	-	-	-
Core Total	1.729E+05	26	-	-	-	-
Lack of fit	1931.25	3	643.75	211.56	0.0001	Significant
Pure Error	54.77	18	3.04	-	-	-
For T_{85}						
Model	9.075E+05	5	1.815E+05	229.56	0.0001	Significant
Residual	16603.09	21	790.62	-	-	-
Core Total	9.241E+05	26	-	-	-	-
Lack of fit	16495.40	3	5498.47	919.08	0.0001	Significant
Pure Error	107.69	18	5.98	-	-	-
For FLT						
Model	4756.68	5	951.34	512.87	0.0001	Significant
Residual	38.95	21	1.85	-	-	-

Core Total	4795.63	26	-	-	-	-
Lack of fit	0.95	3	0.32	0.15	0.9280	Not Significant
Pure Error	38.0	18	2.11	-	-	-

3.12 Studies on Final Formulation

1) Water Uptake Study

The water uptake was determined of F5 batch. It was observed that Water uptake was increase with respect to time. Data for water uptake study is given in the Table 3.13.

Table 3.13: Water Uptake Study of F5 Batch

Time (h)	Water Uptake (%)
1	133.8
2	136.5
3	137.4
4	139.2
5	140.1
6	142.2
7	143.3
8	143.8
9	144.8
10	145.1
11	146.3
12	147.9

2) In-Vitro Drug release for Marketed Tablet, Complex and F5

In vitro release profile of optimized formulation F5 compared with marketed SR tablet (Biaxin-500) and complex. The time for drug release t50% of F5, Biaxin and complex were found to 381.2, 315.36 and 354 minutes respectively. The percentage drug release after 12 hour for F5, Biaxin and complex were found to 95.82, 86.32 and 87.62 respectively shown in Table 3.14, so the release from the optimized formulation and complex were higher compared to marketed product. Release of drug from complex was approximately same so it was concluded that without any polymer drug release is controlled which is shown in Figure 3.27.

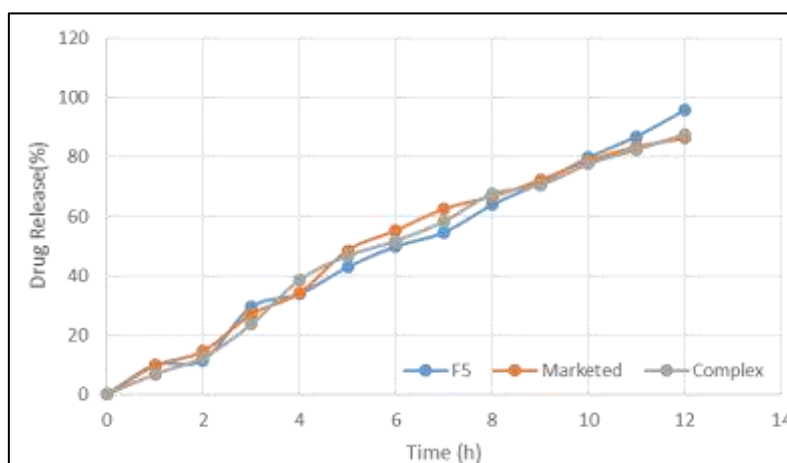


Figure 3.27: Dissolution Profile of marketed formulation with capsule fills with complex and formulated tablet in 0.1N HCL.

Table 3.14: Dissolution data of Marketed Tablet (Biaxin), Complex and F5 in 0.1N HCL

Time (h)	% Drug Release		
	F5	MARKETED TAB.	COMPLEX
0	0.00±0.00	0.00±0.00	0.00±0.00
1	09.85±0.92	09.59±0.36	03.76±0.65
2	11.52±1.32	14.58±0.63	12.45±1.28
3	29.45±2.03	26.94±1.89	23.56±2.43
4	33.81±2.32	34.18±2.92	38.54±1.45
5	42.90±1.45	48.51±1.61	46.68±1.87
6	49.85±1.93	55.26±0.85	51.76±0.69
7	54.61±1.23	62.52±1.44	58.32±0.78
8	63.89±2.04	66.74±0.31	67.54±2.58
9	71.33±0.78	72.23±2.45	70.56±2.65
10	79.84±1.12	78.83±2.68	77.65±1.95
11	87.02±1.67	83.45±1.56	82.56±2.08
12	95.82±2.04	86.32±1.30	87.65±1.71

n=2 (±SD)

3) Optimization

A numerical optimization technique by the desirability approach was used to generate the optimum settings for formulation. The process was optimized for dependent variables Y_1 - Y_3 . The optimized formula arrived by targeting the Y_2 at 650 minute, Y_1 was kept at range 360-400 min. , Y_3 also kept at range 16-62 sec. The optimized results obtained to give 13 results out of that one formula is shown in Table 3.14. The results of optimized formula were compared with the predicted values (Table 3.16), which showed good relationship between experimented and predicted values, which confirms the practicability and validity of the model. The value of n was found to be 0.991.

Table 3.15: Composition of optimized formulation

Ingredients	Quantities (mg)
Complex	500
HPMC K100M	163.5
Citric Acid	38.6
NaHCO ₃	80
PVP K30	60
Mg stearate	5
Lactose	12.9
Total weight	860

Table 3.16: Comparison between the experimented and predicted Values for most probable optimal formulation

Dependent variables	Optimized formulation	
	Experimented value	Predicted value
T _{50%} (Y ₁)	381.2	376.71
T _{85%} (Y ₂)	648.13	649.99
FLT	40.3	38.49

CONCLUSION

The Clarithromycin is poorly water soluble drug and gastric irritant. To overcome these problems attempt was made in present study to form inclusion complex of Clarithromycin with Nanosponges. β -Cyclodextrin (CD) based Nanosponges (NS) are novel class of cross-linked derivatives of Cyclodextrin. The Nanosponges were synthesized by carbonylation of β -Cyclodextrin to exploit its porous structure for drug entrapment. After synthesis of Nanosponges, Drug Clarithromycin was entrapped in it. The Characteristics of Complex was studied by FTIR, DSC, PXRD and SEM. The result of XRPD results showed that the crystallinity of CLA was decreased after loading into Nanosponges. Histopathological study was carried out and it revealed non irritancy of drug-NS complex to gastric mucosa (of rat). Hence drug-NS complex found to be suitable for designing into unit dosage forms. Preliminary Batch were prepared and Evaluated (*in vitro* dissolution) for selection of Polymer. HPMC K100M showed highest release retarding property so it was selected as the polymer for further study. The 3^2 full factorial experimental design was applied and 9 Factorial Design Batches were obtained. Granules were prepared using Wet granulation method and evaluated for their properties. All the batches of tablets were prepared using rotary punch tablet compression machine using 12 mm size punch. Prepared tablets of Batch F1-F9 were evaluated for various tablet properties. Regression analysis was carried out and F5 Batch was found to be optimized Batch. F5 batch showed 95.82 ± 2.48 % Drug Release in 12 hours further it was evaluated for water uptake and compared with the Marketed formulation for % Drug Release.

ACKNOWLEDGEMENT

The authors are very much thankful to PDEAs Shankarrao Ursal College of Pharmaceutical Sciences and Research Centre, Pune, Maharashtra, India and PDEAs Seth Govinds Raghunath Sable College of Pharmacy, Pune, Maharashtra, India for providing the necessary support to complete this work successfully.

CONFLICT OF INTEREST

All authors declared no conflicts of interest.

REFERENCES

- 1) Robinson J R, Lee V H 'Controlled Drug Delivery Fundamentals and Applications'. 1987 Vol. 29, 2nd Edⁿ. Marcel Dekker, INC, New York and Basel: 4-6.
- 2) Khan GM, Review on 'Controlled Release Oral Dosage Forms: Some Recent Advances in Matrix Type Drug Delivery Systems' JPS 2001 (5): 350-354.
- 3) Wise DL, 2005 'Handbook of Pharmaceutical Controlled Release Technology'; Marcel Dekker, INC, New York and Basel: 211, 435-440, 472-473, and 787-788.
- 4) Arora JM, Khar RK 2005 'Gastroretentive Drug Delivery System' AAPS Pharmascitech: 6 (03) Article 47.
- 5) Desai S and Bolton S, "A Floating Controlled Release Drug Delivery System: In vitro-In vivo Evaluation", Pharma. Res., 1993, 10 (9) 1321-325.
- 6) Singh BM and Kim KH, "Floating drug delivery systems: an approach to controlled drug delivery via gastric retention", J. Control. Rel., 2000, 63, 235-259.
- 7) Nakay Y, Fukuoka E, Nakajima S, Yamamoto K. Effects of grinding on physical and chemical properties of crystalline medicinals with microcrystalline cellulose. I. Some physical properties of crystalline medicinals in ground mixtures. Chem. Pharm. Bull. 1977; 25: 3340- 3346.
- 8) D. Ducheⁿe, G. Ponchel, and D. Wouassindjewe: Adv. Drug Del. Rev. 36, 29 B. McCormack and G. Gregoriadis: Int. J. Pharm. 162, 59 (1998).
- 9) Szejtli, J. 1998 'Introduction and general overview of cyclodextrin Chemistry' Chem. Rev. 98, 1743-1754.
- 10) Rekharsky, M.V., Inoue, Y. 1998 'Complexation thermodynamics Of cyclodextrins' Chem. Rev. 98, 1875-1918.
- 11) Salazar Sandoval S, Cortés-Adasme E, Gallardo-Toledo E, Araya I, Celis F, Yutronic N, Jara P, Kogan MJ. β -Cyclodextrin-Based Nanosponges Inclusion Compounds Associated with Gold Nanorods for Potential NIR-II Drug Delivery. Pharmaceutics. 2022 Oct 17;14(10):2206.

- 12) Boscolo Barbara, Trotta Francesco, Ghibaudi Elena 2009 “High catalytic performances of *Pseudomonas fluorescens* lipase adsorbed on a new type of cyclodextrin-based nanosponges” *Journal of Molecular Catalysis B: Enzymatic*.
- 13) <http://www.drugsinformationonline.com>
- 14) Martindale. 2002. The complete drug reference. Sean C.S. 33 rd edition, Pharmaceutical press. Pp.1356-1359.
- 15) Ohtani, Y., Irie, T., Uekama, K., Fukunaga, K., Pitha, J., 1989. Differential effects and β -cyclodextrins on human erythrocytes. *Eur. J. Biochem.* 186, 17–22.
- 16) Israr M, Pugliese N, Farid A, Ghazanfar S, Di Cerbo A, Muzammal M, et al. Preparation and Characterization of Controlled-Release Floating Bilayer Tablets of Esomeprazole and Clarithromycin. *Molecules* 2022;27:3242.
- 17) Chen P, Luo H, Huang S, Liu J, Lin M, Yang F, Ban J, Huang Z, Lu Z, Xie Q, Chen Y. Preparation of high-drug-loaded clarithromycin gastric-floating sustained-release tablets using 3D printing. *AAPS PharmSciTech.* 2021 Apr;22:1-0.
- 18) Shankar Swaminathan Linda Pastero, Loredana Serpe, Francesco Trotta d, Pradeep Vavia, Dino Aquilano b, Michele Trotta a, GianPaolo Zara , Roberta Cavalli “Cyclodextrin-based nanosponges encapsulating camptothecin: Physicochemical characterization, stability and cytotoxicity” *European Journal of Pharmaceutics and Biopharmaceutics*.
- 19) Shanmugam S. Granulation techniques and technologies: recent progresses. *Bioimpacts.* 2015;5(1):55-63.
- 20) Easwari, T S. (2012). Formulation Development and Evaluation of Clarithromycin Oral Dosage Form Against *Helicobacter Pylori* Infection. *INTERNATIONAL JOURNAL OF ADVANCE PHARMACEUTICAL AND BIOLOGICAL SCIENCES.* 3. 281-287.
- 21) Raymond, C.R., Paul, J., 2006. Handbook of Pharmaceutical excipients. 5th edition Alpha pharmaceutical press, London, Chicago. Pp.535-538.
- 22) <https://www.statease.com/docs/v11/>
- 23) Michal Szumilo, Piotr Belniak, Katarzyna Swiader, Ewelina Holody, Ewa Poleszak, Assessment of physical properties of granules with paracetamol and caffeine, *Saudi Pharmaceutical Journal*, Volume 25, Issue 6, 2017, Pages 900-905
- 24) Aulton ME, 1998, *Pharmaceutics: The science of dosage form design*, 1 ed, London Churchill Livinstone. p.247
- 25) Kuchekar, B.S., Singavi, A. A., Late, S.G., Shinde, D.B., 2003. Spectrophotometric estimation of Roxithromycin and Clarithromycin in Pharmaceutical Dosage Forms. *Indian Drugs.* 40(1), 44-45.
- 26) *Indian Pharmacopoeia*, 1996, Govt. of India, Ministry of Health and Family Welfare, Vol., 1, The Controller of Publication, Delhi: 187-191, 382-383.
- 27) Boylan and Cooper . ‘Handbook of Pharmaceutical Excipient’ A Joint Publication of American Pharmaceutical Association And the Pharmaceutical Society of Great Britain : 45-48, 138-140.
- 28) Kibbe AH. 2003. Handbook of Pharmaceutical Excipients, 3rd Ed. American Pharmaceutical Association and Pharmaceutical Press, Washington DC.
- 29) *British pharmacopoeia*. 2003. The Stationary office: London. Vol. 2, 1638
- 30) <https://www.statease.com/docs/v11/contents/optimization/optimization-overview/>



Self-Emulsifying Drug Delivery System (SEDDS) for Enhancement of Solubility and Photostability of Amlodipine Besilate

Prashant H. Khade¹, Gururaj Shahabade², Sachin V.Kotwal³, Priyanka D. Borude⁴,
Jyoti B.Darkunde⁴, Harshal M.Shinde⁵

¹Assistant Professor, PDEAs Shankarrao Ursal College of Pharmaceutical Sciences and Research Centre, Pune, Maharashtra, India.

²Senior Research Scientist at Syngene International Limited, Bengaluru, Karnataka, India.

³Principal, PDEAs Shankarrao Ursal College of Pharmacy (Diploma), Pune, Maharashtra, India.

⁴Lecturer, PDEAs Shankarrao Ursal College of Pharmacy (Diploma), Pune, Maharashtra, India.

⁵Research Scholar, PDEAs Shankarrao Ursal College of Pharmaceutical Sciences and Research Centre, Pune, Maharashtra, India.

For Correspondence -

Prashant H. Khade,

Assistant Professor,

Department of Pharmaceutics,

PDEAs Shankarrao Ursal College of Pharmaceutical Sciences and Research Centre,

Pune, Maharashtra, India.

E-mail Id: phkhade@gmail.com

ABSTRACT

Amlodipine besilate (AMB) with IUPAC name of 3-ethyl-5- methyl-(4RS)-2-((2-aminoethoxy) methyl)-4-(2-chlorophenyl)-1,4-dihydro-6-methyl-3,5-pyridinedicarboxylate monobenzenesulfonate is the most widely used drug for the treatment of hypertension and ischemia by blocking dihydropyridine calcium-channel. Although AMB has excellent performance against the treatment of hypertension, but its low water solubility (2.93 g/L (0.0052 mol/L) in water at 32 °C) is one of the limitations of using AMB in pharmaceutical industry. AMB is in class IV of the biopharmaceutical classification system with slight solubility in water and sparingly soluble in ethanol. To increase the therapeutic efficacy of AMB, the solubility of AMB should be increased in aqueous systems because drugs with low aqueous solubility have poor absorption and low bioavailability. Amlodipine is also known as photosensitive since light catalyzes oxidation of amlodipine to pyridine derivatives that are therapeutically ineffective. To overcome the problem of solubility and photosensitivity, Amlodipine was formulated in the form of Self-Emulsifying Drug Delivery System (SEDDS). Liquid SEDDS was prepared by dissolving amlodipine in various S_{mix} which were further evaluated and F1 and F2 were found to be optimized. F1 and F2 were solidified using spray drying method. After evaluation of Solid SEDDS F1 and F2 batch showed $91.041 \pm 2.96\%$ and $93.059 \pm 1.53\%$ Drug release and increase in Photostability was observed.

KEYWORDS - Amlodipine, Solubility, Absorption, Bioavailability, Photostability, Self-Emulsifying Drug Delivery System (SEDDS)

1. INTRODUCTION

Amlodipine besilate (AMB) with IUPAC name of 3-ethyl-5- methyl-(4RS)-2-((2-aminoethoxy) methyl)-4-(2-chlorophenyl)-1,4-dihydro-6-methyl-3,5-pyridinedicarboxylate monobenzenesulfonate (Figure 1.1) is the most widely used drug for the treatment of hypertension and ischemia by blocking dihydropyridine calcium-channel. Although AMB has excellent performance against the treatment of hypertension, but its low water solubility (2.93 g/L (0.0052 mol/L) in water at 32 °C) is one of the limitations of using AMB in pharmaceutical industry. AMB is in class IV of the biopharmaceutical classification system with slight solubility

in water and sparingly soluble in ethanol. To increase the therapeutic efficacy of AMB, the solubility of AMB should be increased in aqueous systems because drugs with low aqueous solubility have poor absorption and low bioavailability (1). Amlodipine is also known as photosensitive since light catalyzes oxidation of amlodipine to pyridine derivatives that are therapeutically ineffective (2).

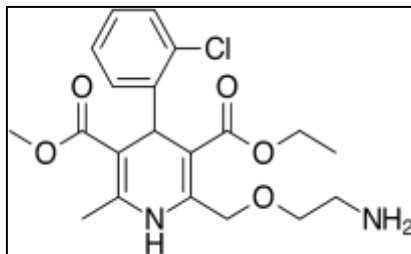


Figure 1.1 – Structure of Amlodipine

Sufficient aqueous solubility is one of the essential requirements for oral administration of a drug. Limited solubility can lead to insufficient dissolution and further reduce the bioavailability of a drug (3, 4). As a result, a variety of effort has been made to enhance the oral bioavailability of poorly water soluble drugs through lipid based emulsion systems, specifically the self-emulsifying drug delivery system (SEDDS) (5-8). SEDDSs are defined as homogeneous mixtures of natural or synthetic oils, surfactants, and co-surfactants that easily form emulsion upon mild agitation and generate a high surface area of interactions between the SEDDS formulation and the gastrointestinal (GI) fluid (9). Moreover, SEDDS has been identified as a prominent technology for drug delivery, because the formulations have great solubilization capacity and a tiny droplet size, which could improve permeation across the GI membrane.

In this present study attempt has been taken to prepare liquid as well as solid self-emulsifying drug delivery system of poorly water soluble and highly photosensitive drug amlodipine. The objective of preparing liquid as well as self-emulsifying drug delivery system is to enhance the solubility of the selected drug which may also increase the dissolution rate and bioavailability of the drug.

2. MATERIAL AND METHOD

2.1. Material

Amlodipine besilate BP, a dihydropyridine calcium-channel blockers was obtained as gift sample from Zydus Cadila, Goa. Capmul PG-8, Capmul MCM, Captex 500 were obtained as Gift sample from Abitec Corporation, US. Labrafil M 1944 CS/ 2125 CS both were gifted by Gattefosse India Pvt Ltd, Mumbai. Oils such as Oleic acid, Isopropyl myristate, Tween 40/60/80, Span 20/80, PEG 200/400/600, Carbitol were purchased from Research lab, Mumbai. Other Solvent used during the Research were of HPLC Grade.

2.2. Screening of Excipients

2.2.1. Solubility study

The solubility of amlodipine in various oils, surfactants, and co-surfactants was measured, respectively. An excess amount of amlodipine was added into 2 ml of each of the selected oils, surfactants, co-surfactants and distilled water in 5-ml stoppered vials separately, and mixed by vortexing. The mixture vials were then kept at $25 \pm 1.0^\circ\text{C}$ in an isothermal shaker for 72 h to reach equilibrium. The equilibrated samples were removed from shaker and centrifuged at 3000 rpm for 15 min. The supernatant was taken and filtered through a $0.45 \mu\text{m}$ membrane filter. The concentration of amlodipine was determined in oils, surfactants, co-surfactants and water using UV- spectrophotometer at 360 nm (9, 10).

2.2.2. Preliminary screening of surfactants

Emulsification ability of various surfactants was screened. Briefly, 300 mg of surfactant was added to 300 mg of the selected oily phase. The mixture was gently heated at $45\text{--}60^\circ\text{C}$ for homogenizing the components. The isotropic mixture, 50 mg, was accurately weighed and diluted with double distilled water to 50 ml to yield fine emulsion. The ease of formation of emulsions was monitored by noting the number of volumetric flask inversions required to give uniform emulsion. The resulting emulsions were observed visually for the relative turbidity. The emulsions were allowed to stand for 2 h and their transmittance was assessed at 360 nm by UV- spectrophotometer (UV V-630, Jasco) using double distilled water as blank (11).

2.2.3. Preliminary screening of co-surfactants

The turbidimetric method was used to assess relative efficacy of the co-surfactant to improve the Nano emulsification ability of the surfactants and also to select best co-surfactant from the large pool of co-surfactants available for peroral delivery. Surfactant, 0.2 gm. was mixed with 0.1 gm. of co-surfactant. Labrafil M 1944 CS, 0.3 gm., was added to this mixture and the mixture was homogenized with the aid of the gentle heat (45–60°C). The isotropic mixture, 50 mg, was accurately weighed and diluted to 50 ml with double distilled water to yield fine emulsion. The ease of formation of emulsions was noted by noting the number of flask inversions required to give uniform emulsion. The resulting emulsions were observed visually for the relative turbidity. The emulsions were allowed to stand for 2 h and their transmittance was measured at 360 nm by UV-spectrophotometer (UV V-630, Jasco) using double distilled water as blank. As the ratio of co-surfactants to surfactant/s is the same, the turbidity of resulting Nano emulsions will help in assessing the relative efficacy of the co-surfactants to improve the nanoemulsification ability of surfactants (12).

2.3. Drug – Excipients Compatibility Study

The Drug – Excipients Compatibility Studies were performed in order to confirm the drug- excipients compatibility. This study mainly include DSC given below, The DSC study was carried out for pure amlodipine, Tween 20, PEG 400, Labrafil M 1944 CS & physical mixtures of all excipients that were expected to be used in the development of formulation like oil phase, emulsifier, surfactant and co-surfactant etc. The DSC patterns were recorded on a METTLER TOLDO DSC1 STAR SYSTEM. Each sample (2-4mg) was heated in crimped aluminium pans at a scanning rate of 10°C/min in an atmosphere of nitrogen using the range of 30⁰-400⁰C. The temperature calibrations were performed periodically using indium as a standard and thermograms obtained were observed for any interaction and reported in the section 3.2. (Table 3.2) (13).

2.4. Construction of Pseudo-ternary phase diagram

A pseudo-ternary phase diagram was constructed by titration of four component mixtures of oil, surfactant and co-surfactant with water at room temperature. After equilibrium, the mixture was visually observed. The generated sample which was clear or slightly bluish in appearance was determined as microemulsion. On the basis of the solubility studies of drug, select the oil phase, surfactants and co-surfactants. Water was used as an aqueous phase for the construction of phase diagrams. Surfactant : co-surfactant (S_{mix}) are mixed in different weight ratios 1:0, 0.5:1(1:2), 1:1, 1:0.5 (2:1), 3:1. These S_{mix} ratios were chosen in increasing concentration of surfactant with respect to co-surfactant and increasing concentration of co-surfactant with respect to surfactant for detailed study of the phase diagrams. For each phase diagram, oil and specific S_{mix} ratio was mixed thoroughly in different weight ratios from 1:9 to 9:1 in different glass vials. Sixteen different combinations of oil and S_{mix} , 1:9, 1:8, 1:7, 1:6, 1:5, 2:8(1:4), 1:3.5, 1:3, 3:7(1:2.3), 1:2, 4:6(1:1.5), 5:5(1:1), 6:4(1:0.7), 7:3 (1:0.43), 8:2(1:0.25), 9:1(1:0.1), were made so that maximum ratios were covered for the study to delineate the boundaries of phases precisely formed in the phase diagrams. Pseudo ternary phase diagrams were developed using aqueous titration method. Slow titration with aqueous phase was done to each weight ratio of oil and S_{mix} and visual observation was carried out for transparent and easily flowable o/w microemulsions. The mixture was visually examined for transparency. After equilibrium was reached, the mixtures were further titrated with aliquots of distilled water until they showed the turbidity. Clear and isotropic samples were deemed to be within the microemulsion region. No attempts were made to completely identify the other regions of the phase diagrams. Based on the results, appropriate percentage of oil, surfactant and co-surfactant was selected, correlated in the phase diagram and were used for preparation of SEDDS containing amlodipine. All studies were repeated thrice, with similar observations being made between repeats and results of phase diagram were reported in section 3.3. (14, 15)

2.5. Selection of Formulation from Pseudo ternary Phase Diagram

From each phase diagram, constructed, different formulations were selected from micro-emulsion region it is reported in section 3.4, so that drug could be incorporated into the oil phase on the following bases.

- The oil concentration should be such that it solubilizes the drug (single dose) completely depending on the solubility of the drug in the oil. 5 mg of amlodipine will dissolve easily in 1 mL of oil.
- To check if there was any effect of drug on the phase behaviour and microemulsion area of the phase diagram.
- The minimum concentration of the S_{mix} used for that amount of oil was taken.

- For convenience purposes, 1mL was selected as the microemulsion formulation, so that it can be increased or decreased as per the requirement in the proportions. (14)

Selected formulations were subjected to different thermodynamic stability and Dispersibility tests.

2.5.1. Thermodynamic stability studies

1. Heating cooling cycle

Six cycles between refrigerator temperature (4°C) and 45°C with storage at each temperature of not less than 48h was studied. Those formulations, which were stable at these temperatures, were subjected to centrifugation test (16, 17).

2. Centrifugation

Passed formulations were centrifuged at 3000 rpm for 30 min. Those formulations that did not show any phase separation were taken for the freeze thaw stress test (16, 18).

3. Freeze thaw cycle

Three freeze thaw cycles between -21°C and +25°C with storage at each temperature for not less than 48 h was done for the formulations (16, 19).

Those formulations, which passed these thermodynamic stress tests, were further taken for the Dispersibility test for assessing the efficiency of self-emulsification.

2.5.2. Dispersibility test

The efficiency of self-emulsification of oral microemulsion was assessed using a standard USP XXII dissolution apparatus 2 (Disso TDT 08L, Electrolab). One millilitre of each formulation was added to 500 mL of water at 37±0.5°C. A standard stainless steel dissolution paddle rotating at 50 rpm provided gentle agitation. The in-vitro performance of the formulations was visually assessed using the following grading system:

Grade A: Rapidly forming (within 1min) Nano emulsion, having a clear or bluish appearance.

Grade B: Rapidly forming, slightly less clear emulsion, having a bluish white appearance.

Grade C: Fine milky emulsion that formed within 2 min.

Grade D: Dull, greyish white emulsion having slightly oily appearance that is slow to emulsify (longer than 2min).

Grade E: Formulation, exhibiting either poor or minimal emulsification with large oil globules present on the surface.

Those formulations that passed the thermodynamic stability and also Dispersibility test in Grade A, Grade B and Grade C was selected for further studies. The results were reported in section 3.4 (Table 3.6 and 3.7)

2.6. Preparation of Liquid SEDDS Formulations

The formulations were prepared by dissolving the formulation amount of amlodipine (5 mg/mL) in the mixture of surfactant, oil and co-surfactant (Table 2.1). Tween 20, Labrafil M 1944 CS, Polyethylene glycol 400 (PEG 400), and amlodipine were accurately weighed and transferred into a borosilicate glass vial. Using magnetic stirrer, the ingredients were mixed for 10 min at 60–65°C until a yellowish transparent formulation was attained. Amlodipine SEDDS formulations were then allowed to cool to room temperature before they were used in subsequent studies (21).

Table 2.1- Data for Preparation of Liquid SEDDS Formulations

Ingredients	Group I (S _{mix} 2:1)			Group II (S _{mix} 3:1)		
	A	B	C	D	E	F
Amlodipine (gm.)	0.005	0.005	0.005	0.005	0.005	0.005
Labrafil M 1944 CS (% w/w)	20	25	30	20	25	30
S _{mix} (% w/w)	80	75	70	80	75	70

Where S_{mix} is Tween 20 and PEG 400

2.7. Evaluation of Liquid SEDDS Formulations

1. Determination of emulsification time

The emulsification time of SEDDS was determined according to United State Pharmacopeia (USP) XXIII, dissolution apparatus II (Disso TDT 08L, Electrolab). In brief, 0.5 mL of each formulation (Table 2.1) was added drop wise to 500mL of purified water at 37°C. Gentle agitation was provided by a standard stainless steel dissolution paddle rotating at 50 rpm (21). The emulsification time was assessed visually as reported by Bachynsky et al. (22) and it was reported in section 3.6. (Table 3.8).

2. Turbidimetric evaluation

Self-emulsifying system (0.2 mL) was added to 0.1 mol L⁻¹ hydrochloric acid (150 mL) under continuous stirring (50 rpm) on a magnetic plate (Remi 5-MLH DX) at ambient temperature, and the increase in turbidity was measured until equilibrium was achieved using a turbidimeter (Digital Nephlo-Turbidity Meter 132, Systronics, India) and it was reported in section 3.6.

3. Drug Content

Amlodipine from pre-weighed SEDDS was extracted by dissolving in 25 mL methanol. Amlodipine content in the methanolic extract was analyzed by UV-spectrophotometer (UV V-630, Jasco) at 360 nm, against the standard methanolic solution of amlodipine and it was reported in section 3.6.(23, 24)

4. Globule size analysis

Droplet size distribution of SEDDS diluted with water was determined using a photon correlation spectrometer (Zetasizer 3000 HAS, Malvern Ltd., UK) based on the laser light scattering phenomenon. Samples were diluted 200 times with purified water. Diluted samples were directly placed into the module and measurements were made in triplicate after 2-min stirring. Droplet size was calculated from the volume size distribution and it is reported in section 3.6. (25, 26)

5. Drug release studies

Drug release studies from SEDDS were performed using USP XXIII, dissolution apparatus II (Disso TDT 08L, Electrolab) with 500 mL of 0.1N HCl as medium at 37±0.5°C. The speed of the paddle was adjusted to 100 rpm. 1 mL of the formulation was (5 mg of drug) and marketed tablet (Amlocard®, Cipla) directly introduced into the medium and an aliquot (2 mL) of sample was collected at designated times and analyzed for the content of amlodipine by UV-spectrophotometer at 360 nm. An equivalent volume (2 mL) of fresh dissolution medium was added to compensate for the loss due to sampling and results of drug release study were reported in section 3.5.(23, 24)

2.8. Preparation of solid SEDDS

Maltodextrin was dissolved in 100 ml distilled water by Magnetic stirring. The liquid SEDDS was then added with constant stirring, and the solution was kept at 50°C for 10 min to obtain a good o/w emulsion. The emulsion was spray dried with a Labultima spray dryer (LU 222 ADVANACED) apparatus. Conditions and parameter for spray drier are shown in Table 2.2. (27)

Table 2.2 - Data for Spray Drying Parameters

Sr. No.	Parameters	Condition at which the formulations were prepared
1	Inlet temperature	120°C
2	Outlet temperature	100°C
3	Feed pump	2.5 mL/min
4	Aspirator Speed	40mmWC
5	Vacuum	25 PSI
6	Cycle time	45 min

Table 2.3 - Data for Preparation of Solid SEDDS Formulations

Ingredients	Group I (S_{mix} 2:1)	Group II (S_{mix} 3:1)
	F ₁	F ₂
Maltodextrin (g)	10	10
Liquid SEDDS (g)	10	10
Water (mL)	100	100

2.9. Evaluation of Solid SEDDS Formulations

1. Reconstitution properties of solid SEDDS

A. Reconstitution

Solid SEDDS (100mg) prepared was dispersed with 10 ml distilled water, respectively, by vortex mixing (30s), and then incubated for 30 min at 25°C and the results of reconstitution was reported in section 3.8.

B. Droplet size of reconstituted emulsions

The average droplet size, size distribution emulsions from solid SEDDS were assessed by photon correlation spectrometer (Zetasizer 3000 HAS, Malvern Ltd., UK) and results of droplet size was reported in section 3.8. (25)(26)

2. Drug Content

Amlodipine from pre-weighed solid SEDDS was extracted by dissolving in 25 mL methanol. Amlodipine content in the methanolic extract was analyzed UV-spectrophotometrically (UV V-630, Jasco) at 360 nm, against the standard methanolic solution of amlodipine and results of drug content was reported in section 3.8.(23)(24)

3. Drug release study

Drug release studies from solid SEDDS were performed using USP XXIII, dissolution apparatus II (Disso TDT 08L, Electrolab) with 500 ml of 0.1N HCl pH 1.2 as a medium at $37 \pm 0.5^\circ\text{C}$. The speed of the paddle was adjusted to 100 rpm. Amlodipine-loaded solid SEDDS (equivalent to 5 mg of amlodipine) were placed in a dissolution tester. At predetermined time intervals an aliquot (2 ml) of the sample was collected, filtered and analyzed for the content of amlodipine by UV-spectrophotometer (UV V-630, Jasco) as mentioned above. An equivalent volume (2 ml) of fresh dissolution medium was added to compensate for the loss due to sampling and results of drug release study was reported in section 3.8. (23)(24)

4. Morphological analysis of solid SEDDS

The outer macroscopic structure of the solid SEDDS was investigated by Scanning Electron Microscope (SEM) with a Scanning Electron Microscope (JEOL JSM- 6360, Japan), operating at 10 kV and results of SEM was reported in section 3.8. (28)

5. Solid state characterization of solid SEDDS

A. DSC

The physical state of amlodipine in solid SEDDS was characterized by the differential scanning calorimetry thermogram analysis. The DSC patterns were recorded on a METTLER TOLDO DSC1 STAR SYSTEM. Each sample (2-4mg) was heated in crimped aluminum pans at a scanning rate of $10^\circ\text{C}/\text{min}$ in an atmosphere of nitrogen using the range of 30-400°C. The temperature calibrations were performed periodically using indium as a standard. The DSC curves are shown in Figure 3.10. (29)

2.10. Photostability study

A. Preparation of sample for irradiation test

All samples were passed through a sieve no. 40 to obtain fine powders with uniform particle sizes before irradiation tests.

B. Irradiation by fluorescent lamp

The irradiation test was employed utilizing a fluorescent lamp (FL-15 Watt, vacuum tube). Each sample of pure amlodipine powder, solid SEDDS of amlodipine was placed and spread uniformly as a thin film

on an aluminium foil. The fine powders on the aluminium foil were discrete enough to allow for uniform irradiation. Irradiation was conducted inside a light cabinet (Photostability chamber TP00000906, Thermolab) to protect samples from extraneous light. The accelerated irradiation test using this lamp was carried out at ambient temperature. Samples were assayed for their content of amlodipine prior to exposure and at 4, 8, 12, 24, 36, and 60 h of continuous exposure using HPLC assay method (30). The obtained chromatograms at different times were shown in Figure 3.11 and 3.12.

3. RESULT AND DISCUSSIONS

3.1. Screening of Excipients

3.1.1. Solubility study

The self-emulsifying formulations consisted of oil, surfactants, co-surfactants and drug should be clear and monophasic liquids at ambient temperature when introduced to aqueous phase and should have good solvent properties to allow presentation of the drug in solution. Solubility studies were aimed at identifying suitable oily phase and surfactant/s for the development of amlodipine SEDDS. Identifying the suitable oil, surfactant/co-surfactant having maximal solubilizing potential for drug under investigation is very important to achieve optimum drug loading (31, 32). The solubility of amlodipine in various oily phases, surfactants and co-surfactant is reported in Table 3.1, 3.2, 3.2 respectively and it is represented graphically in Figure 3.1

According to Solubility tested in this study, Tween 20, a medium-length alkyl chain with HLB 16.7 was selected as appropriate surfactant because non-ionic surfactants are less toxic than ionic surfactants, has good biological acceptance; is powerful permeation enhancer, less affected by pH and ionic strength, and highest solubility of Amlodipine was obtained. Furthermore, Transcutol-P (Diethylene glycol monoethyl ether), Polyethyleneglycol 400 (PEG 400) were selected as a co-surfactants because of their potential to solubilize the drug (33).

Table 3.1 - Data for Solubility study of Amlodipine in Various Oils

Sr No	Oil	*Solubility of Amlodipine (mg/ml) at 25°C
1	Labrafil M 1944 CS	10.24 ±6.23
2	Isopropyl Myristate	11.83 ±4.40
3	Labrafil M 2125 CS	17 ±5.68
4	Capmul PG 8	9.2 ±5.23
5	oleic acid	6.16 ±7.24

* Represents mean ± S.D. (n = 3)

Table 3.2 - Data for Solubility study of Amlodipine in Various Surfactants

Sr No	Surfactant	*Solubility of Amlodipine (mg/ml) at 25°C
1	Tween 20	90.12 ±6.74
2	Span 20	115.93 ±29.42
3	Tween 60	120.68 ±7.25
4	Span 80	74.5 ±22.33

* Represents mean ± S.D. (n = 3)

Table 3.3 - Data for Solubility study of Amlodipine in Various Co-Surfactants

Sr No	Co-Surfactant	*Solubility of Amlodipine (mg/ml) at 25°C
1	Ethanol	160.95 ±5.04

2	PEG 200	204.82 \pm 5.75
3	PEG 400	228.95 \pm 5.39
4	PEG 600	154.16 \pm 4.49
5	Capmul MCM	64.46 \pm 47.66
6	Captex 500	11.66 \pm 1.53
7	Carbitol	330.91 \pm 8.6

* Represents mean \pm S.D. (n = 3)

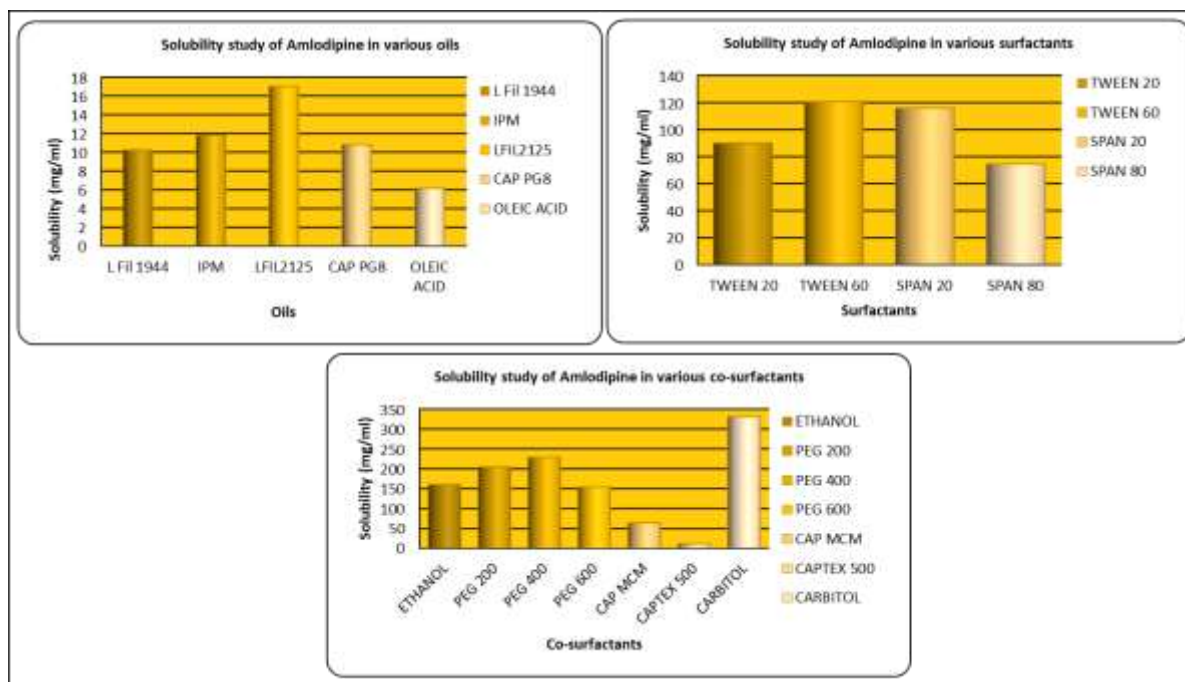


Figure 3.1 – Solubility of Amlodipine in various Oils, Surfactants and Co-surfactants

3.1.2. Preliminary screening of surfactants

Non-ionic surfactants are generally considered less toxic than ionic surfactants. They are usually accepted for oral ingestion. The surfactants were compared for their emulsification efficiencies using different oily phases. It has been reported that well formulated SEDDS is dispersed within seconds under gentle stirring conditions. Transmittance values of different mixtures are demonstrated in Table 3.4. From results it was inferred that the oily phase Labrafil M 1944 CS exhibited the highest emulsification efficiency with Tween 20, requiring only 5 flask inversions for homogenous emulsion formation. On the other hand, Labrafil M 2125 CS showed poor emulsification properties with Tween 20, requiring a minimum of 40 flask inversions (34). The aforementioned results suggested the use of Labrafil M 1944 CS as an oily phase with Tween 20 as a surfactant for further study.

Table 3.4 - Data for Emulsification efficiency of surfactant

Sr. No.	Oils	% Transmittance
		Tween 20
1.	Labrafil M 1944 CS	98
2.	Labrafil M 2125 CS	68

3.1.3. Preliminary screening of co-surfactants

Addition of a co-surfactant to the surfactant-containing formulation was reported to improve dispersibility and drug absorption from the formulation. In view of current investigation, two co-surfactants,

polyethyleneglycol 400, Transcutol-P, were compared for ease of emulsification (34). As reported Table 3.5, the Labrafil M 1944 CS exhibited good emulsification with both co-surfactants, i.e. PEG 400 showing maximum transmittance (98.6%) followed by Transcutol-P (89%).

Table 3.5 - Data for Emulsification efficiency of Co-surfactant

Sr. No.	Co-surfactants	% Transmittance
		Labrafil M 1944 CS
1.	Polyethyleneglycol 400	98.6
2.	Transcutol-P	89

Based on the results of preliminary screening, one distinct system was selected which was:

Labrafil M 1944 CS as oily phase, Tween 20 as surfactant, polyethyleneglycol 400 as co-surfactant for further studies.

3.2. Drug – Excipients Compatibility Study

Compatibility of drug and excipients can be determined by differential scanning calorimetry. Endothermic peaks of Amlodipine at 208° C disappeared in the curves of Labrafil M 1944 CS + Amlodipine, Tween 20+ Amlodipine, PEG 400 + Amlodipine and combination drug & all these excipients. It might be explained as excipients inhibited the crystallization of Amlodipine, because oil, surfactant and co-surfactant produces the molecular dispersion of Amlodipine. According to DSC graph drug and excipients are compatible to each other (35).

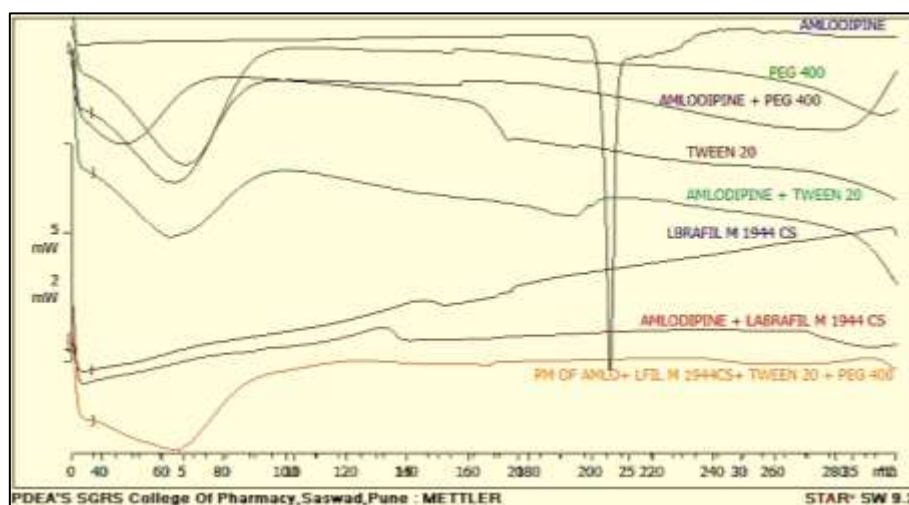


Figure 3.2 - DSC Spectra of Amlodipine and Excipients

3.3. Construction of Pseudo ternary phase diagram

The consideration for screening formulation of SEDDS usually involves: the formulation composition should be simple, safe, and compatible; it should possess good solubility; a large efficient self-emulsification region which should be found in the pseudo-ternary phase diagram, and have efficient droplet size after forming microemulsion. Thus, pseudo-ternary phase diagrams were constructed to identify the self-emulsifying regions with maximum drug loading and to optimize the concentration of oil, surfactant and co-surfactant in the SEDDS formulations and to obtain transparent and stable O/W micro-emulsions. The shaded areas in the pseudo-ternary phase-diagrams shown in Figure 3.3 represented the existence field of stable, clear and transparent O/W micro-emulsions containing Labrafil M1944 as oil and with the Tween 20: PEG 400 fixed mixing ratio, respectively. For any selected composition of surfactant and co-surfactant ratio from self-emulsifying region of ternary phase diagram (shaded) the addition of great volumes of continuous phase allowed the clear system.

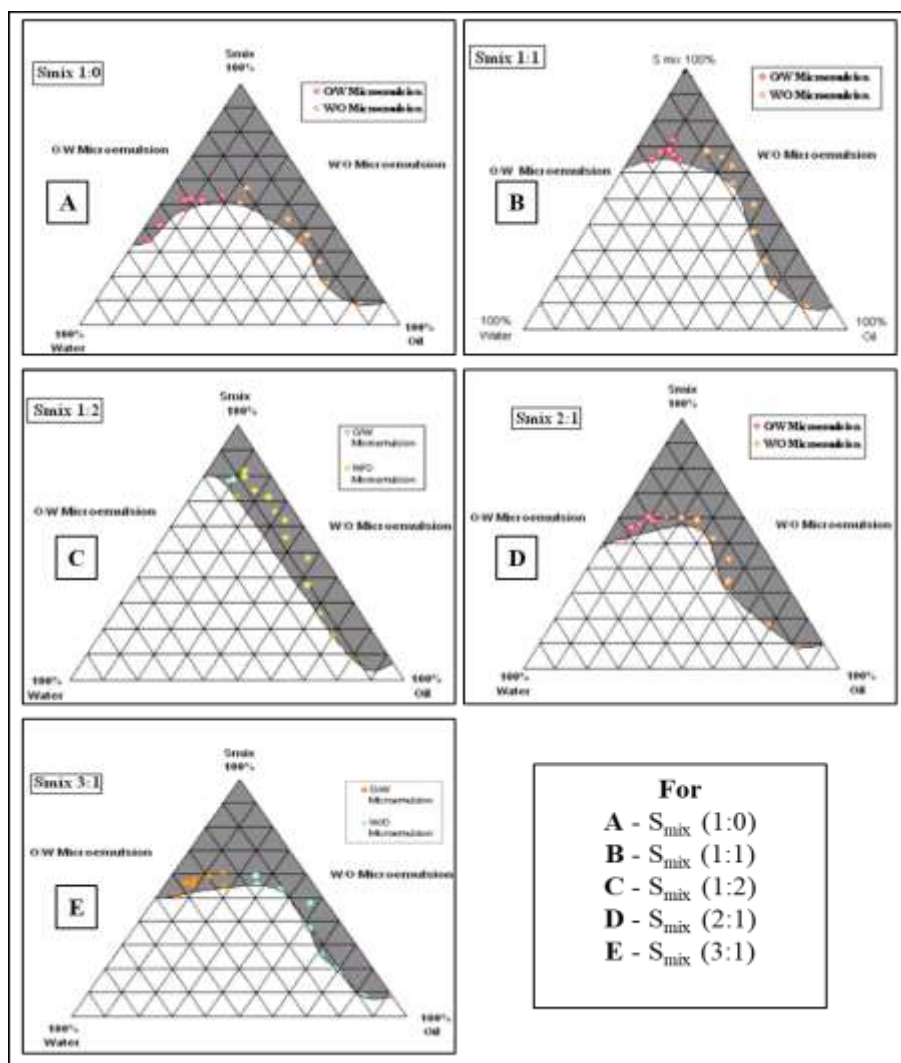


Figure 3.3 - Phase diagram of Labrafil M 1944 CS (oil)- S_{mix} (Tween 20 and Polyethylene glycol 400) were water system having different S_{mix} ratio.

It can be also seen that microemulsion region exists at S_{mix} ratio 1:0 (i.e. without co-surfactant). However, equal mixture of surfactant and co-surfactant decreases the microemulsion region (Figure 3.3 B). Increasing the concentration of surfactant (2:1) resulted in even larger area of microemulsion region (Figure 3.3 D). Further increasing surfactant concentration from 2:1 to 3:1 resulted in no influence on microemulsion region (Figure 3.3 E). The influence of concentration of co-surfactant on the microemulsion region was also seen by constructing the phase diagram in ratio of 1:2. It was seen that the region of microemulsion was decreased with increase in concentration of co-surfactant (Figure 3.3 C). The existence of large or small microemulsion region depends on the capability of a particular surfactant or surfactant mixture to solubilize the oil phase. The extent of solubilization resulted in a greater area with clearer and homogenous solution. It was seen that when the surfactant (Tween 20) was used alone, the oil phase was solubilized to a lesser extent at higher concentration of surfactant implying that surfactant alone was not able to reduce the interfacial tension of oil droplet to a sufficiently low level and thus was not able to reduce the free energy of the system to an ultra-low level desired to produce microemulsions. When a co-surfactant was added, the interfacial tension was reduced to a very low level and very small free energy was achieved which helps in larger microemulsion region. With further increase in surfactant from 1:1 to 2:1 and 3:1 further drop in interfacial tension and free energy was achieved resulting in maximum region of microemulsion/ self-emulsifying formation. Thus, pseudo-ternary phase diagram for S_{mix} 2:1 and 3:1 were selected for the formation of drug loaded self-emulsifying drug delivery system.

3.4. Selection of Formulation from Pseudo ternary Phase Diagram

It is well known that large amounts of surfactants cause GI irritation; therefore, it is important to determine the surfactant concentration properly and use minimum concentration in the formulation. S. Shafiq et al. reported the basis of selecting different nanoemulsion or microemulsion formulations from the phase diagram, as hundreds of formulations can be prepared from nanoemulsion region of the diagram. From the data shown in different pseudo-ternary phase diagrams (D and E), it was understood that oil could be solubilized up to the extent of 50% w/w. Therefore, from phase diagram (D and E) different concentrations of oil, which formed nanoemulsions, were selected at a difference of 5% (20, 25, 30, 35, 40, 45 and 50%) so that maximum formulations could be prepared covering the nanoemulsion/ self-emulsification area of the phase diagram (Tables 3.6 and 3.7). For each percentage of oil selected, only those formulations were taken from the phase diagram, which needed minimum concentration of S_{mix} . There was no sign of change in the phase behavior and nanoemulsion area of phase diagrams when Amlodipine (5 mg) was incorporated in the formulations, which was indicated as the formation and stability of Nano- and microemulsions consisting of nonionic components is not affected by the pH and or ionic strength (36-41).

3.4.1. Thermodynamic stability studies

Nanoemulsions are thermodynamically stable systems and are formed at a particular concentration of oil, surfactant and water, with no phase separation, creaming or cracking. It is the thermostability which differentiates Nano- or microemulsion from emulsions that have kinetic stability and will eventually phase separate (36). Thus, the selected formulations were subjected to different thermodynamic stability testing by using heating cooling cycle, centrifugation and freeze thaw cycle stress tests. Those formulations, which passed thermodynamic stability tests, were taken for dispersibility test (Table 3.6 and 3.7).

Thus it was concluded that the efficiency of surfactant and co-surfactant mixture was unaffected after exposing to extreme conditions.

3.4.2. Dispersibility test

When infinite dilution is done to nanoemulsion formulation, there is every possibility of phase separation, leading to precipitation of a poorly soluble drug as nanoemulsions are formed at a particular concentration of oil, surfactant and water. For oral nanoemulsions the process of dilution by the GI fluids will result in the gradual desorption of surfactant located at the globule interface. The process is thermodynamically driven by the requirement of the surfactant to maintain an aqueous phase concentration equivalent to its CMC (36).

In the present study, we used distilled water as a dispersion medium because it is well reported that there is no significant difference in the nanoemulsions prepared using nonionic surfactants, dispersed in either water or simulated gastric or intestinal fluid (36, 40). Formulations in Group I (Table 3.6) and Group II (Table 3.7) that passed dispersibility test in Grade A, B and C were taken for further study, as Grade A and B formulations will remain as nanoemulsions when dispersed in GIT. Formulation falling in Grade C could be recommended for self-emulsifying drug delivery formulation.

So from the study, total six formulations were selected for further study three from each group i.e. F_1 , F_2 , F_3 from Group I and F_1 , F_2 , F_3 from Group II.

Table 3.6 - Data for Thermodynamic stability test of different formulations selected from Group I (Figs. 10.10 D) at a difference of 5% w/w of oil.

Group I (Fig. 10.10 D) S_{mix} ratio (S:CoS) 2:1	Percentage w/w of different components in formulation		Observations based on the preparation, thermodynamic stability studies and dispersibility tests				Inference
Formulation	Oil	S_{mix}	H/C	Cent.	Freez. Tha.	Disperse.	
F_1	20	80	√	√	√	Grade A	Selected
F_2	25	75	√	√	√	Grade B	Selected
F_3	30	70	√	√	√	Grade C	Selected

F ₄	35	65	√	√	√	Grade D	Rejected
F ₅	40	60	√	√	√	Grade D	Rejected
F ₆	45	55	√	√	√	Grade E	Rejected
F ₇	50	50	√	√	√	Grade E	Rejected

Where, Heating cooling cycle (H/C), Freeze-thaw cycle (Freez. Tha.), Centrifugation (Cent.), Dispersibility test (Disperse.)

Table 3.7 - Data for Thermodynamic stability test of different formulations selected from Group II (Figs. 10.10 E) at a difference of 5% w/w of oil

Group II (Fig. 10.10 E) S _{mix} ratio (S:CoS) 3:1	Percentage w/w of different components in formulation		Observations based on the preparation, thermodynamic stability studies and dispersibility tests				Inference
	Oil	S _{mix}	H/C	Cent.	Freez. Tha.	Disperse.	
F ₁	20	80	√	√	√	Grade A	Selected
F ₂	25	75	√	√	√	Grade B	Selected
F ₃	30	70	√	√	√	Grade C	Selected
F ₄	35	65	√	√	√	Grade D	Rejected
F ₅	40	60	√	√	√	Grade D	Rejected
F ₆	45	55	√	√	√	Grade E	Rejected
F ₇	50	50	√	√	√	Grade E	Rejected

Where, Heating cooling cycle (H/C), Freeze-thaw cycle (Freez. Tha.), Centrifugation (Cent.), Dispersibility test (Disperse.)

3.5. Preparation of Liquid SEDDS Formulations

Formulations selected in section 2.6 were prepared as per the composition reported in Table 2.1 and found to be thermodynamically stable even after addition of a drug.

3.6. Evaluation of Liquid SEDDS Formulations

1. Determination of emulsification time

In SEDDS, the primary means of self-emulsification process is visual evaluation (41). The efficiency of self-emulsification could be estimated by determining the rate of emulsification. The rate of emulsification is an important index for the assessment of the efficiency of emulsification (31) that is the SEDDS should disperse completely and quickly when subjected to aqueous dilution under mild agitation. The emulsification time of liquid SEDDS are presented in Table 3.8. Emulsification time study showed that all the formulations emulsified within 20 s. Among the tested formulations, formulations A and D showed shortest emulsification time than others.

2. Turbidimetric evaluation

The results of turbidimetric evaluation of liquid SEDDS are presented in Table 3.8. Formulations A and D showed low turbidity values (23.1 NTU and 31 NTU, respectively) owing to the presence of adequate amounts of surfactant (Tween 20), which primarily governs the resultant droplet size and its distribution. Formulation C and F, with moderate quality of emulsion formation because of high concentration of oil and showed very high and variable turbidity (94.2±15.8 NTU and 82.1±12.8, mean ± SD, n = 3) and coarser droplets. Formulation B and E showed moderate turbidity values (41.1 NTU and 31.7 NTU, respectively). Thus the droplet size distribution is strongly dependent on concentration of surfactant/co-surfactant.

3. Drug Content

The drug content of all formulations ranged between 5.79 and 7.95 mg/mL (Table 3.8) and passed uniformity of content.

4. Globule size analysis

Droplet size of SMEDDS is a critical parameter in the adapted strategy of enhancing drug bioavailability (42). Droplet size analysis revealed the effect of varying amounts of Tween 20 and PEG 400 in the formulated SEDDS. Changes in Tween 20 to PEG 400 ratios are most likely to alter the resultant HLB of the system and the properties of liquid crystal (LC) interfaces. This in turn governs the size of droplets formed (43). Thus it is the appropriate choice of surfactant and co-surfactant together with their proper concentrations, which provides an optimum self-emulsifying formulation. The mean droplet sizes of the reconstituted microemulsions are reported in Table 3.8. As shown in the table, the average droplet sizes of all microemulsions were less than 700 nm. The data for size distribution for various emulsions containing amlodipine measured by photon correlation spectroscopy are shown in Figure 3.4.

Table 3.8 - Data for Evaluation of Liquid SEDDS formulations

Evaluation Parameters	Group I (S _{mix} 2:1)			Group II (S _{mix} 3:1)		
	A	B	C	D	E	F
Emulsification Time (S) ^a	12±2	17±3	19±4	14±3	16±2	18±1
Turbidity (NTU) ^a	23.1±2.28	41.1±3.41	94.2±15.8	31±4.76	31.7±2.7	82.1±12.8
Drug Content (mg/ml) ^a	5.79±0.05	7.95±0.043	7.11±0.067	6.38±0.9	6.29±0.02	7.87±0.11
Mean Droplet Size (µm)	0.306	0.518	0.690	0.315	0.348	0.366

^aMean ± SD, n = 3.

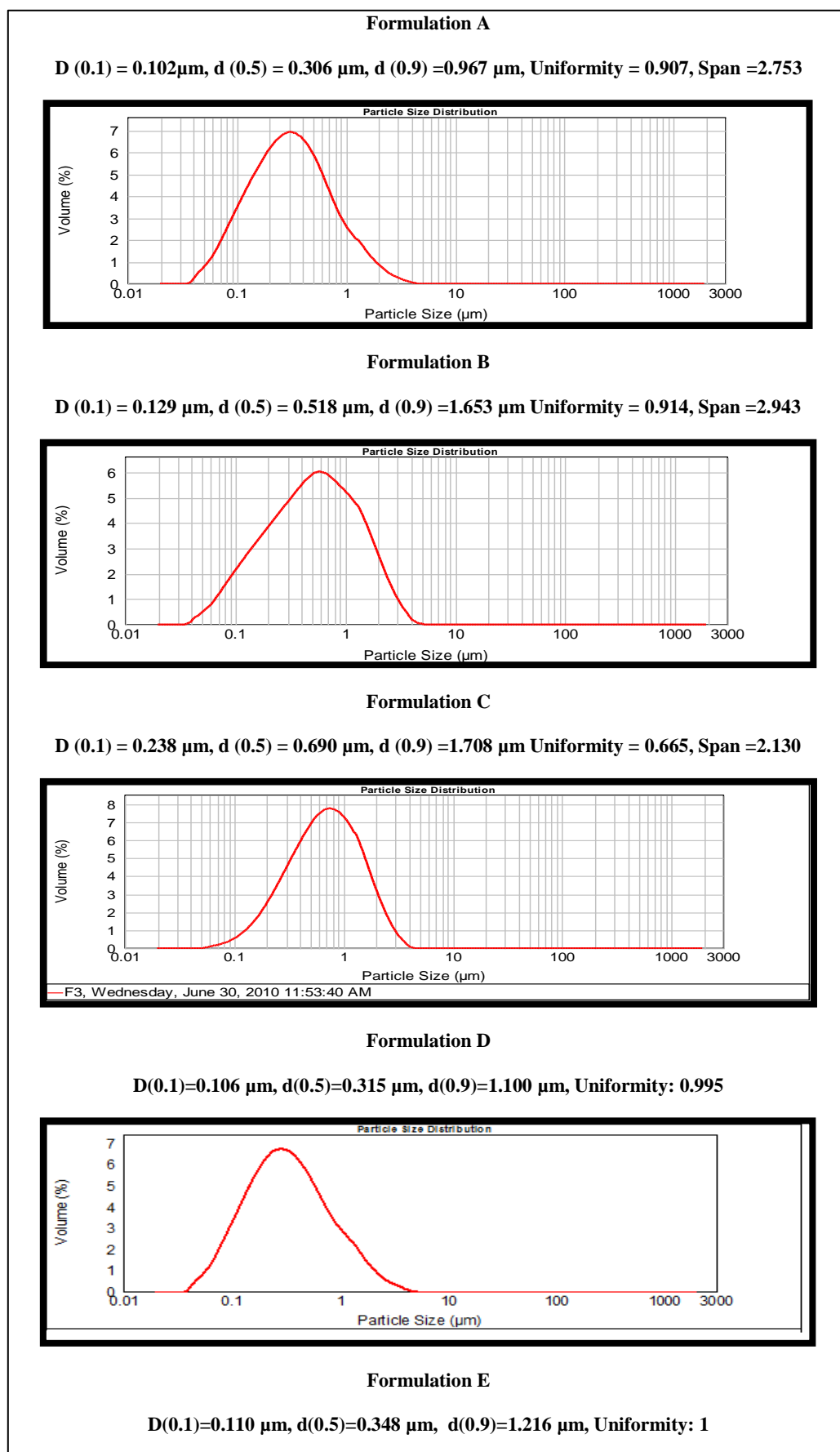


Figure 3.4 - Results of Droplet size distributions of Liquid SEDDS

5. Drug release studies

The in- vitro drug release study of liquid SEDDS were performed in 0.1N HCl. The percent drug release for different formulations is shown in Table 3.9. In the self-emulsifying systems, the free energy required to form an emulsion was very low, thereby allowing spontaneous formation of an interface between the oil droplets and water. It is suggested that the oil/surfactant/co-surfactant and water phases effectively swell and eventually there was increase the release rate. It was clear from the Figure 3.5 and 3.6. The maximum percentage of the drug released within 5min because of fast emulsification. The marketed formulation (Amlocard®) showed only 61% drug release at the end of 60 min. This clearly demonstrated the superior performance of the developed Liquid SEDDS as compared to Amlocard®. The SEDDS represented Amlodipine in solubilized form in gastric fluids after ingestion and hence provided large interfacial area for Amlodipine absorption. Therefore, the optimized formulations (C and F), had higher drug release than marketed preparation, optimum globule size, and stability of emulsion and drug and above all, lower surfactant concentration was selected for the further study (28).

Table 3.9 - Dissolution data for Liquid SEDDS formulations in 0.1N HCl

Time (in min)	*Percent drug dissolved						
	A	B	C	D	E	F	MT
0	0.000	0.000	0.000	0.000	0.000	0.000	0.000
05	96.86±1.3 3	96.09±0.6 5	94.66±1.2 5	97.58±1.2 5	96.59±1.7 8	94.54±1.1 2	59.8±1.23
15	97.48±1.4	96.27±0.5 9	90.92±1.5 7	96.64±1.4 5	96.95±1.0 5	94.47±1.3 6	60.91±1.5 4
30	97.99±2.7 6	96.32±1.0 1	91.45±2.4 5	96.48±1.5 4	96.48±1.1 9	94.59±1.5 5	61.68±0.9 8
60	98.45±2.0 6	96.32±1.3	91.97±2.6 8	96.12±1.6 8	96.89±1.4 5	94.63±1.4 8	61.61±0.8 5

*Represents mean ± S.D. (n = 3), MT: Marketed Tablet of Amlodipine

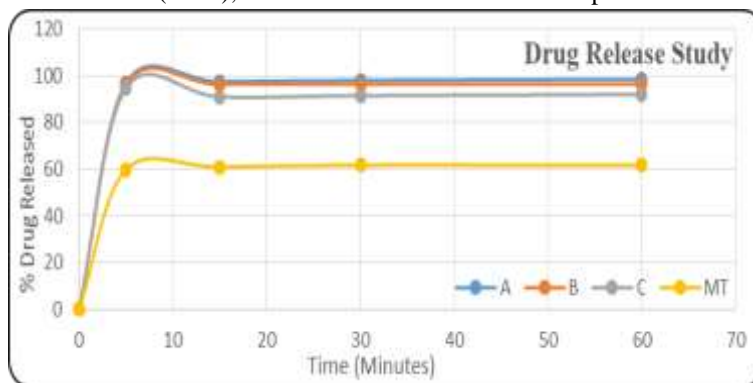


Figure 3.5 - In- vitro drug release profile of Liquid SEDDS Formulations A, B, C and MT in 0.1N HCl

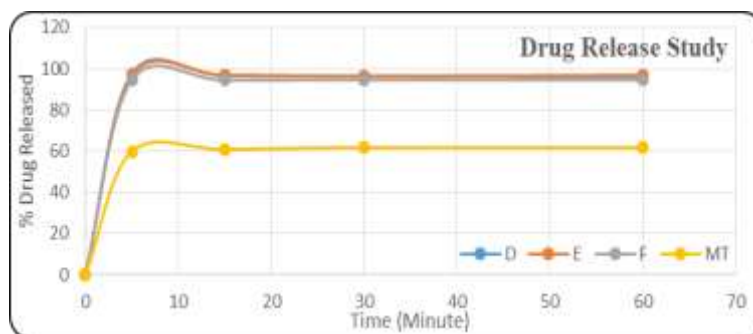


Figure 3.6 - In- vitro drug release profile of Liquid SEDDS Formulations D, E, F and MT in 0.1N HCl

3.7. Preparation of Solid SEDDS

Solid SEDDS were prepared as per the composition reported in Table 2.3.

3.8. Evaluation of Solid SEDDS Formulations

1. Reconstitution properties of solid SEDDS

The mean droplet sizes of the solid SEDDS is presented in Table 3.10. As shown in the table, the z-average droplet sizes of both systems were less than 1 μm . The emulsion droplet size distribution and solid SEDDS (Figure 3.7) further confirmed the self-emulsification nature of the solid SEDDS. The droplet size of the emulsion from the solid SEDDS was slightly increased, compared to the liquid SMEDDS. At the same time, a broader size distribution was observed.

The solid SEDDS preserved the self-emulsification performance of the liquid SEDDS.

Table 3.10 - Data for Evaluation of Solid SEDDS formulations

Evaluation Parameters	Group I (S_{mix} 2:1)	Group II (S_{mix} 3:1)
	F ₁	F ₂
Emulsification Time (S) ^a	20 \pm 2	15 \pm 3
Drug Content (% w/w) ^a	2.59 \pm 0.85	2.52 \pm 0.48
Mean Droplet Size (μm)	0.839	0.623

^aRepresents mean \pm S.D. (n = 3)

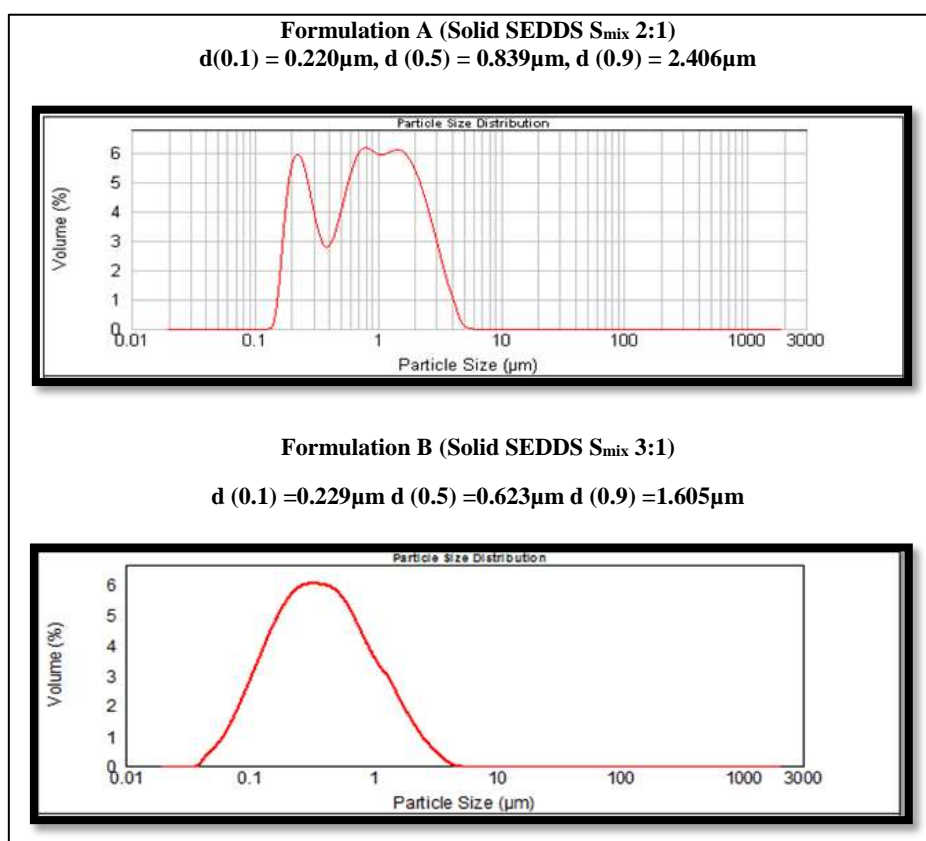


Figure 3.7 - Results of Droplet size distributions of Solid SEDDS

2. Drug Content

The drug content of both formulations ranged between 2.50 and 2.60 % w/w (Table 3.10).

3. Drug Release Study

The in-vitro drug release studies were performed in order to ensure the quick release of the drug in the dissolution medium. In-vitro dissolution studies also give an idea about the self-emulsification efficiency of the developed system. The in-vitro drug release profile of F₁ and F₂ was evaluated in 0.1N HCl (n = 3). It was observed that both the solid SEDDS formulations F₁ and F₂ released more than 90% of Amlodipine within 60

min. Both the formulations dispersed almost instantaneously indicating the high self-emulsion efficiency of the developed formulations.

The graphs of the drug release profile are shown in Figure 3.11. Amlodipine from the solid SEDDS was completely and rapidly dissolved in medium without affecting the dissolution pattern also.

Table 3.11 - Dissolution data for formulations in 0.1N HCl

Time (Minute)	*Percent drug dissolved	
	F ₁	F ₂
0	00.000	00.000
05	88.419±1.06	91.338±1.80
15	89.201±2.60	91.898±3.95
30	89.906±1.10	92.497±1.71
60	91.041±2.96	93.059±1.53

Represents mean ± S.D. (n = 3)

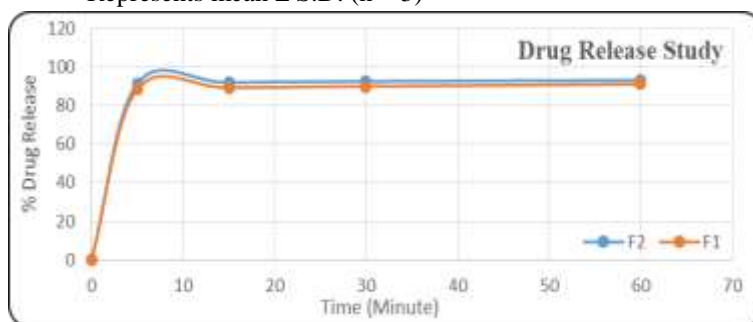


Figure 3.8 - In- vitro drug release profile of Solid SEDDS Formulations F₁ and F₂

4. Morphology of the Solid SEDDS

The outer macroscopic morphology of the Solid SEDDS revealed well separated spherical particle with smooth surface seen in SEM images of the Solid SEDDS. Figure 3.9 shows the scanning electron micrographs of the Maltodextrin powder and Solid SEDDS formulation. Maltodextrin (Figure 3.9 A and 3.9 B) appeared with a rough surface with porous particles. However, the solid SEDDS (Figure 3.9 C and 3.9 D) appeared as smooth-surfaced Maltodextrin particles, indicating that the liquid SEDDS is adsorbed or embedding inside the pores of Maltodextrin. Following spray-drying, maltodextrin is known to produce deep and abundant surface dents and the limited agglomeration of particles was probably due to maltodextrin ability to diminish the degree of particle agglomeration (44, 45) and to the storage of products in closed vials protected from humidity; hence preferred as carrier in the study.

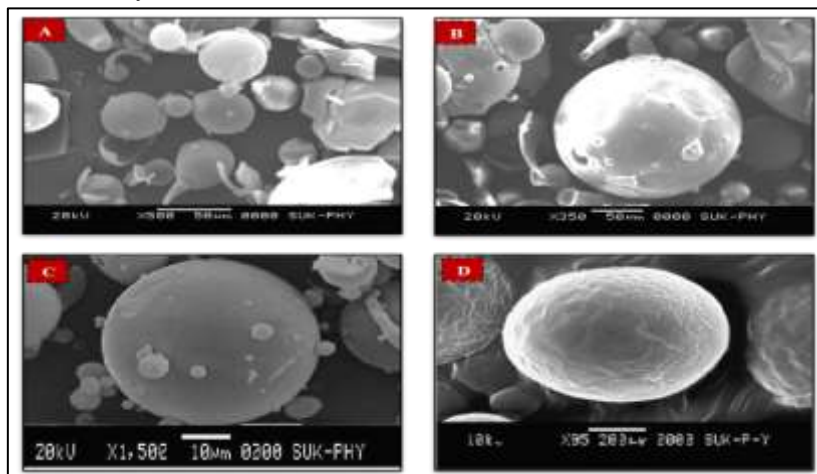


Figure 3.9 - Scanning electron micrographs: (A & B) Maltodextrin; (C & D) Solid SEDDS

5. Solid state characterization of solid SEDDS

1. DSC

The physical state of amlodipine in the solid SEDDS was investigated since it would have an important influence on the in-vitro and in-vivo release characteristics. DSC curves of pure amlodipine, and the solid SEDDS of amlodipine are shown in Figure 3.10. Pure amlodipine showed three sharp endothermic peaks at temperatures between 205^o and 210^oC. No obvious peaks for amlodipine and oil were found in the solid SEDDS of amlodipine. It might be explained that the melting behavior of the oil was changed by maltodextrin and the crystallization of amlodipine was inhibited by maltodextrin and surfactants.

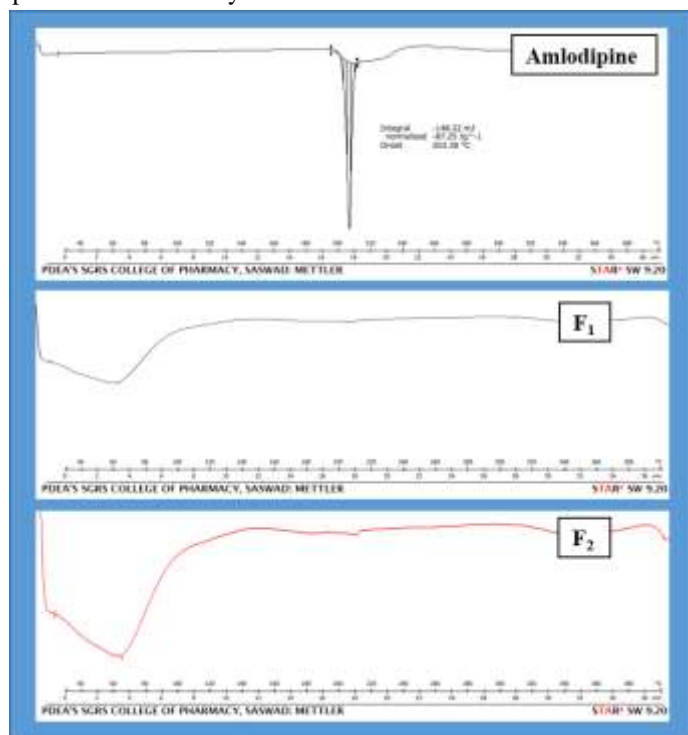


Figure 3.10 - DSC Spectra of pure Amlodipine and Solid SEDDS.

3.9. Photostability study

The Photostability studies of pure amlodipine and Solid SEDDS were done by exposing these samples to the fluorescent light using Photostability chamber (TP 00000906, Thermolab). The Samples were assayed for their content of amlodipine prior to exposure and at 4, 8, 12, and 24 h of continuous exposure using HPLC assay method. The decomposition of pure amlodipine was found to be remarkable upon exposure to fluorescent lamp or sunlight (which is the main source of light during manufacturing, storage and handling). The retention time for amlodipine and its degradation product was found to be 3.3 ± 0.18 and 2.9 ± 0.14 respectively.

In this study, Solid SEDDS was prepared by spray drying the Liquid SEDDS with relatively excess amount of maltodextrin compared to amlodipine. The outer macroscopic morphology of the Solid SEDDS observed by SEM (Figure 3.9 C & 3.9 D) suggests that most of the amlodipine was encapsulated in the maltodextrin matrix. Therefore the improved photostability of Solid SEDDS might be due to the compact physical barrier composed of maltodextrin as observed as the smooth surface of the Solid SEDDS powder (Figure 3.9 C & 3.9 D).

This study indicated that the rate of photo degradation is very slow in Solid SEDDS as compared to pure amlodipine powder; thus Solid SEDDS conferred photostability to drug.

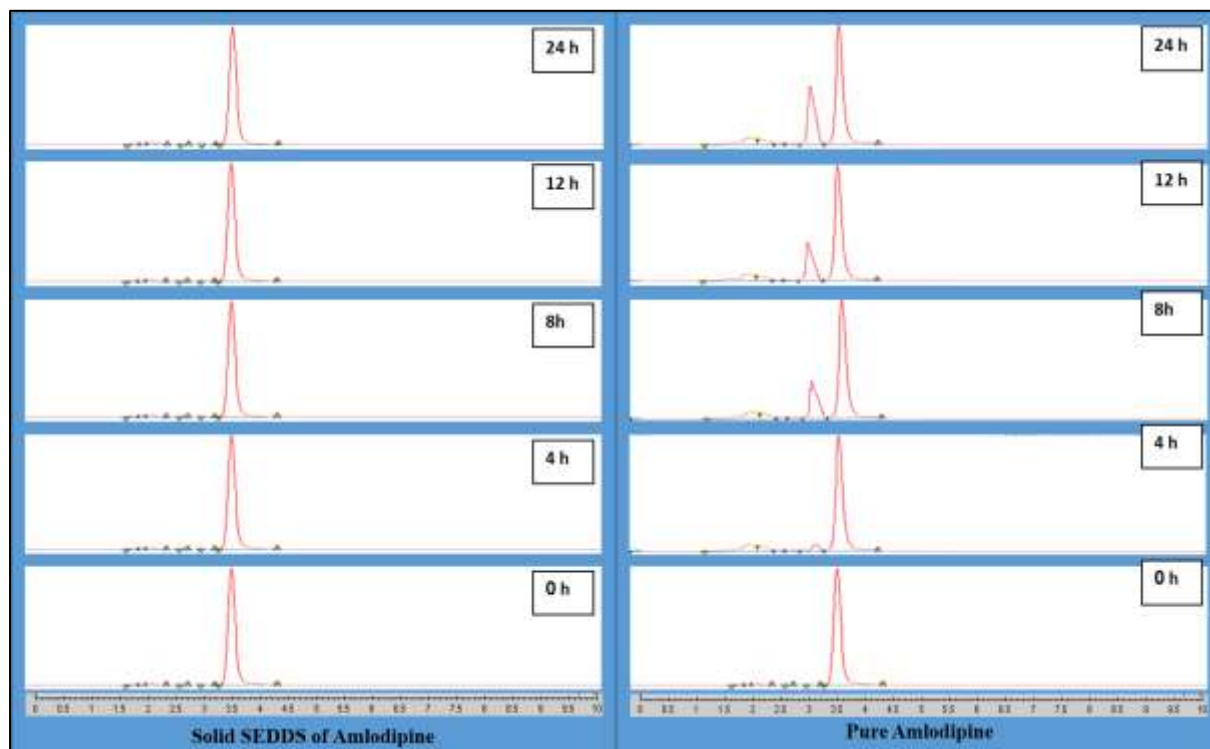


Figure 3.11 - Chromatograms of Solid SEDDS of Amlodipine and Pure Amlodipine at different time interval.

CONCLUSION

In the present study, Amlodipine was formulated in the form of Self-Emulsifying Drug Delivery System (SEDDS) to increase its solubility which will result in enhancement in Dissolution Rate and Bioavailability and also to increase its Photostability. Firstly, Liquid SEDDS was prepared by dissolving Amlodipine in various S_{mix} which were further evaluated and F1 and F2 were found to be optimized. F1 and F2 were solidified using spray drying method and Preparation of Solid SEDDS took place. The in-vitro drug release profile of F₁ and F₂ was evaluated in 0.1N HCl. It was observed that both the solid SEDDS formulations F₁ and F₂ released more than 90% of Amlodipine within 60 min. Further Photostability studies of pure amlodipine and Solid SEDDS (F₁ and F₂) were done by exposing these samples to the fluorescent light using Photostability chamber. The Result of photostability study indicated that the rate of photo degradation is very slow in Solid SEDDS (F₁ and F₂) as compared to pure amlodipine powder; thus we can say that Photostability of amlodipine increase when it is formulated in the form of SEDDS.

ACKNOWLEDGEMENT

The authors are very much thankful to PDEAs Shankarrao Ursal College of Pharmaceutical Sciences and Research Centre, Pune, Maharashtra, India and PDEAs Seth Govinds Raghunath Sable College of Pharmacy, Pune, Maharashtra, India for providing the necessary support to complete this work successfully.

CONFLICT OF INTEREST

All authors declared no conflicts of interest.

REFERENCES

1. Behboudi E, Soleymani J, Martinez F, Jouyban A. Solubility of amlodipine besylate in binary mixtures of polyethylene glycol 400+ water at various temperatures: Measurement and modelling. *Journal of Molecular Liquids*. 2022 Feb 1;347:118394.

2. Jang DJ, Jeong EJ, Lee HM, Kim BC, Lim SJ, Kim CK. Improvement of bioavailability and photostability of amlodipine using redispersible dry emulsion. *European journal of pharmaceutical sciences*. 2006 Aug 1;28(5):405-11.
3. Na YG, Byeon JJ, Wang M, Huh HW, Son GH, Jeon SH, Bang KH, Kim SJ, Lee HJ, Lee HK, Cho CW. Strategic approach to developing a self-microemulsifying drug delivery system to enhance antiplatelet activity and bioavailability of ticagrelor. *International journal of nanomedicine*. 2019;14:1193.
4. Hwang I, Kang CY, Park JB. Advances in hot-melt extrusion technology toward pharmaceutical objectives. *Journal of Pharmaceutical Investigation*. 2017 Mar;47:123-32.
5. Madhav KV, Kishan V. Self microemulsifying particles of loratadine for improved oral bioavailability: Preparation, characterization and in vivo evaluation. *Journal of Pharmaceutical Investigation*. 2018 Jul;48:497-508..
6. Zhao J, Xie P, Ye C, Wu C, Han W, Huang M, Wang S, Chen H. Outside-in synthesis of mesoporous silica/molybdenum disulfide nanoparticles for antitumor application. *Chemical Engineering Journal*. 2018 Nov 1;351:157-68.
7. Rahman MA, Mujahid M, Hussain A, Iqbal Z. Development and pharmacokinetic evaluation of spray-dried self-nanoemulsifying drug delivery system of sertraline. *Journal of Pharmaceutical Investigation*. 2017 Jul;47:325-33.
8. Rashid R, Kim DW, Abid Mehmood Yousaf OM, ud Din F, Park JH, Yong CS, et al. Comparative study on solid self-nanoemulsifying drug delivery and solid dispersion system for enhanced solubility and bioavailability of ezetimibe. *Int J Nanomedicine*. 2015;10:6147-59..
9. SHIVANI RP. Self-Emulsifying Drug Delivery System: A Technique to Improve Oral Bioavailability of Poorly Soluble Drugs. *International Journal of Pharmaceutical Research*. 2021 Jul;13(3).
10. Rana H, Jesadiya B, Mandal S. Development of microemulsion for solubility enhancement of atorvastatin calcium. *International Journal of Pharmaceutical Sciences and Research*. 2013 Aug 1;4(8):3103..
11. Nasr A, Gardouh A, Ghorab M. Novel solid self-nanoemulsifying drug delivery system (S-SNEDDS) for oral delivery of olmesartan medoxomil: design, formulation, pharmacokinetic and bioavailability evaluation. *Pharmaceutics*. 2016 Jun 27;8(3):20.
12. Date AA, Nagarsenker MS. Design and evaluation of self-nanoemulsifying drug delivery systems (SNEDDS) for cefpodoxime proxetil. *International journal of pharmaceutics*. 2007 Feb 1;329(1-2):166-72..
13. Alhamdany AT, Abbas AK. Formulation and in vitro evaluation of amlodipine gastroretentive floating tablets using a combination of hydrophilic and hydrophobic polymers. *International Journal of Applied Pharmaceutics*. 2018 Nov 7;10(6):119-34.
14. Hosmer J, Reed R, Bentley MV, Nornoo A, Lopes LB. Microemulsions containing medium-chain glycerides as transdermal delivery systems for hydrophilic and hydrophobic drugs. *Aaps Pharmscitech*. 2009 Jun;10:589-96.
15. Nastiti CMRR, Ponto T, Abd E, Grice JE, Benson HAE, Roberts MS. Topical Nano and Microemulsions for Skin Delivery. *Pharmaceutics* [Internet]. 2017 Sep 21; 9(4).
16. Florence AT, D Attwood. *Physicochemical principles of pharmacy: in manufacture, formulation, and clinical use*. London: Pharmaceutical Press; 2016.
17. Yang J, Xu H, Wu S, Ju B, Zhu D, Yan Y, et al. Preparation and evaluation of microemulsion-based transdermal delivery of Cistanche tubulosa phenylethanoid glycosides. *Molecular Medicine Reports*. 2017 Jan 25; 15(3):1109–16.
18. Aparna .Formulation and evaluation of solid self-emulsifying drug delivery system of Ranolazine. *Journal of Global Trends in Pharmaceutical Sciences*.2014; 5(4):2238-2247
19. Gupta A.K, Mishra D.K and Mahajan S.C. Preparation and in-vitro evaluation of self-emulsifying drug delivery system of antihypertensive drug, Valsartan.2011;2 (3): 633-639.

20. Yi T, Wan J, Xu H, Yang X. A new solid self-microemulsifying formulation prepared by spray-drying to improve the oral bioavailability of poorly water soluble drugs. *European Journal of Pharmaceutics and Biopharmaceutics*. 2008 Oct 1;70(2):439-44.
21. Chintalapudi R, Murthy TE, Lakshmi KR, Manohar GG. Formulation, optimization, and evaluation of self-emulsifying drug delivery systems of nevirapine. *International journal of pharmaceutical investigation*. 2015 Oct;5(4):205.
22. Bachynsky MO, Shah NH, Patel CI, Malick AW. Factors affecting the efficiency of a self-emulsifying oral delivery system. *Drug development and industrial pharmacy*. 1997 Jan 1;23(8):809-16.
23. Deepan T, Paul Ambethkar K, Vijya Lakshmi G, Dhanaraju M. Analytical Method Development and Validation of RP-HPLC for Estimation of Atorvastatin Calcium and Fenofibrate in Bulk drug and Tablet dosage forms, *Euro. J. App. Sci.*, 2011; 3(2): 35-39.
24. Patil P, Patil V, Paradkar A. Formulation of a self-emulsifying system for oral delivery of simvastatin: in vitro and in vivo evaluation. *Acta pharmaceutica*. 2007 Mar 1;57(1):111-22.
25. Hemangini R, Jesadiya B, Mandal S. Development of microemulsion for solubility enhancement of Atorvastatin Calcium *International Journal of Pharmaceutical Sciences and Research* 2013; Vol. 4(8): 3103-3109.
26. Verma R, Kaushik A, Almeer R, Rahman MH, Abdel-Daim MM, Kaushik D. Improved Pharmacodynamic Potential of Rosuvastatin by Self-Nanoemulsifying Drug Delivery System: An in vitro and in vivo Evaluation. *International Journal of Nanomedicine*. 2021 Feb;Volume 16:905–24.
27. Yi T, Wan J, Xu H, Yang X. A new solid self-microemulsifying formulation prepared by spray-drying to improve the oral bioavailability of poorly water soluble drugs. *European Journal of Pharmaceutics and Biopharmaceutics*. 2008 Oct 1;70(2):439-44..
28. Jaiswal P, Aggarwal G, Harikumar SL, Singh K. Development of self-microemulsifying drug delivery system and solid-self-microemulsifying drug delivery system of telmisartan. *Int J Pharm Investig*. 2014 Oct;4(4):195-206.
29. Truong DH, Tran TH, Ramasamy T, Choi JY, Lee HH, Moon C, Choi HG, Yong CS, Kim JO. Development of Solid Self-Emulsifying Formulation for Improving the Oral Bioavailability of Erlotinib. *AAPS PharmSciTech*. 2016 Apr;17(2):466-73.
30. A. Mohammadi, N. Rezanour, et al., 2007, A stability-indicating high performance liquid chromatographic (HPLC) assay for the simultaneous determination of atorvastatin and amlodipine in commercial tablets, *Journal of Chromatography B*, 846: 215–221.
31. Pouton CW. Formulation of self-emulsifying drug delivery systems. *Advanced drug delivery reviews*. 1997 Apr 14;25(1):47-58.
32. Pouton CW. Lipid formulations for oral administration of drugs: non-emulsifying, self-emulsifying and 'self-microemulsifying' drug delivery systems. *European journal of pharmaceutical sciences*. 2000 Oct 1;11:S93-8.
33. Couvreur P. Dossier: Drug delivery and drug efficacy. *Biomedicine & Pharmacotherapy*. 2004;3(58):141.
34. Pouton CW, Porter CJ. Formulation of lipid-based delivery systems for oral administration: materials, methods and strategies. *Advanced drug delivery reviews*. 2008 Mar 17;60(6):625-37.
35. Nasr A, Gardouh A, Ghorab M. Novel solid self-nanoemulsifying drug delivery system (S-SNEDDS) for oral delivery of olmesartan medoxomil: design, formulation, pharmacokinetic and bioavailability evaluation. *Pharmaceutics*. 2016 Jun 27;8(3):20..
36. Lawrence MJ, Rees GD. Microemulsion-based media as novel drug delivery systems. *Advanced drug delivery reviews*. 2012 Dec 1;64:175-93.
37. Craig DQ, Barker SA, Banning D, Booth SW. An investigation into the mechanisms of self-emulsification using particle size analysis and low frequency dielectric spectroscopy. *International journal of pharmaceutics*. 1995 Jan 31;114(1):103-10..
38. Kreuter J, Swarbrick J, Boyalan JC. *Encyclopedia of pharmaceutical technology*. New York. 1994;10:165-90.

39. Ghosh PK, Murthy RS. Microemulsions: a potential drug delivery system. *Current drug delivery*. 2006 Apr 1;3(2):167-80..
40. Li P, Ghosh A, Wagner RF, Krill S, Joshi YM, Serajuddin AT. Effect of combined use of nonionic surfactant on formation of oil-in-water microemulsions. *International journal of pharmaceutics*. 2005 Jan 6;288(1):27-34.
41. Shah NH, Carvajal MT, Patel CI, Infeld MH, Malick AW. Self-emulsifying drug delivery systems (SEDDS) with polyglycolized glycerides for improving in vitro dissolution and oral absorption of lipophilic drugs. *International journal of pharmaceutics*. 1994 May 16;106(1):15-23..
42. Elnaggar YS, El-Massik MA, Abdallah OY. Self-nanoemulsifying drug delivery systems of tamoxifen citrate: design and optimization. *International journal of pharmaceutics*. 2009 Oct 1;380(1-2):133-41..
43. Patil P, Joshi P, Paradkar A. Effect of formulation variables on preparation and evaluation of gelled self-emulsifying drug delivery system (SEDDS) of ketoprofen. *Aaps Pharmscitech*. 2004 Sep;5:43-50.
44. Dollo G, Le Corre P, Guérin A, Chevanne F, Burgot JL, Leverge R. Spray-dried redispersible oil-in-water emulsion to improve oral bioavailability of poorly soluble drugs. *European Journal of Pharmaceutical Sciences*. 2003 Jul 1;19(4):273-80..
45. Pedersen GP, Fäldt P, Bergenståhl B, Kristensen HG. Solid state characterisation of a dry emulsion: a potential drug delivery system. *International journal of pharmaceutics*. 1998 Sep 15;171(2):257-70.



FORMULATION, EVALUATION AND OPTIMIZATION OF B –CYCLODEXTRIN BASED NANOSPONGES OF CLARITHROMYCIN

Dr. Prashant H. Khade¹, Amol Talware², Sujit S. Kakde¹, Dr. Sachin V. Kotwal³,
Priyanka D. Borude⁴, Harshal M. Shinde⁵

¹Assistant Professor, PDEAs Shankarrao Ursal College of Pharmaceutical Sciences and Research Centre, Pune, Maharashtra, India.

²Sector Manager, Croda India Company Pvt. Ltd, Mumbai, Maharashtra, India.

³Principal, PDEAs Shankarrao Ursal College of Pharmacy (Diploma), Pune, Maharashtra, India.

⁴Lecturer, PDEAs Shankarrao Ursal College of Pharmacy (Diploma), Pune, Maharashtra, India.

⁵Research Scholar, PDEAs Shankarrao Ursal College of Pharmaceutical Sciences and Research Centre, Pune, Maharashtra, India.

For Correspondence -

Prashant H. Khade,

Assistant Professor, Department of Pharmaceutics,

PDEAs Shankarrao Ursal College of Pharmaceutical Sciences and Research Centre,
Pune, Maharashtra, India.

E-mail Id: phkhade@gmail.com

ABSTRACT

The aim of present study was to develop an optimized gastric floating controlled drug delivery system of Clarithromycin (CLA). The Clarithromycin is poorly water soluble drug and gastric irritant. To overcome these problems attempt was made in present study to form inclusion complex of Clarithromycin with Nanosponges. β -Cyclodextrin (CD) based Nanosponges (NS) are novel class of cross-linked derivatives of Cyclodextrin. The Nanosponges were synthesized by carbonylation of β -Cyclodextrin to exploit its porous structure for drug entrapment. A better alternative to β -CD is it's Nanosponges due to low solubility & toxicity of β -CD. The final Nanosponges structure contains both lipophilic cavities of CD and carbonate bridges leading to a network of more hydrophilic channels. NS are solid, insoluble in water, crystalline in nature and thermally stable compounds. They have been used to increase the solubility of poorly water soluble actives, to avoid gastric irritation and control the release of drug. Present study aimed at formulating complex of CLA with NS by solid dispersion technique and absence of interaction of CLA with NS was confirmed by XRPD, DSC and FTIR studies. The result of XRPD results showed that the crystallinity of CLA was decreased after loading into NS. The 3² full factorial experimental designs were applied for tablet formulation. The *in vitro* dissolution studies indicated a slow and prolonged release of drug over the period of 12 h. Histopathological study revealed non irritancy of drug-NS complex to gastric mucosa (of rat). Hence drug-NS complex found to be suitable for designing into unit dosage forms. The release study of drug from tablet as well as capsule as unit dosage forms indicated controlled release of a drug when compared with marketed preparation.

Keywords: Nanosponges, β -Cyclodextrin, Clarithromycin, Solubility, Controlled drug delivery System.

1. INTRODUCTION

The objective of any drug delivery system is to provide therapeutic amount of drug to targeted site in body to achieve the desired therapeutic effect (1). For curing of disease, it is necessary to achieve and maintain the concentration of administered drug within the therapeutically effective range for this drug dosage must be taken several times which results in fluctuating drug levels in plasma. This drawback of conventional dosage form can be overcome by formulation of controlled release dosage forms which provides drug release in an

4999

amount sufficient to maintain the therapeutic drug level over extended period of time, with release profiles controlled by the special technological construction and design of the system (2). The primary objectives of controlled drug delivery are to ensure safety and enhancement of efficacy of drug with improved patient compliance. So the use of these dosage forms is increasing in treatment of acute and chronic diseases as they maintain the concentration of drug in plasma above minimum effective concentration and below the minimum toxic level for extended period of time. Thus, controlled drug delivery results in optimum drug therapy with reduced frequency of dosing and side effects (3).

Effectiveness can also be enhanced by Gastro retentive systems. These are hydro dynamically balanced systems. In these systems dosage form have the specific gravity less than gastric juice, so they float in stomach and retain the drug over for extended period of time. Thus, total residence time in stomach is increased. Also these systems are relatively large in size and passing from pyloric opening is prohibited. This system is useful for drugs which are absorbed in stomach and also for local action of drug (4). Floating Drug Delivery is one of the method to enhance Gastric retention. The drug is released progressively from the swollen matrix, as in the case of conventional hydrophilic matrices (5, 6).

Another most effective method to deliver the insoluble drug at the targeted site is to preparation of Complexation with Nanosponges. A complex is a species of definite substrate-to-ligand stoichiometry that can exist both in solution and in solid state. The distinction between substrate and ligand is arbitrary, and is made solely for experimental convenience. Based on the type of chemical bonding, complexes can be classified into coordination and molecular complexes. The first form coordinate bond then present weak intermolecular force between substrate and ligand. Generally, pharmaceutical systems belong to the second group, being small molecule small molecule complexes, and/or inclusion complexes in which one molecule (host) possess a cavity into which it can admit a guest molecule (7). Nanosponges are prepared from β -Cyclodextrin as nanoporous materials for possible use as carriers for drug delivery. The structure of β -Cyclodextrin-based Nanosponges was principally investigated analyses. Sizes, morphology and toxicity were also examined. The capacity of the Nanosponges to incorporate molecules within their structure was evaluated using drugs with different structures and solubility. The Nanosponges were found capable of carrying both lipophilic and hydrophilic drugs and of improving the solubility of poorly water-soluble molecules (8). Nanosponges are a new class of material made of microscopic particles with cavities a few nanometers wide, characterized by the capacity to encapsulate a large variety of substances that can be transported through aqueous media. The efficacy of some pharmaceuticals adsorbed in the Nanosponges showed an activity 3–4 times higher and exhibited no detrimental side effects. Cyclodextrin based Nanosponges (of dexamethasone, flurbiprofen and Doxorubicin hydrochloride) demonstrated the ability to include either lipophilic or hydrophilic drugs and to release them slowly into physiological media. Thus Nanosponges can be used as a vessel for pharmaceutical principles to improve the aqueous solubility of lipophilic drugs, to protect degradable molecules and to formulate drug delivery systems for various administration routes beside the oral one. Beta Cyclodextrin (β CDs) have been the most widely used of all the Cyclodextrin (9, 10).

2. MATERIALS AND METHODS

2.1 Materials - Clarithromycin was gifted by Cipla pvt Ltd, Kurkumbh, India. Hydroxypropyl Methyl Cellulose K100 was also received as Gift Sample from Colorcon, Goa. Beta – Cyclodextrin was obtained from Gangwal Chemicals, Mumbai. TLC Plate and Diphenyl Carbonate was purchased from S.K. Enterprises. Dimethyl Sulfoxide, Dichloromethane, Acetone, Methanol, Benzene, Chloroform, Hexane, and acetonitrile was purchased from Research lab, Mumbai and all the solvent used were of Analytical Grade.

2.2 Synthesis of Nanosponges

2.2.1 Reaction

The reaction is a nucleophilic substitution where Cyclodextrin is reacted with Carbonyl compound of formula X-CO-X wherein X is Imidazolyl or -OR group in which R is C₁-C₄ alkyl (11). The reaction can be represented by the following scheme:



Where X is the carbonyl compound and n is the integer which can range within 3 to 6 depending upon the conditions used in the reaction which is shown in Figure 3.1.

2.2.2 Procedure

A round-bottomed flask equipped with a reflux condenser with thermometer. Weighed accurate quantities of beta CD and Diphenyl Carbonate (DPC) with DMSO as a solvent. The ratio was varied with 1:2, 1:4, and 1:8 equimolar mixture of beta CD: diphenyl carbonate. The reaction time was 12 h with conventional heating continuously with temperature maintain to 90⁰-100⁰C. The reaction mixture then added to cold water and product obtained was filtered and washed with water to remove excess amount of the beta CD. The product was Soxhlet extracted by ethanol to remove either impurities or unreacted diphenyl carbonate (11).

2.3 Optimization of Synthesized Product (Nanosponges)

The synthesized product was optimized to cross linker used in 1:2, 1:4, 1:8 (β- CD: Diphenyl Carbonate). The optimization for percentage yield is shown in Table 3.1.

2.4 Characterization of Synthesized Product (Nanosponges) (12, 13, 14)

1) Thin Layer Chromatography (TLC)

The TLC was used to evaluate the change in the R_f value of starting and product. Both samples dissolve into appropriate solvent and used for TLC. Chloroform is used as a mobile solvent. The TLC is observed under U.V. chamber. The photograph of TLC was shown in Figure 3.2 and R_f value are shown in Table 3.2.

2) FTIR Spectra

FTIR spectrophotometer was used for recording IR Spectrum of various samples by mixing the sample with dry potassium bromide and the sample was examined at transmission mode over a range 4000-400 cm⁻¹ for studying principle peaks using FTIR spectrophotometer (FTIR-8400, Shimadzu). The FTIR Spectrum of product obtained in synthesis and beta-Cd are shown in Table 3.3 and in Figure 3.3.

3) Differential Scanning Calorimetric analysis (DSC)

Thermogram of the NS was taken on a Mettler Toledo India Pvt. Ltd, Switzerland. (STAR^o SW 9.20). An empty aluminium pan was used as a reference. DSC measurements were performed at a heating rate of 10⁰C/min from 30⁰ to 400⁰C using aluminium sealed pan. During the measurement, the Sample was purged with nitrogen gas. DSC thermograms of Nanosponges are shown in Figure 3.4.

4) Powder X-ray diffraction (PXRD)

The PXRD spectra of samples were recorded using high power powder x-ray diffractometer (Ru-200B, Pune, India) with Cu as target filter having a voltage/current of 40 KV/40 mA at a scan speed of 4^o/min. The samples were analyzed at 2θ angle range of 5^o to 50^o. Step time was 0.5 seconds and time of acquisition was 1 h. The results are reported in Figure 3.5.

5) Nuclear Magnetic Resonance Spectroscopy

The C¹³ NMR of β- CD and NS were recorded in DMSO using as a solvent in NMR Varian-Mercury 30 MHz spectrometer and chemical shifts are given in Parts per million, downfield from tetramethylsilane (TMS) as an internal standard. C¹³ NMR of Nanosponges and beta- CD are shown in Figure 3.6 and Figure 3.7.

2.5 Phase solubility study

Phase solubility equilibrium plots were obtained for binary systems at 25 ⁰C in 0.1 N HCl. The studies were performed as per the procedure of Higuchi and Connors. Studies for binary system were carried out by adding excess amount of the drug to 10 ml of 0.1 N HCl containing increasing amounts of Nanosponges (0–2% w/v). The so formed series of suspensions were equilibrated on a mechanical shaker for 48 h. The equilibrated suspensions were then filtered through a membrane filter (0.45 lm) and absorbances observed by UV-spectrophotometer (13). The phase solubility diagram was constructed by plotting the dissolved clarithromycin concentration against the respective concentration of Nanosponges. The binding constant K_a was calculated from phase solubility diagram using its slope and intercept values (15). The phase solubility graph is shown in Figure 3.8. The stability constant was calculated by using equation 8.1.

$$K_{(a) 1:1} = \frac{\text{Slope}}{S_o (1 - \text{Slope})} M^{-1} \dots\dots\dots (2.1)$$

Where, S_o is intrinsic solubility of drug

M is molar concentration

Ka is apparent stability constant

Slope is calculated from regression equation

2.6 Preparation of binary systems

1) Drug incorporation (13)

Clarithromycin was dissolved in dichloromethane to form a solution. To this solution Nanosponges were added and triturated until the solvent evaporates. The drug and Nanosponges were added in a ratio of 1:1 by weight. The obtained solid dispersion was dried in an oven over night (at 50 °C at atmospheric pressure) to remove any traces of dichloromethane. The obtained powder was sieved through 60 mesh and used for further work.

2) Preparation of Physical mixture

Equimolar physical mixtures were prepared 1:1 by weight homogenously blending exactly weighed amounts of drug and Nanosponges mixture is obtained.

2.7 Characteristics of Complex

1) FT-IR spectroscopy study (16)

FT-IR spectra of selected inclusion complex, Nanosponges and drug were recorded on Jasco FT-IR spectrophotometer using KBr discs. The instrument was operated under dry air purge and the scans were collected at scanning speed 2 mm/sec with resolution of 4 cm⁻¹ over the region 4000-400 cm⁻¹. The scans were evaluated for presence of principle peaks of drug, shifting and masking of drug peaks due to Nanosponges and appearance of new peaks due to complexation. The FT-IR spectra of pure Clarithromycin, pure Nanosponges, physical mixture, and inclusion complex are shown in Figure 3.9.

2) Differential Scanning Colorimetry (DSC) (17)

The DSC study was carried out for pure Clarithromycin, pure Nanosponges, beta-CD, complex of Nanosponges and drug. The DSC patterns were recorded on a Mettler Toledo India Pvt. Ltd, Switzerland (STAR[®] SW 9.20). Each sample (2-4mg) was heated in crimped aluminum pans at a scanning rate of 10°C/min in an atmosphere of nitrogen using the range of 30-400°C. The temperature calibrations were performed periodically using indium as a standard. The DSC curves are shown in Figure 3.10.

3) Powder X-Ray Diffraction Study

The PXRD spectra of samples were recorded using high power powder x-ray diffractometer (Ru-200B, Pune, India) with Cu as target filter having a voltage/current of 40 KV/40 mA at a scan speed of 4°/min. The samples were analyzed at 2θ angle range of 5° to 50°. Step time was 0.5 seconds and time of acquisition was 1 h which is shown in Figure 3.11.

4) Scanning Electron Microscopy

The morphology of the surfaces of the drug loaded Nanosponges and Complex was examined by scanning electron microscopy (SEM). The dried sample was observed under different magnifications with an analytical scanning electron microscope (JEOL-JSM 6360A-Japan). SEM Images of Nanosponges and Complex is shown in the Figure 3.12 and 3.13 respectively.

2.8 Gastric Irritation Test on Rats

As Clarithromycin supposed to cause irritation to gastric mucosa. To determine whether the complex of Clarithromycin and Nanosponges causes gastric irritation or it prevents gastric irritation test was done as follows. Rats weighing about (200-250 g) are selected. They are divided into 3 groups each group contain three rats. One group is treated with control, second group is treated with standard Clarithromycin and another is treated with test i.e. complex. 75 mg of complex is given to test group by oral suspension for 15 days and to standard group is also given 37.5 mg of drug for 15 days. On 16th day all animals are fasted and their stomach is removed and examined for irritation after that histopathology was done (18). The photographs of the stomach tissue of all three groups were shown in Figure 3.14 and the histology reports were shown in Table 3.4.

2.9 Preparation of Preliminary Batches for selection of Polymer

2.9.1 Preparation of Granules

Granules required for controlled release tablet (CRT) formulations were prepared by Wet granulation technique. All the ingredients as given in Table 2.1 were weighed accurately and passed through sieve 30 mesh.

Isopropyl alcohol used as a granulating agent. Required quantity of complex, polymer and diluents were mixed thoroughly in a glass mortar. Sufficient quantity of granulating agent was sprinkled over the powder mixture to obtain enough cohesiveness. This cohesive mass was then sieved through 16 mesh to obtain granules. The granules were then dried at 60°C for 30 min. in hot air oven. Magnesium stearate and talc were finally added as glidant and lubricant mixed well with granules for 5 minutes (19). The prepared dried granules ready for compression was then evaluated for various granule properties as discussed below.

Table 2.1: Data for Composition of Preliminary Batches

Batches		H1	H2	H3	P1	P2	P3	P4	P5
Complex		200	200	200	200	200	200	200	200
HPMC	K4M	100	-	-	-	-	-	-	-
	K15M	-	100	-	-	-	-	-	-
	K100M	-	-	100	30	40	50	60	70
Lactose		50	50	50	120	110	100	90	80
Magnesium Stearate		5	5	5	5	5	5	5	5
Talc		5	5	5	5	5	5	5	5
NaHCO ₃		60	60	60	60	60	60	60	60
Citric Acid		15	15	15	15	15	15	15	15
Total		435	435	435	435	435	435	435	435

*All quantities in mg / tablet

2.9.2 Preparation of Control Release Tablet (CRT)

Different control release tablet (CRT) formulations were prepared by procedure reported in preparation of granules (section 2.9.1) using wet granulation technique. All the batches of tablets were prepared using rotary punch tablet compression machine (Karnavati Rimek minipress II) using 12 mm size punch. Prepared tablets were evaluated for various tablet properties.

2.9.3 Evaluation of CRT (Preliminary Batches)

1) *In vitro* dissolution study for Preliminary batches

In vitro dissolution study was performed using USP Dissolution Testing Apparatus II (Disso TDT 08L, Electrolab). The dissolution test was performed using 900 ml of 0.1 N HCL, at 37 ± 0.5°C and paddle speed was rotated at 50 rpm. A sample (5 ml) of the solution was withdrawn from the dissolution apparatus after every 1hr. for next 12 hrs, and the samples were replaced with fresh dissolution medium equilibrated at the same temperature to maintain the volume. The samples were filtered through Whatman filter paper no. 41. The samples collected were diluted taking dilution factor as 10 i.e. 1ml sample diluted with 2ml of sodium carbonate(20%), 3ml of FCR(2:1 diluted with water) and then 4ml of 0.1N HCL. Samples were then analyzed by UV spectrophotometer at 760 nm using UV spectrophotometer Jasco V-630. The % drug release data is reported in sec 2.9.4, Table 3.6. The graphical presentation of % drug released verses time interval is shown in Figure 3.15 and 3.16. Dissolution tests were performed in duplicate (20).

2.10 Factorial Design Batches (Experimental design) (8, 21,22)

A 3² factorial design was implemented for optimization of oral controlled release tablet. According to the model it contains two independent variables at three levels +1, 0 and -1 (Table 2.2). The translation of coded levels in actual units is enumerated in Table 2.3. According to the model total nine formulations are possible. The composition of different formulations is shown in Table 2.4.

A. Dependent variables

Y1 - Time taken for 50% drug release (%)

Y2 - Time taken for 85% drug release (%)

Y3 - Floating lag time (Seconds)

B. Independent variables:

X1 - HPMC K100M (%)

X2 - Citric Acid

Table 2.2: Factorial Design for Preparation of Batches.

Batch Code	Variable levels in Coded form	
	X ₁	X ₂
F1	+1	+1
F2	+1	0
F3	+1	-1
F4	0	+1
F5	0	0
F6	0	-1
F7	-1	+1
F8	-1	0
F9	-1	-1

Table 2.3: Translation of coded values in actual unit.

Independent Variable levels	Low (-1)	Medium (0)	High (+1)
X ₁ = Concentration of HPMC K100 M (%)	20	30	40
X ₂ = Concentration of Citric Acid (%)	5	7.5	10

Table 2.4: Combination batches by using HPMC K100M & Citric Acid in various concentrations according to 3² factorial designs.

Batch code	F1	F2	F3	F4	F5	F6	F7	F8	F9
Complex	500	500	500	500	500	500	500	500	500
HPMC K100M	100	100	100	150	150	150	200	200	200
Citric Acid	25	37.5	50	25	37.5	50	25	37.5	50
PVP K-30	60	60	60	60	60	60	60	60	60
Mg. Stearate	5	5	5	5	5	5	5	5	5
NaHCO ₃	80	80	80	80	80	80	80	80	80
Lactose	30	17.5	5	30	17.5	5	30	17.5	5
Total	800	800	800	850	850	850	900	900	900

*All quantities in mg/tablet

2.11 Preparation of Factorial Design Batches

2.11.1 Preparation of Granules

Preparation of Granules was done by Wet Granulation Technique using composition mention in Table 2.4. Procedure is mention in the section 2.9.1 was used (19).

2.11.2 Evaluation of Granules

The granule properties include bulk density; tap density, Hausner ratio, and Carr's index were determined using Tap density tester (TD 1025, Lab India).

1) Angle of Repose

Angle of repose has been defined as the maximum angle possible between the surface of pile of powder and horizontal plane. The angle of repose for the granules of each formulation was determined by the funnel method. The granules mass was allowed to flow out of the funnel orifice on a plane paper kept on the horizontal surface. This forms a pile of angle of granules on the paper. The angle of repose was calculated with the help of values of the base radius 'R' and pile height 'H' (23,24).

$$\tan \Theta = h / r \dots\dots\dots (2.2)$$

Where, Θ = angle of repose

h = height of the cone

r = Radius of the cone

Table 2.5: Relationship between angle of repose (Θ) and Flowability

Angle of Repose (Θ)	Flowability
< 20	Excellent
20 – 30	Good
30 – 34	Passable
> 40	Very Poor

2) Bulk Density

The bulk density was obtained by dividing the mass of a powder by the bulk volume in cm³ (23,24). It was calculated by using equation given below:

$$\rho_b = M / V_0 \dots\dots\dots (2.3)$$

Where, ρ_b = bulk density

M = weight of sample in grams

V_0 = Apparent unstirred volume

3) Tapped Density

The tapped density was obtained by dividing the mass of a powder by the tapped volume in cm³ (23,24).It was calculated by using equation given below:

$$\rho_t = M / V_f \dots\dots\dots (2.4)$$

Where, ρ_t = Tap density

M = weight of sample in grams

V_f = final Tap volume

4) Carr's Index

The Carr's index is determined from the tapped density and poured density (bulk density) as per the formula (Eq. (2.4)) given below (23,24).

$$\text{Carr's index (\%)} = \frac{\text{Tapped density} - \text{bulk density}}{\text{Tapped density}} \times 100 \dots\dots\dots (2.5)$$

Table 2.6: Relationship between % compressibility and flowability

% Compressibility	Flowability
5 – 15	Excellent
12 – 16	Good
18 – 21	Fair to Passable
23 – 35	Poor
33 – 38	Very Poor
> 40	Extremely Poor

5) Hausner ratio

Hausner ratio is determined from the ratio of tapped density to poured density using formula given below (23,24).

$$\text{Hausner ratio} = \frac{\text{Tapped density}}{\text{Poured density}} \dots\dots\dots (2.6)$$

The Angle of repose, Bulk density, Tap density, Carr's index and Hausner ratio are reported in sec 3.9.2, Table 3.6.

2.11.3 Preparation of Control Release Tablet (CRT)

Different control release tablet (CRT) formulations were prepared by wet granulation technique. All the batches of tablets were prepared using rotary punch tablet compression machine (Karnavati Rimek minipress II) using 12 mm size punch. Prepared tablets were evaluated for various tablet properties.

2.11.4 Evaluation of Control Release Tablet (CRT)

1) Weight Variation Test

I. P. procedure for uniformity of weight was followed. Twenty tablets were randomly selected from each batch and individually weighed. By using Electronic balance (Shimatzu). The average weight and standard deviation of twenty tablets were calculated .The average weight of tablet and its allowed percent deviation were shown in Table 2.7. Result for Weight Variation test is reported in section 3.9.4, Table 3.7 (25,26).

Table 2.7: Allowable limit for weight variation

Average weight of tablet (X mg)	Percentage deviation
$X \leq 80 \text{ mg}$	10 %
$80 < X < 250 \text{ mg}$	7.5 %
$X \geq 250 \text{ mg}$	5 %

2) Tablet hardness

The resistance of tablet to shipping or breakage, under conditions of storage, transportation and handling before usage depend on its hardness. The hardness of tablet of each formulation was measured by Pfizer hardness tester. The hardness was measured in terms of kg/cm². For each batch three tablets were tested. The average hardness and standard deviation is reported in section 3.9.4, Table 3.7 (25,26).

3) Friability

Friability is the measure of tablet strength. Roche friabilator (FT1020, Labindia) was used for testing the friability. Twenty tablets were weighed accurately and placed in the tumbling apparatus that revolves at 25 rpm dropping the tablets through a distance of six inches with each revolution. After 100 revolutions, the tablets were weighed and the % friability was calculated measured using the formula (Eq. (8.7)). The friability of different formulations is reported section 3.9.4, Table 3.7 (25,26).

$$\text{Friability} = \frac{\text{Initial weight of tablets} - \text{Final weight of tablets}}{\text{Initial weight of tablets}} \times 100 \dots\dots (2.7)$$

4) Thickness

Thickness of tablet is important for uniformity of tablet size. Thickness was measured using Vernier Calliper. It was determined by checking ten tablets from each formulation. Results for thickness are reported in section 3.9.4, Table 3.7 (25,26).

5) Drug Content

Five tablets were weighed individually, crushed to fine powder and about 100 mg of drug was dissolved in 0.1N HCl, the solution was filtered through 0.45μ membrane filter. The absorbance was measured at 760 nm after suitable dilution using F. C. Phenol reagent as a colour forming agent. Results for drug content section 3.9.4, Table 3.7 (25,26).

6) In vitro dissolution study for Factorial batches

In vitro dissolution study was performed using USP Dissolution Testing Apparatus II (Disso TDT 08L, Electrolab). The dissolution test was performed using 900 ml of 0.1 N HCL, at $37 \pm 0.5^{\circ}\text{C}$ and paddle speed was rotated at 100 rpm. A sample (5 ml) of the solution was withdrawn from the dissolution apparatus after every 1hr. for next 12 hrs, and the samples were replaced with fresh dissolution medium equilibrated at the same temperature to maintain the volume. The samples were filtered through Whatman filter paper no. 41. The samples collected were diluted taking dilution factor as 10 i.e. 1ml sample diluted with 2ml of sodium carbonate(20%), 3ml of FCR(2:1 diluted with water) and then 4ml of 0.1N HCL. Samples were then analyzed at 760 nm using UV spectrophotometer (Jasco V-630). The % drug release was calculated using disso software (PCP V3) and is reported in section 3.9.4, Table 3.8 and 3.9. The graphical presentation of % drug released verses time interval is shown in Figure 3.17, 3.18, and 3.19. The FLT for all factorial batches is shown in Figure 3.20. Dissolution tests were performed in triplicate (25,26).

2.12 Curve fitting

Release data were fitted to various mathematical models for describing the release mechanism from controlled release zero-order (Eq.2.8) [Lee, 1984] and Hixon Crowell.

$$M_t/M_{\infty} = k_k P t^n \dots\dots\dots (2.8)$$

Where, M_t/M_{∞} = fraction of drug released at time 't';

$k_k P$ = release rate constant;

n = the release exponent.

$$M_t = M_0 + k_0 \dots\dots\dots (2.9)$$

Where, M_t = the amount of drug released at time 't';

M_0 = the concentration of drug in the solution at $t=0$;

k_0 = the zero-order release constant.

$$M_t = k_H t^{1/2} \dots\dots\dots (2.10)$$

Where, M_t = the amount of drug release at time ' \sqrt{t} ';

k_H = the Higuchi release constant.

All curve fitting, simulation and plotting was carried out by using PCP disso software. The parameters for both zero order and Hixon Crowell models were shown in Table 3.11 (27,28,29).

2.13 Optimization of Factorial Design Batches

2.13.1 Regression analysis

The effect of formulation variables on the response variables were statistically evaluated by applying one way ANOVA at $P < 0.05$ level using a commercially available software package Design-Expert® version 7.1.6 (Stat-Ease Inc.) (8,22). To describe the response surface curvature, the design was evaluated by quadratic model, which bears the form of equation (Eq. 2.11).

$$Y = b_0 + b_1X_1 + b_2X_2 + b_3X_1X_2 + b_4X_1^2 + b_5X_2^2 \dots\dots\dots (2.11)$$

Where, Y is the response variable,

b_0 the constant,

$b_1, b_2 \dots b_5$ the regression coefficient,

X_1 and X_2 stand for the main effect,

X_1X_2 are the interaction terms, show how response changes when

Two factors are simultaneously changed.

1) Regression analysis for response Y_1

The effect of formulation variables on the response variables were statistically evaluated by applying one way ANOVA at $P < 0.05$ level using a commercially available software package Design-Expert® version 7.1.6 (Stat-Ease Inc.) (8, 22).

2) Regression analysis for response Y_2

The effect of formulation variables on the response variables were statistically evaluated by applying one way ANOVA at $P < 0.05$ level using a commercially available software package Design-Expert® version 7.1.6 (Stat-Ease Inc.) (8, 22).

3) Regression analysis for response Y_3

The effect of formulation variables on the response variables were statistically evaluated by applying one way ANOVA at $P < 0.05$ level using a commercially available software package Design-Expert® version 7.1.6 (Stat-Ease Inc.) (8, 22).

4) ANOVA, Pure Error and Lack of Fit

The results for ANOVA, pure error and lack of fit were discussed in section 3.11.1.

2.14 Studies on Final Formulation

1) Water uptake studies

The rate of test medium uptake by the polymer was determined by equilibrium weight gain method similar to Fantasies and Vlachos (2000). The study was carried out in the USP dissolution apparatus II. The FCRT Tablet was accurately weighed, placed in dissolution baskets, and immersed in 0.1 N HCl solution maintained at $37 \pm 0.5^\circ\text{C}$ in the dissolution vessel. At regular intervals, the pre-weighed basket-matrix system was withdrawn from the dissolution vessel, lightly blotted with a tissue paper to remove excess test liquid and re-weighed. The percent water uptake, i.e., degree of swelling due to absorbed test liquid, was estimated at each time point using formula given below:

$$\% \text{ Water uptake} = \frac{(W_t - W_i)}{W_i} \times 100 \dots\dots\dots (2.12).$$

Where, W_t is the weight of the swollen matrix at time, t , W_i is the initial weight of the tablet. The % swelling or water uptake data is reported in section 3.12 in Table 3.13 (26).

2) Comparison of In vitro release study of marketed formulation with capsule fills with complex and formulated tablet

The in vitro profile of optimized formulation and complex were compared with marketed SR tablet (Biaxin-500). *In vitro* dissolution study was performed using USP Dissolution Testing Apparatus II (Disso TDT 08L, Electrolab). The dissolution test was performed using 900 ml of 0.1 N HCL, at $37 \pm 0.5^\circ\text{C}$ and paddle speed was rotated at 100 rpm. A sample (5 ml) of the solution was withdrawn from the dissolution apparatus after every 1hr. for next 12 hrs, and the samples were replaced with fresh dissolution medium equilibrated at the same temperature to maintain the volume. The samples were filtered through Whatman filter paper no. 41. The samples collected were diluted taking dilution factor as 10 i.e. 1ml sample diluted with 2ml of sodium carbonate(20%), 3ml of FCR(2:1 diluted with water) and then 4ml of 0.1N HCL. Samples were then analysed at 760 nm using UV spectrophotometer (Jasco V-630). The % drug release was calculated using disso software (PCP V3) and is reported in section 3.12 (Table 3.14). The graphical presentation of % drug released verses time interval is shown in Figure 3.27 (25,26).

3) Optimization

A numerical optimization technique by the desirability approach was used to generate the optimum settings for formulation. The process was optimized for dependent variables Y_1 - Y_3 . The optimized formula arrived by targeting the Y_2 at 650 minute, Y_1 was kept at range 360-400 min., Y_3 also kept at range 16-62 sec. Results were discussed in section 3.12 (30)

3. RESULTS AND DISCUSSIONS

3.1 Synthesis of Nanosponges

3.1.1 Reaction

Nanosponges was synthesized and purified by ethanol in Soxhlet apparatus. The carbonylation of β -CD and DPC occurred and characterised by various techniques. The reaction is represented in Figure 3.1.

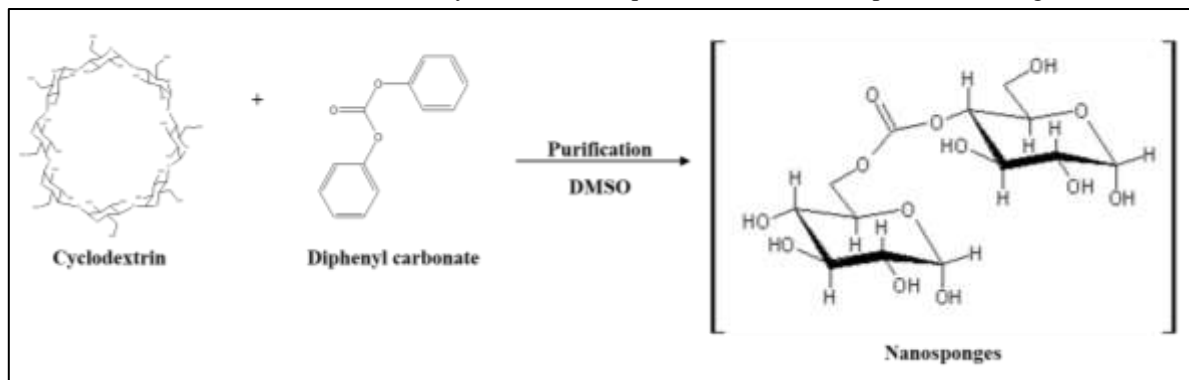


Figure 3.1: Nucleophilic reactions of beta-CD and Diphenyl Carbonate.

3.1.2 Preparation of Nanosponges

Preparation of Nanosponges was carried out according to the procedure mention in the section 2.2.2.

3.2 Optimization of Synthesized Product (Nanosponges)

Reaction was optimised to various concentrations of cross linker. This reaction was optimised in terms of percentage yield. The obtained yield was 55%, 69% and 70% by keeping β -CD: DPC in the ratio 1:2, 1:4 and 1:8. The reactions were carried out batch 1, 2 & 3 for these proportions respectively. The yield obtained in batch 2 and 3 were almost same so combination used in the batch number 2 was finally selected for Nanosponges synthesis.

Table 3.1: Optimization of Synthetic procedure

Batches	BCD:DPC ratio	Energy type	Yield %
1	1:2	Conventional Heating	55
2	1:4	Conventional Heating	69
3	1:8	Conventional Heating	70

3.3 Characterization of Synthesized Product (Nanosponges)

Table 3.2: Characteristics of Nanosponges

Parameters	Characteristics
Colour, State	White, Solid
TLC	Chloroform; $R_f = 0.23$
IR (KBr) cm^{-1}	1775 / cm (C=O group)
DSC	Degradation occurs after 300 $^{\circ}\text{C}$

1) Thin Layer Chromatography (TLC)

TLC showed clear separation between starting material and product. As there was complete consumption of starting material β -CD absence of spot in product the formation of product was confirmed.

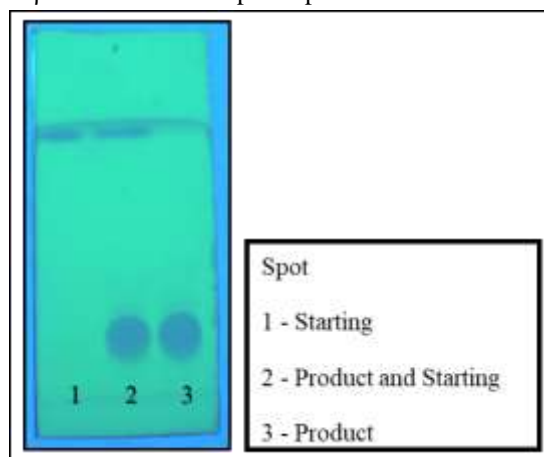


Figure 3.2: TLC Photograph

2) FTIR Spectra

The FTIR spectra of Nanosponges and β -CD were portrayed in Figure 3.3. FTIR spectra of β -CD was characterized by 2925 cm^{-1} (C-H asym./sym. stretch), peak at 1646 cm^{-1} (C=C stretching), 1415 (C-H bend) cm^{-1} and a band with distinct peaks in the region between 1200 and 1000 cm^{-1} . The FTIR spectra of Nanosponges exhibited distinct peaks at 2926 cm^{-1} (C-H asym. /sym. stretch), 1638 cm^{-1} (C=C stretching), 1775 cm^{-1} (Aryl Carbonate), 1026 cm^{-1} (Primary alcohol, C-O stretch), 1413 cm^{-1} (C-H bend) confirming the earlier report. The appearance of peak at 1775 cm^{-1} clearly indicated the carbonylation of β -CD which is shown in Table 3.3. The peak at 1775 / cm confirmed presence of the carbonyl group in the structure of Nanosponges.

Table 3.3: IR peak of β -CD and NS

Group	Beta-CD	Nanosponges
C-H asym./sym. stretch	2925	2926
C=C stretching	1646	1638
Aryl Carbonate	absent	1775
Primary alcohol, C-O stretch	1027	1026
C-H bend	1415	1413

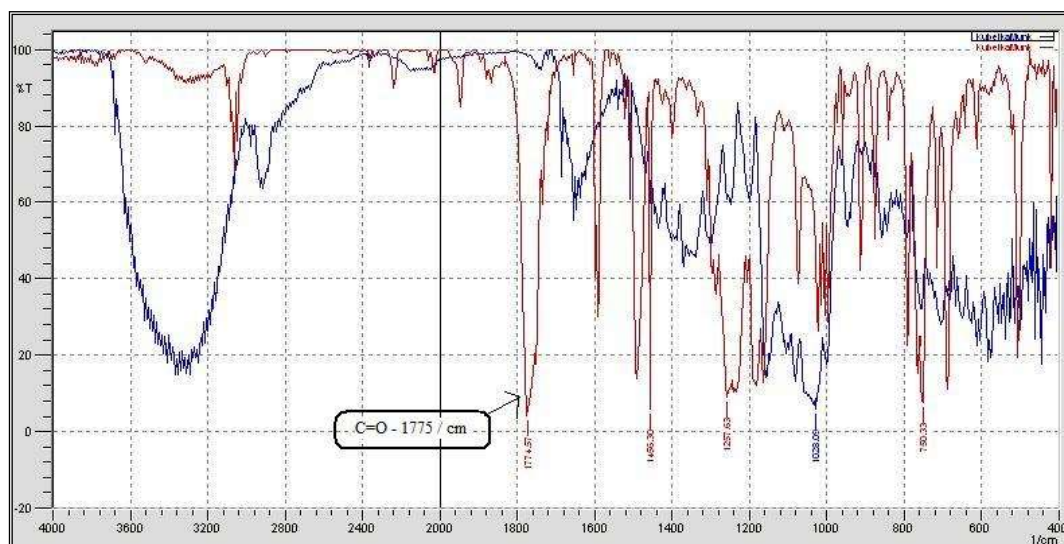


Figure 3.3: FTIR spectra of Nanosponges and Beta-CD

3) DSC Graph

Thermal degradation of Nanosponges is reported after 300°C. The absence of endotherm below 300°C in the present study it was confirmed that the Nanosponges was synthesized. The graph of β -CD and Nanosponges are shown in Figure 3.4.

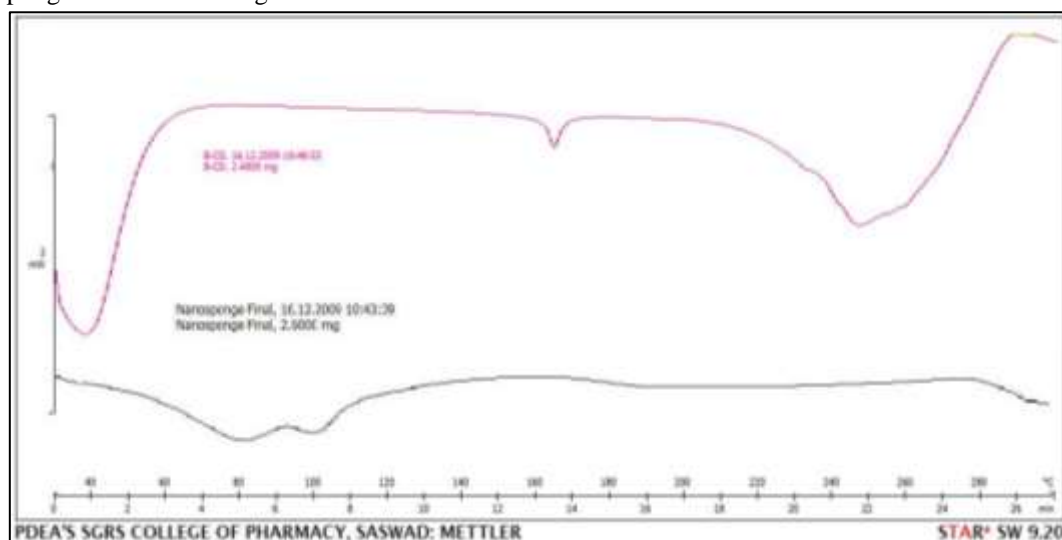


Figure 3.4: DSC graph of Nanosponges and Beta-CD.

4) X-Ray Powder Diffraction (XRPD) Analysis

Formation of Nanosponges was confirmed by XRPD spectra. As shown in Figure 3.5, the number of peaks reduced in Nanosponges as compared to β -CD with peak broadening. This clearly indicated formation of poorly crystalline Nanosponges.

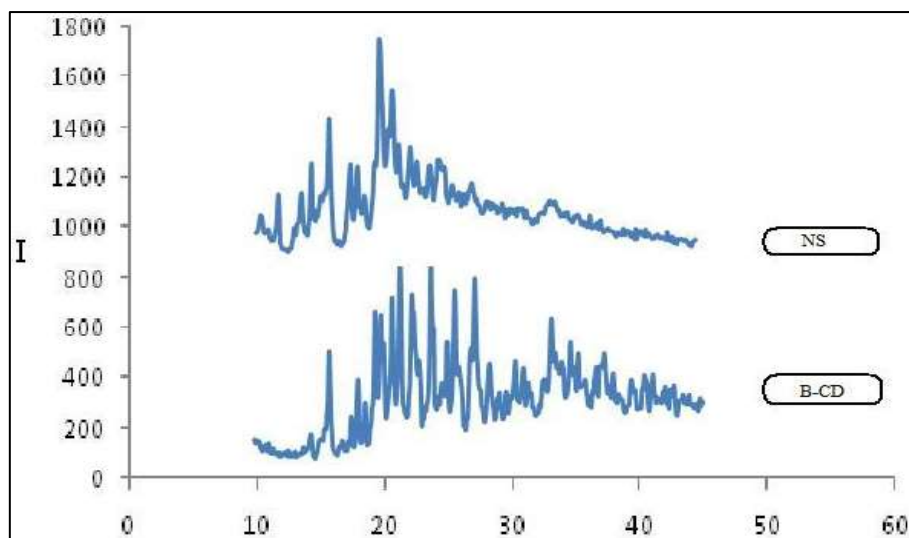


Figure 3.5: PXRD of Nanosponges and Beta-CD

5) NMR

The C^{13} NMR of Nanosponges and β -CD were shown in Figure 3.6 and 3.7 respectively. NMR of NS shows various peaks at different δ - values. The carbonyl bridge between two β -CD showed the peak at 155.5 δ value which confirmed the Nanosponges was synthesized.

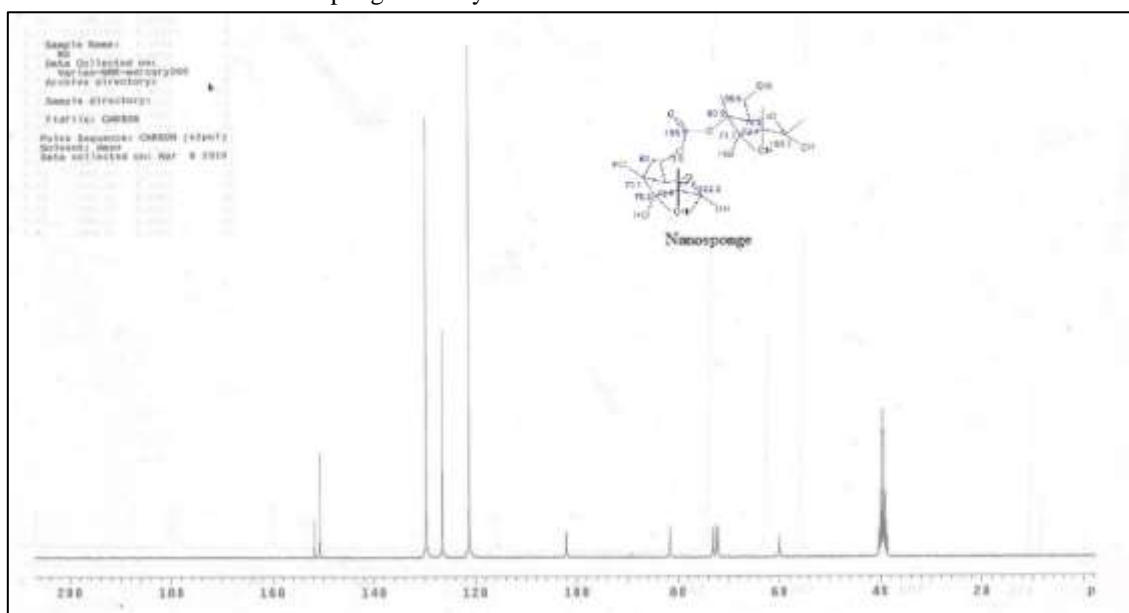


Figure 3.6: NMR of Nanosponges

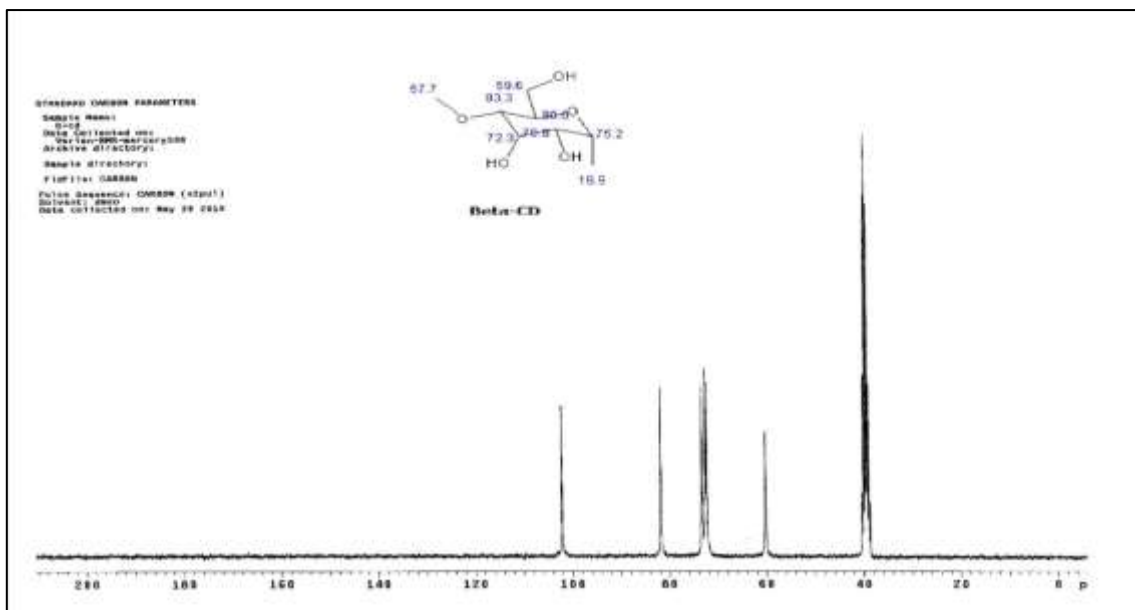


Figure 3.7: NMR of Beta-CD

3.4 Phase solubility studies

The phase solubility studies conducted at 25°C indicated that, solubility of Clarithromycin increased linearly ($R^2=0.961$) as a function of Nanosponges concentration, as shown in Figure 3.8. As apparent solubility of Clarithromycin increased linearly with Nanosponges concentration over the entire concentration range studied; the phase solubility diagram was classified as A_L type. The slope and intercept of the curve were found to be 0.0003047 and 28.21×10^{-8} M, respectively. The stability constant computed from the slope and intercept of the phase solubility diagram was found to be 1080.12 M^{-1} . The value of stability constant obtained indicated a labile association of Clarithromycin and Nanosponges. The solubility of clarithromycin was significantly increased with Nanosponges.

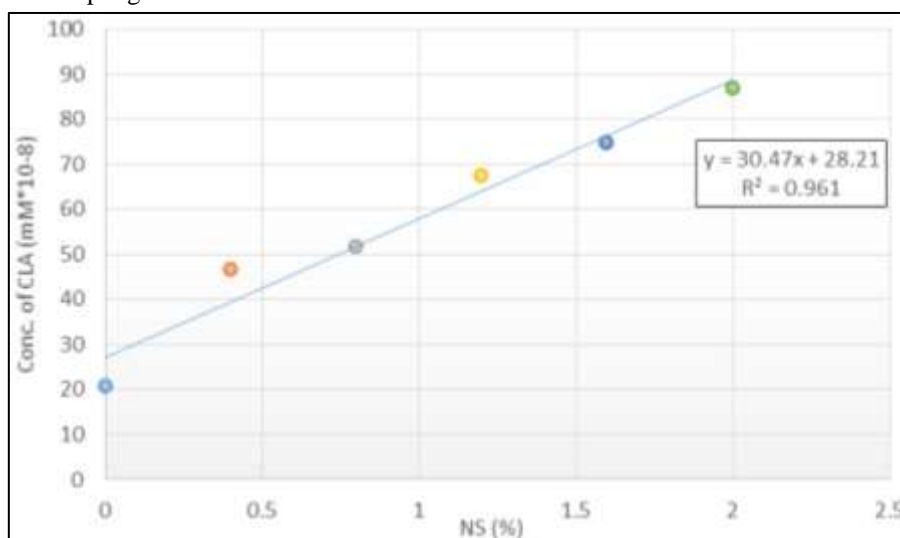


Figure 3.8: Phase solubility study of drug and Nanosponges in 0.1 N HCL

3.5 Preparation of binary systems

Drug Incorporation and Preparation of Physical Mixture was done using the procedure mention in the section 2.6.

3.6 Characteristics of Complex

1) FT-IR spectroscopy study

The FTIR spectra of Nanosponges, Clarithromycin and complex were portrayed in Figure 3.9. The FTIR studies showed that there are weak interactions between NS and CLA that were evident from broadenings and disappearance of the drug peak in case of complexes.

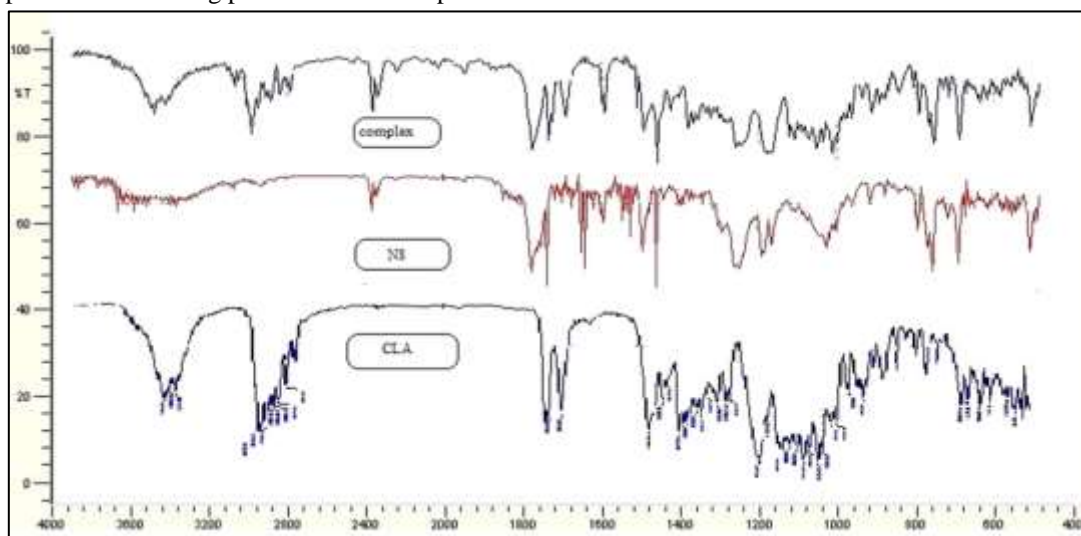


Figure 3.9: FTIR spectra of Nanosponges, Clarithromycin and complex

2) DSC study

The thermal analysis graphs of pure Clarithromycin, complex and Nanosponges are shown in Figure 3.10. Area of enthalpies of the drug progressively decreased in following order Plain drug, Nanosponges, drug Nanosponges PM, and drug Nanosponges solid dispersions.

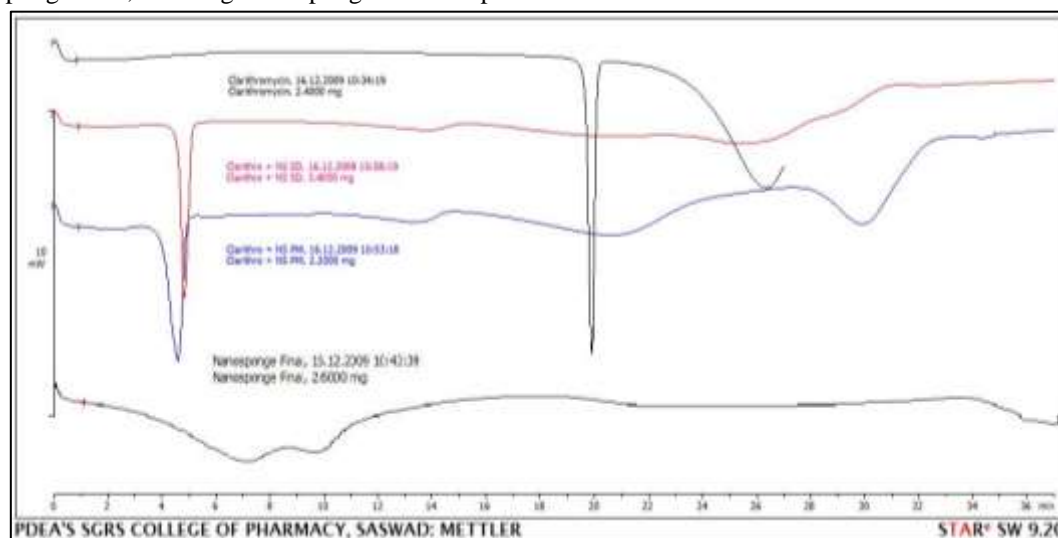


Figure 3.10: DSC graph of pure CLA, complex and Nanosponges

These could be due to change in the state of the drug from crystalline to amorphous. Thus the energy required to melt the drug is reduced i.e. enthalpy reduced. DSC thermograms of the complexes did not show the melting peak corresponding to drug fusion. This indicates that the drug is no longer crystalline and confirms its interaction with NS structure. On the contrary, the binary P.M. presented the melting peak of the drug indicating that CLA maintained its original crystallinity in the P.M. due to a lack of interaction.

3) PXRD Study

The complexation between Clarithromycin and Nanosponges was also confirmed by PXRD. As shown in the PXRD pattern of drug loaded Nanosponges (Figure 3.11), number of peaks of Clarithromycin were reduced. Also, no perfect coincidence was found in PXRD patterns of CLA and CLA- NS complex indicating

the formation of a new ordered phase which might be responsible for increase in the solubility of CLA. Thus it can be predicted that the solubility of CLA is due to its molecular dispersion i.e. complexation with Nanosponges.

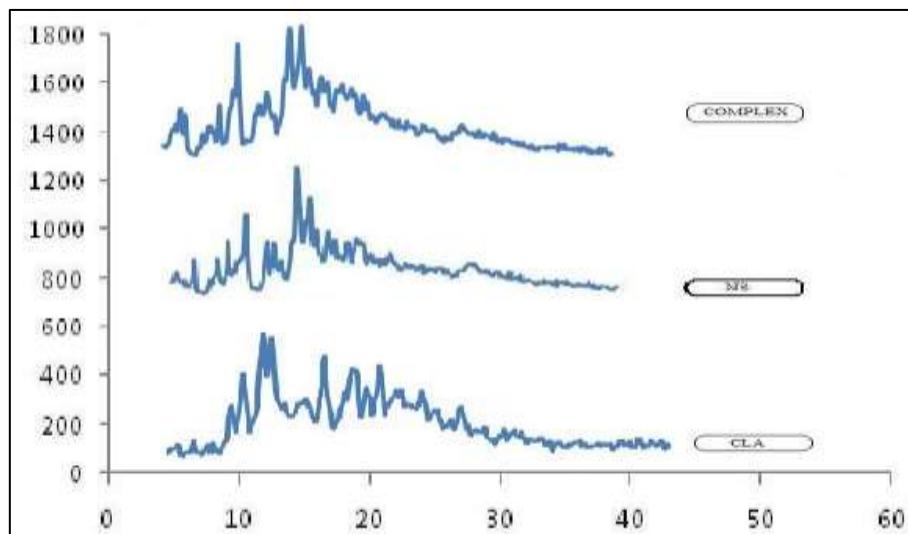


Figure 3.11: PXRD of CLA, NS and Complex

4) Scanning Electron Microscopy

SEM images of NS and complex were shown in Figure 3.12 and 3.13. These images revealed striking difference between the microstructure of plain NS and complex of NS and CLA. Plain NS exhibited highly porous structure while complex was compacted. The SEM of complex confirmed drug loading in the NS as the surface is smooth as compared to porous surface of plain NS.

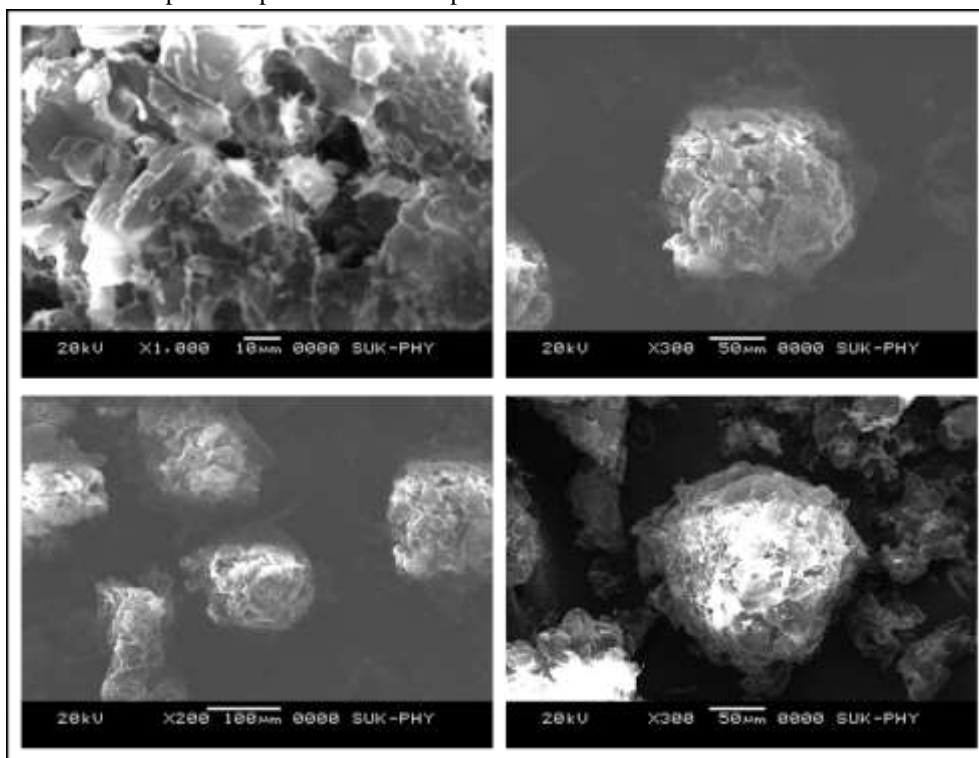


Figure 3.12: SEM Images of NS

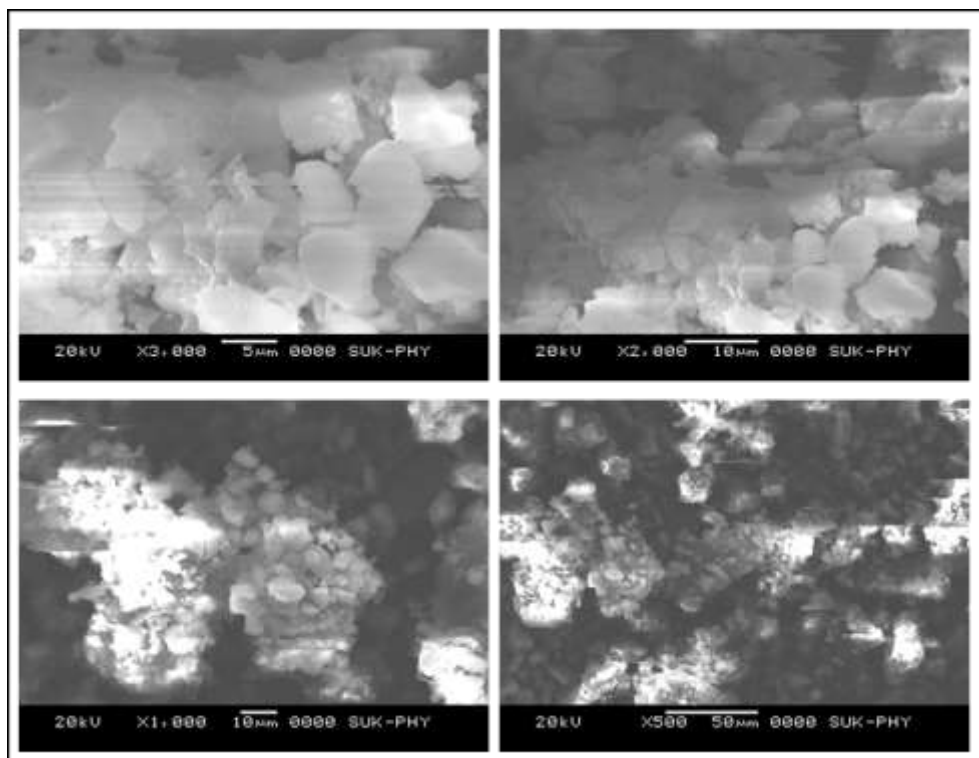


Figure 3.13: SEM Images of Complex

3.7 Gastric Irritation Test

Histopathological examination - Rats treated with Plain drug showed marked mucosal damage. Lesion formation was found to be 75% in these cases whereas in rats which received complex showed reduced gastric lesions as compared with plain drug photographs are shown in Figure 3.14. The results are shown in Table 3.4. From the results it was concluded that severity of ulceration was lowered in test groups than standard group.

Table 3.4: Histopathological report of stomach tissues

Group	Control (A)	Standard(B)	Test (C)
Congestion	00	++	+
Necrosis	00	+++	+
Cellular infiltration	00	++	+
Edema	00	++	+
Ulceration	00	+++	+
Hemorrhages	00	+++	+
Note: 0 indicates no abnormality detected, + indicates pathological changes up to less than 25 %, ++ indicates Pathological changes up to less than 50 % , +++ indicates Pathological changes up to less 75 %, ++++ indicates Pathological changes up to more than 75 %			

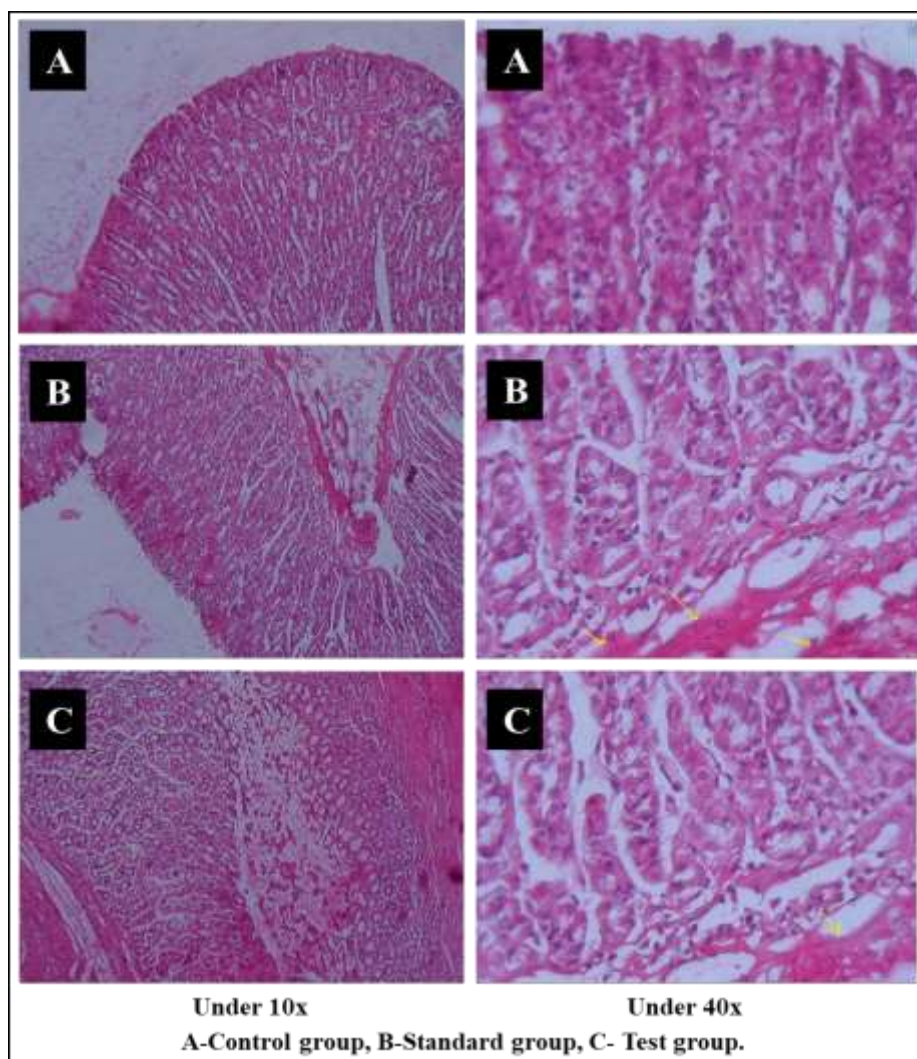


Figure 3.14: Photographs of stomach Tissue

3.8 Preparation of Preliminary Batches for selection of Polymer

3.8.1 Preparation of Granules

Granules were prepared according to the Procedure mentioned in the section 2.9.1.

3.8.2 Preparation of Control Release Tablet (CRT)

Control release tablet of clarithromycin was prepared according to the procedure mentioned in the section 2.9.2.

3.8.3 Evaluation of CRT (Preliminary Batches)

1) *In vitro* dissolution study for Preliminary batches

In vitro dissolution study was performed using USP Dissolution Testing procedure and the result are mention in the Table 3.5. Figure 3.15 shows % Drug Release of Clarithromycin from batches H1-H3. H1 contains HPMC K4M 100 mg alone and released 50% of the drug in 3 hrs. H2 contains HPMC K15M 100 mg alone and released 50% of the drug in 5 hrs. H3 contains HPMC K100M 100 mg alone and released 50% of the drug in 9 hrs which was attributed to its high viscosity as compared to K4M & K15M (Table 3.5). Hence HPMC K100M was used in further studies of preliminary formulations. From the discussion data for batches H1-H3 it was concluded that HPMC K100M showed highest release retarding property.

Table 3.5: *In vitro* dissolution study of preliminary batches in 0.1N HCL

Time (h)	Drug Release %							
	H1	H2	H3	P1	P2	P3	P4	P5
0	0.000	0.000	0.00	0.00	0.00	0.00	0.00	0.00
1	21.76	13.46	01.32	23.12	16.64	08.97	07.54	05.06

2	44.54	23.12	11.65	32.63	22.87	16.86	14.63	18.47
3	57.89	39.54	19.87	43.78	39.56	23.83	21.36	27.90
4	65.43	42.45	24.75	51.75	45.21	35.19	33.69	33.17
5	78.63	58.37	31.21	63.71	53.87	41.09	42.14	35.68
6	89.12	67.84	37.43	72.05	63.97	50.59	47.96	44.01
7	95.27	75.28	41.65	79.24	73.56	59.93	52.41	53.14
8	99.12	82.45	49.08	87.41	81.43	68.48	61.37	58.45
9	99.13	85.63	55.60	94.83	89.54	78.12	68.57	61.45
10	99.19	89.91	57.98	98.67	94.67	82.63	79.63	62.98
11	99.20	92.59	59.12	99.32	99.67	96.94	89.31	75.32
12	99.20	97.61	61.78	99.32	99.68	99.72	95.78	79.92

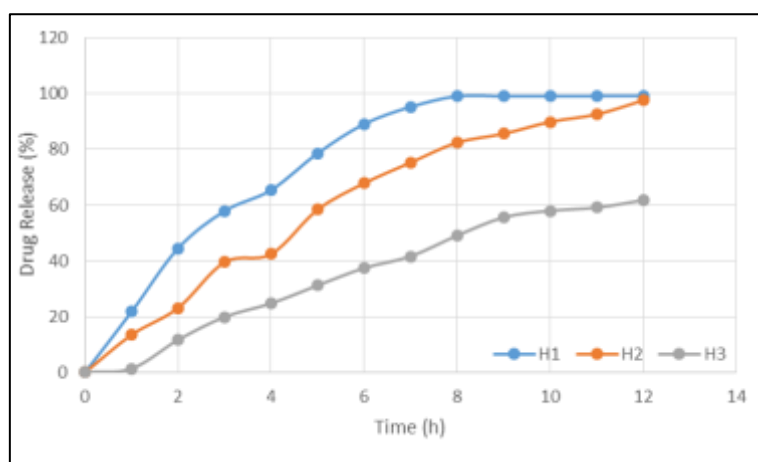


Figure 3.15: % Cumulative Drug release from preliminary Batches H1-H3 in 0.1N HCL

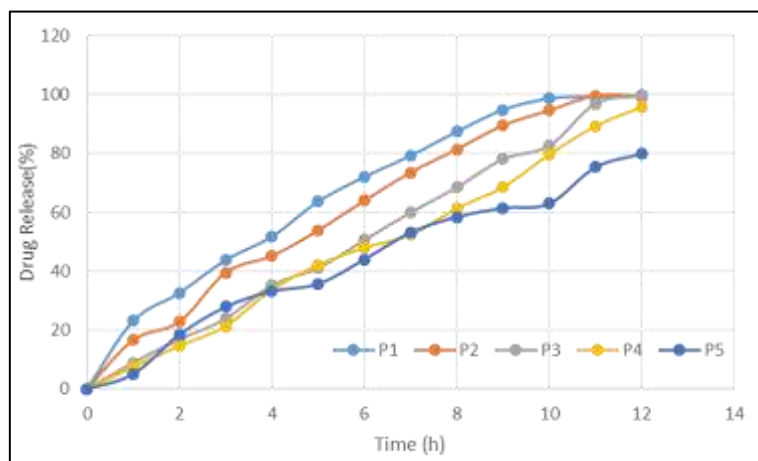


Figure 3.16: % Cumulative Drug release from preliminary Batches P1-P5 in 0.1N HCL

Figure 3.16 shows, Clarithromycin release from batches P1, P2, P3, P4 and P5 contained HPMC K100M alone in increasing concentration from 30, 40, 50, 60 and 70mg /tablet respectively. Preliminary Batches P1, P2, P3, P4 and P5 released its 50% drug content in 230 min., 282min., 355min., 409min. and 407min respectively. As the concentration of HPMC K100M increased the release rate decreased. From the results it was clear that optimized release was from batch P3 and P4 containing 50mg & 60 mg of HPMC K100M per tablet (25% w/w & 30% w/w per tablet). To evaluate the effect of concentration of HPMC K100M and citric acid on in vitro dissolution pattern of drug a statistical model of 3^2 full factorial designs was applied. Hence for further study 20, 30 and 40 % of the HPMC and Citric acid used in 5, 7.5 and 10% used in 3^2 Factorial design.

3.9 Preparation of Factorial Design Batches

3.9.1 Preparation of Granules

Preparation of Granules was done by Wet Granulation Technique using composition mention in Table 2.4.

3.9.2 Evaluation of Granules

The dried granules were evaluated for Angle of repose, Bulk Density, Tapped Density, Carr's index and Hausner's Ratio and the data is shown in Table 3.6.

Table 3.6: Data for Granules properties prepared for Factorial Design Batches

Batch	Angle of Repose	Tapped Density (g/ml)	Bulk Density (g/ml)	Carr's Index %	Hausner ratio
F1	32.80±0.11	0.878±0.05	0.754±0.07	15.09±0.06	0.858±0.05
F2	30.06±0.08	0.899±0.09	0.781±0.09	15.10±0.05	0.86±0.07
F3	31.33±0.16	0.930±0.11	0.784±0.09	15.68±0.09	0.843±0.05
F4	32.97±0.12	0.836±0.08	0.735±0.12	14.52±0.06	0.879±0.09
F5	30.68±0.09	0.891±0.09	0.764±0.14	16.62±0.13	0.857±0.06
F6	32.16±0.11	0.902±0.08	0.782±0.08	15.34±0.08	0.866±0.09
F7	31.83±0.12	0.883±0.13	0.767±0.09	15.12±0.11	0.868±0.07
F8	31.62±0.09	0.895±0.09	0.781±0.12	14.59±0.05	0.872±0.05
F9	30.85±0.13	0.910±0.11	0.792±0.15	14.89±0.05	0.8703±0.07

3.9.3 Preparation of Control Release Tablet (CRT)

Different control release tablet (CRT) formulations were prepared by wet granulation technique. All the batches of tablets were prepared using rotary punch tablet compression machine (Karnavati Rimek minipress II) using 12 mm size punch. Prepared tablets were evaluated for various tablet properties.

3.9.4 Evaluation of compressed tablets:

The Tablets from each batch of factorial design were evaluated for Uniformity in Average weight, Thickness, Hardness, Friability, Drug content and result are reported in Table 3.7.

1) Weight Variation Test

The results indicated was no weight variation as per I.P limit. The average weight of the tablet was found to be in range.

2) Tablet Hardness

The hardness of the tablets was found in the range of 5.2 to 5.8 kg/cm². The results indicated that the tablets having enough hardness and sufficient strength.

3) Friability

Percentage weight loss was measured and found to be less than 1%. As all the batches were within the pharmacopoeial limit (F< 1%).

4) Thickness

Size of tablets was found to be 12 mm in diameter and thickness of tablet was found to range from 3.8 to 4.9 mm.

5) Drug Content

All the formulations complied with the uniformity of drug content test for tablets. The drug content in all the batches of Clarithromycin floating tablets was in the range of 95 to 105%. This ensured good uniformity of the drug content in the tablets

Table 3.7: Data for Tablet properties from Factorial Batches.

Formulation	Average Weight in mg (n=5)	Hardness in Kg/cm ² (n=2)	Thickness in mm (n=2)	Friability in %	Drug Content in % (n=3)
F1	800.03 ±0.64	5.5 ± 0.3	3.9 ± 0.07	0.28	103.03 ±0.31
F2	800.14 ±0.91	5.2 ± 0.6	3.8 ± 0.05	0.32	97.86 ±0.70

F3	800.06 ±1.02	5.5 ± 0.2	3.9 ± 0.11	0.23	96.27 ±1.02
F4	850.52 ±0.83	5.8 ± 0.2	4.5 ± 0.08	0.22	99.61 ±0.73
F5	850.05 ±0.61	5.5 ± 0.4	4.4 ± 0.27	0.33	98.83 ±0.41
F6	850.12 ±0.90	5.8 ± 0.3	4.4 ± 0.13	0.31	104.83 ±1.13
F7	900.05 ±1.24	5.2 ± 0.2	4.9 ± 0.15	0.29	99.94 ±0.42
F8	900.79 ±1.61	5.5 ± 0.2	4.8 ± 0.09	0.33	102.02 ±1.1
F9	900.02 ±1.02	5.8 ± 0.4	4.9 ± 0.07	0.28	99.57 ±0.7

6) In-Vitro Drug release for Factorial batches F1-F9

The matrix tablets displayed a controlled drug release that depended on the total polymer level and citric acid level as well as presence of the drug either in the free or the complexes form. The actual values of % cumulative Drug release of factorial batches F1- F9 are reported in Table 3.8 and Drug release profile of factorial batches F1- F9 are shown in Figure 3.17, 3.18 and 3.19. The values of the release at of T₅₀, T₈₅ and floating lag time are shown in Table 3.9. At lower concentration of polymer % release was more. As concentration of polymer increases the release rate was retarded. The drug release at the end of 12h from the matrix tablets containing Clarithromycin was found to range from 68.15 ± 1.56 to 98.90 ± 1.09 %.

Table 3.8: Dissolution data for Factorial Batches F1-F9 in 0.1N HCL

Time (h)	% Drug Release (n=3)								
	F1	F2	F3	F4	F5	F6	F7	F8	F9
0	0	0	0	0	0	0	0	0	0
1	15.73±1.47	18.68±1.21	21.12±0.52	8.93±1.25	9.85±2.09	11.25±0.37	4.32±1.23	3.95±1.05	4.06±2.09
2	22.15±1.21	29.48±1.93	31.24±1.45	17.84±1.82	11.52±1.27	18.03±1.29	12.49±1.82	16.74±1.25	17.47±2.64
3	34.12±2.67	41.34±1.37	43.49±1.96	23.71±1.57	29.45±1.23	26.87±1.42	17.89±1.62	23.51±2.34	26.9±2.09
4	43.47±1.82	54.93±2.35	57.85±2.31	31.24±2.09	33.81±1.85	37.09±1.65	27.84±1.07	29.21±1.21	32.17±1.84
5	55.42±0.89	58.71±1.83	62.37±1.21	39.71±2.26	42.9±1.07	41.87±1.97	34.16±2.48	30.42±2.14	35.68±1.96
6	61.53±2.41	67.43±1.02	71.81±2.94	43.88±2.67	49.85±1.63	51.74±1.21	38.12±2.09	35.2±1.34	44.03±1.41
7	69.85±1.79	73.84±2.19	79.8±1.57	52.79±1.21	54.61±1.83	56.41±1.32	48.02±2.15	39.41±1.82	52.14±1.82
8	77.6±1.25	79.3±1.07	87.92±1.89	61.82±1.05	63.89±2.09	66.83±1.82	54.56±1.54	48.19±1.52	59.45±1.09
9	85.87±2.09	87.85±2.26	89.8±1.62	69.84±0.59	71.33±1.78	78.41±2.58	62.14±1.71	51.54±1.45	62.64±1.07
10	91.93±1.19	92.73±2.09	94.37±1.97	78.73±0.54	79.84±1.27	81.3±1.67	63.48±1.21	57.58±2.09	63.78±1.48
11	97.3±2.36	97.8±1.27	98.3±1.58	84.67±1.93	87.02±1.82	89.56±2.09	67.73±2.69	63.58±1.26	74.62±1.21
12	98.41±1.63	98.81±2.51	98.9±1.09	94.79±1.37	95.82±2.48	95.87±2.50	68.15±1.56	72.8±1.17	79.5±1.86

The Factorial batches F1, F2 & F3 which had lower total polymer level, were found to release 98.41 ± 1.63 %, 98.81±2.51% and 98.9±1.09 of the drug by the end of 12 h respectively which is shown in Figure 3.17. The Factorial batches F4, F5 & F6 which had medium level of polymer exhibited better drug release as they released 94.79 ± 1.37% ,95.82 ± 2.48 % & 95.87 ± 2.50 % respectively of the drug at the end of 12 h of dissolution , which is shown in Figure 3.18.

The Factorial batches F7, F8 & F9 which had higher polymer level, exhibited an impeded drug release as they released 68.15 ± 1.56 %, 72.8 ± 1.17 % & 79.5 ± 1.86 % respectively of the drug at the end of 12 h of dissolution which is shown in Figure 3.19. An increase in the polymer i.e. HPMC K100M concentration caused the increase in viscosity of diffusion layer and also the formation of gel layer serve as longer diffusional path for drug this might had decreased the effective diffusion coefficient of drug and therefore there was reduction in drug release rate.

Formulation F4, F5 & F6 containing medium polymer level exhibit better drug release in 12 h. So by considering release profile from all factorial batches batch F5 which containing 30% of HPMC K100M and 7.5% citric acid. Formulation F4 & F6 also release nearly same but medium level concentration of citric acid containing F5 was selected. These formulations contain drug in the complexes form exhibited a controlled and complete drug release during the dissolution period due to improved drug solubility.

The 3^2 factorial designs, preliminary trials were carried out to obtain the optimized concentration of polymer. The second variable citric acid was chosen because of its significant effect on the FLT and the drug release profile. All the nine batches showed variable release profile. The polymer concentration being constant and an increase in the concentration of citric acid the dissolution profile was improved significantly. The 3^2 full factorial design was selected to study the effect of independent variables HPMC K100M (X1) and Citric Acid (X2) on dependent variables t50%, t85% and floating lag time (Figure 3.20).

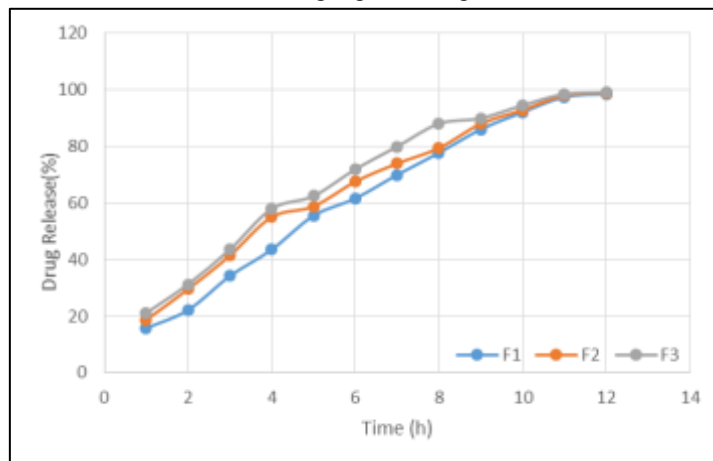


Figure 3.17: % Cumulative Drug release from factorial batches F1-F3

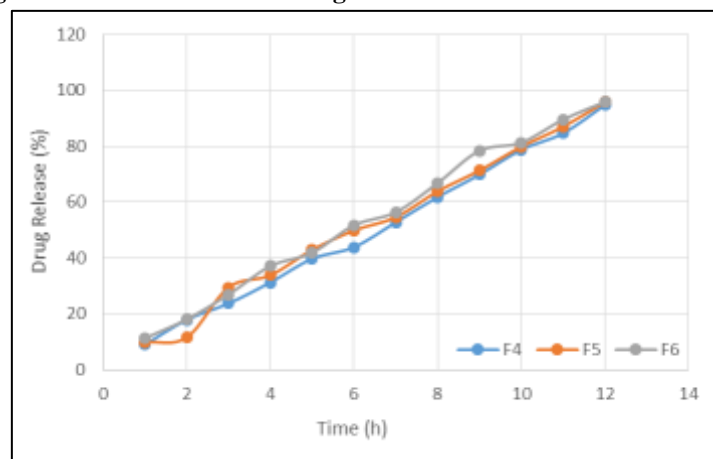


Figure 3.18: % Cumulative Drug release from factorial batches F4-F6

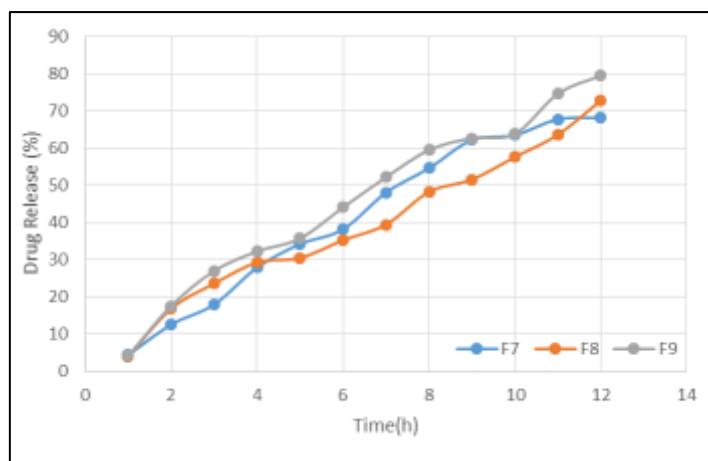


Figure 3.19: % Cumulative Drug release from factorial batches F7-F9

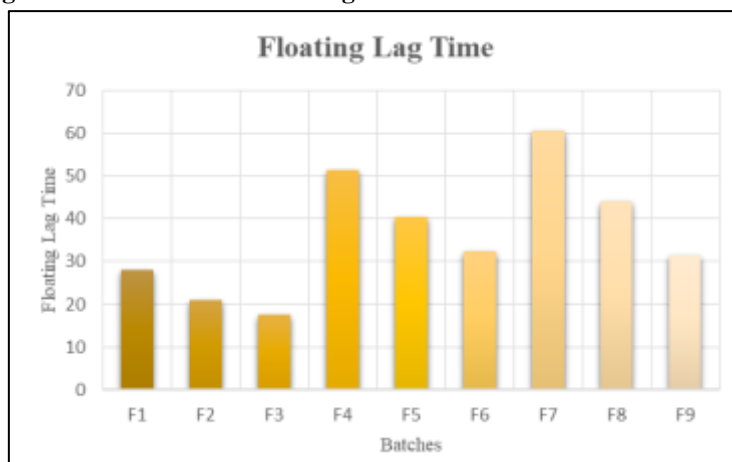


Figure 3.20: Floating Lag Time of Factorial Batches

Table 3.9: Data for Response parameter of Tablet

Batch Code	Clarithromycin release at 12 h (%)	T _{50%} (minutes)	T _{85%} (minutes)	Floating Lag Time (seconds)	Tablet Integrity
F1	98.41±1.63	281.4±1.04	539.5±1.23	28±1	+
F2	98.81±2.51	223.42±1.21	518.41±0.57	21±1	+
F3	98.9±1.09	208.14±1.43	403.83±1.09	17.66±1.52	+
F4	94.79±1.37	394.9±1.62	671.47±1.32	51.33±1.52	+
F5	95.82±2.48	381.2±0.79	648.13±1.54	40.33±2.08	+
F6	95.87±2.5	365.4±1.97	613.40±1.93	32.33±1.53	+
F7	68.15±1.56	444.0±1.34	1008.8±1.46	60.66±1.52	+
F8	72.8±1.17	414.6±1.51	889.5±1.75	44±1	+
F9	79.5±1.86	391.7±1.47	859.9±1.39	31.33±1.52	+
*The values represent the average of three determinations (n=3) + = Good Integrity for 12 h, - =No Integrity.					

3.10 Curve fitting (Release mechanism)

The response Parameter and curve-fitting data of matrix tablet prepared as per 3² Factorial designs are summarized in Table 3.9 and 3.10 respectively, indicated that the possible mechanism of drug release. As most of the batches produced yielded quality adjustment with the Hixon Crowell (average R²=0.9832). However, the best fit model was found to be the Zero order (average R²=0.9942) suggesting that the mechanism of drug release was

combination of diffusion and erosion. Different values for diffusion exponent n in equation represent different drug release mechanisms. When the n value is around 0.45, the Fickian diffusion phenomenon dominates, and when n ranges between 0.45 and 0.89 it is anomalous or non-Fickian release that is, the drug release proceeded by diffusion as well as erosion of the polymer. When the n value exceeds 0.89, the release can be characterized by case II and super case II, which illustrate a zero-order release. The values of the diffusion exponent, as shown in Table 3.10 were found to range from 0.77- 1.0239. Formulations F1, F2 and F3 showed non Fickian type drug release as values of 'n' that is diffusional exponent is lies between 0.45 to 0.89 remaining formulations (F4 – F9) shows Class 2 drug release as the value of 'n' is greater than 0.89. The hydrophilic matrix tablets exhibited $R^2 = (0.9942)$ when analyzed using the Zero-order equation, suggesting that the drug release from most of the batches followed zero-order kinetics.

Table 3.10: Data for study of release mechanism by curve fitting analysis.

Batch code	Zero order			Hixon Crowell		
	K	R ²	n	K	R ²	n
F1	0.64±0.017	0.9946±0.003	0.77±0.01	0.62± 0.033	0.9858±0.005	0.65±0.02
F2	0.65±0.023	0.9933±0.004	0.78±0.01	0.60 ±0.034	0.9887±0.006	0.68±0.02
F3	0.64±0.013	0.9907±0.002	0.78±0.02	0.64±0.024	0.9953±0.004	0.69±0.01
F4	0.15±0.017	0.9983±0.005	0.97±0.03	0.12± 0.017	0.9610±0.008	0.94±0.03
F5	0.16±0.021	0.9971±0.006	0.97±0.02	0.26± 0.021	0.9768±0.007	0.91±0.02
F6	0.14±0.025	0.9964±0.004	0.96±0.02	0.13± 0.034	0.9648±0.003	0.93±0.01
F7	0.11±0.014	0.9940±0.05	1.02±0.03	0.59± 0.016	0.9843±0.008	1.09±0.03
F8	0.10±0.016	0.9910±0.004	1.01±0.02	0.37± 0.021	0.9900±0.007	1.03±0.02
F9	0.11±0.015	0.9927±0.002	1.07±0.02	0.54± 0.021	0.9776±0.005	1.02±0.01

3.11 Optimization of Factorial Design Batches

3.11.1 Regression analysis

1) Effect of formulation variables on T_{50%} Clarithromycin release

The Quadratic model for T_{50%} (Y₁) was found to be significant with an F value 361.54 (P<0.0001). In this case X₁, X₂, X₂² was found to be significant and the model describes the T_{50%} release. The factorial equation for T_{50%} (Y₁) can be written as:

$$T_{50\%} = + 375.40 - 25.50 A + 88.78 B + 6.06 A B + 7.58 A^2 - 52.61B^2 \dots\dots (3.1)$$

As the concentration of HPMC K100M increased it causes an increase in viscosity of swollen gel matrix, which contributes more hindrance for drug diffusion and thus decreases the release rate whereas Citric acid increase the solubilization increase the release rate. The combined effect of X₁ & X₂ shown in response surface plot Figure 3.22 While the increasing amount of HPMC K100M causes the decreases in the drug release, due to formation of high viscous gel matrix. HPMC K100M is swellable polymer which causes a gel layer. The Figure 3.21 shows a graph of observed verses predicted values. The HPMC K100M (X₁) have negative effect on Y₁ & Citric acid (X₂) have positive effect on Y₁, means if we increasing the concentration of X₁ T_{50%} decreases & increase in X₂ the T_{50%} increases due to increased solubilization of drug.

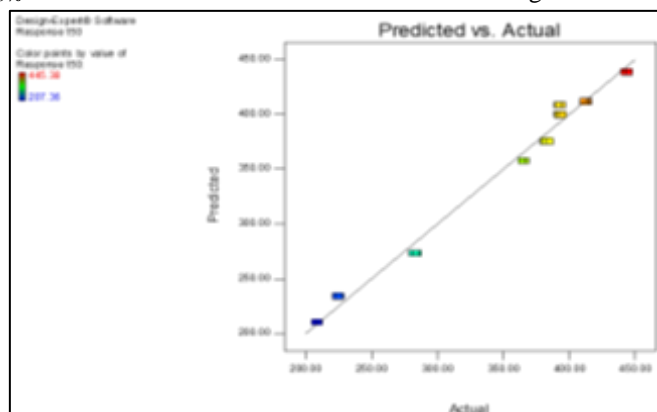


Figure 3.21: Correlation between actual and predicted values for T_{50%} (Y₁)

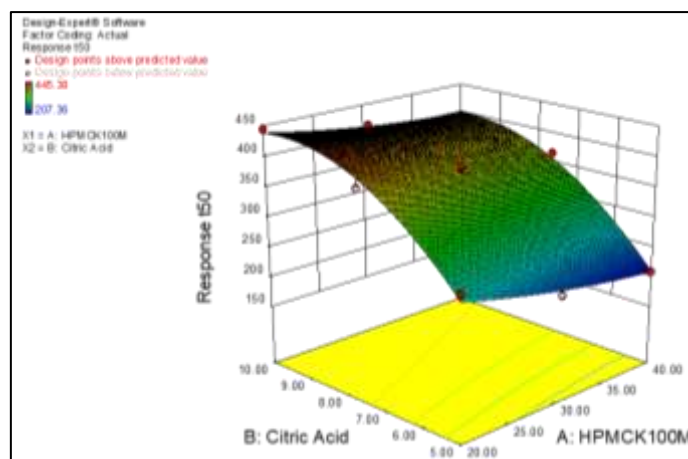


Figure 3.22: Response surface plot showing effect of formulation variables on $T_{50\%}$ (Y_1)

2) Effect of formulation variables on $T_{85\%}$ (Y_2)

The Quadratic model terms for response Y_2 ($T_{85\%}$) were found to be significant with F value of 229.56 ($p < 0.0001$). In this case all the factors except X_1 , X_2 and X_1^2 were found to be significant and the factorial equation for response Y_2 ($T_{85\%}$) can be written as:

$$T_{85} = +645.90 - 56.81 A + 214.75 B - 3.64 A B - 1.16 A^2 + 56.47 B^2 \dots \dots \dots (3.2)$$

As the amount of X_1 increases the corresponding $T_{85\%}$ (time required to release 85% of the drug) also increases. The Figure 3.24 shows the response surface plot. It indicates at all the high levels of X_1 the $T_{85\%}$ value is high. As discussed above this behavior is due to increase in amount of HPMC K100M forms a high viscous gel matrix and thus decreases the drug release and hence $T_{85\%}$ value increases. Whereas X_2 increases the release rate also increases. The Figure 3.23 shows the graph of predicted versus actual data. The HPMC K100M (X_1) has positive effect on $T_{85\%}$ Y_2 and Citric acid (X_2) has negative effect on Y_2 means if we increasing the concentration of X_1 then Y_2 of the drug also increases due to increased viscosity and gel strength and increase in X_2 then decrease in Y_2 means decrease in time require for release.

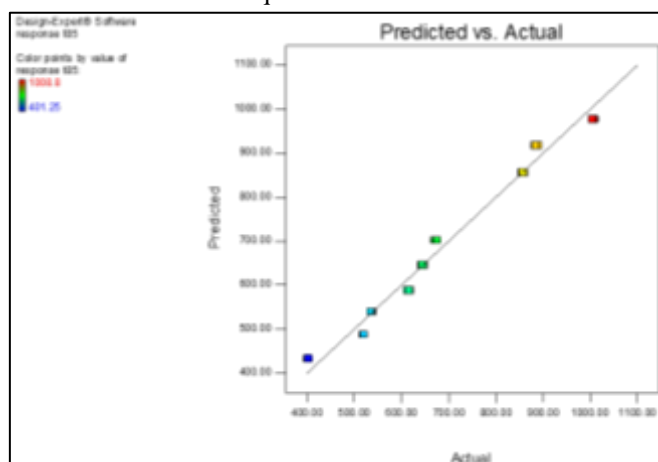


Figure 3.23: Correlation between actual and predicted values for $T_{85\%}$ (Y_2)

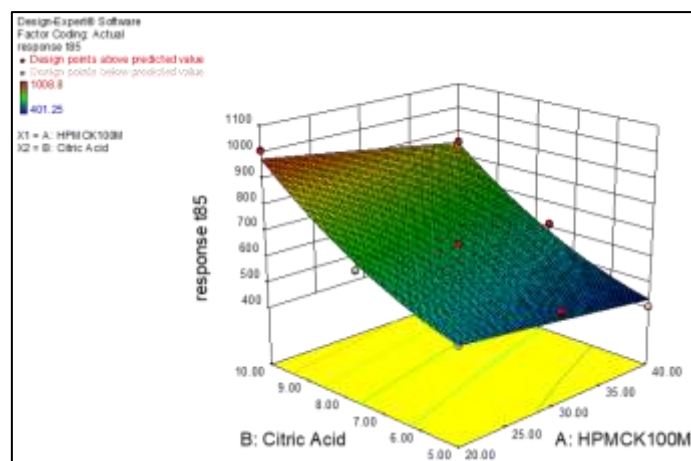


Figure 3.24: Response surface plot showing effect of formulation variables on $T_{85\%}$ (Y_2)

3) Effect of formulation variables on Floating Lag Time (FLT, Y_3)

The Quadratic model terms for response Y_3 (FLT) were found to be significant with F value of 229.56 ($p < 0.0001$). In this case all the factors except X_1^2 were found to be significant and the factorial equation for response Y_3 (FLT) can be written as:

$$FLT = +40.15 - 9.78 A + 11.56 B - 4.75 A B + 1.78 A^2 - 7.56 B^2 \dots \dots \dots (3.3)$$

As the amount of X_1 increases the corresponding FLT (time required to float the tablet) also increases. The Figure 3.26 shows the response surface plot. It indicates at all the high levels of X_1 the FLT value is high. On the contrary X_2 increases the FLT decreases respectively. The Figure 3.25 shows the graph of predicted versus actual data. The HPMC K100M (X_1) has negative effect on Y_3 and Citric acid (X_2) has positive effect on Y_3 means if we increasing the concentration of X_1 then Y_3 of the drug also increases due to increased viscosity and gel strength and increase in X_2 then decrease in Y_3 means decrease in time required for float.

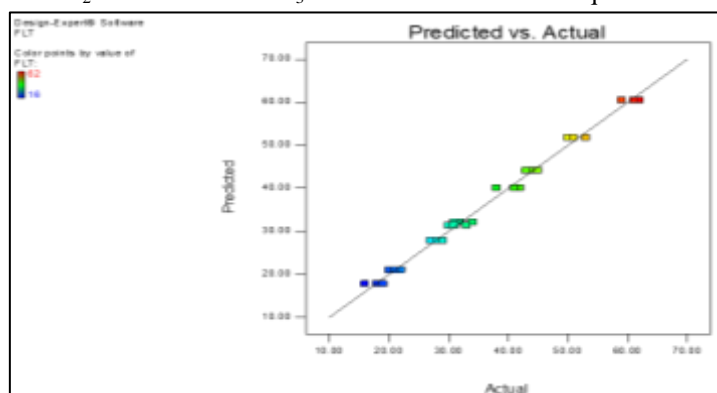


Figure 3.25: Correlation between actual and predicted values for FLT (Y_3)

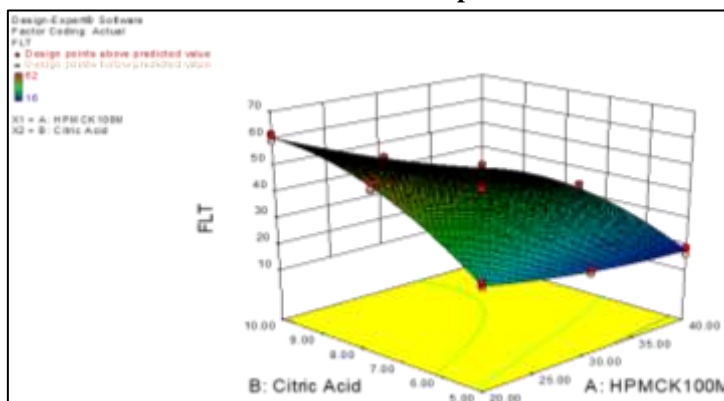


Figure 3.26: Response surface plot showing effect of formulation variables on FLT (Y_3)

4) ANOVA, Pure error, Lack of fit

The results of ANOVA for dependent variables from 3^2 factorial designs shown in Table 3.11 demonstrate that the model was significant for all response variables. Regression analysis was carried out to obtain the regression coefficient shown in Table 3.11 and effects as follows; all factors other than X_1 , X_2 and X_1^2 found significant for response Y_1 and Y_2 whereas for response Y_3 except X_1^2 all other factors found significant. The above results conveyed us that the amount of HPMC K100M & Citric acid plays important role in formulation of Oral Controlled Release matrix tablets of Clarithromycin. The data of pure error and lack of fit are summarized in Table 3.12. The residuals are the difference in the observed and predicted value. Since computed F values were respectively less than critical F values, denotes non-significance of lack of fit.

Table 3.11: Data of ANOVA study for dependent variables from 3^2 factorial designs

Source	d.f.	Sum square	Mean square	F value	Probability
Response (Y_1) = $T_{50\%}$ (h)					
X_1	1	11705.52	11705.52	127.77	< 0.0001*
X_2	1	1.419E+005	1.419E+005	1500.03	< 0.0001*
X_1X_2	1	440.08	440.08	4.65	0.0427
X_1^2	1	345.14	345.14	3.65	0.0698
X_2^2	1	16607.22	16607.22	175.60	< 0.0001*
Response (Y_2) = $T_{85\%}$ (h)					
X_1	1	58084.82	58084.82	73.47	< 0.0001*
X_2	1	8.301E+005	8.301E+005	1049.91	< 0.0001*
X_1X_2	1	158.92	158.92	0.20	0.6585
X_1^2	1	8.13	8.13	0.010	0.9202
X_2^2	1	19130.53	19130.53	24.20	< 0.0001*
Response (Y_3) = FLT(Sec)					
X_1	1	1720.89	1720.89	927.73	< 0.0001*
X_2	1	2403.56	2403.56	1295.76	< 0.0001*
X_1X_2	1	270.75	270.75	145.96	< 0.0001*
X_1^2	1	18.96	18.96	10.22	0.0043
X_2^2	1	342.52	342.52	184.65	< 0.0001*

* -Indicates significant

Table 3.12: Data of ANOVA study for results in analysing lack of fit and pure error

For T_{50}						
Source	Sum of Squares	Degrees of Freedom	Mean Square	F Value	P Value	Model Significant/ Non-significant Relative to Noise
Model	1.710E+05	5	34191.91	361.54	0.0001	Significant
Residual	1986.02	21	94.57	-	-	-
Core Total	1.729E+05	26	-	-	-	-
Lack of fit	1931.25	3	643.75	211.56	0.0001	Significant
Pure Error	54.77	18	3.04	-	-	-
For T_{85}						
Model	9.075E+05	5	1.815E+05	229.56	0.0001	Significant
Residual	16603.09	21	790.62	-	-	-
Core Total	9.241E+05	26	-	-	-	-
Lack of fit	16495.40	3	5498.47	919.08	0.0001	Significant
Pure Error	107.69	18	5.98	-	-	-
For FLT						
Model	4756.68	5	951.34	512.87	0.0001	Significant
Residual	38.95	21	1.85	-	-	-

Core Total	4795.63	26	-	-	-	-
Lack of fit	0.95	3	0.32	0.15	0.9280	Not Significant
Pure Error	38.0	18	2.11	-	-	-

3.12 Studies on Final Formulation

1) Water Uptake Study

The water uptake was determined of F5 batch. It was observed that Water uptake was increase with respect to time. Data for water uptake study is given in the Table 3.13.

Table 3.13: Water Uptake Study of F5 Batch

Time (h)	Water Uptake (%)
1	133.8
2	136.5
3	137.4
4	139.2
5	140.1
6	142.2
7	143.3
8	143.8
9	144.8
10	145.1
11	146.3
12	147.9

2) In-Vitro Drug release for Marketed Tablet, Complex and F5

In vitro release profile of optimized formulation F5 compared with marketed SR tablet (Biaxin-500) and complex. The time for drug release t50% of F5, Biaxin and complex were found to 381.2, 315.36 and 354 minutes respectively. The percentage drug release after 12 hour for F5, Biaxin and complex were found to 95.82, 86.32 and 87.62 respectively shown in Table 3.14, so the release from the optimized formulation and complex were higher compared to marketed product. Release of drug from complex was approximately same so it was concluded that without any polymer drug release is controlled which is shown in Figure 3.27.

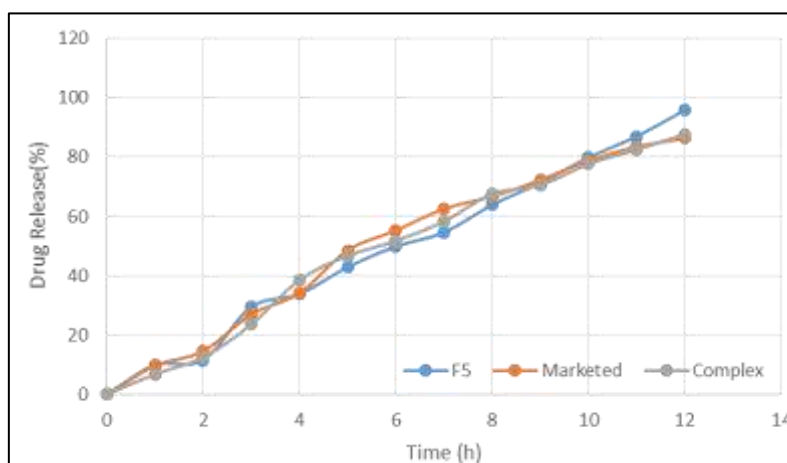


Figure 3.27: Dissolution Profile of marketed formulation with capsule fills with complex and formulated tablet in 0.1N HCL.

Table 3.14: Dissolution data of Marketed Tablet (Biaxin), Complex and F5 in 0.1N HCL

Time (h)	% Drug Release		
	F5	MARKETED TAB.	COMPLEX
0	0.00±0.00	0.00±0.00	0.00±0.00
1	09.85±0.92	09.59±0.36	03.76±0.65
2	11.52±1.32	14.58±0.63	12.45±1.28
3	29.45±2.03	26.94±1.89	23.56±2.43
4	33.81±2.32	34.18±2.92	38.54±1.45
5	42.90±1.45	48.51±1.61	46.68±1.87
6	49.85±1.93	55.26±0.85	51.76±0.69
7	54.61±1.23	62.52±1.44	58.32±0.78
8	63.89±2.04	66.74±0.31	67.54±2.58
9	71.33±0.78	72.23±2.45	70.56±2.65
10	79.84±1.12	78.83±2.68	77.65±1.95
11	87.02±1.67	83.45±1.56	82.56±2.08
12	95.82±2.04	86.32±1.30	87.65±1.71

n=2 (±SD)

3) Optimization

A numerical optimization technique by the desirability approach was used to generate the optimum settings for formulation. The process was optimized for dependent variables Y_1 - Y_3 . The optimized formula arrived by targeting the Y_2 at 650 minute, Y_1 was kept at range 360-400 min. , Y_3 also kept at range 16-62 sec. The optimized results obtained to give 13 results out of that one formula is shown in Table 3.14. The results of optimized formula were compared with the predicted values (Table 3.16), which showed good relationship between experimented and predicted values, which confirms the practicability and validity of the model. The value of n was found to be 0.991.

Table 3.15: Composition of optimized formulation

Ingredients	Quantities (mg)
Complex	500
HPMC K100M	163.5
Citric Acid	38.6
NaHCO ₃	80
PVP K30	60
Mg stearate	5
Lactose	12.9
Total weight	860

Table 3.16: Comparison between the experimented and predicted Values for most probable optimal formulation

Dependent variables	Optimized formulation	
	Experimented value	Predicted value
T _{50%} (Y ₁)	381.2	376.71
T _{85%} (Y ₂)	648.13	649.99
FLT	40.3	38.49

CONCLUSION

The Clarithromycin is poorly water soluble drug and gastric irritant. To overcome these problems attempt was made in present study to form inclusion complex of Clarithromycin with Nanosponges. β -Cyclodextrin (CD) based Nanosponges (NS) are novel class of cross-linked derivatives of Cyclodextrin. The Nanosponges were synthesized by carbonylation of β -Cyclodextrin to exploit its porous structure for drug entrapment. After synthesis of Nanosponges, Drug Clarithromycin was entrapped in it. The Characteristics of Complex was studied by FTIR, DSC, PXRD and SEM. The result of XRPD results showed that the crystallinity of CLA was decreased after loading into Nanosponges. Histopathological study was carried out and it revealed non irritancy of drug-NS complex to gastric mucosa (of rat). Hence drug-NS complex found to be suitable for designing into unit dosage forms. Preliminary Batch were prepared and Evaluated (*in vitro* dissolution) for selection of Polymer. HPMC K100M showed highest release retarding property so it was selected as the polymer for further study. The 3^2 full factorial experimental design was applied and 9 Factorial Design Batches were obtained. Granules were prepared using Wet granulation method and evaluated for their properties. All the batches of tablets were prepared using rotary punch tablet compression machine using 12 mm size punch. Prepared tablets of Batch F1-F9 were evaluated for various tablet properties. Regression analysis was carried out and F5 Batch was found to be optimized Batch. F5 batch showed 95.82 ± 2.48 % Drug Release in 12 hours further it was evaluated for water uptake and compared with the Marketed formulation for % Drug Release.

ACKNOWLEDGEMENT

The authors are very much thankful to PDEAs Shankarrao Ursal College of Pharmaceutical Sciences and Research Centre, Pune, Maharashtra, India and PDEAs Seth Govinds Raghunath Sable College of Pharmacy, Pune, Maharashtra, India for providing the necessary support to complete this work successfully.

CONFLICT OF INTEREST

All authors declared no conflicts of interest.

REFERENCES

- 1) Robinson J R, Lee V H 'Controlled Drug Delivery Fundamentals and Applications'. 1987 Vol. 29, 2nd Edⁿ. Marcel Dekker, INC, New York and Basel: 4-6.
- 2) Khan GM, Review on 'Controlled Release Oral Dosage Forms: Some Recent Advances in Matrix Type Drug Delivery Systems' JPS 2001 (5): 350-354.
- 3) Wise DL, 2005 'Handbook of Pharmaceutical Controlled Release Technology'; Marcel Dekker, INC, New York and Basel: 211, 435-440, 472-473, and 787-788.
- 4) Arora JM, Khar RK 2005 'Gastroretentive Drug Delivery System' AAPS Pharmascitech: 6 (03) Article 47.
- 5) Desai S and Bolton S, "A Floating Controlled Release Drug Delivery System: In vitro-In vivo Evaluation", Pharma. Res., 1993, 10 (9) 1321-325.
- 6) Singh BM and Kim KH, "Floating drug delivery systems: an approach to controlled drug delivery via gastric retention", J. Control. Rel., 2000, 63, 235-259.
- 7) Nakay Y, Fukuoka E, Nakajima S, Yamamoto K. Effects of grinding on physical and chemical properties of crystalline medicinals with microcrystalline cellulose. I. Some physical properties of crystalline medicinals in ground mixtures. Chem. Pharm. Bull. 1977; 25: 3340- 3346.
- 8) D. Duche^{ne}, G. Ponchel, and D. Wouassindjewe: Adv. Drug Del. Rev. 36, 29 B. McCormack and G. Gregoriadis: Int. J. Pharm. 162, 59 (1998).
- 9) Szejtli, J. 1998 'Introduction and general overview of cyclodextrin Chemistry' Chem. Rev. 98, 1743-1754.
- 10) Rekharsky, M.V., Inoue, Y. 1998 'Complexation thermodynamics Of cyclodextrins' Chem. Rev. 98, 1875-1918.
- 11) Salazar Sandoval S, Cortés-Adasme E, Gallardo-Toledo E, Araya I, Celis F, Yutronic N, Jara P, Kogan MJ. β -Cyclodextrin-Based Nanosponges Inclusion Compounds Associated with Gold Nanorods for Potential NIR-II Drug Delivery. Pharmaceutics. 2022 Oct 17;14(10):2206.

- 12) Boscolo Barbara, Trotta Francesco, Ghibaudi Elena 2009 “High catalytic performances of Pseudomonas fluorescens lipase adsorbed on a new type of cyclodextrin-based nanosponges” Journal of Molecular Catalysis B: Enzymatic.
- 13) <http://www.drugsinformationonline.com>
- 14) Martindale. 2002. The complete drug reference. Sean C.S. 33 rd edition, Pharmaceutical press. Pp.1356-1359.
- 15) Ohtani, Y., Irie, T., Uekama, K., Fukunaga, K., Pitha, J., 1989. Differential effects and β -cyclodextrins on human erythrocytes. Eur. J. Biochem. 186, 17–22.
- 16) Israr M, Pugliese N, Farid A, Ghazanfar S, Di Cerbo A, Muzammal M, et al. Preparation and Characterization of Controlled-Release Floating Bilayer Tablets of Esomeprazole and Clarithromycin. Molecules 2022;27:3242.
- 17) Chen P, Luo H, Huang S, Liu J, Lin M, Yang F, Ban J, Huang Z, Lu Z, Xie Q, Chen Y. Preparation of high-drug-loaded clarithromycin gastric-floating sustained-release tablets using 3D printing. AAPS PharmSciTech. 2021 Apr;22:1-0.
- 18) Shankar Swaminathan Linda Pastero, Loredana Serpe, Francesco Trotta d, Pradeep Vavia, Dino Aquilano b, Michele Trotta a, GianPaolo Zara , Roberta Cavalli “Cyclodextrin-based nanosponges encapsulating camptothecin: Physicochemical characterization, stability and cytotoxicity” European Journal of Pharmaceutics and Biopharmaceutics.
- 19) Shanmugam S. Granulation techniques and technologies: recent progresses. Bioimpacts. 2015;5(1):55-63.
- 20) Easwari, T S. (2012). Formulation Development and Evaluation of Clarithromycin Oral Dosage Form Against Helicobacter Pylori Infection. INTERNATIONAL JOURNAL OF ADVANCE PHARMACEUTICAL AND BIOLOGICAL SCIENCES. 3. 281-287.
- 21) Raymond, C.R., Paul, J., 2006. Handbook of Pharmaceutical excipients. 5th edition Alpha pharmaceutical press, London, Chicago. Pp.535-538.
- 22) <https://www.statease.com/docs/v11/>
- 23) Michal Szumilo, Piotr Belniak, Katarzyna Swiader, Ewelina Holody, Ewa Poleszak, Assessment of physical properties of granules with paracetamol and caffeine, Saudi Pharmaceutical Journal, Volume 25, Issue 6, 2017, Pages 900-905
- 24) Aulton ME, 1998, Pharmaceutics: The science of dosage form design, 1 ed, London Churchill Livinstone. p.247
- 25) Kuchekar, B.S., Singavi, A. A., Late, S.G., Shinde, D.B., 2003. Spectrophotometric estimation of Roxithromycin and Clarithromycin in Pharmaceutical Dosage Forms. Indian Drugs. 40(1), 44-45.
- 26) Indian Pharmacopoeia, 1996, Govt. of India, Ministry of Health and Family Welfare, Vol., 1, The Controller of Publication, Delhi: 187-191, 382-383.
- 27) Boylan and Cooper . ‘Handbook of Pharmaceutical Excipient’ A Joint Publication of American Pharmaceutical Association And the Pharmaceutical Society of Great Britain : 45-48, 138-140.
- 28) Kibbe AH. 2003. Handbook of Pharmaceutical Excipients, 3rd Ed. American Pharmaceutical Association and Pharmaceutical Press, Washington DC.
- 29) British pharmacopoeia. 2003. The Stationary office: London. Vol. 2, 1638
- 30) <https://www.statease.com/docs/v11/contents/optimization/optimization-overview/>



Investigation for determination of therapeutic potential for antitubercular activity with special reference to *Caesalpinia crista* fruits



Vipul Dhasade and M. Komala*

Department of Pharmaceutics, School of Pharmaceutical Sciences, Vels Institute of Science, Technology and Advanced Studies (VISTAS), Chennai - 600117, Tamil Nadu, India

E-mail/Orcid Id:

VD, vipuldhasade2009@gmail.com, <https://orcid.org/0000-0002-0959-9465>;

MK, komala.sps@velsuniv.ac.in, <https://orcid.org/0000-0001-8357-535X>

Article History:

Received: 01st Feb., 2023

Accepted: 15th Apr., 2023

Published: 30th Apr., 2023

Keywords:

Alkaloids, antitubercular activity, *Caesalpinia crista*, MABA

Abstract: In recent years, plant biochemistry has played a significant role due to plant-derived products' phytochemical details. One of the difficulties of phytochemistry nowadays is performing the aforementioned procedures with limited material due to the wide variety and low yield of phytochemicals. The secondary metabolites found in *Caesalpinia crista* have a wide range of applications. To better understand the antitubercular properties of *Caesalpinia crista*, a major medicinal plant, this study examines the most essential compounds in its fruits. Results from both quantitative and phytochemical screening revealed high concentrations of a wide variety of bioactive compounds, including alkaloids, phenols, amino acids, flavonoids, saponins, tannins, proteins, terpenoids, and glycosides. Microplate-based Alamar blue assay demonstrates their efficacy against TB. In addition, the results confirmed the presence of antitubercular potential in specific phytochemicals extracted from *Caesalpinia crista* fruits.

Introduction

Over time, nature has provided many benefits to human health, including the materials for early attempts at therapeutic intervention. People in the past often turned to plants for relief from a wide range of medical conditions. Plants have long been studied for potential of new medicines, and many different plants have been used as models for developing new pharmaceuticals, food additives, agricultural chemicals, and industrial chemicals, making plant-derived products an invaluable tool in the fight against disease (Borris, 1996). The photochemical defence mechanism relies on bioactive compounds present naturally in plants. There are two types of phytochemicals, known as main and secondary components, and each serves a specific purpose in plant metabolism. Among 2.5–5 million plant species worldwide only a small percentage of the estimated have had their phytochemicals investigated (Zambari et al., 2023).

Both plant biochemistry and organic chemistry now provide special attention to the phytochemical analysis of plant products. It is concerned with the wide range of organic compounds that plants store, and it contributes to our understanding of their chemical composition, distribution, and biological function. Understanding phytochemistry requires both the effective application of tried and true methodologies and the constant development of novel approaches to meet new difficulties. A major challenge in phytochemistry is carrying out all of these processes with only a small amount of starting material. To address a biological problem linked to plant growth control, the biochemistry of plant-animal interactions, or the evolution of ancient plants, it is usually necessary to identify a wide range of complicated chemical compounds that may only be available for analysis in microgram levels.

As many economically significant crops and animals, including humans, are susceptible to fungal and bacterial diseases, Finding cures for these diseases will need the



methodical investigation of plant species in search of novel bioactive compounds. The value of plants comes from the chemical substances they contain, which have an observable impact on human physiology. The most well-known of these bioactive plant elements are alkaloids, tannins, flavonoids, and phenolic compounds. Low mammalian toxicity, target selectivity, and biodegradability are just a few of the ways in which these natural pesticides excel over their synthetic counterparts (Rajaiah et al., 2022).

Several primary and secondary metabolites as well as their intermediates, were found in the *Caesalpinia crista* (*Caesalpinia bonduca*, *Caesalpinia bonducella*) species of the family *Caesalpinaceae* (Fabaceae). They can potentially prevent and treat various disease conditions in humans (Panda et al., 2022). Its global reach included Southeast Asia and the rest of the tropics and subtropics. This plant can be found up to 2,500 feet above sea level in some of the woodlands along the coast and inland (Joshi et al., 2023).



Figure 1. *Caesalpinia crista* Plant

Bonducin (Bonducellin), Steroidal saponins, 1, 5, 6, 7, 14-Voucapanepentol derivative, Caesalpin, (1-ketone 6, 7-diacetylcassane), acetic acid, myristic acid, viniticolic, vouncapenic and cassaic acids, cassanefuranoditerpenoid as bonducellpin E, F, lupeol acetate, β -amyrin and α -amyrin are reported in plant fruit cells (Dhulap et al., 2023; Almeleebia et al., 2022).

Mycobacterium tuberculosis is the primary pathogen responsible for tuberculosis (TB), a bacterial lung illness (*M. tuberculosis* [MTB]). Throughout the past few decades, it has been recognised as a serious problem since it is home to many of the world's most infectious and potentially fatal diseases. White plaque smear-positive tuberculosis is an infectious illness caused by *Mycobacterium tuberculosis* and related organisms. Several mycobacteria species include *M. africanum*, *M. bovis*, *M. caprae*, *M. microti*, *M. pinnipedi* and *M. canettii* (Wijaya et al., 2022).

People have different preferences for which *Caesalpinia crista* plants to use while treating disease symptoms. The goal of this research was, therefore, to determine whether or not *Caesalpinia crista* fruit contains any phytoconstituents with anti-tuberculosis properties.

Materials and Methods

Collections of Plant Material and Drying

Harvested in September, the ripe fruits of the plant are fresh and ready to eat. Raw medication is stored in the dark for regular room-temperature drying. Coarse powder in airtight containers was stored to avoid from direct sunlight and moisture until making the extract.

Authentication

Dr. Priyanka A. Ingle (Scientist, Botanical Survey of India, Pune) confirmed the authenticity of this plant specimen (Dated October 1, 2020, voucher specimen VVD 01 of *Caesalpinia crista* was submitted (Ref. No. BSI/WRC/IDEN.CER./2020/92)).

Crude Extract preparation

Two 12-hour sessions of Soxhlet apparatus refluxing with different organic solvents were applied to 100 grammes of dry powdered fruit components. Hexane, ethanol, chloroform, ethyl acetate, and distilled water were chosen as solvents for the extraction process due to their varying degrees of polarity. Keeping the solvent at a rolling boil throughout the extraction process is crucial for obtaining the highest possible yield. The extracted dried concentrate was then packaged in sterile containers, labelled, and stored in the fridge for later analysis.

Phyto-chemical Screening:

Caesalpinia crista fruit extracts were analysed for their physical properties and yield percentage after being concentrated and dried. In addition, a preliminary qualitative test was conducted on all extracts to check for primary and secondary phytochemicals, as is customary practice (Mukherjee, 2002; Harborne, 1998; Gokhale, 2020; Trease, 2002; Khandelwal, 2005; Wagner, 1996).

Phytochemical analysis of *Caesalpinia crista* crude extracts

Extracted phytochemicals may show a reaction in qualitative and quantitative phytochemical analysis. The phytochemicals in each extract were identified and quantified using the following techniques.

Determination of total phenolic compounds

The sample extract was diluted with 100 ml of distilled water after being weighed out at 100 mg. After removing 1 mL of the solution, 0.5 mL of 2N Folin-Ciocalteu reagent and 1.5 mL of 20% Na_2CO_3 solution were added to a test tube. The volume was then increased

to 8 millilitres using distilled water, and the resulting mixture was vigorously shaken before being given two hours to settle. At 765 nm, we measured the absorption. The solubility of a 0.5 mg/ml standard gallic acid solution in methanol was determined using the same conditions. The results of every test were measured three times for accuracy (Silva et al., 2022).

Determination of total flavonoids

The move towards relies on the absorptivity maximum at 415nm, which is achieved through the production of the flavonoids-aluminium combination. Twenty percent aluminium trichloride in methanol was added to 100µl of sample extracts in methanol (10 milligrammes per millilitre). Add 0.1 millilitre acetic acid and a 5-millilitre methanol mixture. After waiting 40 minutes, the absorbance at 415 nm was measured. We followed the same laboratory protocols and created 100 cc of blank samples. Under the same laboratory conditions, quercetin absorption from a 0.5 mg/ml quercetin solution in methanol was tested as a reference. The results of every test were measured three times for accuracy (Donga et al., 2022).

Determination of total alkaloids

1 g of test extract was macerated in 20 ml of ethanol containing 20% sulfuric acid (1:1 v/v). 1 ml of the filtrate was mixed with 4 ml of the 60% H₂SO₄ solution. The aforesaid combination was left to stand for 3 hours after being combined with 5 ml of 0.5% formaldehyde in 60% H₂SO₄ for 5 minutes. At 565 nm, the absorbance was measured.

Determination of total tannins

3.75 ml of distilled water, 0.5 ml of 35% sodium carbonate solution, 0.25 ml of Folin Phenol reagent, and 0.5 millilitres of test extract was mixed carefully. The solution mentioned above was tested for its absorbance at 725 nm. Tannic acid standard solutions ranged from 0 to 0.5mg/ml. The concentration of tannic acid in the extract is reported as many milligram's per millilitre (Govindaram et al., 2023; Roghini et al., 2018).

Determination of total glycosides

We used 50 millilitres of distilled water to macerate 1 gramme of extract. Alkaline pirate solution (about 4 ml) was added to the filtrate (1 millilitre). After boiling the mixture for 5 minutes we let it cool down. Then, we measured the light absorbance of the mixture at a wavelength of 490 nm, as reported by Chen et al. (2022) and Mobin et al. (2021).

Test for Terpenoids

A 1 gramme sample was macerated in 50 ml of ethanol before being filtered. Combine 2.5 ml of filtrate with the same volume of concentrated hydrogen peroxide

and 5% aqueous phosphomolybdic acid solution. Let for 30 minutes, then add enough ethanol to make up 12 ml. At 700 nm, we measured the absorption (Juvatkar et al., 2021).

Test for Steroids

A 1-gramme sample was macerated in 20 millilitres of ethanol before being filtered. A volume of 2 mL of the chromogenic solution was added into the filtrate and the solution was allowed to sit for thirty minutes. 550 nm was used to measure the absorbance. The concentration of individual phytocomponents in test extract can be estimated by measuring the colour difference between test and blank samples. All the quantitative information shown above is given in milligrams per dry material (Juvatkar et al., 2021).

Column chromatographic isolation

As per observation, ethanol and ethyl acetate extracts containing components were separated with isocratic manner. The *in-vitro* anti-tubercular activity of isolated fractions was tested (Bhandari et al., 2022).

In-vitro Anti-Tubercular activity

Microplate Alamar Blue Assay (MABA)

Screening against mycobacterial pathogens (*Mycobacterium tuberculosis*) (H37Rv) (ATCC No-27294), employing 96 well plates in the microplate Alamar blue assay (MABA), is in the works.

Requirement

Microbial strain *M. tuberculosis* (H37Rv) (ATCC No-27294), Almar Blue reagent, Tween 80, parafilm, incubator, Middlebrook 7H9 culture media, and 96 well plates are all required.

Test sample: Several phytocomponents were detected in an ethanol extract of *Caesalpinia crista* fruit, and these components were separated using isocratic column chromatography. Microplate Alamar Blue Assay assessed the concentration and quality of all collected fractions to identify the most active and purified phytocomponents. Preparations were made for test concentrations ranging from 0.8 to 100 µg/ml (Silva et al., 2022; Shirsat et al., 2021).

Microplate Alamar Blue Assay

M. tuberculosis (H37Rv) (ATCC No. 27294) was used to test the fractions' antitubercular activity. This approach strongly correlates with the proportionate and BACTEC radiometric methods and uses a thermally stable reagent. *M. tuberculosis* (MTB) was grown in 7H9 medium with and without the test plant components at dilutions of 0.8, 1.6, 3.12, 6.25, 12.5, 25, 50, and 100 µg/ml in a 96-well plate. To avoid medium evaporation during incubation 200 µl of sterile deionized water was added to the external wall wells of a sterile 96-well plate.

Table 1. Characteristics of *Caesalpinia crista* fruit extracts.

Extract particulars	Percent Yield (%W/W)	Characteristics	
		Colour	Appearance/ Consistency
Hexane extract (CFH)	04.11%	Green	Solid
Chloroform extract (CFC)	08..31%	Brown	Semisolid
Ethyl acetate extract (CFEA)	14.25%	Dark brown	Semisolid
Ethanol extract (CFET)	10.25%	Dark brown	Semisolid
Aqueous (Water) extract (CFA)	07.67%	Brown	Liquid

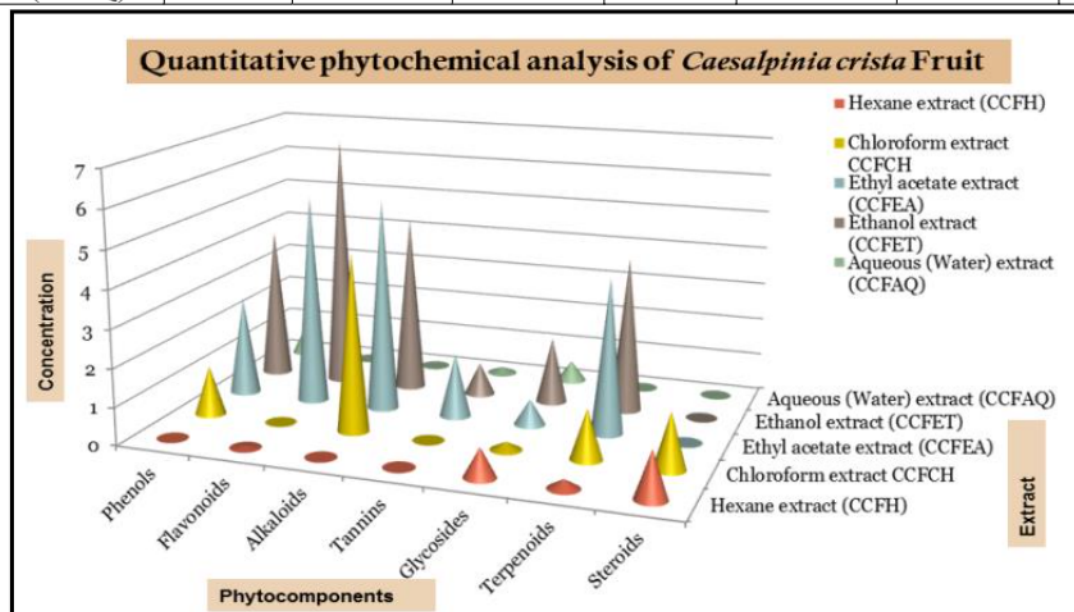
Table 2. Qualitative analysis of *Caesalpinia crista* Fruits extract.

Sr.No.	Tests	CFH	CFC	CFEA	CFE	CFA
1.	Tests for Acidic compounds	-	-	-	+	-
2	Test for carbohydrate					
	Molish's test	-	-	-	+	-
	Fehling test	-	+	+	+	-
	Benedicts test	-	-	+	-	-
	Barfoed test	-	-	-	+	-
	Selivanoffs test	-	+	+	-	-
	Osazone formation test	-	-	-	-	-
3	Test for Proteins					
	Biuret Test	-	-	-	+	+
	Millons Test	-	-	-	-	-
4	Test for amino acids					
	Ninhydrine test	-	+	-	+	+
5	Test for Steroids					
	Salkowski test	+	+	-	-	-
	Liebermann test	+	-	-	+	-
	Liebermann-Burchard reaction	-	+	-	-	-
6	Test for Glycosides					
	Anthraquinone glycoside test	-	+	-	+	-
	Cardiac glycoside test	-	+	-	+	-
	Cynogentic glycosides test	-	-	+	-	-
7	Test for Terpenoids:	-	+	+	+	-

8	Test for Saponin					
	Foam test	-	+	-	-	+
9	Test for Alkaloids					
	Dragondorff's test	-	+	+	+	-
	Mayer's test	-	-	-	-	-
	Hager's test	-	-	+	+	-
	Wagner's test	-	-	-	+	-
10	Test for Tannins and Phenolic compounds					
	5% FeCl ₃ test	-	-	+	+	-
	Lead acetate solution	-	-	+	+	-
11	Test for Flavonoids					
	Shinoda test	-	-	+	+	-
	Sulphuric acid test	-	-	+	-	-
Abbreviations: HE- Hexane; CH- Chloroform; EA-Ethyl Acetate; EO; Ethanol; AQ; Aqueous, Note: (-): Absent, (+): Presence						

Table 3. Quantitative Analysis of *Caesalpinia crista* Fruits extracts

Extracts/ Test	Phytochemical Mean \pm STD						
	Phenols	Flavonoids	Alkaloids	Tannins	Glycosides	Terpenoids	Steroids
<i>Caesalpinia crista</i> Fruits extracts							
Hexane extract (CFH)	-	0.06 \pm 0.003	-	-	0.77 \pm 0.003	0.24 \pm 0.021	1.23 \pm 0.083
Chloroform extract CFCH	1.30 \pm 0.030	-	4.65 \pm 0.024	-	0.21 \pm 0.002	1.31 \pm 0.071	1.47 \pm 0.012
Ethyl acetate extract (CFEA)	2.62 \pm 0.011	5.58 \pm 0.013	5.61 \pm 0.042	1.68 \pm 0.012	0.68 \pm 0.001	4.08 \pm 0.004	-
Ethanol extract (CFET)	4.05 \pm 0.027	6.75 \pm 0.019	4.70 \pm 0.020	0.85 \pm 0.011	1.75 \pm 0.087	4.10 \pm 0.052	-
Aqueous (Water) extract (CFAQ)	0.87 \pm 0.021	-	-	0.16 \pm 0.003	0.54 \pm 0.020	-	-

Figure 2. Concentration vs Test compound of *Caesalpinia crista* Fruits extract

Each well of a plate was then filled with 100 μ l of Middlebrook 7H9 broth, allowing for the serial dilution of compounds. The detected drug concentrations ranged from 0.80 to 100 g/ml.

Parafilm was used to seal the plates, and then they were incubated at 37 degrees Celsius for five days. The plate was then incubated for 24 hours after adding 25 μ l of a freshly prepared 1:1 mixture of Almar Blue reagent and 10% Tween 80. Wells that tested blue indicated no bacterial growth, whereas those that tested pink indicated growth. The rate at which the dye was diluted was used as a proxy for bacterial proliferation. If the standard's result for the percentage reduction of Almar blue dye was lower, then the extracts were declared effective. All assay variables were kept in triplicate wells. The lowest drug concentration that prevented the blue-to-pink colour change was established as the minimum inhibitory concentration (MIC) (Martolia et al., 2021; Bansal et al., 2020).

Results and Discussion

Phyto-chemical screening test

The following findings were reported from the detailed phytochemical analysis of *Caesalpinia crista* fruit extracts conducted in this study. The properties of each extract are listed in Table 1. The results showed the highest percentage yield for the extracts made using chloroform, ethyl acetate, and ethanol. The results for various phytochemicals in the extract showed promise. Table 2 shows that the different complex metabolites in the fruits of *Caesalpinia crista* were more clearly separated using the polarity gradient solvent selection. Hexane, chloroform, ethyl acetate, and ethanol extracts revealed steroids, saponins, glycosides, alkaloids, phenolic chemicals, and flavonoids, respectively. Proteins and saponins were extracted aqueously.

Caesalpinia crista's (Crude extract) phyto-chemical quantification

Seven phytochemicals (phenol, flavonoids, alkaloids, tannin, glycosides, terpenoids, and steroids) were screened for quantitatively in the extract was carried out using methods described in the literature, and the findings are presented in Table 3 and Figure no. 2. Alkaloids, phenolic compounds, flavonoids, and glycosides are some examples of secondary metabolites that contribute to a plant's potential for medicinal use. Phytochemical components in the extract were also quantified through additional analytical testing.

The ethanol extract found phenols, terpenoids, and flavonoids in the highest quantity. Ethyl acetate extract has the highest concentration of alkaloid and some trace flavonoids. The chloroform extract contained measurable amounts of alkaloids and steroids. It is shown that plant metabolites can be isolated under controlled circumstances.

In-vitro Anti-Mycobacterial activity

Microplate Alamar Blue Assay (MABA)

Caesalpinia crista ethanol extracts showed the most promise in the tests, inhibiting the development of mycobacteria. Take note of what is shown in Figure 3. The best inhibition and MIC values came in at 3.2 and 6.25 μ g/ml for tests 6 and 7, respectively.

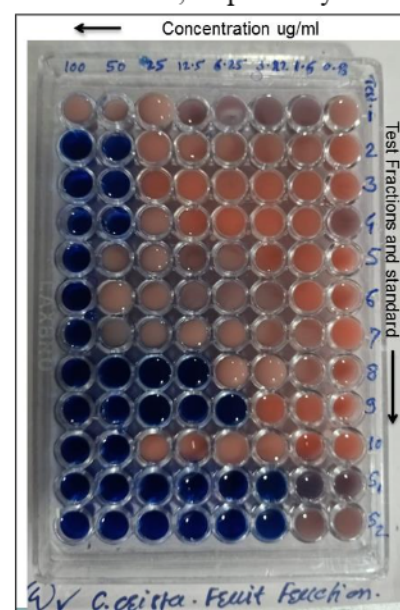


Figure 3. Image of Microplate Alamar Blue Assay (MABA)

Table 4. Minimum Inhibitory concentration (MIC) of specimens

Sr. No.	Samples	MIC μ g/ml	Sr. No.	Samples	MIC μ g/ml
1.	Fraction 1	100	7	Fraction 7	100
2.	Fraction 2	50	8	Fraction 8	12.5
3.	Fraction 3	50	9	Fraction 9	6.25
4.	Fraction 4	50	10	Fraction 10	50
5.	Fraction 5	100	11	Std. 1: Isoniazid	3.12
6.	Fraction 6	100	12	Std. 2: Rifampicin	3.12

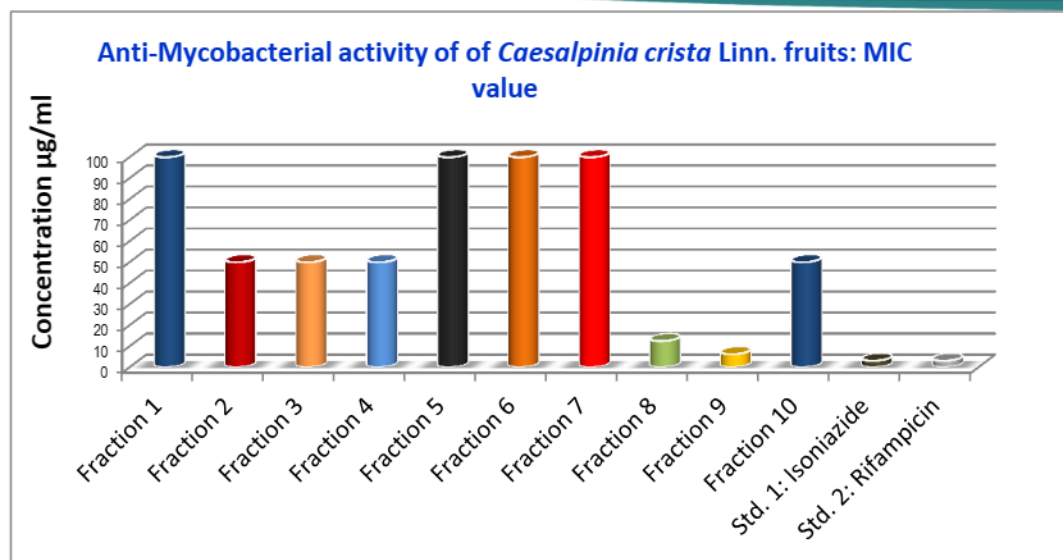


Figure 4. Graphical Illustration of Minimum Inhibitory concentrations vs fractions

The concentrations shown in Table 5 of the *in-vitro* anti-tubercular activity that results were effective in inhibiting the growth of *Mycobacterium*. Table 6 and Figure 2 reveal that the minimal inhibitory concentrations (MICs) for fractions 8 and 9 of the crude extract are 12.5 and 6.25 µg/ml, respectively. Hence, the separated phytochemicals in this fraction exhibited promising effectiveness against *M. tuberculosis*, especially when compared to other fractions and conventional medicines.

Conflict of Interest

There is no known conflict of interest in this publication.

Acknowledgement

The authors acknowledge the help of the research and library facilities provided by the CSIR-Central Drug Research Institute Sector 10, Lucknow - 226021, India.

Conclusion

The fruits of *Caesalpinia crista* were extracted using a solvent and then tested for several phytochemicals. Qualitative analysis alongside sugars, proteins, and lipids also detected secondary metabolites like alkaloids, flavonoids, phenols, tannins, terpenoids, and glycosides. Some of the components necessary for biosynthesis that produces higher derivatives might be found in the fruits of plants. Alkaloids, flavonoids, phenols, tannins, terpenoids, and glycosides, among other phytochemicals, were abundant when the samples were analysed quantitatively. In particular, the ethyl acetate and ethanol extracts of *Caesalpinia crista* fruits had significantly more of this compound than the other three extracts. Alkaloids are necessary for substance metabolism as well as the protective function of animals.

The use of flavonoids to treat malignant tumors is attributed to their capability to halt the growth and spread of malignant tumours. Numerous more disease manifestations have demonstrated the antioxidant ability of phenolic and flavonoid compounds. Several studies have found that combining phenols with plant flavonoid components increases the antioxidant, anticarcinogenic, anti-inflammatory, and other beneficial effects. The inclusion of tannins improves the antibacterial action of extracts, and they also inhibit pathogenic fungi.

Ethyl acetate extract fractions 8 and 9 were found to have identified phytochemical compounds with promising antimycobacterial activity. They have the potential to develop into a game-changing lead medication source for the prevention of tuberculosis due to their promising activity against the *M. tuberculosis* (H37Rv) strain. To sum up, *Caesalpinia crista*'s extracted bioactive fractions and phytochemicals are promising candidates for use as antimycobacterial medicines in future pharmaceutical and light-emitting diode (LED) innovations. We need to better understand the active portions of ethyl acetate and isolate the functional groups responsible for its antibacterial effects.

References

- Almeleebia, T. M., Alsayari, A., & Wahab, S. (2022). Pharmacological and Clinical Efficacy of *Picrorhizakurroa* and Its Secondary Metabolites: A Comprehensive Review. *Molecules*, 27(23), 8316. <https://doi.org/10.3390/molecules27238316>
- Bansal, T., Kaur, H., Kaur, S., & Kaur, S. (2020). Investigation of anticancer and antitubercular activity of some medicinal plants. *Plant Archives*, 20(2), 2764-2768.

- Bhandari, C. B., Rakholiya, K. D., & Kaneria, M. J. (2022). Pharmacognostic and phytochemical evaluation of *Caesalpinia crista* L. leaf. *Journal of Medicinal Plants*, 10(6), 37-39.
- Borris, R. P. (1996). Natural products research: perspectives from a major pharmaceutical company. *Journal of Ethnopharmacology*, 51(1-3), 29-38. [https://doi.org/10.1016/0378-8741\(95\)01347-4](https://doi.org/10.1016/0378-8741(95)01347-4)
- Chen, X. M., Lu, W., Zhang, Z. H., Zhang, J. Y., Tuong, T. M. L., Liu, L. L., & Gao, J. M. (2022). Cassanediterpenoids from the aerial parts of *Caesalpinia pulcherrima* and their antibacterial and anti-glioblastoma activity. *Phytochemistry*, 196, 113082. <https://doi.org/10.1016/j.phytochem.2021.113082>
- Dhulap, S., Mandhare, A., & Deval, K. (2023). Bio-evaluation studies of phytoconstituents-A review of the patents granted and filed by CSIR. *Indian Journal of Natural Products and Resources (IJNPR)[Formerly Natural Product Radiance (NPR)]*, 13(4), 434-450.
- Donga, S., & Chanda, S. (2022). *Caesalpinia crista* seeds mediated green synthesis of zinc oxide nanoparticles for antibacterial, antioxidant, and anticancer activities. *BioNanoScience*, 12(2), 451-462. <https://doi.org/10.1007/s12668-022-00952-8>
- Gokhale, S.B., Purohit, A.P., & Kokate, C.K. (2020). Pharmacognosy, 57th edn. NiraliPrakashan, Pune, pp.157-166.
- Govindaram, D., Kumar, A. R., Krishnan, R., & Savithri, N. (2023). Anti-cariogenic property of *Carica papaya*, *Trachyspermum ammi*, *Caesalpinia cristallinn* extracts and their effect on human oral keratinocytes. *Journal of Oral and Maxillofacial Pathology*, 27(1), 26-32.
- Harborne JB (1998). Phytochemical Methods. Springer International, London. p.7
- Joshi, Y., Rani, H., Kaur, G., Kumar, M., Sindhu, R. K., Kushwah, A. S., & Mittal, R. (2023). Herbal and Ayurvedic Plants as Remedial Approach for Viral Diseases with Focus on COVID-19: A Narrative Review. *Current Traditional Medicine*, 9(3), 66-86. <https://doi.org/10.2174/2215083808666220822124541>
- Juvatkar, P. V., & Jadhav, A. G. (2021). *Caesalpinia bonducella*: A medicinal potential value. *Journal of Pharmacognosy and Phytochemistry*, 10(4), 206-214.
- Khandelwal, K.R. (2005). Practical Pharmacognosy Technique and Experiments. NiraliPrakashan, Pune, pp. 149-156.
- Martolia, J., Soni, H., & Falguni, T. (2021). In Vitro Anti Tubercular Activity and Physicochemical Standardization of Selected Medicinal Plant Extracts. *Indian Journal of Pharmaceutical Sciences*, 83(2), 230-237. <https://doi.org/10.36468/pharmaceutical-sciences.768>
- Mobin, L., Saeed, S. A., Ali, R., Naz, S., & Saeed, S. G. (2021). Antibacterial antioxidant and phenolic fractions analysis of *Caesalpinia crista* seed coat extract and its different fractions. *Pak. J. Bot*, 53(2), 597-603. [https://doi.org/10.30848/PJB2021-2\(18\)](https://doi.org/10.30848/PJB2021-2(18))
- Mukherjee, P.K. (2002). Quality Control of Herbal Drugs, Business Horizon Pharmaceutical Publishers, New Delhi, pp.380-422.
- Panda, N., Mishra, B., Kar, N. R., Panigrahi, S. P., Dash, R. N., & Gangopadhyay, A. (2022). Phytochemical constituent and its pharmacological application of various Types of chemical compounds present in *Cocculushirsutus* (L.) diels. *Journal of Positive School Psychology*, 6(8), 992-1000.
- Rajaiah, E., & Singisala, N. R. (2022). Antibacterial and anti fungal efficacy of some medicinal plants used in Indian herbal medicine. *Journal of Medicinal Plants*, 10(1), 36-42. <https://doi.org/10.22271/plants.2022.v10.i1a.1361>
- Roghini, R., & Vijayalakshmi, K. (2018). Phytochemical screening, quantitative analysis of flavonoids and minerals in ethanolic extract of *Citrus paradisi*. *International Journal of Pharmaceutical Sciences and Research*, 9(11), 4859-4864.
- Shirsat, R., Kengar, A., & Rai, A. (2021). In-vitro callogenesis and screening of antimicrobial activity of callus and seed of *Caesalpinia bonducella* F.: A threatened medicinal plant of Western Ghats. *Journal of Pharmaceutical Research International*, 33(31A), 76-89. <https://doi.org/10.9734/jpri/2021/v33i31A31666>
- Silva, D., Lopes, M. V., Petrovski, Ž., Santos, M. M., Santos, J. P., Yamada-Ogatta, S. F., & Branco, L. C. (2022). Novel Organic Salts Based on Mefloquine: Synthesis, Solubility, Permeability, and In vitro Activity against *Mycobacterium tuberculosis*. *Molecules*, 27(16), 5167. <https://doi.org/10.3390/molecules27165167>

- Trease, GE, Evans, WC (2002). Phytochemicals. In: Pharmacognosy. Saunders Publishers, London., p. 42-393.
- Wagner H, Bladt S. (1996), Plant Drug Analysis: A Thin Layer Chromatography Atlas. Springer publication Germany, pp.1-381.
<https://doi.org/10.1007/978-3-642-00574-9>
- Wijaya, V., Jand'ourek, O., Křoustková, J., Hradiská-Breiterová, K., Korábečný, J., Sobolová, K., et al. (2022). Alkaloids of *Dicranostigma franchetianum* (Papaveraceae) and Berberine Derivatives as a New Class of Antimycobacterial Agents. *Biomolecules*, 12(6), 844.
<https://doi.org/10.3390/biom12060844>
- Zambari, I. F., Muhamad, N. A., & Hafid, S. R. A. (2023). A Comparative Study of Anti-Inflammatory Properties and Activities of Green and Red *Christiavespertilionis* Leaves. *Sains Malaysiana*, 52(1), 211-222.
<https://doi.org/10.17576/jsm-2023-5201-17>

How to cite this Article:

Vipul Dhasade and M. Komala (2023). Investigation for determination of therapeutic potential for antitubercular activity with special reference to *Caesalpinia crista* fruits. *International Journal of Experimental Research and Review*, 30, 321-329.

DOI :<https://doi.org/10.52756/ijerr.2023.v30.029>



This work is licensed under a Creative Commons Attribution-NonCommercial-NoDerivatives 4.0 International License.



Pune District Education Association's
**Shankarrao Ursal College of Pharmaceutical
Sciences & Research Centre, Kharadi, Pune-14.**



Academic Year 2021-22



**International Journal of Biology, Pharmacy
and Allied Sciences (IJBPAS)**

'A Bridge Between Laboratory and Reader'

www.jibpas.com

DEVELOPMENT AND EVALUATION OF FLOATING TABLET USING NOVEL FLOATING AGENT *SACCHAROMYCES BOULARDII* AND HYDROPHILIC POLYMERS

CHITTAM SS^{*1}, BHOSALE AV¹ AND CHAVAN RS²

1: Department of Pharmaceutics, PDEA'S Seth Govind Raghunath Sable, College of
Pharmacy, Saswad, Pune, Maharashtra, India

2: Department of Pharmaceutical Chemistry, PDEA'S Seth Govind Raghunath Sable, College
of Pharmacy, Saswad, Pune, Maharashtra, India

***Corresponding Author: Suvarna Sudhakar Chittam: E Mail: cssgrs@gmail.com**

Received 16th Sept. 2021; Revised 20th Oct. 2021; Accepted 19th Dec. 2021; Available online 1st Aug. 2022

<https://doi.org/10.31032/IJBPAS/2021/11.8.6316>

ABSTRACT

Saccharomyces boulardii, is the unique yeast probiotic that has been effectively used as a good biotherapeutic agent. In aerobic respiration it produces CO₂ and H₂O and in anaerobic alcoholic fermentation it generates ethanol and CO₂. In present investigation this property of yeast is used to generate carbon dioxide in floating tablet. Furosemide is selected as model drug for the development of a floating drug delivery system. Floating tablet prepared by direct compression using *Saccharomyces boulardii* probiotics formulations as floating agent due to its ability to generate carbon dioxide gas and its safety. Different grades of Hydroxy propyl methyl cellulose (HPMC), Carboxy methyl cellulose sodium (CMC sodium) are used as hydrophilic polymers. Calcium hydroxide is used as PH modifier which enhance solubility of furosemide and also maintain integrity of matrix. we concluded that HPMC has capacity to form a more stable gel than CMC sodium. *In vitro* buoyancy study and dissolution study showed that floating tablet containing HPMC E 15 LV floated for more than 24 hr and 85.36 ± 0.53 % drug release up to 12hr. *Saccharomyces boulardii* formulation was good floating agent and it's very easy to prepare tablet using this novel floating agent in combination with different hydrophilic polymers.

Keywords: *Saccharomyces boulardii*, probiotics, facultative anaerobe, hydrophilic polymers, furosemide

INTRODUCTION

Yeasts are eukaryotic microorganisms prevalent in natural environments including the normal microbial flora of humans, on plants, on airborne particles, in water, in food products, and in many other ecological niches. Yeasts are heterotrophic organisms,

in other words, energy metabolism and carbon metabolism are closely linked. In aerobic respiration yeast produces CO₂ and H₂O and in anaerobic alcoholic fermentation it generates ethanol and CO₂. In present

investigation this property of yeast used to generate carbon dioxide in floating tablet [1]. *Saccharomyces boulardii*, is the unique yeast probiotic that has been effectively used as a good biotherapeutic agent to prevent and/or treat variety of gastrointestinal diseases. *Sacchchromyces boulardii* is generally administered in lyophilized powder form. Lyophilized products are stable at room temperature, have the benefit of portability and maintain high viability counts for extended periods [2]. *Saccharomyces boulardii* retains many properties that make it an impending probiotic agent, i.e. it survives during GI transit, it grow well at temperature 37°C, both in vitro and in vivo [3], its high tolerance to gastric acidity, proteolysis enables it to attain high populations in the GI tract. They can forever colonise in the colon and do not easily translocate out of the intestinal tract [4]. They can also be perceived alive throughout the GIT, if they are given in lyophilized form [5]. *Sacchchromyces boulardii* is facultative anaerobe so that it can grow under aerobic or anaerobic conditions [6].

Furosemide is BCS class IV drug having poor aqueous solubility and permeability. It is mainly absorbed in stomach and the upper part of gastrointestinal tract and has a short half life of less than 2hrs. The conventional dosage form shows erratic absorption which results in poor bioavailability (30–60%) [7]. It shows high permeability and better absorption through stomach. Thus furosemide have pH dependent solubility and permeability [8]. So it is selected as model drug for the development of a floating drug delivery system. In present investigation, an attempt has been made to improve the bioavailability of Furosemide by prolonging its duration in the stomach via floating

dosage forms using *Saccharomyces boulardii* probiotics formulation. It is used as floating agent due to its ability to generate carbon dioxide gas and its safety. Solubility and release rate of furosemide controlled by choosing best hydrophilic polymers among HPMC E LV 15, HPMC 50 cp, CMC sodium 200 and 2000 cps. Calcium hydroxide used as PH modifier which increase rate of dissolution of furosemide and also maintain integrity of matrix.

MATERIALS & METHODS

Materials

Furosemide was gifted by (FU) Suleshvari Pharm, Ankaleshwar, Gujarat. Hydroxy propyl methyl cellulose E LV 15 was gifted by Loba chemie pvt.ltd , Hydroxy propyl methyl cellulose 50 cps purchased from John Baker INC., Carboxy methyl cellulose sodium 200 cps and 2000 cps purchased from SDFCL S D Fine Chem Ltd and Fisher Scientific respectively, *Saccharomyces boulardii* probiotic preparation purchased from local market, Hydrochloric acid was gifted by Themis Research lab, Mumbai. Calcium hydroxide, Magnesium stearate and Sodium hydroxide purchased from Poona chemical laboratory, Pune.

Methods

Preparation of Floating tablet of Furosemide
Floating tablets of furosemide were formulated by direct compression technique using polymers like HPMC E 15 LV, HPMC 50 cp , CMC Sodium 200 and 2000 CPs and other ingredients like calcium hydroxide, magnesium stearate, and *Saccharomyces boulardii* probiotic formulation. All ingredients were passed through sieve no # 40, except yeast preparation. First HPMC E 15 LV, calcium hydroxide and furosemide were first mixed using mortar and pestle to get a uniform tablet blend. Finally

Sacchromyces boulardii preparation and magnesium stearate were mixed delicately to above prepared mixture blend. The mixture was then weighed accurately according to the formula and compressed into tablets using

Minipress tablet punching machine (Karnavati) to obtain tablets of desired specifications [9, 10]. Similarly, different formulations were prepared as given in **Table 1**.

Table 1: Composition of Furosemide floating tablets (mg/ tablet)				
Formulation code	PF1	PF2	PF3	PF3
Ingredients (mg)				
Furosemide	20	20	20	20
Calcium hydroxide	10	10	10	10
<i>Saccharomyces boulardii</i> preparation	20	20	20	20
Magnesium stearate	2	2	2	2
HPMC E 15 LV	50	-	-	-
HPMC 50 cp	-	50	-	-
CMC sodium 200 cps	-	-	50	-
CMC sodium 2000 cps	-	-	-	50

EVALUATION TEST

Hardness Test

Monsanto hardness tester was used for evaluation of hardness [10].

Thickness

Vernier caliper was used for evaluation of thickness of tablets [10].

Friability

Friability was expressed in terms of percentage weight loss. For determination of friability Roche Friabilator was used. % friability was evaluated using following formula [11].

Friability (%) = $\frac{W1 - W2}{W1} \times 100$

Where,

W1 = Weight of Tablets (Initial / Before Tumbling) &

W2 = Weight of Tablets (After Tumbling or friability)

Drug content

10 tablets were weighed and crushed using motor pestle. The crushed powder equivalent to average weight of tablets was weighed accurately and put in 100 ml 0.1N NaoH solution for complete extraction of drug and stirred continuously. The solution was filtered using the whatsman filter paper, diluted with 0.1N NaoH solution and the

drug content was determined spectrophotometrically [12].

Uniformity of weight

Twenty tablets were selected randomly, weighed individually using electronic balance and the average weight was calculated. The % weight variation was calculated and checked for weight variation as per IP [13].

$$\% \text{ Weight variation} = \frac{\text{Average weight} - \text{Individual weight}}{\text{Individual weight}} \times 100$$

Tablet Floating Behavior

The floating lag time and total floating duration was determined by visual inspection. The test was performed using USP type II (paddle) apparatus at speed of 50 rpm in 900 mL 0.1N HCl at 37 ± 0.5°C to simulate *in vivo* conditions [14].

In vitro dissolution studies

In vitro dissolution studies were conducted by using paddle dissolution apparatus (Electerolab) at 50 rpm using 900 mL of 0.1 N HCl, (pH 1.2) as a dissolution medium at 37 ± 0.5°C. The absorbance of the sample solution was recorded using UV spectrophotometer at 274 nm. Calculation was carried using disso software (PCP disso

V3) and *in vitro* release profile was determined [15].

RESULTS AND DISCUSSION

The prepared FDDS tablets were evaluated and data enclosed in table 2. From this data it was clear that evaluation parameters of all batches were in acceptable range. uniformity of weight, uniformity of drug content not much deviate from the mean value.

The best release was found to be with lower viscosity grade of HPMC E 15 LV containing formulation PF1, while comparing with higher viscosity grade of HPMC and CMC sodium .

Drug release rate of formulation PF2 was slow as compare to PF1 formulation. The reduction in gel formation. Highly viscous gels cause retardation of drug release [16, 17]. Thus the higher viscosity gel layers of HPMC 50 cps matrices provided a more tortuous and resistant barrier to diffusion, resulting in slower release of drugs from these matrices [18].

In formulation PF3 and PF4 CMC sodium 200 and 2000 cps used as matrix former respectively. CMC sodium a polyelectrolyte gel, is very sensitive to pH changes. The neutralization of charges in acid medium affects the polymer chain conformation and results in a tight network structure. The chain arrangement generates a system of drug release rate as polymer (HPMC) content or viscosity increase may be attributed to stronger connected channels with in the gel matrix that controls the drug release process in a biological environment [19]. And thus it shows lower drug release as compare to PF1 and PF2 but unexpectedly PF3 batch which contain CMC sodium having 200 cp viscosity shows higher drug release than PF2 formulation because HPMC has capacity to

form a more stable gel than CMC sodium. In other words the gel layer formed by the CMC sodium polymer seems to be lower in strength and therefore could not entrap the evolved gas efficiently [20]. hence it breaks down slowly into pieces or erode and shows rapid drug release than PF1.

PF4 formulation which containing higher viscosity grade of CMC sodium shows slow drug release due to formation of tight network structure..

HPMC has capacity to form a more stable gel than CMC sodium [21] and hence formulation PF1 and PF2 shows higher floating duration. This might be due to the faster swelling rate and rapid formation of thick gel around the tablets at higher polymer concentration causing rapid entrapment of generated CO₂. The gas generated is imprisoned and protected within the gel formed by hydration of the polymer, thus lowering the density of the tablet below that of gastric contents, causing buoyancy or floatation [20].

The tablet consisting solely of low viscosity Na CMC eroded in simulated gastric solution so temporary floating or break down in pieces was observed for these formulations.

Formulation PF 4 contain Na CMC having high viscosity, as a polyelectrolyte gel, is very sensitive to pH changes. The neutralization of charges in acid medium affects the polymer chain conformation and leads to a tight network structure and due to this tight network structure it forms rigid tablet [19] and so it shows temporary floating or sinks at a bottom. However, further investigation should be carried out to establish stability and reproducibility of this dosage form.

Table 2: Evaluation of physical parameters of Furosemide floating tablet

Formulation code	Hardness (kg/cm ²) mean ±SD	Thickness (mm) mean ±SD	Friability (%) ±SD	Drug Content Uniformity (%) mean ± SD	Weight variation Average wt in (mg) ± SD	Total Floating time(h)
PF1	5.0±0.25	3.36±0.05	0.49±0.08	100.29±1.30	101.7±2.86	>12
PF2	5.16±0.04	3.33±0.08	0.55±0.06	102.59±1.97	101.1±3.00	>12
PF3	5.13±0.12	3.26±0.12	0.48±0.17	100.57±1.55	100.9±3.23	Float (< 12)
PF4	5.26±0.12	3.2±0.08	0.61±0.048	102.63± 1.92	101.65±2.81	Temporary Float or sink at bottom

*Represents mean ± S.D (n =3)

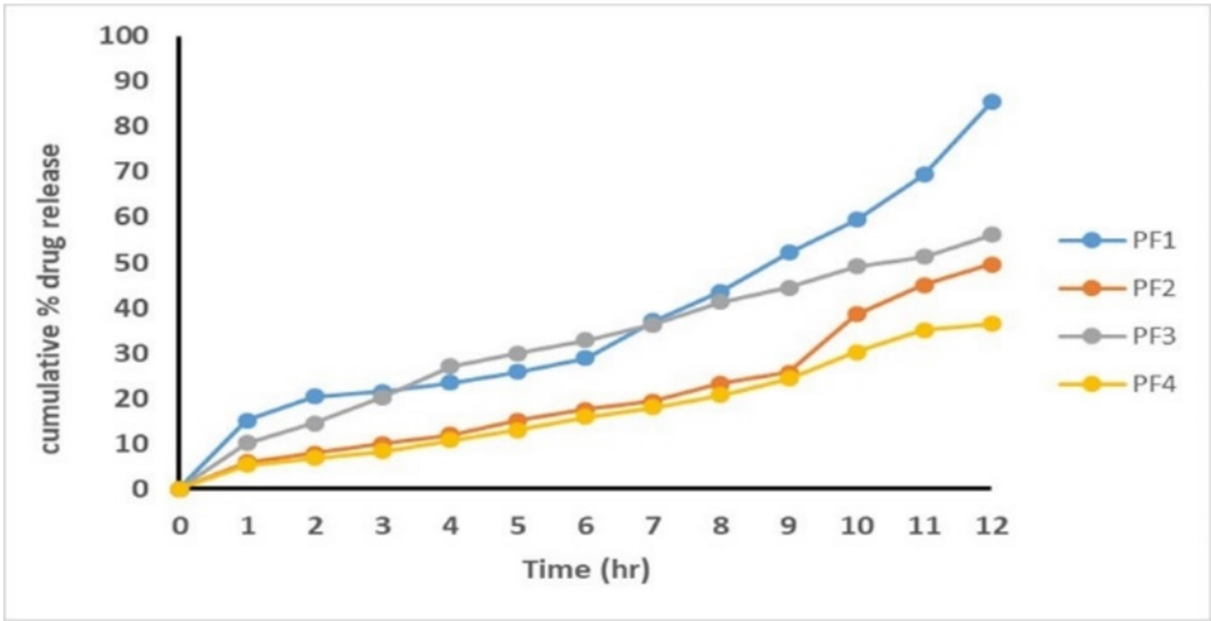


Figure 1 : In vitro Drug Release profiles of all the formulations

CONCLUSION

From present study we concluded that floating tablets of furosemide were successfully developed using novel floating agent *Sacchromyces boulardii* formulation. HPMC E LV 15 is more suitable polymer for designing of GRDDS. However, further studies should be carried out, including *in vivo* investigations, to confirm the findings of this work and to establish stability and reproducibility of this dosage form.

ACKNOWLEDGEMENTS

Author would like to thanks College of Pharmacy, Akluj and College of pharmacy, Saswad for providing necessary facilities and support.

FUNDING

Nil

AUTHORS CONTRIBUTIONS

All the authors have contributed equally.

CONFLICT OF INTEREST

The authors declare no conflict of interest.

ABBREVIATIONS

HPMC: Hydroxy propyl methyl cellulose; carboxy methyl cellulose sodium : CMC sodium ; NaoH: Sodium hydroxide; Hcl :hydrochloric acid; FDDS: Floating Drug Delivery System

REFERENCES

[1] Hatoum R, Labrie S and Fliss I (2012) Antimicrobial and probiotic properties of yeasts: from fundamental to novel applications. Front. Microbio. 3:421. doi: 10.3389/fmicb.2012.00421

[2] Theodoros Kelesidis and Charalabos Pothoulakis. Efficacy and safety of the probiotic *Saccharomyces boulardii* for the prevention and therapy of gastrointestinal disorders. Ther Adv Gastroenterol (2012) 5(2) 111–125. DOI: 10.1177/1756283X11428502

- [3] Czerucka D, Piche T, Rampal P. Review article: yeast as probiotics – *Saccharomyces boulardii*. *Aliment Pharmacol Ther.* 2007;26:767–778.
- [4] Boddy, A.V., Elmer, G.W., McFarland, L.V., Levy, R.H. 1991. Influence of antibiotic on the recovery of *Saccharomyces Boulardii* in rats. *Pharma Res.*, 8 : 796-800.
- [5] Dixit K, Gandhi DN. Biotherapeutic properties of probiotic yeast *Saccharomyces* in fermented dairy products. 2006. Available from <https://www.dairyscience.info/index.php/probiotics/232-yeast-probiotics.html>. Accessed 21 March 2021.
- [6] Dickinson, J.R., and Schweizer, M. (1999). “Carbon Metabolism”. *The Metabolism and Molecular Physiology of S. cerevisiae*. 23.
- [7] Sharad SD, Pradeep RV. Design of a gastroretentive mucoadhesive dosage form of furosemide for controlled release. *Acta Pharm. Sin. B.* 2012;2(5):509–517.
- [8] Patel RC, Keraliya RA, Patel MM, and Patel MM, Patel NM. Formulation of furosemide solid dispersion with micro crystalline cellulose for achieve rapid dissolution. *J Adv Pharm Technol Res.* 2010; 1(2): 180–189. PMID: 22247844; PMCID: PMC3255424.
- [9] Pawar HA, Gharat PR, Dhavale RV, Joshi PR, Rakshit PP. Development and evaluation of gastro retentive floating tablets of an antihypertensive drug using hydrogenated cottonseed oil. *ISRN Pharm.* 2013; 2: 1-9.
- [10] Aswatha Ram HN, Lachake P, Kaushik U, Shreedhara CS. Formulation and evaluation of floating tablets of liquorice extract. *Pharmacognosy Res.* 2010;2(5): 304–308.
- [11] Chauhan YS, Kataria U, Dashora A. Formulation and evaluation of floating tablet for indomethacin. *J Drug Delivery Ther.* 2018; 8(4):338-345.
- [12] Oussama M, Ghenwa I, Mostafa I, Mais A. Assessment of physicochemical properties of furosemide (40mg) tablets marketed in Syria. *J. Chem. Pharm. Sci.*, 2016; 9(4): 2879-2881. 18).
- [13] Puthoori H, Murthy T, Kaushik A, Murthy K. Formulation and evaluation of floating tablets of niacin for sustained release. *Asian J Pharm.* 2012; 6: 31-7.
- [14] Tavakoli N, Varshosaz J, Dorkoosh F, Motaghi S, Tamaddona L. Development and Evaluation of a Monolithic Floating Drug Delivery System for Acyclovir. *Chem. Pharm. Bull.* 2012; 60(2) 172- 177.
- [15] Tiwari SB, Murthy TK, Pai MR, Mehta PR, Chowdary PB. Controlled release formulation of tramadol hydrochloride using hydrophilic and hydrophobic matrix system. *AAPS PharmSciTech.* 2003; 4(3): E31.
- [16] Viral F, Patel NM. Statistical evaluation of influence of viscosity and content polymer on dipyridamole release from floating matrix tablets: A technical note. *AAPS PharmSciTech.* 2007; 8(3): E1-E5.
- [17] Garg R, Gupta G. Preparation and evaluation of gastroretentive

- floating tablets of silymarin. Chem Pharm Bull 2009; 57(6): 545-549.
- [18] Srisagul S, Pornsak S, Satit P. Design of Floating HPMC Matrix Tablets: Effect of Formulation Variables on Floating Properties and Drug Release. Advanced Materials Research 2011; 311-313: 1140-1143.
- [19] Sokar MS, Hanafy AS, El-Kamel AH, El-Gamal S S. Pulsatile core-in-cup valsartan tablet formulations: In vitro evaluation. Asian journal of pharmaceutical sciences 2013; 8: 234-243.
- [20] Farnaz F, Seyed AM. Preparation and In-vitro Evaluation of Gastroretentive Bupropion Hydrochloride Tablets. Tropical Journal of Pharmaceutical Research 2012; 11 (3): 351-359
- [21] Nigusse B, Gebre-Mariam T, Belete. A(2021) Design, development and optimization of sustained release floating, bioadhesive and swellable matrix tablet of ranitidine hydrochloride. PLOS ONE 2021; 16(6): e0253391.

How to Cite:

Sukre, M., Barge, V., Kasabe, A., Shinde, T., & Kandge, M. (2022). Formulation and evaluation of econazole nitrate microemulsion. *International Journal of Health Sciences*, 6(S3), 9181–9190. <https://doi.org/10.53730/ijhs.v6nS3.8243>

Formulation and evaluation of econazole nitrate microemulsion

Manisha Sukre

Department of Pharmaceutical Quality Assurance, P.D.E.A's Shankarrao Ursal College of Pharmaceutical Sciences and Research Centre, Kharadi, Pune, Maharashtra, India

*Corresponding author email: manishasukre21@gmail.com

Vijaya Barge

Department of Pharmaceutical Quality Assurance, P.D.E.A's Shankarrao Ursal College of Pharmaceutical Sciences and Research Centre, Kharadi, Pune, Maharashtra, India

Amit Kasabe

Department of Pharmaceutical Quality Assurance, P.D.E.A's Shankarrao Ursal College of Pharmaceutical Sciences and Research Centre, Kharadi, Pune, Maharashtra, India

Trupti Shinde

Department of Pharmaceutical Quality Assurance, P.D.E.A's Shankarrao Ursal College of Pharmaceutical Sciences and Research Centre, Kharadi, Pune, Maharashtra, India

Mansi Kandge

Department of Pharmaceutical Quality Assurance, P.D.E.A's Shankarrao Ursal College of Pharmaceutical Sciences and Research Centre, Kharadi, Pune, Maharashtra, India

Abstract---Econazole Nitrate microemulsion is presently considered as the novel drug delivery system. It shows prolonged action. It is considered as the imidazole antifungal agent which shows broad spectrum activity. Antifungal agent contains the lipophilic groups which are administered in the microemulsions as they are able to penetrate the system easily. It belongs to BCS Class II drug. i.e., low soluble and highly permeable. The drug efficacy of topical formulation is limited to instability due to poor solubility and low permeability. These are the basic reasons which increase the scope for designing of microemulsion. The topical microemulsion containing Econazole Nitrate prepared using oleic acid as the oil phase, tween 20 as

surfactant and propylene glycol as co- surfactant. The optimized formulation B1 was evaluated for various tests such as Particle size, Zeta potential, pH, Viscosity, Scanning electron microscopy and Electrical conductivity.

Keywords---econazole nitrate, microemulsion, antifungal.

Introduction

The concept of microemulsion was introduced by Hoar and Schulman in the 1940s, it was a clear single-phase solution by triturating a milky emulsion with hexanol¹. Microemulsion are stable, isotropic and clear mixture of oil, water, surfactant and co- surfactant. These are the thermodynamically stable mixtures². Topical drug delivery is defined as the application of pharmaceutical dosage form to skin for direct treatment of cutaneous disorder or cutaneous manifestations of general diseases^{3,4}. The primary advantage of topical application is the avoidance of first pass metabolism. The skin is properly structured membrane and mainly consists of three layers. Stratum corneum is considered as the outermost layer and is considered as the layer for permeation of drugs. It is mainly composed of dead and keratinized cells⁵.

Microemulsion are defined as the good delivery system for delivery of hydrophobic drugs⁶. The main antifungal drugs like azole and imidazole are lipophilic in nature and it is very difficult to incorporate in aqueous gel. To solve that microemulsion came into picture. Lipophilic drugs can be easily incorporated in droplets of o/w microemulsion⁷. Econazole nitrate is an antifungal drug containing imidazole ring which interacts with 14 demethylase a cytochrome P-40 enzyme which converts to lanosterol to ergosterol. Econazole inhibits the ergosterol synthesis which is the essential component of fungal cell membrane, this increases the cellular permeability causing leakage of cellular components, resulting in fungal cell death^{8,9}. Due to low solubility of Econazole Nitrate is incompletely absorbed after oral administration¹⁰. It is also topically applicable in the treatment of cutaneous candidiasis and tinea infections of skin¹¹. The objective of present research was to formulate a stable microemulsion with good consistency, bioavailability, prolonged action and penetration of Econazole Nitrate.

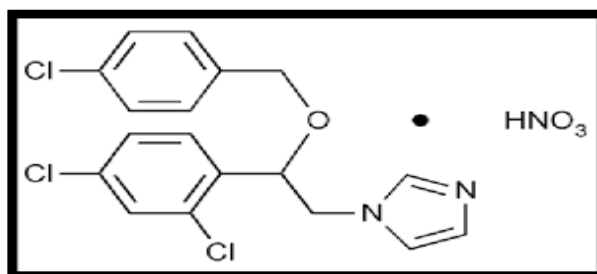


Fig 1. Structure of Econazole Nitrate

Materials and Methods

Materials

Econazole nitrate are procured from Solanki suppliers (Pune, India). Oleic acid and Tween 20 were purchased from Solanki suppliers (Pune, India). All the chemicals and solvent used were of analytical grade.

Methods

Identification of pure drug

Identification of pure drug was carried was by Fourier transform Infra-red Spectrophotometry (Shimadzu 8400S) scanned in the range of 200-400 nm.

Identification of drug by FTIR

FTIR (Shimadzu 8400S) spectrophotometer were used in the range of 400-4000 cm^{-1} using potassium bromide discs (Mixing ratio 1:1) The samples were hermetically sealed in aluminium pans and heated at a constant rate of $10^{\circ}\text{C}/\text{min}$ over a temperature range of 40 to 300°C .

Determination of melting point

Melting point of drug was determined by Thiele's tube method. The small amount of drug in one end closed capillary attached to graduated thermometer and constant heat was supplied to the assembly suspended in the paraffin bath. The temperature at which the drug melts is noted.

Preparation of Microemulsion

Weighed required quantity of drug (Econazole nitrate). Econazole drug was dissolved in oil (oleic acid). The Econazole nitrate was then dissolved with the mixture of surfactant and co-surfactant (Tween 20 and propylene glycol). Finally, the appropriate amount of water is added to the solution mixture drop by drop to get microemulsion.

Table 1
Preparation of Optimized microemulsion

Ingredients	Batch 1	Batch 2	Batch 3	Batch 4
Econazole nitrate (gm)	1	1	1	1
Oleic acid (ml)	7	7	7	7
Tween 20 (ml)	30	25	20	15
Propylene glycol (ml)	30	28	26	24
Distilled (ml)	32	39	49	53

Evaluation of Microemulsion

- **pH¹²:**

The pH of Microemulsion was determined using digital pH meter (Model EQ-610). Before measuring the pH of optimized microemulsion, the pH meter was calibrated with phosphate buffer 4 and 7. Then microemulsion was taken in glass beaker and electrode of pH meter was dipped into it for a minute and pH was noted.

- **Viscosity^{13,14}:**

Viscosity of microemulsion was determined by using Brookfield viscometer (Model LV) using spindle no 62. The apparent viscosity was measured at 10, 20, 30, 50 and 100 rpm. The Brookfield viscometer consist of cup which is stationery and spindle which is rotating. Different rotating size spindles are used and immersed in liquid. For liquids with low viscosity, large sized spindles are used (large diameter and surface area) are used and for higher viscosity small spindles (small diameter and surface area) are used. Rotate the spindle in microemulsion till we get a constant dial reading in the display of viscometer. This procedure is repeated for three times to get a reproducible result.

- **Electrical conductivity¹⁵:**

The conductivity measurement helps in determining whether the formulation is water continuous or oil continuous type. The solubilization of selected oily mixture was measured quantitatively by measuring the electrical conductivity. The conductivity of formulated samples was measured using conductivity meter (Model Systonics- Conductivity meter 304).

- **Drug content^{16,17}:**

Drug content of microemulsion was determine by dissolving accurately weighed 1ml of microemulsion in 10 ml of methanol. After suitable dilution absorbance was recorded by using UV- visible spectrophotometer (UV – 1800 Shimadzu, Japan) at 270 nm.

- **Zeta potential¹⁸:**

HORIBA Scientific SZ -100 measures the Zeta potential of microemulsion to determine the charge on the surface of particles. The material is introduced into the disposable cell, and the Zeta potential is calculated by measuring particle electrophoretic moiety.

- **Particle size determination¹⁹:**

Samples were diluted using distilled water followed by measurement of particle size and Zeta potential in the triplicates and average values. Particle size of microemulsions was determined using HORIBA sz-100 (z type) and the average values \pm SD were recorded.

- **Scanning Electron Microscopy²⁰:**

Scanning electron microscopy provides high resolution imaging that may be used to evaluate diverse materials for surface cracks, defects contaminants and corrosion. When a focused stream of secondary electron interacts with atoms in sample, multiple singles produced that include information about the surface topography using Nova NanoSEM NPEP. All the images are canned at 10000 x with a 5 m dimension scale 303.

Result and Discussion

Fourier Transform Infrared Spectroscopy (FT-IR)

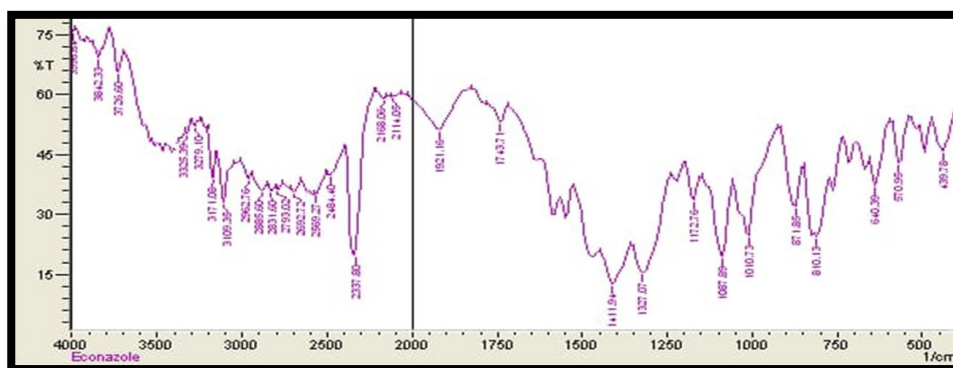


Fig 2. Fourier Transform Infrared Spectroscopy (FT-IR)

Identification and confirmation of pure drug (Econazole Nitrate) was carried out by observing obtained spectra. It showed characteristics peak at 3325.39 (-C-N stretching) imidazole ring; 3109.35 (-C-H stretching); 1411.94 (-C-C stretching); 640 (-C-Cl stretching). These peaks value was in accordance with previously reported spectra of Econazole Nitrate.

UV spectroscopy

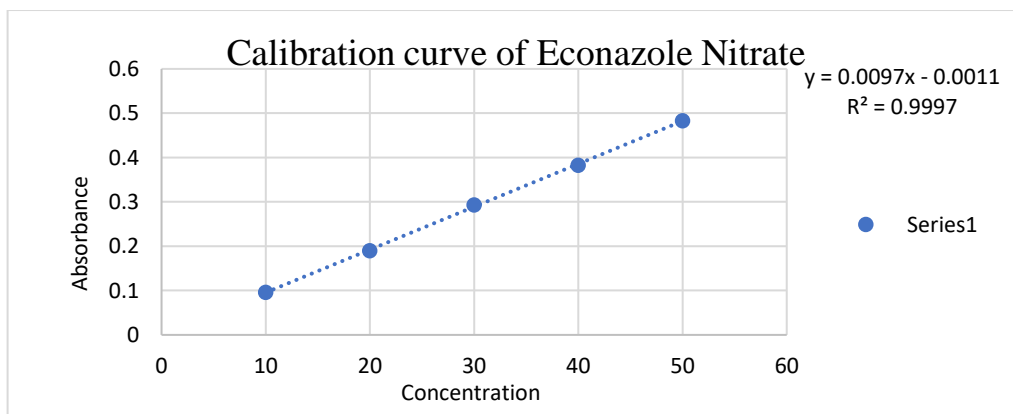


Fig 3. Calibration curve of Econazole Nitrate

The standard calibration curve of Econazole Nitrate was obtained by plotting absorbance against concentration. The calibration curve obeys Beers- Lamberts law and it shows good linearity. Econazole Nitrate in methanol showed maximum absorbance at 270 nm. The concentration range of 0- 50 $\mu\text{g/ml}$ at 270 nm showed coefficient of correlation value of 0.9997.

Melting Point

The melting point of Econazole Nitrate was found to be 162°C.

pH, Drug content (%)

The pH value of optimized Econazole Nitrate microemulsion formulation (B1) was suitable for topical application because the pH of skin in the range 5.5 to 7.0. pH of different microemulsion was checked and it was shown in table. Drug content of all microemulsions was done and result was shown in table:

Table 2
Characterisation of microemulsion

Batches	pH	Drug Content (%)
1	6.2	98.45
2	5.8	96.05
3	5.6	93.67
4	6.1	94.34

Viscosity

Viscosity was determined and result was shown in table

Table 3
Viscosities of microemulsion

Viscosity (RPM)	Batch 1 (cP)	Batch 2 (cP)	Batch 3 (cP)	Batch 4 (cP)
10	126	138	255	348
20	147	157.5	199	238.5
30	153	163	175	192
50	158	166	150	149.4
100	160.5	169	121.5	109

The rheological properties of the microemulsion are evaluated by Brookfield viscometer. These viscosities determination confirm whether the system is o/w or w/o microemulsion.

Determination of Particle size and Zeta potential

Table 4
Determination of Particle size and Zeta potential

Batches	Particle size (nm)	Zeta Potential (mV)
1	35.2	17.5
2	89.6	17.3
3	544.8	21.7
4	1732.6	19.0

The droplet size of microemulsion determines the rate and extent of drug release absorption. The small of particle size of microemulsion lead to more rapid absorption as well enhanced the bioavailability of the formulation. Particle size of

optimized microemulsion (B1) was found to be 35.2 nm; such globules were considered to be suitable for topical administration. The zeta potential governs the stability of microemulsion, it measures the value for stability sample. The high value of zeta potential indicates electrostatic repulsion between droplets. Zeta potential of B1 was found to be 17.5mV.

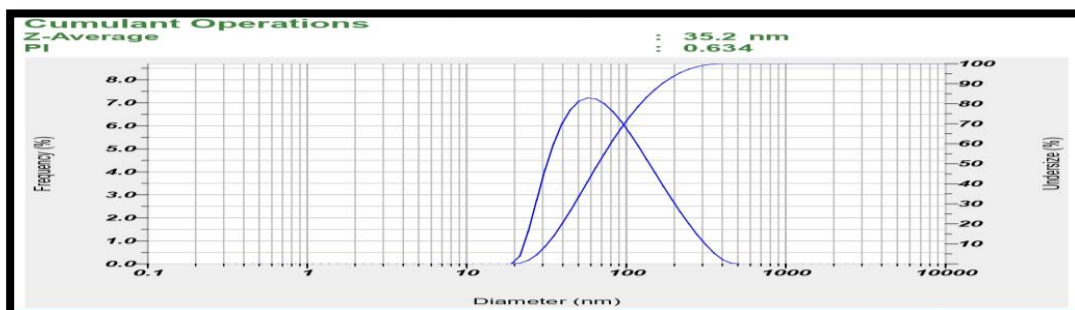


Fig 4. Particle size of optimized formulation (B1)

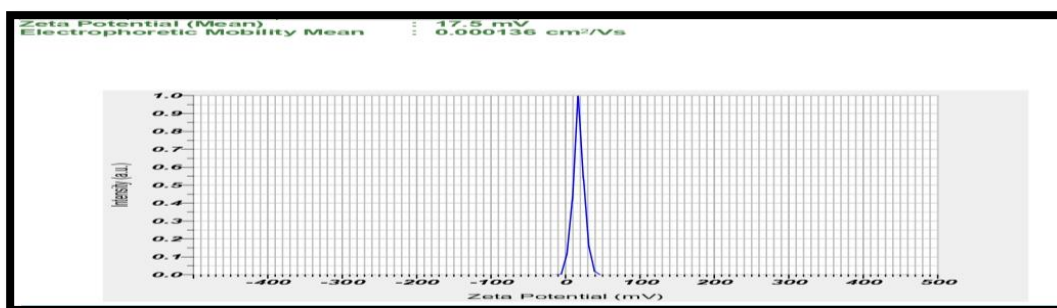


Fig 5. Zeta potential of optimized formulation (B1)

Electrical Conductivity

Table 5
Determination of electrical conductivity

Batches	200 ms	20 ms	2 ms	200 μ s	20 μ s
1	000	00.2	0.19	190	1.
2	000	00.2	0.22	1	1.
3	000	00.2	0.22	1	1.
4	000	00.1	0.18	177	1.

Electrical conductivity is utilized to identify nature of o/w or w/o microemulsion. It is measured using electro conductometer, used to identify whether there is an oil or water as continuous phase. It also identifies the phase inversion phenomenon.

Scanning Electron Microscopy

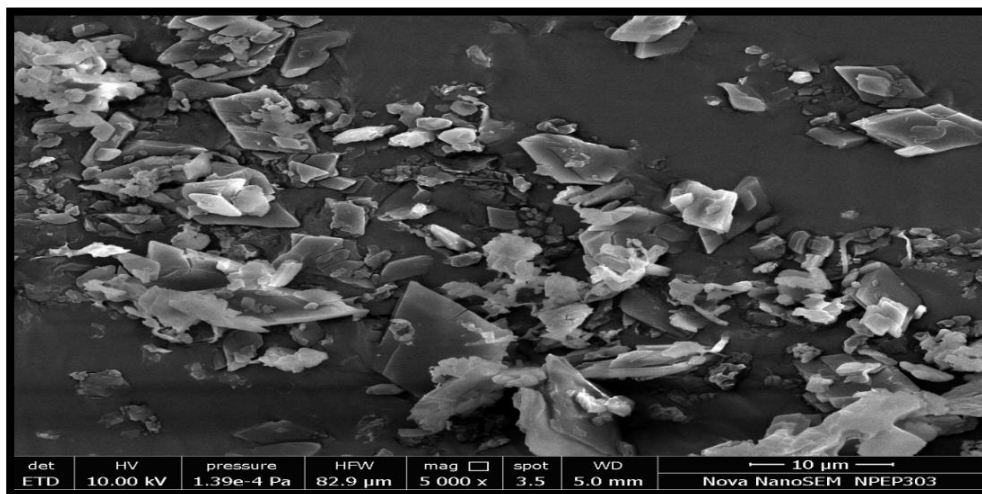


Fig 5. SEM of optimized formulation

The optimized batch of microemulsion was subjected to SEM analysis for morphology and surface topography. The SEM analysis of the microemulsion shows hexagonal and bicontinuous structure.

Conclusion

The topical route is most popular and successful for controlled and targeted drug delivery. The aim of this work is to develop Econazole Nitrate microemulsion for prolonged release based on topical delivery and for also treating skin fungal infection in short duration of time. The microemulsion containing Econazole Nitrate for solubility enhancement was prepared by phase titration method. The microemulsion is most accepted for topical drug delivery as it shows prolonged shelf life. The various formulation was prepared as per the different composition. The prepared formulation of B1 was optimized for results such as particle size, zeta potential and scanning electron microscopy. The stability behaviour can be determined using zeta potential. The formula is prepared with complete and extend release of poorly soluble antifungal drug can be prepared with expected higher penetration through the skin due to small particle size.

Acknowledgment

For the completion of the research work the authors would like to show sincere gratitude to PDEA'S Shankarrao Ursal College of Pharmaceutical Sciences & Research Centre, Kharadi, Pune to provide with a lot of support and help whenever needed.

References

1. Hoar TP, Schulman JH. Transparent water-in-oil dispersions, the oleopathichydromicelle. *Nature* 1943;152:102-3.
2. J. H. Schulman et al. Mechanism of formation and structure of micro emulsions by electron microscopy. *The Journal of Physical Chemistry* 1959; 63: 1677–1680.
3. Kaur J, Kaur J, Jaiswal S, Gupta GD. Recent advances in topical drug delivery system. *Pharm Res.*, 2016; 6(07): 6353-59.
4. Joshi B et al; "Emulgel: A Comprehensive Review on the Recent Advances in Topical Drug Delivery." *International Research Journal of Pharmacy*. 2011, 2(11), 66-70.
5. Patel Rahul R., Kanu R Patel, Mukesh R Patel. Formulation and Characterization of Microemulsion based Gel of Antifungal Drug. – Review.
6. Kumar. K. Senthil et al. Microemulsions as Carrier for Novel Drug Delivery: A Review. *International Journal of Pharmaceutical Sciences Review and Research* 2011; 10: 37-45.
7. Gurjot Kaur, Bedi PMS and Jasjeet K Narang. Topical Nanoemulgel: A Novel Pathway for Investigating Alopecia. *Journal of Nanomedicine & Nanotechnology*. 2017; 8(6): 1-5
8. Gajra B, Pandya, Singh S and Rabari: Mucoadhesive hydrogel films of econazole nitrate formulation and optimization using factorial design. *Journal of Drug Delivery* 2014: 1-14.
9. Gupta PC, Kapoor A and Pandey P: Designing and characterization of econazole nitrate nanostructured lipid carriers gel for topical delivery. *European Journal of Pharmaceutical and Medical Research* 2018; 5(6): 559-67.
10. Shaikh NM and Kulkarni KB: Formulation and evaluation of nanoemulsion for topical application. *Journal of Drug Delivery and Therapeutics* 2019; 9(4): 370-75
11. Patel H C, Parmar G, Seth A K, Patel J D and Patel S R, "Formulation and evaluation of o/w nanoemulsion of ketoconazole", *International Journal of Pharmaceutical Sciences*, 2013, 4(4): 338-351.
12. M Joyce Nirmala, N Chandrasekaran, Amitava Mukherjee. Enhanced solubilization of aqueous insoluble anti-hypertensive drug. *Int J Pharm Pharm Sci* 2012;4:366-8.
13. Zhai G., Zhu W., Guo C., Yu A., Gao Y., Microemulsion-based hydrogel formulation of penciclovir for topical delivery, *International journal of pharmaceutics*, 2009, 378, 152- 158
14. Chena H, Changa X, Dub D, Jin L, "Microemulsion-Based Hydrogel Formulation of Ibuprofen for Topical Delivery", *International Journal of Pharmaceutics*; 2006, 52–58.
15. Patel MR, Patel RB, Parikh JR, and Patel BG, "Effect of Formulation Components on the In vitro Permeation of Microemulsion Drug Delivery System of Fluconazole", *American Association of Pharmaceutical Scientists*; Vol. 10 (3): 2009, 917-923
16. Gui S., Pan E., Liu P., Lu c, Development of Novel Microemulsion-based Hydrogel for Topical Delivery of Sinomenium, *Latin American journal of pharmacy*, 2011,30(5), 931- 936.

17. Vishal Yadav, Prakash Jadhav, Shailaja Dombé, Anjali Bodhe, Pranali Salunkhe. Formulation and evaluation of micro sponge gel for topical delivery of the antifungal drug. *Int J Appl Pharm* 2017;9:30-7
18. Moghimipour E, Salimi A, "Design and Characterization of Microemulsion Systems for Naproxen", *Advanced Pharmaceutical Bulletin*; Vol 3(1): 2013, 63-71.
19. Thansungnoen T, Daduang J and Priprem A: Formulation and evaluation of niosomes encapsulated with KT2 and RT2: antimicrobial and anticancer peptides derived from crocodile leukocyte extract. *International Journal of Pharmaceutical Science and Research* 2020: 11(2); 623-30.
20. Karthik. T.V.K., Martinez, V., Agrawal. V., Porous silicon ZnO/SnO₂ structures for CO₂ detection, *Journal of alloys and Compounds* , 731, 2008, 853-863

How to Cite:

Bhavana, S., Vijaya, B., Amit, K., Shubhangi, K., & Parijat, S. (2022). Formulation and evaluation of a topical gel containing dapsone and fexofenadine HCl. *International Journal of Health Sciences*, 6(S2), 12033–12044. <https://doi.org/10.53730/ijhs.v6nS2.8237>

Formulation and evaluation of a topical gel containing dapsone and fexofenadine HCl

Sakpal Bhavana

Department of Pharmaceutical Quality Assurance, PDEA'S Shankarrao Ursal
College of Pharmaceutical Sciences & Research center, Kharadi, Pune,
Maharashtra, India
Corresponding author email: sakpalbhavana@gmail.com

Barge Vijaya

Department of Pharmaceutical Quality Assurance, PDEA'S Shankarrao Ursal
College of Pharmaceutical Sciences & Research center, Kharadi, Pune,
Maharashtra, India

Kasabe Amit

Department of Pharmaceutical Quality Assurance, PDEA'S Shankarrao Ursal
College of Pharmaceutical Sciences & Research center, Kharadi, Pune,
Maharashtra, India

Karkhile Shubhangi

Department of Pharmaceutical Quality Assurance, PDEA'S Shankarrao Ursal
College of Pharmaceutical Sciences & Research center, Kharadi, Pune,
Maharashtra, India

Suryawanshi Parijat

Department of Pharmaceutical Quality Assurance, PDEA'S Shankarrao Ursal
College of Pharmaceutical Sciences & Research center, Kharadi, Pune,
Maharashtra, India

Abstract---Topical drug administration is a localized method of delivering drugs to specific areas of the body via topical channels such as ophthalmic, rectal, vaginal, and cutaneous. The major route of topical medication delivery is through the skin, which is one of the most easily accessible organs on the human body for topical drug administration. The present investigation involves formulation of topical gel using Dapsone and Fexofenadine HCl. For the treatment of chronic spontaneous urticaria, Dapsone is an effective and well-tolerated second-line treatment. Topical Dapsone is used to treat acne. Dapsone belongs to the sulfone antibiotics family of drugs. It works by reducing inflammation and delaying or preventing bacteria growth. Fexofenadine HCl is an antihistamine medicine that helps with the

symptoms of allergies. Topical gel of Dapsone and Fexofenadine HCl was prepared by using High molecular weight water soluble polymer Hydroxy propyl methyl cellulose such as K35 grade and other excipients including Propyl paraben, oleic acid, Triethanolamine and purified water were reported in the formation of gel. In the present investigation combination of Dapsone and Fexofenadine HCl gel. The formulated gel was evaluated for pH, viscosity, spreadability, extrudability, conductivity, particle size, zeta potential, in vitro drug diffusion studies. Among the formulated gel batch 1 has met all the specifications and was found to be optimized. Efficient delivery of drug to skin application was found to be highly beneficial in localizing the drug to desired site in the skin and reduced side effects associated with conventional treatment.

Keywords---dapsone, fexofenadine HCl, urticaria, topical.

Introduction

Transdermal drug delivery systems (TDDS), are dosage forms that are meant to distribute a therapeutically effective quantity of medicine over a patient's skin. The full morphological, biophysical, and physicochemical features of the human skin must be examined in order to transfer medicinal substances via the human skin for systemic effects. Transdermal administration has an advantage over injectables and oral methods because it improves patient compliance and avoids first-pass metabolism.¹ Transdermal delivery has a variety of advantages compared with the oral route. In particular, it is used when there is a significant first-pass effect of the liver that can prematurely metabolize drugs. Transdermal delivery also has advantages over hypodermic injections, which are painful, generate dangerous medical waste and pose the risk of disease transmission by needle re-use, especially in developing countries. In addition, transdermal systems are noninvasive and can be self-administered. They can provide release for long periods of time (up to one week). They also improve patient compliance and the systems are generally inexpensive.^{2,3} Gels are semisolid formulations that may be applied to the skin or to mucous membranes that are easily accessible, such as the mouth. Colloidal particles, also known as the gelator or gallant, are equally disseminated throughout a dispersion media or solvent to produce a three-dimensional matrix known as the gel.^{4,5} They are normally prepared with the aid of suitable gelling agent like HPMC K35. Substances such as stabilizers and preservatives are used as additives in the formulation of gel.⁶ Chronic spontaneous urticaria (CSU), a subtype of chronic urticaria, is characterised as the development of itchy hives (wheals), angioedema, or both on a daily, or nearly daily, basis for 6 weeks or more with no obvious external cause.^{7,8} Chronic spontaneous urticaria (CSU) is a mast cell-driven condition that causes wheals, angioedema (AE), or both for more than 6 weeks. The autoimmune processes are hypothesised to be involved in the etiopathogenesis of CSU.^{9,10} Second-generation drugs (cetirizine, loratadine, Fexofenadine HCl, desloratadine, levocetirizine, ebastine, and bilastine) are preferable for the treatment of urticaria. Due to their severe drowsiness and adverse effects, as well as their short duration of action, first-generation H1 antihistamines are less favoured. Dapsone is a sulfone

antibiotic with antimicrobial and anti-inflammatory properties. Only 2 small, randomized clinical trials exist on the use of Dapsone in CSU.^{11,12} Dapsone is a sulfone antibiotic having antibacterial and anti-inflammatory effects. Dapsone is bacteriostatic as well as anti-inflammatory. Its antibacterial activity originates from its sulfonamide-like capacity to block dihydrofolic acid production. Dapsone also has a number of anti-inflammatory effects.¹³ Antibiotic and antihistaminic drugs are combined in a gel formulation to treat urticaria. Dapsone was utilised as an antibiotic and Fexofenadine HCl was used as an antihistaminic to treat allergic conditions and reduce wheals and sores on the body. The focus in this study was developing a gel using HPMC K35 which is used as polymer and mixture of excipients using oleic acid, Propyl Paraben, triethanolamine and purified water. The API were added and mixed well in the formulation. Formulated gel were subjected to physical stability. The pH of formulated ranged from 6.8 to 7.2 which is suitable for topical application.

Materials and Methods

Dapsone was purchased from Research-lab Fine Chem Industries (Mumbai, India). Fexofenadine HCl was purchased from Sreekara Organics (Telangana). Oleic acid was purchased from Research-lab Fine Chem Industries (Mumbai, India). Propyl paraben was purchased from Research-lab Fine Chem Industries (Mumbai, India). HPMC K35 was purchased from Ashland Inc. Netherland. Triethanolamine was purchased from Research-lab Fine Chem Industries (Mumbai, India). All the chemicals were of analytical grade.

Methods^{14,15}

Identification of pure drug

Identification of pure drug was carried out by Fourier Transform Infra-red Spectrophotometry (Shimadzu 8400s) scanned in the range of 200-400nm.

Drug-excipient compatibility study

Studies of drug-excipient compatibility are important to ascertain drug and excipients are compatible with each other. DSC graph and IR spectra are used to study drug-excipient compatibility.

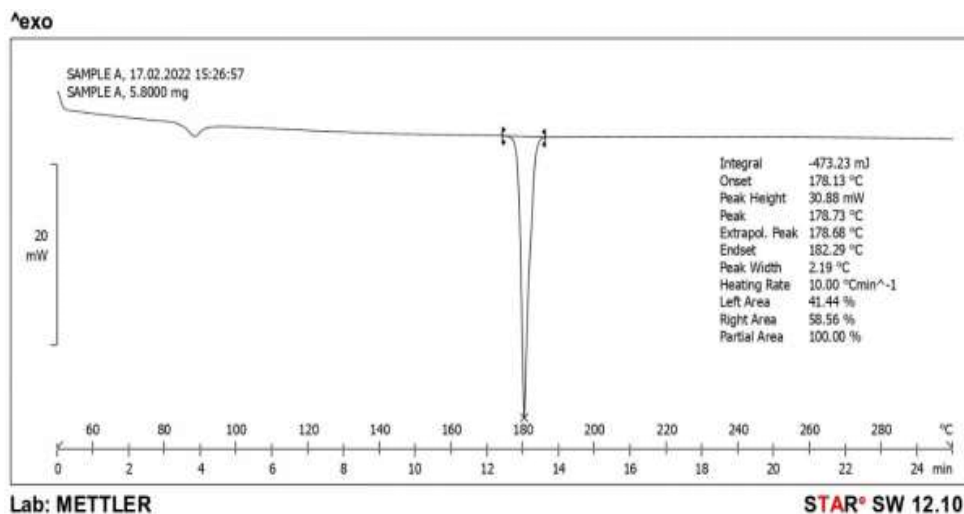
FTIR study

FTIR (Shimadzu 8400s) spectrophotometer were used in the range of 400-4000 cm^{-1} using potassium bromide discs (Mixing ratio 1:1). The samples were hermetically sealed in aluminium pans and heated at a constant rate of $10^\circ\text{C}/\text{min}$ over a temperature range of 40 to 300°C .

DSC study

The DSC thermograms of the Dapsone alone show the peak onset temperature (T_{onset}) is $[178.13^\circ\text{C}]$ and peak transition temperature (T_{peak}) is $[178.73^\circ\text{C}]$. (Fig. 1)

Fig. 1: DSC graph of pure Dapsone



FTIR spectroscopy

The FTIR spectrums of pure Dapsone as well Fexofenadine HCl and physical mixtures of drugs and polymers were studied separately as per the excipients used in the formulation. It was observed that there were no major shifts in the main peaks of either drug. This indicates that there were no compatibility problems with the drug with the polymers and excipients used in the formulation. Dapsone had peaks at 3063.06 (=C-H stretching), 3333.10 (N-H stretching), 1589.40 (C=C stretching), 1280.78 (C-N stretching), and 1134.18 (S=O stretching), while Fexofenadine HCl showed characteristic peak values at 3037 (C-H stretching); 1705 (-COOH stretching); 3294 (O-H stretching) and 1334 (C-N stretching). These peak values were in accordance with previously reported spectra of Fexofenadine HCl(Fig. 3)

Fig.2 FTIR of Dapsone

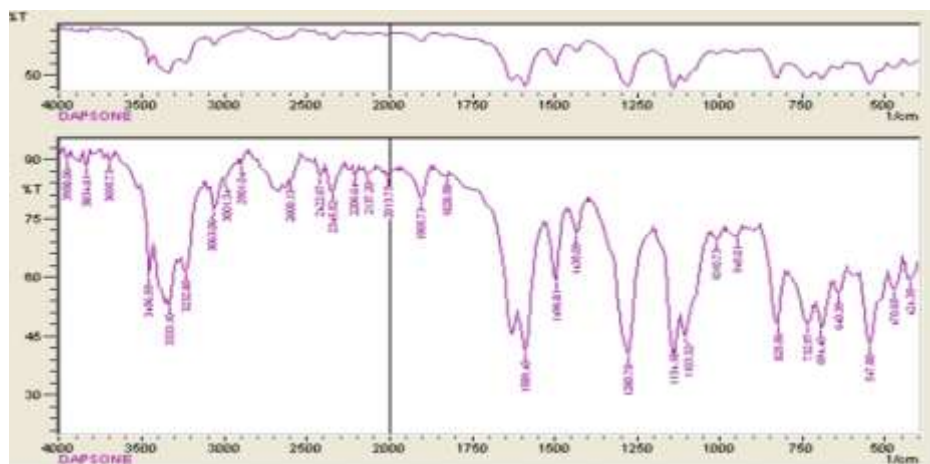
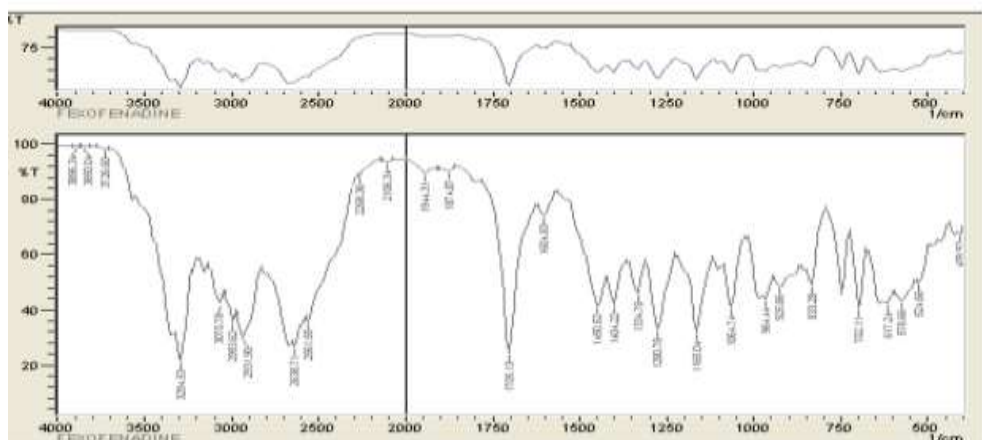


Fig 3 FTIR of Fexofenadine HCl



UV spectroscopy

The linearity of the responses of both drugs was verified at 2–10 $\mu\text{g/ml}$ concentrations. The calibration curve was obtained by plotting the absorbance versus the concentration data and was treated by linear regression analysis. The equation of the linearity curve for Dapsone obtained was $y = 0.1238x + 0.0066$. The linearity curve was found to be linear in the a for mentioned concentrations (the correlation coefficient (r^2) of determination was 0.9996) (Fig.4). Similarly, the equation of the linearity curve for Fexofenadine HCl obtained was $y = 0.036x + 0.0555$. The linearity curve was found to be linear for mentioned concentrations. (the correlation coefficient (r^2) of determination was 0.9991) (Fig.5)

Fig 4: Calibration curve of dapsone

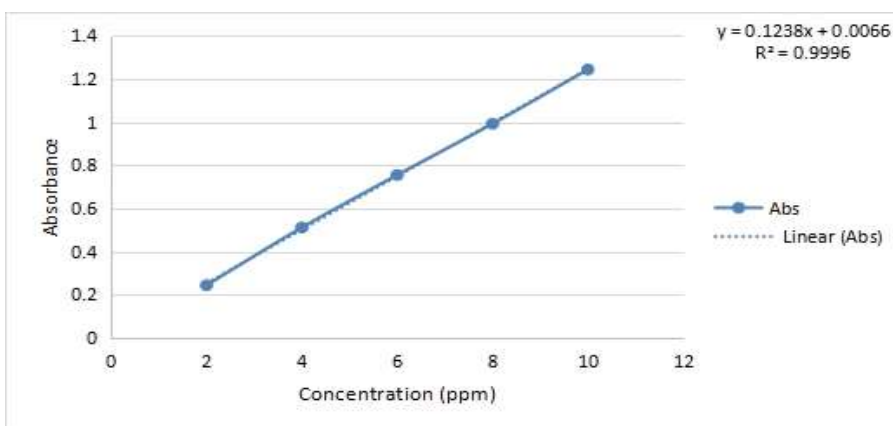
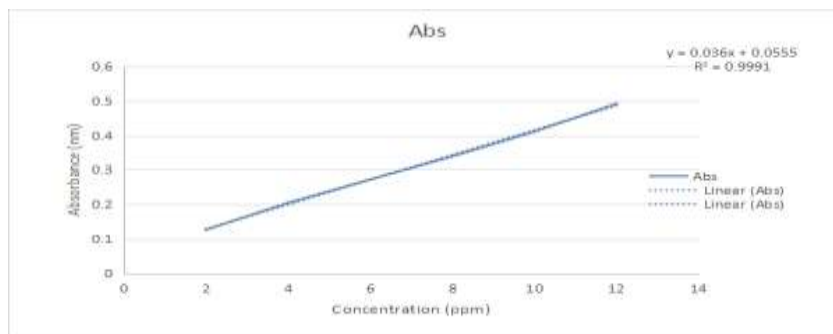


Fig 5: Calibration curve of Fexofenadine HCl



Preparation of Gel

To obtain O/W gel formulation HPMC K35 polymer was solubilized in purified water with constant trituration. In polymer dispersion oleic acid was added slowly with continuous stirring along with Dapsone, Fexofenadine HCl and propyl paraben and was mixed well by continuous trituration. Finally gel was made by adjusting the pH of the mixture to 7.0 using triethanolamine and resulted in desired gel consistency good homogeneity and spreadability.

Table 1- Composition of gel (DF1-DF4)

Name of ingredient	DF1	DF2	DF3	DF4
Dapsone (gm)	0.375	0.375	0.375	0.375
Fexofenadine HCl(gm)	0.25	0.25	0.25	0.25
Propyl paraben (gm)	0.01	0.01	0.01	0.01
HPMC K35 (gm)	0.025	0.05	0.075	0.125
Oleic acid (gm)	1.875	1.875	1.875	1.875
Triethaloamine	Q.S	Q.S	Q.S	Q.S
Purified water	Q.S	Q.S	Q.S	Q.S

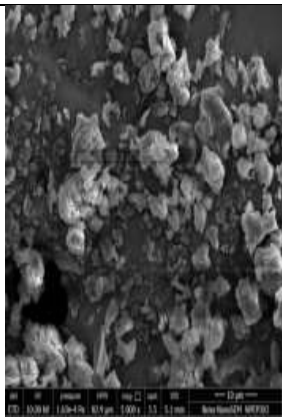
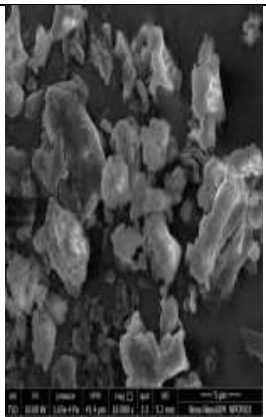
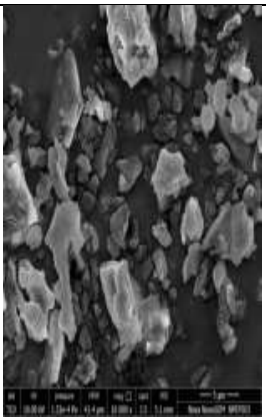
Evaluation of Gel

1. Appearance - Patient compliance is aided by the use of colour. The prepared gels were examined visually for clarity, colour, and particle presence.
2. pH^{16,17} :- A digital pH metre (Model EQ-610) was used to determine the pH of the gel. In distilled water, 1 gm gel was swirled until a homogeneous suspension was obtained. The volume of the solution was increased to 100 mL, and the pH was determined. The pH of each formulation was done in triplicate and average value are determine.
3. Viscosity^{18,19}:- The gel's viscosity was determined using a (LV) Brookfield viscometer. The spindle no. 96 is utilised since the system is non-Newtonian. The viscosity was tested for 2 minutes.

4. Conductivity²⁰:- A direct reading digital conductivity meter (Systronics model no. 304) and dipping type conductivity cell.
5. Zeta Potential²¹:- The charge on the surface of particles is characterized by the HORIBA Scientific SZ-100 by measuring the zeta potential of a gel. The sample is injected into a disposable cell and a measurement of the particle electrophoretic mobility results in the calculated zeta potential.
6. Particle size²²:- Horiba sz-100 windows [z type] were used to investigate the particle size (PS) of the gel. Particle size and zeta potential were measured in triplicates after dilution with distilled water, and the average values \pm SD were recorded.
7. Spreadability²²⁻²⁴:- Excess sample was sandwiched between the two glass slides, and a 100 g weight was used to compress the sample to a uniform thickness for 5 minutes. The pan was filled with weight (250 g). The time it took to separate the two slides in seconds was used as a measure of spreadability.
8. Extrudability^{25,26}:- Measure the force required to extrude the material from tube. Extrudability was based upon the quantity in percentage of gel and gel extruded from lacquered aluminium collapsible tube on application of weight in grams required to extrude at least 0.5 cm ribbon of gel in 10 seconds. +++ excellent ++ very good + average
9. Scanning electron microscopy²⁷:- Scanning electron microscopy (SEM) provides high-resolution imaging that may be used to evaluate diverse materials for surface cracks, defects, contaminants, or corrosion. When a focused stream of secondary electrons interacts with atoms in the sample, multiple signals are produced that include information about the surface topography and sample composition using the Nova NanoSEM NPEP, all pictures were scanned at 10000x with a 5 m dimension scale 303.
10. Content uniformity²⁸:- Drug content of gel was determine by dissolving accurately weighed 1gm of gel in methanol. After suitable dilution absorbance was recorded by using UV- visible spectrophotometer (UV – 1800 Shimadzu, Japan) at 290 and 225nm. Drug content was determined using slope of standard curve.
11. Diffusion studies^{29,30} :- The study was performed using Franz diffusion cells with dialysis membrane with the use of the instrument Jasco V-630 model no V-630. Here the microemulsion based gel equivalent to 10mg of dapsone was placed on the donor compartment and the receptor compartment was filled with mixture of phosphate buffer solution (pH 7.4) and 30% methanol, maintained at 37 ± 10 °C for in vitro diffusion studies, artificial dialysis membrane was soaked in the same buffer solution for 24hrs before mounting on the diffusion cells. Receptor liquid was withdrawn after each hours and sink condition was maintained by replacing liquid kept at same temperature. Dapsone concentration was assayed using UV spectrophotometer. Using the photometric mode for noting absorbance of UV/VIS bandwidth was taken at wavelength of Fexofenadine HCl was taken at wavelength of 225nm and diffusion study of gel was performed.

Evaluation table

Particulars	DF1	DF2	DF3	DF4
Appearance	Off-white to yellow	Off-white to yellow	Off-white to	Off-white to yellow

	gel with suspended particles	gel with suspended particles	yellow gel with suspended particles	gel with suspended particles
Fill volume (gm)	5	5	5	5
pH	6.8-7.2	6.8-7.2	6.8-7.2	6.8-7.2
Conductivity				
1)200ms	1)001	1)001	1)000	1)000
2)20ms	2)00.7	2)00.6	2)00.1	2)00.5
3)2ms	3)0.67	3)0.69	3)0.12	3)0.54
4)200 μ s	4)1	4)1	4)148	4)1
5)20 μ s	5)1	5)1.0	5)1	5)1.0
Zeta potential (mV)	-33.7	-20.0	-20.5	-5.4
Particle size (nm)	1.8	1139.1	1173.0	1423.5
Spredability (gm.cm/sec)	3.2 \pm 0.0156	4.1 \pm 0.0264	3.9 \pm 0.057	4.6 \pm 0.0284
Extrudibility	++	+++	++	+++
Scanning electron microscopy				
Uniformity of content(%)1)Dapsone	99.2	98.7	95.1	99.7
2)Fexofenadine HCl	99.3	99.8	94.6	98.4

In vitro Diffusion studies

Table 2- Data of In-vitro drug release studies of gel of Dapsone (%)

Time (min)	D1	D2	D3	D4
5	12.1273	12.87677	8.42995	11.5277
10	18.7725	18.58268	19.1023	20.56662
15	27.4263	33.5069	29.5947	32.4627

20	33.6169	44.55907	32.6775	42.3556
25	43.72966	50.19503	47.2471	49.0408
30	59.3684	64.28993	62.3163	68.2321
45	79.1093	82.1021	74.6275	79.0193
60	100.9287	95.062	77.2706	97.07143

In-vitro drug release profile of gel of Dapsone

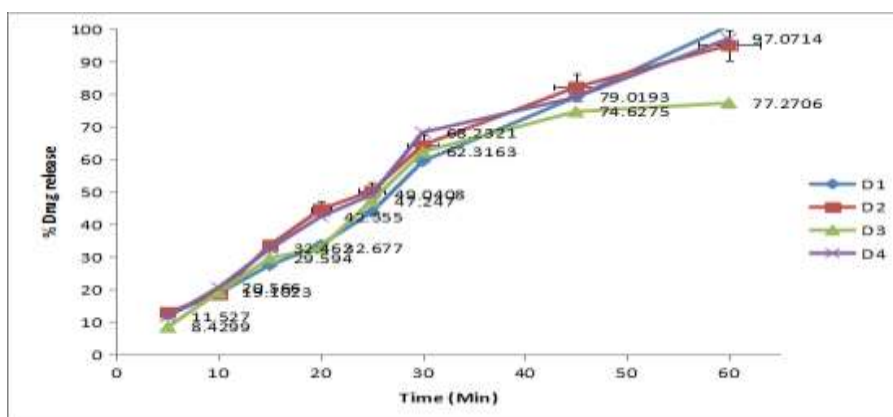
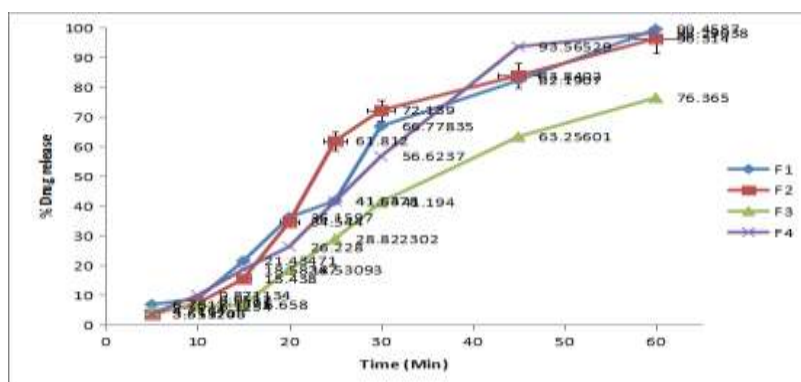


Table 3- Data of In-vitro drug release studies of gel of Fexofenadine HCl (%)

Time (min)	F1	F2	F3	F4
5	6.761168	3.5137	4.7164	3.6512
10	8.6512	7.1391	6.1254	9.87113
15	21.4347	15.4381	6.65807	18.582
20	36.1597	34.544	18.5309	26.2285
25	41.6408	61.8127	28.8230	41.5378
30	66.7783	72.1391	41.1941	56.6237
45	82.190	83.8402	63.256	93.5652
60	99.458	96.3144	76.365	98.2903

Fig. 6: In-vitro drug release profile on gel of Fexofenadine HCl



Viscosity results DF1 (Spindle number-96)

RPM	Surface (cP)	Middle (cP)	Bottom (cP)
5	12380	39940	93560
10	10220	21870	52220
20	3328	11970	28080
30	1500	3806	19220
40	1519	3413	12300
50	1250	2797	10410
60	7781	1603	6659

Viscosity results DF2 (Spindle number-96)

RPM	Surface (cP)	Middle (cP)	Bottom (cP)
5	33560	87000	10820
10	22780	51660	55030
20	10270	28550	30520
30	9750	28550	29810
40	3431	13070	13820
50	3078	11270	12710
60	1641	7566	7594

Viscosity results DF3 (Spindle number-96)

RPM	Surface (cP)	Middle (cP)	Bottom (cP)
5	25880	31540	56250
10	25865	35038	19450
20	7688	21450	19360
30	6719	19630	7913
40	3394	7669	8325
50	3094	10170	8750
60	2897	6009	7828

Viscosity results DF4 (Spindle number-96)

RPM	Surface (cP)	Middle (cP)	Bottom (cP)
5	2531	30630	43910
10	2625	22970	28590
20	13590	12890	16920
30	8438	7625	12780
40	3031	3581	9469
50	2953	2750	8188
60	2531	1528	6563

Conclusion

Dapsone is a sulfone derivative, used for the topical as well as systemic microbial infections. Fexofenadine HCl is an antihistamine used to relieve the symptoms of

allergies. In the present study, an attempt was made to formulate topical gel of Dapsone and Fexofenadine HCl for efficient delivery of drug across the skin. Various formulation (F1, F2, F3, F4, F5) were developed by using suitable polymer (HPMC K35). Developed formulations of gel were evaluated for the physiochemical parameters such as drug content, viscosity, spreadability, in vitro diffusion, zeta potential and particle size. Viscosity studies of various formulations revealed that formulation F1 was better when compared to other formulation. pH of the formulation was within the accepted limit of 6.8-7.2 and did not produce skin irritation. Zeta potential of the optimized batch was -33.7 which indicates good stability of the formulation. Particle size was seen to be 1.8 due to which it has good permeation through the skin barriers. From among all the developed formulation of batch 1 was selected as the best formulation. The objective of the present work of formulation and evaluating of topical gel has been achieved.

Acknowledgement

For the completion of the research work the authors would like to show sincere gratitude to PDEA'S Shankarrao Ursal College of Pharmaceutical Sciences & Research center, Kharadi, Pune to provide with a lot of support and help whenever needed.

References

1. Loyd V. Allen Jr, Nicholas G. Popovich, Howard C. Ansel. Pharmaceutical dosage forms and drug delivery systems, 8th Edition., Wolter Kluwer Publishers, New Delhi, 2005 pp. 298-299.
2. Miller, M.A. & Pisani, E. The cost of unsafe injections. *Bull. World Health Organ.* 77, 808-811 (1999).
3. Guy, R.H. & Hadgraft, J. (eds.) *Transdermal Drug Delivery* (Marcel Dekker, New York; 2003).
4. Lieberman HA, Rieger MM, Banker GS. *Pharmaceutical Dosage Forms: Disperse Systems*, 2nd ed., Marcel Dekker, New York, 1998.
5. Buerkle LE, Rowan SJ. Supramolecular gels formed from multi-component low molecular weight species. *Chem Soc Rev.* 2012;41:6089-6102.
6. Abhishek Soni 1 *, Dr. Amit Chaudhary 1, Dr. Shivali Singla 2, Dr. Sachin Goyal 2. (2019). REVIEW ON: NOVEL APPROACH IN PHARMACEUTICAL GEL. *Journal of Pharma Research*, 8(6), 429-435.
7. Gimenez Arnau AM, Valero Santiago A, Bartra Tomas J et al (2019) Therapeutic strategy according to differences in response to omalizumab in patients with chronic spontaneous urticaria. *J Investig Allergol Clin Immunol* 29(5):338348. <https://doi.org/10.18176/jiaci.0323>.
8. Westby EP, Lynde C, Sussman G (2018) Chronic urticaria: following practice guidelines. *Skin Therapy Lett* 23(3):1-4.
9. S.W. Lanigan *et al.* Association between urticaria and hypothyroidism *Lancet* (1984)
10. M. Caproni *et al.* Chronic idiopathic urticaria: infiltrating cells and related cytokines in autologous serum-induced wheals *Clin Immunol* (2005).
11. Lang DM. Evidence-based diagnosis and treatment of chronic angioedema. *Allergy Asthma Proc.* 2014;35:10-6. urticaria

12. Zhu YI, Stiller MJ. Dapsone and sulfones in dermatology: overview and update. *J Am Acad Dermatol.* 2001;45(3):420-434. doi:10.1067/mjd.2001.114733.
13. Coleman MD. Dapsone: modes of action, toxicity and possible strategies for increasing patient tolerance. *Br J Dermatol* 1993; 129: 507–513.
14. Nappinnai M., Pakalapati S, Arimilli R. Rofecoxib gels-preparation and evaluation. *Indian Drugs.* 2006; 43(65):13-51.
15. Cartensen JT, Rhodes CT (2005) Preformulation. In: Cartensen JT, Rhodes CT (eds.). *Drug Stability principles and practices* (3rd edn)., Marcel Dekker Inc., New York, USA.
16. Murthy TGEK, Kishore VS. Formulation and evaluation of transdermal gels of diltiazem hydrochloride. *Indian J. Pharm. Educ. Res.* 2008; 42(3): 272-276.
17. Rupal J, Kaushal J, Setty MC, Dipti P. Preparation and evaluation of topical gel Valdecoxib. *Inter J. Pharm. Sci. Research.* 2010; 2(1):51-54.
18. Kauri LP, Garg R, Gupta GD. Development and evaluation of topical gel of minoxidil from different polymer bases in application of alopecia. *Int. J. Pharmacy Pharm. Sci.* 2010; 2(3): 43-47
19. <https://www.brookfieldengineering.com>
20. Kumar Nrendra (2014), Study Of extraction, Isolation and Physico-Chemical Properties of Psidium Gaujava, *International Journal Of Research Science and Management*, ISSN: 2349- 5197
21. Hiemenz, *Principles of Colloid and Surface Chemistry*, Marcel Decker, 1977
22. Chowhan ZT. Role of binders in moisture-induced hardness increase in compressed tablets and its effect on in vitro disintegration and dissolution. *J. Pharm. Sci.* 1980; 69; 1-4.
23. Rupal J, Kaushal J, Setty MC, Dipti P. Preparation and evaluation of topical gel Valdecoxib. *Inter J. Pharm. Sci. Research.* 2010; 2(1):51-54
24. Gupta A, Mishra AK, Singh AK, Gupta V, Bansal P. Formulation and evaluation of topical gel of diclofenac sodium using different polymers. *Drug Invent. Today.* 2010; 2: 250-253.
25. Ahmed M, Gendy E, Alaa A. In vitro Release Studies of Flurbiprofen from Different Topical Formulations. *Drug Dev. Ind. Pharm.* 2002; 28(7):823-831.
26. Goyal S, Sharma P, Ramchandani U, Shrivastava SK. et al. Formulation development and characterization of aceclofenac gel containing linseed oil and ginger oleoresin. *Int. J. Pharm. Biol. Arch.* 2011; 3(3):1087-1094.
27. Karthik. T.V.K., Martinez, V., Agrawal. V., Porous silicon ZnO/SnO₂ structures for CO₂ detection, *Journal of alloys and Compounds* , 731, 2008, 853-863
28. Michaels A.S, Chandrasekaran S. K, Shaw J.E. Drug permeation through human skin: Theory and invitro experimental measurement. *AIChE J.* 2004;21(5) 16 Williams AC, Barry BW. Penetration enhancers. *Adv drug deliv rev.* 2004;56(5):603-618.
29. Belgamwar V, Patel H, Joshi A, Agrawal A, Surana S. Design and development of nasal mucoadhesive microspheres containing tramadol HCl for CNS targeting. *Drug Delivery, Informa Healthcare*, 2011;18(5):353-360.
30. Patel, J., Ketkar, S., Patil, S., Fearnley, J., Mahadik, K. R., & Paradkar, A. R. (2015). Potentiating antimicrobial efficacy of propolis through niosomal-based system for administration. *Integrative medicine research*, 4(2), 94-101

How to Cite:

Shinde, T., Barge, V., Kasabe, A., Sukre, M., & Kandge, M. (2022). Formulation and evaluation of microemulsion containing griseofulvin. *International Journal of Health Sciences*, 6(S3), 9206–9215. <https://doi.org/10.53730/ijhs.v6nS3.8245>

Formulation and evaluation of microemulsion containing griseofulvin

Trupti Shinde

Department of Pharmaceutical Quality Assurance P.D.E.A's Sankarrao Ursal
College of Pharmaceutical Sciences and Research Centre, Kharadi, Pune,
Maharashtra, India

*Corresponding author email: truptiss89@gmail.com

Vijaya Barge

Department of Pharmaceutical Quality Assurance P.D.E.A's Sankarrao Ursal
College of Pharmaceutical Sciences and Research Centre, Kharadi, Pune,
Maharashtra, India

Amit Kasabe

Department of Pharmaceutical Quality Assurance P.D.E.A's Sankarrao Ursal
College of Pharmaceutical Sciences and Research Centre, Kharadi, Pune,
Maharashtra, India

Manisha Sukre

Department of Pharmaceutical Quality Assurance P.D.E.A's Sankarrao Ursal
College of Pharmaceutical Sciences and Research Centre, Kharadi, Pune,
Maharashtra, India

Mansi Kandge

Department of Pharmaceutical Quality Assurance P.D.E.A's Sankarrao Ursal
College of Pharmaceutical Sciences and Research Centre, Kharadi, Pune,
Maharashtra, India

Abstract---The aim of the following research is to formulate a microemulsion containing drug Griseofulvin. Griseofulvin is an antifungal agent which inhibits the mitosis. It is recommended orally for treatment of fungal disease. It is used to treat skin infections such as jock itch, athletes foot and ringworm. Also it is used to treat the fungal infections of scalp, toenails and fingernails. Griseofulvin is a BCS II class drug. It is highly lipophilic poorly soluble drug with low oral bioavailability. The present aim was to increase the solubility by microemulsion system for topical delivery. Microemulsions are clear, stable and isotropic liquid. They show advantages such as spontaneous preparation, scale up, ease of preparation, improving

drug solubility of hydrophobic drugs. It is also used to increase the bioavailability of drug. These also aim at controlling the bioavailability of various drug molecules. The review put forward the development in microemulsion containing system. They improve solubility, chemical stability and oral bioavailability of poorly water soluble drugs. There is formulation of four different batches. The batches differ in quantity of surfactant and co- surfactants.

Keywords---griseofulvin, microemulsion, particle size, zeta potential, scanning electron microscopy.

Introduction

The formulation and development of novel drug delivery system with the nature of enhancing the effectiveness of the existing of drug is an ongoing process in pharmaceutical research. The microemulsion concept was introduced in 1940s by Hoar and Schulman who generated a clear single phase solution by triturating milky emulsion with hexanol¹. Microemulsion are clear, transparent, thermodynamically stable dispersions of oil and water, stabilized by an interfacial film of surfactant frequently in combination with a co-surfactant². Alternative names for this system are often used such as swollen micelle, transparent emulsion, solubilized oil and micellar solution. Microemulsions are bicontinuous system that are essentially composed of bulk phases of water and oil separated by a surfactant/cosurfactant rich interfacial region³. These systems have advantages over conventional emulsions in that they are thermodynamically stable liquid systems and are spontaneously formed.

Griseofulvin is an effective antifungal drug for several species of fungi, such as *Microscopium*, *Epidermophyton* and *Trichophyton*⁴. Griseofulvin is practically insoluble in water and is a biopharmaceutics classification system Class II drug, which means that it has a low solubility and a high permeability⁵. Due to its low water solubility, Griseofulvin has a dissolution rate, which lead to low drug bioavailability. Low Griseofulvin absorption can be increased by formulating it as a microemulsion, which lead to selection of Griseofulvin microemulsion gel preparation as the topic for this study⁶. Griseofulvin may cause some systemic side effects if given orally over the long term. Side effects that may arise include proteinuria, nephrosis, leukopenia, hepatitis, clotting disorders, liver enzyme elevation, hyperbilirubinemia, and bleeding in the digestive tract. To avoid these adverse effects, a Griseofulvin microemulsion gel preparation for topical use was formulated to overcome these problem.

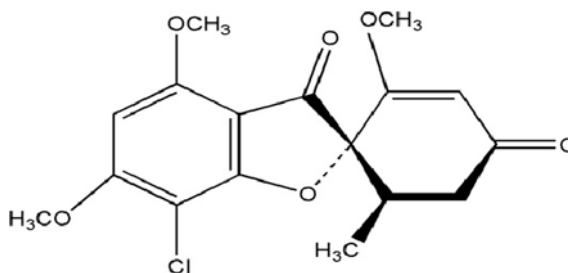


Fig 1. Structure of Griseofulvin

Materials and Methods

Materials

Griseofulvin was purchased from the Solanki suppliers (Pune, India). All the Chemicals used as oleic acid, propylene glycol, Tween 20 were of analytical grade.

Methods

Identification of pure drug

Identification of pure drug was carried by Fourier Transform Infra-red spectrophotometry (Shimadzu 800s) scanned in the range of 200-400 nm.

Identification of drug by FTIR

FTIR (Shimadzu 8400s) spectrophotometer were used in the range of 400- 4000 cm^{-1} using potassium bromide discs (mixing ratio 1:1). The samples were hermetically properly sealed in aluminium pans and heated at a constant rate of 10°C /min over a temperature range of 40-300°C.

Determination of Melting point

Melting point of drug was determined by Thiele's tube method. The small amount of drug in one closed end closed capillary attached to graduated thermometer and constant heat was supplied to the assembly suspended in paraffin bath. The temperature at which the drug melts is noted.

Formulation of Microemulsion

Weighed required quantity of drug (Griseofulvin). Griseofulvin drug was dissolved in oil (oleic acid) and this phase is sonicated for 5 min. The phase of surfactant and co- surfactant was prepared. Both the phases are mixed together by using magnetic stirrer. The addition of dropwise water was done to obtain 100 ml microemulsion. 100 ml microemulsion was prepared.

Table 1
Preparation of Optimized Microemulsion

Ingredients	Batch 1	Batch 2	Batch 3	Batch 4
Griseofulvin (gm)	1	1	1	1
Oleic acid(ml)	7	7	7	7
Tween 20 (ml)	30	25	20	15
Propylene glycol(ml)	30	28	26	24
Distilled water (ml)	32	39	46	53

Evaluation of Microemulsion

pH

The pH of Microemulsion was determined using digital pH mete (Model EQ-610). Before measuring the pH of optimized microemulsion, the pH meter was calibrated with phosphate buffer 4 and 7. Then microemulsion was taken in glass beaker and electrode of pH meter was dipped into it for a minute and pH was noted. As pH of skin is usually 5.1 to 5.6, the pH of microemulsion of topical delivery should be always considered within this range.

Viscosity

The viscosity of microemulsion was determined by using Brookfield viscometer (Model LV) using spindle no 62. The apparent viscosity was measured at 10, 20, 30, 50 and 100 rpm. The Brookfield viscometer consist of cup which is stationery and spindle which is rotating. Different rotating size spindles are used and immersed in liquid. For liquids with low viscosity, large sized spindles are used (large diameter and surface area) are used and for high viscosity small spindles (small diameter and surface area) are used. Rotate the spindle in microemulsion till we get a constant dial reading in the display of viscometer. This procedure is repeated for three times to get a reproducible result.

Electrical conductivity

The conductivity measurement helps in determining whether the formulation is water continuous or oil continuous type. The solubilization of selected oily mixture was measured qualitatively by measuring the electrical conductivity. The conductivity of formulated samples was measured using conductivity meter (Model Systonics -Conductivity meter 304).

Drug content

Drug content of microemulsion was determined by dissolving accurately weighed 1 ml of microemulsion in 10 ml of methanol. After suitable dilution absorbance was recorded by using UV-visible spectrophotometer (UV-1800 Shimadzu, Japan) at 270 nm. The drug content is determined using an equation that includes a liner regression analysis of the calibration curve.

Zeta potential

Zeta potential is used to determine the stability of the prepared microemulsion. The charge on the surface of the particles is characterized by HORIBA SZ-100 by measuring the Zeta potential of the microemulsions. The sample is injected into a disposable cell and measurement of the particle electrophoretic moiety results in the calculation of Zeta potential.

Particle size determination

Samples were diluted using distilled water followed by measurement of particle size and Zeta potential in the triplicates and average values. Particle size of microemulsions was determined using HORIBA sz-100 (z type).

Conductivity

The Conductivity of prepared microemulsion was measured by digital conductivity meter. Voltage is applied between two electrodes in a probe immersed in a sample. The drop in voltage caused by resistance of sample is used to calculate the conductivity per centimetre

Scanning Electron Microscopy

SEM provides detailed image of the structure which is not possible by TEM. It is also used in the particle counting and size determination. The average magnification of scanning electron microscopy is 20X to 30,000X.

Results and Discussion

UV Spectroscopy

Calibration is defined as the process of assessment and refinement of the accuracy and precision method. It is the general method for determining the concentration of substance in an unknown sample by comparing to the unknown to set of standard samples of unknown concentration.

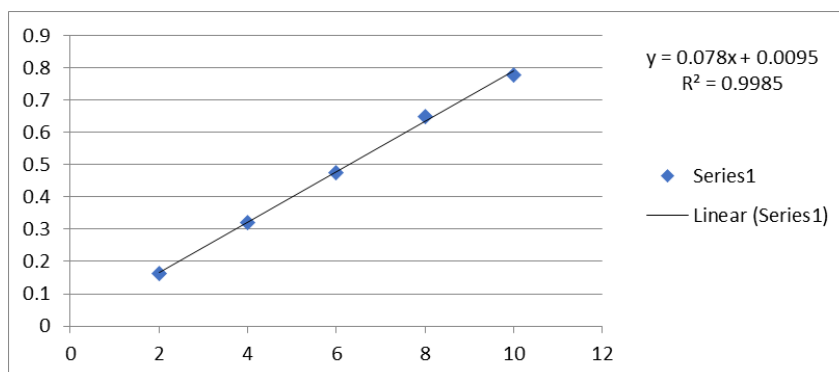


Fig 2. Calibration curve of Griseofulvin

IR Spectroscopy

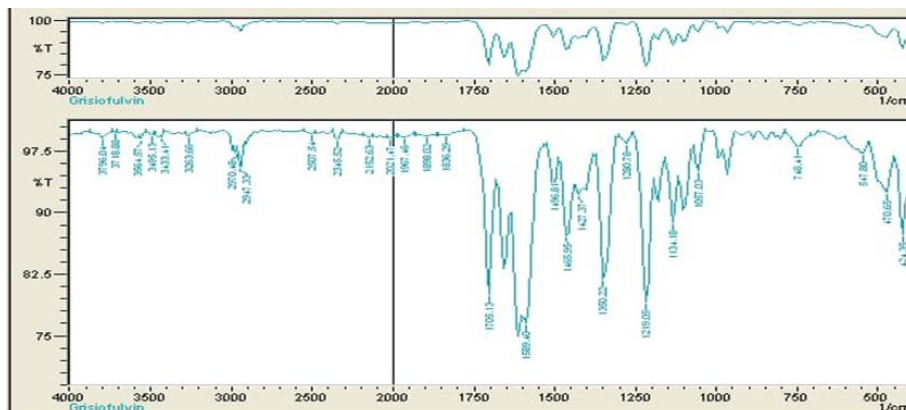


Fig 3. Interpretation of IR of Griseofulvin

Table 2
Interpretation of IR of Griseofulvin

S. No	Reference wavenumber	peak	Observed wavenumber	peak	Functional groups
1	1500-1600		1589		C=C
2	600-1500		1465		C-H
3	3200-3400		3263		O-H
4	1680-1760		1705		C=O

Melting Point

The melting point of Griseofulvin was found to be 220°C.

pH, Drug Content

The pH of microemulsion of topical delivery should be always considered within this range. pH of different microemulsions was checked and it was shown in table. Drug content of all microemulsions was done and result was shown in table:

Table 3
Determination of pH, drug content

Batches	pH	Drug content (%)
1	5.8	94.89
2	6.5	92.78
3	6.2	98.89
4	5.6	90.70

The higher the amount of drug more it will show concentrated formulation. These formulations range from concentrated aqueous.

Viscosity

Viscosity was determined and results was shown in table

Table 4
Viscosities of microemulsion

Viscosity (RPM)	Batch 1 (cP)	Batch 2 (cP)	Batch 3 (cP)	Batch 4 (cP)
10	000	00.0	0.03	1.
20	000	00.0	0.03	1.
50	000	00.0	0.03	1.
100	000	00.0	0.01	1.2

Determination of Particle size and Zeta potential

Table 5
Determination of Particle size and zeta potential

Batches	Particle size	Zeta Potential (mV)
1	5237.3	-36.4
2	785.9	-46.2
3	377.3	-46.5
4	2156.2	-44.5

The particle size of microemulsion is determines the rate and extent of drug release absorption. The small of particle size is required for lead to more rapid absorption as well enhanced the bioavailability of the formulation. Particle size of optimized microemulsion was found to be 377.3 nm; such globules were considered to be suitable for topical administration. The zeta potential governs the stability of microemulsion, it measures the value for stability sample. The negative zeta potential indicates the droplets of microemulsion having no charge i.e. the system is stable. Zeta potential was found to be -46.5mV.

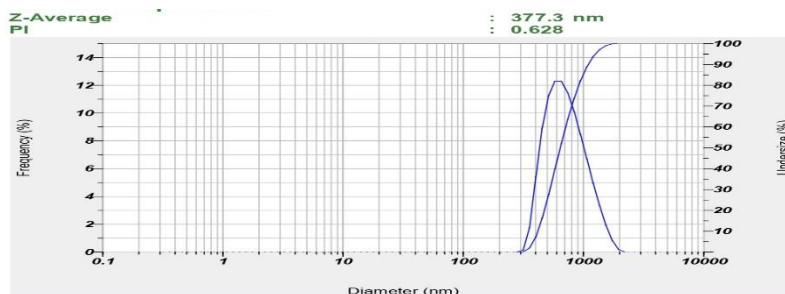


Fig 4. Particle size of optimized formulation(G3)

Zeta Potential (Mean) : -46.5 mV
Electrophoretic Mobility Mean : -0.000360 cm²/Vs

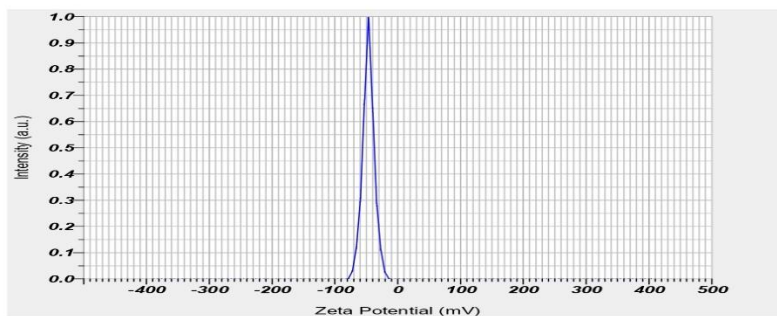


Fig 5. Zeta Potential of optimized formulation(G3)

Electrical Conductivity

Table 6
Determination of electrical conductivity

Batches	200 ms	20 ms	2 ms	200 μ s	20 μ s
1	000	00.0	0.03	026	1.
2	000	00.0	0.03	031	1.
3	000	00.0	0.03	028	1.
4	000	00.0	0.01	012	1.

Electrical conductivity is utilized to identify nature of o/w or w/o microemulsion. It is measured using electro conductometer, use to identify whether there is an oil or water as continuous phase. It also identifies the phase inversion phenomenon.

Scanning Electron microscopy

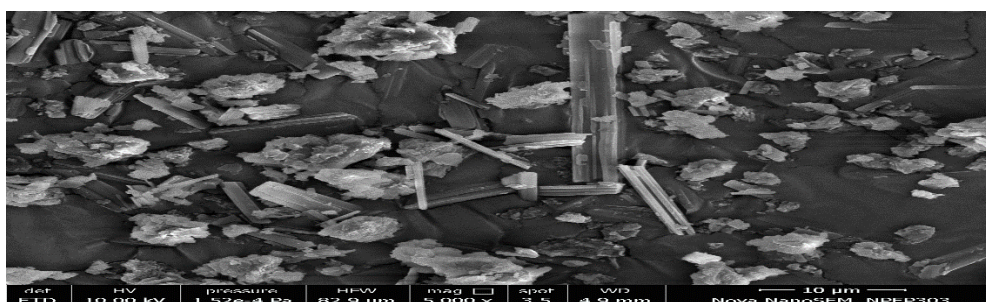


Fig 6. SEM of optimized formulation

The optimized batch of microemulsion was subjected to SEM analysis for morphology and surface topography. The SEM analysis of the microemulsion shows hexagonal and bicontinuous structure.

Conclusion

The current research work is focused on the preparation of safe, efficient and more compatible microemulsion which will enhance utility of these novel vehicles. The microemulsion protects labile drug, control drug release and reduce patient variability. The microemulsion can be used to optimize drug targeting without a concomitant increase in systemic absorption. The role of microemulsion is used to overcome problems of poor aqueous solubility of highly lipophilic drug compound. It provides high, consistent and reproducible bioavailability. The microemulsion preparation shows transparent yellow colour. The zeta potential determines the stability of formulation. To avoid the adverse side effect, a Griseofulvin microemulsion for topical use was formulated.

Acknowledgement

For the completion of the research work the authors would like to show sincere gratitude to PDEA'S Shankarrao Ursal College of Pharmaceutical Sciences and Research Centre. Kharadi, Pune to provide with a lot of support and help whenever needed.

References

1. International Agency for Research on Cancer. IARC Monographs on the Evaluation of Carcinogenic Risks to Humans. Vol. 79. Lyon, France: IARC Press; 2001. p. 75-89.
2. Tanaka Y, Waki R, Nagata S. Species differences in the dissolution and absorption of
3. griseofulvin and albendazole, biopharmaceutics classification system class II drugs, in the gastrointestinal tract. *Drug Metab Pharmacokinet* 2013;28(6):485-90.
4. Aggarwal N, Goindi S, Khurana R. Formulation, characterization and evaluation of an optimized microemulsion formulation of griseofulvin for topical application. *Colloids Surf B Biointerfaces* 2013;105:158-66.
5. Moghimipour E, Salimi A, Hassanvand S. Permeability assessment of griseofulvin microemulsion through rat skin. *Int J Pharm Chem Biol Sci* 2013;3(4):1061-5.
6. U.S. National Library of Medicine. Griseofulvin-Griseofulvin Tablet; 2016. Available from: <http://www.dailymed.nlm.nih.gov/dailymed/drugInfo.cfm?setid=6149c044-58bb-402c-a4b5-18b96dd9b3b9>. [Last accessed on 2016 Jan 11].
7. Lahenmeier DW. Safety evaluation of topical applications of ethanol on the skin and inside the oral cavity. *J Occup Med Toxicol* 2008;3:26.
8. Shinde U, Pokharkar S, Modani S. Design and evaluation of microemulsion gel system of nadifloxacin. *Indian J Pharm Sci* 2012;74(3):237-47.
9. Kumar A, Kushwaha V, 11. Júnior AA, Baldo JB. The behavior of zeta potential of silica suspensions. *N J Glass Ceram* 2014;4:29-37
10. Sharma PK. Pharmaceutical microemulsion: Formulation, characterization and drug deliveries across skin. *Int J Drug Dev Res* 2014;6(1):1-21.
11. T.P. Hoar and J.H. Schulman. Transparent water-in-oil dispersions, the oleopathic hydro micelle. *Nature* 1943; 152: 102-103.

12. J. H. Schulman et al. Mechanism of formation and structure of micro emulsions by electron microscopy. *The Journal of Physical Chemistry* 1959; 63: 1677–1680.
13. Danielsson and B. Lindman. The definition of a microemulsion, *Colloids and Surfaces* 1981; 3: 391–392.
14. Shinoda K and Lindman B. Organised surfactant systems: Microemulsions. *Langmuir* 1987; 3: 135–149.
15. M. Jayne Lawrence and Gareth D. Rees. Microemulsion-based media as novel drug delivery systems. *Advanced Drug Delivery Reviews* 2000; 45: 89–121.
16. Kumar. K. Senthil et al. Microemulsions as Carrier for Novel Drug Delivery: A Review. *International Journal of Pharmaceutical Sciences Review and Research* 2011; 10: 37-45.
17. Patel R. Mrunali. Microemulsions: As Novel Drug Delivery Vehicle. 2007; 5.
18. Madhav. S and Gupta. D. A review on microemulsion based system. *International Journal of Pharmaceutical Sciences and Research* 2011; 2 (8): 1888.
19. Shiokawa T. et al. Effect of Polyethylene Glycol Linker Chain Length of Folate-Linked Microemulsions Loading Aclacinomycin A on Targeting Ability and Antitumor Effect In vitro and In vivo. *Clinical Cancer Research* 2005; p11.
20. Talegaonkar S and Mishra P. Intranasal delivery: An approach to bypass the blood brain barrier. *Indian Journal of Pharmacology* 2004; 36: 140-147.
21. Hasse. A. and Keipert S. Development and characterisation of microemulsions for ocular application. *European Journal of Pharmaceutics and Biopharmaceutics* 1997; 43: 179–183.
22. Malmsten. M. Microemulsions in pharmaceuticals In *Handbook of Microemulsion. Science and Technology*. Marcel Dekker. Inc. New York. 1999; p 755.

How to Cite:

Kulkarni, O., Kasabe, A., Barge, V., Kerle, V., & Pate, A. (2022). Formulation and evaluation of serratiopeptidase and salbutamol tablet for dysphagia. *International Journal of Health Sciences*, 6(S3), 9154–9169. <https://doi.org/10.53730/ijhs.v6nS3.8241>

Formulation and evaluation of serratiopeptidase and salbutamol tablet for dysphagia

Onkar Kulkarni

Dept of Pharmaceutical Quality Assurance, Pune District Education Association's Shankarrao Ursal College of Pharmaceutical Sciences & Research Centre, Kharadi
*Corresponding author email: Onkarkulkarni9011@gmail.com

Amit Kasabe

Dept of Pharmaceutical Quality Assurance, Pune District Education Association's Shankarrao Ursal College of Pharmaceutical Sciences & Research Centre, Kharadi

Vijaya Barge

Dept of Pharmaceutical Quality Assurance, Pune District Education Association's Shankarrao Ursal College of Pharmaceutical Sciences & Research Centre, Kharadi

Vikram Kerle

Dept of Pharmaceutical Quality Assurance, Pune District Education Association's Shankarrao Ursal College of Pharmaceutical Sciences & Research Centre, Kharadi

Abhijeet Pate

Dept of Pharmaceutical Quality Assurance, Pune District Education Association's Shankarrao Ursal College of Pharmaceutical Sciences & Research Centre, Kharadi

Abstract---Oral Dispersible Tablet of Serratiopeptidase and salbutamol were prepared, evaluated and different types of concentration and dissolution of tablets were studied. In FTIR, drug and excipients with their mixture showed that there is no interaction between the drug molecule and excipients used. The Percentage of drug content of tablets in the formulations was found to be 95 % to 105% which complies with the limits of pharmacopoeia. By the process of direct compression method was used to prepare oral Dispersible tablet containing 300 mg of Serratiopeptidase and salbutamol. formulation was conducted using different concentrations of croscarmellose, micro crystalline cellulose, as a super disintegrants. And their interaction with Serratiopeptidase and salbutamol also evaluated using FTIR.

Keywords---fast dissolving tablets, mouth dissolving tablets, orally disintegrating tablets.

Introduction

Oral Dispersible Tablets are a type of tablet that dissolves when it comes into contact with saliva. The drug is released from the dosage form as a result of this. Super disintegrants like croscarmellose can increase the disintegration of tablets in the oral cavity, making the dosage form acceptable for youngsters, the elderly, bedridden patients, and dysphagia sufferers. The United States Food and Drug Administration defines an oral dispersible tablet as "a solid substance or active component that is easily dispersible when the tablet is placed on the tongue and should disintegrate within a few seconds." The oral tablet is also known as a rapid disintegrating tablet, a mouth dissolving tablet, a fast-dissolving tablet, and a quick dissolving tablet. This dosage form is widely used in children's, the patients who have difficulties in swallowing in case of Dysphagia, Bedridden patients. Or Psychiatric patients.

Serratiopeptidase it is the proteolytic enzyme, that is used to be reduce the inflammation i.e. it works as anti-inflammatory and analgesic agent. Serratiopeptidase is soluble in water and insoluble in alcohol. This proteolytic enzyme is quickly absorbed and delivered into the bloodstream through the colon. There are several issues with serratiopeptidase for oral delivery when there is a high chance of enzymatic breakdown in the GIT tract. Salbutamol is a beta2-adrenergic receptor agonist with a short half-life that is used to treat asthma and COPD. Bronchodilator is another name for it. Salbutamol dissolves quickly in water with no lag time. The focus of this research is to develop oral dispersible tablets containing serratiopeptidase and salbutamol in order to achieve quick dissolution, absorption, and increased drug bioavailability. Salbutamol and Serratiopeptidase oral dispersible tablets developed to improve patient compliance and give a faster onset of action.

Materials and Methods

Materials

Serratiopeptidase and Salbutamol were purchased from Arti distributor, Mumbai, India. Similarly Micro crystalline cellulose, Croscarmellose, Magnesium stearate and talc were obtained from pharmaceutical department.

Methods

DSC

Differential scanning calorimetry is the thermo-analytical techniques. Heat input or output of a sample was measured with the help of calorimeter. DSC thermograms of Serratiopeptidase and salbutamol were established by analysing the drug. The drug component was placed in an aluminium pan and subjected to DSC instrument (METTLER, STAReSW 12.10.) Indium was used as reference

standard. During heating the sample from 250°C to 300°C at a rate of 10°C/ min the DSC spectrum were recorded.

FTIR

Fourier Transform Infrared Spectroscopy was carried out for solid samples to identify the presence of various functional groups present in drug. The samples were prepared by the potassium bromide disc method. Powders (20mg drug in 280mg KBr) were triturated in agate mortar and pestle to produce fine and uniform mixture. Prepared sample disc was placed in a sample holder and transferred to sample compartment. Samples were scanned in the region of 4000-400 cm⁻¹ using a Bruker FTIR spectrometer and it was compared with standard.

Preparation of Serratiopeptidase and Salbutamol Sulphate

Direct compression method was used to prepare oral dispersible tablet of Serratiopeptidase and salbutamol. At first all the ingredients excluding lubricant, glidant, sweetner and diluent (Micro crystalline cellulose) were passed through sieve and the remaining ingredients were passed through sieve of mesh size 50. Then all the ingredients except glidant and lubricant were weighed correctly and mixed thoroughly. Finally lubricant and glidant were added to the powder and mixed thoroughly to obtain uniform particle size. The prepared powder blend was then compressed with tablet compression machine using die of 7 mm diameter.

Formula

Table 1
Formulation of Serratiopeptidase and Salbutamol ODT

Ingredients	F1	F 2	F 3	F 4
Serratiopeptidase	80	80	80	80
Salbutamol	10	10	10	10
Croscarmellose	40	45	55	60
Mg. Stearate	30	30	30	30
MCC	120	115	110	105
Talc	20	20	20	20

#Total tablet– 300mg

Evaluation of pre-compression flow properties of powder blend Organoleptic properties

Organoleptic properties of drug like colour, odour and solubility were observed and recorded. Solubility was observed in Water and Ethanol.

Bulk Density

Bulk density was measured using bulk density apparatus. Fixed weight of powder was poured in the measuring cylinder and volume was recorded.

Bulk density = Bulk weight/Bulk volume

Tapped Density

Fixed weight of powder was poured in the measuring cylinder and tapped 50 cycles multiple times. Volume was recorded after each 50 tapping cycles until fixed (concurrent) reading was obtained. The tapped density was obtained by using following equation:

Tapped Density = Bulk weight/Tapped volume

Carr's Index

Carr's index was obtained by using following equation:

$$\text{Carr's index (\%)} = \frac{\text{tapped density} - \text{bulk density}}{\text{Tapped Density}} \cdot X100$$

Tapped density Value less than 1.25 indicate good flow (=20% Carr), where greater than 1.25 indicates poor flow.

Angle of Repose

Fixed weight of powder was poured through funnel. The height and diameter of the power pile was noted. Angle of repose was obtained by using following equation:

$$\text{Angle of repose } \theta = \tan^{-1} (2h/d)$$

height

diameter

Where, h = maximum

D = Average

Hausner's ratio

Flow properties of the powder can also be examined using hausner's ratio. Hausner's ratio was obtained by using following equation:

$$\text{Hausner's ratio} = \frac{\text{Tapped Density}}{\text{Bulk Density}}$$

The value of ratio below 1.25 indicates good flow while above 1.35 indicates the poor flow

Post Compression Studies **Weight variation**

For each batch, 20 tablets were taken and weighed for weight of each tablet using a digital balance. The average weight of tablet for was determined and minimum and maximum deviation was calculated for each batch.

Thickness

Dimension of 10 tablets for each batch was determined using vernier caliper and the average diameter and thickness was determined.

Hardness

Using Monsanto Hardness tester, the hardness of 10 tablets was measured and average hardness of tablets was determined.

Friability

The weight of tablets equal to 6.5 grams were taken and rotated for 100 cycles in a friabilator. After 100 revolutions, the tablets were weighed and percentage loss was calculated.

Dissolution Test

The in-vitro dissolution study was carried out with the USP dissolution test apparatus. 900ml of dissolution medium (6.8 phosphate buffer) was taken in covered vessel and the temperature was maintained at $37 \pm 0.5^\circ\text{C}$. The speed of the paddle was set at 100rpm. Sampling was done every 10min interval. For each sample 10ml of dissolution medium was withdrawn and the same amount of dissolution medium at 37°C was replaced. The sample withdrawn was filtered with Whatman filter paper and diluted with 6.8 phosphate buffer and then analysed in the UV spectrophotometer. The absorbance was measured at 660nm and percentage drug release was calculated.

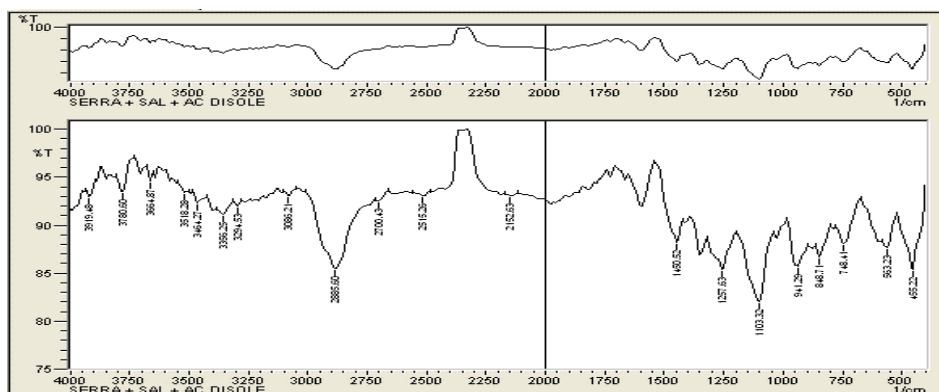
Disintegration test

For most tablets the first important step toward solution is break down of tablet into smaller particles or granules, a process known as disintegration. This is one of the important quality control tests for disintegrating type tablets. Six tablets are tested for disintegration time using USP XXII apparatus. Disintegration type sustained release tablets are tested for disintegrating time.

Results and Discussion**FTIR**

FTIR studies were done to evaluate whether there is any interaction between the active ingredient serratiopeptidase and salbutamol and the excipients used in the formulations. The peaks of the active ingredient serratiopeptidase and salbutamol with the mixture of excipients with one another, the peak positions are at the same wave number, Serratiopeptidase + salbutamol + AC DI SOLE
The FT-IR Spectroscopy Was done and following spectra were observed.

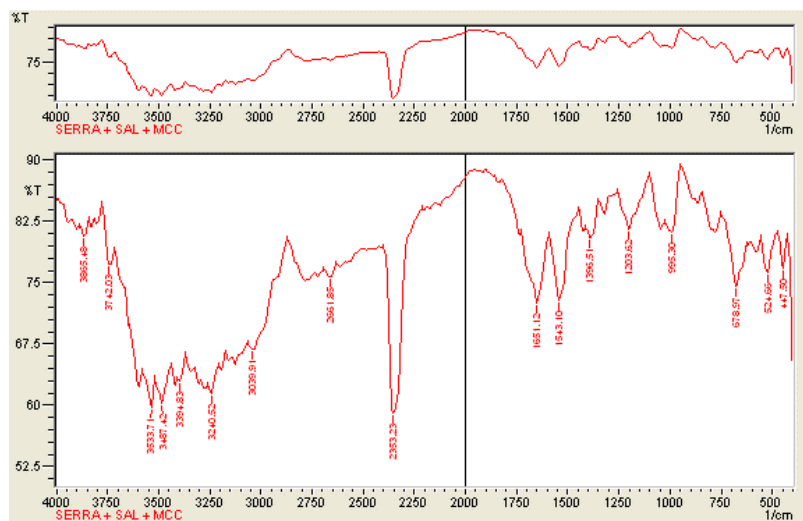
Serratiopeptidase + Salbutamol + AC DI Sole



Graph :- FTIR spectra of mixture of Serratiopeptidase + Salbutamol + AC DI Sole

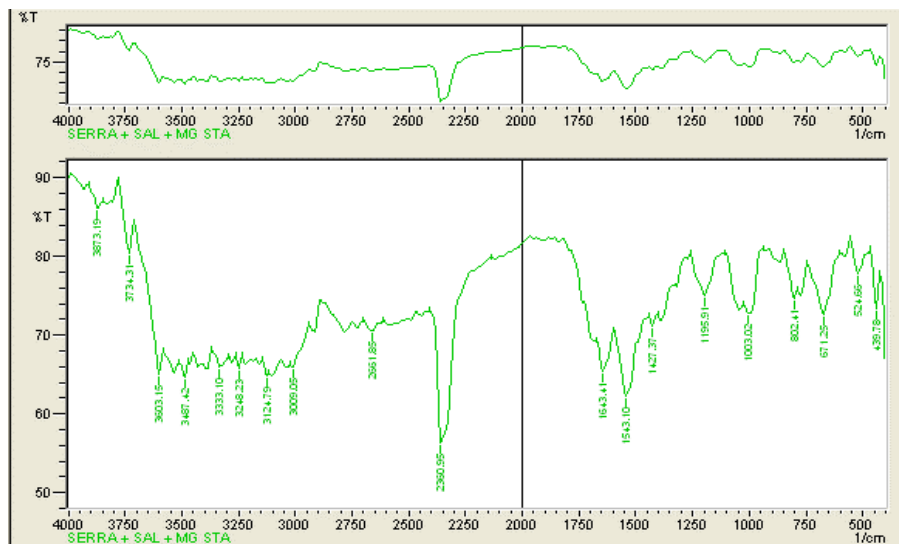
Observation: Identification and Confirmation of active pharmaceutical ingredients was carried by observing the FT-IR Spectra. Mixture of Serratiopeptidase + Salbutamol+ Ac DI Sole Showed characteristics peak at Values 3294.53(=O-H Stretching);2885.60(=N-H Stretching);2700.43(=O-H Stretching);1103.32(=C-O Stretching);1257.63(=C-H Stretching)

Serratiopeptidase + salbutamol+Mcc



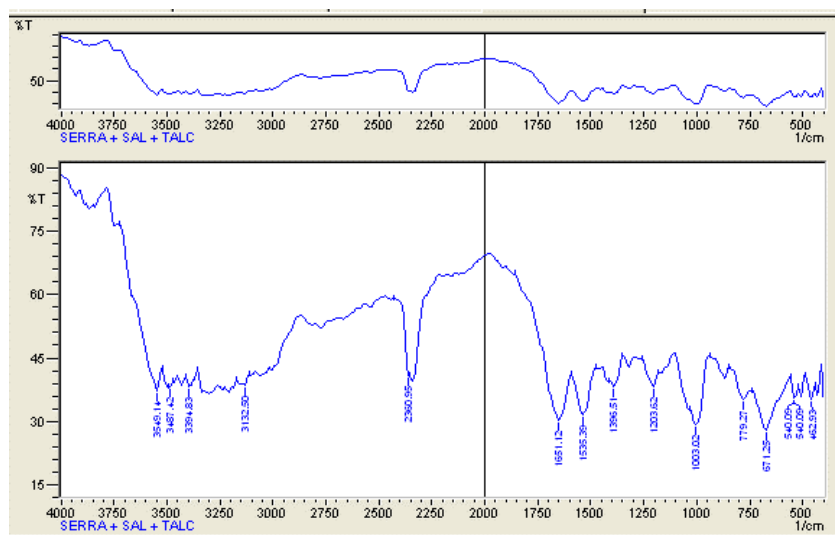
Observation: Mixture of Serratiopeptidase + Salbutamol + MCC Showed characteristics peak at values 3394.83(=N-H Stretching);3533.71(=O-H Stretching);1651.12(=C-C Stretching);1543.10(=N-O Stretching);3039(=O-H Stretching).

Serratiopeptidase + Salbutamol + Mg. Stearate



Observation: Mixture of Serratiopeptidase + Salbutamol + Mg. Stearate Showed Characteristics peak at values 3603.15(=O-H Stretching);2661.85(=C-H Stretching);1543.10(=N-O Stretching);1195.91(=C-O Stretching) 2533.23 (=N=C=O Stretching)

Serratiopeptidase + Salbutamol + Talc

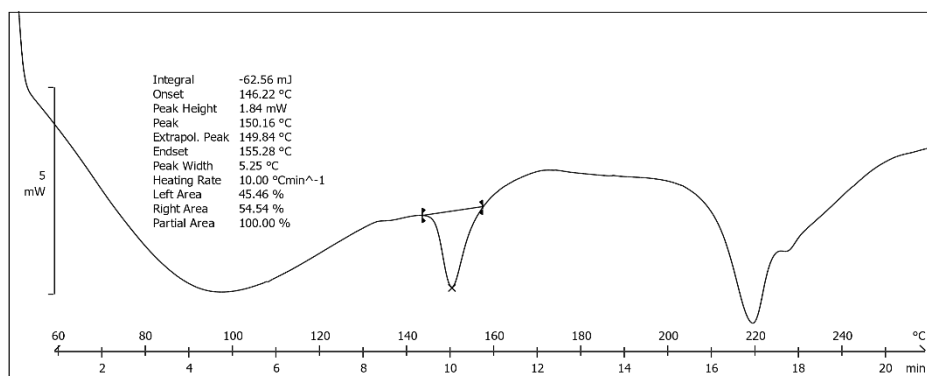


Observation: Mixture of Serratiopeptidase + salbutamol + Talc showed characteristics peak at values 3549.14(=O-H Stretching);3394.83(=N-H Stretching);3132.50(=O-H Stretching);1535.39(=N-O Stretching);1203.62(=C-O Stretching).

DSC (Differential Scanning Calorimetry)

Sample A:- Serratiopeptidase

The Melting Point of Serratiopeptidase is 146°C -148°C



Lab: METTLER

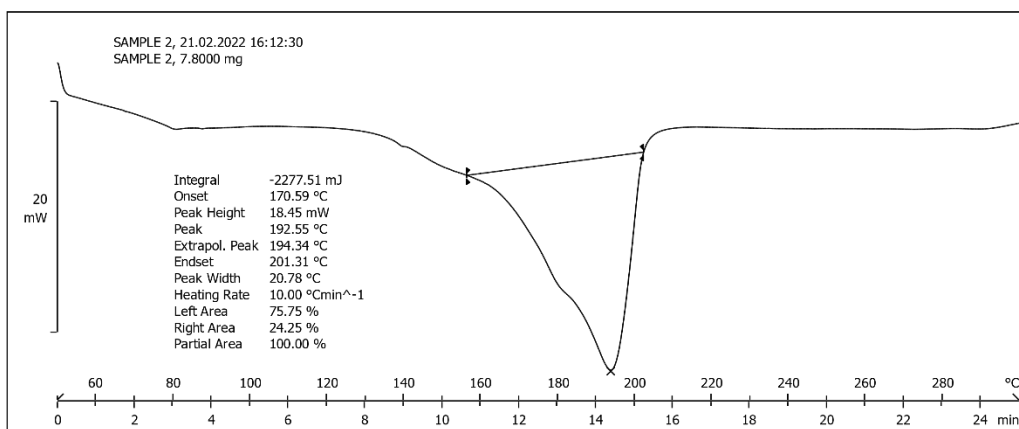
STAR® SW 12.10

Graph: Differential Scanning Calorimetry Serratiopeptidase

A Curve is observed in the graph. The onset temperature is 146.22°C and the peak transition temperature is 150.16°C that is the melting point of Serratiopeptidase. So, the thermal identification of Serratiopeptidase is done with the help of DSC.

Sample B: - Salbutamol

The Melting Point of Salbutamol 170°C – 180°C



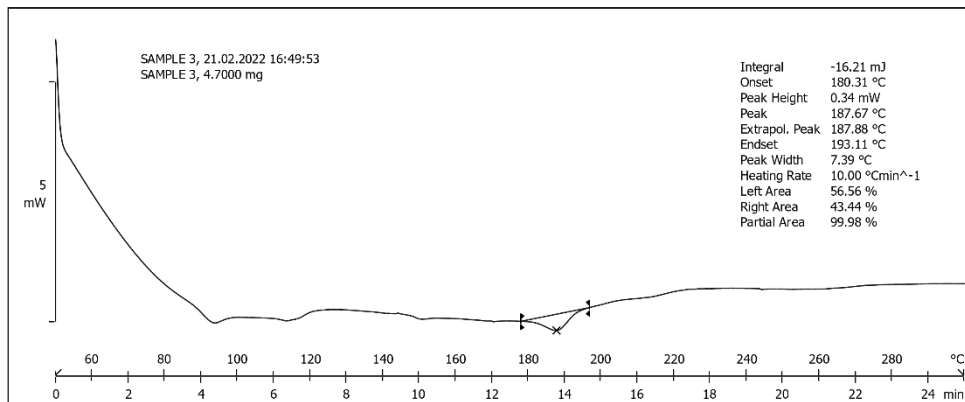
Lab: METTLER

STAR® SW 12.10

Graph:Differential Scanning Calorimetry of salbutamol

A Curve is observed in the graph. The onset temperature is 170.59°C and the peak transition temperature is 192.55°C that is the melting point of Salbutamol. So, the thermal identification of Salbutamol is done with the help of DSC.

Sample C: - Mixture (Serratiopeptidase and Salbutamol)

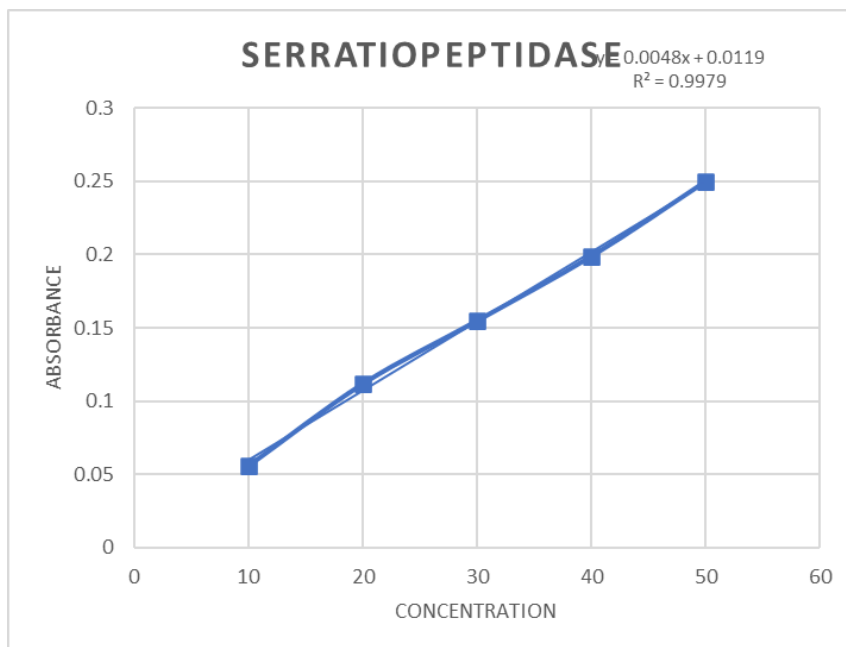


Lab: METTLER STAR® SW 12.10
Graph: Differential Scanning Calorimetry of Serratiopeptidase and salbutamol combination

A curve is observed on the graph. The onset temperature is 180.31 °C. It shows the melting point of salbutamol, so the combination shows compatibility so the thermal compatibility of this combination is done with the help of DSC.

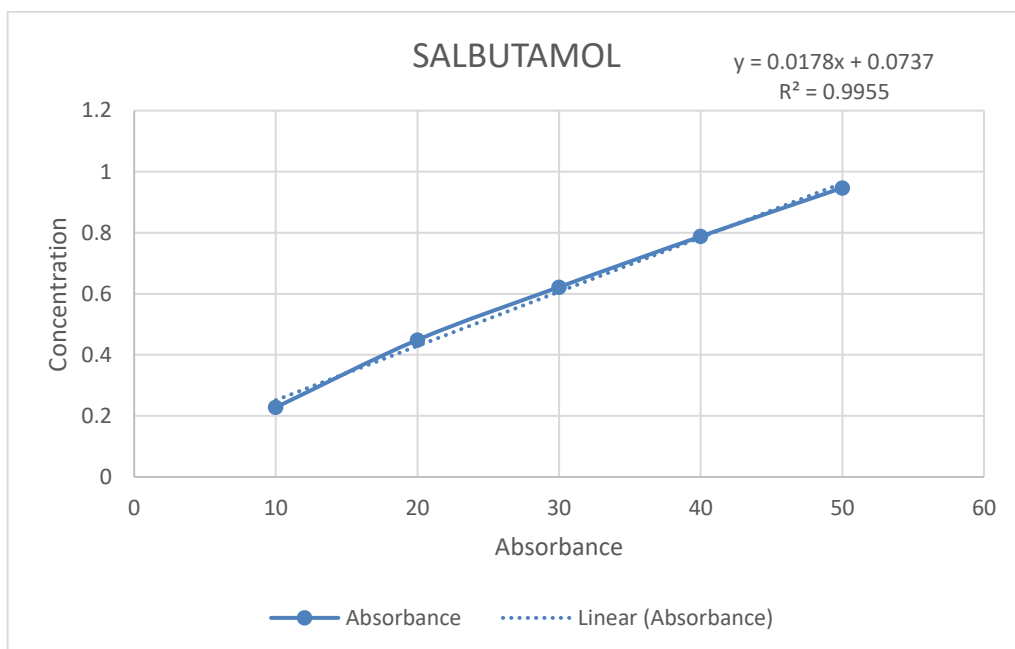
Standard Graph of Serratiopeptidase

When absorbance v/s concentration was plotted, a straight line was obtained which suggests that the process used to measure the absorbance of sample is validated.



Concentration($\mu\text{g/ml}$)	Absorbance
10	0.059
20	0.112
30	0.155
40	0.199
50	0.250

Standard Graph of Salbutamol



Concentration($\mu\text{g/ml}$)	Absorbance
10	0.228
20	0.449
30	0.622
40	0.788
50	0.947

General appearance

Visual observation revealed that all the tablets of four formulations were round.

Table 2
Formulation Table for Post Compression Studies

Batch	Weight Variation	Thickness	Hardness	Friability	Disintegration Time
F1	0.112	3.1	3.3	0.21	4m30sec
F2	0.121	3.3	3.5	0.33	5m20sec
F3	0.13	3.2	3.1	0.38	3m50sec
F4	0.129	3.1	3.4	0.45	6m10sec

Physical Parameters

Formulation	Bulk Density (gm/ml)	Tapped Density (gm/ml)	Angle of Repose	Carr's Index (%)	Hausners Ratio (HR)
F1	0.4247	0.5135	26.15	17.29	1.20
F2	0.3903	0.5448	26.95	30.08	1.40
F3	0.3563	0.5270	25.70	32.39	1.47
F4	0.4159	0.5150	25.34	19.24	1.23

Pre-Compression Study

Table 3
Formulation Table for Pre-Compression Studies

Wavelength 276 Nm	F 1	F 2	F 3	F 4
5 Min	0.012	0.004	0.006	0.009
15 Min	0.0128	0.006	0.012	0.015
30 Min	0.013	0.0087	0.0178	0.025
45 Min	0.0145	0.0115	0.0205	0.0268
60 Min	0.0149	0.0138	0.0235	0.0299

Comparative Dissolution profile of formulations.

Table 4
Formulation table for Dissolution Study.

Sr No	Time	Absorbance
1	0	0
2	5	0.0038
3	15	0.0074
4	30	0.013
5	45	0.0178
6	60	0.0235

Sr.no	Time (Min)	Absorbance
1	0	0
2.	5	0.005
3.	15	0.0021
4.	30	0.0087
5.	45	0.0113
6.	60	0.0158

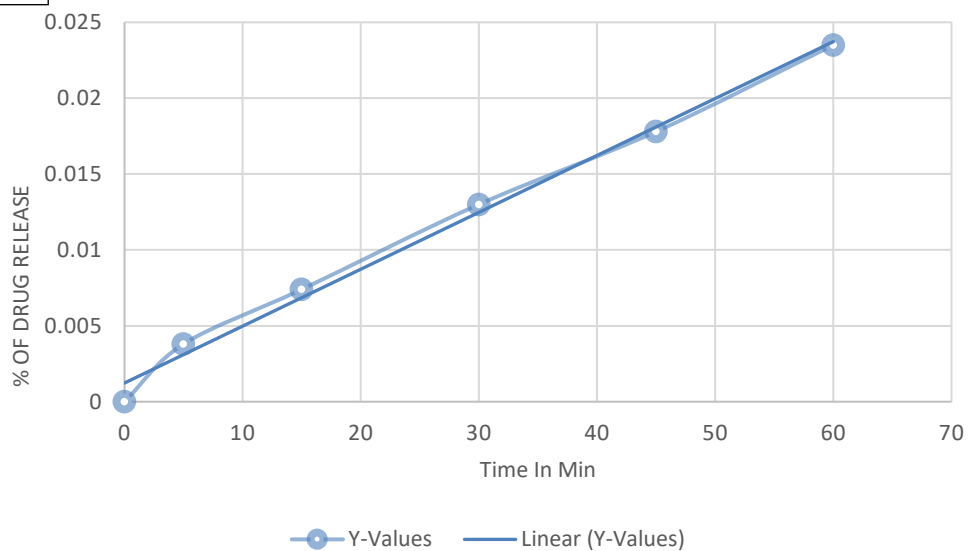
Sr.no	Time (Min)	Absorbance
1.	0	0
2.	5	0.004
3.	15	0.009
4.	30	0.0149
5.	45	0.0215
6.	60	0.0275

Sr.no	Time (Min)	Absorbance
1	0	0
2	5	0.0052
3	15	0.0103
4	30	0.0175
5	45	0.0255
6	60	0.0326

F1

Y-Values

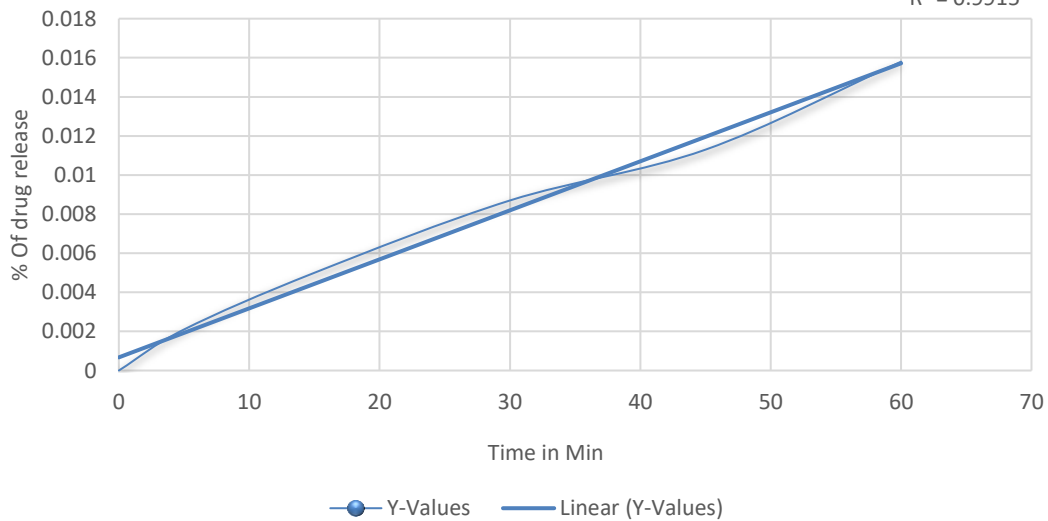
$$y = 0.0004x + 0.0012$$
$$R^2 = 0.9931$$

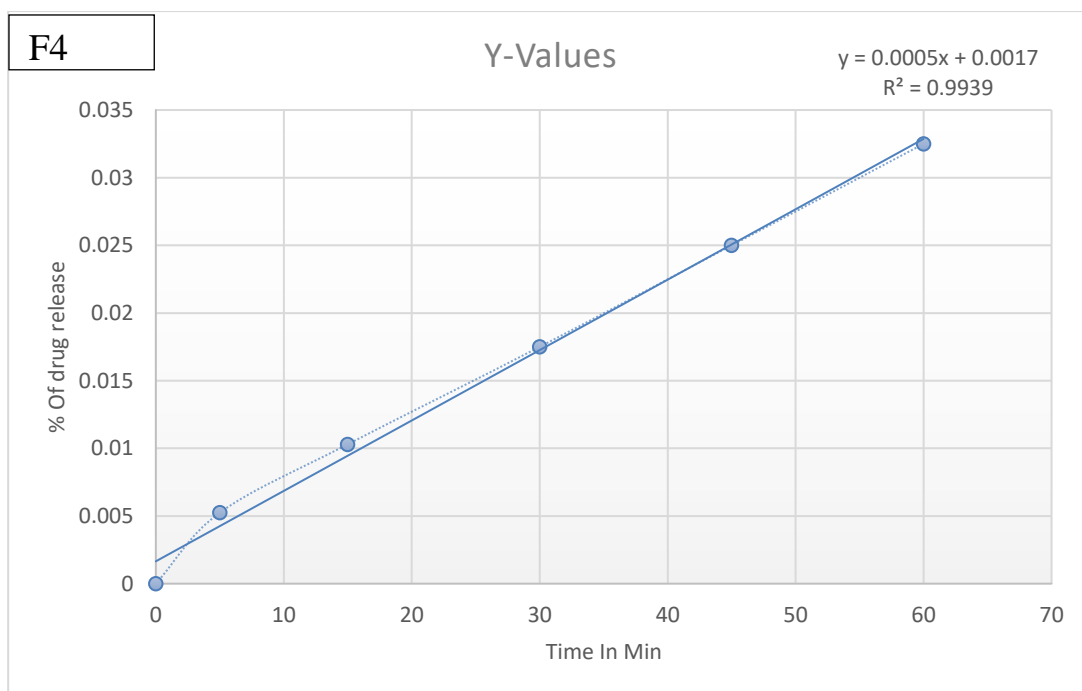
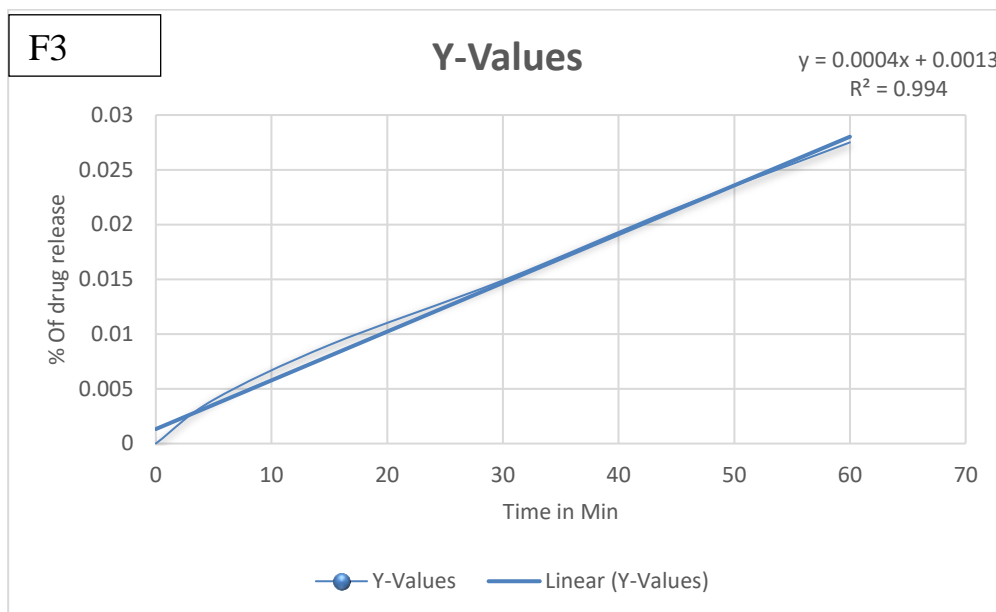


F2

Y-Values

$$y = 0.0003x + 0.0007$$
$$R^2 = 0.9915$$





Discussion

IR spectrum of Serratiopeptidase sample was interpreted. From these, we can say that the given sample may be Serratiopeptidase. The oral dispersible of Serratiopeptidase and salbutamol were formulated and evaluated. The use of super disintegrants for the formulation of the ODTs was satisfactory and commercially feasible. The use of super disintegrants caused quick disintegration

and prompt dissolution of the tablet. The FTIR study of the drug molecule and its mixture with the excipients were performed to show the compatibility of the drug molecule and the excipients. The FTIR peak correlates with the mixture to show that there is no interaction between component. By using Super disintegrants, they show better results in case of hardness, disintegration, etc. All the tablets passed the weight variation test as the percentage weight variation was within USP limits. The hardness of the tablets was in between 3.1 to 3.5 kg/cm². The friability of the tablets was in between 0.21% to 0.45%. The disintegration time of the formulated batches was between 4 min 30sec to 6 min 10 Sec.

Conclusion

The oral Dispersible tablet of Serratiopeptidase and salbutamol were prepared successfully by the use of direct compression method. Different formulations were designed to evaluate the influence of different concentrations of super disintegrants on ODTs of Serratiopeptidase and salbutamol. Four formulations with different concentrations of super disintegrants were prepared. FTIR studies using the drug and its mixtures with the excipients showed that the peaks correlate with one another which signify that there is no interaction between the drug molecule and the excipients used. This suggests that the composition of Serratiopeptidase and salbutamol ODTs could be optimized so as to obtain rapid disintegration and drug dissolution along with acceptable tablets hardness and friability. This could be helpful to improve the drug's absorption and bioavailability, which helps to better patient compliance and convenience.

Conflict of Interest

None declared by the authors.

Acknowledgement

For the completion of the research work the authors would like to show sincere gratitude to PDEA'S Shankarrao Ursal College of Pharmaceutical Sciences & Research centre, Kharadi, Pune, to provide with a lot of support and help whenever needed.

References

1. Manish Khadka, Dharma Prasad Khanal, Deepti Piya Baniya, Prakash Karki and Saurav Shrestha, Formulation and evaluation of oral disintegrating tablets of furosemide, 2021; 3(6): 149-156.
2. Abay Fb, Ugrulu T. Orally disintegrating tablet : a short review .journal of pharmaceutics and drug development, 2015;3:3-303
3. Tejas K, Ganesh D. A Review on orodispersible tablet: A novel Approach. Research journal of pharmacy and technology .2019;12-8-3993
4. Babu A, Akhtar M. The overview of formulation and evaluation of fast dissolving tablet: A promising tablet dosage journal of applied pharmaceutical Research .2020;8:2.
5. Parmar Kinjal, Patel Pinkal, Parate Pandurang, Patel Janki, Development and Validation of Analytical Method for Simultaneous Estimation of Diclofenac

- Sodium and Serratiopeptidase in Bulk and Tablet Dosage Form, *Journal of Drug Delivery and Therapeutics*, 2019; 9(4):395-405.
6. S. Dineshmohan, K. Vanitha, A. Ramesh, G. Srikanth and S. Akila, Formulation and Evaluation of Salbutamol Sulphate Fast Dissolving Tablet, *International Journal of Research in Pharmaceutical and Biomedical Sciences*, 2010; 105-108.
 7. Harsh Vora, Darshan Modi, Vikram Pandya, Praful Bharadia, Maulik Patel, Oral Dispersible Tablet: A Popular Growing Technology, *Asian Journal of Pharmaceutical Research and Development*, 2013: 138-155
 8. Shivani Bhagat, Monika Agarwal, Vandana Roy, Serratiopeptidase: A systematic review of the existing evidence, *International Journal of Surgery*, 2013, 209, 207.
 9. Shirisha Vardhineedi, Haribabu Y, Sheeja VK, Parasuraman R, DEVELOPMENT AND VALIDATION OF FT-IR SPECTROMETRIC METHOD FOR SIMULTANEOUS ESTIMATION OF SERRATIOPEPTIDASE AND ROXITHROMYCIN IN BULK AND DOSAGE FORM, *Acta Biomedica Scientia*, 2016; 3(4): 258-263
 10. G. Mahendar, S. Jaya, FORMULATION AND EVALUATION OF FLOATING TABLETS OF SALBUTAMOL SULPHATE, *International Research Journal of Pharmaceutical and Applied Sciences*, 2012; 2(6): 97-109.

How to Cite:

Suryawanshi, P. S., Barge, V. U., Kasabe, A. J., Sakpal, B. R., & Karkhile, S. N. (2022). Development and evaluation of tablet formulation containing combination of dapsone and acetazolamide for treatment of severe burn. *International Journal of Health Sciences*, 6(S2), 12014–12032. <https://doi.org/10.53730/ijhs.v6nS2.8236>

Development and evaluation of tablet formulation containing combination of dapsone and acetazolamide for treatment of severe burn

Parijat S. Suryawanshi

Department of Pharmaceutical Quality Assurance, PDEA's Shankarrao Ursal College of Pharmaceutical Sciences and Research Centre, Kharadi, Pune-411014, Maharashtra, India
Corresponding author email: psuryawanshi2704@gmail.com

Vijaya U. Barge

Department of Pharmaceutical Quality Assurance, PDEA's Shankarrao Ursal College of Pharmaceutical Sciences and Research Centre, Kharadi, Pune-411014, Maharashtra, India

Amit J. Kasabe

Department of Pharmaceutical Quality Assurance, PDEA's Shankarrao Ursal College of Pharmaceutical Sciences and Research Centre, Kharadi, Pune-411014, Maharashtra, India

Bhavana R. Sakpal

Department of Pharmaceutical Quality Assurance, PDEA's Shankarrao Ursal College of Pharmaceutical Sciences and Research Centre, Kharadi, Pune-411014, Maharashtra, India

Shubhangi N. Karkhile

Department of Pharmaceutical Quality Assurance, PDEA's Shankarrao Ursal College of Pharmaceutical Sciences and Research Centre, Kharadi, Pune-411014, Maharashtra, India

Abstract---The aim of this study was to develop and optimise a bilayer tablet containing Dapsone and Acetazolamide for the effective treatment of severe burns. Preformulation studies, including drug excipient compatibility, were studied for both drugs. The compatibility studies showed that there was no interaction between the drug and excipients and also drug-drug. The bilayer tablet was formulated in such a way that the immediate release layer contains Dapsone and the sustained release layer contains Acetazolamide. The formulated batches of bilayer tablets F1-F4 were evaluated. The parameters t₉₀%, Drug release, Friability, Hardness, Drug content, and Angle of repose

are considered for the evaluation of a tablet. The kinetic study showed that the drug release follows the matrix model as the best fit model. In vitro dissolution studies of bilayer tablets in USP type II apparatus resulted in 98.04% drug release of Dapsone for 60 minutes and 94.21% drug release of Acetazolamide for a period of 12 hours. According to the findings of this study, the drug and excipients used in the formulation were at the appropriate concentrations.

Keywords---bilayer tablets, angioedema, diuretic agent, antibiotic agent, immediate release, sustained release, kinetic analysis.

Introduction

Recent advancements in drug pharmacokinetics and pharmacodynamics behaviour have enabled a more rational approach to the development of optimal drug delivery systems. Nowadays, more focus has been devoted to the development of controlled and immediate release drug delivery systems. Conventional dosage forms cause a wide range of fluctuations in drug concentrations in the bloodstream and tissues, resulting in undesired toxicity and inefficiency. In the last decade, interest in developing a combination of two or more active pharmaceutical ingredients (API) in a single dosage form (bilayer tablet) has increased. [1,2] The main objectives of combination therapy are to encourage the use of lower doses of drugs to treat patients and also to minimise dose-dependent side effects and adverse reactions. [3-6] To overcome the drawbacks of single-layer combination tablets, this concept came into force. [7] Bilayer tablets can be a primary option to avoid chemical incompatibilities between APIs by physical separation and to enable the development of different drug release profiles (i.e., immediate release with extended release). [2]

In severe burn cases, an edematous condition occurs, also known as angioedema. This results in swelling of the lower layer of skin (dermis) and tissue just beneath the skin (subcutaneous tissue) or mucous membranes. Therefore, in such cases, a combination of treatment with an antibiotic, for example, Dapsone, to treat the bacterial infection at the site of action along with a diuretic agent for reduction of swelling, is used. The objective of the present study was to develop and evaluate a bilayer tablet containing Dapsone as an antibiotic agent and Acetazolamide as a diuretic agent.

Materials and Methods

Dapsone was purchased from Research-Lab Fine Chem Industries, Mumbai. Acetazolamide was purchased from Nakoda Chemicals Ltd., Telangana. Benecel™ E4M polymer was supplied as a gift sample by Ashland Co. Netherland. Croscarmellose Sodium- Ac-Di-Sol®, Microcrystalline cellulose- AVICEL PH102, Magnesium stearate, Talc, and Sodium saccharin were supplied as a kind gift from Fine Chem Ltd., Mumbai. All other chemicals and reagents used were of analytical grade and were purchased from local suppliers.

Methods

Identification of Pure drug

a) *FTIR* [8]

Identification of pure drug Dapsone and Acetazolamide was carried out by Fourier Transform Infra-red Spectrophotometry (Shimadzu 8400s) scanned in the range of 400-4000 cm^{-1} .

b) *DSC*

A differential scanning calorimeter (Mettler Toledo) was used for thermal analysis of both drugs for identification purposes. Individual drugs were weighed directly into the DSC aluminium crucible. The samples were scanned in a dry nitrogen atmosphere at a temperature ranging from 200-400 °C. The heating rate was 10°C·min⁻¹ and the thermograms obtained were observed for the identification of pure drugs.

c) *UV-spectroscopy* [9,10]

The absorption maximum for both Dapsone and Acetazolamide drugs was determined by running the spectrum of the drug solution in a double-beam ultraviolet spectrophotometer. (UV-1800, Shimadzu) A stock solution of 200 ppm was made by accurately weighing 100 mg of Dapsone drug and dissolving it in 0.1N hydrochloric acid in a 100 ml volumetric flask. 0.1ml, 0.2ml, 0.3ml, 0.4ml, and 0.5ml aliquots of drug solution were transferred into a series of 10ml volumetric flasks and brought to final volume with 0.1N hydrochloric acid. The spectrum of this stock solution was run in the 200–400 nm range in an ultra-visible spectrophotometer. (UV-1800, Shimadzu) Similarly, a stock solution of 100 ppm was made by accurately weighing 10 mg of Acetazolamide drug and dissolving it in distilled water in a 100ml volumetric flask. 0.2ml, 0.4ml, 0.6ml, 0.8ml, and 1.0ml aliquots of drug solution were transferred into a series of 10ml volumetric flasks and brought to final volume with distilled water. The spectrum of this stock solution was run in the 200–400 nm range in an ultra-visible spectrophotometer. (UV-1800, Shimadzu)

Drug-excipient compatibility study

Drug-excipient compatibility studies are necessary to ensure that drugs and excipients are compatible. DSC graph and IR spectra are used to study drug-excipient compatibility.

a) *FTIR study* [11]

FTIR (Shimadzu 8400s) spectrophotometer were used in the range of 400-4000 cm^{-1} using potassium bromide discs [Mixing ratio- 1:1 (Drug: Excipient/s)] to study drug-excipient compatibility.

b) *DSC study* [12,13]

A differential scanning calorimeter (Mettler Toledo) was used for thermal analysis of drug and excipient mixtures. Individual drug and excipient samples, as well as physical mixtures, were weighed directly into the DSC aluminium crucible [Mixing ratio- 1:1 (Drug: Excipient/s)]. The samples were scanned in a dry nitrogen atmosphere at a temperature ranging from

200-400°C. The heating rate was 10°C·min⁻¹ and the thermograms obtained were observed for interactions.

Preparation of immediate release layer and sustained release layer

The compressed tablets of the immediate release layer according to batches (D1-D4) were formulated by using Croscarmellose Sodium- Ac-Di-Sol® as a superdisintegrant. All ingredients were weighed accurately. The composition of the immediate release layer is listed in Table 1. The above mixture was triturated for 5 minutes and lubricated with magnesium stearate and talc. Similarly, the compressed tablets of the sustained release layer according to batches (A1-A4) were formulated by using Benecel™ E4M polymer. All ingredients were weighed accurately. The composition of the sustained release layer is listed in Table 2. The above mixture was triturated for five minutes and lubricated with magnesium stearate and talc.

Table 1- Composition of Dapsone as Immediate release tablet of batches D1-D4

Ingredients / Batch	Dapsone (mg)	Ac-Di-Sol (mg)	Avicel PH102 (mg)	Talc (mg)	Magnesium stearate (mg)	Sodium saccharin (mg)
D1	50	50	88	8	2	2
D2	50	40	98	8	2	2
D3	50	30	108	8	2	2
D4	50	20	118	8	2	2

Table 2- Composition of Acetazolamide as Sustained release tablet of batches A1-A4.

Ingredients / Batch	Acetazolamide (mg)	E4M polymer (mg)	Avicel PH102 (mg)	Talc (mg)	Magnesium stearate (mg)	Sodium saccharin (mg)
A1	250	50	38	8	2	2
A2	250	40	48	8	2	2
A3	250	30	58	8	2	2
A4	250	20	68	8	2	2

Preparation of bilayer tablets

The direct compression method was used for the preparation of bilayer tablets. The sustained release layer was poured first into the die cavity, followed by the immediate release layer, which was poured and compressed into the tablets using a 12 station tablet compression machine (Rimek, Mini Press-II MT, Karnavati Engineering Ltd., 12 station) with an average hardness of 4.0-6.0 kg/cm². (Monsanto hardness tester)

Evaluation of powder blends (Pre compression study) [14,15]

- Angle of Repose θ

The angle of repose of the powder blend was determined by the fixed funnel method. The accurately weighed powder blend was allowed to flow through the funnel, which was adjusted to a height of 2 cm. The angle of repose was calculated using the following equation:

$$\theta = \tan^{-1} \frac{h}{r} \quad \text{----- Equation 1}$$

Where, θ , h , r are the angle of repose, pile height, and pile base radius, respectively.

- **Bulk density (BD)**

Bulk density is the ratio of the mass of powder to the bulk volume. It is usually expressed as g/ml. Bulk density was calculated using the following equation:

$$\rho_b = \frac{M}{V_b} \quad \text{----- Equation 2}$$

Where, ρ_b = Bulk density, M = mass in grams, and V_b = bulk volume in milliliters.

- **Tapped density (TD)**

The tapped density of a powder is the ratio of the powder's mass to the volume occupied by the powder after it has been tapped for a specified time. The tapped density of a powder is measured in g/ml and represents its random dense packing. Tapped density was calculated using the following equation:

$$\rho_t = \frac{M}{V_t} \quad \text{----- Equation 3}$$

Where, ρ_t = Tapped density, M = mass in grams, and V_t = Tapped volume in milliliters.

- **Carr's Index**

This property is also known as percent compressibility and is indirectly related to the flow rate, cohesiveness, and particle size. Carr's index was calculated using following equation:

$$\text{Carr's Index} = \frac{\rho_t - \rho_b}{\rho_t} \times 100 \quad \text{----- Equation 4}$$

Where, ρ_t = Tapped Density; ρ_b = Bulk Density

- **Hausner's Ratio**

It is the ratio of the tapped density to the bulk density. A good flow has been indicated by a Hausner's ratio greater than 1.25, and a poor flow may have a value of 1.5. It is calculated using following equation:

$$\text{Hausner's ratio} = \frac{\text{Tapped density } (\rho_t)}{\text{Bulk density } (\rho_b)} \quad \text{----- Equation 5}$$

Evaluation of tablets (Post compression study) [14,15,16,18]

- **Weight Variation**

About 20 tablets from each batch F1-F4 were selected and weighed collectively and individually. From the collective weight, an average weight was calculated. Each tablet's weight was then compared with the average weight to determine whether it was within permissible limits or not. To pass the test, not more than two of the individual weights deviated from the average weight by more than 5.0%. Randomly selected tablets from all batches were tested for thickness using a vernier caliper. (Mitutoyo Corporation, Japan) Standard deviation values were determined and were found within the range.

- *Hardness*
- The hardness of tablets from batches F1-F4 was determined by using the Monsanto hardness tester (n=3) and expressed in Kg/cm². The lower plunger of the hardness tester was placed in contact with the tablet and a zero reading was taken. The plunger was then forced against a spring by turning a threaded bolt until the tablet fractured. As the spring is compressed, a pointer rides along a gauge in the barrel to indicate the force.
- *Friability test*
- The friability test was performed by weighing the initial weight of 20 tablets of batches F1-F4 individually and placing them in the Roche Friabilator (Electrolab, Mumbai, India). The drum of the friabilator was rotating at 25 rpm for 4 minutes. Pre-weighed samples of tablets were placed in the friabilator and subjected to 100 revaluation, dedusted and reweighed. The percent friability for each formulation was determined using the following equation:

$$\% \text{ Friability} = \frac{\text{Initial weight} - \text{Final weight}}{\text{Initial weight}} \times 100 \quad \text{----- Equation 6}$$

Drug content [19]

All tablets of formulated batches D1-D4 were subjected for %drug content. For all batches, about 20 tablets were weighed and finely powdered. Transferred an accurately weighed quantity of the powder equivalent to about 50mg of Dapsone in a 200ml volumetric flask. Add 150 ml of methanol and sonicate the solution for 15 minutes at 35°C. Then the solution was cooled to room temperature and made up to the mark by using methanol. Filter the solution through the whatmann filter paper to get the clear solution. Filled a 50ml volumetric flask with 5ml of clear solution, diluted with methanol, and mixed. Withdraw 0.8ml, 1.0ml, and 1.2ml of the stock solution to prepare 8ppm, 10ppm, and 12ppm solutions, respectively. The absorbance was measured spectrophotometrically (UV-1800, Shimadzu) by scanning wavelengths in the range of 400 nm to 200 nm, using methanol as a blank.

Twenty tablets from formulated batches A1-A4 were taken to calculate the percent drug release. The tablets were weighed and crushed into fine powder, and from this, 10 mg of powder was weighed and transferred into a 100ml volumetric flask. To this, 70 ml of methanol was added and sonicated for 30 minutes to dissolve completely. After attaining room temperature, the volume was made up with the same solvent and shaken well to obtain a homogeneous solution. After discarding

the first 20 ml of solution, the tablet solution was filtered through whatmann filter paper. The resultant clear solution was a 100 µg/ml sample stock solution, which was further diluted with methanol to obtain working stock solutions of 8 ppm, 10 ppm, and 12 ppm, respectively. These working stock solutions were prepared in triplicate and scanned at 263.00nm using an UV-spectrophotometer. (UV-1800, Shimadzu)

In vitro Dissolution studies

A dissolution study for formulated batches was performed separately for the immediate and sustained release layers as per USP by using USP-II apparatus (paddle type) dissolution test apparatus (Electrolab TDT08L, Mumbai, India). The dissolution medium for the immediate release tablet layer and for the sustained release layer were 900ml of 0.1N hydrochloric acid and 900ml of 0.01N hydrochloric acid, respectively. The medium was allowed to equilibrate to a temperature of 37±0.5°C. A tablet from each batch was placed in the vessel and covered; the apparatus was operated for up to 1 hour at 100 rpm for the immediate release layer and 12 hours for the sustained release layer. The sample was withdrawn at specified time intervals and replaced with a fresh 1ml of medium. The aliquots were filtered through Whatmann filter paper No. 42. The absorbance of the sample solution was measured using UV spectroscopy against the corresponding media as a blank for the immediate release layer and the sustained release layer at 290 nm and 265 nm, respectively.

Kinetic analysis of In vitro drug release study [14,16]

The data from the in vitro dissolution study were plotted to investigate release kinetics in various kinetic models, including zero order, first order, matrix, korsmeyer-peppas, and Hixon–Crowell.

- *Zero order*

In-vitro dissolution data was evaluated as cumulative percent drug release *vs.* time. It was expressed in concentration/ time. Where, K is the zero order release constant and t is time in hours.

$$C = K_0 t \quad \text{----- Equation 7}$$

- *First order model*

Drug release data in this model depends on concentration. Where, C is concentration, C_0 is the initial concentration, and K is the first order constant.

$$\log C = \log C_0 - kt / 2.303 \quad \text{-----Equation 8}$$

- *Korsmeyer-peppas model*

In this model, drug release data is constructed as log cumulative % drug release *vs.* log time.

$$Mt / M_\infty = K t n \quad \text{----- Equation 9}$$

Where, M_t / M_∞ is a fraction of drug release at time t , K is release rate constant, n is release exponent.

- Hixson and Crowell model [17]

In this type, particle regular area is proportional to the cubic root of its volume and is described by the following equation:

$$M_0^{1/3} - M^{1/3} = K_{HC} t \quad \text{----- Equation 10}$$

Where, M_0 is the initial amount of drug, M amount of remaining drug on time t , K_{HC} is constant of incorporation.

Results and Discussion

Identification of Pure drugs

FTIR study

Identification and confirmation of pure drugs were carried out by observing the obtained spectra. Dapsone showed characteristic peak values at 3063.06 (=C-H stretching); 3333.10 (N-H stretching); 1589.40 (C=C stretching); 1280.78 (C-N stretching) and 1134.18 (S=O stretching). These peak values were in accordance with previously reported spectra of Dapsone. (Fig. 1) Acetazolamide showed characteristic peak values at 3302.24 (C=O stretching); 1365.65 (S=O stretching); 2353.23 (C=N stretching) and 1674.27 (R-C(=O)NH₂ stretching). These peak values were in accordance with previously reported spectra of Acetazolamide. (Fig. 2)

Fig. 1: FTIR spectra of pure Dapsone.

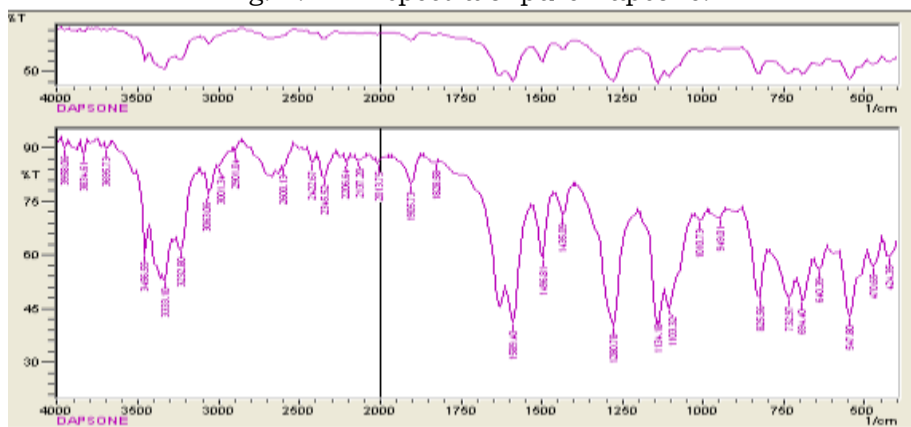
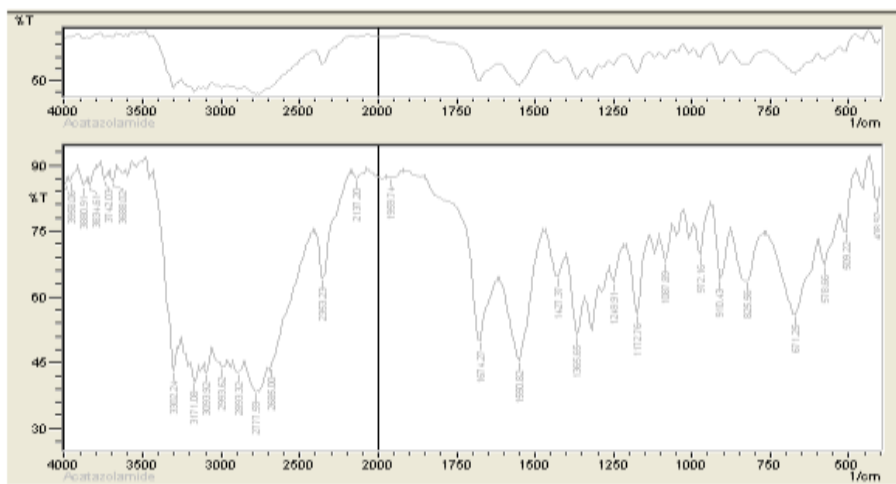


Fig. 2: FTIR spectra of pure Acetazolamide



DSC study

The DSC thermograms of the Dapsone alone show the peak onset temperature (Tonset) is [178.13°C] and peak transition temperature (Tpeak) is [178.73°C].(Fig.3) Similarly for Acetazolamide alone, the peak onset temperature (Tonset) is [271.16°C] and the peak transition temperature (Tpeak) is [272.11°C]. (Fig.4). These results indicate the purity of the drug.

Fig. 3: DSC graph of pure Dapsone.

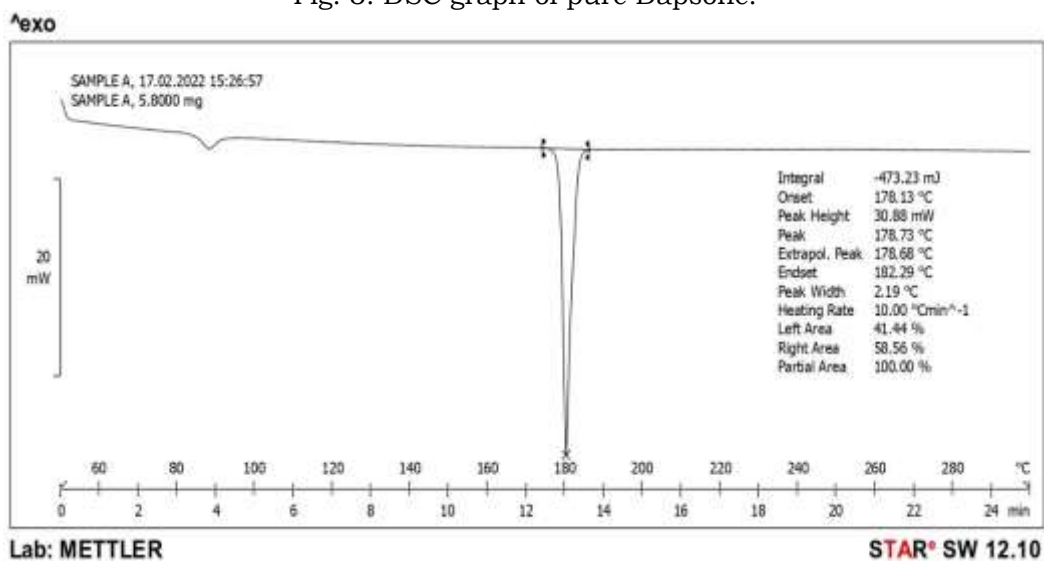
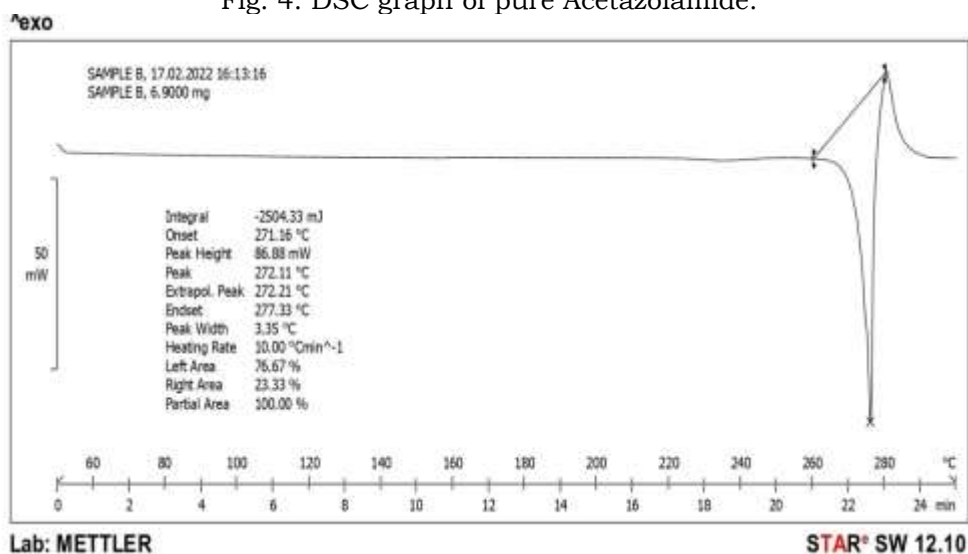


Fig. 4: DSC graph of pure Acetazolamide.



UV spectroscopy

The linearity of the responses of both drugs was verified at 2–10 µg/ml concentrations. The calibration curve was obtained by plotting the absorbance versus the concentration data and was treated by linear regression analysis. The equation of the linearity curve for Dapsone obtained was $y = 0.1238x + 0.0066$. The linearity curve was found to be linear in the aforementioned concentrations (the correlation coefficient (r^2) of determination was 0.9996) (Fig.5). Similarly, the equation of the linearity curve for Acetazolamide obtained was $y = 0.0823x + 0.0074$. The linearity curve was found to be linear in the aforementioned concentrations. (The correlation coefficient (r^2) of determination was 0.9992) (Fig.6)

Fig. 5: Calibration Curve for Dapsone

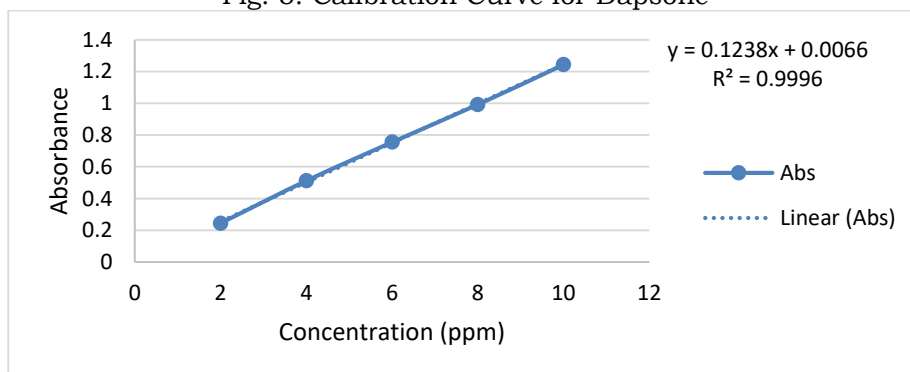
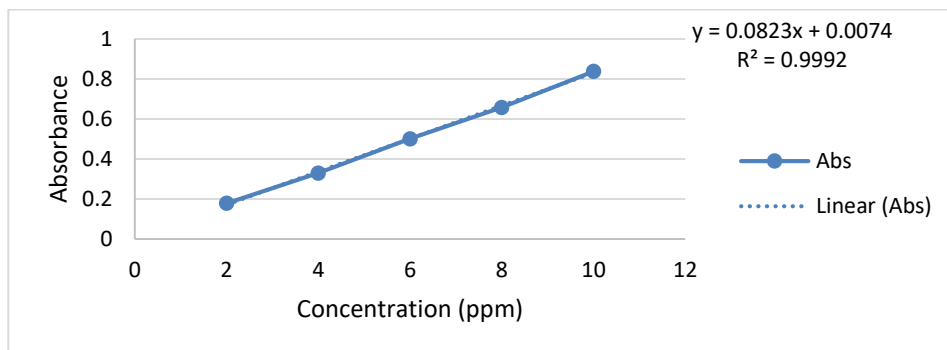


Fig. 6: Calibration Curve for Acetazolamide



Drug-excipient compatibility study

FTIR spectroscopy-

The FTIR spectrums of pure Dapsone as well as Acetazolamide and physical mixtures of drugs and polymers were studied separately as per the excipients used in the formulation. It was observed that there were no major shifts in the main peaks of either drug. This indicates that there were no compatibility problems with the drug with the polymers and excipients used in the formulation. Dapsone had peaks at 3063.06 (=C-H stretching), 3333.10 (N-H stretching), 1589.40 (C=C stretching), 1280.78 (C-N stretching), and 1134.18 (S=O stretching), (Fig.7,8) while Acetazolamide had peaks at 3302.24 (C=O stretching), 1365.65 (S=O stretching), 2353.23 (C=N stretching), and 1674.27 (R-C(=O)NH₂ stretching). These peak values were in accordance with previously reported spectra of Dapsone and Acetazolamide. (Fig. 9, 10)

Fig.7 : FTIR spectra of Dapsone + Ac-Di-Sol

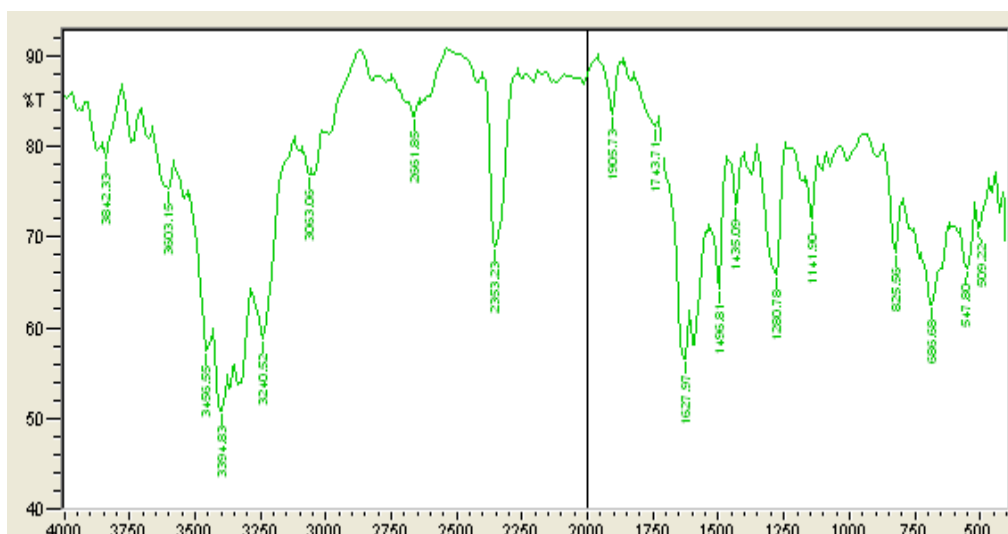


Fig.8 : FTIR spectra of Dapsone + MCC + Talc + Magnesium stearate + Sodium saccharin

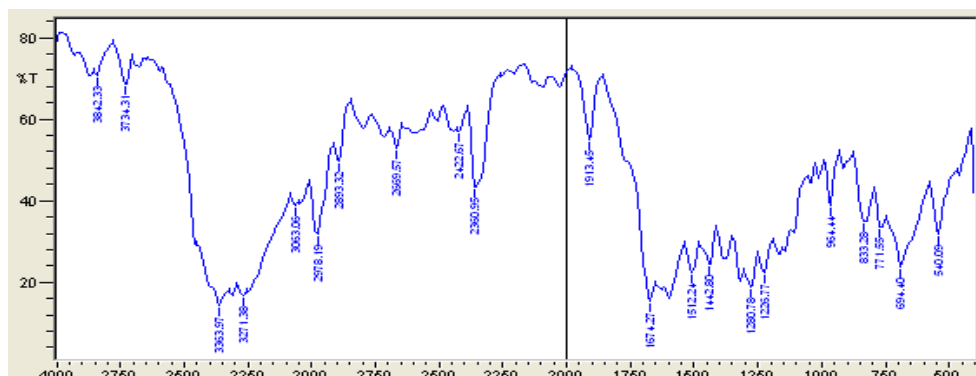


Fig.9 : FTIR spectra of Acetazolamide + E4M polymer

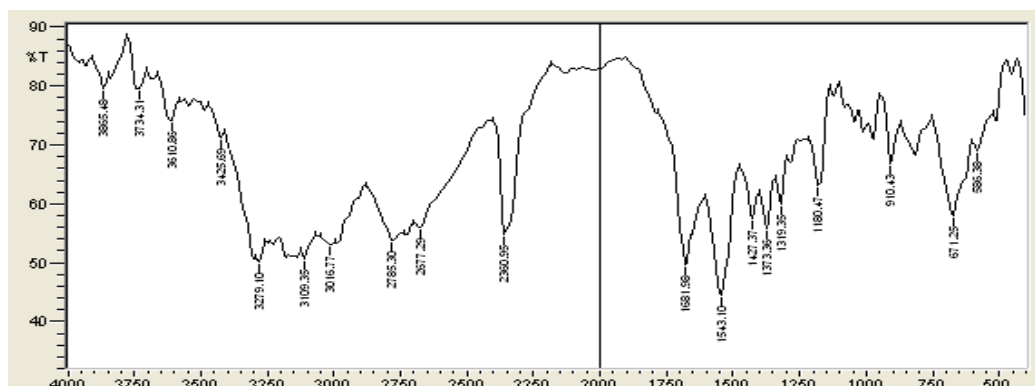
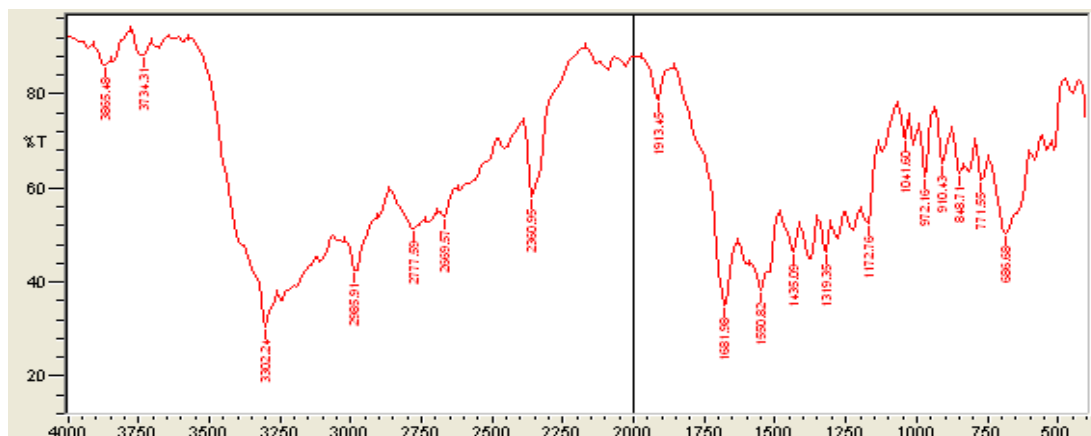


Fig.10 : FTIR spectra of Acetazolamide + MCC + Talc + Magnesium stearate + Sodium saccharin



DSC study

The DSC thermogram for Dapsone in combination with various excipients shows the peak onset temperature (Tonset) [176.86°C] and peak transition temperature (Tpeak) [179.10°C]. The thermogram of Dapsone showed a sharp endothermic peak at ~180°C and a peak onset ~176°C. In this thermogram, the melting endotherm of Dapsone (T onset and T peak) was well preserved, with light broadening shifting towards the lower temperature range. (Fig. 11) Similarly, Acetazolamide in combination with various excipients shows an onset temperature (Tonset) [258.66°C] and a peak transition temperature (Tpeak) [264.99°C]. The thermogram of Acetazolamide showed a sharp endothermic peak at ~269°C and a peak onset ~258°C. In this thermogram, the melting endotherm of Acetazolamide (T onset and T peak) was well preserved, with light broadening shifting towards the lower temperature range. (Fig. 12) These shifts in peak in both graphs to a lower temperature range might be due to the drug being mixed with excipients and do not necessarily indicate probable incompatibility.

Fig. 11: DSC graph for Dapsone with excipients

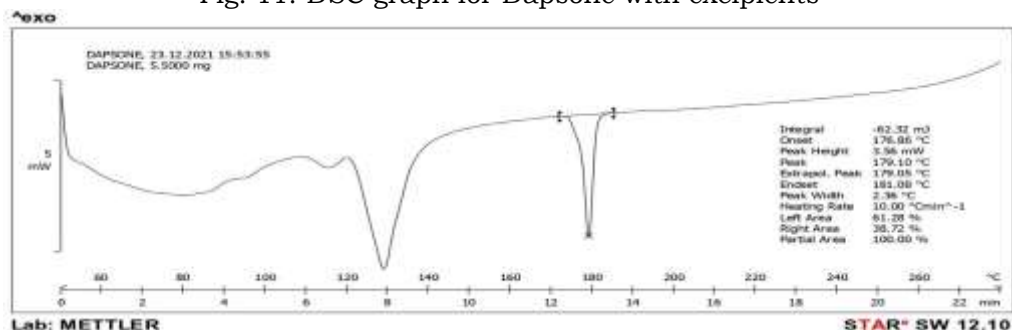
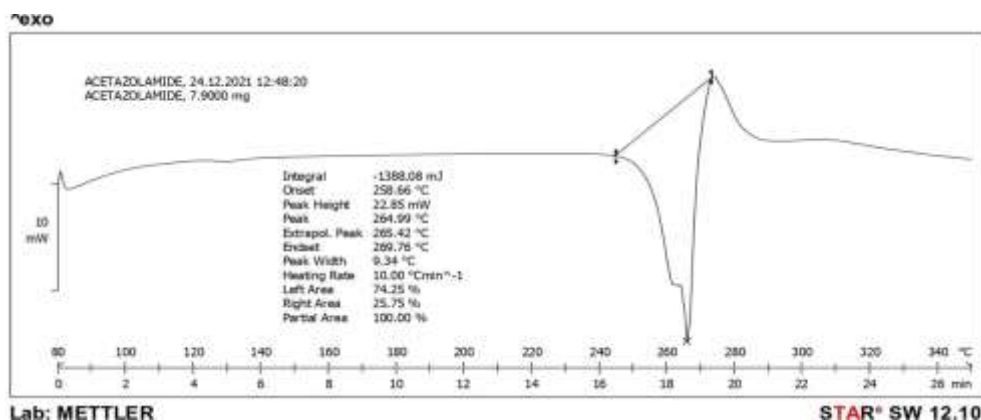


Fig. 12: DSC graph for Acetazolamide with excipients



Evaluation of powder blends (Pre compression study)

The directly compressible blends of the immediate release layer of Dapsone reveal that the angle of repose was found between 26.31 ± 0.5 to 28.80 ± 0.8 , Hausner's Ratio between 1.02 to 1.05 and Carr's index between 2.38 to 4.76 %. The directly

compressible blends of the sustained release layer of Acetazolamide reveal that the angle of repose was found between 26.76 ± 0.7 to 29.51 ± 0.5 , Hausner's Ratio for all batches is 1.03, and Carr's index for all batches is 3.63%. These pre-compression studies indicate good flow and compression characteristics of all the immediate release and sustained release blends as per USP limits. In these immediate release and sustained release directly compressible powder blends, magnesium stearate and talc are used as lubricant and diluent, respectively, which imparts good flow and compressibility to the blends as given in table no. 3 and 4.

Table 3- Pre-compression parameters of Immediate release layer of Dapsone (D1-D4)

Formulation Code	Angle of Repose (θ)	Bulk density (g/ml)	Tapped density (g/ml)	Carr's Index (%)	Hausner's Ratio
D1	28.22 ± 0.5	0.41 ± 0.005	0.42 ± 0.005	2.38	1.02
D2	27.29 ± 0.1	0.40 ± 0.005	0.42 ± 0.005	4.76	1.05
D3	26.31 ± 0.5	0.41 ± 0.005	0.42 ± 0.005	2.38	1.02
D4	28.80 ± 0.8	0.41 ± 0.005	0.42 ± 0.005	2.38	1.02

\pm S.D. n=3

Table 4- Pre-compression parameters of Sustained release layer of Acetazolamide (A1-A4).

Formulation Code	Angle of Repose (θ)	Bulk density (g/ml)	Tapped density (g/ml)	Carr's Index (%)	Hausner's Ratio
A1	26.76 ± 0.7	0.53 ± 0.006	0.55 ± 0.005	3.63	1.03
A2	28.71 ± 0.4	0.53 ± 0.006	0.55 ± 0.005	3.63	1.03
A3	28.61 ± 0.4	0.53 ± 0.006	0.55 ± 0.005	3.63	1.03
A4	29.51 ± 0.5	0.53 ± 0.006	0.55 ± 0.005	3.63	1.03

\pm S.D. n=3

1. *Evaluation of tablet (Post compression study)*

The general appearance of the batch (F1-F4) formulated tablets was evaluated. These tablets were round in shape, white in colour, and had a smooth texture.

2. *Weight Variation*

The tablets from batches F1-F4 were evaluated for % weight variation, which showed a % weight variation of between 0.18-4% from the average weight of the tablet complying as per standard (for $>324\text{mg} \pm 5.0\%$ deviation).

3. *Thickness*

Randomly selected tablets from all batches were tested for thickness and were found to be $0.50 \pm 0.005\text{cm}$. Standard deviation values were determined and were found to be within the range.

Hardness

The compressed tablets from all batches F1-F4 were found to be within the limit as per standard record, which lies in between 5.3 ± 0.057 to 5.5 ± 0.115 kg/cm² (n=3).

Friability Test

For all batches F1-F4, friability values were found to be within the range of 0.48-0.87, which conforms to the standard limit (1%, n=3).

Drug content

The formulated tablets, batches D1-D4, were tested for assay by UV spectroscopy. Dapsone absorbance in methanol is measured at 296nm (λ_{max}). The assay was found to be in the range of 98.0% to 99.70%, which is within the standard record limit (92.5%-107.5%). The formulated tablets, batches A1-A4, were tested for assay by UV spectroscopy. Acetazolamide absorbance in methanol is measured at 263nm (λ_{max}). The assay was found to be in the range of 99.30% to 102.07%, which is within the standard record limit (95%-105%).

Table 5- Post-compression evaluation parameters

Formulation Code	Average weight (gm)	Thickness (cm)	Hardness (Kg/cm ²)	Friability (%)	Assay (%)	
					Dapsone	Acetazolamide
F1	0.448	0.55±0.00 5	5.5	0.87	99.70	100.60
F2	0.527	0.55±0.00 5	5.5	0.56	98.00	99.30
F3	0.533	0.55±0.00 5	5.5	0.56	99.65	102.07
F4	0.531	0.55±0.00 5	5.5	0.48	99.33	101.69

±S.D. n=3

In vitro Dissolution studies

The release profile of Dapsone from different batches of formulated matrix tablets was plotted in Figure 13. Based on the results of in-vitro dissolution testing, it was known that the formulations were compressed with different concentrations of superdisintegrant and showed different rates of drug release. The t90% increases with an increase in the quantity of superdisintegrant. These values are for a 60-minute period. But the formulation D1 showed the maximum amount of drug release, i.e., 98.04% for a period of 60 minutes. Similarly, the release profile of Acetazolamide from different batches of formulated matrix tablets was plotted in Figure 14. Based on the results of in-vitro dissolution testing, it was known that the formulations were compressed with different concentrations of E4M polymer and showed different rates of drug release. An increase in polymer

concentration results in a decrease in $t_{90\%}$. These values are for a 12-hour period. But the formulation A4 showed the maximum amount of drug release, i.e., 94.21% for a period of 12 hours.

Fig. 13: In-vitro drug release profile of immediate release matrix tablet of Dapsone

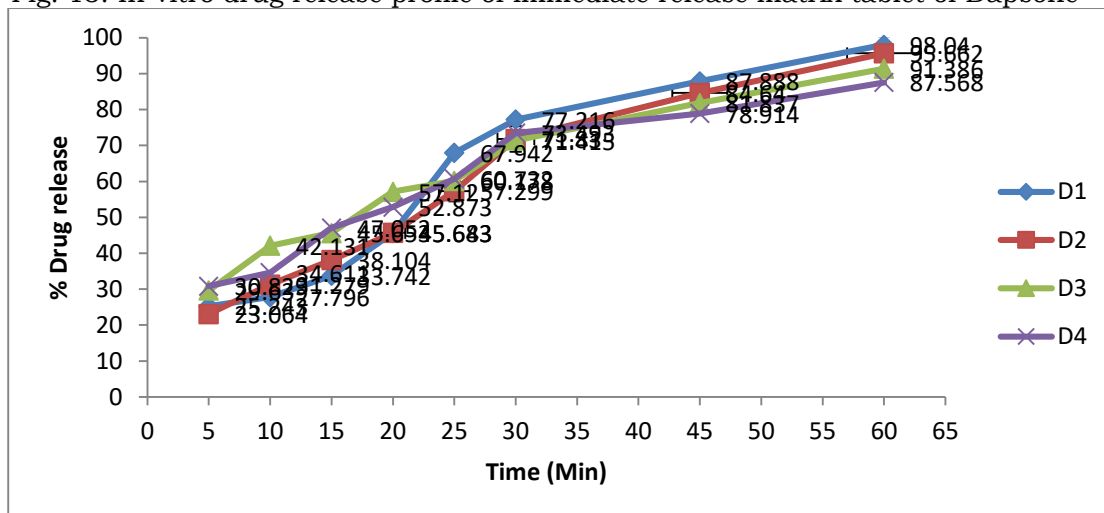
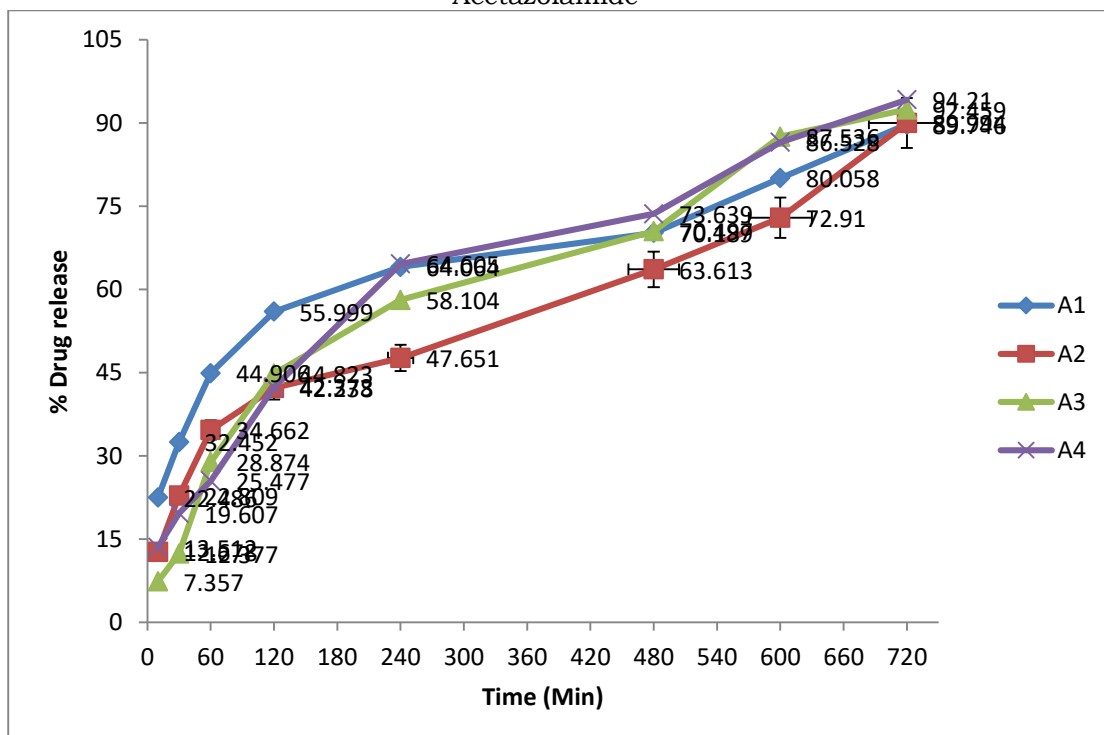


Fig. 14: In-vitro drug release profile of Sustained release matrix tablet of Acetazolamide



Kinetic analysis of In vitro drug release study [18]

In-vitro drug release profiles for prepared batches of Dapsone and Acetazolamide were applied to different kinetic models such as the zero order model, first order model, matrix model, and Haxson-Crowell model, etc. The kinetic data for all the batches is illustrated separately in tables 6 and 7. The highest correlation coefficient resulted from the matrix model, which indicates that the drug is released by dissolution with the changes in surface area and diameter of particles or tablets. The rate of dissolution is determined by the surface area of the solvent; the larger the area, the faster the dissolution.

Table 6 – Kinetics of drug release profile for Dapsone

Results		Zero order model	First order model	Matrix model	Hix. Crow. model
Sr. No.	Time (min)	29	41	229	36
1.	0	0.000	0.000	0.000	0.000
2.	5	6.186	7.869	0.780	7.254
3.	10	7.725	11.134	0.848	9.877
4.	15	6.378	10.535	0.980	8.987
5.	20	2.861	6.252	0.812	4.951
6.	25	0.013	0.885	0.749	0.439
7.	30	5.596	2.542	0.819	3.430
8.	45	0.701	0.396	0.974	0.492
9.	60	0.011	1.047	0.920	0.565

Table 7 – Kinetics of drug release profile for Acetazolamide

Results		Zero order model	First order model	Matrix model	Hix. Crow. model
Sr. No.	Time (min)	1	1	7	1
1.	10	0.000	0.000	0.000	0.000
2.	15	0.011	0.011	0.830	0.011
3.	30	0.001	0.000	0.848	0.001
4.	60	0.063	0.054	0.835	0.057
5.	120	0.199	0.171	0.704	0.180
6.	240	0.113	0.082	0.595	0.091
7.	480	0.509	0.563	0.860	0.544
8.	600	0.069	0.072	0.978	0.071
9.	720	0.237	0.276	2.980	0.263

Conclusion

The study of formulating bilayer tablets containing Dapsone and Acetazolamide was successfully achieved by using direct compression technology. Bilayer tablets contained Dapsone as an immediate release layer and Acetazolamide as a sustained release layer. This formulation was prepared using Ac-Di-Sol as the

superdisintegrant in the immediate release layer and E4M polymer in the sustained release layer. DSC and IR studies revealed that there were no compatibility issues between the API and the excipients used in the formulation. The dissolution study was performed separately for each layer for 60 min for the immediate release layer and 12 hours for the sustained release layer, which was taken as the ideal formulation to fulfil all requirements of the bilayer tablet. Analyzing regression coefficients in drug release kinetic studies, it was found to fit the matrix model. All other evaluation studies performed were found to be within the official limit range.

Acknowledgement

The authors are greatly thankful to Ashland Inc. Ltd., Netherlands for providing a gift sample of Benecel™ E4M polymer.

Conflict Of Interest

The authors declare no conflict of interest.

References

1. Roop K Khar, SP Vyas, Farhan J Ahmad, Gaurav K Jain (2013). Lachman/Lieberman's The Theory and Practice of Industrial Pharmacy. CBS Publishers & Distributors Pvt. Ltd., Fourth edition, 872.
2. Vishwakarma A. G., Mogal R. T., Pawar A. Y. (2014). Bi-Layer Tablet- A New Ways in Oral Drug Delivery System. *Int. J. PharmTech Res.* 6(5)pp, 1416-1428.
3. Reddy P. T., Rao D. V., Kumar R. K. (2013). Bi-layer technology- an emerging trend: a review. *Int. J. Res. Dev. Pharm. L. Sci.* 2(3), 404-411.
4. Priyamvada B., Ganarajan G., Preeti K. (2013). Bilayer: a review. *International Journal of Pharmaceutical and Chemical Sciences*, 2(4), 1788-1797.
5. V. Rajani, Y. Rajendra Prasad, A. Lakshmana Rao (2018). Formulation and In-vitro evaluation of Dapagliflozin and Saxagliptin bilayered tablets. *International Journal of Research in AYUSH and Pharmaceutical Sciences*, 2(11), 296-305.
6. Deepika KL, Sanjeev Kumar P. (2013). Design, development and evaluation of Domperidone maleate bilayer tablets. *International Journal of Pharmacy and Pharmaceutical Sciences*, 5(4), 701-710.
7. Mohideen S. et al. (2011). Development and evaluation of two layered tablet of Glimepiride and Metformin hydrochloride for treatment of hyperglycemia. *Int. J. Bio.* 2(1), 31-35.
8. Fan, Jia, (2011) Study of controlled release of dapsone from modified montmorillonite and polymer matrices. Theses. 80. (<https://digitalcommons.njit.edu/theses/80>).
9. Reddy N. R., Sreedevi G., Prabhavathi K., Chakravarthy I. E. (2003). A simple and rapid spectrophotometric determination of Dapsone and its dosage form. *Asian Journal of Chemistry*. 14(2), 1146-1148.
10. Reddy P. S., Dayakar M., Srinivasulu D., Reddy N. V., Akhila G., Venkatesh P., Jyothi M. (2020). Method development and validation of Acetazolamide by using UV spectroscopy. *IJESC*. 10(6), 26146-26154.

11. Suresh Jain, Anil Bhandari & Suresh Purohit. (2009). Spectrophotometric determination of nateglinide in bulk and tablet dosage forms. *Asian Journal of Pharmaceutics*. July-September. pp218-221.
12. Interpreting Unexpected Events and Transitions in DSC Results- TA Instruments. <http://www.tainstruments.com/pdf/literature/TA039.pdf>.
13. How to Interpret the Unexpected Transitions in DSC Results- TA Instruments. <https://www.azom.com/article.aspx?ArticleID=12101>.
14. Mohd Abdul Handi, V. Lokeswara Babu, Narottam Pal (2012). Formulation and evaluation of sustained release matrix tablets of Glimepiride based on combination of Hydrophilic and hydrophobic polymers. *Journal of Applied Pharmaceutical Science*. 2(6), 101-107.
15. Radhika P. R., Pal T. K., Sivakumar T. (2009). Formulation nad evaluation of sustained release matrix tablet of Glipizide. *Iranian Journal of Pharmaceutical Sciences*. 5(4), 205-214.
16. Chinta R., Pilli R. (2020). Formulation design of Empagliflozin and Metformin hydrochloride extended release tablets: Optimization of formulation using statistical experimental design. *Int. J. Pharm. Sci. & Res*. 11(12), 6434-6447.
17. Marcos Luciano Bruschi (2015). 5 - Mathematical models of drug release. Strategies to Modify the Drug Release from Pharmaceutical Systems. *Woodhead Publishing*, 63-86. (<https://doi.org/10.1016/B978-0-08-100092-2.00005-9>)
18. Salih O. S. (2015). Study the sustained release effect of different polymers used in the formulation of Aspirin-Rosuvastatin tablets. *International Journal of Pharmacy and Pharmaceutical Sciences*. 7(12), 166-172.
19. Dudhe P.B., Lahane A. V., Borhade K. D., Shelke P.S., Chavare P.D. (2017). Spectrophotometric Determination of Acetazolamide in Bulk and Tablet Dosage Form by Area Under Curve and First Order Derivative Methods. *International Journal of ChemTech Research*. 10(6)pp, 261-268.

How to Cite:

Kerle, V., Kasabe, A., Barge, V., Kulkarni, O., & Pate, A. (2022). Formulation and evaluation of topical gel containing combination of dapsone and acetazolamide. *International Journal of Health Sciences*, 6(S3), 9216–9229.
<https://doi.org/10.53730/ijhs.v6nS3.8246>

Formulation and evaluation of topical gel containing combination of dapsone and acetazolamide

Vikram Kerle

Department of Pharmaceutical Quality Assurance, PDEA'S Shankarrao Ursal
College of Pharmaceutical Sciences & Research Centre, Kharadi, Pune,
Maharashtra, India

*Corresponding author email: Vikramkerle008@gmail.com

Amit Kasabe

Department of Pharmaceutical Quality Assurance, PDEA'S Shankarrao Ursal
College of Pharmaceutical Sciences & Research Centre, Kharadi, Pune,
Maharashtra, India

Vijaya Barge

Department of Pharmaceutical Quality Assurance, PDEA'S Shankarrao Ursal
College of Pharmaceutical Sciences & Research Centre, Kharadi, Pune,
Maharashtra, India

Onkar Kulkarni

Department of Pharmaceutical Quality Assurance, PDEA'S Shankarrao Ursal
College of Pharmaceutical Sciences & Research Centre, Kharadi, Pune,
Maharashtra, India

Abhijit Pate

Department of Pharmaceutical Quality Assurance, PDEA'S Shankarrao Ursal
College of Pharmaceutical Sciences & Research Centre, Kharadi, Pune,
Maharashtra, India

Abstract---The idea of innovation is to formulate a gel containing the combination of Dapsone and Acetazolamide for the treatment of Angioedema. Dapsone being a sulfone has antibacterial and antibiotic properties whereas Acetazolamide has a Diuretic property. So, a combination of these drugs helps to obtain a formulation with antibacterial, antibiotic and diuretic effect for the treatment of Angioedema. Various excipients such as a gelling agent, preservative, solubilizing agent etc. are used to form a stable and flawless gel formulation. The gel formulation prepared is used in the treatment of Angioedema that is a rapid oedema or swelling at specific areas such

as face, genitals, hands, feet's etc. The formulation has a comparatively greater effect for treatment of angioedema. Marketed formulations in treatment of angioedema have a specific action on the body such as antibiotic or diuretic whereas this new formulated gel has a combination of drugs that have a dual effect for the treatment of Angioedema. The swelling caused by the disease and the spread of infection is more effectively treated by this combination used in the gel formulation.

Keywords---topical drug delivery system (TDDS), gel formulation, angioedema, HPMC, dapsone, acetazolamide, antibiotic, diuretic.

Introduction

Topical Drug Delivery System (TDDS) has now become a more progressive way for the treatment of diseases related to skin. This delivery system has a more target-oriented way of action. It includes formulations such as gels, creams, ointments, lotions etc. These formulations are directly administered at the site of skin injury, infection or diseases related to skin. Gels have a significant mechanism of action by optimal cutaneous and percutaneous drug delivery. They avoid the GIT (Gastro-Intestinal Tract) which helps in avoiding enzymatic activity and drug interactions with food and drinks thus avoiding the first pass effect. ¹ Dapsone is a synthetic sulphone that has antibiotic and antibacterial property. It is a white crystalline powder that is odourless in nature. It is soluble in alcohol, methanol, acetone and Dil. Hcl. Dapsone acts against bacteria and protozoa in the same way as sulphonamides, that is by inhibiting the synthesis of dihydrofolic acid through competition with para-amino-benzoate for the active site of dihydropteroate synthetase. The anti-inflammatory action of the drug is unrelated to its antibacterial action and is still not fully understood. 5% of Dapsone gel is available in the market for the treatment of Acne Vulgaris. The antibacterial property of dapsone helps to cease the spread of infection. ²

Acetazolamide is potent carbonic anhydrase (CA) inhibitor. It is a white crystalline powder which is odourless in nature. It is soluble in ethanol and slightly in water. The diuretic effect of acetazolamide is due to its action in the kidney on the reversible reaction involving hydration of carbon dioxide and dehydration of carbonic acid. The result is renal loss of bicarbonate (HCO_3^- ion), which carries out sodium, water, and potassium. The removal of water from the site of infection helps in treating swelling in case of angioedema. ³ The combination of Dapsone and Acetazolamide provide a dual effect in treatment of angioedema. The antibiotic and antibacterial effect of dapsone helps to cease the infection whereas the diuretic effect of acetazolamide helps in decreasing the swelling from the site of infection. Polymer or the gelling agent used is Hydroxy Propyl Methyl Cellulose (HPMC) that acts by stabilizing the gel molecules.

Materials and Methods

Materials

Dapsone and Acetazolamide were purchased from Aarti Distributors, Mumbai. HPMC K750 was obtained from Ashland Inc, Netherland. Other chemicals such as Tween 80, Methyl Paraben and Triethylamine were obtained in co-ordination from the Department of Pharmaceutical Quality Assurance. Dapsone is an antibacterial and antibiotic agent. Acetazolamide acts as a diuretic agent are main active pharmaceutical ingredient are used in the formulation. HPMC (Hydroxy Propyl Methyl Cellulose) is a polymer and is used as a gelling agent to form a stable gel formulation. The HPMC is mixed with water by continuous stirring to form a polymer complex which acts as a gel base for the formulation. Methyl Paraben used acts as a preservative and helps in maintaining the drug properties for a longer time. Tween 80 is used in as a surfactant; it helps in increasing the viscosity at acidic Ph. It also reduces the surface tension leading to increase in spreading and wetting properties of the gel. Tween 80 being in liquid form has an additive effect of increasing the volume of the formulation. Triethylamine used acts as an alkalizing agent or pH stabilizing agent. It is added in the formulation in quantity that is sufficient to make the gel neutral in nature to avoid any skin problems after application such as skin irritation, itching, redness etc. Purified water is added to the formulation with continuous stirring to avoid flocculation and formation of water bubbles. Water is added in sufficient quantity to make up the volume to desired quantity. These materials used were obtained in pure form and formulation was prepared. Each and every chemical was certified pure and free of any contamination or impurities. The purity of the drugs is important to formulate a stable gel, free from any contaminations or impurities.

Methods⁷

There are some of the processes like Hydrolysis and polycondensation (SOL-GEL), gelation, aging, drying, densification, and crystallization for the formulation of gel formulation. SOL-GEL: This process involves hydrolysis and polycondensation reactions. In this method a colloidal suspension is converted to a gel. It is compatible to polymer and polymerisation. DISPERSION: In this method the gelling agent or the polymer is dispersed in water with continuous stirring at 1200 rpm for 30 minutes. Then the API are directly added to the dispersion with a suitable preservative. We have used Dispersion method for successful formulation of the gel.

Dispersion method ⁸

HPMC was dispersed in water with stirring at 1200 rpm for 30 minutes. Next step involves addition of API with continuous stirring. Dapsone and Acetazolamide are mixed with the dispersion of HPMC. Finally, the addition of excipients is done such as methyl paraben, Tween 80 and Triethylamine. Water is used as a vehicle to increase the consistency of the formulation and to make the volume to required quantity. During all the processes, continuous stirring of the formulation is required to avoid formation of water bubbles which may mess with the consistency of the formulation. The gel formulation then prepared is kept still for

30 mins to check whether it solidifies or not. This gel formulation prepared by dispersion method with firm and continuous stirring is free from flocculation or water bubbles. The polymer used is HPMC that acts as a gelling agent forms the dispersion with water and acts as a gelling base for the formulation. A stable gel formulation is prepared with the help of this dispersion method.

Formula

Table 1
Formulation Table for All Batches

Name of the ingredient	Batch I	Batch II	Batch III	Batch IV
Dapsone (gm)	0.375	0.375	0.375	0.375
Acetazolamide (gm)	0.25	0.25	0.25	0.25
Methyl paraben (gm)	0.01	0.01	0.01	0.01
HPMC K750 (GM)	0.025	0.050	0.075	0.125
Tween 80 (ml)	1.875	1.875	1.875	1.875
Triethylamine	Q. S	Q. S	Q. S	Q. S
Purified water	Q. S	Q. S	Q. S	Q. S

Analytical Tests Performed

Preformulation tests

UV-spectrophotometry: ⁹

This technique is used to determine the absorbance of light in ultraviolet and visible ranges of electromagnetic spectra. A light in UV spectra is incident on the sample and the amount of light absorbed is determined. Method carried out in this test is as follows; Stock solution was prepared by weighing 10mg of drug and adding it in 0.1N Hcl. Dilutions were prepared of concentration of 2ppm, 4ppm, 6ppm, 8ppm, 10ppm and volume was makeup with 0.1N Hcl. Absorbance of each concentration was taken at 290 nm and calibration curve was plotted.

FT-IR Spectroscopy: ¹⁰

This technique is used to determine the absorption of light in infrared spectra. It was used to determine different functional groups present in a drug or sample. FT-IR spectrum was recorded between 4000-400 cm^{-1} . This technique is mainly used in identification and confirmation of unknown materials.

DSC (Differential Scanning Calorimetry): ¹⁴

A Differential Scanning Calorimetry, or DSC, is a thermal analysis technique that looks at how a material's heat capacity (C_p) is changed by temperature. A sample of known mass is heated or cooled and the changes in its heat capacity are tracked as changes in the heat flow. This technique helps in establishing a connection between the enthalpy and the physical properties of a substance.¹⁵ The instrument used for DSC is a device thermal analysis instrument that

determines the temperature and heat flow associated with material transitions as a function of time and temperature.¹⁶

Postformulation tests

- pH determination:
pH was recorded using digital pH meter. 5g gel was dispersed in 45ml distilled water at 27°C and solution pH was measured.
- Conductivity:
The conductivity of the sample depends on the dielectric constant of the solvent used. The conductivity may differ for each and every formulation depending upon the solvent used.

Particle size determination

It is a measurement of size distribution of individual particles of gel or any other formulation. It is a fundamental physical property that determine the physical nature and stability of the formulation.

Technique used

Laser diffraction spectrometry

It is the most widely used technique for determination of particle size distribution of any sample. This technique is widely used due to its rapid results and simplicity of use. It provides immediate experimental results compared to other techniques. Particle size distribution affects various physical parameters of a formulation are as follows; drug release rate for various sustained and delayed release formulations. Dissolution rate and bioavailability of various drugs. Dose uniformity and content of the formulation.

Figure 2

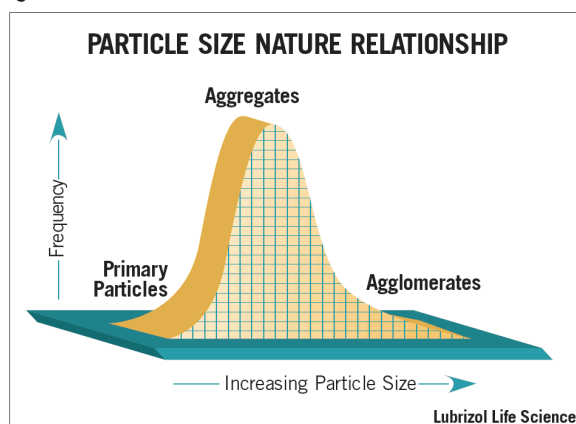


Figure: Relation between particle size and frequency of particles

Zeta potential: ¹⁷

This process is used to determine the charge on the surface of particles present in the gel formulation. A greater positive and negative values of zeta potential indicate a good physical stability of the individual particles. This test helps in determining the physical stability of the formulation as well as the binding tendency of the particles of gel formulation. It is the key to electrostatic dispersion control. It is used to optimize the formulation and increase the stability of the formulation. It is used in determining long-term stability.

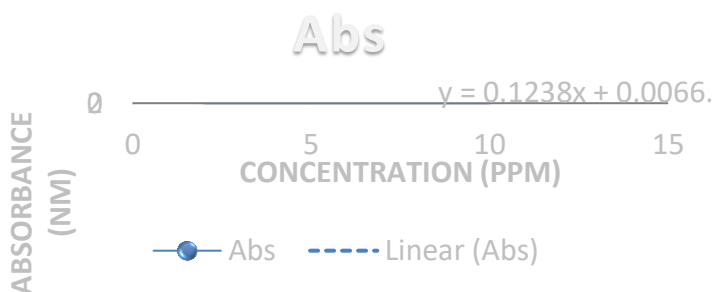
Table 2
Parameters of zeta potential

Manitude of Zeta potential (mV)	Stability behavior
0 to 5	Rapid coagulation or flocculation
10 to 30	Incipient instability
30 to 40	Moderate stability
40 to 60	Good stability
Greater than 61	Excellent stability

Result and Discussion**UV-spectrophotometry:**⁹**Dapsone**

Stock solution was prepared by weighing 10 mg of drug and adding it in 0.1N Hcl. Dilutions were prepared of concentration of 2 ppm, 4 ppm, 6 ppm, 8 ppm, 10ppm and volume was makeup with 0.1N Hcl. Absorbance of each concentration was taken at 290 nm and calibration curve was plotted. Calibration curve was determined by plotting the values of Absorbance versus Concentration.

Sr No.	Concentration (in ppm)	Absorbance (in nm)
1.	2	0.245
2.	4	0.512
3.	6	0.755
4.	8	0.992
5.	10	1.243

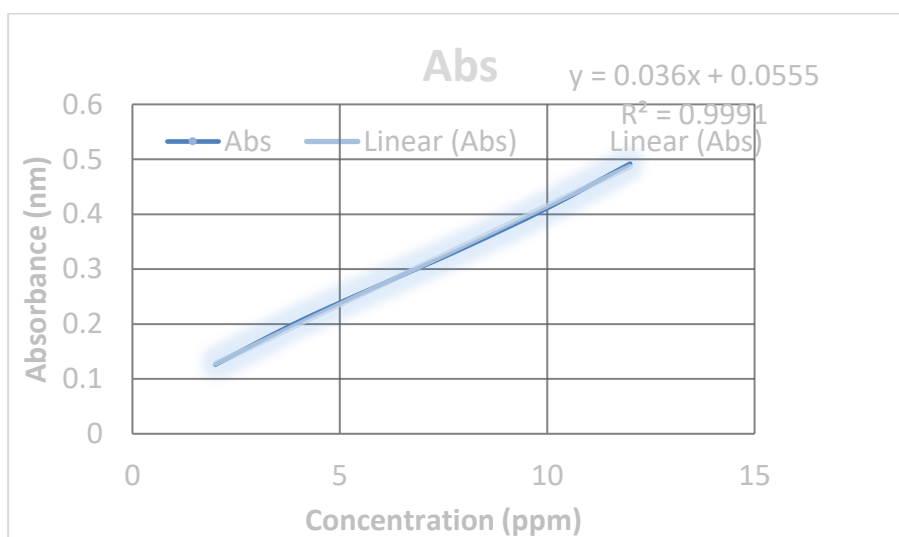


Graph: Calibration Curve of Dapsone by UV-Spectrophotometry

Acetazolamide

Acetazolamide (10 mg) was accurately weighed and dissolved in 100 ml of 0.00 1 N HCl to give a stock solution of concentration 100 g/ml. This was the primary stock solution of 100 g/ml. It was shaken to get the drug dissolved. UV spectrum was recorded in the wavelength range 278.94nm. Calibration curve was determined by plotting the values of Absorbance versus Concentration.

Sr No.	Concentration (in ppm)	Absorbance (in nm)
1.	2	0.126
2.	4	0.204
3.	6	0.272
4.	8	0.339
5.	10	0.411
6.	12	0.492

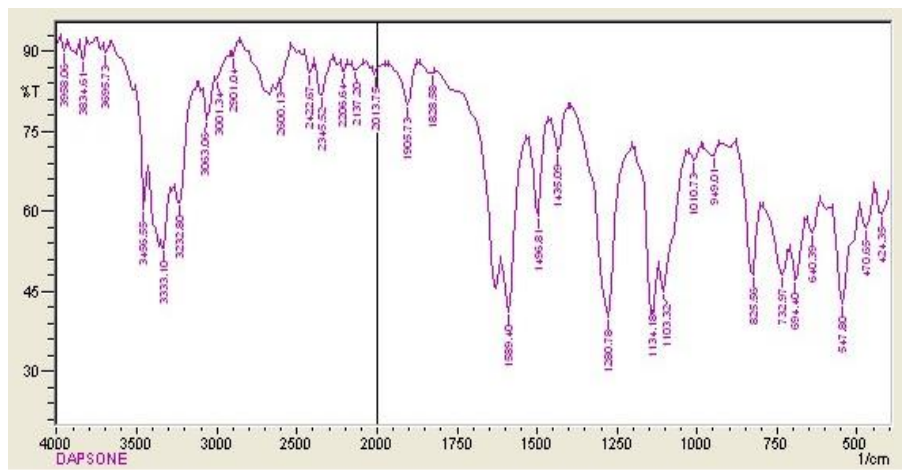


Graph: Calibration Curve of Acetazolamide by UV-Spectrophotometry

FT-IR Spectroscopy

The FT-IR spectroscopy was done and the following spectra were observed:

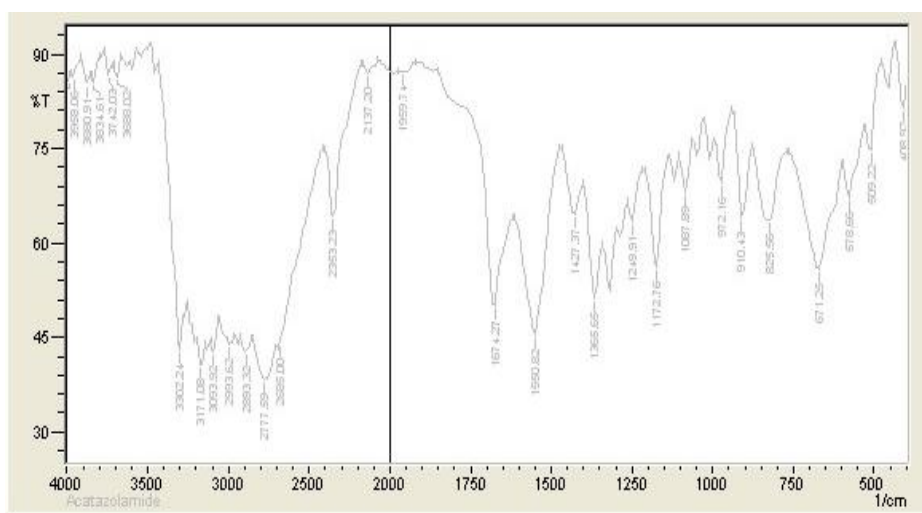
Dapsone



Graph: FT-IR spectra of Dapsone

Identification and confirmation of active pharmaceutical ingredients was carried out by observing the obtained FT-IR spectra. Dapsone showed characteristic peak values at 3063.06 (C-H stretching); 3333.10 (N-H stretching); 1589.40 (C=C stretching); 1280.78 (C-N stretching) and 1134.18 (S=O stretching). These peak values were determined by observed spectra of Dapsone as shown in above graph.

Acetazolamide

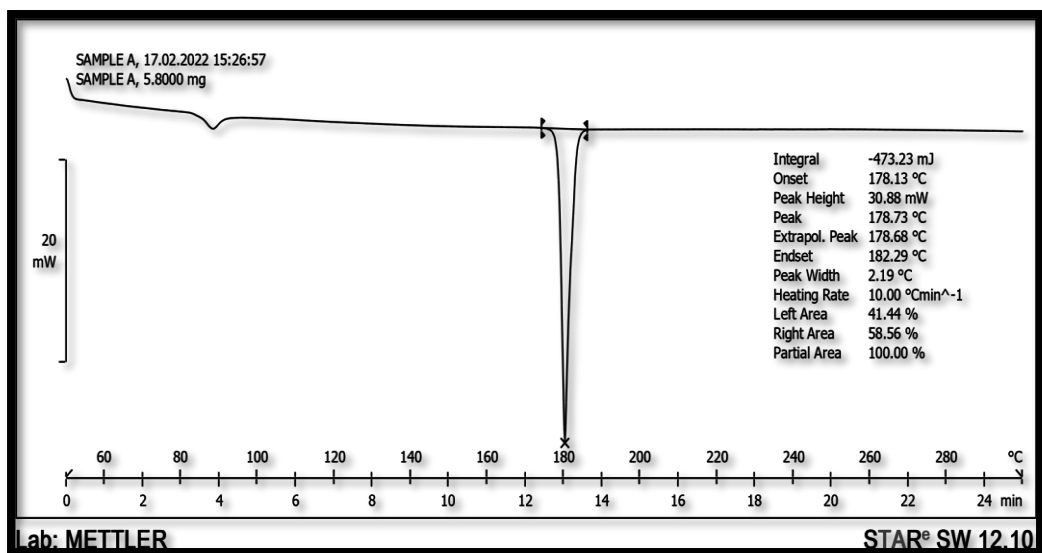


Graph: FT-IR spectra of Acetazolamide

Acetazolamide showed characteristic peak values at 3302.24 (C=O stretching); 2353.23 (C=N stretching); 1365.65 (S=O stretching) and 1674.27 (R-C(=O)NH_2 stretching). These peak values were determined by observed spectra of Acetazolamide as shown in the above graph.

DSC (Differential Scanning Calorimetry):

SAMPLE A: Dapsone: The melting point of Dapsone is 175-178 °C.

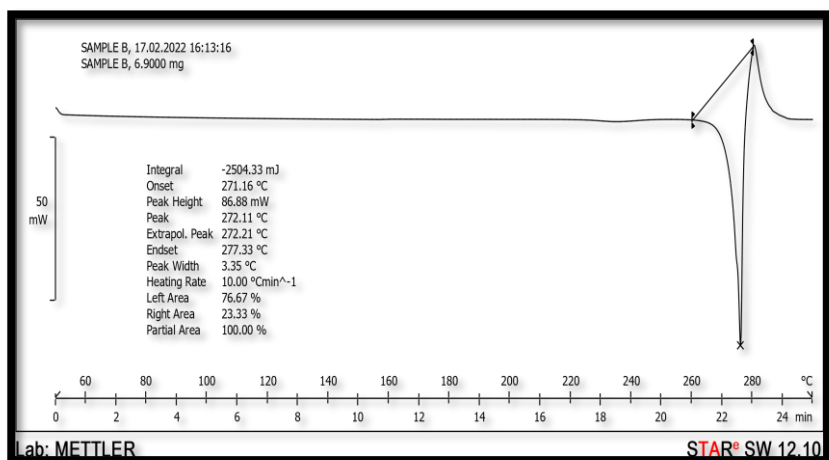


Graph: Differential Scanning Calorimetry of Dapsone

A curve is observed in the graph. The onset temperature is 178.13° C and the peak transition temperature is 178.73° C that is the melting point of Dapsone.so the thermal identification of Dapsone is done with the help of DSC.

Sample B: Acetazolamide:

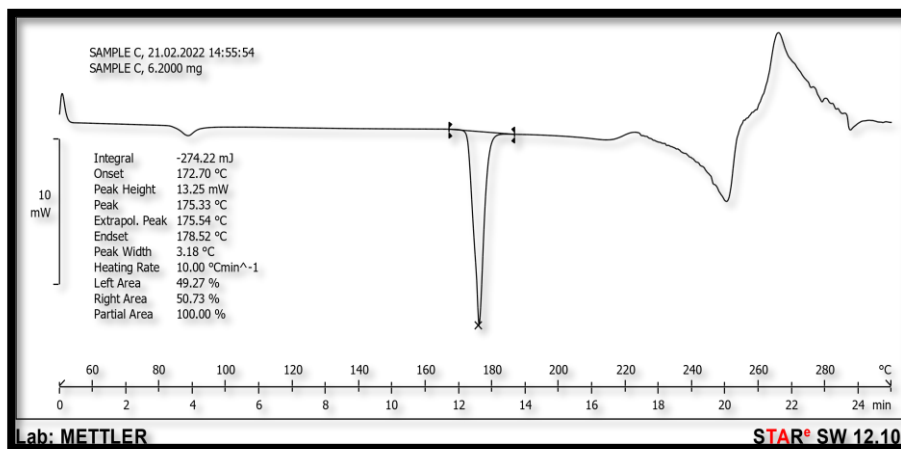
The melting point of Acetazolamide is 258-271° C.



Graph: Differential Scanning Calorimetry of Acetazolamide

A curve is observed in the graph. The onset temperature is 271.16°C and the peak transition temperature is 272°C that is the melting point of Acetazolamide. so the thermal identification of Acetazolamide is done with the help of DSC.

Sample C: Dapsone + Acetazolamide:



Graph: Differential Scanning Calorimetry of Dapsone and Acetazolamide in combination

A curve is observed in the graph. The onset temperature is 172°C . It shows the melting point of Dapsone. So, the combination shows a compatibility. So, the thermal compatibility of this combination is done with the help of DSC.

Post Formulation Analysis PH Determination

Batch no.	pH value
I	6.9
II	5.8
III	6.2
IV	6.4

Conductivity

Sr no.	200 ms	20 ms	2 ms	200 μs	20 μs
Batch I	000	00.2	0.19	190	1
Batch II	000	00.2	0.22	1	1
Batch III	000	00.2	0.22	1	1
Batch IV	000	00.1	0.18	177	1

Particle size determination

The test was done on 4 batches of gel and particle size data was obtained. Among them 4th batch had the best particle size. The graph of the 4th batch is as shown below:

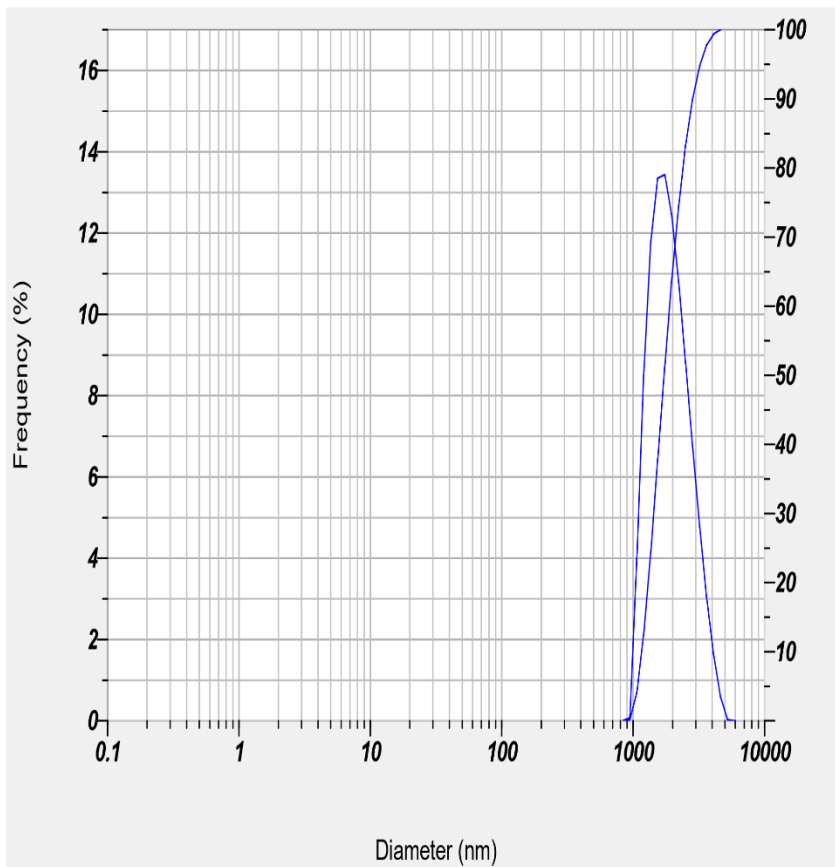
Cumulant Operations

Z-Average

: 941.0 nm

PI

: 0.901



Graph: particle size determination of Batch IV

Zeta Potential (17)

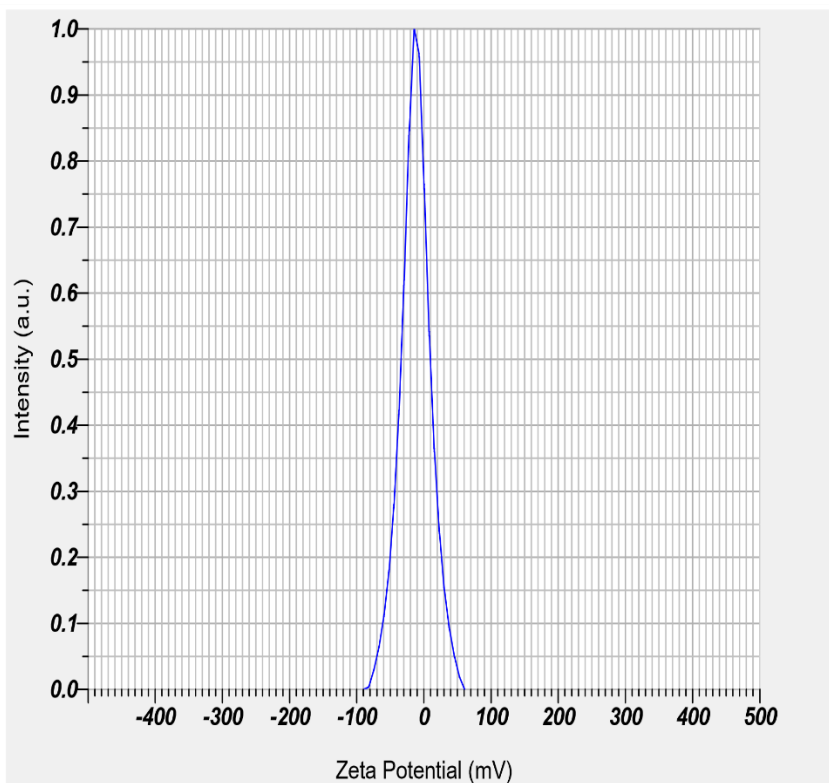
The test was done on 4 batches of gel and particle size data was obtained. Among them 4th batch had the best particle size. The graph of the 4th batch is as shown below:

Calculation Results

Peak No.	Zeta Potential	Electrophoretic Mobility
1	-12.1 mV	-0.000094 cm ² /Vs
2	--- mV	--- cm ² /Vs
3	--- mV	--- cm ² /Vs

Zeta Potential (Mean) : -12.1 mV

Electrophoretic Mobility Mean : -0.000094 cm²/Vs



Graph: Zeta potential of Batch IV

Conclusion

The prepared formulation has a greater effect and stability compared to other present marketed formulations. Various marketed formulations present in the form of tablets, oral suspensions and i formulations have a synergic effect on treatment of angioedema. But the gel formulation prepared has a greater action because (1) The administration is done at the site of infection or cell injury so a greater drug absorption is caused which leads to more efficient action on the diseases. (2) The topical drug delivery avoids the First Pass Metabolism thus avoids the enzymatic degradation and acidic degradation of drug. (3) The

administered drugs are readily absorbed in the body and cause a dual action of antimicrobial as well as diuretic action which totally treat angioedema to minimize all its symptoms. (4) The systemic side effects caused are relatively low compared to other marketed formulations. Drug degradation leading to lower action of drug is minimized by use of preservative. So, a stable and long use gel formulation is obtained. Thus, a stable gel formulation is prepared that is effective in the treatment of angioedema.

Acknowledgment

For the completion of the research work the authors would like to show sincere gratitude to PDEA'S Shankarrao Ursal College of Pharmaceutical Sciences & Research centre, Kharadi, Pune, to provide with a lot of support and help whenever needed.

References

1. Gupta, S. and Pandit, K.R., In; Concepts of Pharmaceutical Dosage Form, 9th Edition, B.S. Shah Publication, Delhi, 1997, pg.no.155-156.
2. Tripathi, K.D., In; Essentials of Medical Pharmacology, 5th Edition, Jaypee Brothers Medical Publisher Pvt. Ltd, New Delhi, 2004, pg no.8-16.
3. Ahuja, M., Bodake, S.H., Gupta, S. and Jayal, V., In; Piyush Synopsis for Pharmacy, 2nd Edition., Piyush Book Publication Pvt. Ltd., 2005, pg no.443.
4. Brahmankar, D.M. and Jaiswal, S.B., In; Biopharmaceutics and Pharmacokinetic, A Treatise, 1st Edition, Vallabh Prakashan, Delhi, 1995, pg no.7-8.
5. Kumar B, Antimicrobial resistance in leprosy. Clinical microbiology and infection: the official publication of the European Society of Clinical Microbiology and Infectious Diseases. 2018 Dec 21.
6. Kassamali R, Sica DA. Acetazolamide: a forgotten diuretic agent. Cardiol Rev. 2011 Nov-Dec; 19(6):276-8.
7. Mikami R, Mishra B, Rajnikant P S, Balasubramaniam J. Development and evaluation of a novel floating in situ gelling system of amoxicillin for eradication of Helicobacter pylori. International Journal of Pharmaceutics, 335(1): 114-122, 2007.
8. Bakhle S. S., Upadhye K.P., Dixit G.R., Wadetwar R.N. Solubility and Dissolution Improvement of Poorly Soluble Drug Using Solid Dispersion Technique. International Journal of Pharmacy and Technology. 2 (4); 1230-1240; 2010.
9. Skoog, Douglas A; Holler, F. James; Crouch, Stanley R. (2007). Principles of Instrumental Analysis (6th edition). Belmont, CA: Thomson Brooks/Cole.
10. Tamm, L.K. and Tatulian, S.A. Infrared spectroscopy of proteins and peptides in lipid bilayers. pg no. 365-429.
11. Seshadri, S., Khurana, R. and Fink, A.L. Fourier transform infrared spectroscopy in analysis of protein deposits. Methods Enzymol. pg no. 559-576.
12. Barth, A. Infrared spectroscopy of proteins. Biochim Biophys Acta 1767, 1073-1105 (2007)
13. Doglia, S.M., Ami, D., Natalello, A., Gatti-Lafranconi, P. and Lotti, M. Fourier transform infrared spectroscopy analysis of the conformational quality of recombinant proteins within inclusion bodies.

14. Privalov PL, Potekhin SA. Scanning microcalorimetry in studying temperature induced changes in proteins.
15. Hohne G, Hemminger W, Flammersheim H-J. Differential Scanning Calorimetry: An introduction for practitioners.
16. Haines PJ, Reading M, Wilburn FW. Differential thermal analysis and differential scanning calorimetry. In Brown ME. (ed); Handbook of Thermal Analysis and Calorimetry, vol I.
17. Kumar A, Dixit CK (2017). "Methods for characterization of nanoparticles". Advances in Nanomedicine for the Delivery of Therapeutic Nucleic Acids. pg no. 43-58.

How to Cite:

Shubhangi, K., Amit, K., Bhavana, B. V. S., & Parijat, S. (2022). Formulation and evaluation of a dapson and fexofenadine HCl immediate release combination tablet. *International Journal of Health Sciences*, 6(S3), 9191–9205.
<https://doi.org/10.53730/ijhs.v6nS3.8244>

Formulation and evaluation of a dapson and fexofenadine HCl immediate release combination tablet

Karkhile Shubhangi

Department of Pharmaceutical Quality Assurance, PDEA'S Shankarrao Ursal College of Pharmaceutical Sciences & Research centre, Kharadi, Pune, Maharashtra, India

*Corresponding author email: Shubhangi3347@gmail.com

Kasabe Amit

Department of Pharmaceutical Quality Assurance, PDEA'S Shankarrao Ursal College of Pharmaceutical Sciences & Research centre, Kharadi, Pune, Maharashtra, India

Barge Vijaya Sakpal Bhavana

Department of Pharmaceutical Quality Assurance, PDEA'S Shankarrao Ursal College of Pharmaceutical Sciences & Research centre, Kharadi, Pune, Maharashtra, India

Suryawanshi Parijat

Department of Pharmaceutical Quality Assurance, PDEA'S Shankarrao Ursal College of Pharmaceutical Sciences & Research centre, Kharadi, Pune, Maharashtra, India

Abstract---The purpose of the study was to formulate a conventional (immediate release) tablet using a combination of Dapsone and Fexofenadine HCl. Dapsone is a sulfone with anti-inflammatory, immunosuppressive, antibiotic, and antibacterial properties. Fexofenadine HCl is a non-sedating antihistamine approved for the treatment of allergies, whereas Dapsone is used to prevent bacteria from growing and causing red, itching welts. Fexofenadine HCl is an antihistamine that is used to treat allergic symptoms by blocking a natural substance called histamine. Direct compression methods were used to formulate the tablets, which contained super disintegrating polymers such as Ac-di-sol (Croscarmellose sodium). Four tablet formulations were compounded using the direct compression method, with polymer varying ratios. According to the evaluation results, formulations met the specifications when compared to official pharmacopoeias and standards. Different parameters, such as

hardness, friability, weight variation, and dissolution studies, were used to evaluate tablets. This formulation of tablet combination of Dapsone and Fexofenadine HCl releases the drug within 60 minutes. Thus, the trial was a success in terms of achieving our goal of developing a tablet with few excipients and a simple manufacturing method.

Keywords---dapsone, fexofenadine HCl, urticaria, immediate release, super disintegrant.

Introduction

This research work is concerned with design and characterization of oral immediate release tablet of Dapsone and Fexofenadine HCl in combination in order to provide immediate relief from pain, swelling, itching and to inhibit the growth of bacteria. Immediate release drug delivery systems are designed to provide immediate drug levels in short period of time. Immediate release drug delivery is desirable for drugs having long biological half life, high bioavailability, lower clearance and lower elimination half life. But main criterion for immediate release dosage form is poor solubility of the drug and the need of immediate action of drug to treat unwanted defect condition or any allergic condition¹. Drug delivery systems (DDS) distribute therapeutic medications throughout the body as needed to produce the intended therapeutic impact safely. Typically, such systems are created to enhance active compounds' water solubility and chemical stability, and ii) in-vitro ,iii) decrease side effects while increasing pharmaceutical activity.² Therapeutic effectiveness and short and long-term biological effects are influenced by drug delivery routes and the physicochemical features of those routes. Each delivery technique has advantages, disadvantages and each requires a unique delivery vehicle design.

Oral delivery has emerged as the most appealing route, owing to its ability to produce solid formulations with a long shelf life, convenience of administration, and enhanced immunological response.³ Immediate release tablets are designed to dissolve and release their dose form without the need of special coatings or other rate-controlling procedures. Immediate release tablets crumble quickly and dissolve quickly to release the medication. Disintegration, solubility and different physiological variables all affect medication bioavailability in the mouth.^{4,5} The word "instant relief" comes to mind, when any pharmacological formulation in which galenic modifications do not significantly or purposely slow the rate of drug release from the formulation or drug absorption. In this scenario, immediate release may be achieved by using a suitable pharmaceutically acceptable diluent or carrier that does not significantly slow down the rate of drug release and/or absorption. As a result, the phrase excludes formulations that have been adjusted to give "modified," "controlled," "sustained," "prolonged," "extended," or "delayed" drug release.⁵⁻⁶ Urticaria, sometimes known as "hives," is a common skin condition that affects between 15 and 25% of the population at some point in their lives. Adults are more often than children, and women are more likely than males, with peak frequency in the third to fifth decades of life.

The emergence of pruritic "wheals," which are well-circumscribed patches of non-pitting edema with blanched centres and elevated borders that affect only the superficial sections of the dermis and are visible in association with surrounding erythema of the skin, characterises this disorder.^{8,9} Angioedema affects around 40% of urticaria suffers swelling that occurs beneath the skin.¹⁰⁻¹² Fewer studies show that second-generation antihistamines are effective in the treatment of acute urticaria, a biologic condition that normally disappears in a few of weeks. We can find controlled research that show that any antihistamine is superior in the treatment of acute Urticaria. Second-generation H1 antihistamines are preferred for therapy.¹³ Because of their substantial drowsiness and adverse effects, as well as their short duration of action, first-generation H1 antihistamines are less favoured.¹³ For the treatment of urticaria, second-line antihistamines and an antibiotic are compounded in single-unit dose form. Dapsone is an antibiotic that is used to regulate and minimise bacterial development, while antihistaminics are used to treat allergic diseases and diminish wheals and sores on the body.

Materials and Methods

Dapsone was provided as a complimentary sample by Research-lab Fine Chem Industries (Mumbai, India). Sreekara Organics supplied the Fexofenadine HCl (Telangana). Ashland Inc. Netherland provided the E4M polymer as a free sample. Fine Chem Ltd supplied Ac-Di-Sol and microcrystalline cellulose (Avicel pH 102). (Mumbai, India). Fine Chem Ltd provided the magnesium stearate, talc, and sodium saccharine (Mumbai, India). All of the reagents used in this experiment were of analytical quality.

Methods¹⁴

Identification of pure drug

Identification of pure drug was carried out by Fourier Transform Infra-red Spectrophotometry (Shimadzu 8400) scanned in the range of 200-400nm.

Drug-excipient compatibility study

Studies of drug-excipient compatibility are important to ascertain drug and excipients are compatible with each other. DSC graph and IR spectra are used to study drug-excipient compatibility.

FTIR study

FTIR (Shimadzu 8400s) spectrophotometer were used in the range of 400-4000 cm^{-1} using potassium bromide discs (Mixing ratio 1:1) The samples were hermetically sealed in aluminium pans and heated at a constant rate of 10°C/min over a temperature range of 40 to 300°C.

Drug-excipient compatibility study

DSC study

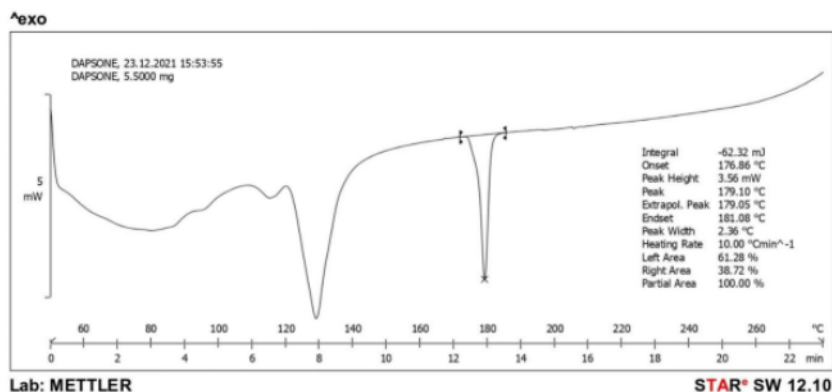


Fig. DSC graph for Dapsone with excipients

The DSC thermogram for Dapsone in combination with various excipients shows the peak onset temperature (Tonset) [176.86°C] and peak transition temperature (Tpeak) [179.10°C]. The thermogram of Dapsone showed a sharp endothermic peak at ~180°C and a peak onset ~176°C. In this thermogram, the melting endotherm of Dapsone (T onset and T peak) was well preserved, with light broadening shifting towards the lower temperature range.

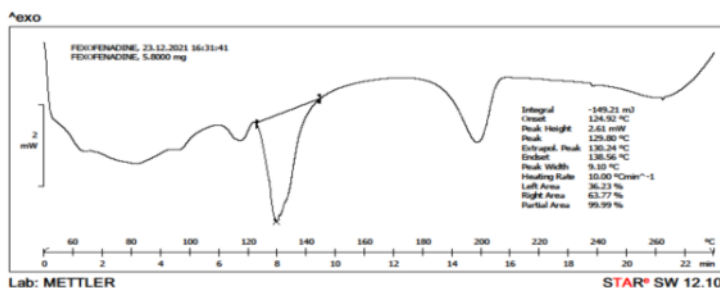


Fig- DSC graph for Fexofenadine HCl with excipients

Similarly, Fexofenadine HCl in combination with various excipients shows an onset temperature (Tonset) [124.92°C] and a peak transition temperature (Tpeak) [129.80°C]. The thermogram of Fexofenadine HCl showed a sharp endothermic peak at ~129°C and a peak onset ~125°C. In this thermogram, the melting endotherm of Fexofenadine HCl (T onset and T peak) was well preserved, with light broadening shifting towards the lower temperature range. These shifts in peak in both graphs to a lower temperature range might be due to the drug being mixed with excipients and do not necessarily indicate probable incompatibility.

FTIR spectroscopy

The FTIR spectrums of pure Dapsone as well Fexofenadine HCl and physical mixtures of drugs and polymers were studied separately as per the excipients used in the formulation. It was observed that there were no major shifts in the main peaks of either drug. This indicates that there were no compatibility problems with the drug with the polymers and excipients used in the formulation. Dapsone had peaks at 3063.06 (=C-H stretching), 3333.10 (N-H stretching), 1589.40 (C=C stretching), 1280.78 (C-N stretching), and 1134.18 (S=O stretching), while Fexofenadine HCl showed characteristic peak values at 3037 (C-H stretching); 1705 (-COOH stretching) ; 3294 (O-H stretching) and 1334 (C-N stretching). These peak values were in accordance with previously reported spectra of Fexofenadine HCl

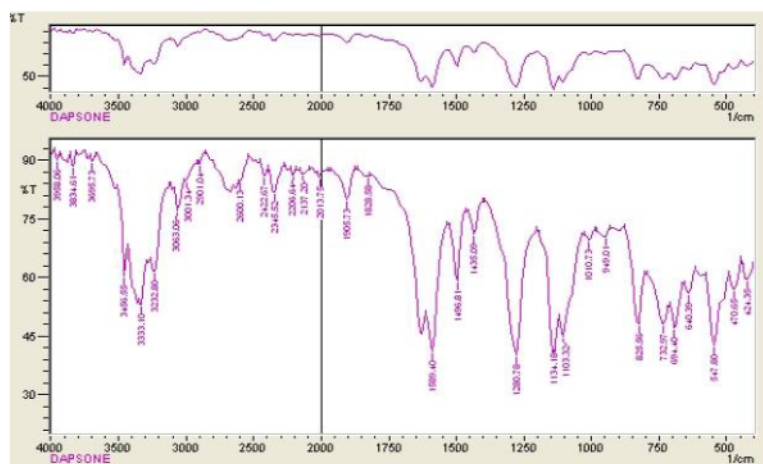


Fig. FTIR of Dapsone

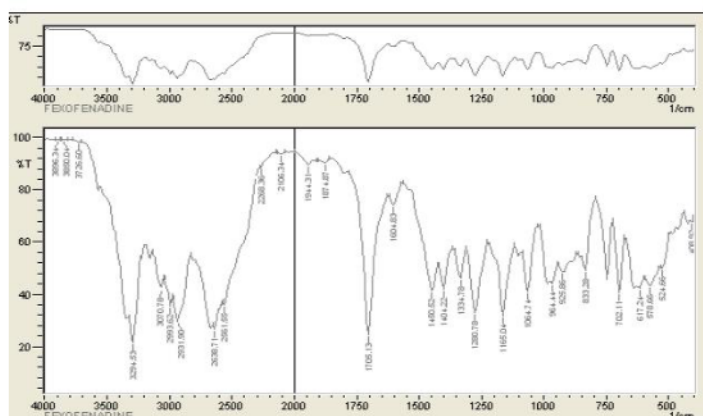


Fig FTIR of Fexofenadine

UV spectroscopy

The linearity of the responses of both drugs was verified at 2–10 µg/ml concentrations. The calibration curve was obtained by plotting the absorbance

versus the concentration data and was treated by linear regression analysis. The equation of the linearity curve for Dapsone obtained was $y = 0.1238x + 0.0066$. The linearity curve was found to be linear for mentioned concentrations (the correlation coefficient (r^2) of determination was 0.9996) (Fig.5). Similarly, the equation of the linearity curve for Fexofenadine HCl obtained was $y = 0.036x + 0.0555$. The linearity curve was found to be linear for mentioned concentrations. (the correlation coefficient (r^2) of determination was 0.9991)

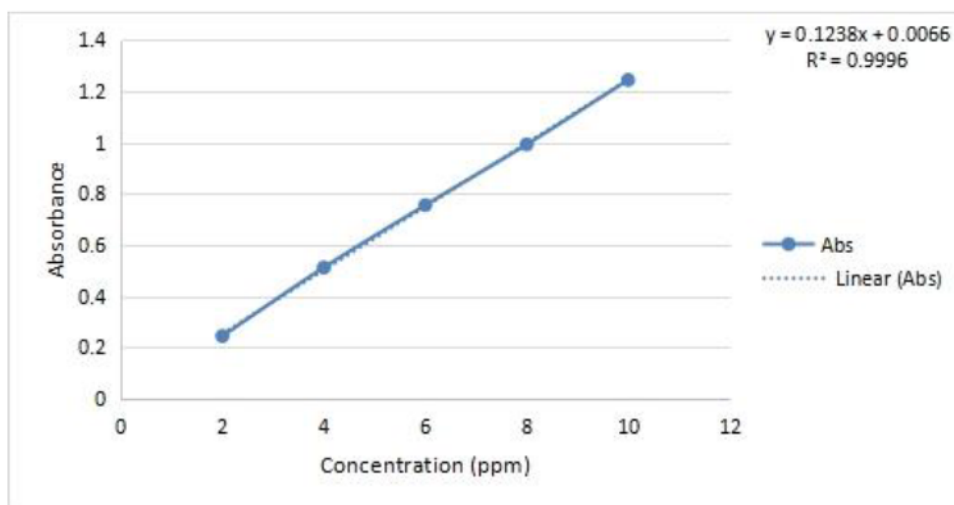


Fig. Calibration curve of Dapsone

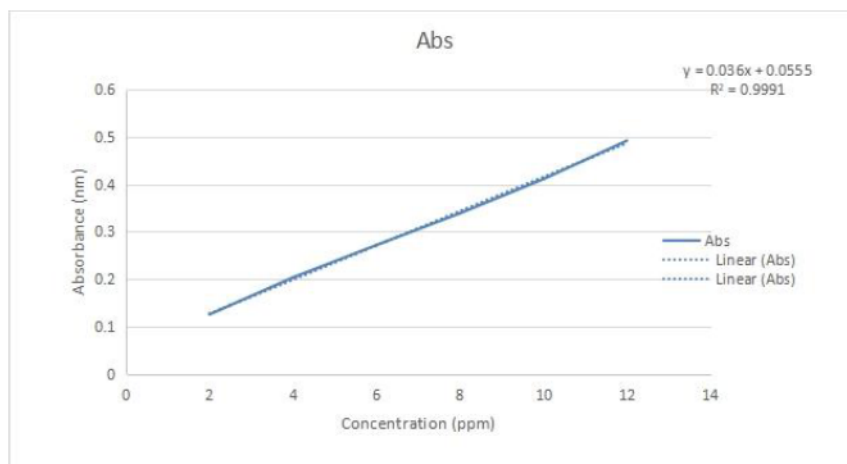


Fig. Calibration curve of Fexofenadine HCl

Precompression studies

Angle of repose^{15,16}- The highest angle achievable between the surface of a pile of powder and the horizontal plane is known as angle of repose. The angle of repose may be used to calculate the frictional force in a loose powder. It is a measure of the powder's flow characteristics. Angle of repose is the maximum angle that may be achieved between the surface of a pile of powder and the horizontal plane. The

frictional force in a loose powder may be calculated using the angle of repose. It is a measurement of the powder's ability to flow through the funnel's sides. Angle of repose and powder flow characteristic are related.

$$\theta = \tan^{-1}(H/R)$$

Angle of repose=

Where, H = Height of pile in centimeter

R = Radius of pile in centimeter

When the angle of repose is less than 25°, the flow was said to be excellent, and if the angle of repose is more than 40°, the flow is considered to be poor.

Bulk density (ρ_b)¹⁷- Using an electronic digital balance, weigh a 20g sample and pour carefully from the side wall into a 100 ml capacity "Class A" graduated measuring glass cylinder. Slowly level the surface of the sample in the cylinder and examine the occupied volume.

$$\rho_b = \frac{M}{V_b}$$

where, ρ_b = Bulk density
M = Mass of power blend
Vb = Bulk volume of powder blend

Tapped density- By dividing the mass of a powder by the tapped volume in cm³, the tapped density was calculated. A sample of around 50 cm³ of powder is carefully put into a 100 ml graduated cylinder after passing through a standard sieve no. 20. The cylinder was dropped 100 times from a height of 1 inch at 2-second intervals onto a hard wood surface. The final tapped volume in cm³ of the sample contained in the cylinder was then divided by the weight of the sample in grammes to obtain the tapped density of each formulation. It was determined using the following equation:

$$\rho_t = \frac{M}{V_t}$$

where, ρ_t = Tapped Density
M = Mass of powder blend
Vt = Tapped volume of powder blend

Hausner's ratio:-It is the ratio of the tapped density to the bulk density. It is calculated as follows-

$$\text{Hausner's ratio} = \frac{\text{Tapped density (pt)}}{\text{Bulk density (pb)}}$$

A good flow has been indicated by a Hausner's ratio greater than 1.25, and a poor flow may have a value of 1.5.

Carr's index:-It is also called as Carr's Index or Carr's Compressibility Index, an indication of the compressibility of a powder. It is calculated as follows-

$$\text{Carr's Index} = \frac{\rho_t - \rho_b}{\rho_t} \times 100$$

Where, ρ_t = Tapped Density

ρ_b = Bulk Density

Preparation of tablet by direct compression method

Tablets were prepared by using tablet compression machine. Accurately weighed amount of powder mixture for different batches was fed manually into die. The weighed amount of powder mixture was and into the die and release to compressed at a predetermined compression pressure of 5-6 N at optimum speed of rotation, using standard concave punches. (Brand Name-Rimek, Mini Press-II, Karnavati Engineering Ltd., Ahmadabad, Gujarat).

Table 1
Composition of Sustained release tablet of batches DF1-DF4

Name of ingredients	DF1	DF2	DF3	DF4
Dapsone (mg)	50	50	50	50
Fexofenadine HCl(mg)	120	120	120	120
Ac-di-sol(mg)	X	XX	XXX	XXXX
Avicel pH102 ((mg)MCC	XXX	XX	XXX	XXXX
Talc (mg)	8	8	8	8
Magnesium stearate(mg)	2	2	2	2
Sodium saccharine(mg)	2	2	2	2

(MCC indicates microcrystalline cellulose)

Evaluation of tablets

Thickness

The thickness of the tablet was measured by using Vernier calliper by picking the tablets randomly. Randomly selected tablets from all batches were tested for thickness and were found to be 0.50 ± 0.005 cm. Standard deviation values were determined and were found to be within the range.

Hardness¹⁸

Using a Monsanto hardness tester, the force required to crush the tablet is calculated. Three tablets from a batch are tested for hardness. Hardness is measured in Kg/cm². The compressed tablets from all batches F1-F4 were found to be within the limit as per standard record, which lies in between 5.3 ± 0.057 to 5.5 ± 0.115 kg/cm² (n=3).

Weight variation test

The weight variation test is also called as uniformity of weight; it is the official quality control test. It is performed to ensure that each tablet dosage form has the accurate amount of drug. As per the U.S.P., randomly select 20 tablets and then accurately weigh selected 20 tablets individually and calculate the average weight. The tablets from batches F1-F4 were evaluated for % weight variation, which showed a % weight variation of between 0.18-4% from the average weight of the tablet complying as per standard (for $>324\text{mg} \pm 5.0\%$ deviation).

Friability test ¹⁹

Friability Test: The Roche Friabilator was used to determine the tablets' friability. Five tablets were carefully weighed and placed in the tumbling chamber, where they were tumbled at 25 rpm for 4 minutes. The % weight loss was calculated using the formula below after the tablets were weighed again.

$$\% \text{friability} = \frac{\text{Initial weight} - \text{Final weight}}{\text{Initial weight}} \times 100$$

Drug content²⁰

The formulated tablets batches DF1-DF4 were tested for assay by UV spectroscopy. Absorbance of NTG in methanol is recorded at 225nm and 290nm (λ_{max}) over concentration range 5 μg -50 μg . % assay was found to be in between 96.23 to 101.69, which is complying as per the standard record limit (95%-105%).

Dissolution study

A dissolution study for formulated batches was performed separately for the immediate and sustained release layers as per USP by using USP-II apparatus (paddle type) dissolution test apparatus (Electrolab TDT08L, Mumbai, India). The dissolution medium for the immediate release tablet layer and for the sustained release layer were 900ml of 0.1N hydrochloric acid and 900ml of 0.01N hydrochloric acid, respectively. The medium was allowed to equilibrate to a temperature of $37 \pm 0.5^\circ\text{C}$. A sample (1 ml) of the solution was withdrawn from the dissolution apparatus at 5, 10, 15, 20, 25, 30, 45, 60 min time intervals and the samples were replaced with fresh dissolution medium. A tablet from each batch was placed in the vessel and covered; the apparatus was operated for up to 1 hour at 100 rpm for the immediate release layer and 12 hours for the sustained release layer. The sample was withdrawn at specified time intervals and replaced with a fresh 1ml of medium. The aliquots were filtered through Whatmann filter paper No. 42. The absorbance of the sample solution was measured using UV spectroscopy against the corresponding media as a blank for the immediate release layer and the sustained release layer at 290 nm and 225 nm, respectively.

Table 2
Pre compression evaluation parameters- Angle of Repose (θ)

Batch	Sample weight (gm)	Height of pile (h) in cm	Radius (r) in cm			Angle of Repose (θ)			Mean θ	S.D (+-)	Angle of repose
			r1	r2	r3	θ_1	θ_2	θ_3			
DF1	5.004	1.5	2.8	2.7	2.6	27.92	28.81	29.68	28.80	± 0.8	Excellent
DF2	5.002	1.5	2.8	2.7	2.8	27.92	28.81	27.92	28.21	± 0.5	Excellent
DF3	5.001	1.6	2.8	2.8	2.6	29.68	29.68	31.38	30.24	± 0.9	Excellent
DF4	5.002	1.5	2.6	2.7	2.6	29.68	28.81	29.68	29.39	± 0.5	Excellent

\pm S.D. n=3

Table 3
Pre compression evaluation parameters- Bulk density

Batch	Mass of powder M (gm)	Bulk volume of powder V_0			Bulk density D_b			Mean D_b	S.D. \pm
		V_{01}	V_{02}	V_{03}	D_{b1}	D_{b2}	D_{b3}		
DF1	25.004	61	59	60	0.41	0.42	0.41	0.41	± 0.005
DF2	25.002	61	59	60	0.41	0.42	0.41	0.41	± 0.005
DF3	25.001	59	61	60	0.42	0.41	0.41	0.41	± 0.005
DF4	25.002	59	61	60	0.42	0.41	0.41	0.41	± 0.005

\pm S.D. n=3

Table 4
Pre compression evaluation parameters- Tapped Density

Batch	Mass of powder M (gm)	Bulk Volume	Tapped volume of powder V_t			Tapped density D_t			Mean D_t	S.D. \pm
			V_{t1}	V_{t2}	V_{t3}	D_{t1}	D_{t2}	D_{t3}		
D	25.00	61	59	60	59	0.42	0.41	0.42	0.43	± 0.005

F 1	3									
D F 2	25.00 1	62	60	61	59	0.42	0.41	0.42	0.42	±0.005
D F 3	25.00 2	62	60	61	59	0.42	0.41	0.42	0.42	±0.005
D F 4	25.00 4	62	60	61	59	0.41	0.41	0.42	0.42	±0.005

Table 6
Pre compression evaluation parameters- Carr's Index

Batch	Tapped Density (Dt)	Bulk Density (Db)	Carr's Index $100 \times (Dt) - (Db) / (Dt)$	Flow Character
DF1	0.42	0.41	2.38	Excellent
DF2	0.42	0.40	4.76	Excellent
DF3	0.42	0.41	2.38	Excellent
DF4	0.42	0.41	2.38	Excellent

Table 7
Pre compression evaluation parameters- Hausner's ratio

Batch	Tapped Density (Dt)	Bulk Density (Db)	Hausner Ratio	Flow Character
DF1	0.42	0.41	1.02	Excellent
DF2	0.42	0.40	1.05	Excellent
DF3	0.42	0.41	1.02	Excellent
DF4	0.42	0.41	1.02	Excellent

Table 8
Post-compression evaluation parameters

Formulation Code	Average weight (gm)	Thickness (cm)	Hardness (Kg/cm ²)	Friability (%)	Assay (%)	
					Dapsone	Fexofenadine HCl
F1	0.301	0.49±0.01 1	5.5	0.48	99.00	98.55
F2	0.296	0.49±0.00 5	5.4	0.48	98.21	98.00
F3	0.305	0.51±0.00 0	5.4	0.36	99.62	96.72
F4	0.299	0.49±0.00	5.5	0.32	99.36	96.30

±S.D. n=3

In vitro Dissolution studies

Table 9
Data of In-vitro drug release studies of immediate release matrix tablet of Dapsone (%)

Time (min)	D1	D2	D3	D4
5	11.20297	20.2315	20.646	21.2058
10	20.28646	28.895	28.7803	32.26288
15	29.08516	39.552	32.093	48.20146
20	32.41277	39.552	43.899	57.52977
25	44.2393	53.062	67.062	62.34132
30	57.29994	68.0722	78.7995	74.20282
45	77.53543	80.1135	88.907	87.44833
60	89.05718	98.425	96.551	97.64602

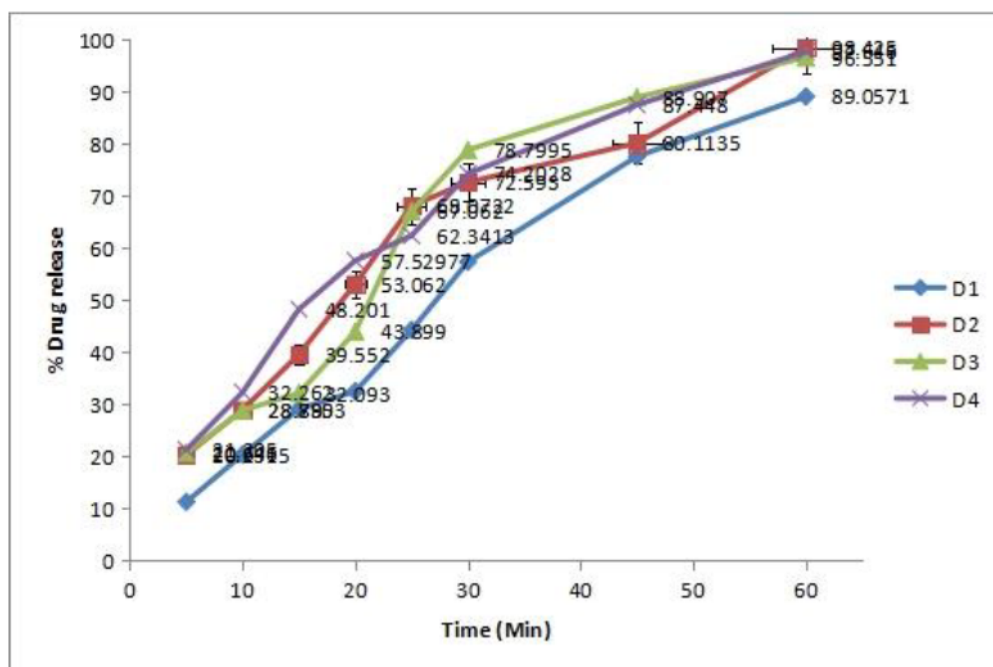


Fig. : In-vitro drug release profile of immediate release matrix tablet of Dapsone

Table 10
Data of In-vitro drug release studies of sustained release matrix tablet of
Fexofenadine HCl (%)

Time (min)	F1	F2	F3	F4
5	9.3728	10.4725	4.08	6.8986
10	19.0807	26.658	17.053	24.527
15	35.9707	35.558	32.104	36.692
20	44.819	44.939	56.7096	46.846
25	57.225	67.7234	70.6615	61.8642
30	78.6855	73.8402	82.6375	78.3934
45	90.8505	83.6168	89.2869	88.2388
60	96.9501	97.8299	96.6237	97.3281

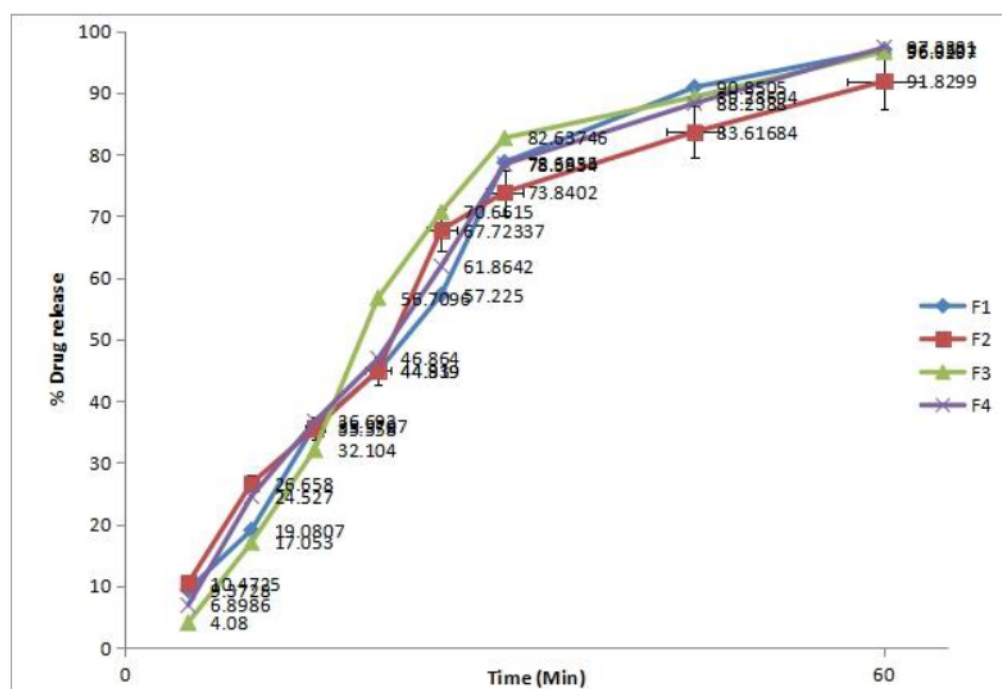


Fig. In-vitro drug release profile of Sustained release matrix tablet of Fexofenadine HCl

Conclusion

The purpose of this study was to develop, assess and evaluate the tablet and the objectives were met. Based on the findings of the completed tests of differential scanning calorimetry and IR studies it was stated that there is no substantial drug excipient interaction. As a result, we may determine that drug and other excipients are compatible. The dissolution time of tablet was less than one minute for release of certain amount of drug from all the tablet formulations. The drug release in optimized formulation of batch 2 was found to be 98.425 % for Dapsone and 98.7299 Fexofenadine HCl % in 60 mins. The optimized

formulation also showed satisfactory hardness, friability, drug content, weight variation, dissolution. The objective of the present work of formulation and evaluation of immediate release tablet for treatment of urticaria has been achieved.

Acknowledgement

For the completion of the research work the authors would like to show sincere gratitude to PDEA'S Shankarrao Ursal College of Pharmaceutical Sciences & Research Centre, Kharadi, Pune to provide with a lot of support and help whenever needed.

References

1. Patel HP, Patel JK, Patel RR; Formulation Development & Optimization of Multiple Unit Particles System (mups) Containing Ramipril and Hydrochlorothiazide. *International Journal of Pharmaceutical Sciences*, 2010; 2(1): 448- 456
2. Park K. Controlled drug delivery systems: past forward and future back. *J Control Release* 2014;190:3-8.
3. Hodayun B, Lin X, Choi HJ. Challenges and Recent Progress in Oral Drug Delivery Systems for Biopharmaceuticals. *Pharmaceutics*. 2019;11(3):129. Published 2019 Mar 19. doi:10.3390/pharmaceutics11030129.
4. Jadhav SB, Mali AD, Rajeghadage SH and Bathe ARS: Formulation and evaluation of immediate release tablets of Imipramine hydrochloride. *International Journal of Biomedical and Advance Research* 2014; 5(11): 559-65.
5. Patel N, Natarajan R and Rajendran NN: Formulation and evaluation of immediate release bilayer tablets of Telmisartan and Hydrochlorothiazide. *International Journal of Pharmaceutical Sciences and Nanotechnology* 2011; 4(3): 1477-82.
6. Jon Gabrielsson, Nils-Olof Lindberg and Torbjorn Lundstedt , *Multivariate Methods in Pharmaceutical Applications*, J.Chemom 2002; 16:141-160
7. Dedhiya et al, "Lercanidipine immediate release compositions" United States Patent Application 2006 0134212
8. Eriksson et al, "New oral immediate release dosage form" United States Patent Application 20060034 911
9. Poonawalla T, Kelly B. Urticaria : a review. *Am J Clin Dermatol*. (2009) 10:9–21. doi: 10.2165/0128071-200910010-00002
10. PubMed Abstract | CrossRef Full Text | Google Scholar
11. Kanani A, Betschel SD, Warrington R. Urticaria and angioedema. *Allergy Asthma Clin Immunol*. (2018) 14 (Suppl. 2):59. doi: 10.1186/s13223-018-0288-z
12. Powell RJ, Leech SC, Till S, Huber PA, Nasser SM, Clark AT, British Society for Allergy and Clinical Immunology. BSACI guideline for the management of chronic urticaria and angioedema. *Clin Exp Allergy*. 2015;45(3):547–65
13. Lee, E.E., Maibach, H.I. Treatment of Urticaria. *Am J Clin Dermatol* 2, 27–32 (2001). <https://doi.org/10.2165/00128071-200102010-00005>.
14. Mahdy AM, Webster NR. *Pharmacology*. Elsevier Ltd; 2011. Histamine and antihistamines; pp. 324–9.

15. Cartensen JT, Rhodes CT (2005) Preformulation. In: Cartensen JT, Rhodes CT (eds.). *Drug Stability principles and practices* (3rd edn)., Marcel Dekker Inc., New York, USA.
16. Maurya SD, Tilak VK, Dhakar RC, Verma KK, Soni U, Gupta, Preparation and evaluation of floating tablet of famotidine through solid dispersion, *International Journal of Current Research and Review*, 2011; (2)1: 21-30.
17. Thoke SB, Sharma Y., Rawat S, Nangude, S Formulation development & evaluation of effervescent tablet of Alendronate sodium with vitamin D3, *Journal of Drug Delivery & Therapeutics*; 2013; 3(5):65-74.
18. Tomar M, Singh AK, Sinha AR. Physical parameter of microcrystalline cellulose and the most acceptability in pharmaceutical industries: *J of inno in p'ceutical and bio Sci.*, 2015; 570-578.
19. RaoNGR, Kumar M, Reddy MS, Kistayya C, Reddy BM. Development and evaluation of fast dissolving tablets of fosinopril by a sublimation method. *Int J Pharm Sci Drug Res* 2012;4:230-5.
20. Chavan PM and Ughade S: Preparation, characterization and evaluation of tablet for colonic delivery. *Int J Pharm Sci & Res* 2018; 9(5):2027-33. doi: 10.13040/IJPSR.0975-8232.9(5).2027-33.
21. Michaels A.S, ChandrasekaranS.K, Shaw J.E. Drug permeation through human skin: Theory and invitro experimental measurement. *AIChE J.* 2004;21(5) 16 Williams AC, Barry BW. Penetration enhancers. *Adv drug deliv rev.* 2004;56(5):603-618.

How to Cite:

Kandge, M., Kasabe, A., Sukre, M., & Shinde, T. (2022). Formulation and evaluation of microemulsion containing miconazole nitrate. *International Journal of Health Sciences*, 6(S3), 9145–9153. <https://doi.org/10.53730/ijhs.v6nS3.8240>

Formulation and evaluation of microemulsion containing miconazole nitrate

Mansi Kandge

Department of Pharmaceutical Quality Assurance, P.D.E.A's Shankarrao Ursal College of Pharmaceutical Sciences and Research Centre, Kharadi, Pune, Maharashtra, India

*Corresponding author email: mansikandge8@gmail.com

Amit Kasabe

Vijaya Barge, Department of Pharmaceutical Quality Assurance, P.D.E.A's Shankarrao Ursal College of Pharmaceutical Sciences and Research Centre, Kharadi, Pune, Maharashtra, India

Manisha Sukre

Department of Pharmaceutical Quality Assurance, P.D.E.A's Shankarrao Ursal College of Pharmaceutical Sciences and Research Centre, Kharadi, Pune, Maharashtra, India

Trupti Shinde

Department of Pharmaceutical Quality Assurance, P.D.E.A's Shankarrao Ursal College of Pharmaceutical Sciences and Research Centre, Kharadi, Pune, Maharashtra, India

Abstract---The aim of the present research is to formulate a microemulsion containing miconazole nitrate as it provides various advantages over conventional dosage form. It also put forward the idea for the formulation of microemulsion containing miconazole nitrate with the use of varying surfactant and co- surfactants with an objective to increase the better drug loading, high transparency, high thermodynamic stability, better bioavailability and ease of preparation. Miconazole nitrate is hydrophobic imidazole antifungal agent. The studies show that it is highly effective in the topical treatment of fungal infections. Due to the presence of both lipophilic and hydrophilic domains, a wide range of lipophilic and hydrophilic domains are incorporated in these systems.

Keywords---formulation, microemulsion, miconazole nitrate.

Introduction

Skin diseases can be generally treated by topical or delivering directly drug into dermis. These are normally applicable to superficial infections, also which are restrained to stratum corneum. A wide range of technologies have been developed to overcome these problems such as liposomes, chemical penetration, microemulsion, sonophoresis, iontophoresis, electroporation, and stratum corneum abscission. Miconazole nitrate is an imidazole antifungal agent which shows fungistatic activity in opposition to normal pathogenic fungi as well as yeasts. Depending upon the structure, microemulsions are of different types as w/o, o/w or bicontinuous system. Microemulsion is defined as clear, stable and isotropic mixtures of oil, water, surfactant and co- surfactant. This drug delivery is used for topical, percutaneous, transdermal, oral, parenteral and ocular application of medicinal agents. All microemulsion are fluids with low viscosity. The miconazole nitrate is primarily known for its antifungal activity. It is clinically used for superficial treatment of superficial mycoses, dermatophytes, cutaneous candidiasis and other infections. Topical drug therapy is appropriate for management of local diseases in order to restrict therapeutic effect to target size and decrease systemic drug absorption. Miconazole Nitrate is generally applied topically for treating various diseases on skin surface like athlete's foot, jock itch, ringworm and perioral candidiasis.

Materials and Methods

Miconazole nitrate was purchased from Solanki Suppliers (Pune, India). Oleic acid and Tween 20 were purchased from Solanki Suppliers (Pune, India). Chemicals such as propylene glycol was obtained from the laboratory. All the chemicals obtained were of analytical grade.

Methods

Identification of pure drug

Identification of pure drug was carried by Fourier Transform Infra-red spectrophotometry (Shimadzu 800s) scanned in the range of 200-400 nm.

FTIR Study

FTIR (Shimadzu 8400s) spectrophotometer was used in the range of 400-400 cm^{-1} using potassium bromide discs (mixing ratio 1:1). The samples were properly sealed in aluminium pans and heated at a constant rate of 10 $^{\circ}\text{C}/\text{min}$ over a temperature range of 40-300 $^{\circ}\text{C}$.

Determination of Melting point

Melting point of drug was determined by Thiele's tube method. The small amount of drug was taken in one end closed capillary tube is attached to graduated thermometer and constant heat was supplied to the assembly suspended in paraffin bath. The temperature at which the drug melts is noted.

Preparation of Microemulsion

The required amount of miconazole nitrate was weighed. The weighed amount of drug was dissolved in oil phase (mixture 1). This mixture was sonicated for 10 min. The mixture 2 is prepared by mixing surfactant and co- surfactant. The prepared mixture was mixed together using magnetic stirrer. The drop wise addition of water was done for making up the volume. The 100 ml microemulsion was prepared.

Table 1
Preparation of Microemulsion (Batch 1- Batch 4)

Ingredients	Batch 1	Batch2	Batch 3	Batch 4
Griseofulvin (gm)	1	1	1	1
Oleic acid (ml)	7	7	7	7
Tween 20(ml)	30	25	20	15
Propylene glycol (ml)	30	28	26	24
Distilled water(ml)	32	39	46	53

Evaluation of microemulsion

pH

The pH of prepared microemulsion was measured using digital pH meter. It is measurement of alkanity or acidity for the prepared microemulsion

Viscosity

Viscosity was determined using (LV) Brookfield Viscometer using. Spindle no. 62. Microemulsion shows Newtonian type of flow. Viscosity was measured for fixed time 2 min

Zeta potential

Zeta potential is used to determine the stability of the prepared microemulsion. The charge on the surface of the particles was characterized by HORIBA SZ-100 by measuring the Zeta potential of the microemulsions. The sample was injected into a disposable cell and measurement of the particle electrophoretic moiety results in the calculation of Identification potential.

Particle size

Samples were diluted using distilled water followed by measurement of particle size and Zeta potential in the triplicates and average values. Particle size of microemulsions was determined using HORIBA sz-100 (z type).

Conductivity

The Conductivity of prepared microemulsion was measured by digital conductivity meter. Voltage was applied between two electrodes in a probe immersed in a sample. The drop in voltage caused by resistance of sample was used to calculate the conductivity per centimetre

Scanning Electron Microscopy

Scanning electron microscopy provides high resolution imaging that may be used to evaluate diverse materials for surface cracks, defects contaminants and corrosion. When a focused stream of secondary electron interacts with atoms in sample, multiple singles produced that include information about the surface topography using Nova NanoSEM NPEP. All the images are canned at 10000 x with a 5 m dimension scale 303.

Content Uniformity

Drug content was performed by dissolving accurately weighed 1 ml of microemulsion in methanol. After suitable dilution absorbance was recorded by using UV visible spectrophotometer (UV 1800, Shimadzu, Japan) at 232 nm. Drug content was measured by slope of standard curve.

Results

FTIR Study

Identification and confirmation of drug was carried out by observing the spectra.

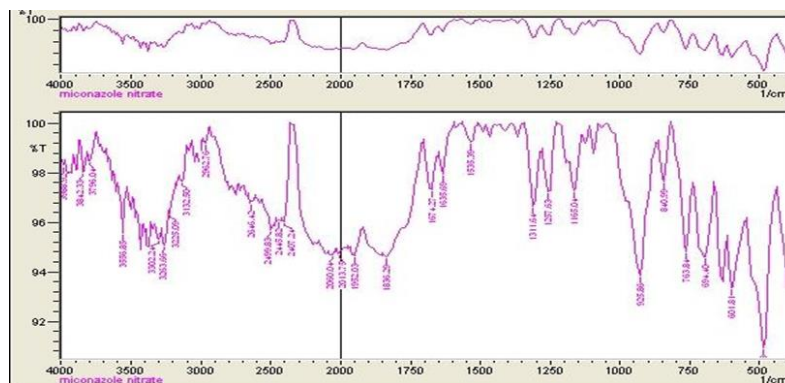


Fig 1. Interpretation of IR of Miconazole Nitrate

Identification of pure drug shows C - C stretching vibrations at 1505 cm^{-1} , C- H bending at 1468 cm^{-1} , the C-N vibration of imidazole group at 3151 cm^{-1}

UV Spectroscopy

The calibration curve was obtained by plotting the absorbance versus the concentration data was treated by linear regression analysis. The equation of

linearity curve for miconazole nitrate was obtained by the equation $y = 0.0275x + 0.0335$. The linearity curve was found to be linear for the above-mentioned concentrations. The correlation coefficient R of drug was found to be 0.9965.

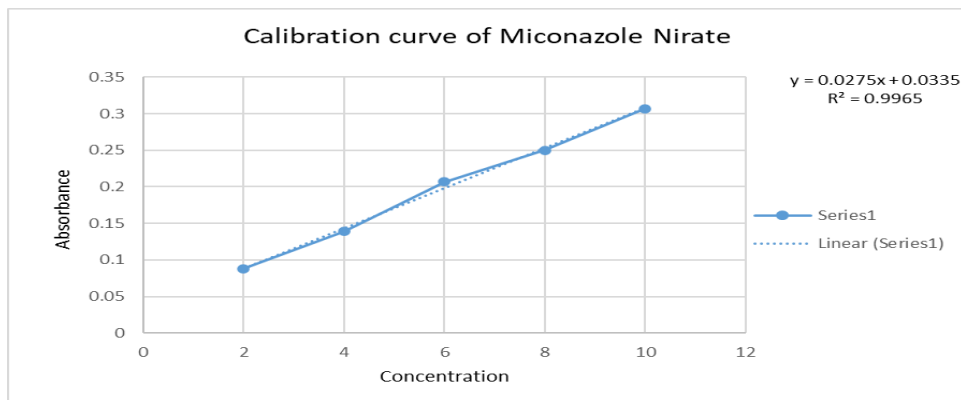


Fig 2. Calibration curve of Miconazole Nitrate

Melting point

The melting point of Miconazole nitrate was found to be 180°C.

pH, Drug content

Table 2
Characterisation of microemulsion

Batch	pH	Drug content (%)
1	6.2	96.89
2	6.5	92.54
3	5.8	94.23
4	6.1	90.65

The pH of microemulsion should be always considered within the suitable range. The pH of different microemulsion was checked as followed in the table. Drug content is determined as shown in the table. The higher amount of drug will show concentrated formulation. These formulation ranges from concentrated to aqueous.

Particle Size and zeta potential

Table 3
Determination of Particle size and Zeta potential

Batch	Particle Size(nm)	Zeta Potential(mV)
1	215.0	-20.5
2	226.9	-18.9
3	802.7	-17.9
4	172.4	23.6

The particle size of microemulsion determines the rate and extent of drug release absorption. The small particle size of microemulsion show more rapid absorption as well as it increases the bioavailability of the formulation. Particle size of optimized microemulsion (M1) was found to be 215.0 nm these globules are suitable for topical delivery administration. The Zeta potential plays a crucial role in the stability factor of the formulation. The high value of Zeta potential indicates the electrostatic repulsion between the two droplets. The negative charge characterizes the more stability of the formulation. The Zeta potential value for optimized batch M1 was determined to be -20.5. It shows better stability.

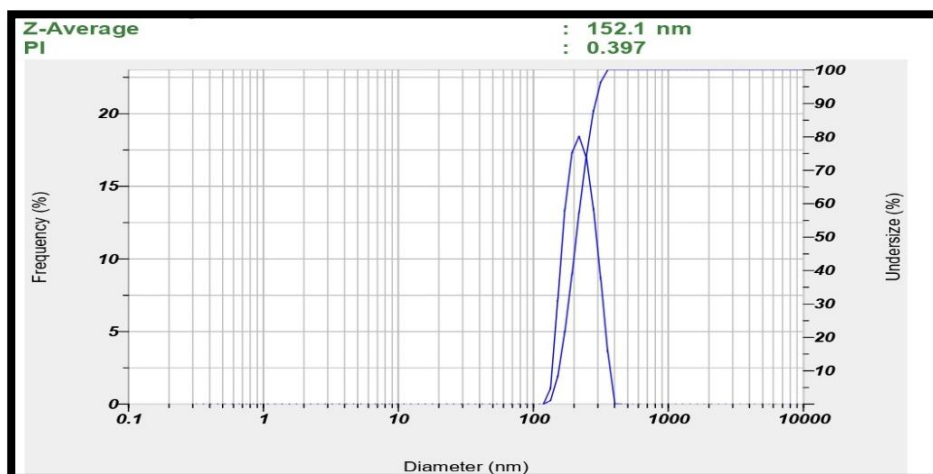


Fig 3. Particle size of optimized formulation (M1)

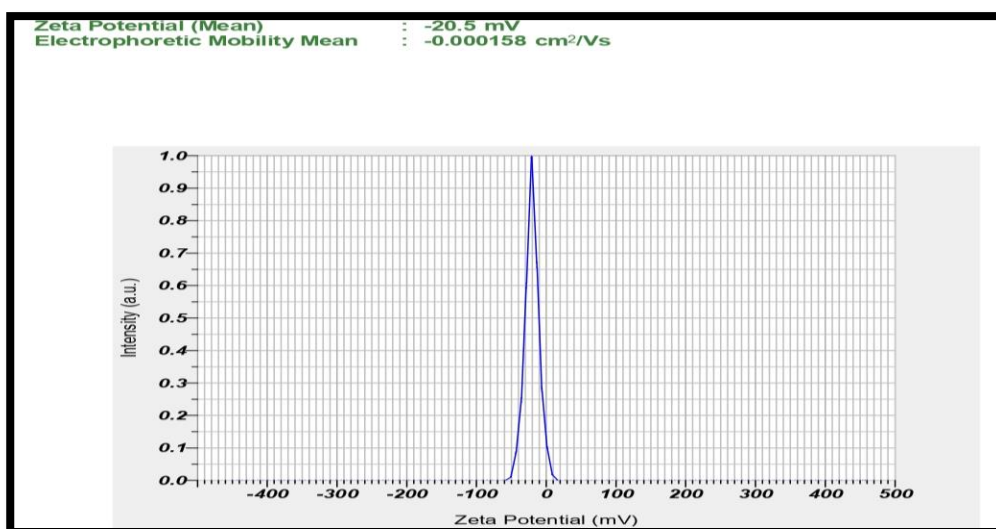


Fig 4. Zeta potential of optimized formulation (M1)

Viscosity

The viscosity values for different formulation are considered in the table:

Table 4
Viscosities of microemulsion

RPM	Batch 1	Batch 2	Batch 3	Batch 4
10	144	193	264	1428
20	165	155	185	936
30	168	149	149	737
50	171	151	110	553.2
100	172.3	152	84.30	551

Conductivity

Table 5
Determination of electrical conductivity

Batches	200ms	20ms	2 ms	200 μ s	20 μ s
1	000	00.0	0.02	023	1.
2	000	00.0	0.04	036	1.
3	0.0	00.0	0.03	031	1.
4	000	00.0	0.01	014	1.

Electrical conductivity is used to determine the nature of w/o or o/w microemulsion. It is measured using electric conductometer. It is used to identify whether there is oil or water as a continuous phase. It is also used to identify the phase inversion process.

Scanning Electron Microscopy

The optimized batch of. Microemulsion which is analysed for SEM Analysis shows the hexagonal or bicontinuous structure. It is also further analysed for surface topography and morphology of the sample.

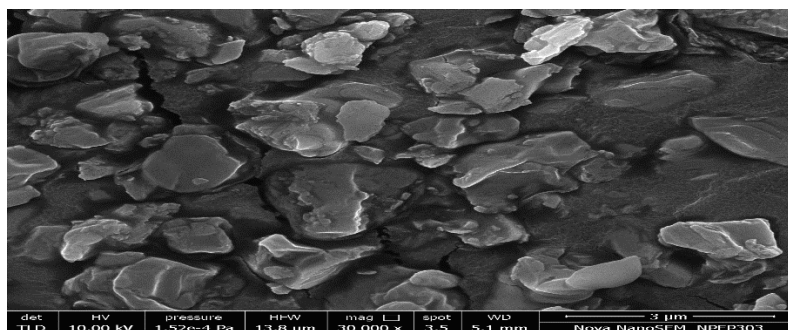


Fig 5. SEM of optimized formulation

Conclusion

Different administration of drug is considered as the basic criteria for the choice of drug as well as its route. Microemulsion shows thermodynamic stability, choice of route for control delivery. The above formulation shows good consistency. Miconazole nitrate is considered from the azole group of antifungals. They prove to be best formulation in the novel drug delivery system since they have prolonged shelf life, improved drug solubilization and ease of preparation and administration. The idea behind the study was to develop a topical microemulsion for sparingly soluble antifungal agent. Another advantage for formulation of microemulsion is most of the lipophilic groups are easy to penetrate through the microemulsion as compared to other drug delivery. The above optimized microemulsion shows all the parameters within the suitable criteria. The Zeta potential characterizes the stability of the optimized microemulsion. These is considered as important factor for the optimized batch.

Acknowledgement

For the completion of the research work the authors would like to show sincere gratitude to PDEA'S Shankarrao Ursal College of Pharmaceutical Sciences & Research Centre, Kharadi, Pune to provide with a lot of support and help whenever needed.

References

1. Shahzadi, I., M.I. Masood, F. Chowdhary, A.A. Anjum, M.A. Nawaz, I. Maqsood, et al. (2014) *Int. J. Pharm. Sci. Rev. Res.* 24: 30-6.
2. Williams, H. D., P. Sassene, K. Kleberg, J.C. Bakala-N'Goma, M. Calderone, V. Jannin, et al. (2012) *J. Pharm. Sci.* 101: 3360-80.
3. Haroon K.S. & K.P. Kok (2014) *Acta Pol. Pharm.* 71: 301-9.
4. Osborne, D., A. Ward & K. O'Neill (1991) *J. Pharm. Pharmacol.* 43: 451-4.
5. Haroon, K.S., A.I. Muhammad, A.H. Rosenani & K.P. Kok (2015) *J. Coordin. Chem.* 68: 1088- 100.
6. Saraf, S., S. Sahu, C.D. Kaur & S. Saraf (2010) *J. Cosm. Dermatol.* 6: 223-8.
7. Pignatello, R., M. Vandelli, P. Giunchedi & G. Puglisi (1997) *STP Pharma Sci.* 7: 148-57.
8. Sahoo, S.K., A.A. Mallick, B. Barik & P.C. Senapati (2005) *Trop J. Pharm Res.* 4: 369-75.
9. Dey, S., S. Pramanik & A. Malgope (2011) *ISRN Pharma.* 2011:627623.
10. Hanaoka, T., T. Hatsuta, T. Tago, M. Kishida & K. Wakabayashi (2000) *App. Catal. A* 190: 291- 6.
11. Park, E.-S., Y. Cui, B.-J. Yun, I.-J. Ko & S.C. Chi (2005) *Arch. Pharmacol Res.* 28: 243-8.
12. Abd-Allah, F. I., H.M. Dawaba & A. Ahmed (2010) *Drug. Discov. Ther.* 4: 257-66.
13. Ehan, O., M.I. Qadir, S.A. Malik, W.S. Abbassi & B. Ahmad (2012) *J. Chem. Soc. Pak.* 34: 365- 70.
14. Qadir, M.I., I. Hasan & T. Mobeen, (2018)VVVV

15. Heuschkel S, Goebel A, Neubert RHH, MicroemulsionsModern Colloidal Carrier for Dermal and Transdermal Drug delivery, Journal of Pharmaceutical Sciences, 97(2), 2008, 602-631.
16. Bhat JI, Alva VDP, Inhibition effect of Miconazole nitrate on the Corrosion of Mild steel in Hydrochloric acid medium, International Journal of Electrochemistry, 2(1), 2011, 1-8.
17. Janjale MV, Patil SH, Patil DK, Formulation and Evaluation of Miconazole nitrate solid dispersion for Dissolution rate Enhancement, International Journal of Pharmaceutical & Biological Archives, 2(6), 2011, 192-196.



Pune District Education Association's
**Shankarrao Ursal College of Pharmaceutical
Sciences & Research Centre, Kharadi, Pune-14.**



Academic Year 2020-21

Original Article

DEVELOPMENT AND CHARACTERIZATION OF DICLOFENAC SODIUM LOADED EUDRAGIT RS100 POLYMERIC MICROSPONGE INCORPORATED INTO *IN SITU* GEL FOR OPHTHALMIC DRUG DELIVERY SYSTEM

RAJASHRI B. AMBIKAR^{1*}, ASHOK V. BHOSALE²

¹PDEA's Seth Govind Raghunath Sable College of Pharmacy, Saswad, Purandar, Pune, Maharashtra, India, ²PDEA's Shankarrao Ursal College of Pharmaceutical Sciences and Research Centre, Kharadi, Pune, Maharashtra, India
Email: rajashriwin@gmail.com

Received: 14 Jun 2021, Revised and Accepted: 28 Jul 2021

ABSTRACT

Objective: Purpose of the study to design and formulate Diclofenac sodium (DIC) microsponges.

Methods: With varied polymer: drug ratio DIC loaded microsponges were prepared with Eudragit RS100 polymer by quasi solvent diffusion method. Microsponges evaluated for particle size, entrapment efficiency, drug content, *in vitro* drug release, Fourier Transform Infrared Spectroscopy (FTIR), Differential scanning calorimetry (DSC) and Scanning electron microscopy (SEM). DIC loaded microsponges incorporated into ocular *in situ* gel to attained controlled release by microsp sponge and improved residence time by gelling system. Ocular *in situ* gel evaluated for pH, drug content determination, gelling capacity, *in vitro* drug release and sterility study.

Results: DSER4 microsp sponge formulation having polymer to drug ratio 1:7 showed satisfactory production yield (68.13%), entrapment efficiency (62.86%), drug content (80.73%), requisite particle size (less than 10 μ m) (7.52 μ m) and *in vitro* release 87.94% after 6 h. Selected DSER4 formulation was incorporate into *in situ* gel. Carbopol 940 forms stiff gel at higher pH so used as a gelling agent, whereas Hydroxypropyl Methylcellulose E4M was used as a viscosity-enhancing agent for the formulation of *in situ* gel in varied compositions. *In situ* gel formulation IG4 showed sustained release of 76.92% till the end of 8 h and satisfactory gelling capacity so IG4 further evaluated for sterility test. Rheological studies reveal the sol-gel transition of *in situ* gel occur at the physiological condition to form stiff gel.

Conclusion: Prepared *in situ* gel formulations showed sustained drug release for a period of 8 h, which is satisfactory for management of ocular pain.

Keywords: Microsp sponge, Ocular *in situ* gel, Controlled release, Ophthalmic drug delivery, Kinetic release

© 2021 The Authors. Published by Innovare Academic Sciences Pvt Ltd. This is an open access article under the CC BY license (<https://creativecommons.org/licenses/by/4.0/>)
DOI: <https://dx.doi.org/10.22159/ijpps.2021v13i9.42405>. Journal homepage: <https://innovareacademics.in/journals/index.php/ijpps>.

INTRODUCTION

Microsponges are polymeric particulate delivery systems having 5 to 300 μ m diameter with a porous spherical structure formed with polymer enclosing active drug ingredients and thereby control drugs release [1]. Microsponges are drug-contained polymeric sponge-like structures with large porous surface and non-collapsible structure made through numerous of interconnecting voids. Microsponges display good stability for extreme acidic (pH 1) to extreme basic (pH 11) conditions also stable at high temperatures (up to 130 °C). This entrapment technologies offer high drug payload than others [2].

Several different research works of microsponges explored on various areas like colonic delivery [3-5], topical delivery [6, 7], gastroretentive delivery [8] and percutaneous delivery [9] for controlled and sustained drug release. Fewer attempts have been made for ophthalmic drug delivery [10-12] of microsponges.

Ophthalmic drug delivery systems have the main problem of fast and substantial precorneal loss, caused by high turnover of tear fluid and further draining of tear fluid from eye [13]. Particulate system suffers from this nasolacrimal drainage. This possibility of short residence time is eliminated by the incorporation of particulate system *in situ* gel and increases its retention in eye. A lot of attempts have been made on the incorporation of particulate system in ocular *in situ* gel [14, 15]. But lesser studies are carried out on microsp sponge-loaded ocular *in situ* gel.

In situ gels, upon installation in ocular cul-de-sac, go through a sol-gel phase transition to form a stiff gel. Phase transition occurs from droppable low viscous solution to stiff gel by the influence of physicochemical changes i.e. pH, temperature and ions composition, caused by tear fluid. This system allows administration of accurate

doses in the form of drop and augmented residence time which in turn improves bioavailability at ocular area [16].

Carbopol is a polyacrylic acid (PAA) polymer, which go through a sol to gel conversion in an aqueous solution with a change in pH above its pKa of about 5.5. However, the high amount of carbopol required to get stiff gel results in highly acidic solutions. Such acidic polymeric solution is unable to neutralize with the buffering capacity of the tear fluid. So to good gelling capacity could be achieved with no further increment in the amount of carbopol in polymer solution; by adding HPMC polymer as viscosity enhancing polymer [17]. HPMC E4M was selected for *in situ* gel formulation as its frequent use in ophthalmic drug delivery, reliability, superior transparency and less incompatibility [18].

Diclofenac sodium is effectively used for pain management in cases of corneal epithelial defects followed by surgery or accidental trauma, and prevention of intraoperative miosis during cataract surgery, treatment of postoperative ocular inflammations, chronic non-infectious inflammations and for symptomatic relief of seasonal allergic conjunctivitis [19].

The purpose of this study is to attain controlled release through microsp sponge and improve its residence time by incorporating microsponges in *in situ* gel. Eudragit RS100 is used as a polymer for the preparation of microsponges. Further microsponges were added to HPMC E4M and carbopol *in situ* gel.

MATERIALS AND METHODS

Materials

Diclofenac Sodium (DIC) was gifted by Nulife Pharmaceuticals, Pune, India. Eudragit RS 100 (ERS) and Hydroxypropyl Methylcellulose E4M (HPMC E4M) was gifted from Evonik India Pvt. Ltd., Mumbai and

Colorcon Asia Pvt. Ltd., Goa, India respectively. Carbopol 940, Dichloromethane (DMC), Triethylcitrate, Polyvinylalcohol 30,000–70,000 (PVA) were procured from Research lab fine chem. Industries, Mumbai. All other chemicals used for analysis were analytical grade.

Preparation of DIC loaded microsponges

For the preparation of DIC-loaded microsponges with ERS polymer; the quasi-emulsion solvent diffusion method was considered. To prepare internal phase ERS polymer and triethylcitrate (1% w/v) dissolved in dichloromethane. To the prepared solution of polymer, DIC was added and homogeneously dispersed by ultrasonication to achieve particle size reduction. Polymer: drug ratio was varied as 1:1 to 1:13. The internal phase was added dropwise to 100 ml of 1% w/v PVA solution. This emulsion was stirred for 4hr using magnetic stirrer at 1000 rpm. The DIC loaded microsponges were filtered, washed with double distilled water and then dried for 48 h at room temperature. DIC-loaded microsponges stored for further characterization [5, 20].

Characterization of DIC loaded microspunge

Determination of Percentage Yield

The percentage yield of obtained microsponges was determined by calculating the percentage of the weight of the DIC loaded microsponges and the collective weight of DIC and ERS polymer.

$$\text{Production yield} = \frac{W_{Pr}}{W_{Th}} \times 100 \dots (\text{Equation 1})$$

Where,

W_{Pr} = Practical mass of DIC loaded microsponges

W_{Th} = Theoretical mass (Total weight of DIC and ERS polymer added to formulation)

Drug content

DIC-loaded microspunge formulation equivalent to 10 mg of DIC of each batch was finely crushed in a glass mortar. Further to this add 60 ml of phosphate buffer (pH 7.4) and the solution was shaken for 4 h. to dissolve DIC and, filtered. Filtered solution was diluted to 100 ml with 7.4 phosphate buffer. The resultant solution was analyzed on UV spectrophotometer (Jasco V-530) at 275.5 nm. The DIC content of the microsponges (D_{At}) was calculated.

Entrapment Efficiency (%)

Entrapment Efficiency (%) of DIC contained microspunge was calculated with an equation,

$$\text{Entrapment Efficiency (\%)} = \frac{D_{At}}{D_{Th}} \times 100 \dots (\text{Equation 2})$$

Where,

D_{At} = Actual drug content in Dried microsponges

D_{Th} = Practical drug content (Weight of DIC added in microsponges)

Particle size

Optical microscopy was used to measure particle size of microspunge by using digital microscope (Motic CV5-2), calibrated with ocular micrometer (AmScope MR400 Microscope calibration slide). Selected microspunge formulation was dispersed in water and few drops were placed on a glass slide. The drop of dispersion was observed under a digital microscope. The mean of particle size for 300 particles was calculated [21].

In vitro drug release from DIC loaded microsponges

Franz diffusion cell was used to carry out *in vitro* drug release of DIC-loaded microsponges. Freshly prepared STF of pH 7.4 was filled in the receptor compartment of the Franz diffusion cell and with a

small magnetic bar STF was constantly stirred at 100 rpm. A dialysis membrane (12 000–14 000 Dalton MW, Hi-media, India) soaked for 12 h in the STF and stretched in between donor and receptor chambers. DIC loaded microspunge dispersed in distilled water and placed in donor compartment; and covered with a coverslip. Samples each of 1 ml, were withdrawn for at predetermined time intervals from the receptor chambers and replaced with fresh STF and sink conditions. *In vitro* drug release was performed thrice for each formulation; further samples were analyzed by measuring the absorbance at 275.5 nm using UV spectrophotometer [22].

In vitro drug release kinetic study of DIC loaded microsponges

Drug Kinetic model studies of *in vitro* release data of microspunge formulations were performed to conclude the DIC release mechanism. *In vitro* release data was fitted to the following models and regression coefficient values (r^2) were calculated.

- Zero-order kinetic model ($d_0 - d = Kt$)
- First order kinetic model ($\log d = \log d_0 - Kt/2.303$)
- Hixson-crowell kinetic model ($d_0^{1/3} - d^{1/3} = Kt$)
- Higuchi kinetic model ($d_0 - d = Kt^{1/2}$)

Where d is the quantity of the DIC remaining in the microspunge at time t and d_0 is the initial amount of the DIC in the microspunge. Diffusion mechanism was explained by the diffusion exponent (n) value of Korsmeyer-Peppas equation ($d_0 - d/d_0 = Kt^n$). The diffusion exponent value $n < 0.45$ signifies the release follows fickian mechanism. If exponent value indicates $0.5 < n < 0.8$ signifies the release follows the non-fickian mechanism [23].

Fourier transform infrared spectroscopy (FTIR)

FTIR spectra of DIC, physical mixture of DIC and ERS polymer and; selected microspunge formulations were recorded in ATR mode with a Perkin Elmer (Model: SPECTRUM BX).

Differential scanning calorimetry (DSC)

Thermal analysis of DIC and the selected microspunge were scanned at a rate of 20 °C/min on a Differential scanning calorimetry (Mettler Toledo, Model: StareSW920, Mumbai) between 40 °C and 320 °C under dynamic nitrogen atmosphere DSC studies were carried out intend to find out any incompatibility.

Scanning electron microscopy (SEM)

A Field Emission Scanning Electron Microscope (FEI Nova NanoSEM 450) operated at 3.00 kV and magnification of $\times 500$ and $\times 5000$; was used to study the morphology of microsponges. Selected microspunge need to coat with gold-palladium alloy for 45s under an argon atmosphere before observation.

Formulation of DIC loaded microsponges containing ocular in situ gel

Ocular *in situ* gel formulations containing varied concentrations of Carbopol 940 and HPMC E4M were prepared as per the composition summarized in table 1. Accurately weighed HPMC E4M was dispersed in 50 ml of distilled water and carbopol 940 was dispersed over this solution and kept to hydrate 12h. The solution was stirred with an overhead stirrer. DIC-loaded microsponges (equivalent to 0.1 gm DIC) were dispersed in distilled water and added to the polymeric solution. Benzalkonium chloride was mixed to the prepared solution. Required amount of distilled water was added to make up the volume to 100 ml. Prepared in situ gel formulation thoroughly agitated and sterilized in an autoclave at 121 °C for 20 min [24, 25].

Table 1: Composition of DIC loaded microspunge containing ocular *in situ* gel formulations

Ingredient (%W/V)	IG1	IG2	IG3	IG4
Carbopol 940	0.1	0.1	0.1	0.1
HPMC E4M	0.2	0.4	0.6	0.8
Benzalkonium chloride	0.02	0.02	0.02	0.02
Distilled water qs	100	100	100	100

Characterization of DIC loaded microsponges containing ocular *in situ* gel

Determination of visual appearance and clarity

The appearance and clarity ocular *in situ* gel formulations were evaluated by observing gel in front of black and white background in fluorescent light inside a bright, lightened cabinet.

Determination of pH

The pH of *in situ* gel formulation was determined using a pH meter (Labindia, Mumbai, Model: GMPH) which was calibrated before use with the buffered solution at pH 4 and 7. Three readings were taken for every sample and the average of three samples was calculated.

Drug content determination

In situ gel formulation was added to 100 ml volumetric flask. To this add 60 ml of pH 7.4 phosphate buffer was added and shaken for 4 h. and filtered. Filtered solution was further diluted to 100 ml with 7.4 phosphate buffer. Analyzed using UV spectrophotometer (UV1Jasco, Japan, Model: V-530) with phosphate buffer (pH 7.4) as blank. The drug content of the microsponges was calculated.

Determination of gelling capacity

To vial containing 2 ml of freshly prepared STF (maintained at 37 °C), drop of the *in situ* gel was added. The drop of *in situ* gel was observed and the time taken by drop for gelation was noted also the time taken for the gel formed to dissolve was noted [12]. Gelling capacity of formed *in situ* gel was noted as follows.

- (-) No gel formation
- (+) The gel formation occur after few minutes and dissolves quickly
- (++) Instantaneous gel formation and resides for few hours
- (+++) Instantaneous stiff gel formation which resides for long period of time

Rheological studies

Brookfield digital viscometer (DVII+PRO) was used to measure the viscosity (in cps) of the prepared *in situ* gel formulations. The spindle (T-D) was rotated at 20 rpm. Three readings were reported 30 sec after putting the motor on and an average calculated.

In vitro drug release from *In situ* ocular gel containing DIC loaded microsponges

The *in vitro* drug release from the *in situ* ocular gel was carried out as per procedure described above under '*In vitro* drug release from DIC loaded microsponges'. The *in situ* ocular gel was placed on donor compartment. To the top of the *in situ* gel 250 μ l of the STF was added to simulate the small amount of tear secreted on the eye surface and covered with a coverslip. 1 ml of samples were taken out at time intervals 0.25, 0.5, 1, 2, 3, 4, 5, 6, 7 and 8 h with timely maintenance of sink condition. Samples were analyzed by using UV

spectrophotometer [22]. *In vitro* drug release studies performed thrice for each *in situ* gel formulation.

In vitro drug release kinetic study of *in situ* ocular gel containing DIC loaded microsponges

Kinetic study of drug release data was performed ocular *in situ* gel as described above under '*In vitro* drug release kinetic study of DIC loaded microsponges'.

Sterility study

The sterility study was performed according to Indian Pharmacopoeia [26]. *In situ* ocular gel formulation was directly inoculated aseptically into fluid thioglycolate medium (20 ml), and incubated for 14 d at 30 °C to 35 °C. Separately, *In situ* ocular gel formulation was directly inoculated aseptically into soyabean-casein digest medium (20 ml) and incubated for 14 d 20 °C to 25 °C. Microbial contamination was tested with a Fluid thioglycolate medium and the presence of fungi tested with soybean-casein digest medium with incubation under aerobic conditions. The tests were performed in triplicate under aseptic conditions to avoid accidental contamination. The positive and negative controls were performed for the examination of growth promotion and sterility, respectively.

RESULTS

Characterization DIC loaded microsphere formulations

Production yield (%), drug content (%) and entrapment efficiency (%)

With increase in polymer: drug ratio there is increment in production yield, drug content and entrapment efficiency. Production yield varied between 27.50% and 72.50%. At low DIC concentration production yield was found extremely low (27.50%). Drug content varied from 27.27% to 90.15% (table 2).

Particle size analysis

Particle size is an important parameter in ocular administration of particular system. Particle size range from $20.39 \pm 4.21 \mu\text{m}$ and $0.78 \pm 0.11 \mu\text{m}$. Particle size decreased as an increase in Polymer: drug ratio. This finding is in accordance with literature [2].

In vitro drug release of DIC loaded microsponges

In vitro drug release is graphically presented in fig. 1. Formulation DERS4 (87.94%) and DERS5 (90.73%) showed relatively comparable drug release as compared to DERS3 (79.41%) at the end of 6 h. Study revealed that the highest cumulative drug release after 6 h is 90.73%.

Kinetic analysis of the *in vitro* release data of DIC loaded microsphere formulations

The release of DIC in both DIC-loaded microsponges formulations DERS3 and DERS4 showed more adherence to Higuchi's diffusion kinetic model, with regression coefficient (r^2) value 0.9730 and 0.9655, respectively (table 3).

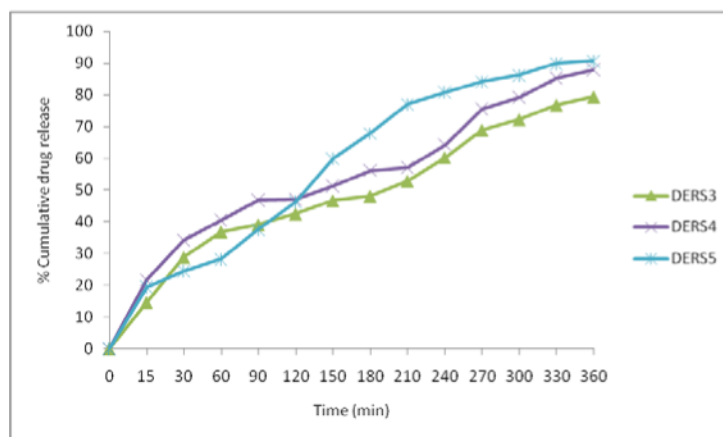


Fig. 1: *In vitro* release profiles of DIC loaded microsphere formulations (DERS3, DERS4 and DERS5). The data is expressed as mean \pm SD, n=3

Table 2: Characterization data of DIC loaded microsponges

S. No.	Formulation code	Polymer: drug ratio	Particle size (μm)	Production yield (%)	Drug content (%)	Entrapment efficiency (%)
1	DERS1	1: 1	20.39 \pm 4.21	27.50 \pm 3.54	27.27 \pm 5.43	15.00 \pm 3.15
2	DERS2	1:3	13.14 \pm 2.63	43.75 \pm 2.51	45.71 \pm 4.92	26.67 \pm 4.84
3	DERS3	1: 5	8.32 \pm 1.94	57.50 \pm 4.13	73.91 \pm 3.46	51.00 \pm 3.61
4	DERS4	1:7	7.52 \pm 2.29	68.13 \pm 3.98	80.73 \pm 3.51	62.86 \pm 5.49
5	DERS5	1: 9	6.98 \pm 1.45	64.00 \pm 4.56	86.72 \pm 1.36	61.67 \pm 2.27
6	DERS6	1:11	1.64 \pm 0.82	68.75 \pm 1.32	87.88 \pm 2.40	65.91 \pm 3.65
7	DERS7	1: 13	0.78 \pm 0.11	72.50 \pm 2.12	90.15 \pm 4.22	70.38 \pm 1.74

*n=3, mean \pm SD

Table 3: Release kinetics study of DIC loaded microsphere formulations

Formulation code	Zero-order model (r^2)	First-order model (r^2)	Higuchi model (r^2)	Hixson-crowell model (r^2)	Korsmeyer-peppas model (n)
DSER3	0.9271	0.9602	0.9730	0.9625	0.67
DSER4	0.9139	0.9301	0.9655	0.9483	0.67
DSER5	0.9373	0.9883	0.9772	0.9861	0.72

DERS5 followed first-order drug release kinetic, with regression coefficient (r^2) value 0.9883. The diffusion exponents (n) of all microsphere formulations have a value more than 0.5 but less than 0.8. This indicates that the DIC release mechanism from microspheres is non-Fickian diffusion.

Microsphere formulation DERS4 was selected as having requisite particle size, sustained release and satisfactory Production yield, Entrapment efficiency and Drug content. DERS4 was further studied for FTIR, DSC and SEM.

Fourier transform infrared spectroscopy (FTIR)

Drug-polymer compatibility in the selected microspheres DERS4 was evaluated by FTIR. The principle IR peaks of DIC appeared at wavenumbers of 3361.34 cm^{-1} (NH stretching of secondary amine groups), 1302.12 cm^{-1} (C-N stretching), 1503.46 cm^{-1} (C=C ring stretching) and 1548.76 cm^{-1} (C=O stretching of the carboxyl ion) and 757.12 cm^{-1} (C-Cl stretching) [27]. The characteristic DIC peaks were present in the physical mixture as well as in the DIC-loaded microspheres DERS4 (fig. 2) with no significant changes in frequencies.

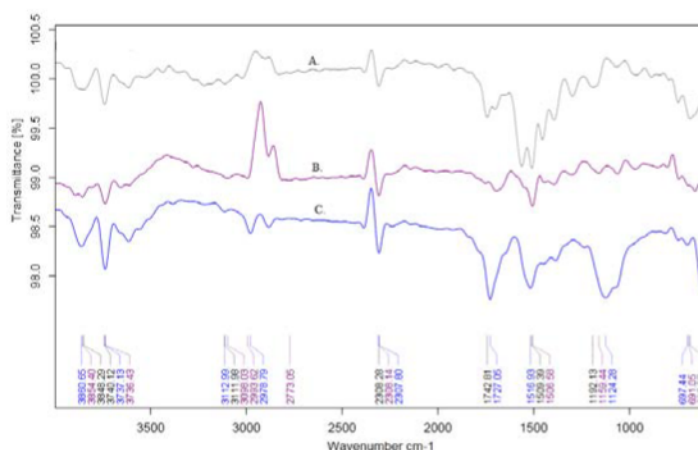


Fig. 2: FTIR spectrum of (a) DIC (b) Physical mixture of DIC and ERS polymer (c) Selected microsphere formulation DERS4

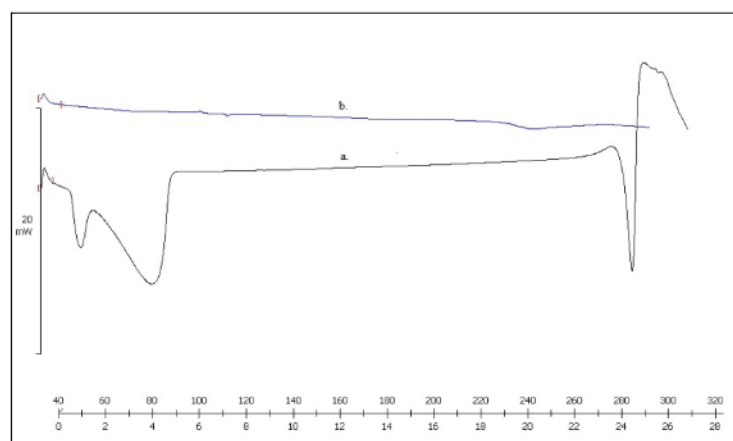


Fig. 3 DSC thermogram of (a) Pure DIC and (b) Selected microsphere DERS4

Differential scanning calorimetry (DSC)

The thermal behavior of the DIC, and selected microsp sponge DERS4 are presented in (fig. 3).

DSC thermogram of DIC exhibited endothermic peaks, initial peak due to loss of water followed by the other sharp endothermic peak at 291.97 °C, indicating to melting point of DIC in crystalline form; reflecting DIC purity [9]. The DSC curves of DERS4 formulation exhibited suppressed peak of the DIC at 280.40 °C.

Scanning electron microscopy (SEM)

Morphology DIC loaded microsponges were studied by SEM analysis. The representative SEM images of microsp sponge (DERS4) are shown in (fig. 4 and 5).

Formulation and characterization of *in situ* ocular gel containing DIC loaded Microsponges

In situ ocular gel found clear with suspended microsp sponge particles. The pH of *in situ* gel solution was found in range 6.03 to 6.13.

The formulation have an optimum viscosity at Non-Physiological conditions that will give ease in instillation to eye in the form of drop, which go through a quick sol to gel transition (triggered by pH) at physiological conditions (37 °C and 7.4 pH) as shown in table 4.

The *in vitro* drug release from *in situ* ocular gel showed sustained release. The % cumulative drug release from formulations was found to be IG1 (89.25%), IG2 (84.23%), IG3 (76.92%), and IG4 (69.64%) after 8 h as shown in fig. 6.

The drug release kinetic of all *in situ* gel formulations suggests Higuchi kinetic model (table 5) and diffusion exponent showed non-fickian diffusion mechanism.

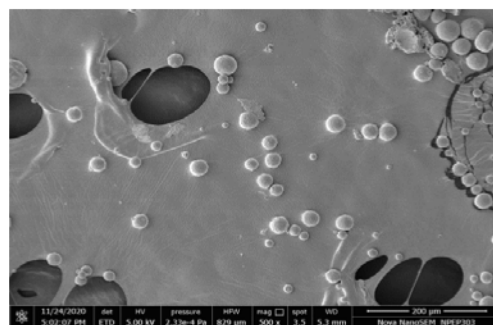


Fig. 4: SEM of selected microsp sponge DERS4 (Magnification x 500)

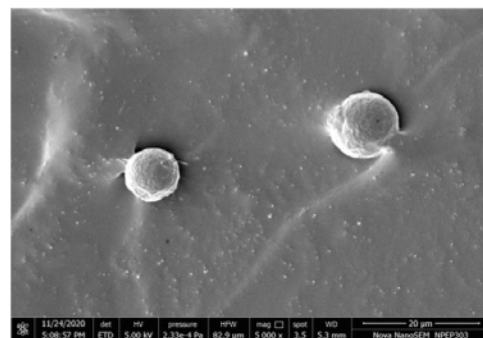


Fig. 5: SEM of selected microsp sponge DERS4 (Magnification x 5000)

Table 4: Characterization of DIC loaded microsp sponge containing ocular *in situ* gel

Formulation code	IG1	IG2	IG3	IG4
Gelling capacity	+	++	++	+++
pH	6.04	6.03	6.13	6.10
Viscosity At Non-Physiological conditions	860±120	1008±142	1843±176	2308±241
(cP) At Physiological conditions (pH 7.4 and 37 °C)	1852±194	4340±241	6651±186	7035±108
Drug content (%)	86.54±1.74	90.73±1.40	94.26±1.61	89.83±2.24

*n=3, mean±SD

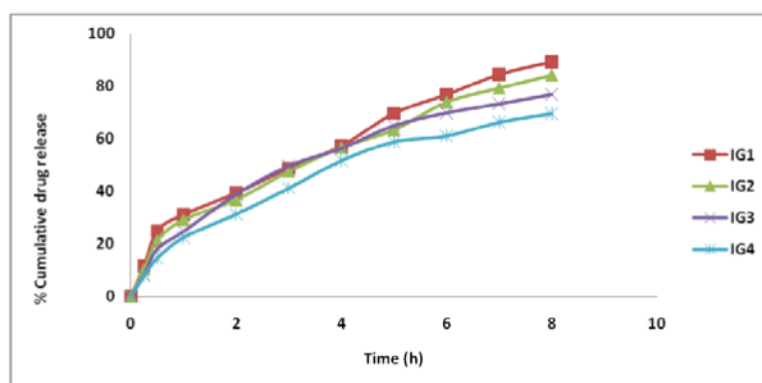


Fig. 6: *In vitro* release profiles of DIC loaded microsp sponge containing ocular *in situ* gel. The data is expressed as mean±SD, n=3

Table 5: Release kinetics study of DIC loaded microsp sponge containing ocular *in situ* gel

Formulation code	Zero order model (r ²)	First order model (r ²)	Higuchi model (r ²)	Hixson-crowell model (r ²)	Korsmeyer-peppas model (n)
IG1	0.9536	0.9755	0.9900	0.9880	0.68
IG2	0.9536	0.9884	0.9936	0.9904	0.68
IG3	0.9260	0.9904	0.9941	0.9753	0.69
IG4	0.9410	0.9877	0.9931	0.9763	0.68

Sterility study

The study results of the sterility study are summarized in table 6, the prepared ocular *in situ* gel formulation passed the sterility test. There was zero growth found in fluid thioglycollate medium and soyabean casein digest medium.

Table 6: Sterility test of ocular *in situ* gel formulation IG3

Organism	Bacteria	Fungi
+ve Control	Turbid	Turbid
-ve Control	Clear	Clear
IG3	Clear	Clear

*n=3, mean±SD

DISCUSSION

DIC-loaded microsponges were prepared by the quasi emulsion solvent diffusion method using ERS polymer. In literature, this method is considered to be simple, replicable, rapid and solvent toxicity also got eliminated [3]. With the increase in drug concentration in polymer: drug ratio; production yield, drug content and entrapment efficiency increases. As more drug are available for entrapment leading to high amount of drugs in microsponges leading to increased values of production yield, drug content and entrapment efficiency. The lower values of entrapment efficiency (15.00%) could be due to dissolution of some fraction of DIC in PVA solution during the emulsification process [20]. With an increase in level of DIC (besides drug dissolution), more drugs available for entrapment in ERS polymer matrix. As a result entrapment efficiency increases with increment in polymer: drug ratio.

High PVA concentration and high stirring speed yield small particle size which is requisite for this study. In the quasi emulsion solvent diffusion method, organic phase i.e. dichloromethane diffuses out to yield particles in which drug particle surrounded by polymer. At high polymer: drug ratio less polymer amounts surrounds the drug causing decreased particle sizes of microsponges [2].

As in the polymer: drug ratio the concentration of drug increased, polymer units surrounding drug units is less than at low. During phase transition process less polymer got bound to the drug giving smaller size microsphere. Particle size of less than 10 µm is required for ocular administration [11]. Hence microsphere formulations above 10 µm were not further investigated. Microsponges have particle size range from 5-300 µm. So microsponges below 5 µm were also excluded from further studies.

Sustained release of drug was as a result of incorporation of drug in polymer Matrix [28]. Drug release is inversely related to the Polymer: drug ratio. High Polymer: drug ratio yield smaller particles having more active surface area which coming in contact with diffusion media. Also smaller particle exhibit shorter path length drug need to travel through microsphere pores into the diffusion media [8]. Drug release rates were increased with an increasing amount of DIC in microsphere. At a high Polymer: drug ratio, the corresponding polymer amount is lesser. As more drug got released more void channels formed which allows more diffusion media to enter and in turn increases release rate.

FTIR studies confirms that no interaction between drug and ERS polymer. The thermogram of microsphere formulation showed suppressed peak signify uniform dispersion of DIC in polymeric matrix and altered crystallinity of DIC. Absence of any other significant endothermic peak, in the melting point range of DIC (melting point found as 286.26 °C) indicates that absence of any interaction between the DIC and ERS polymer, and verify the aptness of microsphere preparation technique [27].

SEM results indicated that DERS4 microsponges were tiny, porous and spherical. Surface integrity of microsphere got retained. Microsponges particles are free from aggregates. This might be due to aqueous solution of PVA which is used during the quasi emulsion solvent diffusion method. PVA reduces surface charge on the particle giving aggregate free microsponges [29].

In the present investigation, incorporation of DIC-loaded ERS polymeric microsponges was performed into *in situ* gel formulated using polymers Carbopol 940 and HPMC E4M. Carbopol 940 and HPMC E4M were used in combination as alone high concentration of carbopol 940 yield a highly acidic solution, which is not suitable for ocular administration (pH of lacrimal fluid 7.4) [30]. So moderate concentration of Carbopol 940 (0.1% w/v) along with viscosity-enhancing polymer HPMC E4M (0.2-0.8 % w/v) [31] was used to formulate *in situ* gel. The pH of formulation would raises instantly to pH 7.4 (an ideal ocular pH) after instillation into eye due to pH of lacrimal secretion. Thus, the formulations were considered to be suitable for ocular administration and may not cause any irritation to ocular tissues upon instillation [25].

At Physiological conditions formulation form stiff gel which increases residence time of microsponges incorporated in gel. In *in situ* gel formulation contains HPMC E4M and carbopol 940 which are known to gel reversibly on elevation of temperature and pH respectively [31]. Hence at physiological conditions viscosity of formulation increases to form a stiff gel, as both pH and temperature increases.

Formed stiff gel should display good integrity and not to get dissolve and erode for extended period of time. Formulations IG2 and IG3 exhibited satisfactory “++” grade of gelling capacity [12].

In situ gel formulation IG3 showed sustained release with a satisfactory “++” grade of gelling capacity. Hence, IG3 formulation was taken for further Sterility test. Sterility study results proved the efficiency of autoclaving for sterilization of ocular *in situ* gel.

CONCLUSION

With the present study, the potential of DIC loaded microsponges as drug carriers for ocular delivery was investigated. Microsponges showed good practical yield, entrapment efficiency, drug content and suitable particle size for ocular administration. Controlled release of up to 6 h observed through DIC loaded microsponges. DIC loaded microsponges successfully incorporated in *in situ* gels. The clarity, pH, drug content, gelling capacity and rheological studies of DIC loaded microsponges containing ocular *in situ* gel formulations were found to be acceptable. Further, *in situ* gel formulations showed sustained drug release for a period of 8 h, which is satisfactory for management of ocular pain.

ACKNOWLEDGEMENT

The authors express sincere thanks to Dr. R. S. Chavan, Principal, PDEA's S. G. R. S. College of Pharmacy, Saswad, Purandar, Pune, Maharashtra, India for providing the facilities needed to undertake this research work.

ETHICS APPROVAL AND CONSENT TO PARTICIPATE

Not applicable

ABBREVIATIONS

DIC: Diclofenac Sodium; ERS: Eudragit RS 100; HPMC E4M: Hydroxypropyl Methylcellulose E4M; DMC: Dichloromethane; PVA: Polyvinylalcohol; FTIR: Fourier Transform Infrared Spectroscopy; DSC: Differential scanning calorimetry; SEM: Scanning electron microscopy; STF: Simulated tear fluid.

FUNDING

This research did not receive any specific grant from funding agencies in public, commercial or not-for-profit sectors.

AUTHORS CONTRIBUTIONS

All authors have read and approved the manuscript. Rajashri B. Ambikar designed the study, carried out experimental work, Analyzed data and Drafted the manuscript. Dr. Ashok V. Bhosale contributed in designing of study, checked the paper content, helped in data interpretation and critical revision of the manuscript for intellectual content.

CONFLICT OF INTERESTS

The authors declare no competing interests.

REFERENCES

- Osmani RA, Aloorkar NH, Kulkarni AS, Thaware BU, Kulkarni PK. Microsponge based drug delivery system for augmented gastroparesis therapy: formulation development and evaluation. *Asian J Pharm Sci* 2015;10:442-51.
- Nokhodchi A, Jelvehgari M, Siahi MR, Mozafari MR. Factors affecting the morphology of benzoyl peroxide microsponges. *Micron* 2007;38:834-40.
- Kumari A, Jain A, Hurkat P, Tiwari A, Jain SK. Eudragit S100 coated microsponges for Colon targeting of prednisolone. *Drug Dev Ind Pharm* 2018;44:902-13.
- Sareen R, Nath K, Jain N, Dhar KL. Curcumin loaded microsponges for colon targeting in inflammatory bowel disease: fabrication, optimization, and *in vitro* and pharmacodynamic evaluation. *J Biomed Biotechnol* 2014. DOI:10.1155/2014/340701.
- Srivastava R, Kumar D, Pathak K. Colonic luminal surface retentive Meloxi-cam microsponges delivered by erosion based colon targeted matrix tablet. *Int J Pharm* 2012;427:156-62.
- Bhatia M, Saini M. Formulation and evaluation of curcumin microsponges for oral and topical drug delivery. *Prog Biomater* 2018;7:239-48.
- Abdelmalak NS, El-Menshaweh SF. A new topical fluconazole microsphere loaded hydrogel: preparation and characterization. *Int J Pharm Pharm Sci* 2012;4:460-9.
- Arya P, Pathak K. Assessing the viability of microsponges as gastro retentive drug delivery system of curcumin: Optimization and pharmacokinetics. *Int J Pharm* 2014;460:1-12.
- Maiti S, Kaity S, Ray S, Sa B. Development and evaluation of xanthan gum-facilitated ethyl cellulose microsponges for controlled percutaneous delivery of diclofenac sodium. *Acta Pharm* 2011;61:257-70.
- Ambikar RB, Bhosale AV. Formulation and evaluation of eudragit RL100 polymeric drug loaded microsphere for ophthalmic use. *J Pharm Res Int* 2021;33:45-51.
- Abd-Elal RMA, Elosaily GH, Gad S. Full factorial design, optimization, *in vitro* and *ex vivo* studies of ocular timolol-loaded microsponges. *J Pharm Innov* 2020;15:651-63.
- Obiedallah MM, Abdel-Mageed AM, Elfaham TH. Ocular administration of acetazolamide microsponges in situ gel formulations. *Saudi Pharm J* 2018;26:909-20.
- Ali J, Fazil M, Qumbar M, Khan N, Ali A. Colloidal drug delivery system: amplify the ocular delivery. *Drug Delivery* 2016;23:710-26.
- Kesarla R, Tank T, Vora PA, Shah T, Parmar S, Omri A. Preparation and evaluation of nanoparticles loaded ophthalmic *in situ* gel. *Drug Delivery* 2016;23:2363-70.
- Upadhyay P, Kumar M, Pathak K. Norfloxacin loaded pH triggered nanoparticulate *in-situ* gel for extraocular bacterial infections: optimization, ocular irritancy and corneal toxicity. *Iran J Pharm Sci* 2016;15:3-22.
- Al-Kinani A, Zidan G, Elsaid N, Seyfoddin A, Alani AW, Alany R. Ophthalmic gels: past, present and future. *Adv Drug Delivery Rev* 2018;126:113-26.
- Wu Y, Liu Y, Li X, Kebebe D, Zhang B, Ren J, *et al.* Research progress of in-situ gelling ophthalmic drug delivery system. *Asian J Pharm Sci* 2019;14:1-15.
- Khangtragool A. Methocel E4M: preparation and properties as a vehicle for the ocular drug delivery of vancomycin. *Chiang Mai J Sci* 2014;41:166-73.
- Adelli GR, Balguri SP, Bhagav P, Raman V, Majumdar S. Diclofenac sodium ion exchange resin complex loaded melt cast films for sustained release ocular delivery. *Drug Delivery* 2017;24:370-9.
- Jelvehgari M, Siahi Shadbad MR, Azarmi S, Martin GP, Nokhodchi A. The microsphere delivery system of benzoyl peroxide: preparation, characterization and release studies. *Int J Pharm* 2006;308:124-32.
- Martin A, Bustamante P, Chun A. Micromeritics. In: *Physical pharmacy-physical chemical principles in the pharmaceutical science*. 5th ed. B I Waverly Pvt. Ltd; 2002. p. 446-8.
- Nair AB, Shah J, Jacob S, Al-Dhubiab BE, Sreeharsha N. Experimental design, formulation and *in vivo* evaluation of a novel topical in situ gel system to treat ocular infections. *PLoS One* 2021;16:e0248857.
- Son GH, Lee BJ, Cho CW. Mechanisms of drug release from advanced drug formulations such as polymeric-based drug-delivery systems and lipid nanoparticles. *Int J Pharm Investig* 2017;47:287-96.
- Li SS, Li GF, Liu L, Jiang X, Zhang B, Liu ZG, *et al.* Evaluation of paeonol skin-target delivery from its microsphere formulation: *in vitro* skin permeation and *in vivo* microdialysis. *PLoS One* 2013;20;8:e79881.
- Song J, Bi H, Xie X, Guo J, Wang X, Liu D. Preparation and evaluation of sinomenine hydrochloride in situ gel for uveitis treatment. *Int. Immunopharmacol* 2013;17:99-107.
- Indian Pharmacopoeia. The controller of publication, New Delhi; Ministry of health and family welfare. India. 6th Ed. Volume II; 2010. p. 59-66.
- Kucukturkmen B, Oz UC, Bozkir A. *In situ* hydrogel formulation for intra-articular application of diclofenac sodium-loaded polymeric nanoparticles. *Turk J Pharm Sci* 2017;14:56-64.
- Kumar PM, Ghosh A. Development and evaluation of metronidazole loaded microsphere based gel for superficial surgical wound infections. *J Drug Delivery Sci Technol* 2015;30:15-29.
- Deshmukh K, Poddar SS. Tyrosinase inhibitor-loaded microsphere drug delivery system: new approach for hyperpigmentation disorders. *J Microencapsul* 2012; 29:559-68.
- Charoo NA, Kohli K, Ali A. Preparation of in situ-forming ophthalmic gels of ciprofloxacin hydrochloride for the treatment of bacterial conjunctivitis: *in vitro* and *in vivo* studies. *J Pharm Sci* 2003;92:407-13.
- Makwana SB, Patel VA, Parmar SJ. Development and characterization of in-situ gel for ophthalmic formulation containing ciprofloxacin hydrochloride. *Results Pharma Sci* 2016;6:1-6.
- Sheshala R, Ming NJ, Kok YY, Singh TRR, Dua K. Formulation and characterization of pH induced in situ gels containing sulfacetamide sodium for ocular drug delivery: a combination of carbopol®/HPMC polymer. *Indian J Pharm Educ Res* 2019;53:654-62.

NOVEL FLOATING AGENT *SACCHAROMYCES BOULARDII* FORMULATION BASED FLOATING DRUG DELIVERY SYSTEM

SUVARNA CHITTAM*, ASHOK BHOSALE

Department of Pharmaceutics, PDEA'S Seth Govind Raghunath Sable, College of Pharmacy, Saswad, Pune (Maharashtra, India)
Email: cssgrs@gmail.com

Received: 30 May 2021, Revised and Accepted: 28 Jul 2021

ABSTRACT

Objective: The objective is to design and optimize a floating tablet of furosemide using a novel floating agent *Saccharomyces boulardii*.

Methods: In this study floating tablet based on principle of combination of floating and swelling prepared by direct compression technique. *Saccharomyces boulardii* probiotics preparation is used as a floating agent due to its bloating property i.e. production of CO₂ gas and hydrophilic polymer HPMC E LV 15 used as swellable polymer. Furosemide is a BCS class IV drug selected as model drug which shows pH dependent solubility and permeability and it is better absorbed from the gastric region, hence to improve dissolution and residence at absorption site of such drug, floating drug delivery system is needed. Calcium hydroxide used as pH modifier which increase rate of dissolution of furosemide and also maintain integrity of tablet matrix. Formulation designed and developed using central composite design response surface methodology technique, so as to explore the effect of formulation variables such as amount of *Saccharomyces boulardii* preparation and calcium hydroxide on floating lag time and % drug release after 12h.

Results: The numerical and graphical optimization technique were used to choose the optimal formulation. Floating lag time was found to be 12.6 min and 88.18% drug release for the optimized formulation. *In vivo* buoyancy studies depicted that formulation stay more than 6h in stomach.

Conclusion: Study indicate that *Saccharomyces boulardii* is a promising floating agent, and the formulation containing this novel floating agent is suitable for gastro retention and it increases bioavailability of furosemide.

Keywords: *Saccharomyces boulardii*, Probiotics, Furosemide, Response surface methodology, Bloating

© 2021 The Authors. Published by Innovare Academic Sciences Pvt Ltd. This is an open access article under the CC BY license (<https://creativecommons.org/licenses/by/4.0/>)
DOI: <https://dx.doi.org/10.22159/ijap.2021v13i5.42237>. Journal homepage: <https://innovareacademics.in/journals/index.php/ijap>

INTRODUCTION

Yeasts are a significant source for procurement products with probiotic activity and a good alternative to probiotic bacteria [1]. *Saccharomyces boulardii* is the unique yeast probiotic that has been effectively used as both a preventive and therapeutic agent for diarrhea and other GI complaints. *Saccharomyces boulardii* retains many properties that make it an impending probiotic agent, i.e. it survives during GI transit, it grow well at temperature 37 °C, both *in vitro* and *in vivo* [2], its high tolerance to gastric acidity, proteolysis and are able to attain higher populations in the GI tract. They can forever colonize in the colon and do not easily move out from the intestinal tract [3]. They can also be perceived alive throughout the GIT, if they are given in lyophilized form [4]. *Saccharomyces boulardii* is generally administered in lyophilized powder form [5]. *Saccharomyces boulardii* is used in a variety of gastrointestinal disorders but its major drawback is it's certain side effects such as gas and bloating [6]. Bloating is a feeling of increased gas in the stomach that subsides over a few days [7].

Saccharomyces boulardii is an anaerobe, which means it can grow under aerobic or anaerobic conditions. *Saccharomyces boulardii* consume sugars from the simplest form to the complex form by tapping order i.e. they first consume glucose, fructose and secondly lactose and finally, they devour starch, resulted in the manufacture of ethanol and carbon dioxide [8]. *Saccharomyces boulardii* are a heterotrophic organism, meaning they cannot produce its own food but obtain their energy or nutrition from carbon source. Though it prefer to use glucose, it can also use monosaccharides, polysaccharides, oligosaccharides, alcohol, organic acids, pyruvate, and lactate. *Saccharomyces boulardii* prefers fermentation over respiration 98 to 2%. The fermentation pathway is documented as Embden-Myer of Pathway (EMP), which prepares ethanol products. The depletion of glucose ultimately will lead to a condition known as "cell depression", which generate product like carbon dioxide and water from oxidation of ethanol [9]. Thus in aerobic respiration, it produces CO₂ and H₂O and in anaerobic alcoholic fermentation, it generates ethanol and CO₂.

In the present work, an attempt has been made to develop a floating tablet using novel floating agent and which based on the principle of combination of floating and swelling. *Saccharomyces boulardii* probiotics formulation used as floating agent due to its bloating property as well as its resistance to gastric acidity and high temperature and hydrophilic polymer HPMC used as the swellable polymer. Furosemide is a loop diuretic used in the recovery of hypertension [10]. Furosemide is a weekly acidic drug having pKa 3.9 [11] and having a short half-life of 2h. Oral bioavailability of conventional tablet is 30 to 60% due to its variable and erratic absorption. It is a BCS class IV drug having insignificant aqueous solubility and permeability. It is mainly absorbed from the stomach and the upper part of the gastrointestinal tract [12]. It shows high permeability and better absorption through the stomach. Thus furosemide having a pH-dependent solubility and permeability [13]. So it is selected as a model drug for the development of a floating drug delivery system. In present investigation, an attempt has been made to improve the bioavailability of furosemide by prolonging its duration in the stomach via the floating dosage forms using novel floating agent such as *Saccharomyces boulardii* formulation and also enhance its solubility by using hydrophilic polymers such as HPMC and calcium hydroxide used as pH modifier which increase rate of dissolution of furosemide and also maintain integrity of matrix.

MATERIALS AND METHODS

Materials

Furosemide was gifted by (FU) Suleshvari Pharma, Ankaleshwar (Gujarat). Hydroxypropyl methylcellulose was gifted by Loba Chemie Pvt. Ltd. *Saccharomyces boulardii* probiotic preparation was purchased from local market. Hydrochloric acid was gifted by Themis Research lab, Mumbai. Calcium hydroxide, Magnesium stearate and Sodium hydroxide purchased from Poona chemical laboratory, Pune.

Methods

Preparation of floating tablet of furosemide

Floating tablets containing *Saccharomyces boulardii* formulation and furosemide were formulated by direct compression technique using

polymer like HPMC E 15 LV and other ingredients like calcium hydroxide, magnesium stearate, and probiotic preparation containing *Saccharomyces boulardii*. All ingredients were passed through sieve no # 40, except *Saccharomyces boulardii* preparation. HPMC E 15 LV, calcium hydroxide and furosemide were first mixed using a mortar and pestle to get a uniform tablet blend. Finally, *Saccharomyces boulardii* preparation and magnesium stearate were mixed delicately to the above-prepared mixture blend. The mixture was then weighed accurately according to the formula and compressed into tablets using Minipress tablet punching machine (Karnavati) to obtain tablets of desired specifications [14, 15]. The different formulations were prepared as given in table 1.

Evaluation test

Hardness test

Monsanto hardness tester used for evaluation of hardness [15].

Thickness

Vernier caliper was used for the evaluation of tablet thickness [15].

Friability

Friability was expressed in terms of percentage weight loss. % friability was evaluated using the following formula [16].

$$\% \text{ Friability} = \frac{W1 - W2}{W1} \times 100$$

Where,

W1 = Weight of Tablets (Initial/Before Tumbling) and

W2 = Weight of Tablets (After Tumbling or friability)

Determination of swelling index

Swelling degree defines the change of dimension or weight gain of the dosage form. First, a tablet was weighed (W₁) and placed in a glass beaker containing hot 0.1 N HCl (PH 1.2) having temp. 37±0.5 °C. Tablets were removed at intervals of 1, 2, 3, 4, 6 and 8 h; excess water was carefully removed using filter paper and tablets were again weighed. Water uptake is measured in terms of percent weight gain. The % swelling index (SI) was measured by the following formula [17].

$$\% \text{ Swelling index} = \frac{\text{Final Weight of tablet (W}_2\text{)} - \text{Initial weight of tablet (W}_1\text{)}}{\text{Initial weight of tablet (W}_1\text{)}} \times 100$$

Uniformity of weight

Twenty tablets were selected randomly weighed individually using electronic balance and the average weight was calculated. The % weight variation was calculated and checked for weight variation as per IP [18].

$$\% \text{ Weight variation} = \frac{\text{Average weight} - \text{Individual weight}}{\text{Individual weight}} \times 100$$

Drug content

10 tablets were weighed and crushed using motor pestle. The crushed powder equivalent to an average weight of tablets was weighed accurately and put in 100 ml 0.1N NaOH solution for complete extraction of drug and stirred continuously. The solution is filtered using a Whatman filter paper, diluted with 0.1N NaOH solution and the drug content is determined spectrophotometrically [19].

Tablet floating behavior

The floating lag time and total floating duration were determined using USP type II (paddle) apparatus at speed 50 rpm in 900 ml 0.1N HCl at 37±0.5 °C to simulate *in vivo* conditions. And on the basis of visual inspection, time were recorded [20].

In vitro dissolution studies

In vitro dissolution studies were conducted by using paddle dissolution apparatus (Electrolab) at 50 rpm using 900 ml of 0.1 N HCl, (pH 1.2) as a dissolution medium at 37±0.5 °C and the absorbance of the sample solution was recorded using UV spectrophotometer at 274 nm. The *in vitro* dissolution study calculation was conducted using disso software (PCP disso V3). The *in vitro* release profile was determined [21].

Drug Release mechanism and model fitting

In the present study, several mathematical models such as zero-order, first-order, matrix, Higuchi's, Peppas and Hixson-Crowell model can be tested to determine the best fit model [22, 23].

Statistical analysis and optimization

Design-Expert software used for statistical analysis of the data and optimization polynomial models. The best-fitting model was elected on the basis of comparisons of several statistical parameters. ANOVA used to ascertain the significant effect of factors on responses. The relationship between the factors and response was further clarified using response surface plots. Subsequently, a numerical optimization techniques used to engender the best-optimized solution [24].

In vivo buoyancy study by using X ray

The tablets are prepared by replacing some quantity of drug with barium sulfate. The *in vivo* buoyancy study conducted using healthy albino rabbits. Prepared optimized tablet containing barium sulphate administered to rabbits. X ray was taken at intervals of 1, 2, 4, 6 and 12 h [25].

RESULTS AND DISCUSSION

The prepared FDDS tablets were evaluated and data is enclosed in table 2. From this data, it was clear that the evaluation parameters of all batches were in the acceptable range. Uniformity of weight, uniformity of drug content not much deviate from the mean value.

Table 1: Composition of furosemide floating tablets (mg/tablet)

Formulation code	Ingredients (mg)				
	Furosemide	HPMC E 15 LV	<i>Saccharomyces boulardii</i> preparation	Calcium hydroxide	Magnesium stearate
F1	20	40	25	15	2
F2	20	45	20	15	2
F3	20	50	15	15	2
F4	20	45	25	10	2
F5	20	50	20	10	2
F6	20	55	15	10	2
F7	20	50	25	5	2
F8	20	55	20	5	2
F9	20	60	15	5	2

HPMC E 15 LV-Hydroxy Propyl Methyl Cellulose E 15 LV

The percentage swelling index, which is expressed in terms of weight gain of all batches shown in fig. 1. As the concentration of calcium hydroxide increases, swelling index decreases and as the concentration of hydrophilic polymer HPMC E15 LV increases, swelling index increases. hence formulation F9 shows a higher

swelling index and formulation F1 shows a lower swelling index. Buoyancy is achieved due to hydration of swelling material like polymer Hydroxypropyl methylcellulose and carbon dioxide gas [26] generation from *Saccharomyces boulardii* formulation when it come in contact with water from acidic media.

Table 2: Evaluation of physical parameters of furosemide floating tablets

Batch code	Hardness (kg/cm ²)	Thickness (mm)	Friability (%)	Weight variation	Drug content uniformity (%)	Total floating time (h)
F1	5.1±0.22	3.4±0.08	0.62±0.09	103.1±3.6	97.66±2.45	>12
F2	5.2±0.08	3.5±0.08	0.49±0.08	101±3	98.70±2.98	>12
F3	5.0±0.21	3.36±0.05	0.56±0.05	101±4.17	100.20±1.85	>12
F4	5.2±0.21	3.33±0.05	0.53±0.05	100.5±3.26	102.91±2.87	>12
F5	5.0±0.25	3.36±0.05	0.49±0.08	101.7±2.86	100.29±1.30	>12
F6	5.4±0.12	3.33±0.12	0.45±0.12	102.8±3.06	97.57±1.73	>12
F7	5.2±0.12	3.43±0.12	0.55±0.10	102.9±3.38	101.41±2.66	>12
F8	5.3±0.24	3.5±0.08	0.48±0.08	102.4±5.31	99.35±2.32	>12
F9	5.3±0.24	3.46±0.09	0.55±0.05	102.5±3.80	103.66±1.87	>12

*Represents mean±SD (n =3)

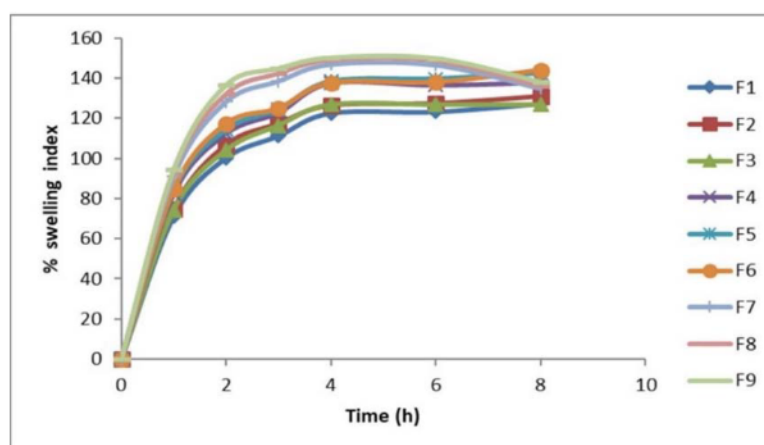


Fig. 1: Maximum % swelling index of all the formulations

From data of factorial design, it is clear that floating lag time changes as the amount of floating agent (*Saccharomyces boulardii* preparation) and calcium hydroxide changes. As the amount of floating agent is changed from 15 to 25 mg the floating lag time decreased because more amount of floating agent contain more Colony Forming Unit of *Saccharomyces boulardii*, which produce more amount of carbon dioxide gas, but as the concentration of calcium hydroxide changed from 5 to 15 mg floating lag time increased because swellability and viscosity of polymer layer also affect on floating lag time, hence as the quantity of calcium hydroxide increased it affect on the viscosity of HPMC layer. The reduction in viscosity at lower pH is mainly because of the more coiling nature of HPMC when ionic strength increased. At the lowest pH i. e in acidic pH of dissolution medium, the coiling of polymer molecules takes place, which preferred HPMC-water interaction and the possibility for polymer-polymer interaction is less prominent [26]. In the case of basic pH due to the addition of calcium hydroxide, which act as pH modifier for the microenvironment of tablet, the HPMC molecules are relatively extended and due to the extended conformation of polymer molecules, the polymer-polymer interaction is preferred, which leads the molecules to overlap and coiling and then entangles to become a thermo co reversible gel, which leads to polymer-polymer interactions. Thus their was an upsurge in velocity and viscosity of HPMC at a higher pH range [27] and a good gel layer is formed due to the addition of calcium hydroxide. This gel layer prevents matrix disintegration and any further rapid water penetration [28]. As water penetrate slowly in matrix of the tablet, activation of *Saccharomyces boulardii* and carbon dioxide formation rate also slows down and this is one reason of increased floating lag time with an increase in calcium

hydroxide, but an increased concentration of calcium hydroxide also increased integrity of matrix due to formation of good gel layer.

And thus, it was found that as we change the quantity of calcium hydroxide, it affects on floating lag time, in a formulation containing F1 to F3 where the concentration of calcium hydroxide is high it changes its viscosity and ability of polymer to swell and hence tablet from these batches require more floating lag time then further batches which consists of less calcium hydroxide thus floating lag time is influenced by both quantity of floating agent and amount of calcium hydroxide in the formulation. Total floating duration and matrix integrity also increases with an increase in the quantity of calcium hydroxide.

% drug releases of all floating tablets were represented in fig. 2a and 2b. Average % drug release from batch F1 to F9 varies from 90.01% to 77.79% also affected by the quantity of both calcium hydroxide and floating agent. Cumulative % drug release increases with an increase in the quantity of calcium hydroxide (pH modifier) and *Saccharomyces boulardii* preparation. Addition of calcium hydroxide in the tablet as a pH modifier maintained a microenvironment gel matrix pH greater than pH with buffer ions in the surrounding media (pH 1.2), but without the pH modifier, the internal matrix was essentially retained same pH as that of surrounding media. If an acidic drug-like furosemide is buffered to a pH above its pKa and is ionized, the drug may have a greater solubility, resulting in faster drug-release rates; this is the reason why formulation F1, F2 and F3 shows higher drug release though the swelling index is lower due to thermoreversible gel formation. This emphasizes pH modifiers play an important role to alter drug solubility and to change microenvironment pH, which might increase drug release [29]. Second reason for an increase in drug

release with an increase in quantity of calcium hydroxide is pH gradient. pH of the gel matrix microenvironment plays an important role in drug release. The gel matrix cannot maintained a neutral environment inside the tablet matrix in the presence of pH modifier

and the pH of an internal matrix was higher than the acidic buffer of the surrounding media. There might be pH gradient developed across the gel structure, with the outer gel layer having a lower pH than the inner layer, which exist near to tablet core [29].

Table 3: Experimental design and observed response of the formulation in central composite design

Std	Run	Factor 1 A: <i>Saccharomyces boulardii</i> preparation (mg)	Factor 2 B: calcium hydroxide (mg)	Response 1 Floating lag time (min)	Response 2 Cumulative % drug release after 12 h
4	1	25	15	16.5	90.81
8	2	20	15	18	87.84
3	8	15	15	19.5	84.36
6	3	25	10	12.3	88.82
11	4	20	10	14	85.92
12	5	20	10	14.5	84.83
10	7	20	10	15.5	85.31
13	9	20	10	15	85.06
9	11	20	10	15.2	85.32
5	12	15	10	17	82.53
2	10	25	5	9.5	84.22
7	13	20	5	11.1	81.11
1	6	15	5	13	77.79

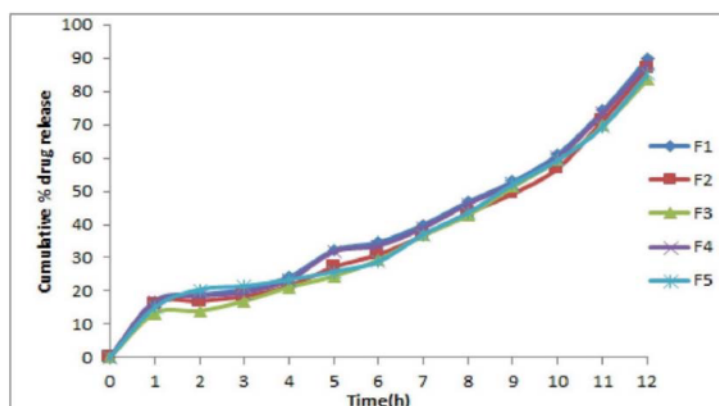


Fig. 2a: Drug release profiles of batch F1 to F5

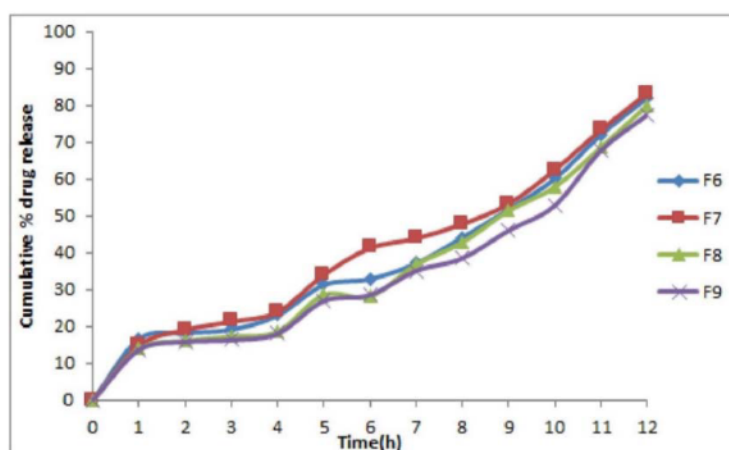


Fig. 2b: Drug release profiles of batch F6 to F9

From regression coefficient (R^2) of release data of formulation from F1 to F9 found by curve fitting method displays zero-order model is best fit model for formulation. In Korsmeyer-Peppas model, the release exponent i.e. n value, is in range from 0.45 to 0.85 for all batches.

Data analysis

Thirteen formulations were prepared as per the central composite design using Design-Expert version 13 software. All dependent variable responses of formulation shown in table 3. From fit

summary using Design-Expert software, It was clear that and linear model for floating lag time and quadratic model was suggested for cumulative % drug release after 12h (table 4).

Statistical summary of response shown in table 5 which indicate R^2 value 97.46% and 99.33% for response floating lag time and % drug release after 12h respectively. The values of Prob>F were found to be 0.05 for all responses again, indicating that the models are significant. Moreover, the Lack of Fit F-values of 0.44 and 0.47

implies the Lack of Fit is not significant relative to the pure error of the above two parameters. This model can be used to direct the design space.

By using response surface methodology following regression equations obtained (A: *Saccharomyces boulardii* preparation, B: calcium hydroxide)

$$\text{Floating lag time (Y1)} = 15.36 - 0.37 \cdot A + 0.68 \cdot B \text{ ----- (1)}$$

$$\begin{aligned} \text{\% Drug Release after 12 h (Y2)} &= 63.46 + 0.4557 \cdot A + 1.52 \cdot B + 0.0002 \cdot A \cdot B \\ &+ 0.0045 \cdot A^2 - 0.043 \cdot B^2 \text{ ----- (2)} \end{aligned}$$

In Eq. (1), the coefficient of A is negative and the coefficient of B is positive. It indicates that floating lag time (Y1) decreases with an increasing amount of *Saccharomyces boulardii* preparation (A) and Floating Lag Time increases with increasing value of independent variable calcium hydroxide.

It is observed from Eq. (2) that all the coefficients are positive. It signifies % drug release after 12 h (Y2) increases on increasing the amount of *Saccharomyces boulardii* preparation and calcium hydroxide [30].

Table 4a: ANOVA for linear model for response 1: floating lag time

Source	Sum of squares	Df	Mean square	F-value	p-value	
Model	90.27	2	45.13	191.78	<0.0001	Significant
A- <i>Saccharomyces boulardii</i> preparation	20.91	1	20.91	88.84	<0.0001	
B-calcium hydroxide	69.36	1	69.36	294.73	<0.0001	
Residual	2.35	10	0.2353			
Lack of Fit	0.9413	6	0.1569	0.4444	0.8208	not significant
Pure Error	1.41	4	0.3530			
Cor total	92.62	12				

Table 4b: ANOVA for the quadratic model for response 2: cumulative % drug release after 12 h

Source	Sum of squares	Df	Mean square	F-value	p-value	
Model	130.74	5	26.15	203.51	<0.0001	Significant
A- <i>Saccharomyces boulardii</i> preparation	61.25	1	61.25	476.69	<0.0001	
B-calcium hydroxide	65.94	1	65.94	513.17	<0.0001	
AB	0.0001	1	0.0001	0.0008	0.9785	
A ²	0.0354	1	0.0354	0.2758	0.6157	
B ²	3.26	1	3.26	25.39	0.0015	
Residual	0.8994	7	0.1285			
Lack of Fit	0.2367	3	0.0789	0.4763	0.7157	not significant
Pure Error	0.6627	4	0.1657			
Cor Total	131.64	12				

Table 5: Statistical summary of the response

Fit statics	Floating lag time (min)	% Drug release after 12 h
Std. Dev.	0.4851	0.3584
Mean	14.70	84.92
C. V. %	3.30	0.4221
R ²	0.9746	0.9932
Adjusted R ²	0.9695	0.9883
Predicted R ²	0.9610	0.9800
Adeq Precision	45.1997	53.466

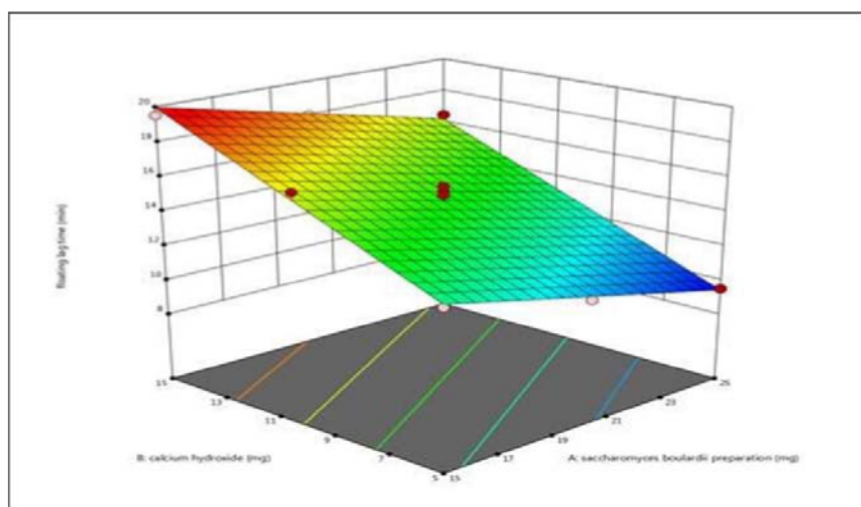


Fig. 3: Response surface plot showing the effect of the amount of *Saccharomyces boulardii* preparation and calcium hydroxide on floating lag time

Response surface analysis

3D surface plot for Floating lag time shown in fig. 3 indicate that floating lag time increases with decreasing amount of *Saccharomyces boulardii* preparation and it increases with an increasing amount of calcium hydroxide.

3D surface plot shown in fig. 4 demonstrates the relation of % drug release after 12 h with *Saccharomyces boulardii* preparation and calcium hydroxide. The effect of *Saccharomyces boulardii* preparation and calcium hydroxide was found to be in an ascending manner i.e. increasing the amount of both increases the response.

By using numerical and graphical optimization techniques best solution found. The statistically optimized formulation selected contained 25 mg of A (*Saccharomyces boulardii* preparation) and 9.98 mg of B (calcium hydroxide) as shown in overlay plot fig. 5. The observed value for floating lag time and cumulative % drug release after 12h were 12.6 min. and 88.18%. Model predicted value of floating lag time was 12.8 min, % drug release after 12 h was 88.66%. The observed values and predicted values of an optimized batch are in close agreement with each other, which confirm the predictability and validity of the model.

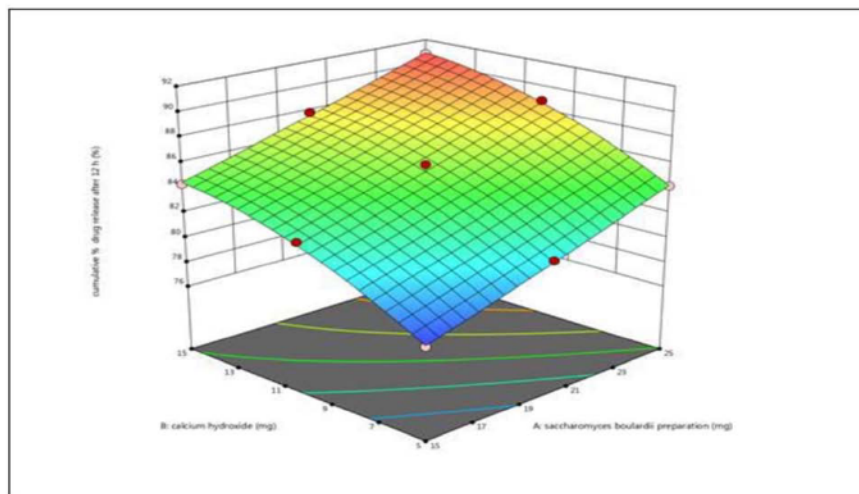


Fig. 4: Response surface plot showing the effect of the amount of *Saccharomyces boulardii* preparation and calcium hydroxide on % drug release after 12 h from furosemide floating tablet

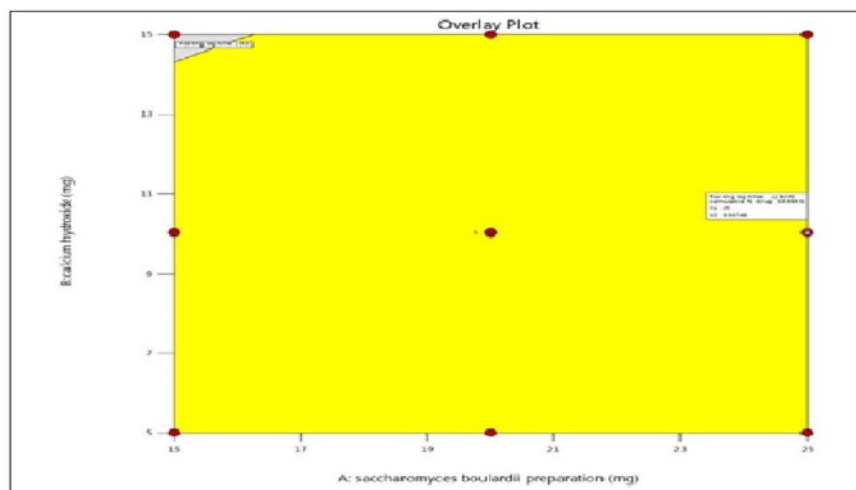


Fig. 5: Optimization of floating tablet's overlay plot

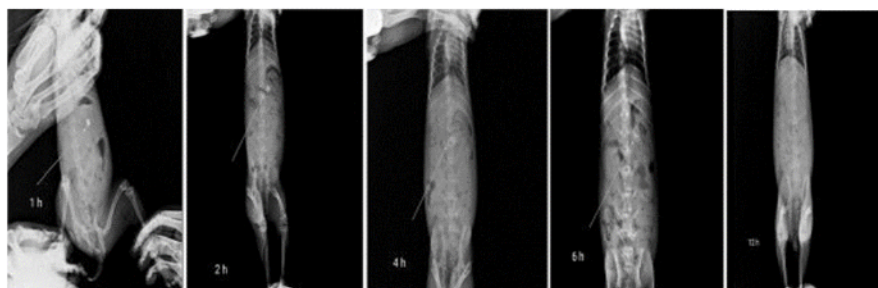


Fig. 6: X ray pictures of tablet at 1, 2, 4, 6 and 12 h

In vivo tablet behavior is shown in X-ray picture of fig. 6 from this it was clear that tablet float intact more than 6h and less than 12h.

CONCLUSION

We conclude that *Saccharomyces boulardii* formulation was the good floating agent and it's very easy to prepare tablet using this novel floating agent. The response variables of the formulation was optimized by the response surface methodology technique. The optimized formulation F(0) shows 88.18 % cumulative drug release after 12h and 12.6 min floating lag time. *In vitro* and *in vivo* buoyancy studies and *in vitro* % drug release study indicate that the formulation is suitable for gastro retention and it increases the bioavailability of furosemide.

ACKNOWLEDGEMENT

Author would like to thanks the College of Pharmacy, Akulj and College of Pharmacy, Saswad for providing necessary facilities and support.

ABBREVIATIONS

HPMC: Hydroxypropyl methylcellulose; *S. boulardii*: *Saccharomyces boulardii*; NaOH: Sodium hydroxide; HCl: hydrochloric acid; FDDS: Floating Drug Delivery System

FUNDING

Nil

AUTHORS CONTRIBUTIONS

All the authors have contributed equally.

CONFLICT OF INTERESTS

The authors declare no conflict of interest.

REFERENCES

- Agarbatl A, Canonico L, Marini E, Zannini E, Ciani M, Comitini F. Potential probiotic yeasts sourced from natural environmental and spontaneous processed foods. *Foods* 2020;9:1-25.
- Czerucka D, Piche T, Rampal P. Review article: yeast as probiotics—*saccharomyces boulardii*. *Aliment Pharmacol Ther* 2007;26:767-78.
- Boyle RJ, Roy MRB, Tang ML. Probiotic use in clinical practice: what are the risks?. *Am J Clin Nutr* 2006;83:1256-64.
- Dixit K, Gandhi DN. Biotherapeutic properties of probiotic yeast *saccharomyces* in fermented dairy products; 2006. Available from: <https://www.dairyscience.info/index.php/probiotics/232-yeast-probiotics.html>. [Last accessed on 10 Apr 2021]
- Sindhu SC, Khetarpaul N. Effect of probiotic fermentation on antinutrients and *in vitro* protein and starch digestibilities of indigenously developed RWGT food mixture. *Nutr Health* 2002;16:173-81.
- The health benefits of *saccharomyces boulardii* a yeast that may help with diarrhea and more. Available from: <https://www.verywellhealth.com/the-benefits-of-saccharomyces-boulardii-89509>. [Last accessed on 10 Apr 2021].
- Can probiotics cause side effects? Probiotics are healthful strains of live bacteria and yeast. Taking probiotics can provide a range of benefits, but it can also cause side effects. Available from: <https://www.medicalnewstoday.com/articles/323821>. [Last accessed on 10 Apr 2021].
- Mousa AH, Bakry AM. Efficacy of *saccharomyces boulardii* metabolism during fermentation of milk fortified with wheat grain juice. *Food Sci Technol Res* 2019;25:657-65.
- Dickinson JR. Carbon metabolism. In: Dickinson JR, Schweizer M. eds. *The metabolism and molecular physiology of Saccharomyces cerevisiae*. London and Philadelphia PA: Taylor and Francis; 1999. p. 23-24.
- Kumar S, Nand A. Formulation, optimization and *in vitro* evaluation of gastroretentive mucoadhesive microspheres of furosemide. *Int J Pharm Pharm Sci* 2016;8:392-8.
- Meka L, Kesavan B, Kalamata VR, Eaga CM, Bandari S, Vobalaboina V, et al. A design and evaluation of polymeric coated minitables as multiple unit gastroretentive floating drug delivery systems for furosemide. *J Pharm Sci* 2009;98:2122-32.
- Darandale SS, Vavia PR. Design of a gastroretentive mucoadhesive dosage form of furosemide for controlled release. *Acta Pharm Sin B* 2012;2:509-17.
- Patel RC, Keraliya RA, Patel MM, Patel MM, Patel NM. Formulation of furosemide solid dispersion with microcrystalline cellulose for achieve rapid dissolution. *J Adv Pharm Technol Res* 2010;1:180-9.
- Pawar HA, Gharat PR, Dhavale RV, Joshi PR, Rakshit PP. Development and evaluation of gastro retentive floating tablets of an antihypertensive drug-using hydrogenated cottonseed oil. *ISRN Pharm* 2013;2:1-9.
- Aswatha Ram HN, Lachake P, Kaushik U, Shreedhara CS. Formulation and evaluation of floating tablets of liquorice extract. *Pharmacogn Res* 2010;2:304-8.
- Patil MS, Vidyasagar G, Patil VB. Formulation, optimization and evaluation of floating tablets clarithromycin. *Int J Pharm Pharm Sci* 2015;7:320-6.
- Shaikh SA, Shaikh SN, Patel SM, Khalifa MY, Makrani SI, Siddiqi HA, et al. Design expert supported formulation development, mathematical optimization and predictability study of floating tablets of bisoprolol fumarate. *Int J Appl Pharm* 2021;13:242-8.
- Tekade BW, Jadhao UT, Patil SG, Patil VR. Formulation and *in vitro* evaluation of floating tablets of cefpodoxime proxetil. *Int J Curr Pharm Res* 2017;9:18-22.
- Oussama M, Ghenwa I, Mostafa I, Mais A. Assessment of physicochemical properties of furosemide (40 mg) tablets marketed in Syria. *J Chem Pharm Sci* 2016;9:2879-81.
- Tavakoli N, Varshosaz J, Dorkoosh F, Motaghi S, Tamaddona L. Development and evaluation of a monolithic floating drug delivery system for acyclovir. *Chem Pharm Bull* 2012;60:172-7.
- Tiwari SB, Murthy TK, Pai MR, Mehta PR, Chowdary PB. Controlled release formulation of tramadol hydrochloride using hydrophilic and hydrophobic matrix system. *AAPS PharmSciTech* 2003;4:E31.
- Rashmitha V, Madhusudan Rao Y, Pavani S. Formulation and evaluation of fenoverine floating tablets. *Asian J Pharm Clin Res* 2021;14:175-80.
- Siepmann J, Siepmann F. Mathematical modeling of drug delivery. *Int J Pharm* 2008;364:328-43.
- Mohapatra S, Barik B, Kar RK, Sahoo SK, Barik BB. Design, development and optimization of gastro retentive floating tablets of cefixime trihydrate. *Asian J Chem* 2013;25:7599-606.
- Arza RAK, Gonugunta CSR, Veerareddy PR. Formulation and evaluation of swellable and floating gastroretentive ciprofloxacin hydrochloride tablets. *AAPS PharmSciTech* 2009;10:220-6.
- Dios P, Nagy S, Pal S, Pernecker T, Kocsis B, Budan F, et al. Preformulation studies and optimization of sodium alginate-based floating drug delivery system for eradication of *Helicobacter pylori*. *Eur J Pharm Biopharm* 2015;96:196-206.
- Punitha S, Uvarani R, Panneerselvam A. Effect of pH in aqueous (Hydroxy Propyl Methyl Cellulose) polymer solution. *Results Materials* 2020;100120:1-6.
- Chi LL, Luigi GM, James L, Ford MR. The use of hypromellose in oral drug delivery. *J Pharm Pharmacol* 2005;57:533-46.
- Bashar M Al-Taani, Bassam M Tashtoush. Effect of microenvironment pH of swellable and erodible buffered matrices on the release characteristics of diclofenac sodium. *AAPS PharmSciTech* 2003;4:1-6.
- Acharya S, Patra S, Panib NP. Optimization of HPMC and carbopol concentrations in non-effervescent floating tablet through factorial design. *Carbohydrate Polymers* 2014;102:360-8.

Solubility Enhancement of Azilsartan by Self Micro Emulsifying Drug Delivery System

Ashwini Thongire¹, Prof. Prashant Khade², Prof. Sujit Kakade³, Dr. Ashok Bhosale⁴

^{1,2,3,4}Department of Pharmaceutics, Shankarrao Ursal College of Pharmacy, Kharadi, Pune, Maharashtra, India

ABSTRACT

Azilsartan is a BCS class II drug with poor aqueous solubility. The research work mainly contains on the enhancement of solubility of Azilsartan by developing Self Microemulsifying Lipid Formulations. The solubility of Azilsartan was determined in various lipid excipients by UV Spectroscopy analysis. Based on the solubility data and IR studies the excipients were selected. Cinnamon(oil), Tween 80 (Surfactant) and Polyethylene glycol 400 (PEG 400) were Selected as co-surfactants and formulation were developed. The pseudo ternary phase diagrams were constructed to determine the emulsification area. Various compositions of oil and surfactant mixture were titrated with water to determine the limit of emulsification and microemulsion region by keeping one component constant at one time. Four selected formulations were further evaluated for self-emulsification time, phase separation, Thermodynamic stability studies, Droplet size distribution and zeta potential. Out of there four formulations F3 shows less emulsification time, less particle size and high drug release. The present studies indicates that SMELFs can be potentially used a drug delivery system for poorly water-soluble drugs.

Keywords: Azilsartan, Oils, Surfactants, Co-surfactants, Pseudo ternary phase diagram, solubility study.

INTRODUCTION

Azilsartan medoxomil (AZL) is a particular AT1 subtype angiotensin II receptor antagonist. In view of the impeding of the pressor effects of angiotensin II, it shows antihypertensive activity. AZL is a poorly water-soluble drug. It shows between subject changeability in oral bioavailability. Attributable to the hydrophobic nature of AZL, different methodologies can be utilized to improve on its solubility. Different techniques have been effectively applied to improve the dissolution profile of poorly water-soluble drug likesolid dispersion, nanocrystals,nanoparticles,liposomes, self-nonoemulsionand self-microemulsion. Among them, self-microemulsifying Drug delivery system (SMEDDS) is a somewhat more up to date lipid-based technology with gigantic unique solution on the rate and degree of assimilation of poorly water-soluble drugs. A lipid-based dosage forms regularly comprises of at least one drug dissolved in the mix of lipophilic excipients, for example, triglycerides, surfactants or co-surfactants. Lipid-based formulations are isotropic combinations of drug, lipid and surfactants, generally with at least one co-surfactant. At the point when such a systemcomes to in the lumen of the gastrointestinal (GI) tract, it dispersed to a fine emulsion (micro/nano) with the aid of GI fluid. Self-micro-emulsifying lipid formulations usually improve the bioavailability of hydrophobic drug.

MATERIALS AND METHODS

Materials: Azilsartan Gift samples from Emcure Pharma (Pune), Castor oil, sesame oil, soybean oil, oleic acid, cinnamon oil, clove oil, olive oil, PEG 400, Propylene glycol, Ethanol, span 80, Tween 80, span 20 were purchased from the ResearchlabFinechem. Industries,Mumbai.

METHODS^[11-14]

Solubility studies

The saturation solubility of Azilsartan was done in different excipients like oils, surfactants, and co-surfactants. The solubility of Azilsartan was controlled by adding excess amount of drug to each screw covered glass vials containing 2 ml of excipient. The mixture was mixed by vertexing for drug solubilization. At that point the blends were heated in thermostatic water bath at 40°C for 5 minutes further to improve Solubilization. The mixture was magnetically stirred for 30 min and the vials were sonicated for 1 h. Further mixing was done by kept aside for carried out for 72 h using a mechanical shaker to achieve equilibrium. The vials were centrifuged at 2000 rpm for 15 min. The clear supernatant was diluted with methanol and analysed to determine the amount of dissolved AZL using UV-spectrophotometer.

Screening of surfactants for emulsification efficiency

The selection of best surfactant from a large pool of surfactants was done on the basis of transparency percentage and ease of emulsification. For emulsification study, oil and surfactant (1:1 ratio by weight) were mixed gently at 50°C for

2 min and further stirred to form homogeneous mixture. This oil surfactant mixture was diluted with distilled water in 1:100 ratio in a glass stoppered flask. The stoppered flasks were inverted several times and the number of flask inversions required to form a homogenous microemulsion (with no turbidity or phase separation) were counted. For the percentage transmittance study, emulsions were allowed to stand for 2 h and examined for percentage transmittance using an UV spectrophotometer. The percentage of transmittance was calculated for each emulsion in triplicate. The surfactant forming a clear emulsion with fewer inversions and higher percentage transmittance was selected for further studies.

Screening of co-surfactants for emulsification efficiency

The selected oil phase and surfactant were used for further screening of the different co-surfactants. For determining emulsification efficiency, a mixture of 200 μ l, 400 μ l and 600 μ l ml of co-surfactant, selected surfactant and selected oil, respectively. The emulsions were allowed to stand for 2 h and examined for percentage transmittance using an UV spectrophotometer. The percentage of transmittance was calculated for each emulsion in triplicate. The surfactant forming a clear emulsion with fewer inversions and higher percentage transmittance was selected for further studies.

Construction of pseudo ternary phase diagram^[15-16]

A pseudo ternary phase diagram was constructed by titration of four segment combinations of oil, surfactant and co-surfactant with water at room temperature after balance the mixture was outwardly observed the produced mixture which was clear or somewhat pale blue in appearance was resolved as microemulsion. The presence of microemulsions areas were dictated by utilizing pseudo-ternary phase graphs. SMEDDS were diluted under agitation conditions utilizing water titration strategy: The combination of oil and surfactant/cosurfactant at certain weight proportions were diluted with water in a dropwise way. Distilled water was utilized as an aqueous phase for the development of phase diagrams. Oil, surfactants and co surfactants were gathered in four distinct blends for phase studies. Surfactant and cosurfactant (Smix) in each gathering were blended in various weight proportions (1:0, 1:1, 2:1, 3:1). These Smix proportions were picked in expanding convergence of surfactant regarding cosurfactant and expanding centralization of cosurfactant as for surfactant for definite investigation of the phase diagram for plan of SMEDDS. For each phase diagram, oil and Smix proportion was blended completely in various weight proportions from 1:0 to 3:1 in various glass vials. Seventeen distinct blends of oil and Smix were made with the goal that most extreme proportions were covered for the examination to depict the limits of stages exactly framed in the phase diagrams. The oil and Smix are taken and readings are taken with firstly when oil is taken as fix quantity and changing the ratio of Smix and vice versa. Pseudo-ternary phase diagrams were created utilizing aqueous titration strategy. The convergence of water at which turbidity-to-transparency and transparency- to-turbidity changes happened was gotten from the weight estimations. These qualities were then used to decide the limits of the microemulsion area relating to the picked worth of oils, just as the S/CoS blending proportion. All investigations were accounted for thrice.

Preparation of SMELFs

The formulations were prepared by solubilizing dose of azilsartan in the mixture of surfactant, oil and co-surfactant. Azilsartan, Cinnamon oil, Tween 80, PEG-400 were precisely weighed and transferred into a borosilicate glass vial. Using magnetic stirrer, the mixtures were blended for 10min. at 60-65⁰C until a yellowish transparent formulation was attained. Azilsartan SMEDDS were then permitted to cool to room temperature before they were utilized in evaluations.

Characterization of SMEDDS^[17-24]

Thermodynamic stability studies

Heating cooling cycle-

six cycles between refrigerator temperature 4⁰c and 45⁰c with capacity at each temperature of not less than 48 hr was studied. Those formulations which were stable at these temperatures were exposed to centrifugation test.

Centrifugation-

Passed formulations were centrifuged at 3500 rpm for 30 min. Those formulations that didn't show any phase separation were taken for the freeze thaw stress test.

Freeze thaw cycle-

Three freeze thaw cycle between - 21⁰c and 25⁰c with capacity at every temperature for at the at least 48 hr was accomplished for the formulations. Those formulations which finished these thermodynamic stress tests were additionally taken for the dispersibility test for surveying the adequacy of self-emulsification.

Dispersibility Test

The adequacy of self-emulsification of oral microemulsion was surveyed utilizing a standard USP disintegration mechanical assembly 2. One millilitre of every formulation was added to 500 ml of water, 0.1 N HCl at 37 \pm 0. 5⁰c. A

standard treated steel disintegration paddle pivoting at 50 rpm gave gentle agitation. The in-vitro evaluation of formulations was outwardly evaluated.

Grade a-Rapidly shaping Nonoemulsion having clear or pale blue appearance.

Grade b-Quickly framing somewhat less clear emulsion having a pale blue white appearance.

Grade c-Fine milky emulsion that formed inside 2 min.

Grade d-Dull, greyish white emulsion having somewhat oily appearance that is delayed to emulsify (longer than 2min.)

Grade E-Formulation showing either poor or minimal emulsification with enormous oil globules present on a superficial level.

Effect of Dilution-

Formulations are diluted with excess of Water, 0.1N HCL and the diluted samples are stored for 24hrs and visually observed for precipitation (or) phase separation of drug. No precipitation (or) phase separation is found which indicates that the formulations are stable on dilution.

Determination of emulsification time-

The emulsification time of SMEDDS was resolved by United state Pharmacopeia USP dissolution apparatus 2. In brief 1 ml of every formulation was added drop astute to 500 ml of distilled water at 37°C. Gentle agitation was given by a standard treated steel disintegration paddle pivoting at 50 rpm.

Percent transmittance-

The percent transmittance of the system is measured at particular wavelength using UV-spectrophotometer keeping distilled water as blank. Stability of optimized micro emulsion formulation with respect to dilution is checked by measuring Transmittance through U.V. Spectrophotometer. Transmittances of samples are measured and for each sample three replicate assays are performed. 1 ml of formulation was diluted with 100 and 1000 fold water (ml), and % transmittance was determined using UV spectrophotometer.

Cloud point determination-

Dilute the formulation 1ml with 1000 ml of water in beaker and placed on a water bath with gradually increasing the temperature until the diluted formulation turned to cloudy or turbid. It gives the information about the stability of the micro emulsion at body temperature.

Refractive Index-

Refractive index proved the transparency of formulation. The refractive index measured using digital refractometer.

Drug loading efficiency-

For determining the AZL content, 1 ml of SMEDDS containing 40 mg AZL was diluted with methanol in a volumetric flask and mixed well by shaking or inverting the flask 2 to 3 times. Samples were prepared in triplicate and absorbance was measured after suitable dilutions at 250 nm using an UV spectrophotometer. The amount of AZL present in each formulation was calculated from a calibration curve.

Determination of Viscosity-

The rheological properties of the micro emulsion are evaluated by Brookfield viscometer. These viscosities determination conform whether the system is w/o or o/w. If system has low viscosity, then it is o/w type of the system and if high viscosities then it is w/o type of the system. The Viscosity is determined by the viscosity at 12 rpm with spindle number S18 of Brookfield viscometer.

Determination of droplet size and poly-dispersibility index-

Droplet size is an important factor affecting self-emulsification performance as it determines the rate and extent of drug release. Prior to measurement, 1 ml of each SMEDDS formulation was diluted 100 times with distilled water. The globule size and poly-dispersibility index (PDI) of the formed microemulsion were determined by dynamic light scattering (DLS) using a photon correlation spectrometer, which analyses the fluctuation in light scattering due to Brownian motion of the particles. Light scattering was monitored at 25°C at a scattering angle of 90.

Determination of zeta potential-

The zeta potential of the diluted SMEDDS was determined using Zetasizer. Samples were placed in a clear disposable cuvette and the results were recorded. The charge on emulsion droplets and their zeta potential values were obtained.

Invitro drug release study-

The in-vitro dissolution study of SMELFs were carried out using USP-Type II dissolution test apparatus in 500mL 0.1 N HCl at 50 rpm rotating speed. In – Vitro drug release study was performed for 60 mins in 0.1NHCl. Samples were

withdrawn at 0, 5, 10, 15, 30, 45, 60, minute's time intervals. An equal volume of dissolution medium (1ml) was replenished after every sampling to maintain constant volume. Samples were analysed using UV-Spectrophotometer at 250 nm. Percentage drug release and cumulative percentage drug release were calculated from absorbance and concentration that were obtained with the help of standard graph of Azilsartan.

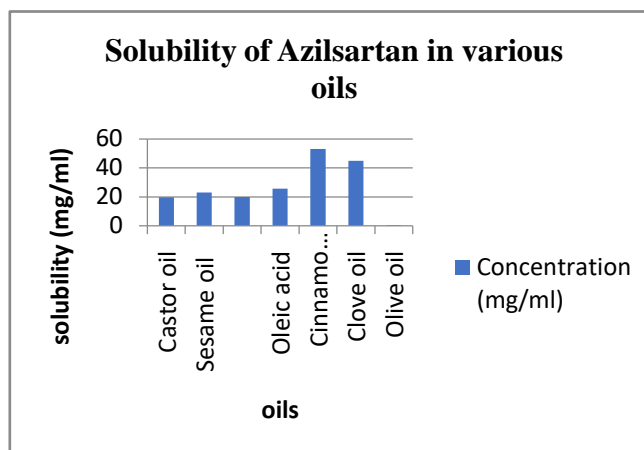
RESULTS AND DISCUSSION

Solubility of Azilsartan in various Oils

Solubility of Azilsartan in various oils was determined by UV-spectrophotometer. The saturation solubility of Azilsartan in various oils is shown in Table 1 and Fig 1. Cinnamon oil was selected for the formulation which shows the highest solubility of AZL.

Table1: Solubility of Azilsartan in various oils Fig 1: Solubility of Azilsartan in various oils

Sr.No.	Oils	Concentration(mg/ml)
1	Castor oil	19.63±3.24
2	Sesame oil	22.98±2.98
3	Soybean oil	20.01±1.35
4	Oleic acid	25.78±1.26
5	Cinnamon oil	53.05±2.45
6	Clove oil	45.03±2.74
7	Olive oil	0.49±0.05



(All as values are expressed mean n=3)

Solubility of Azilsartan in various Surfactants

Solubility of Azilsartan was determined in various Surfactants. Surfactants Tween80 is selected for formulation which has highest solubility and good emulsifying ability among all other formulations. Results are shown in Table 2 and Fig 2.

Table 2: Solubility in various Surfactants

Sr No.	Surfactant	Solubility(mg/ml)
1	Span 80	13.78±3.25
2	Tween 80	67.98±1.95
3	Span 20	3.36±0.05

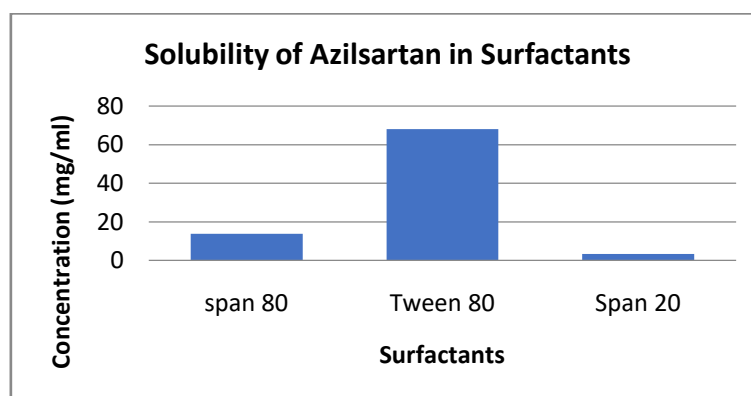


Fig: 1 Solubility in various Surfactant

Solubility in various Co-Surfactants

Solubility of Azilsartan in various Co-Surfactants was determined. PEG 400 is selected for the formulation which shows highest solubility than other co-surfactants. Solubilities of various Co-Surfactants are shown in Table3 and Fig 3.

Table 3: Solubility of Azilsartan in various Co-Surfactants

Sr.No.	Co-surfactant	Solubility(mg/ml)
+1	Ethanol	45.69±1.43
2	Propylene glycol	58.67±1.68
3	PEG 400	70.04±1.23

(All as values are expressed mean n=3)

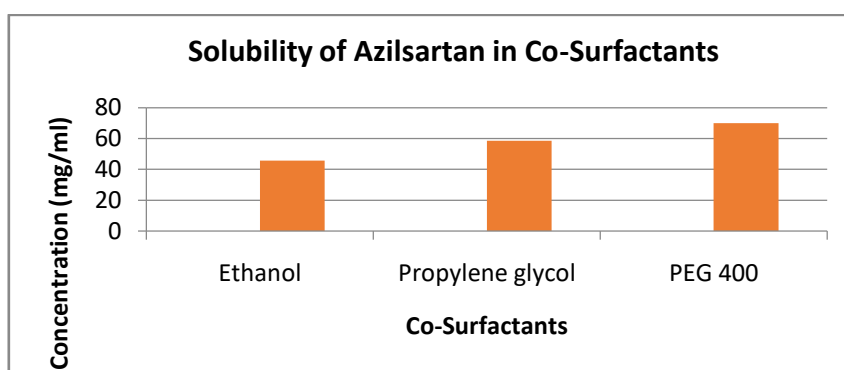


Fig 3: Solubility in various co-surfactants

Screening of surfactants for emulsification efficiency:

Among the oils Cinnamon oil is choose since the drug is highly soluble into it. Among the different surfactants which surfactant shows the highest emulsification efficiency and % transmittance is choosing from screening of surfactants. Tween 80 show the highest emulsification efficiency and % Transmittance. Hence among different surfactants Tween 80 is selected.

Table 4: Screening of surfactant

Surfactants	% Transmittance	No. of inversions
Span 80	53.4	14
Tween 80	98.5	4
Span 20	40.7	17

Screening of co-surfactants for emulsification efficiency

The selected surfactant and oil are gone for the evaluation of co-surfactants for emulsification efficiency. Among the different co-surfactants which co-surfactant shows the highest emulsification efficiency and % transmittance is choosing from screening of co-surfactants. Both propylene glycol and PEG 400 show the highest emulsification efficiency and % Transmittance. Among them PEG 400 is selected because of its highest % transmittance.

Table 5: Screening of co-surfactant

Co-Surfactants	% Transmittance	No. of inversions
Ethanol	89.1	6
Propylene glycol	98.6	5

PEG 400	99.3	4
---------	------	---

Selection of excipients:

Based on the solubility studies done on various oils, surfactants and co surfactants, excipients which has shown more solubility was selected for the formulation.

- Oil: Cinnamon oil
- Surfactant: Tween 80
- Co-Surfactant: PEG 400

Drug -Excipient compatibility studies by FTIR spectroscopy

The IR spectrum of AZL revealed characteristic peak at 3433 cm^{-1} for the O–H group, a peak at 3302 cm^{-1} for N–H group and a sharp peak at 1705 cm^{-1} for the C=O group. The spectrum of AZL also showed C=N stretching 1655 and C–O stretching peaks were recorded at 1219 , 1249 and $\text{c}=\text{c}$ at 1620 cm^{-1} . The results are in accordance to the Radl et al.

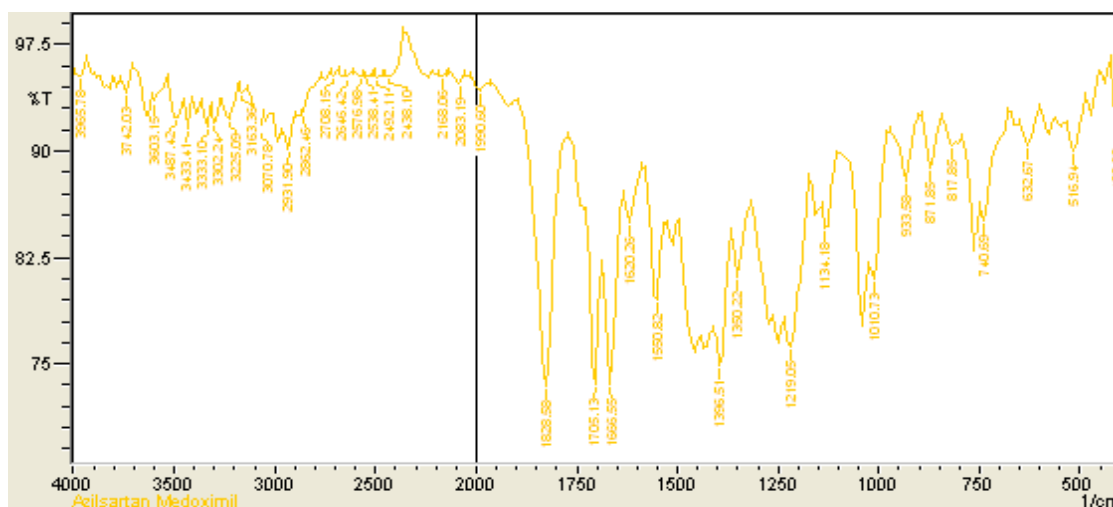


Fig 4: FT-IR Spectra of Azilsartan Medoximil

drug + excipient mixture-

The absence of interfering peaks indicating no interaction between AZL and excipients.

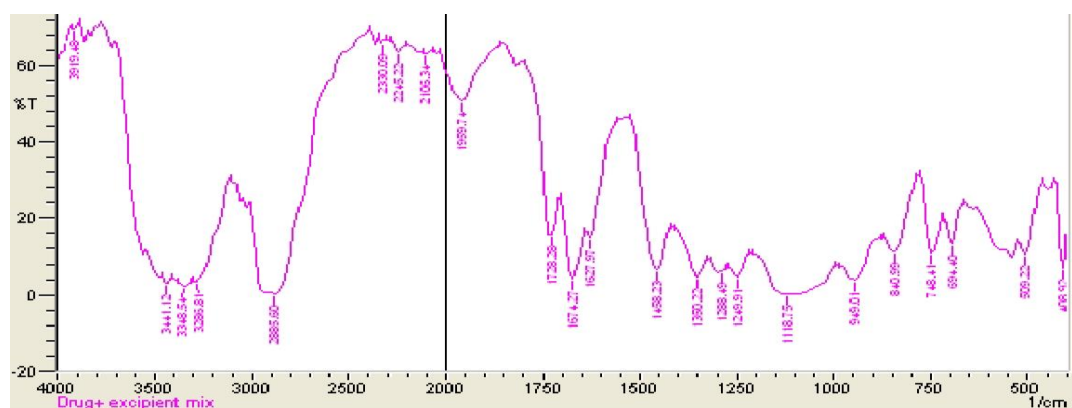


Fig 5: FT-IR Spectra of Azilsartan Medoximil+ excipients

Pseudo – ternary Phase Diagrams:

Pseudo – ternary Phase Diagrams are constructed to identify the microemulsion regions and to identify suitable composition of oil, surfactant and co-surfactant for the formulation of SMELFs. From Pseudo – ternary phase diagrams it has been found that the systems consisting of Cinnamon as oily phase, Tween 80 as surfactant and PEG 400 as co-surfactant showed good micro emulsify property. pseudo-ternary phase diagrams were constructed to identify self-micro-emulsifying regions, to select a suitable concentration of oils, surfactants, and co-surfactants for the formulation of SMEDDS. Phase diagrams were mapped at surfactant/co-surfactant ratio (1:0, 1:1, 2:1 and 3:1). The size of the

micro-emulsion region in the diagrams was compared; a larger size indicates greater self-micro-emulsification efficiency. The micro-emulsion was identified as the area is clear and transparent formulation was obtained on dilution based on visual inspection of samples. Pseudoternary phase diagrams showed that the zone of micro-emulsion was largest in the case of a formulation containing Tween 20– propylene glycol mixture (Smix) at 2:1 and 3:1 ratio (Fig 6)

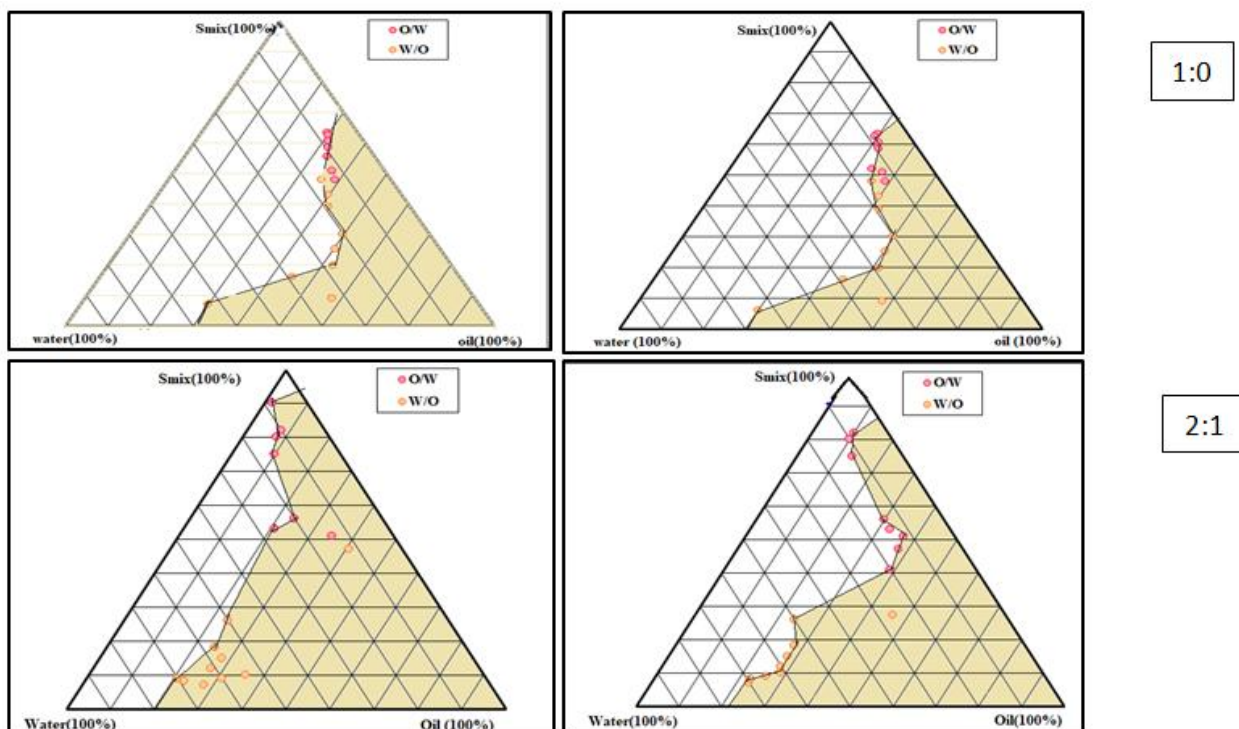


Fig 6: Pseudo ternary phase diagrams

Evaluation of azilsartan medoxomil SMEDDS-

Table 6- Thermodynamic stability test data

Smix (2:1)	Percentage w/w of components		Observations			Dispersibility	
	Oil	Smix	Centrifugation	Freeze Thaw	H/C		
F1	50	50	✓	✓	✓	Grade D	Grade D
F2	40	60	✓	✓	✓	Grade C	Grade C
F3	30	70	✓	✓	✓	Grade A	Grade A
F4	20	80	✓	✓	✓	Grade B	Grade B
Smix (3:1)							
F5	50	50	✓	✓	✓	Grade D	Grade D
F6	40	60	✓	✓	✓	Grade C	Grade C
F7	30	70	✓	✓	✓	Grade A	Grade A
F8	20	80	✓	✓	✓	Grade B	Grade B

The formulations which are shows grade A and grade B are selected for further studies.

Effect on dilution-

Table 7- Effect on dilution

Sr. No.	Formulation	Distilled water	0.1 N HCl
1	F3	NO	NO
2	F4	NO	NO
3	F7	NO	NO
4	F8	NO	NO

All formulations are passed the dilution test there is no phase separation on the infinite dilution of formulations.

Determination of emulsification time-

In the SEDDS, the essential methods for self-emulsification measure are visual assessment. The proficiency of self-emulsification could be assessed by deciding the rate of emulsification. The rate of emulsification is a significant file for the evaluation of the productivity of emulsification that is the SEDDS ought to disperse totally and immediately when exposed to aqueous dilution under gentle agitation. Among all F3 shows lowest emulsification time and F8 shows highest emulsification time. Formulations F3 and F7 show less emulsification time than other formulations.

Percentage Transmittance-

All the selected formulations show the % Transmittance more than 95 % which is indication of clear emulsion. Among the formulations formulation F3 and F7 shows greater transmittance than F4 and F8.

Cloud point determination-

Cloud point of microemulsion is the temperature at which the transparent microemulsion solution becomes cloudy. All the formulations show the cloud point at nearly same temperature. F3 shows the cloud point at highest temperature than other formulations. F8 shows the cloud point at low temperature than other formulations.

Refractive Index-

The refractive index is important for determining formulation transparency. The refractive Index of Formulation F3 and F7 is less as compared to Formulation F4 and F8.

Drug loading-

The selected formulations show the drug loading more than 90% and hence suggest good drug loading capacity. Formulation F3 shows highest drug loading. All the formulations show the drug loading greater than 90.

Table 8- Data for Evaluation of SMEDDS

Sr. No.	Formulation	Emulsification Time (s)	% Transmittance	Cloud point (°C)	Refractive Index	Viscosity(cp)	Drug Loading
1	F3	26.05±0.25	98.5±0.43	83	1.34	80.15±0.5	98.5±0.5
2	F4	37.26±0.69	93±1.43	79	1.41	93.36±1.5	91.2±0.2
3	F7	29.35±1.5	97.4±1.42	81	1.38	85.63±0.75	96.1±1.5
4	F8	39.48±0.50	92.8±1.5	76	1.43	102.77±1.5	90.4±0.7

(All as values are expressed mean n=3)

Viscosity-

Formulation F3 is less viscous than formulation F8 show high viscosity. According to Viscosity values it is clear that the formulations are o/w type microemulsions.

Droplet size and polydispersibility Index-

A microemulsion is a thermodynamically stable fluid. It is different from kinetically stable emulsions which will be break into oil and water over time. The particle size of microemulsions ranges from about 10 to 300 nm. Because of the small particle sizes, microemulsions appear as clear or translucent solutions. The particle size of all formulations is within range of microemulsion. F3 shows low particle size (138 nm) as compared to other. All the formulations show the droplet size and PDI values in the microemulsion range.

Table 9- Droplet size and polydispersibility Index-

Sr. No.	Formulation Code	Droplet size (nm)	PDI	Zeta potential
1	F3	138	0.321	-42.0
2	F4	160.7	0.367	-23.8
3	F7	140.3	0.320	-41.1
4	F8	161.2	0.367	-29.5

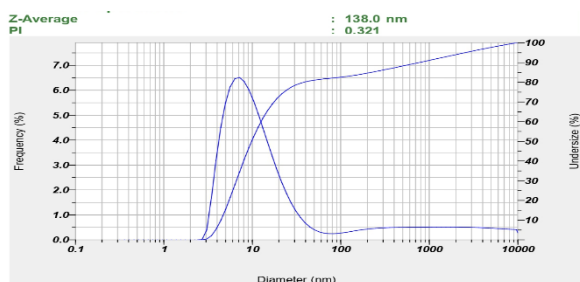


Fig 7: Particle size for formulation F3

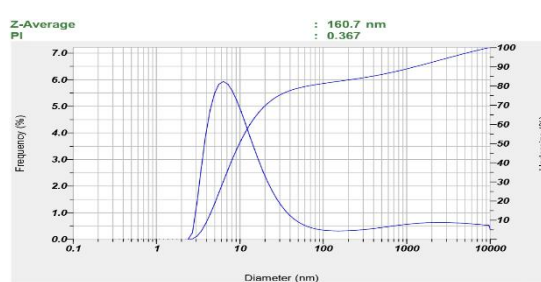


Fig 8: Particle size for formulation F4

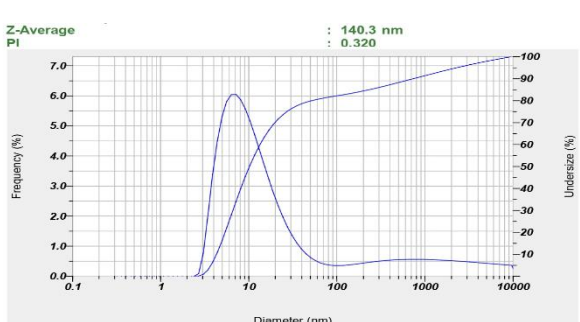


Fig 9: Particle size for formulation F7

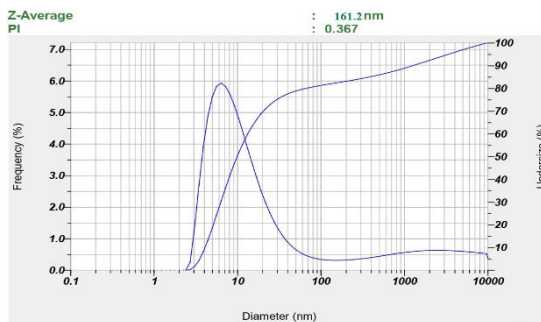


Fig 10: Particle size for formulation F8

Zeta Potential-

Zeta potential is essential to determine the stability of microemulsion. All the formulation selected shows zeta potential value which is required in the microemulsion. All the selected formulation is stable. F3 shows the zeta potential which is more negative and hence give the better stability. All other formulations possess zeta potential values with optimum range which shows the stability of microemulsion. F3 shows the optimum zeta potential value than other formulations.

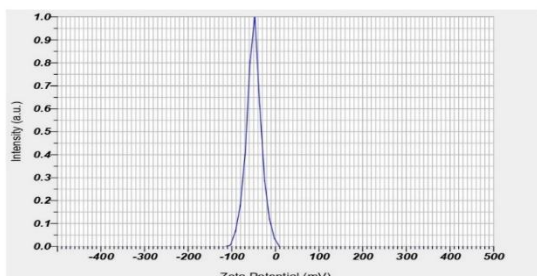


Fig 11: Zeta potential F3

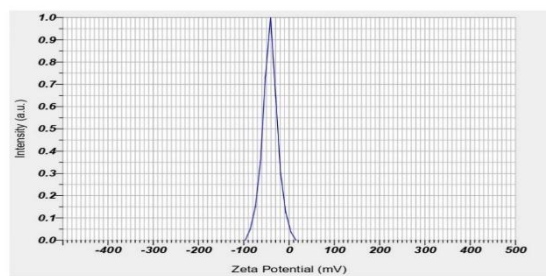


Fig 12: zeta potential F4

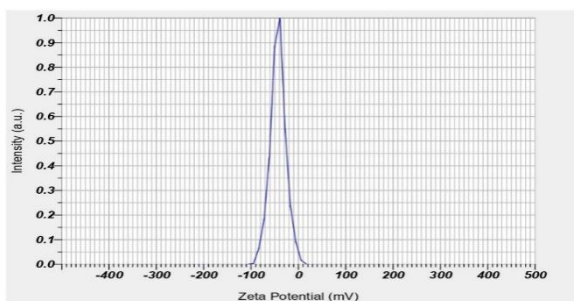


Fig 13: Zeta potential F7

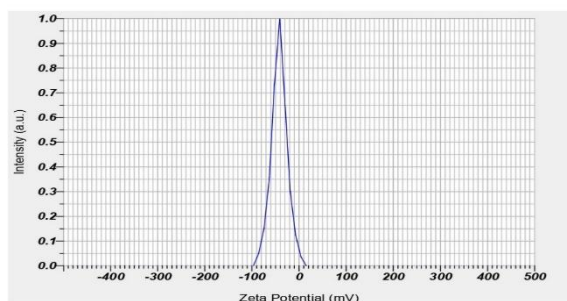


Fig 14: zeta potential F8

Invitro drug release study-

All formulations show the Drug release of greater percent than pure azilsartan. Formulation F3 and F7 shows more than 80% drug release within 5 min. Formulation F3 and F7 shows more than 95% drug release within 1 hr. The formulation F3 shows highest drug release than other formulations.

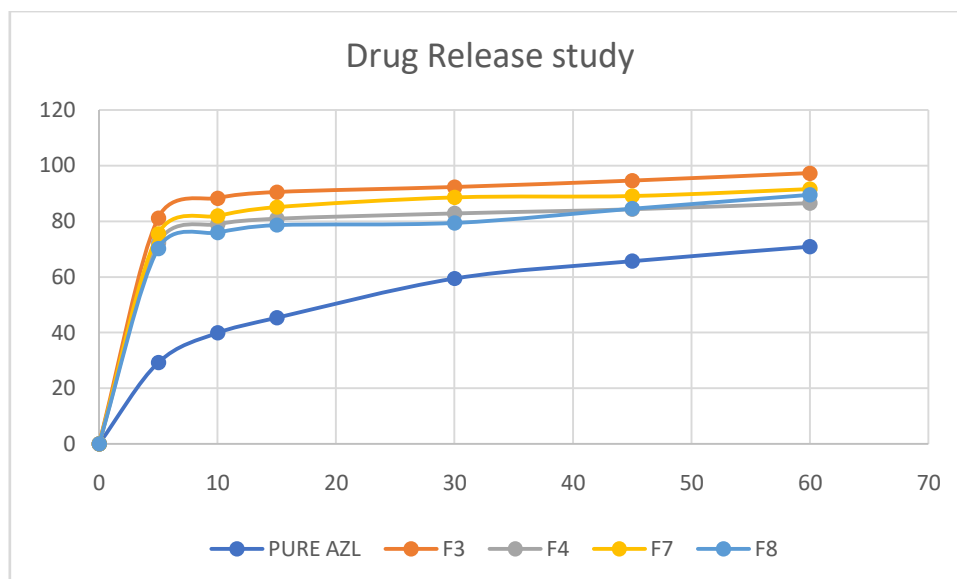


Fig15: Drug release study of Azilsartan in 0.1 N HCl

SUMMARY AND CONCLUSION

The drug azilsartan which was ineffectively soluble drug was chosen for SMELFs because of its poor water solubility and its oral bioavailability which is around under 60%. Self-micro-emulsifying lipid formulations was created to work on its solubility and dissolution rate. Solubility of azilsartan is determined in various Oils, Surfactants and Co-surfactants by UV Spectrophotometric technique. Azilsartan has been shown most extreme solubility in oil cinnamon oil, surfactant Tween 80 and co surfactant PEG 400. A series of Pseudo ternary stage diagrams are developed to recognize micro emulsion area. Different composition of Oil and Smix are titrated with water to distinguish microemulsion locale. From pseudo ternary stage diagrams frameworks comprising of cinnamon oil as oil stage, Tween 80 surfactant, PEG 400 as co surfactant are chosen for detailing. SMELFs are ready by choosing oil: Smix proportion (1:9 to 9:1) and Smix proportion 1:0, 1:1, 2:1 and 3:1. From the ternary phase diagrams the Smix ratio 2:1 and 3:1 shows the highest emulsification region and hence is selected for the further formulation's preparation. Eight formulations were prepared out of which 4 passes the thermodynamic stability and dispersibility tests and formulations which shows the Grade A and Grade B emulsions are selected. Prepared formulations are evaluated for Self-emulsification and visual assessment, Phase separation and precipitation of the drug, Robustness to dilution, Percentage Transmittance, drug loading efficiency, Thermodynamic stability studies, Droplet size, PDI and Zeta potential. All four formulations are emulsified in less than 1min. No formulation had showed precipitation and phase separation of drug. All formulation shows effect on dilution. All the selected formulations show the % Transmittance more than 95 % which is indication of clear emulsion. Among the formulations formulation F3 and F7 shows greater transmittance than F4 and F8. The selected formulations show the drug loading more than 90% and hence suggest good drug loading capacity. Formulation F3 shows highest drug loading. All the formulations show the drug loading greater than 90. F3 shows low particle size (138 nm) as compared to other. All the formulations show the droplet size and PDI values in the microemulsion range. F3 shows the zeta potential which is more negative and hence give the better stability. All other formulations possess zeta potential values with optimum range which shows the stability of microemulsion. All formulations show the Drug release of greater percent than pure azilsartan. Formulation F3 and F7 shows more than 80% drug release within 5 min. Formulation F3 and F7 shows more than 95% drug release within 1 hr. The formulation F3 shows highest drug release than other formulations. The SELFs obviously showed improved and increased drug dissolution for poorly soluble drug. This assists with helps to keep the poorly soluble drug. So, the pre-arranged SMELFs have ability for conveying poorly water soluble drug azilsartan in soluble state in GIT.

REFERENCES

- [1] Jones, J. D.; Jackson, S. H.; Agboton, C.; Martin, T. S. Azilsartan Medoxomil (Edarbi): The Eighth Angiotensin II Receptor Blocker. P T 2011, 36, 634.
- [2] Pande, V. V.; Sanklecha, V. M.; Arote, S. R. Formulation and Development of Extended-Release Matrix Pellets of Water Insoluble Azilsartan Medoxomil with Solid Dispersion. Indian Drugs 2019, 56, 21.
- [3] Webb, N. J.; Wells, T.; Tsai, M.; Zhao, Z.; Juhasz, A.; Dudkowski, C. Single-Dose Pharmacokinetics and Safety of Azilsartan Medoxomil in Children and Adolescents with Hypertension as Compared to Healthy Adults. Eur. J. Clin. Pharmacol. 2016, 72, 447–457. DOI: 10.1007/s00228-015- 1987-8.

- [4] Lu, T.; Sun, Y.; Ding, D.; Zhang, Q.; Fan, R.; He, Z.; Wang, J. Study on Enhanced Dissolution of Azilsartan-Loaded Solid Dispersion, Prepared by Combining Wet Milling and SprayDrying Technologies. *AAPS PharmSciTech.* 2017, 18, 473–480. DOI: 10.1208/s12249-016-0531-1.
- [5] Ma, J.; Yang, Y.; Sun, Y.; Sun, J. Optimization, Characterization and in Vitro/Vivo Evaluation of Azilsartan Nanocrystals. *Asian J. Pharm. Sci.* 2017, 12, 344–352. DOI: 10.1016/j.ajps.2016.09.008.
- [6] Nassar, T.; Rom, A.; Nyska, A.; Benita, S. A Novel Nano capsule Delivery System to Overcome Intestinal Degradation and Drug Transport Limited Absorption of P-Glycoprotein Substrate Drugs. *Pharm. Res.* 2008, 25, 2019–2029. DOI: 10.1007/s11095-008-9585-4.
- [7] Sinswat, P.; Overhoff, K. A.; McConville, J. T.; Johnston, K. P.; Williams, R. O. III, Nebulization of Nanoparticulate Amorphous or Crystalline Tacrolimus-Single-Dose Pharmacokinetics Study in Mice. *European J. Pharm. Biopharm.* 2008, 69, 1057–1066. DOI: 10.1016/j.ejpb.2008.01.037.
- [8] Lee, M. J.; Straubinger, R. M.; Jusko, W. J. Physicochemical, Pharmacokinetic and Pharmacodynamic Evaluation of Liposomal Tacrolimus (FK 506) in Rats. *Pharm. Res.* 1995, 12, 1055–1059. DOI: 10.1023/A:1016222817860.
- [9] Park, Y. J.; Ryu, D. S.; Li, D. X.; Quan, Q. Z.; Oh, D. H.; Kim, J. O.; Seo, Y. G.; Lee, Y. I.; Yong, C. S.; Woo, J. S.; Choi, H. G. Physicochemical Characterization of Tacrolimus-Loaded Solid Dispersion with Sodium Carboxymethyl Cellulose and Sodium Lauryl Sulphate. *Arch. Pharm. Res.* 2009, 32, 893–898. DOI: 10.1007/s12272-009-1611-5.
- [10] Yamashita, K.; Nakate, T.; Okimoto, K.; Ohike, A.; Tokunaga, Y.; Ibuki, R.; Higaki, K.; Kimura, T. Establishment of New Preparation Method for Solid Dispersion Formulation of Tacrolimus. *Int. J. Pharm.* 2003, 267, 79–91. DOI: 10.1016/j.ijpharm.2003.07.010. [11] Rahman, M. A.; I
- [11] Dixit RP, Nagarsenker MS. Self-nanoemulsifying granules of ezetimibe: design, optimization and evaluation. *Eur J Pharm Sci.* 2008;35(3):183.
- [12] Date AA, Nagarsenker MS. Design and evaluation of Self-Nanoemulsifying drug delivery systems (SNEDDS) for cefpodoxime proxetil. *Int J Pharm.* 2007;329(1-2):166-72.
- [13] Patel AR, Vavia PR. Preparation and in vivo evaluation of SMEDDS (Self-Microemulsifying Drug Delivery System) containing fenofibrate. *AAPS J.* 2007;9(3): E344-52.
- [14] Nasr A, Gardouh A, Ghorab M. Novel solid Self-Nanoemulsifying drug delivery system (S-SNEDDS) for oral delivery of olmesartan medoxomil: design, formulation, pharmacokinetic and bioavailability evaluation. *Pharmaceutics.* 2016;8(3):20.
- [15] Atef E, Belmonte AA. Formulation, in-vitro and in-vivo Characterization of phenytoin Self-Emulsifying Drug Delivery System. *Eur J Pharm Sci.* 2008; 35:257-63.
- [16] Kang MJ, Kim HS, Jeon HS, Park JH, Lee BS, Ahn BK, Moon KY, Choi YW. In situ intestinal permeability and in vivo absorption characteristics of olmesartan medoxomil in self-microemulsifying drug delivery system. *Drug Dev Ind Pharm.* 2012;38(5):587-96.
- [17] Patel PV, Patel HK, Panchal SS, Mehta TA. Self-micro-emulsifying drug delivery system of tacrolimus: formulation, in vitro evaluation and stability studies. *Int J Pharm Investig.* 2013;3(2):95-104.
- [18] Nekkanti V, Karatgi P, Prabhu R, Pillai R. Solid selfmicroemulsifying formulation for candesartan cilexetil. *AAPS PharmSciTech.* 2010;11(1):9-17.
- [19] Khoo SM, Humberstone AJ, Porter CJH, Edwards GA, Charman WN. Formulation design and bioavailability assessment of lipidic self-emulsifying formulations of halofantrine. *Int J Pharm.* 1998;167(1-2):155-64.
- [20] Onoue S, Uchida A, Kuriyama K, Nakamura T, Seto Y, Kato M, Hatanaka J, Tanaka T, Miyoshi H, Yamada S. Novel solid self-emulsifying drug delivery system of coenzyme Q10 with improved photochemical and pharmacokinetic behaviors. *Eur J Pharm Sci.* 2012;46(5):492-9.
- [21] Ghosh PK, Majithiya RJ, Umrethia ML, Murthy RSR. Design and development of microemulsion drug delivery system of acyclovir for improvement of oral bioavailability. *AAPS PharmSciTech.* 2006;7(3):77.
- [22] Chudasama AS, Patel VV, Nivsarkar M, Vasu KK, Shishoo CJ. In vivo evaluation of self-emulsifying drug delivery system for oral delivery of nevirapine. *Indian J Pharm Sci.* 2014;76(3):218-24.
- [23] Odeberg JM, Kaufmann P, Kroon KG, Haglund P. Lipid drug delivery and rational formulation design for lipophilic drugs with low oral bioavailability, applied to cyclosporine. *Eur J Pharm Sci.* 2003;20(4-5):375-82.
- [24] Avachat AM, Patel VG, Drug SN. Self-nanoemulsifying drug Delivery system of stabilized ellagic acid-phospholipid complex with improved dissolution and permeability. *Saudi Pharm J.* 2015;23(3):276-89.



High Performance Thin Layer Chromatography Fingerprinting Analysis of *Piper betle* L. Leaves

Ramdas N. Kale^{1*} and Ravindra Y. Patil²

¹Department of Pharmacognosy, SVPM's College of Pharmacy, Malegaon (Bk) Tal- Baramati Dist- Pune 413115, India.

²Department of Pharmacognosy, PDEA's Shankarrao Ursal College of Pharmaceutical Science and Research Centre, Kharadi, Pune 411014, India.

Authors' contributions

This work was carried out in collaboration among all authors. All authors read and approved the final manuscript.

Article Information

DOI: 10.9734/JPRI/2020/v32i4831120

Editor(s):

(1) Dr. Mohamed Fathy, Assiut University, Egypt.

Reviewers:

(1) Jasenka Gajdoš Kljusurić, University of Zagreb, Croatia.

(2) Amamer Redwan, Alzaitona University, Libya.

Complete Peer review History: <http://www.sdiarticle4.com/review-history/65395>

Original Research Article

Received 28 November 2020

Accepted 02 February 2021

Published 08 February 2021

ABSTRACT

Introduction: Many modern medicines used today based on plants and plant products. *Piper betle* is generally known as the betle vine, it is an important medicinal and recreational plant. High performance thin layer chromatography (HPTLC) is an advanced powerful analytical method with more separation power, high performance and superior reproducibility than classic thin layer chromatography (TLC). A chromatographic fingerprint of a plant extract is a chromatographic pattern of some common chemical constituents of pharmacologically active and/or chemical characteristics. Chromatographic fingerprints are useful in authentication and identification of plant.

Objectives: Objectives of present research was to establish HPTLC fingerprinting of methanolic extract of *Piper betle* L. leaves.

Materials and Methods: Methanolic extract of *Piper betle* leaves was prepared using soxhlet apparatus. HPTLC studies were performed using a CAMAG HPTLC system equipped with automatic TLC sampler-4 (ATS 4), TLC scanner 4, and vision CATS 3.0 software.

Results: The study revealed the presence of alkaloids with R_f value 0.65, flavonoids with R_f values 0.19, 0.29, 0.72, 0.95., and phenolic compound with R_f value 0.7.

*Corresponding author: E-mail: ramdas.kalesvpm@gmail.com;

Conclusion: The HPTLC fingerprinting profile developed for the methanolic extract of *Piper betle* L. leaves will help in proper identification of the plant.

Keywords: *Piper betle*; HPTLC; alkaloids; flavonoids; phenolic compounds.

1. INTRODUCTION

The chemistry of plants is divergent as the great variety of forms in which plants occur. The therapeutically important constituents are usually found to be associated with many other substances. Owing to the medicinal properties pertaining to a crude drug, it is important to retain its quality and purity. With the advent of new analytical tools and sophisticated instruments it is possible to suggest a practicable quality assurance profile for a crude drug [1]. HPTLC is a modern powerful analytical technique with high separation power, performance and reproducibility superior to classic TLC. A chromatographic fingerprint of a plant extract is a chromatographic pattern of some common chemical constituents of pharmacologically active and/or chemical characteristics. Chromatographic fingerprints are useful in authentication and identification of plant [2].

Piper betle Linn. is a perennial dioecious climber, with large leaves, 15-20 cm long, broadly ovate, slightly cordate, shortly acuminate, acute, entire, glabrous, yellowish or bright green, shining on both side [3]. It is generally known as the betle vine, it is an important medicinal and recreational plant [4]. *Piper betle* is extensively found in damp forest and is propagated in India, Vietnam, China and other countries [5]. The leaves of betle vine are nutritive and posses antitumor activity [6], antibacterial [7], antioxidant [8], gastro protective [9], neuroprotective [10], antifilarial [11], anti malarial [12] and analgesic activity [13]. The current investigation aims to analyze the HPTLC fingerprinting profile of alkaloids, flavonoids, phenolic compounds and glycosides for methanolic extract of *Piper betle* L. leaves (MEPBL).

2. MATERIALS AND METHODS

2.1 Collection of Plant Material

The leaves of *Piper betle* L. were obtained from the rural areas of Baramati Dist-Pune (Maharashtra) and identified in the Department of Botany, Agricultural Development Trust's Sharda Bai Pawar Mahila Mahavidyalaya, Sharda nagar Tal-Baramati Dist-Pune, India and was

deposited at the college herbarium (Voucher specimen No. PASR-142).

2.2 Preparation of Extract

The fresh leaves of *Piper betle* washed under tap water, air dried, and powdered. Powdered material was subjected to soxhlet extraction with methanol as a solvent. The Extract so obtained was concentrated by evaporating the solvent. The Percent yield was calculated. Extract was stored at room temperature and protected from direct sunlight.

2.3 HPTLC Analysis

2.3.1 Preparation of sample

100 mg MEPBL was dissolved in 5 ml of methanol and solution is sonicated for 15 min and centrifuged for 5 minutes.

2.3.2 Developing solvent system

A number of solvent systems were tried during HPTLC analysis. The satisfactory resolution obtained for the different phytochemical constituent was in the solvent system toluene-ethyl acetate- formic acid (70:30:1), for alkaloid was toluene- ethyl acetate- methanol-ammonia (25%) (30:30:15:1), for flavonoid was ethyl acetate-formic acid-acetic acid-water (100:11:11:26), for Phenolic compounds was cyclohexane-ethyl acetate-formic acid (4:6:1) and for the glycoside was ethyl acetate-methanol-water (20:2.8:2).

2.3.4 Chromatography

A 2 μ L, 4 μ L, 6 μ L, 8 μ L, 10 μ L and 12 μ L sample solution were loaded as 8 mm band length on a 100 X 100 mm silica gel 60F₂₅₄ TLC aluminum plates using Hamilton syringe and Automatic TLC sampler (ATS 4) instrument.

2.3.5 Development of chromatogram

The samples loaded plate was kept in Twin trough glass chamber 10X10 cm saturated with mobile phase for 20 min.

2.3.6 Detection of spot

The developed plate was dried at room temperature for 5 min., to evaporate solvents from the plate. The images were captured in white light, UV254 nm and UV366 nm. The developed plate was sprayed with Anisaldehyde sulphuric acid reagent for different unknown compounds, Dragendorffs reagent for Alkaloids, Natural product reagent A for Flavonoids, Alcoholic FeCl_3 for Glycosides and Alcoholic KOH for Phenolic compounds.

2.3.7 Scanning

After derivatization the plates were scanned in CAMAG TLC Scanner 4. The Peak table, Peak display and Peak densitogram were recorded.

Retention factor (R_f), and % area were calculated using vision CATS 3.0 software.

3. RESULTS

HPTLC chromatogram of MEPBL showed different peaks of phytoconstituents. Fig. 1. is the image of TLC plate at 366nm, Fig. 2. is the chromatogram and Table 1. shows the presence of various unknown compounds with retention factor, peak height and peak area.

Presence of alkaloid was confirmed with R_f value 0.65 after derivatization with Dragendorffs reagent as a orange zone is observed. Fig. 3 is the image of TLC plate before derivatization and Fig. 4 is the image of TLC plate derivatized with Dragendorffs reagent captured in white light.

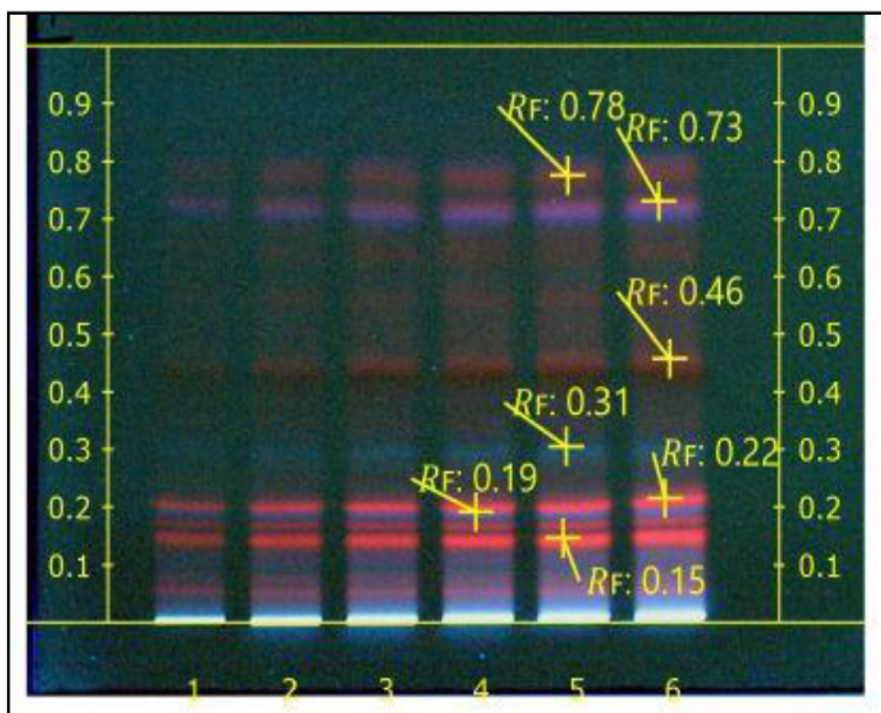


Fig. 1. Image of TLC plate at 366 nm

Table 1. Peak table with R_f values, height and area of unknown compounds

Peak	R_f	Height	Area
1	0.061	0.0162	0.00019
2	0.156	0.2023	0.00400
3	0.182	0.0597	0.00089
4	0.216	0.2124	0.00452
5	0.485	0.0281	0.00040
6	0.724	0.0697	0.00280
7	0.797	0.0275	0.00107

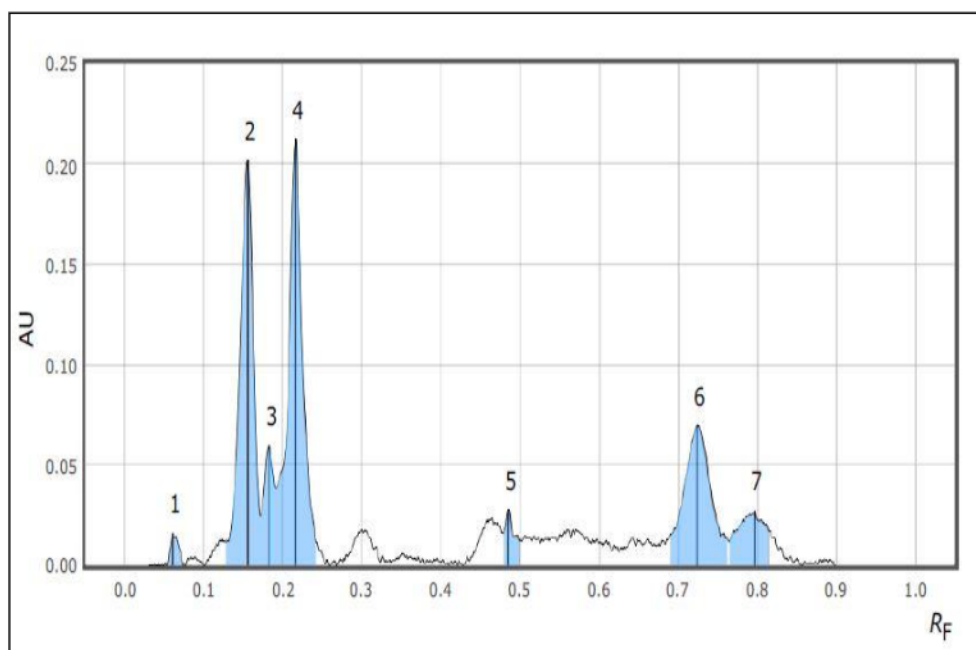


Fig. 2. HPTLC chromatogram of MEPBL at 366 nm

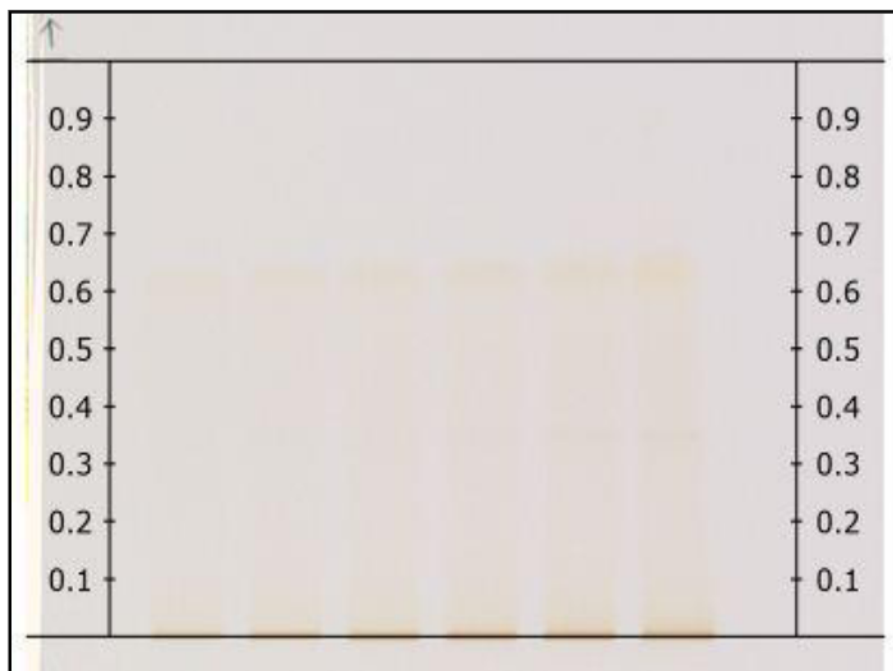


Fig. 3. Image of TLC plate before derivatization in white light

Four flavonoids are detected in MEPBL after derivatization with Natural product reagent A. R_f values was found to be 0.19, 0.29, 0.72 and 0.95. Fig. 5. is the image of TLC plate before derivatization and Fig. 6. is the image of TLC

plate derivatized with natural product reagent A captured at 366nm.

Phenols are detected in MEPBL after derivatization with ferric chloride as dark blue

zone (Fig. 7) with R_f value 0.7. However it was not observed before derivatization with ferric chloride (Fig. 8).

Glycosides are not detected as before and after derivatization with alc. KOH dark blue bands are not observed (Fig.9).

4. DISCUSSION

The universal role of plants in the treatment of diseases is exemplified by their employment in

all the major systems of medicine irrespective of the underlying philosophical premise [14]. In developing countries 80% of the population depends on medicinal plants as a source for their medicine [15]. By considering the demand for the herbs, there is need of simple and rapid analytical method for the plant based medicine. The results from HPTLC fingerprint analysis of MEPBL confirmed the presence of alkaloids with R_f value 0.65, presence of flavonoids are confirmed with R_f values 0.19, 0.29, 0.72 and 0.95 and phenolic compound was confirmed with

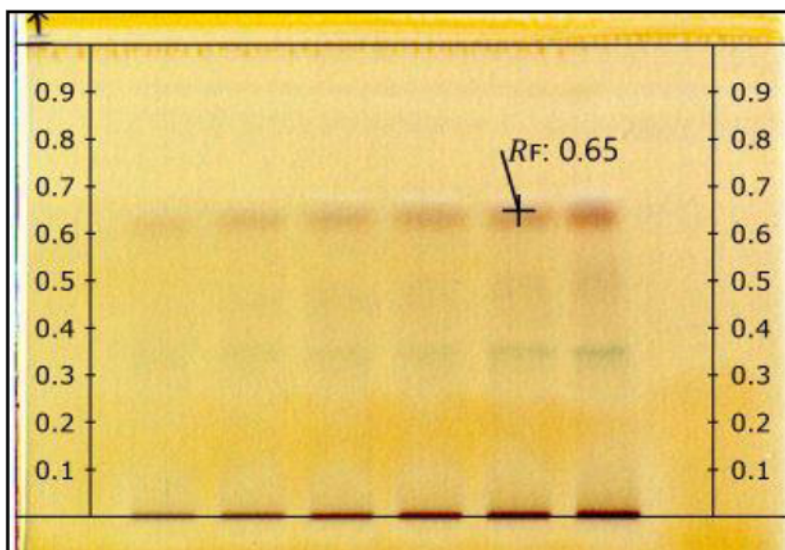


Fig. 4. Image of TLC plate derivatized with dragendorffs reagent captured in white light

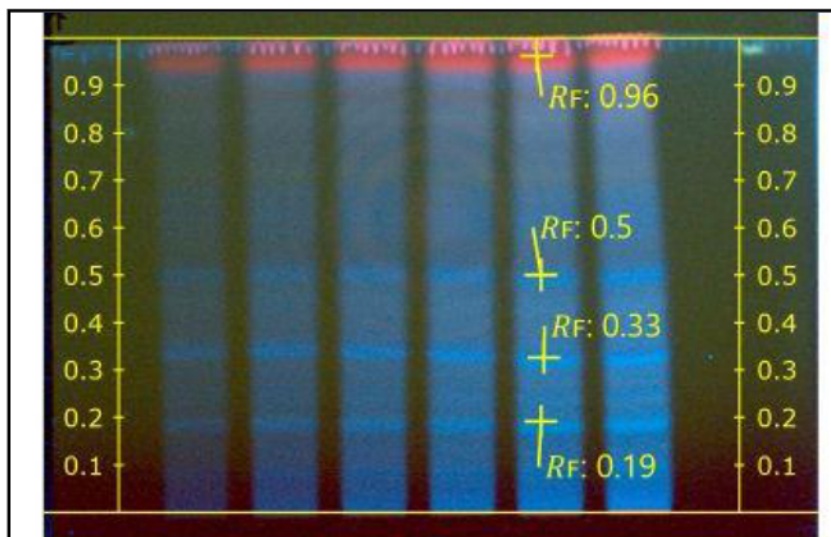


Fig. 5. Image of TLC plate before derivatization captured at 366 nm

R_f value 0.7. However glycoside was found to be absent in MEPBL. HPTLC fingerprint analysis can be used as a diagnostic tool for the correct identification of the plant. A method for HPTLC

analysis of *P. betle* has been presented along with results that show the presence of alkaloids, flavonoids and phenolic compounds in the methanolic extract of the plant material.

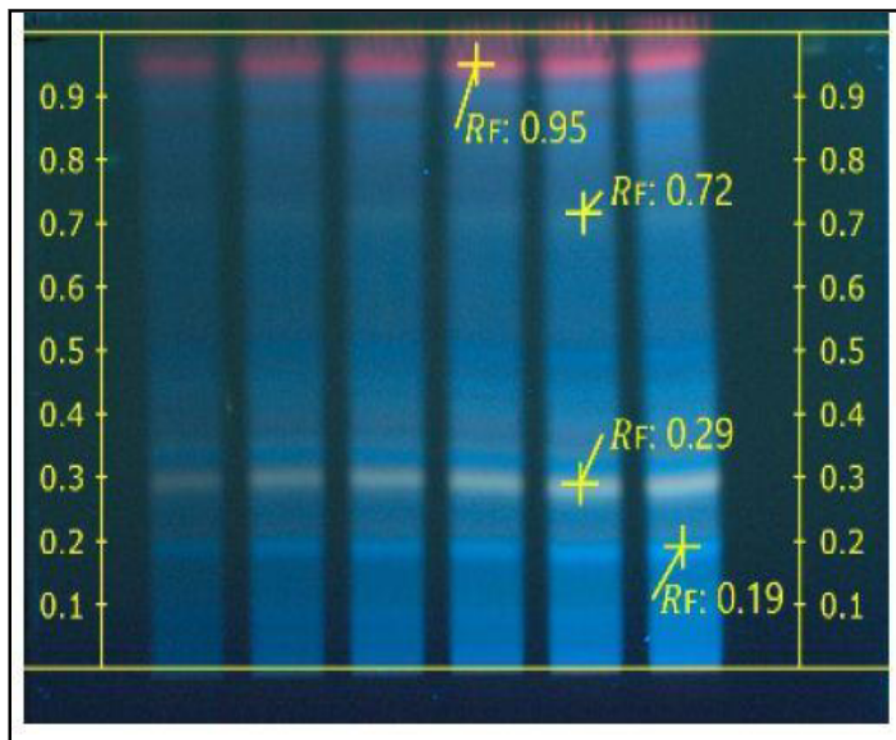


Fig. 6. Image of TLC plate after derivatization with natural product a captured at 366 nm

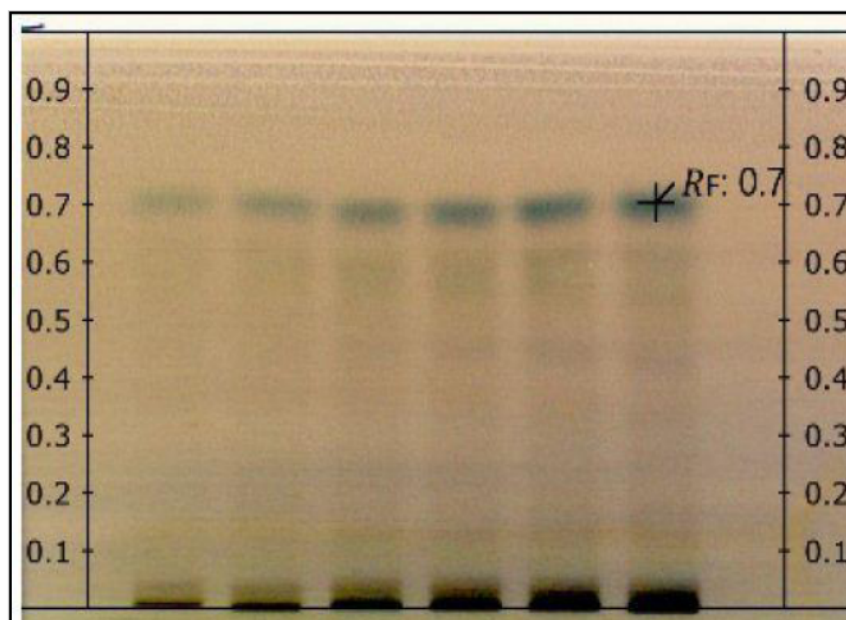


Fig. 7. Image of TLC plate after derivatization with ferric chloride captured in day light



Fig. 8. Image of TLC plate before derivatization with ferric chloride captured in day light

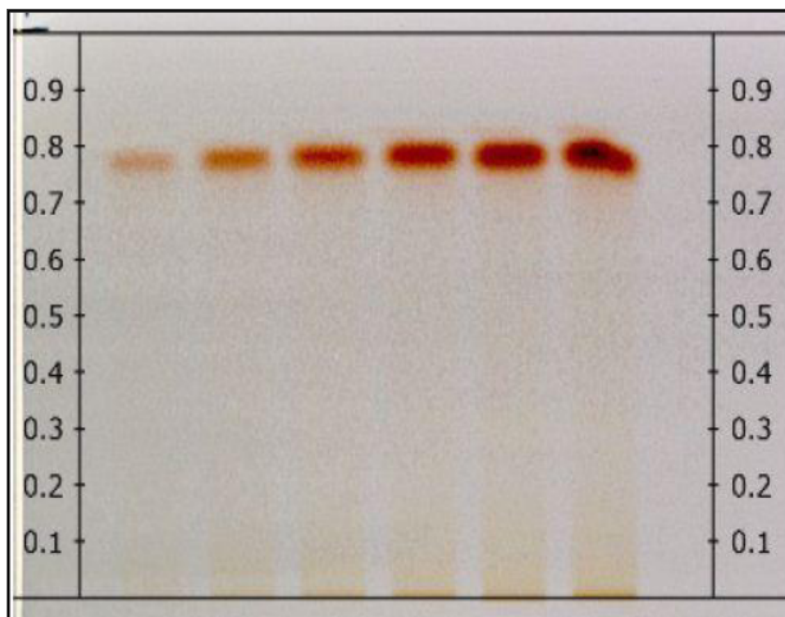


Fig. 9. Image of TLC plate after derivatization with alc KOH captured in day light

5. CONCLUSION

The HPTLC fingerprinting profile developed for the methanolic extract of *Piper betle* L. leaves will help in proper identification of the plant.

CONSENT

It is not applicable.

ETHICAL APPROVAL

It is not applicable.

ACKNOWLEDGEMENTS

We express our sincere thanks to Management and Principal of SVPMS College of Pharmacy, Malegaon Bkll Tal Baramati Dist Pune for

providing necessary research facility for this study. We also express our gratitude to Prof. R.B. Deshmukh, Head, Dept. of Botany, Agri cultural Development Trust's Shardabai Pawar Mahila Mahavidyalaya Shardanagar Tal-Baramati for the authentication of plant.

COMPETING INTERESTS

Authors have declared that no competing interests exist.

REFERENCES

- Kokate CK, Purohit AP, Gokhale SB. Pharmacognosy. Edn 46, Nirali Prakashan, Pune, 2010;6:1.
- Chothani DL, Patel MB, Mishra SH. HPTLC fingerprint profile and isolation of marker compound of *Ruellia tuberosa*. Chromatogr. Res Int. 2012;1-6
- Warrier PK, Nambier VPK, Ramanakutty C. Indian Medicinal Plants. Orient Long man Publishers Ltd .Madras: India. 1996; 279.
- Kumar N, Misra P, Dube A, Bhattacharya S, Dikshit M, Ranade S. Piper betle Linn. A maligned pan-asiatic plant with an array of pharmacological activities and prospects for drug discovery. Curr Sci. 2010;99:922-32
- Bhattacharya S, Banerjee D, Bauri AK, Chattopadhyay S, Bandyopadhyay SK. Healing property of the Piper betel phenol, allylpyrocatechol against indomethacin-induced stomach ulceration and mechanism of action. World J Gastroenterol 2007;13(27):3705-13.
- Gundala SR, Aneja R. *Piper betel* leaf: A reservoir of potential xenohormetic nutraceuticals with cancer-fighting properties. Cancer Prev Res 2014;7(5): 477-86.
- Agarwal T, Singh R, Shukla AD, Waris I, Gujrati A. Comparative analysis of anti bacterial activity of four *Piper betle* varieties. Adv Appl Sc Res, 2012;3:698-05.
- Jaiswal SG, Patel M, Saxena DK, Naik SN. Antioxidant properties of *Piper betle* (L.) leaf extracts from six different geographical domain of India. J Biores. Engg. Technol. 2014; 2(2):12-20.
- Majumdar B, Chaudhuri SGR, Ray A, Bandyopadhyay SK. Effect of ethanol extract of *Piper betle* Linn leaf on healing of NSAID-induced experimental ulcer a novel role of free radical scavenging action. Indian J Exp Biol, 2003;41:311-5.
- Chan EWC, Wong SK. Phytochemistry and pharmacology of three Piper species: An update. J Phcog. 2014; 1(9): 534-44.
- Singh M, Shakya S, Soni VK, Dangi A, Kumar N, Bhattacharya SM. The n-hexane and chloroform fractions of *Piper betle* L. trigger different arms of immune responses in BALB/c mice and exhibit anti filarial activity against human lymphatic filarid *Brugia malayi*. Int Immunopharmacol. 2009;9(6):716-28.
- Pal M, Chandrashekar K. Mosquito repellent activity of *Piper betel* Linn. Int J Pharm Life Sci. 2010; 1(6):313-5.
- Badrul AM, Fahima A, Nahida P, Rashna SP, Akter S, Chowdhury J et al. Antioxidant, analgesic and anti-inflammatory activities of the methanolic extract of *Piper betle* leaves. Avicenna J. Phytomed. 2012; 1-14.
- Evans WC. Pharmacognosy. Edn 16. Saunders Elsevier.2009;3-7.
- Duraisamy G, Ganesan R, Manokaran K, Balasubramaniam V, Chandrasekar U. HPTLC fingerprinting analysis of *Evolvulus alsinoides*(L.) L. J. Acute Med. 2012;(2): 77-82.

© 2020 Kale and Patil; This is an Open Access article distributed under the terms of the Creative Commons Attribution License (<http://creativecommons.org/licenses/by/4.0>), which permits unrestricted use, distribution, and reproduction in any medium, provided the original work is properly cited.

Peer-review history:
The peer review history for this paper can be accessed here:
<http://www.sdiarticle4.com/review-history/65395>



In Vivo Antidiabetic Activities of Polyherbal Extracts against Streptozotocin-Nicotinamide Induced Type 2 Diabetic Mice Model

Pradnya Jagtap¹, Yashashri Nimbalkar¹, Vidya Patil^{2*} and Ravindra Y. Patil³

¹PDEA'S Seth Govind Raghunath Sable College of Pharmacy, Saswad, Maharashtra, India

²Department of Botany, Waghire College, Saswad Pune, Maharashtra, India

³PDEA's Shankarro Ursal College of Pharmaceutical Sciences and Research Centre, Pune, Maharashtra, India

*Corresponding author, email: patilvidya14@gmail.com

Co-authors' e-mails: pnj1511@gmail.com, yashashri159@gmail.com, rypatil1971@yahoo.co.in

Received 9 May 2021, Revised 11 Jul 2021, Accepted 20 Jul 2021, Published Aug 2021

DOI: <https://dx.doi.org/10.4314/tjs.v47i3.1>

Abstract

Diabetes mellitus is a chronic metabolic disorder and rapidly increasing cases of diabetes throughout the world are major concerns in both developed and developing countries. Currently available oral antidiabetic medicines have limitations in efficacy and safety, which in conjunction with the emergence of diabetes mellitus as a global epidemic have aided the popularity of alternative therapies to manage the disease safely and more efficiently. Herbal medicines are accepted as alternative therapies for blood sugar control. *Gymnema sylvestre*, *Boerhavia diffusa*, *Tinospora cordifolia*, and *Argyreia nervosa* are some potent herbs used for the management of diabetes. Mixing of these plants in different ratios may produce synergistic antidiabetic actions which may have greater antidiabetic activity. Hence, the present study aimed to determine the antidiabetic activities of polyherbal extracts in streptozotocin-nicotinamide induced type 2 diabetic mice. The administration of polyherbal extract orally at doses of 100, 200 and 400 mg/kg significantly decreased the blood glucose levels compared to the control diabetic mice. The polyherbal extract significantly lowered the elevated total cholesterol, triglycerides and low-density lipoprotein levels, while increased the high-density lipoprotein indicating antihyperlipidemic activity. The present study reveals that polyherbal extract at a dose of 400 mg/kg body weight resulted in a significant decline ($p < 0.001$) in blood glucose level.

Keywords: Polyherbal extracts, diabetes mellitus, Oral glucose tolerance test, Streptozotocin-Nicotinamide.

Introduction

Diabetes mellitus (DM) is a chronic metabolic disorder characterized by hyperglycaemia caused by reduced insulin secretion, decreased glucose utilization and increased glucose production (Undale et al. 2014, Mouri and Badireddy 2019). Glucose homeostasis is a balance between hepatic glucose production and peripheral glucose uptake and utilization. Insulin is the most

important regulator of glucose homeostasis (Simon and Wittmann 2019, Yari et al. 2020). Diabetes mellitus is classified into general categories like type 1, type 2, gestational diabetes, among other specific types of diabetes. Type 1 diabetes is caused by B-cell destruction, usually leading to absolute insulin deficiency. Type 2 diabetes is a result of progressive insulin secretory defects in conjunction with insulin resistance. Gestational

diabetes mellitus (GDM) is a diabetes type usually diagnosed in the second or third trimester of pregnancy and is not clearly evident in diabetes. Other uncommon diabetes types include monogenic diabetes syndromes such as neonatal diabetes, maturity-onset diabetes of the young (MODY), diabetes resulting from diseases of the exocrine pancreas (such as cystic fibrosis), and drug or chemical induced diabetes such as in the treatment of HIV/AIDS or after organ transplantation (American Diabetes Association,

<https://www.diabetes.org/diabetes>). Diabetes mellitus is a serious metabolic disease that has significant impacts on the health, quality of life and life expectancy of patients (Sancheti and Seo 2009). According to the reports of the World Health Organization, the rapid increase of diabetes in India is indicative of a potential epidemic with over 62 million individuals currently diagnosed and future projections indicating a rapid increase in numbers (Wild et al. 2004). In 2000, India had the highest number of people with diabetes mellitus (31.7 million) followed by China (20.8 million) and United States (17.7 million) in second and third places. The global prevalence of diabetes is predicted to double from 171 million in 2000 to 366 million in 2030 with India seeing the highest increase with numbers nearing 80 million (Wild et al. 2004).

There are various synthetic drugs used for the treatment of hyperglycaemia. The synthetic drugs have various side effects such as causing hyperglycaemia at higher doses, dermatological reactions, liver problems, nausea, vomiting, generalized hypersensitivity reactions, lactic acidosis and diarrhoea. These anti-diabetic drugs also cause weight gain which may further contribute to the progression of type 2 diabetes. The secondary complications arising from the use of synthetic

drugs lead to limitations in their uses and potentially create issues in the management of diabetes (Chaudhuri and Sharma 2016). So, there is a need to develop safe and economic alternative treatments for diabetes mellitus. Therefore, there is considerable interest in the field of medicinal plants due to their natural origins and fewer side effects (El-Shafey et al. 2013). The World Health Organization also recommended and encouraged the practice of herbal medicines especially in countries where access to the conventional treatments of diabetes is inadequate.

The pharmacological activity of a single plant is less when compared to polyherbal formulations that contain combinations of various plants. Polyherbal formulations produce synergistic actions which are more potent and also diminish the concentrations of individual herbs, thereby reducing adverse effects (Shah et al. 2019).

In the present study, polyherbal formulations which consisted of extracts of *Gymnema sylvestre*, *Boerhavia diffusa*, *Tinospora cordifolia*, and *Argyreia nervosa* were used to determine hypoglycaemic activities. The herbs used in the formulations are reported in traditional medicines to treat diabetes mellitus and their active phytoconstituents like gymnemic acids, gymnemosides a, b, c, d, e, and f and gymnemosaponins (Kanetkar et al. 2007, Mishra et al. 2014), punarnavine-1, β -sitosterol (Sharma et al. 2019), tinosporin (Galani et al. 2010), quercetin and kaempferol (Gosh 1984) etc. Their details are given in Table 1. Therefore, in the present investigation, the polyherbal formulations were evaluated for hypoglycaemic activity in streptozotocin-nicotinamide (STZ-NIC) induced diabetes in mice.

Table 1: Phytoconstituents of polyherbs used for polyherbal extract preparation

Sr.No.	Plant name	Phytochemical constituents
1	<i>Gymnema sylvestre</i> R. Br.	Gymnemic acid I-IV, Gymnemasaponins, Gymnemosides a, b, c, d, e, and f, Kaempferol 3-O- β -D-glucopyranosyl-(1-4)- α -L-rhamnopyranosyl-(1-6)- β -D-galactopyranoside, Stigmasterol, Conduritol A and Quercitol (Kanetkar et al. 2007)
2	<i>Boerhavia diffusa</i> L.	Punarnavine-1 & 2, Boeravinone A-I, 9-O-Methyl-10-hydroxy coccineone E, 10-dimethyl boeravinone C, Coccineone E, β -Sitosterol β -Sitosterol-D-glucoside, β -Sitosteryl oleate, Sitosteryl palmitate, Liriodendrin, Stringarsionol and Mono-D-glucoside and β -D-glucoside (Mishra et al. 2014)
3	<i>Tinospora cordifolia</i> (Thunb.) Miers	Tinosporide, Furanolactone diterpene, Furanolactone clerodane diterpene, furanoid diterpene, Tinosporaside, Giloinsterol, β -Sitosterol, 20a- Hydroxy ecdysone, Giloin, Tinosporan acetate, Tinosporal acetate, Tinosporidine, Heptacosanol, Octacosanol, sinapic acid, Tinosponone, and 2- phytoecdysones (Sharma et al. 2019)
4	<i>Argyreia nervosa</i> (Burm.f.) Bojer	1-Triacontanol, Epifriedelinol Acetate, Epifriedelinol and β -Sitosterol, N-Triacontanol, B-Sitosterol, P-Hydroxycinnamoyl Octadecanolate, Caffeic acid, p-Hydroxycinnamate, Hexadecanyl p-hydroxycinnamate, L-Ester coumarin and Tetradecanyl palmitate (Galani et al. 2010, Gosh 1984)

Materials and Methods

Plant materials

The leaves of *Gymnema sylvestre* (Asclepiadaceae), whole plant of *Boerhavia diffusa* (Nyctaginaceae), stem and leaves of *Tinospora cordifolia* (Menispermaceae) and whole plant of *Argyreia nervosa* (Convolvulaceae) were collected from local regions around Purandar town in Maharashtra and Pune University campus. Freshly collected plants were pressed in a herbarium press and dried plant specimens mounted on herbarium sheet. All the information provided and herbaria were submitted to the Botanical Survey of India (BSI) Herbarium in Pune for authentication; the corresponding voucher numbers are VP-11, VP-10, VP-9 and VP-7. The plant parts were washed with distilled

water to remove dirt and soil, and then shade dried.

Preparation of extracts

The selected parts of plants were washed and dried under shade for 20 days. The dried plants were pulverized using a mechanical grinder and powdered for further studies and extracted with 80% absolute ethanol using Soxhlet apparatus for 6 hours. The extracts were evaporated to dryness (resinous material) under reduced pressure at 60 °C and stored at 4 °C until use. The polyherbal formulation was developed by combining the dried extracts of the plant extracts (Mandlik 2008, Maurya et al. 2011).

Preparation of polyherbal mixture

Polyherbal mixture was prepared by mixing individually extracted powders of plants *Gymnema sylvestre*, *Boerhavia diffusa*, *Tinospora cordifolia*, and *Argyreia nervosa*. The concentration of each plant in the plant polyherbal extract mixture was decided according to their potent antidiabetic activity at that concentration. *Gymnema sylvestre* shows potent antidiabetic activity at a dose of 400 mg/kg (Aralelimath and Bhise 2012), and the average weight of the experimental animal is 27 g, so, 10.8 mg of *Gymnema sylvestre* was used in the polyherbal mixture. *Boerhavia diffusa* shows potent antidiabetic activity at a dose of 200 mg/kg (Malhotra et al. 2014), so 5.4 mg of *Gymnema sylvestre* was used in the polyherbal mixture. *Tinospora cordifolia* shows potent antidiabetic activity at a dose of 400 mg/kg (Puranik et al. 2010), so 10.8 mg of *Gymnema sylvestre* was used in the polyherbal mixture. *Argyreia nervosa* shows potent antidiabetic activity at a dose of 500 mg/kg (Kumar and Alagawadi 2010), so 13.5 mg of *Gymnema sylvestre* was used in the polyherbal mixture. All these powders were mixed well to make polyherbal mixtures, and this prepared polyherbal mixture was administered to an animal with water at different concentrations (100, 200 and 400 mg/kg).

Chemicals and reagents

Streptozotocin, nicotinamide and glucose were obtained from Sigma. Other chemicals and reagents used in the study were of analytical grade.

Determination of in vivo antidiabetic activity

Animals: Swiss albino mice bred in the animal house facility of PDEA's SGRS College of Pharmacy were used. The animals were maintained under controlled temperature, humidity and light cycle as prescribed by the Committee for the Purpose of Control and Supervision of Experiments on Animals (CPCSEA). Standard animal pellet diet and water were provided *ad libitum*. The experimental protocol was approved by the

Institutional Animal Ethics Committee (IAEC) (SGRS/ IAEC/ 07/2018-19) and experiments were conducted according to the guidelines of the CPCSEA.

Experimental design

Acute oral toxicity tests of the polyherbal extract

An acute oral toxicity study was carried out according to OECD guidelines 423. In this method pre-specific fixed doses of the test substances were used, i.e., 5 mg/kg, 50 mg/kg, 300 mg/kg, 2000 mg/kg, 5000 mg/kg and the mortality rates due to these doses were observed. Generally, the female was used for this study and each dose Group consisted of 3 animals.

Effect of polyherbal formulation on oral glucose tolerance test (OGTT)

The oral glucose tolerance test was performed in overnight fasted (12-14 hrs) mice. The mice were divided into six Groups (n = 6).

Group I: served as normal control mice, administered drinking water daily.

Group II: had glucose control mice.

Group III: mice were administered standard drug metformin (250 mg/kg).

(The dose of metformin administered to mice in this study was calculated according to a clinically relevant human dose based on body surface area. Metformin 250 mg/kg)

Group IV: mice were administered polyherbal extract of 100 mg/kg.

Group V: mice were administered polyherbal extract of 200 mg/kg.

Group VI: mice were administered polyherbal extract of 400 mg/kg.

Glucose (2 g/kg) was fed to mice of groups II to VI, 30 minutes before the administration of the extracts and standard drug. Blood was withdrawn from the retro-orbital sinus after 0, 30, 60, 90 and 120 minutes of extract and standard drug administration, and the plasma obtained after centrifugation at 3000 rpm was estimated for fasting plasma glucose levels glucometer (Turner 1965, Gosh 1984, Zhang et al. 2002, Chaudhuri and Sharma 2016).

Induction of diabetes mellitus (non-insulin dependent diabetes mellitus)

In overnight fasted mice, streptozotocin (STZ) was injected (50 mg/kg in 0.1 mL citrate buffer pH 4.5 i.p.) 15 min after nicotinamide (NIC) injection (120 mg/kg in 0.1 mL normal saline) in all the groups except for Group I which was the non-diabetic control i.e., Normal control. Animals were fed with glucose solution (5%) for 12 hrs to avoid hypoglycaemia. Hyperglycaemia was confirmed after 3 days. Mice having serum glucose >250 mg/dl were selected for the study (Birgani et al. 2018).

Evaluation of antidiabetic activity

The animals were divided into six Groups (I-VI) of six mice each as mentioned previously and Groups III to VI were treated with test drugs. The fasting glucose levels were determined on days 0, 7, 14, 21 and 28 of extract administration. During the experimental period, the mice were weighed daily and the mean changes in body weights were calculated.

Estimation of biochemical parameters

On day 28, the animals were sacrificed by cervical dislocation to determine the biochemical parameters. triglycerides (TGL), low density lipoprotein (LDL), cholesterol and high-density lipoprotein (HDL) were determined (Rakieten et al. 1963, Nagja et al. 2017, Sheikh et al. 2015).

Statistical analysis

Results were analysed statistically using the One-Way ANOVA method followed by Bonferroni Test (multiple comparison test). The minimum level of significance was set at $p < 0.05$. The data are presented as the mean \pm SEM.

Results**Acute oral toxicity according to OECD guidelines 423**

In acute oral toxicity study, oral administration of the polyherbal extracts at the doses of 5 mg/kg, 50 mg/kg, 300 mg/kg, 2000 mg/kg, 5000 mg/kg body weight did not induce any changes in behaviour and no mortality was observed during the study. There was no significant difference in the body weight and food consumption when compared to the normal control group. On the 7th day, macroscopic pathology observations revealed no visible lesions in any animals after sacrifice. The observed data suggested that the oral LD₅₀ value of polyherbal extract is greater than 2000 mg/kg body weight. Therefore, polyherbal extract can be safely used as a dose up to 2000 mg/kg body weight for therapeutic use. Selected doses: 100 mg/kg, 200 mg/kg, 400 mg/kg.

Effects of polyherbal extracts on body weight

The effects of the polyherbal extracts on the bodyweight of animals were checked, the results of which are presented in Table 2. The body weight measured in grams in Group II (Disease control) was observed to be 20.17 ± 0.5426 g on the 28th day. Significantly ($p < 0.001$) decreased level of bodyweight in Group II (Disease control) was observed as compared to Group I (Normal control). In Groups III, IV, V and VI significant ($p < 0.001$) increase in body weight was observed as compared to Group II (Disease control). In Group VI, significant ($p < 0.01$) increase in body weight as compared to Group III (Standard control). All data were subjected to the One-Way ANOVA method followed by Bonferroni's multiple comparisons test and given in Figure 1.

Table 2: Effects of polyherbal extracts on body weight of STZ-NIC induced diabetic mice

S.No.	Treatment Group	Body weight (g)				
		0 Day	7 th Day	14 th Day	21 th Day	28 th Day
I	Normal	27 ±	26.5 ±	26.5 ±	26.83 ±	27.17 ±
	Control	0.5164	0.4282	0.3416	0.4779	0.4014
II	Disease (Diabetic) control	28.33 ±	26.33 ±	24.5 ±	23.17 ±	20.17 ±
		0.3073 ^{NS}	0.3333 ^{NS}	0.4282 ^{NS}	0.7032 [*]	0.5426 ^{***}
III	Standard Treated	27.33 ±	26.37 ±	27.5	26.17 ±	25.67 ±
		0.8433 ^{NS}	1.022 ^{NS}	± 0.8062 ^{NS}	0.9804 ^{NS}	0.8028 ^{***}
IV	Polyherbal extract treated I 100 mg/kg	30.5 ±	28.67 ±	27.5 ±	26.50 ±	25 ±
		0.9916 ^{NS,NS}	0.9545 ^{NS,NS}	0.8062 ^{NS,NS}	0.5627 ^{*,NS}	0.5164 ^{**,NS}
V	Polyherbal extract treated II 200 mg/kg	30 ±	29.17 ±	28.5 ±	27.67 ±	27.17 ±
		0.4472 ^{NS,NS}	0.4773 ^{NS,NS}	0.6708 ^{**,NS}	0.5578 ^{**,NS}	0.8333 ^{***,NS}
VI	Polyherbal extract treated III 400 mg/kg	28.33	28	27.33	27.50	29.17
		±1.145 ^{NS,NS}	±1.211 ^{NS,NS}	±1.054 ^{NS,NS}	±1.057 ^{**,NS}	±0.8724 ^{***,##}

Notes: All values are expressed as mean ± SEM. N = 6. All data are subjected to One Way ANOVA followed by Bonferroni's multiple comparisons test; here Group II is compared with Group I and Groups III, IV, V and VI are compared with Group II. *p < 0.05, **p < 0.01, ***p < 0.001, NS: Not Significant. Multiple Comparison: Groups IV, V, VI are compared with Group III. # p < 0.05, ## p < 0.01, ### p < 0.001, NS: Not Significant.

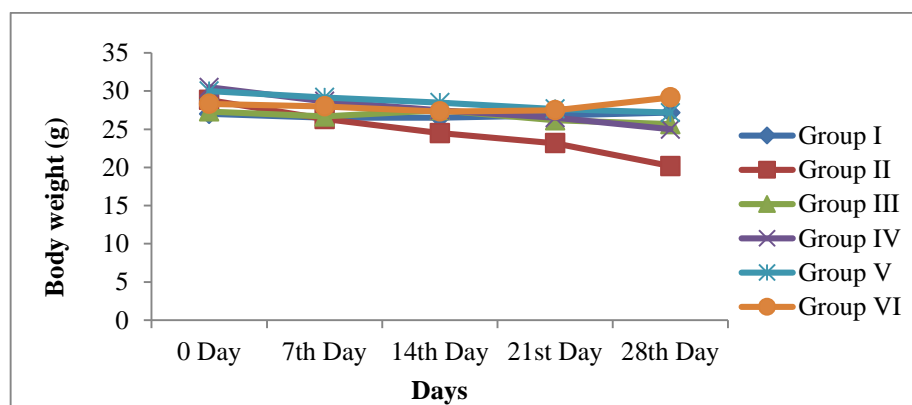


Figure 1: Effects of polyherbal extracts on body weights in STZ-NIC induced diabetic mice; values are expressed as mean ± SEM, n = 6. Where, Group I: Normal control, Group II: Disease control, Group III: Standard control, Group IV: polyherbal extract treated 100 mg/kg, Group V: polyherbal extract treated 200 mg/kg, Group VI: polyherbal extract treated 400 mg/kg.

Effects of the polyherbal extracts on oral glucose tolerance

The effects of the polyherbal extracts on the blood glucose level measured with Glucopoint One-touch glucometer in Group II (Disease control) were observed to be 320.2 ± 9.513 mg/dl at 120 min. All the readings are given in Table 3 and significant ($p < 0.001$) increase in blood glucose level in Group II (Disease control) was observed as compared to Group I (Normal Control). In Group VI polyherbal extract-treated III 400 mg/kg, a

significant ($p < 0.001$) decrease in blood glucose level at 60, 90 and 120 min was observed as compared to Group II (Disease control). In a similar comparison against Group III (Standard control) treated with metformin (250 mg/kg, p.o.), Group VI polyherbal extract-treated III 400 mg/kg showed a significant ($p < 0.001$) decrease in blood glucose level at 90 min and 120 min. The results suggest the potential effects of polyherbal extract-treated at dose of 400 mg/kg at 90 and 120 mins of treatment (Figure 2).

Table 3: Effects of polyherbal extracts on oral glucose tolerance test in STZ-NIC induced diabetic mice

S.No	Treatment Group	Plasma glucose concentrations (mg/dl)					
		0 min	30 min	60 min	90 min	120 min	
I	Normal Control	93.67	± 129.2	± 146.7	± 129.3	± 94.33	
		1.145	1.537	1.453	2.108	0.8819	
II	Disease (Diabetic) control	326.0	$\pm 350.7 \pm 10.7$	± 371.2	± 349.2	± 320.2	
		8.839***	***	9.41***	10.03***	9.513***	
III	Standard Control	313.3	$\pm 329.0 \pm 9.29$	± 309.3	± 292.2	± 263.8	
		9.510 ^{NS}	NS	9.59***	7.026***	9.888***	
IV	Polyherbal extract treated I 100 mg/kg	324.3	± 342	± 354.0	± 343.5	± 329.8	
		8.804 ^{NS}	8.021 ^{NS}	6.127 ^{NS,##}	6.339 ^{NS,###}	6.041 ^{NS,#}	
V	Polyherbal extract treated II 200 mg/kg	326.2	± 334.3	± 330.5	± 324.8	± 317.2	
		9.228 ^{NS,NS}	8.920 ^{NS,NS}	9.66 ^{NS,NS}	9.428 ^{NS,#}	9.407 ^{NS,#}	
VI	Polyherbal extract treated III 400 mg/kg	310.0	± 328.5	± 295.8	± 249.2	± 199.7	
		8.14 ^{NS,NS}	11.95 ^{NS,NS}	7.300 ^{NS,NS}	3.745 ^{NS,##}	0.9888 ^{NS,###}	

Notes: All values are expressed as mean \pm SEM, n = 6. All data are subjected to One Way ANOVA followed by Bonferroni's multiple comparisons test; here Group II is compared with Group I and Groups III, IV, V and VI are compared with Group II. * $p < 0.05$, ** $p < 0.01$, *** $p < 0.001$, NS: Not Significant. Multiple Comparison: Groups IV, V and VI are compared with Group III. # $p < 0.05$, ## $p < 0.01$, ### $p < 0.001$, NS: Not Significant.

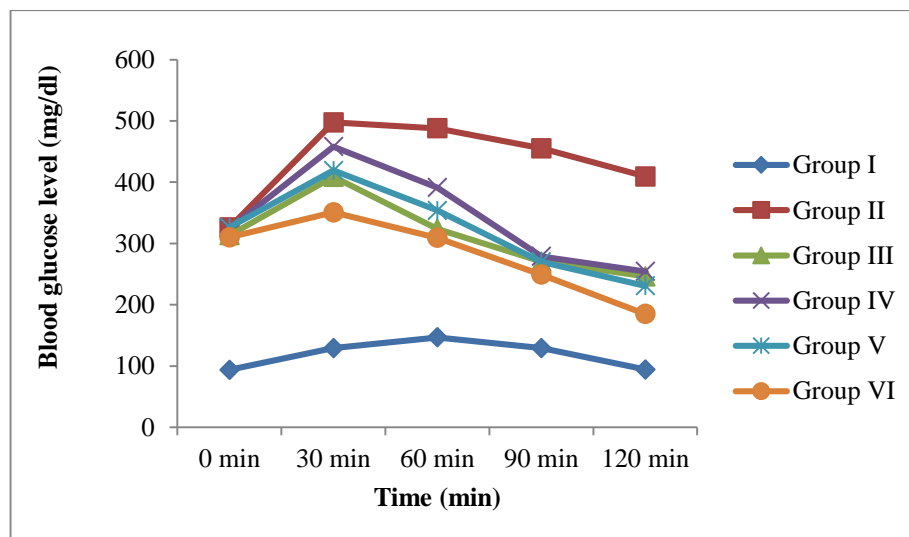


Figure 2: Effects of polyherbal extracts on oral glucose tolerance test in STZ-NIC induced diabetic mice; values are expressed as mean \pm SEM, n = 6. Where, Group I: Normal control, Group II: Disease control, Group III: Standard control, Group IV: polyherbal extract treated 100 mg/kg, Group V: polyherbal extract treated 200 mg/kg, Group VI: polyherbal extract treated 400 mg/kg.

Effects of the polyherbal extracts on non-insulin-dependent diabetes mellitus

In the sub-acute study conducted in the STZ-NIC induced diabetic mice, the blood glucose level in Group II (Disease control) was found to be 316.7 ± 6.800 mg/dl (Table 4). Significant ($p < 0.001$) increase in blood glucose level in Group II (Disease control) was observed as compared to Group I (Normal control). At the end of 28 days of treatment schedule, significant ($p < 0.001$) decrease in the blood glucose level was observed in

Groups III, IV, V and VI compared to Group II (Disease control). In Group VI, significant ($p < 0.01$) decrease in blood glucose level at 28 days was observed as compared to Group III (Standard control) treated with metformin (250 mg/kg, p.o.). While in Groups IV and V, no significant decrease in blood glucose level at 28 days was observed as compared to Group III. The results suggest the potential effects of polyherbal extract-treated at dose of 400 mg/kg at 14, 21 and 28 days of treatment (Figure 3).

Table 4: Effects of polyherbal extracts on blood glucose level in STZ-NIC induced diabetic mice

Sr. No	Treatment Group	Fasting plasma glucose concentration (mg/dl)				
		Day 0	7 th Day	14 th Day	21 st Day	28 th Day
I	Normal Control	96 ± 0.6831	96.17 ± 0.4014	96.33 ± 0.3333	97.50 ± 0.4232	97.67 ± 0.4216
II	Disease (Diabetic) control	309.5 ± 7.018***	311.5 ± 6.662***	316.7 ± 7.592***	314.2 ± 7.609***	316.7 ± 6.800***
III	Standard Control	325 ± 7.043 ^{NS}	316.7 ± 7.592 ^{NS}	221.3 ± 10.93***	165.6 ± 8.036***	101.3 ± 1.874***
IV	Polyherbal extract treated I 100 mg/kg	325 ± 7.043 ^{NS,NS}	289.5 ± 6.893 ^{NS,#}	238.0 ± 6.061***, ^{NS}	196.3 ± 3.964***, ^{##}	146.8 ± 3.745***, ^{NS}
V	Polyherbal extract treated II 200 mg/kg	329 ± 7.033 ^{NS}	287.7 ± 4.197 ^{NS,#}	232.5 ± 5.464***, [#]	164.2 ± 4.534***, ^{NS}	112.3 ± 2.060***, ^{###}
VI	Polyherbal extract treated III 400 mg/kg	323.8 ± 5.231 ^{NS}	283.3 ± 5.783 ^{*,##}	218.7 ± 9.050***, ^{##}	156.0 ± 3.416***, ^{##}	100.8 ± 1.352***, ^{##}

Notes: All values are expressed as mean ± SEM, n = 6. All data are subjected to One Way ANOVA followed by Bonferroni's multiple comparisons test; here Group II is compared with Group I, and Groups III, IV, V and VI are compared with Group II. *p < 0.05, **p < 0.01, ***p < 0.001, NS: Not Significant. Multiple Comparison: Group IV, V and VI are compared with Group III. # p < 0.05, ## p < 0.01, ### p < 0.001, NS: Not Significant.

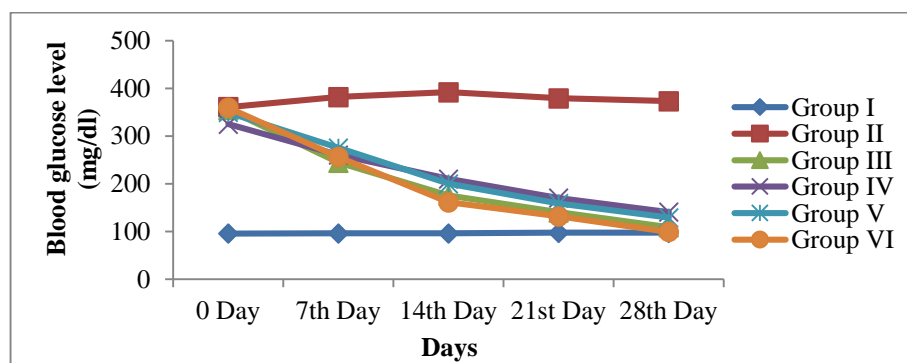


Figure 3: Effects of polyherbal extracts on blood glucose level in STZ-NIC induced diabetic mice; values are expressed as mean ± SEM, n = 6. Where, Group I: Normal control, Group II: Disease control, Group III: Standard control, Group IV: polyherbal extract treated 100 mg/kg, Group V: polyherbal extract treated 200 mg/kg, Group VI: polyherbal extract treated 400 mg/kg.

Effects of polyherbal extracts on lipid profile

The levels of serum lipids are usually elevated in DM and such an elevation represents a risk factor for coronary heart disease. This abnormally high level of serum lipids is mainly due to the uninhibited actions

of lipolytic hormones on the fat deposits due to the action of insulin. The regulation of lipid profiles in different groups of mice is exhibited in Table 5. A significant increase in TGL, total cholesterol and LDL, and a decrease in HDL was observed in Group II Disease control mice

compared with Group I Normal control mice (Table 5). Groups IV, V and VI polyherbal extract-treated and Group III standard drug-treated mice showed significantly decreased TGL, total cholesterol, LDL, and increased HDL compared to Group II Disease control mice. The results of the study indicate the anti-

hyperlipidaemic activity of the polyherbal extracts. The Group VI polyherbal extract-treated at dose of 400 mg/kg produced extreme anti-hyperlipidemic activity compared with Groups IV and V polyherbal extract-treated at doses of 100 mg/kg and 200 mg/kg (Figure 4).

Table 5: Effects of polyherbal extracts on lipid profile in STZ-NIC induced diabetic mice

Sr. No.	Treatment Groups	Lipid profile mg/dl			
		Cholesterol	Triglycerides	LDL	HDL
I	Normal Control	73.50 ± 2.078	85.50 ± 0.3416	51.83 ± 0.3074	69.07 ± 0.2108
II	Disease (Diabetic) control	126.2 ± 1.078***	200.00 ± 0.3651***	194.8 ± 0.5426***	24.0 ± 0.3651***
III	Standard Control	82.33 ± 0.8433***	86.17 ± 1.621***	51.27 ± 0.3073***	71.33 ± 0.3333***
IV	Polyherbal extract treated I 100mg/kg	95.50 ± 1.839***,###	95.83 ± 0.3073***,###	58.33 ± 0.4126***,###	74.50 ± 0.6191***,###
V	Polyherbal extract treated II 200 mg/kg	90.33 ± 0.5578***,###	87.33 ± 0.6146***,###	54.83 ± 0.3073***,###	68.17 ± 0.1666***,###
VI	Polyherbal extract treated III 400 mg/kg	71.17 ± 0.4773***,###	83.33 ± 0.4216***,ns	52.00 ± 0.3651***,###	59.00 ± 0.3651***,###

Notes: All values are expressed as mean ± SEM, n = 6. All data are subjected to One Way ANOVA followed by Bonferroni's multiple comparisons test; here Group II is compared with Group I and Groups III, IV, V and VI are compared with Group II. *p < 0.05, **p < 0.01, ***p < 0.001, NS: Not Significant. Multiple Comparison: Groups IV, V and VI are compared with Group III. # p < 0.05, ## p < 0.01, ### p < 0.001, NS: Not Significant.

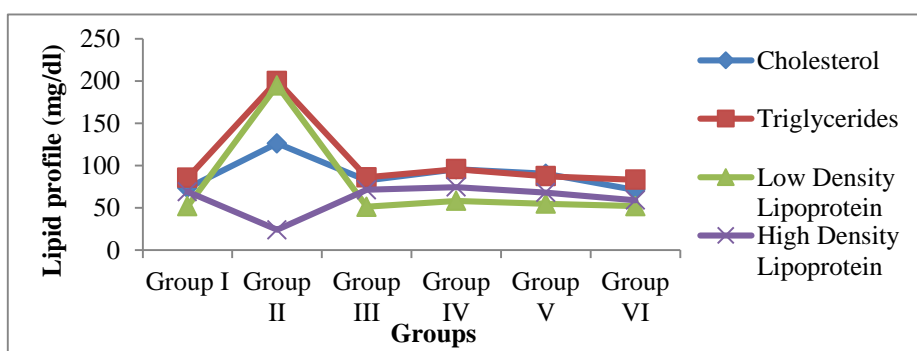


Figure 4: Effects of polyherbal extracts on lipid profile in STZ-NIC induced diabetic mice; values are expressed as mean ± SEM, n = 6. Where, Group I: Normal control, Group II: Disease control, Group III: Standard control, Group IV: polyherbal extract treated 100 mg/kg, Group V: polyherbal extract treated 200 mg/kg, Group VI: polyherbal extract treated 400 mg/kg.

Histopathologic analysis of pancreas

At the end of the study, the histopathology of the pancreas was done; results are shown in Figure 5. In Group II (Disease control), the histopathologic analysis of the pancreas revealed severe congestion, a huge decrease in the number of islets of Langerhans and β cells, and fibrosis and inflammatory cell infiltration into the islets of Langerhans. Group III (Standard control) treated with drug metformin showed moderate congestion with a comparatively lower decrease in the number of

islets of Langerhans and β cells and lymphocytic infiltration of mild nature. Groups IV and V, i.e., polyherbal extracts at doses of 100 and 200 mg/kg, respectively also showed moderate congestion with a moderate decrease in the number of islets of Langerhans and β cells and mild lymphocytic infiltration. While the Group VI polyherbal extract at the dose of 400 mg/kg showed mild congestion and mild decrease in the number of islets of Langerhans with normal β cell population indicating a significant amount of recovery.

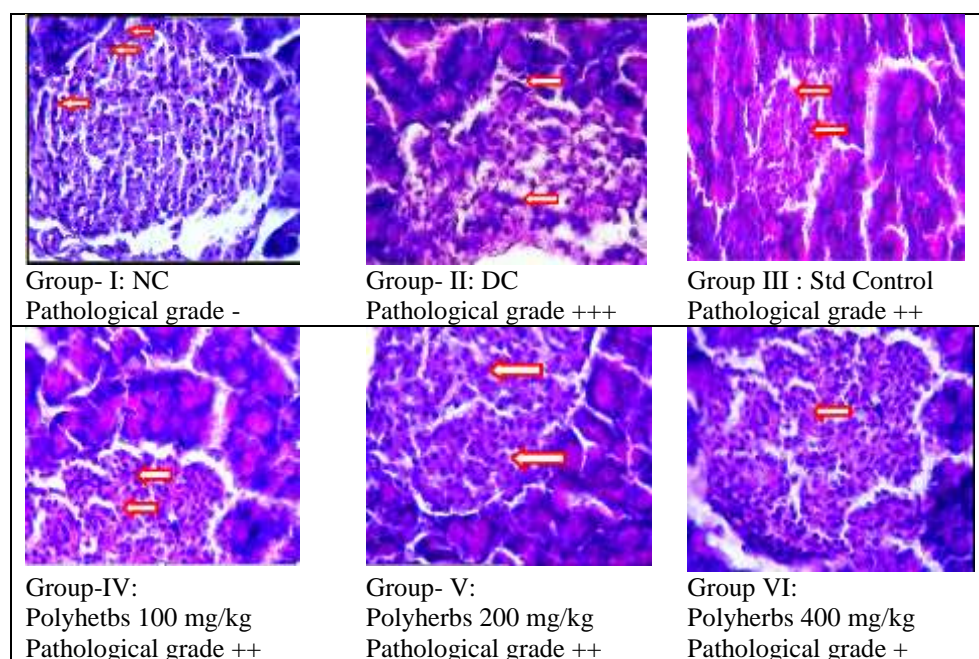


Figure 5: Pathological grades; Grade: -- no injury; Grade: +++ severe injury; Grade: ++ moderate injury; Grade: + mild injury.

Figure 5: Group I Normal control show “-” pathological grade which indicates no injury in tissue. The histopathologic analysis of pancreas revealed severe congestion, huge decrease in the number of islets of Langerhans and β cells, and fibrosis and inflammatory cell infiltration into the islets of Langerhans in Group II Disease control which shows +++ pathological grade indicating severe injury. Group III Standard drug metformin treatment shows ++ pathological grade, i.e., moderate congestion with moderate decrease in the number of islets of Langerhans and β cells, and mild lymphocytic infiltration. Groups IV and V, i.e. polyherbal extracts at doses of 100 and 200 mg/kg, respectively also shows ++ pathological grade indicating moderate congestion with moderate decrease in the number of islets of Langerhans and β cells and mild lymphocytic infiltration. While the group VI of polyherbal extract at 400 mg/kg showing + pathological grade indicates mild congestion and mild decrease in the number of islets of Langerhans with normal β cell population, thereby indicating significant amount of recovery.

Discussion

Various synthetic drugs are used for the treatment of hyperglycaemia, like insulin and oral hypoglycaemic agents. These synthetic drugs are associated with side effects which lead to limitations in their use and create issues in the management of diabetes. So, there is a need to develop safe and economic alternative treatments for diabetes mellitus. As such, there is considerable interest in the field of medicinal plants due to their natural origins and fewer side effects. In recent times, herbal formulations have gained greater importance mainly due to their efficacy and easy availability, as well as fewer side effects when compared to synthetic drugs. These advantages have led the people to move toward herbal preparations for disease treatment and prevention, as they are claimed to display synergistic, potentiate, and agonistic/antagonistic actions and the mixtures of species in them show better therapeutic effects than individual species on their own (Petchi et al. 2014, Mohapatra et al. 2016). Srivastava et al. (2012) noted that the concept of polyherbalism has been highlighted in Sharangdhar Samhita, Ayurvedic literature dating back to 1300 AD. Also, they highlighted any single herb concentration of polyherbal formulation is reduced which is also responsible for reducing the adverse effects. In the present study, polyherbal formulations containing extracts of leaves of *Gymnema sylvestre*, whole plant of *Boerhavia diffusa*, stem and leaves of *Tinospora cordifolia*, and whole plant *Argyreia nervosa* were selected for the antidiabetic study. The individual plants have already been determined to have antidiabetic activity. The polyherbal formulations were formulated using the ethanolic extracts of the leaves of *Gymnema sylvestre*, the whole plant of *Boerhavia diffusa*, stem and leaves of *Tinospora cordifolia*, and whole plant *Argyreia nervosa*. The antidiabetic activity of the individual plants has been proven. The leaves of the *Gymnema sylvestre* showed significant antidiabetic activity against STZ-induced diabetes at a dose of 400 mg/kg

(Aralelimath and Bhise 2012), *Boerhavia diffusa* shows potent antidiabetic activity at dose of 200 mg/kg (Malhotra et al. 2014), *Tinospora cordifolia* shows potent antidiabetic activity at a dose of 400 mg/kg (Puranik et al. 2010), *Argyreia nervosa* shows potent antidiabetic activity at dose of 500 mg/kg (Kumar et al. 2010). The administration of polyherbal mixture exhibited significant antidiabetic effects and shows synergistic and potential actions against diabetes. The concentrations of the extracts were calculated from the references mentioned in the present study and worked for polyherbal extracts. The findings of the present study indicate the significant effects of the polyherbal extracts on streptozotocin-nicotinamide induced type 2 diabetic animals (mice).

Streptomyces achromogenes is a source of STZ, which is an antibiotic. Structurally, is a glucosamine derivative of nitrosourea. The nitrosourea moiety of this derivative is responsible for beta cell toxicity, while deoxyglucose moiety helps transport across the cell membrane. STZ causes alkylation or breakage of DNA strands and a consequent increase in the activity of poly-ADP-ribose synthetase, an enzyme depleting NAD in beta cells finally leading to energy deprivation and death of beta cells (Srinivasan and Ramarao 2007).

Recently, Undale et al. (2014) stated that a new animal model of type 2 diabetes has been produced by the combination of STZ and NIC administration in adult rats. The rats administered NIC (230 mg/kg, ip) 15 min before STZ (65 mg/kg, iv) have shown to develop moderate and stable non-fasting hyperglycaemia without any significant changes in plasma insulin levels. As NIC is an antioxidant, it exerts a protective effect on the cytotoxic action of STZ by scavenging free radicals and causes only minor damage to pancreatic beta-cell mass-producing type 2 diabetes. Therefore, this model has been found to be an advantageous tool for the investigation of insulinotropic agents in the treatment of type 2 diabetes (Undale et al. 2014).

The principle objective in the treatment of diabetes mellitus is to decrease the elevated blood glucose to normal physiological level to prevent further micro and macrovascular complications. In this study, metformin was used as a standard drug. Metformin is accepted as a first-line antidiabetic agent for the management of type 2 diabetes. It is suited for the treatment irrespective of body weight, age, severity of hyperglycaemia and provides an agreeable pharmacological base for therapy in conjunction with other antidiabetic agents (Scarpello and Howlett 2008). Metformin has lower mortality and cardiovascular risks as compared to other insulin secreting agents such as glimepiride, glibenclamide, glipizide and tolbutamide in patients with type 2 diabetes mellitus. Metformin also does not produce hyperglycaemia since it does not stimulate insulin secretion when administered alone in patients with type 2 diabetes mellitus (Wright et al. 2006). As shown in Table 1, reduction in body weight observed in diabetic mice might be the result of degradation of structural proteins and fats due to deficiency of carbohydrates for the energy metabolism and significant increase in body weight of diabetic mice treated with polyherbal extracts showed the blood glucose stabilization effect which in turn prevents the loss of body weight.

Glucose tolerance test is a standard procedure that determines how rapidly exogenous glucose can be cleared from the blood. Insulin is important for regulating the uptake of glucose from the blood by cells. Soni et al. (2018), explained impairment of glucose tolerance, which means takes a longer time to clear a given amount of glucose divulges problems with the maintenance of glucose homeostasis (insulin resistance, carbohydrate metabolism, diabetes, etc).

As seen in Table 2, in Group VI mice treated with a polyherbal extract at the dose of 400 mg/kg, a significant ($p < 0.001$) decrease in blood glucose level at 90 min and 120 min was observed as compared to Group-III treated with standard drug metformin. The results indicated that the polyherbal extract at the dose

of 400 mg/kg increases the clearance of the glucose from the blood which might be due to enhanced uptake of glucose from the cells which is regulated by insulin.

The diabetes was induced in mice after administration of streptozotocin-nicotinamide. As shown in Table 3, a consistent decrease in the blood glucose level was observed in the groups treated with metformin (Group III) and polyherbal extract-treated Groups IV, V and VI. In Group VI, polyherbal extracts at the dose of 400 mg/kg, a significant ($p < 0.001$) decrease in blood glucose level at 28 days was observed as compared to Group III treated with metformin (250 mg/kg, p.o.). While in Groups IV and V no significant decrease in blood glucose level at 28 days was observed as compared to Group III. The results suggest the potential effects of polyherbal extract-treated at dose of 400 mg/kg at 14, 21 and 28 days of treatments. The possible mechanism by which polyherbal extract brings about its hypoglycemic action in diabetic mice maybe by potentiating the insulin effect of plasma by increasing either the pancreatic secretion of insulin from the existing beta cells or by its release from the bound form.

Dyslipidaemia is a secondary complication accompanied by long term effects of diabetes and had been discussed many times during the past decades. During diabetes, the levels of TGL, cholesterol and LDL increase and the HDL levels decline significantly. In the diabetic model, abnormal concentrations of serum lipids might be due to a disturbance in hormone-sensitive enzyme lipase. The lipase enzyme concentration allows the mobilisation of free fatty acids from the peripheral fat repository because of insulin deficiency (Soni et al. 2018). The administration of polyherbal extract significantly restored cholesterol, TGL, LDL and HDL levels to their normal values in diabetic mice, which might be due to its lipid-lowering activity. Therefore, this polyherbal extract also plays a significant role against diabetes-associated complications.

Histopathology of the pancreas of STZ-NIC diabetic animals showed a severe decrease in

the number of islets of Langerhans and β cells, with fibrosis and inflammatory cell infiltration into the islets of Langerhans. Polyherbal extract and metformin treatment to the animals reduced the severity of the histopathologic changes caused by STZ.

Conclusion

Chemically active principles present in the studied plants may be responsible for the observed antidiabetic effect of the polyherbal extracts. The hypoglycaemic effect produced by the polyherbal formulations may be due to the glycosides, flavonoids, tannins, and saponins present in the extracts. From the present study, it could be concluded that the administration of polyherbal formulations containing extract of *Gymnema sylvestre*, *Boerhavia diffusa*, *Tinospora cordifolia* and *Argyreia nervosa* exhibited significant antidiabetic effects by controlling the blood glucose levels. Additionally, the polyherbal formulations decreased total cholesterol, triglycerides and LDL, with an increase in HDL at the end of the treatments. The polyherbal extract-treated Group VI (400 mg/kg) exhibited maximum antidiabetic activity compared to the polyherbal extract-treated Group IV (100 mg/kg) and Group V (200 mg/kg). The significant hypoglycaemic activity of the polyherbal formulation might be due to the varied mechanism of action of each herbal drug present in the formulations. Hence, the developed polyherbal formulation might prove to be a potential safe alternative for the existing anti-diabetic synthetic drugs.

Acknowledgement

The authors are thankful to Pune District Education Association for providing animal house facilities during study. The author Dr. Patil is thankful to the DS Kothari Fellowship program, University Grants Commission and Savitribai Phule Pune University for the financial support during the post-doctoral research, this research idea emerged during the study.

Ethics Approval and Ethical statement

The experimental protocols were approved by the Institutional Animal Ethical Committee of PDEA's Seth Govind Raghunath Sable College of Pharmacy, Saswad (Ref. No. SGRS/IAEC/07/2019-20).

References

- American Diabetes Association 2451 Crystal Drive, Suite 900, Arlington, VA 22202 1-800-DIABETES <https://www.diabetes.org/diabetes>
- Aralelimath VR and Bhise Sb 2012 Anti-diabetic effects of *Gymnema Sylvestre* extract on streptozotocin induced diabetic rats and possible B-cell protective and regenerative evaluations. *Digest J. Nanomater. Biostruct.* 7: 135-142.
- Birgani GA, Ahangarpour A, Khorsandi L and Moghaddam HF 2018 Anti-diabetic effect of betulinic acid on streptozotocin-nicotinamide induced diabetic male mouse model. *Braz. J. Pharm. Sci.* 54(2): 1-7
- Chaudhuri A and Sharma S 2016 Evaluation of antidiabetic activity of polyherbal formulation in streptozotocin induced diabetic rats. *Pharm. Biosci. J.* 4: 01-06.
- El-Shafey AAM, El-Ezabi MM, Selim MME, Ouda HHM and Ibrahim DM 2013 Effect of *Gymnema sylvestre* R. Br. leaves extract on certain physiological parameters of diabetic rats. *J King Saud Uni. Sci.* 25: 135-141.
- Galani VJ, Patel BG and Patel NB 2010 *Argyreia speciosa* (Linn. f.) sweet: a comprehensive review. *Pharmacogn. Rev.* 4(8): 172-178.
- Gosh MN 1984 Toxicity studies, Fundamentals of Experimental Pharmacology, Scientific Book Agency, Calcutta, pp. 153-158.
- Kanetkar P, Singhal R and Kamat M 2007 *Gymnema sylvestre*: a memoir. *J. Clin. Biochem Nutr.* 41(2): 77-81.
- Kanetkar P, Singhal R, and Kamat M 2007 "Gymnema sylvestre: a memoir. *J. Clin. Biochem. Nutr.* 41(2): 77-81.
- Kumar S and Alagawadi KR 2010 Hypoglycemic effect of *Argyreia nervosa* root extract in normal and streptozotocin-diabetic rats. *Der Pharmacia Lettre* 2(2): 333-337.
- Malhotra D, Ishaq F and Khan A 2014 Antihyperglycemic activity of *Boerhaavia diffusa* in streptozotocin induced diabetic rats. *Int. J. Chem. Anal. Sci.* 5(1): 21-23.
- Mandlik RV, Desai SK, Naik SR, Sharma G and Kohli RK 2008 Antidiabetic activity of a

- polyherbal formulation (DRF/AY/ 5001), *Indian J. Exper. Biol.* 46: 599-606.
- Maurya AK, Tripathi S, Kahrana M, Ahmed Z and Sahu RK 2011 Evaluation of antidiabetic effects of *Ficus racemosa* extracts in diabetic induced rats, *Pharmacologyonline* 3: 907-914.
- Mishra S, Aeri V, Gaur P and Jachak SM 2014 Phytochemical, therapeutic, and ethnopharmacological overview for a traditionally important herb: *Boerhavia diffusa* Linn. *BioMed Res. Int.* 2014: 808302, 19 pages.
- Mohapatra L, Bhattamishra SK, Panigrahy R, Parida S and Pati P 2016 Antidiabetic effect of *Sargassum wightii* and *Ulva fasciata* in high fat diet and multi low dose streptozotocin induced type 2 diabetic mice. *Pharm. Biosci. J.* 4: 13- 23.
- Mouri MI and Badireddy M 2019 Hyperglycaemia, Stat Pearls, Treasure Island, FL, USA, pp1-5.
- Nagja T, Kumar V and Sanjeev A 2017 Antidiabetic activity of a polyherbal formulation in streptozotocin induced type 2 diabetic rats. *J. Nat. Remed.* 16(4): 148-152.
- Petchi RR, Vijaya C and Parasuraman S 2014 Antidiabetic activity of polyherbal formulation in streptozotocin–nicotinamide induced diabetic Wistar rats. *J. Tradit. Complement. Med.* 4:108-117.
- Puranik N, Kammar K and Devi S 2010 Antidiabetic activity of *Tinospora Cordifolia* (willd.) in streptozotocin diabetic rats; does it act like sulfonylureas? *Turk. J. Med. Sci.* 40: 265-270.
- Rakieten N, Rakieten ML and Nadkarni MV 1963 Studies on the diabetogenic action of streptozotocin, *Cancer Chemother. Rep.* 29: 91-98.
- Sancheti SS and Seo SY 2009 *Chaenomeles sinensis*: A potent α -and- β glucosidase inhibitor. *Am. J. Pharmacol. Toxicol.* 4: 8-11.
- Scarpello JHB and Howlett HC 2008 Metformin therapy and clinical uses. *Diab. Vasc. Dis. Res.* 5: 157-167.
- Shah S, Manigauha A and Dubey B 2019 Formulation and evaluation of antidiabetic and antihyperlipidemic activities of polyherbal formulation in streptozotocin induced diabetic rat. *Pharm. Biosci. J.* 7(1): 26-30.
- Sharma P, Dwivedee BP, Bisht D, Dash AK and Kumar D 2019 The chemical constituents and diverse pharmacological importance of *Tinospora cordifolia*, *Heliyon* 5(9): e02437.
- Sheikh Y, Manral MS, Kathait V, Prasara B, Kumar R and Sahu RK 2015 Computation of in vivo antidiabetic activity of *Holarrhena antidysenterica* seeds extracts in Streptozotocin-induced diabetic rats. *Iranian J. Pharmacol. Therapeut.* 14(2): 22-27.
- Simon K and Wittmann I 2019 Can blood glucose value really be referred to as a metabolic Parameter? *Rev. Endocr. Metab. Disord.* 20: 151-160.
- Soni L, Dobhal M, Arya D, Bhagour K, Parasher P and Gupta R 2018 In vitro and in vivo antidiabetic activity of isolated fraction of *Prosopis cineraria* against streptozotocin-induced experimental diabetes: a mechanistic study. *Biomed. Pharmacother.* 108: 1015-1021.
- Srinivasan K and Ramarao P 2007 Animal models in type 2 diabetes research: an overview, *Indian J. Med. Res.* 125: 451-472.
- Srivastava S, Lal VK and Pant KK 2012 Polyherbal formulations based on Indian medicinal plants as antidiabetic phytotherapeutics, *Phytopharmacology* 2: 1-15.
- Turner RA 1965 Screening Method in Pharmacology, Academic Press, New York, pp. 22-41.
- Undale VR, Bhosale AV and Upasani CD 2014 Study of pharmacodynamic interaction between a polyherbal formulation BSL-150 and Metformin, *Pharm. Crops* 5: 67-76.
- Wild S, Roglic G, Green A, Sicree R and King H 2004 Global prevalence of diabetes-estimates for the year 2000 and projections for 2030. *Diabetes Care* 27(3): 1047-1053.
- Wright AD, Cull CA, Macleod KM and Holman RR 2006 Hyperglycaemia in type 2 diabetic patients randomized to and maintained on monotherapy with diet, sulfonylurea, Metformin, or insulin for 6 years from diagnosis: UKPDS73, *J. Diabet. Compl.* 20: 395-401.
- Yari Z, Behrouz V, Zand H and Pourvali K 2020 New insight into diabetes management from Glycemic index to dietary Insulin index, *Curr. Diabetes Rev.* 16(4): 293-300.
- Zhang P, McGrath B, Li S, Frank A, Zambito F, Reinert J, Gannon M, Ma K, McNaughton K and Cavener DR 2002 The PERK eukaryotic initiation factor 2 α kinase is required for the development of the skeletal system, postnatal growth and the function and viability of the pancreas. *Mol. Cell. Biol.* 22: 3864-3874.



Effect of *Solanum melongena* Linn. Leaves Extracts on Clonidine Induced Catalepsy and Milk Induced Leukocytosis and Eosinophilia in Mice

Ramdas N. Kale ^{1*}, Ravindra Y. Patil ²

¹ Department of Pharmacognosy, SVPM's College of Pharmacy, Malegaon BkII Tal- Baramati Dist- Pune 413115. India

² PDEA's Shankarrao Ursal College of Pharmaceutical Science and Research Centre, Kharadi, Pune 411014, India.

Address for Correspondence: Ramdas N. Kale, ramdas_udct@yahoo.com

Received:

24.12.2019

Accepted:

22.04.2020

Published:

15.04.2021

Keywords

Solanum melongena,
Catalepsy,
Leukocytes,
Eosinophilia.

ABSTRACT: Objective: To study the Effect of *Solanum melongena* Linn. leaves extracts on Clonidine induced catalepsy and milk induced Leukocytosis and Eosinophilia in mice. Methods: Methanolic and chloroform extracts of *Solanum melongena* Linn. leaves were prepared. Preliminary phytochemical screening of the prepared extracts was carried out. Effects of prepared extracts were studied on Clonidine induced catalepsy and milk induced leukocytosis and eosinophilia in mice. Results: Maximum duration of catalepsy was observed at 90 min after the clonidine administration. There was significant inhibition ($p < 0.05$) of clonidine induced catalepsy in the animals pretreated with chlorpheniramine maleate, methanol and chloroform extract of *S. melongena*. Administration of milk (4mg/kg) subcutaneous route exhibited significant increase in leucocyte and eosinophil count after 24 hrs of administration. Chloroform extract at the dose of 500mg/kg body weight showed significant inhibition ($p < 0.05$) of milk induced leukocytosis and eosinophilia. Conclusions: These results suggest that *Solanum melongena* leaves extract may have the potential therapeutic value in the treatment of allergic diseases. © 2020 iGlobal Research and Publishing Foundation. All rights reserved.

Cite this article as: Kale, R.N.; Patil, R.Y. Effect of *Solanum melongena* Linn. leaves extracts on clonidine induced catalepsy and milk induced Leukocytosis and Eosinophilia in mice. Indo Global J. Pharm. Sci., 2021; 11(2): 110-114 . DOI: <http://doi.org/10.35652/IGJPS.2021.112005> .

INTRODUCTION

Solanum melongena Linn (Solanaceae) is an erect or suffrutescent, herbaceous, armed or unarmed plant[1]. It is a culinary vegetable, has been in use in the Indian system of medicine[2]. Besides, having many traditional uses *Solanum melongena* is reported to exhibit many important pharmacological actions. Various parts are reported to have analgesic & antipyretic[3], anti-inflammatory[4], hypolipidemic[5], Anti asthmatic[6], spasmogenic[7] and hypotensive action[8]. Flavonoids isolated from *S. melongena* showed potent antioxidant activity[9]. *S. melongena* is also a natural source of vitamin A. It would play an important role for vision and eye health[10]. The plant has been investigated for the presence of chemical constituents, quercetin 3-O-rhamnoside, kaempferol-3-O-rhamnoside[11] and alkaloidal fractions were isolated from the leaves.

Catalepsy is a condition in which the animal maintains imposed posture for long time before regaining normal posture. Catalepsy is the sign of extrapyramidal effect of drugs that inhibit dopaminergic transmission or increase histamine release in brain. Clonidine, a α_2 adrenoreceptor agonist induces dose dependent catalepsy in mice, which is inhibited by H_1 receptor antagonist but not by H_2 receptor antagonist[12].

During asthmatic inflammation leukocyte release cytokines, histamine and major basic protein promote ongoing inflammation[13]. An abnormal increase in peripheral eosinophils count more than 4% of total leukocyte is termed as eosinophilia[14]. In the present investigation we have evaluated effect of *Solanum melongena* Linn. leaves extracts on Clonidine induced catalepsy and milk induced Leukocytosis and Eosinophilia in mice.

MATERIALS AND METHODS

Collection of plant material

The leaves of *Solanum melongena* were collected from the rural areas of Baramati Dist-Pune (Maharashtra) and identified in the Department of Botany, Agricultural Development Trust's Shardabai Pawar Mahila Mahavidyalaya, Shardanagar Malegaon BkII Tal-Baramati Dist-Pune, Maharashtra, India. (Voucher specimen PASR-140)

Drugs and chemicals

The drugs used were: clonidine (Neon Lab. Ltd., India), chlorpheniramine maleate (Pfizer Ltd.) and dexamethasone (Zydus Healthcare Ltd); all were purchased from commercial source. Chemicals used were: Methanol and chloroform (Research Lab. Industries, India)

Extract preparation and phytochemical screening

The leaves of *Solanum melongena* were dried and crushed to coarse powder. Powdered material was subjected to soxhlet extraction with methanol and chloroform as a solvent. Extracts so obtained were concentrated to dryness by evaporating the solvent. Yields were calculated. Extracts were stored at room temperature and protected from direct sunlight. Both the extracts were separately subjected to preliminary phytochemical screening using standard tests.

Animals

Swiss albino mice (20-30gm) of either sex were obtained from National Institute of Biosciences, Pune, India. Animals were maintained in our animal house under standard laboratory condition. Animals were exposed to day night light cycle and room temperature (24 ± 2)⁰C. All animals are allowed free access to ready-made food pellets and water. Animals were handled according to standard protocols for the use of laboratory animals[15]. The experimental protocol was approved by the Institutional Animal Ethics Committee (1214/ac/08/CPCSEA).

Acute toxicity study

Acute toxicity study was performed by oral route in mice as per OECD guidelines 423.

Clonidine induced catalepsy in mice

Bar test was performed to study effect of clonidine induced catalepsy[16-18]. Clonidine (1mg/kg, s.c.) was injected to mice (n=6). Before 1 h of clonidine treatment, group I received dist. Water (1ml/kg i.p.) group II received Chlorpheniramine maleate (10mg/kg body weight, i.p.) group III received methanolic extract (250mg/kg body weight i.p.) group IV received methanolic extract (500mg/kg body weight i.p.) group V received chloroform extract (250mg/kg body weight i.p.) and group VI received chloroform extract (500mg/kg body weight i.p.) Forepaws of mice were placed on horizontal bar and time required to remove the paws for each animal was noted and duration of catalepsy were measured at 15, 30, 60, 90 and 120 min.

Milk induced Leukocytosis and Eosinophilia in mice

Swiss albino mice of either sex weighing between 20-30g were divided into six groups of five animals each. All animals received boiled (boiling temp 70°C and boiling time 20 min) and cooled milk in dose of 4 ml/kg subcutaneously. Animal belong to group I treated as control and received distilled water 10 ml/kg. p.o. Group II received methanolic extract 250mg/kg.p.o.(MESML250), Group III received methanolic extract 500mg/kg.p.o.(MESML500) Group IV received chloroform extract 250mg/ kg.p.o.(CESML250) Group V received chloroform extract 500mg/ kg.p.o.(CESML500), whereas group VI received Dexamethasone 50mg/kg i.p. All the extracts and standard drug were administered 1h before milk injection. Blood samples were collected before and 24 h after milk administration from the retro orbital plexus, under light ether anesthesia. Difference in total leukocyte and eosinophil count before and after 24h drug administration were calculated [19].

Statistical analysis

The mean \pm SEM values were calculated for each group. The statistical analysis was performed using one way analysis of variance (ANOVA) followed by Dunnett's test for individual groups comparison with control. A probability value less than 0.05 were considered as significant.

RESULTS AND DISCUSSION

Acute toxicity study

Treatment with methanol and chloroform extract up to 2000mg/kg orally to mice did not induce mortality. Hence LD₅₀ was considered to be more than 2000 mg/kg. Based on acute toxicity results 250 and 500 mg/kg doses were selected.

Preliminary phytochemical screening

Table 1 represents the results of the phytochemical screening for both methanolic extract as well as chloroform extract.

Table1. Phytochemical screening of the extracts

Phytoconstituents	Methanol extract	Chloroform extract
Alkaloids	+++	+++
Flavonoids	++	+++
Saponins	+	-
Tannins	++	++
Steroids	+	+

+++; strong intensity reaction, ++: medium intensity reaction, +: Weak intensity reaction, -:Not detected

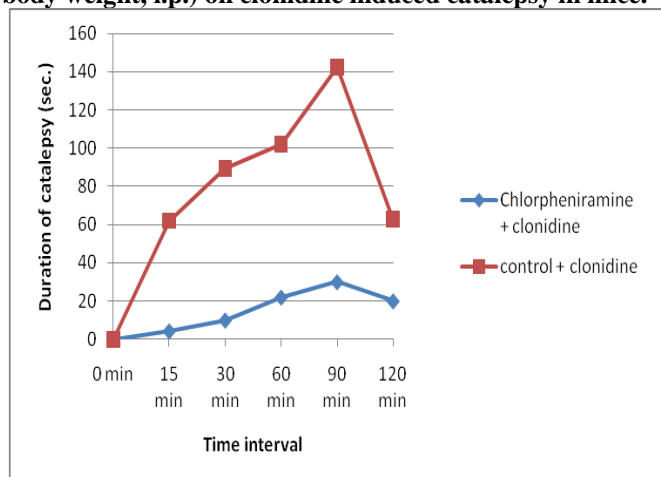
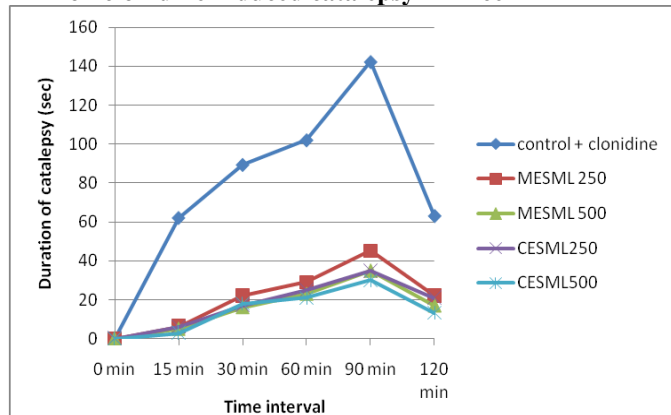
Clonidine induced catalepsy

All the groups showed maximum duration of catalepsy at 90 min after the clonidine administration. There was significant inhibition ($p < 0.05$) of clonidine induced catalepsy in the animals pretreated with chlorpheniramine maleate, methanolic extract and chloroform extract (**Table 2, Figure 1 and 2**).

Table 2. Effect of various extracts of *Solanum melongena* on clonidine induced catalepsy in mice

Group	Duration of catalepsy (Sec), Mean±SEM				
	15min	30 min	60 min	90 min	120min
Contr ol	62.00±4.465	89.33±4.828	102.00±.819	142.33±12.387	63.00±5.190
Std	4.33±0.667*	10.00±1.461*	22.00±3.367*	30.00±2.295*	20.00±1.414*
MES ML 250	6.33±1.116*	22.00±3.055*	29.00±3.215*	45.167±7.692*	22.167±3.911*
MES ML 500	5.00±0.856*	16.167±2.27*	23.00±2.324*	35.00±2.530*	17.00±2.422*
CESM L 250	6.00±0.966*	17.00±1.317*	25.00±2.887*	35.00±2.221*	21.00±1.653*
CESM L500	3.00±0.577*	18.00±1.065*	21.00±1.571*	30.00±2.422*	13.33±0.882*

*p<0.05

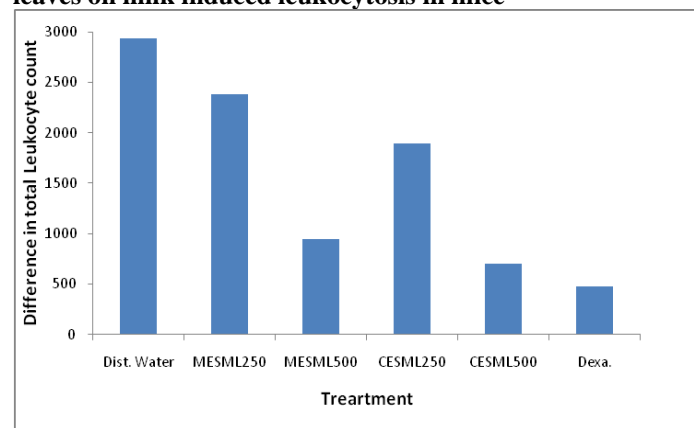
Figure 1. Effect of Chlorpheniramine maleate (10mg/kg body weight, i.p.) on clonidine induced catalepsy in mice.**Figure 2. Effect of various extracts of *Solanum melongena* Linn on clonidine induced catalepsy in mice****Milk induced Leukocytosis and Eosinophilia in mice**

Subcutaneous administration of boiled and cooled milk at dose of 4ml/kg. showed a significant increase in the leukocytes and eosinophils count after 24h as compared to leukocyte count before milk administration (Table 3 and 4; Figure 3 and 4).

Table 3. Effect of various extracts of *Solanum melongena* leaves on milk induced Leukocytosis in mice

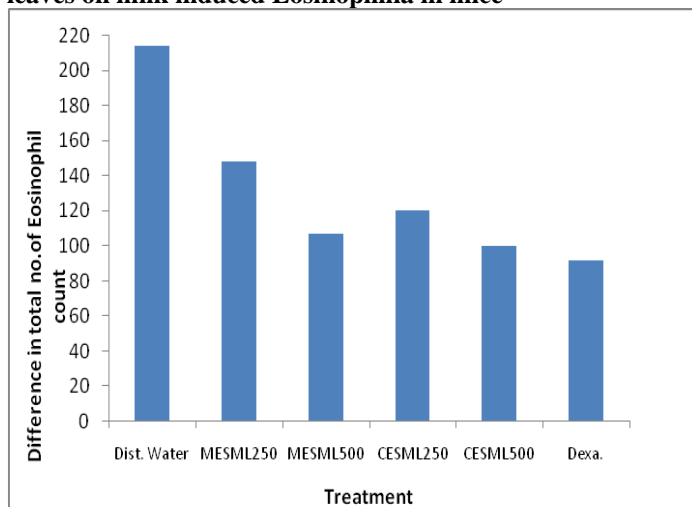
Group	Treatment	Difference in Total leukocyte count (Per cu mm) (Mean ± SEM)
I	Dist. Water	2936.00 ± 487.13
II	MESML250	2386.00 ± 374.13
III	MESML500	943.00 ± 98.78*
IV	CESML250	1891.00 ± 191.19
V	CESML500	706.00 ± 172.81**
VI	Dexamethasone (50mg/kg i.p.)	476.00 ± 110.40***

*p<0.004, **P<0.003, ***p <0.001

Figure 3. Effect of various extracts of *Solanum melongena* leaves on milk induced leukocytosis in mice**Table 4. Effect of various extracts of *Solanum melongena* leaves on milk induced Eosinophilia in mice**

Group	Treatment	Difference Total eosinophil count (Per cu mm) (Mean ± SEM)
I	Dist. Water	214.00 ± 38.64
II	MESML250	148.00 ± 15.29**
III	MESML500	107.00 ± 11.35
IV	CESML250	120.00 ± 18.16
V	CESML500	100.00 ± 22.36*
VI	Dexamethasone (0.5mg/kg i.p.)	92.00 ± 22.00***

*p<0.03, **P<0.029, ***p <0.025

Figure 4. Effect of various extracts of *Solanum melongena* leaves on milk induced Eosinophilia in mice

It is known that clonidine releases histamine from mast cells[20]. Clonidine induced release of histamine from mast cells is inhibited by α_2 adrenoceptor blocker. In the present investigation, all groups showed maximum duration of catalepsy at 90 min after the clonidine administration. There was significant inhibition ($p < 0.05$) of clonidine induced catalepsy in the animals pretreated with *Solanum melongena* extract. This indicates antihistaminic activity of the *Solanum melongena*.

After parenteral administration of milk there is increase in total leukocyte and eosinophil count, this stressful condition can be normalized by administration of an antistress or adaptogenic drug. The involvement of eosinophil in bronchial mucosa, in which allergic inflammation occurs, is a critical contributor to the late asthmatic reaction of congestion and mucus hypersecretion. In the late phase, especially in the development of allergic asthma, eosinophil plays role as inflammatory cell. Eosinophil secretes mediators such as eosinophil cationic protein, tumor necrosis factor, eosinophil derived neurotoxin and prostaglandin results in epithelial shedding, bronchoconstriction and promotion of inflammation in respiratory tract often allergic. In the present study it has been found that, parenteral administration of milk at a dose of 4ml/ kg significantly induced the total leukocyte and eosinophil count ($p < 0.001$) after 24 hours. Animals of the group treated with chloroform extract (500mg/ kg body weight) of *S. melongena* significantly inhibited increase in number of total leukocyte and eosinophil count.

CONCLUSION

The results of present study revealed that *Solanum melongena* leaves extract inhibit the clonidine induced catalepsy and milk induced leukocytosis and eosinophilia in mice, suggests its potential antihistaminic and antiallergic activities. However we are screening *Solanum melongena* leaves extract for other animal models of asthma to evaluate its efficacy in the management of asthma. We are also working on

phytochemical investigation of these extracts to pin point the chemical constituents responsible for the activity

ACKNOWLEDGEMENTS

We express our sincere thanks to Management and Principal of SVPMs College of Pharmacy, Malegaon BkII Tal Baramati Dist Pune for providing necessary research facility for this study. We also express our gratitude to Prof. R.B. Deshmukh, Head, Dept. of Botany, Agricultural Development Trust's Shardaibai Pawar Mahila Mahavidyalaya, Shardanagar Tal-Baramati for the authentication of plant.

CONFLICT OF INTEREST

The authors have no conflict of interest.

FUNDING SOURCE

There is no source of funding.

DATA AVAILABILITY

Not declared.

REFERENCES

- [1] Warrier PK, Nambier VPK, Ramanakutty C. Indian Medicinal Plants. Orient Longman Publishers Ltd .Madras: India; 1996; 157
- [2] Mutalik S, Paridhavi K, Mallikarjuna Rao C, Udupa N. Antipyretic and analgesic effect of leaves of *Solanum melongena* Linn. in rodents. Indian Journal of Pharmacology 2003; 35: 312-315.
- [3] Vohora SB, Kumar I, Khan MS. Effect of alkaloids of *Solanum melongena* on the central nervous system. J Ethnopharmacol. 1984; 11:331-336.
- [4] Han SW, Tae J, Kim JA, Kim DK, Seo GS, Yun KJ, et al. The aqueous extract of *Solanum melongena* inhibits PAR2 agonist-induced inflammation. Clin Chim Acta 2003; 328:39-44.
- [5] Sudheesh S, Presannakumar G, Vijaykumar S, Vijayalakshmi N.R., Hypolipidemic effect of Flavonoids from *Solanum melongena*. Plant Food Human Nutr. 1997; 51, 321-330.
- [6] Bello SO, Muhammad B, Gammaniel KS, Aguye AI, Ahmed H, Njoku CH, et al. Randomized double blind placebo controlled clinical trial of *Solanum melongena* L. fruit in moderate to severe asthmatics. J Med Sci 2004; 4:263-269.
- [7] Mans DRA, Toelsie J, Mohan S, Jurgens S, Muhringen M, Illes S, et al. Spasmogenic effect of a *Solanum melongena* leaf extract on guinea pig tracheal chains and its possible mechanism(s) J. Ethnopharmacol 2004; 95: 329-333.
- [8] Shum OL, Chiu KW. Hypotensive action of *Solanum melongena* on normotensive rats. Phytother Res. 1991; 5:76-81.
- [9] Sudheesh S, Sandhya C, Asha S.K, Vijayalakshmi N.R., Antioxidant activity of Flavonoids from *Solanum melongena* Phytother Res 1999; 13, 393-396.
- [10] Nish P, Abdul Nazar P, Jayamurthy P., A comparative study on antioxidant activities of different varieties of *Solanum melongena*. Food and chemical Technology 2009; 47: 2640-2644.
- [11] Barnabas CGG, Nagarajan S., Chemical and pharmacological studies on the leaves of *Solanum melongena* Fitoterapia. 1989; 60(1): 77-78.
- [12] Jadhav JH, Balsara JJ, Chandorkar AG. Involvement of histaminergic mechanisms in the cataleptogenic effect of clonidine in the mice. J Pharm Pharmacol 1983; 35: 671-673.

- [13] Brekhman LI, Dardymov IV. New specific substances of plant origin, which increases nonspecific resistance. *Ann Rev Pharmacol* 1969; 9: 419-428.
- [14] Mali RG, Dhake AS Evaluation of effects of Bauhina variegata bark extracts against milk induced eosinophilia in mice *J Adv Pharm Technol Res* 2011; 2(2): 132-134.
- [15] National Research Council. Guide for the care and use of laboratory animals. Washington DC: Institute for Laboratory Animal research, National Academics Press; 2011; 11-40.
- [16] Ferre S, Guix T, Prat G, Jane F, Casas M. Is experimental catalepsy properly measured? *Pharmac Biochem Behav.* 1990; 35: 753-757.
- [17] Taur DJ, Nirmal SA, Patil RY. Effect of various extracts of Ficus bengalensis bark on clonidine and haloperidol-induced catalepsy in mice. *Pharmacologyonline.* 2007; 3: 470-477.
- [18] Ghaisas MM., Bulani VD., Suralkar AA., Limaye R.P. Effect of *Calotropis gigantea* on clonidine and haloperidol induced catalepsy. *Pharmacologyonline* 2009; 3:484-488.
- [19] Bhargava, K.P., Singh, N. Anti-stress activity of *Ocimum sanctum* Linn. *Indian J Med Res* 1981; 73: 443-451.
- [20] Lakadwala AD, Dadkar NK, Dohadwala AN. Action of clonidine on mast cells of rats. *Pharm Pharmacol.* 1980; 32: 790-791.



Contents lists available at UGC-CARE

International Journal of Pharmaceutical Sciences and Drug Research

[ISSN: 0975-248X; CODEN (USA): IJPSPP]

journal home page : <http://ijpsdr.com/index.php/ijpsdr>

Research Article

Studies on Nephroprotective Effect of Methanolic and Aqueous Extract of Bark of *Pithecellobium Dulce* Roxb. in Rats

Ravindra Patil¹, Surekha Yamgar^{2*}¹Department of Pharmacognosy, PDEA's Shankarrao Ursal College of Pharmaceutical Sciences and Research Center, Kharadi, Pune, Maharashtra, India²Department of Pharmacognosy PDEA's Seth Govind Raghunath Sable College of Pharmacy, Saswad, Pune, Maharashtra, India

ARTICLE INFO

Article history:

Received: 03 August, 2021

Revised: 29 August, 2021

Accepted: 08 September, 2021

Published: 30 September, 2021

Keywords:

Creatinine,
Nephroprotective,
Pithecellobium Dulce,
Tannins.

DOI:

10.25004/IJPSDR.2021.130516

ABSTRACT

Kidney failure is a major problem of worldwide proportions. Kidney injury is a sudden loss of kidney function resulting in the accretion of waste materials such as creatinine and urea in the body. There are various agents that exert nephrotoxic effects through distinctive morbid defence mechanisms. Gentamicin, cisplatin and paracetamol are among common nephrotoxicity agents. In recent years, natural compounds are being expanded used in the treatment of kidney diseases. With this backdrop the study has been designed with the aim to studies on nephroprotective effect of methanolic and aqueous extract of bark of *Pithecellobium Dulce* Roxb. in rats. The methanolic and aqueous extracts of bark of *P. Dulce* was studied for nephroprotective effect in female Wistar rats against cisplatin, gentamicin and paracetamol induced nephrotoxicity, by estimating serum creatinine, blood urea and serum albumin levels. The dried bark of *P. Dulce*, Roxb (*Leguminosae*), contains tannins, flavonoids, triterpenoids, beta-sitosterol and saponin glycoside. Treatments with the methanolic and aqueous extracts could significantly ($P < 0.001$) reduce the elevated serum levels of creatinine, blood urea and serum albumin. *P. Dulce* bark extracts significantly prevented the physical, biochemical, histological and structural changes induced by cisplatin, gentamicin and paracetamol in the kidney. The present study reports with the exploration of *P. Dulce* bark extracts possessed *implicit* nephroprotective activity. This activity may be attributed due to the abundant phytoconstituents of the plant extracts.

INTRODUCTION

Nephrosis is a chronic disorder of environmental toxicant, noxious chemicals, and drugs, including antibiotics, drugs used in chemotherapy like cisplatin, almighty alter the structure or internal functioning of several organs and create harmful effects on kidney, heart, pancreas and intestine etc.^[1] Polygenic disorder like diabetes is the most common cause of kidney failure, accounting for nearly 44 percent of the diabetic cases.^[2]

Even when diabetes is controlled, the disease can lead to kidney failure. Many people with diabetes do not develop chronic kidney disease (CKD) that is severe enough to progress to kidney failure. Nearly 24 million people in the United States have diabetes.^[3] Nephrogenic fibrosing dermopathy is a common significance of chronic kidney failure. In all cases, the expanse of production

and deposition of extracellular matrix (ECM) proteins in the kidney firmly correlates with disease asperity, impairment of renal function and subsequent progression to end-stage renal disease (ESRD).^[4]

Kidney being one of the indispensable organs of human body performing the function of removing toxic substances needs protection for healthy life. As stated above, the prevalence of the kidney disorders needs to be seriously viewed. Ethno-medicinal plants can be acclimated to advice apprehend the charge for dialysis by treating the causes and after effect of kidney failure, as well as reducing the many adverse effect of dialysis. In the established pharmacopoeia, *P. dulce* bark reduced into powder percolated in alcohol or water is used to pyrexia and diarrhea, injury chancres, sickness, and seizure.^[5] *P. dulce* prohibited *Naja kaouthia* venom activities by

*Corresponding Author: Surekha Yamgar

Address: Department of Pharmacognosy PDEA's Seth Govind Raghunath Sable College of Pharmacy, Saswad, Pune, India

Email ✉: surekhayamgar@gmail.com

Tel.: +91-9987919468

Relevant conflicts of interest/financial disclosures: The authors declare that the research was conducted in the absence of any commercial or financial relationships that could be construed as a potential conflict of interest.

Copyright © 2021 Ravindra Patil *et al.* This is an open access article distributed under the terms of the Creative Commons Attribution- NonCommercial-ShareAlike 4.0 International License which allows others to remix, tweak, and build upon the work non-commercially, as long as the author is credited and the new creations are licensed under the identical terms.

precipitating venom proteins due to condensed tannins.^[6] In fact, relating to aqueous and alcoholic stem bark extract contains excessive amounts of phenolic compounds including, flavonoids and pro-anthocyanidin. The dried bark of *P. dulce*, (*Leguminosae*), is tree indigenous to the America, central Asia and India. The bark yields 37% tannins of the catechol type while the leaves yield quercetin, kaempferol, dulcitol and afezilin.^[7] The bark of *P. dulce* is utilized for treatment of liver disorders.^[8] It also acts probably by scavenging the free radicals and inhibition of generation of oxygen species.^[9] The drug has not yet explored for the treatment of kidney disorders and there is a high probability that the drug would prove to be beneficial in offering protection against the kidney failure in patients suffering from diabetes, hypertension and cardiac disorders.

The bark has found to lower the blood glucose levels of alloxan induced diabetes in rats.^[10] With this background the study has been designed with the aim to evaluate the bark of *P. Dulce*, Roxb (*Leguminosae*), for its nephroprotective activity so that the drug can be utilized to protect kidneys, as the organ needs serious attention in the contemporary lifestyle.

MATERIALS AND METHODS

Plant Material

The barks of *P. Dulce* (family- *Leguminosae*) were collected from Chopda area of the district-Jalgaon, during the months of April to June and authenticated by department of Biodiversity and Palaeobiology, Maharashtra Association for the Cultivation of Science, Agharkar Research Institute, Pune-411004 (Certificate number AUTH 19-129 and Reference No – COPS/2661/2018-19). The sample has been critically studied with the help of microscope, organoleptic characters and TLC profile.

Drugs and Chemicals

The following chemicals were used for the study, cisplatin injection (Cismax 50 GLS Pharma limited), gentamicin injection (Gentalab, Laborate Pharmaceutical India Ltd), paracetamol (Paracip500, Cipla) urea estimation kit (Yucca Diagnostics), creatinine estimation kit (Delta Lab) and albumin kit (Pathozyme diagnostics).

Preparation of the Extract

The barks were shade dried for weeks. The dried barks were further chopped into small pieces and reduced to powder. *P. Dulce* bark powdered (250 gm) were defatted by extracting with petroleum ether (60–80°C), followed by extraction with methanol using soxhlet extractor. The methanolic extract was then concentrated rotary flash evaporator to a syrupy consistency. The residual solvent was removed by drying the extract in vacuum oven (yield - 25.5 gm). The aqueous extract of the plant was prepared by using the cold maceration process.

The extract was then evaporated to dryness and the yield was noted (23.40 gm) and stored in air-tight, amber colored containers at room temperature for further proposed experimental studies.

Phytochemical Screening

The extract obtained was subjected to qualitative tests for identification of different phytoconstituents like alkaloids, tannins, glycosides, phenolic, flavonoids, proteins and steroids, by using standard and simple qualitative methods.^[11]

Acute Toxicity Studies

Acute oral toxicity studies were performed as per OECD Guidelines 423. The study required female rats to be tested at the dose of 300 and 2000 mg/kg b.w.p.o. The animal was observed continuously first 30, 60, 120, 180 and 240 minutes after dosing, with special attention and once daily thereafter, for a total of 14 days. All animal showed no clinical signs of intoxication. Extracts did not cause mortality in the female rats.

Pharmacological Study

Animals

Healthy female wistar rats (180–200 gm each) were used for the study. The animals were housed in polypropylene cages with stainless steel grill top and maintained under standard environmental conditions such as temperature ranging from $22 \pm 3^\circ\text{C}$, relative humidity $55 \pm 5\%$ and illumination cycles set to 12 hours dark/light cycle. All the animals were fed with rodent pellet diet and water *ad libitum* under strict hygienic conditions. All procedures were performed in accordance with CPCSEA guidelines after approval from the Institutional Animal and Ethics Committee (IAEC) of the Crystal Biological solution [No. CRY/2021/006 & 2030/PO/RcBiBt/S/18/CPCSEA].

Evaluation of Nephroprotective Activity

Cisplatin-induced Nephrotoxicity^[12]

Nephrotoxicity was induced by administering dose of cisplatin 5 mg/kg b.w.i.p. for seven consecutive days.

Gentamicin-induced Nephrotoxicity^[13]

Nephrotoxicity was induced by administering dose of gentamicin 100 mg/kg b.w.i.p. for seven consecutive days.

Paracetamol-induced Nephrotoxicity^[14]

Nephrotoxicity was induced by administering dose of paracetamol (2 g/kg) per orally on 7th day.

Treatment Schedule: The female Wistar rats (180-200 g) were divided into ten groups (n=6). The animals are given the following treatment in the study.

- **Group I:** Normal control (vehicle) group received gum acacia mucilage 2% w/v.
- **Group II:** Disease control group received single dose of cisplatin (5mg/kg b.w. i.p.) on day one.

- **Group III:** Cisplatin + methanolic extract of *P. Dulce* (500 mg/kg b.w.p.o) once a day, from day 1 to day 6.
- **Group IV:** Cisplatin + aqueous extract of *P. Dulce* (500 mg/kg b.w.p.o) once a day, from day 1 to day 6.
- **Group V:** Disease control group were injected with gentamicin (100 mg/kg b.w.i.p) for seven consecutive days.
- **Group VI:** Rats in this group were injected with gentamicin (100 mg/kg b.w.i.p) and administered methanolic extract of *P. Dulce* (500 mg/kg b.w.p.o) for seven consecutive days.
- **Group VII:** Rats in this group were injected with gentamicin (100 mg/kg b.w.i.p) and administered aqueous extract of *P. Dulce* (500 mg/kg b.w.p.o) for seven consecutive days.
- **Group VIII:** Disease control group were given paracetamol (2 g/kg b.w.p.o) per orally on 7th day.
- **Group XI:** Rats in this group the methanolic extract of *P. Dulce* (500 mg/kg b.w.p.o) were given for seven consecutive days followed by paracetamol (2 g/kg b.w.p.o) on the last day.
- **Group X:** Rats in this group the aqueous extract of *P. Dulce* (500 mg/kg b.w.p.o) were given for seven consecutive days followed by paracetamol (2 g/kg b.w.p.o) on the last day.

At the end of the experiment, blood sample were collected by puncturing retro-orbital plexus. Collected blood samples were centrifuged for separation of serum. The serum was separated and processed for estimation of biochemical parameters like serum creatinine, blood urea level and albumin.

Biochemical Estimations and Histopathological Studies

On 7th day, blood was withdrawn from retro-orbital plexus and serum was separated. The serum and urea samples were used for biochemical estimations like serum creatinine, urea, and albumin. All biochemical analysis was conducted using standard test kits. These kits were used as per the directions given along with it; Smart 5 Semi auto Biochemistry analyzer was used for the analysis. After end of the study, the animals from each group were sacrificed and kidneys were isolated. The rat kidney identified and carefully dissected for histopathological examination. All the preserved organs/tissues samples such as skin from all the groups were processed routinely and embedded in paraffin. The sections of 3-5 μ thickness were cut and stained with hematoxylin-eosin stain and observed under 40x. Histopathology examinations of all the thin sections were examined carried out and noted down.

Estimation of Serum Creatinine: Creatinine levels were estimated using the standardized kits which followed the Jaffe's reaction. Creatinine reacts with alkaline picrate (in ratio of 1:1) a colored creatinine picrate complex produces reddish color. The absorbance of the color complex is

directly proportional to creatinine concentration in sample. It was measured at 492 nm (480-520 nm).

Estimation of Urea: Urea reacts with urease GLDH reagent and then urea decomposes to form ammonia, which further reduces to form NAD⁺. The rate of formation of NAD⁺ is directly proportional to the amount of urea present in the sample and it is estimated by monitoring absorbance change within fixed time at 340 nm wavelength

Estimation of Serum Albumin: Albumin reacts with a dye bromocresol green in a buffered medium to form a green colored complex. The intensity of the color formed is directly proportional to the amount of albumin present in the sample. The absorbance of sample was measured at 546 nm.

Statistical Analysis

The experimental data was obtained from the biochemical estimations were expressed as mean \pm SEM for each group. The statistical analysis was conducted using one-way analysis of variance (ANOVA) followed by Dunnett's multiple comparison tests. Values $p > 0.05$ were considered non-significant, $p < 0.05$ as significant, $p < 0.01$ as highly significant and $p < 0.001$ as very highly significant respectively. All experimental data was computed for statistical analysis by using graph pad prism software.

RESULTS AND DISCUSSION

Phytochemical Screening: Phytochemical screening results showed the presence of carbohydrates, flavonoids, proteins, phenol, steroid and tannin.

Acute Toxicity Studies: Acute oral toxicity for methanolic and aqueous extracts of *P. dulce* Roxb. bark using wistar rats, according to the OECD Guidelines, 423, was found to be in GHS Category 5, > 2000–5000 mg/kg body weight, with a LD₅₀ cut off at 5000 mg/kg body weight. Animal did not cause any mortality during the study. All the animals showed no clinical signs of toxicity immediately after dosing and appeared normal up to four hours and showed no clinical signs of intoxication at daily observations up to 14 days. As the oral LD₅₀ cut off value of the extracts of was found to be safe for use.

Biochemical Estimations

cisplatin (CP), gentamicin (GM) and paracetamol (PC) treated rats developed polyuric acute renal failure as assessed by measuring different biochemical parameters like blood urea, plasma creatinine and plasma albumin. The blood urea level in CP, GM, and PC treated rats increased significantly (** $P < 0.001$) compared with the vehicle treated group. Plasma creatinine levels were also increased very highly significantly in CP, GM, and PC treated rats. CP and GM treatment plasma albumin level increased significantly, and PC treated animals were having significantly (* $P < 0.05$) changes compared with vehicle treated animals. (Table 1).



After treatment with the methanolic extract, values of urea, creatinine and albumin were reduced significantly as compared to disease control but it seems less effective than methanolic extract (Figs. 1–3).

After treatment with the methanolic extract values of urea, creatinine and albumin were reduced significantly as compared to disease control was observed in GM-treated animals. In aqueous treated

group values for urea, creatinine and albumin were decreased significantly as compared to disease control but it seems less effective than methanolic extract (Fig. 4–6).

After treatment with the methanolic extract, values of urea, creatinine and albumin were reduced significantly as compared to disease control, but it seems less effective than methanolic extract (Fig. 7–9).

Table 1: Effect of administration of methanolic and aqueous extracts of *P. Dulce* bark on various biochemical parameters in cisplatin (CP), gentamicin (GT) and paracetamol (PC) induced renal damage.

Sr. No	Group	Urea (mg/dL)	Creatinine (mg/dL)	Albumin (g/dL)
I	Vehicle	38.342 ± 2.139	0.546 ± 0.140	2.900 ± 0.051
II	Disease Control- Cisplatin	72.392 ± 3.606***	1.142 ± 0.388***	3.855 ± 0.064 ***
III	Cisplatin + Methanol extract	51.217 ± 3.324 ***	0.586 ± 0.067 ***	2.978 ± 0.154 ***
IV	Cisplatin + Aqueous extract	63.713 ± 2.839 ***	0.632 ± 0.059 **	3.612 ± 0.062 ***
V	Disease Control -Gentamicin	144.601 ± 9.238 ***	1.897 ± 0.341 ***	3.815 ± 0.045 ***
VI	Gentamicin + Methanol extract	57.875 ± 4.186 ***	0.735 ± 0.098 ***	2.820 ± 0.055***
VII	Gentamicin + Aqueous extract	82.939 ± 5.664 ***	0.995 ± 0.145 ***	3.213 ± 0.046 ***
VIII	Disease control - Paracetamol	76.343 ± 5.779 ***	1.152 ± 0.396 ***	2.978 ± 0.050 *
XI	Paracetamol+ Methanol extract	39.243 ± 3.312 ***	0.566 ± 0.074 ***	2.860 ± 0.034 ***
X	Paracetamol+ Aqueous extract	43.231 ± 3.656 ***	0.580 ± 0.076 ***	2.887 ± 0.042 **

Values are expressed as Mean ± S.E.M. (n=6). The disease control group is compared with vehicle group and the treated groups are compared with the disease control group by One way ANOVA test followed by Dunnette's multiple comparison test ***P < 0.001 **P < 0.01, *p < 0.05.

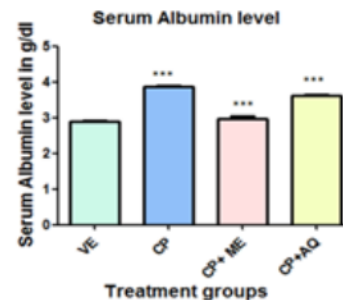
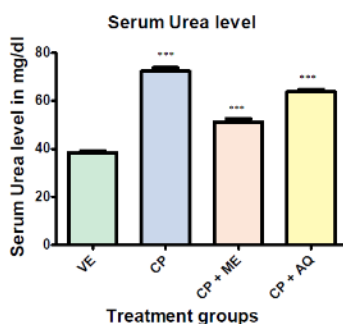
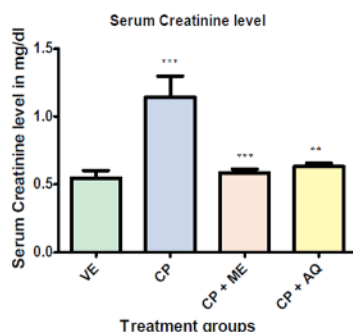


Fig. 1 & 2: Effect of *P. Dulce* on Serum Creatinine and Urea in Cisplatin induced nephrotoxicity in rats

Fig. 3: Effect of *P. Dulce* on Serum Albumin in Cisplatin-induced nephrotoxicity in rats.

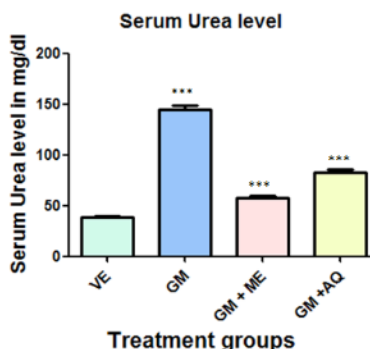
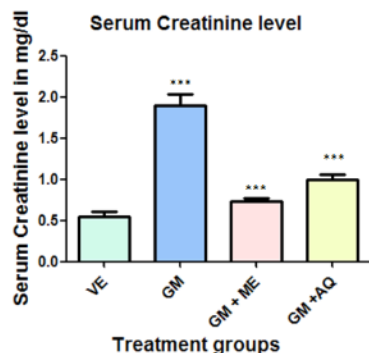


Fig. 4 & 5: Effect of *P. Dulce* on Serum Creatinine and Urea in Gentamicin induced nephrotoxicity in rats

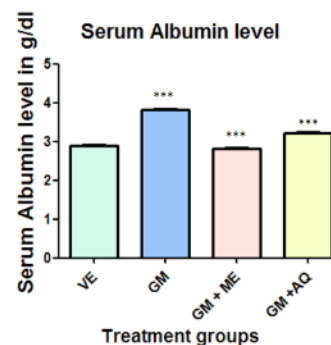


Fig.6: Effect of *P. Dulce* on Serum Albumin in Gentamicin induced nephrotoxicity in rats

Body Weight of Animals

Animals were measured for their body weights at day 1 and just before sacrifice. Bodyweight was increased but not significantly observed in all the animals. In groups II and V body weight gained was not considered as compared to the vehicle control group (Table 2).

Histopathological Studies

Microscopic examination of the kidney showed the highest toxicity in diseased groups induced with cisplatin and gentamicin compared to paracetamol. At the same time, it was found that methanolic extracts were found to have more significant recovery as compared to aqueous extract. The aqueous extract was also significantly improved the pathological condition of the kidney. The histopathological changes in each kidney were observed for changes in glomerular membrane, endothelial tissue, interstitial congestion, tubular hemorrhage, inflammatory cell infiltrates and degeneration of cells.

DISCUSSION

Cisplatin is currently used as one of the most important drugs in the treatment of a wide range of solid tumors of the

head, ovary, and lung cancer. Gentamicin is used to gram-negative bacterial infections such as meningitis, lung, bone, joint and urinary tract infections.^[15] Paracetamol treats to acute pain, aches and reduce fever.^[16] Cisplatin gets accumulated in the tubular epithelial cells of the proximal kidney tubule, thus specifically causes nephrotoxicity. Gentamicin induces nephrotoxicity by inhibiting protein synthesis in renal cells, leading to necrosis of cells in the proximal renal tubule, resulting in acute necrosis, followed by acute renal failure. *Renal toxicity* in *paracetamol* is followed by reductions in glomerular filtration rate and cellular injury confined to the proximal tubule. CP, GM & PC induced renal impairment is evidenced by a very highly significantly ($p < 0.001$) increase in blood urea, serum creatinine, and serum albumin as well as acute necrosis that was evidenced through the histopathological examination of the kidney due to administration of cisplatin, gentamicin, and paracetamol in the regimen of nephroprotective effects. After treatment with the methanolic extract, values reduced significantly in CP, GM & PC treated animals. In the aqueous treated group, urea, creatinine, and albumin values decreased significantly compared to disease control, but it seems less effective than methanolic extract.

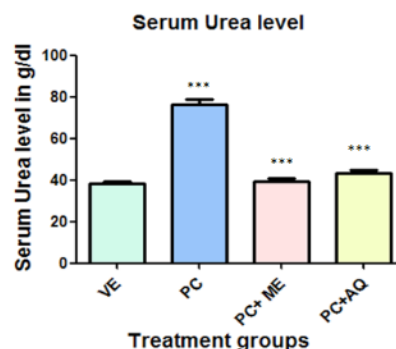
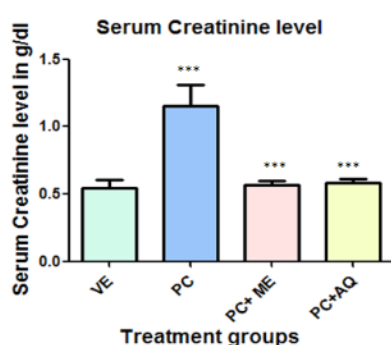


Fig. 7 and 8: Effect of *P. Dulce* on Serum Creatinine and Urea in Paracetamol induced nephrotoxicity in rats.

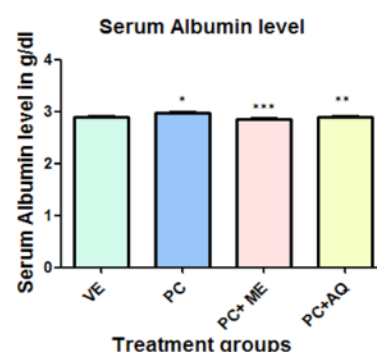


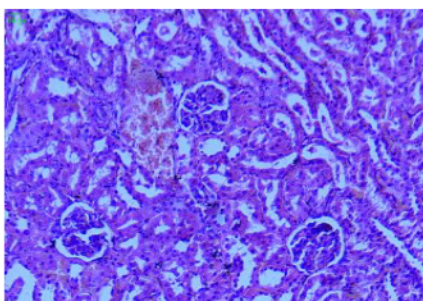
Fig.9: Effect of *P. Dulce* on Serum Albumin in Paracetamol induced nephrotoxicity in rats.

Table 2: Effect of administration of methanolic and aqueous extracts of *P. Dulce* bark on body weight in induced renal damage.

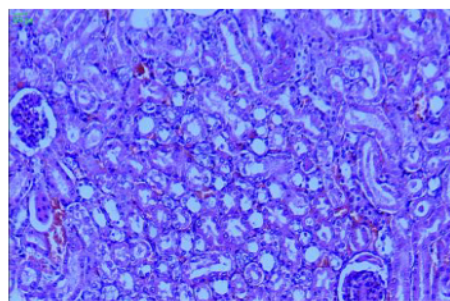
Sr. no	Group	Day 0 (gm)	On day of scarification (gm)
I	Vehicle	190.25 ± 4.27	197.92 ± 4.14
II	Disease Control- Cisplatin	188.08 ± 4.57	194.42 ± 4.55
III	Cisplatin + Methanol extract	188.33 ± 4.76	195.33 ± 5.13
IV	Cisplatin + Aq extract	188.83 ± 4.46	195.25 ± 4.06
V	Disease Control -Gentamicin	189.00 ± 4.80	194.08 ± 4.60
VI	Gentamicin + Methanol extract	188.67 ± 4.52	194.92 ± 4.50
VII	Gentamicin + Aq extract	188.92 ± 4.83	195.25 ± 5.15
VIII	Disease control - Paracetamol	189.33 ± 4.80	198.00 ± 4.84
XI	Paracetamol+ Methanol extract	188.83 ± 5.57	197.42 ± 5.94
X	Paracetamol+ Aq extract	188.67 ± 5.70	197.58 ± 5.54

Values are expressed as Mean ± S.E.M. (n=6). The Disease control group is compared with vehicle group, and the treated groups are compared with the Disease control group by One way ANOVA test followed by Dunnette's multiple comparison test ***P < 0.001 **P < 0.01, *P < 0.05.

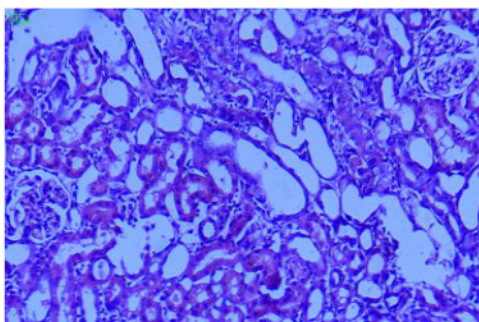




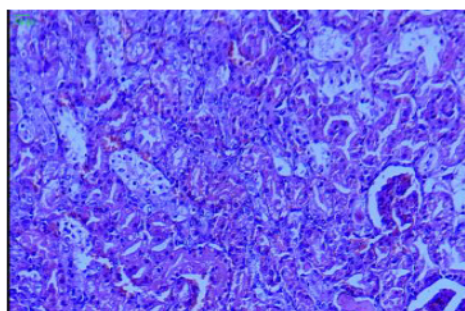
Group I: Vehicle- Saline
Normal Nephrons were observed, no any pathological changes were observed



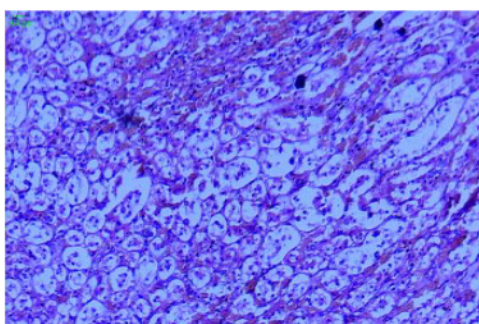
Group II: Disease Control- Cisplatin
Moderate inflammation and thickened basal membrane, loss of endothelial tissue, higher glomerular fibrosis, and tissue necrosis was observe



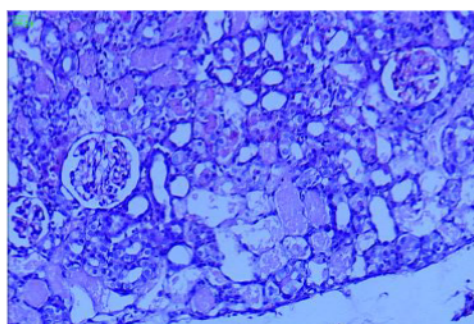
Group III: Protective group Cisplatin + Methanol extract
Mild inflammation of nephrons along with mild necrosis, no damage to glomerular membrane, mild inflammation, but no hemorrhage was observed



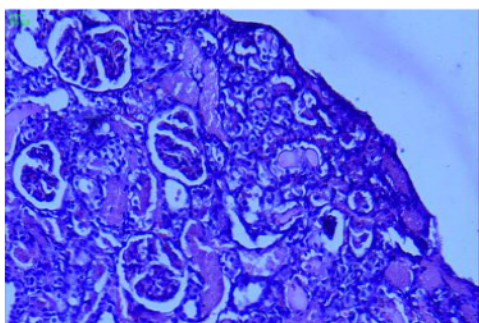
Group IV: Protective group- Cisplatin + Aq extract
Inflammation and tissue necrosis was moderate, whereas some endothelial loss was observed. Mild fibrosis and hemorrhage was observed



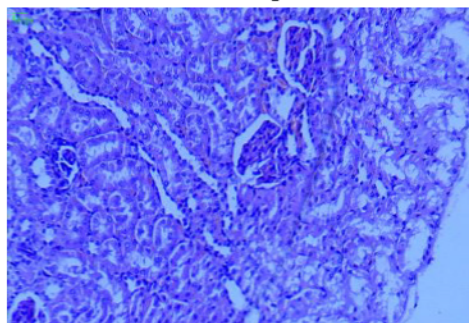
Group V: Disease Control -Gentamicin
Severe Inflammation and thickened basal membrane, moderate haemorrhage, severe endothelial swelling and disruption along with loss of endothelial tissue, higher glomerular fibrosis and tissue necrosis was observe



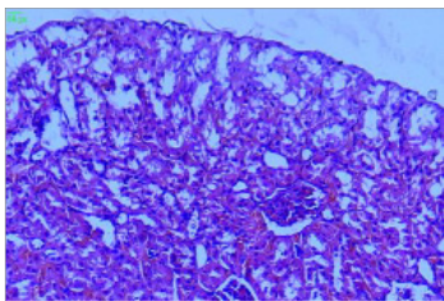
Group VI: Protective group - Gentamicin + Methanol extract
Mild inflammation of nephrons along with mild necrosis, no damage to glomerular membrane, mild inflammation but no haemorrhage was observed



Group VII: Protective group- Gentamicin + Aq extract
Inflammation and tissue necrosis was moderate, whereas some endothelial loss was observed. Mild fibrosis and haemorrhage was observed



Group VIII: Disease control - Paracetamol
Moderate Inflammation and haemorrhage, Severe Endothelial swelling and disruption along with loss of endothelial tissue, moderate glomerular fibrosis in animals and no tissue necrosis was observed

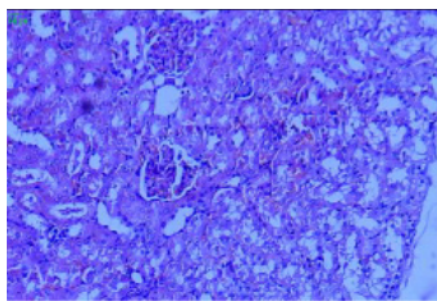


Group XI: Protective group- Paracetamol+ Methanol extract
Mild inflammation and no haemorrhage were observed. No loss of endothelium but moderate tissue fibrosis in some of the animals was observed

The methanolic extract was found to have a more significant recovery as compared to aqueous extract. The aqueous extract was also significantly improved the pathological condition of the kidney. The histopathological changes in each kidney were observed for changes in the glomerular membrane, endothelial tissue, interstitial congestion, tubular hemorrhage, inflammatory cell infiltrates, and degeneration of cells. The bark of *P. dulce* exhibited good nephroprotective activity due to various chemical constituents such as tannins, flavonoids, steroids, and phenols containing drugs.

REFERENCES

- Hussain T, Gupta RK, Sweetey K, Eswaran B, Vijayakumar M and Rao CV. Nephroprotective activity of *Solanum xanthocarpum* fruit extract against gentamicin-induced nephrotoxicity and renal dysfunction in experimental rodents. *Asian Pacific Journal of Tropical Medicine*. 2012;5:68691. Available from: DOI: 10.1016/S1995-7645(12)60107-2
- Fioretto P, Steffes W, Sutherland E, Goetz C, Mauer M. Reversal of Lesions of Diabetic-II. National Diabetes Information Clearinghouse. Diabetes Control and Complications Trial, U. S. Government Printing Office, NIH publication, Washington D.C, 1994;97: 3874-3875. Available from: DOI: 10.1056/NEJM199807093390202
- Barbosa J, Steffes W, Sutherland E, Connert E, Rao V. Effect Of Glycemic Control on Early Diabetic Renal Lesions. *Journal of American Medical Association*. 1994;272(8):600-606. Available from: PMID: 8057515
- Becker J, Perkovic V, Hewitson T. Pharmacological intervention in renal fibrosis and vascular sclerosis. *Journal of Nephrology*. 2001; 14:332-339. Available from: PMID: 11730265
- Nagmoti DM, Khatri DK, Juvekar PR, Juvekar AR. Antioxidant activity and free radical-scavenging potential of *Pithecellobium dulce* Benth seed extracts. *Free Radicals and Antioxidants*. 2012; 2(2):37-43. Available from :DOI: 10.5530/ax.2012.2.7
- Pithayanukul P, Ruenraroengsak P, Bavovada R, Pakmanee N, Suttisri R, Saen-oon S. Inhibition of *Naja kaouthia* venom activities by plant polyphenols. *Journal of Ethnopharmacology*. 2005;97(3): 527-533. Available from:doi: 10.1016/j.jep.2004.12.013.
- Zapesochyna GG, Yarosh EA, Syanidze NV, Yarosh GI. Flavonoids of the leaves of *Pithecellobium dulce*. *Khimiya Prirodnykh Soedineni*. 1980;2:252-253. Available from: doi:000/890/000890138.
- Singh L, Mamta S. Oxidative DNA damage protective activity and antioxidant and hepatoprotective potentials of *Pithecellobium dulce* plant. 2nd International Conference and Exhibition on Nutritional Science & Therapy. Courtyard by Marriott Philadelphia Downtown, USA. *Journal of Nutrition & Food Sciences*. 2013;15-17. Available from:doi:10.1016/j.jfct.2009.01.034.
- Shankar K, Maheshkumar K. Antioxidant and free radical scavenging activity of *Pithecellobium dulce* (Roxb.) Benth wood bark and leaves. *Free radicals and antioxidants*. 2012;2(3):47-57. Available from : doi.org/10.5530/ax.2012.3.7
- Raghu P, Hari P, Venkatesh P, Venkata K, Sudheer B. Antidiabetic activity of bark extract of *Pithecellobium dulce* benth in alloxan-induced diabetic rats. *Natural product: An Indian journal*.2010; 6 (4):201-204.
- Khandelwal KR. *Practical Pharmacognosy*. Pune: Nirali Prakashan; 2008; 19thed. 149-56, 157-159.
- Annie S, Rajagopal P, Malini S. Effect of *cassia auriculata* linn. Root extract on cisplatin and gentamicin – induced renal injury. *Phytomedicine*. 2005; 12(8): 555-560. Available from: doi: 10.1016/j.phymed.2003.11.010.
- Harlalka GV, Patil CR, Patil MR. Protective effect of *Kalanchoe pinnata* pers. (crassulaceae) on gentamicin-induced nephrotoxicity in rats. *Indian Journal of Pharmacology*. 2007; 39(4): 201-205. Available from :DOI: 10.4103/0253-7613.36540
- Ngangbam d, sayeri d, rajesh d, subhalakshmi d, meena d, Sucheta Devi. Nephroprotective effect of *elsholtzia blanda* benth. In paracetamol induced toxicity in albino rats. *International Journal of Recent Scientific Research*. 2018; 9(7): 28186-28189. Available from: DOI: 10.24327/IJRSR
- Gentamicin sulfate. The American Society of Health-System Pharmacists. 16 August 2015.
- Warwick C. Paracetamol and fever management. *Journal of the Royal Society for the Promotion Health*. 2008; 128 (6): 320-323. Available from: doi.org/10.1177/1466424008092794



Group X: Protective group- Paracetamol +Aq extract
Moderate Inflammation and mild haemorrhage, slight endothelial swelling and disruption along with loss of endothelial tissue, moderate glomerular fibrosis and mild tissue necrosis was observed.

How to Cite this Article: Patil R, Yamgar S. Studies on Nephroprotective Effect of Methanolic and Aqueous Extract of Bark of *Pithecellobium Dulce* Roxb. in Rats. *Int. J. Pharm. Sci. Drug Res.* 2021;13(5):574-580. DOI: 10.25004/IJPSDR.2021.130516





Pune District Education Association's
**Shankarrao Ursal College of Pharmaceutical
Sciences & Research Centre, Kharadi, Pune-14.**



Academic Year 2019-20

EVALUATION OF THE EFFECT OF *PIPER BETLE* L. LEAVES EXTRACT AGAINST CLONIDINE-INDUCED CATALEPSY AND MILK-INDUCED LEUKOCYTOSIS AND EOSINOPHILIA IN MICE

RAMDAS N KALE^{1*}, RAVINDRA Y PATIL²

¹Department of Pharmacognosy, SVPM's College of Pharmacy, Malegaon (Bk), Baramati, Pune, India. ²Department of Pharmacognosy, PDEA's Shankarrao Ursal College of Pharmaceutical Sciences and Research Center, Kharadi, Pune, India. Email: ramdas.kalesvpm@gmail.com

Received: 05 August 2020, Revised and Accepted: 10 September 2020

ABSTRACT

Objective: The objective of the study was to evaluate the effect of *Piper betle* L. leaves extract against clonidine-induced catalepsy and milk-induced leukocytosis and eosinophilia in mice.

Methods: Methanolic extract of *P. betle* L. leaves was prepared using Soxhlet apparatus. Preliminary phytochemical screening of the prepared extract was carried out using standard chemical tests. Effect of the prepared extract was evaluated against clonidine-induced catalepsy and milk-induced leukocytosis and eosinophilia in mice model.

Results: Maximum duration of catalepsy was observed at 90 min after the clonidine administration. There was a significant inhibition ($p < 0.05$) of clonidine-induced catalepsy in the animals pretreated with chlorpheniramine maleate and extract of *P. betle* leaves. Administration of milk (4 mg/kg) subcutaneous route exhibited a significant increase in leucocytes and eosinophil count after 24 h of administration. Methanolic extract of *P. betle* L. leaves showed significant inhibition ($p < 0.05$) of milk-induced leukocytosis and eosinophilia.

Conclusion: These results suggest that *P. betle* leaves extract may have the potential therapeutic value in the treatment of allergic diseases.

Keywords: Catalepsy, Leukocytosis, Eosinophilia.

© 2020 The Authors. Published by Innovare Academic Sciences Pvt Ltd. This is an open access article under the CC BY license (<http://creativecommons.org/licenses/by/4.0/>) DOI: <http://dx.doi.org/10.22159/ajpcr.2020.v13i11.39321>

INTRODUCTION

Piper betle Linn. is a perennial dioecious climber; stems are semi-woody, much thickened at nodes; leaves large, 15–20 cm long, broadly ovate, slightly cordate, shortly acuminate, acute, entire, glabrous, yellowish or bright green, shining on both sides [1]. It is commonly known as the betle vine, it is an important medicinal and recreational plant [2]. *P. betle* is extensively found in damp forests and is propagated in India and other Southeast Asia, such as Vietnam and China [3]. The five main cultivars of *P. betle* Linn. are Bangla, Desawari, Karpooori, and Sanchi [4]. The betle leaves are nutritive and possess antitumor [5], wound healing [6], antimicrobial [7], antibacterial [8], antioxidant [9], gastroprotective [10], neuroprotective [11], antifilarial [12], antimalarial [13], and analgesic activity [14]. The leaves contain a variety of biologically active components like hydroxychavicol, chavicol, piperbetol, chavibetol, piperol A, methylpiperbetol, and piperol. The key component of the leaf is a volatile oil known as betle oil [15]. Karpooori variety possesses highest content of eugenol [16]. The primary goal of this research was to evaluate the effect of *P. betle* L. leaves extract against clonidine-induced catalepsy and milk-induced leukocytosis and eosinophilia in mice.

MATERIALS AND METHODS

Collection of plant material

The leaves of *P. betle* were collected from the rural areas of Baramati Dist., Pune (Maharashtra) and identified in the Department of Botany, Agricultural Development Trust's Shirdabai Pawar Mahila Mahavidyalaya, Shirdanagar Malegaon (Bk), Tal., Baramati Dist., Pune, Maharashtra, India (Voucher specimen PASR-142).

Drugs and chemicals

The drugs used were clonidine (Neon Lab. Ltd., India), chlorpheniramine maleate (Pfizer Ltd.), and dexamethasone (Zydus Healthcare Ltd.);

all were purchased from a commercial source. Chemical used were methanol (Research Lab. Industries, India).

Extract preparation and phytochemical screening

The leaves of *P. betle* were dried and crushed to a coarse powder. Powdered material was subjected to Soxhlet extraction with methanol as a solvent. The extract so obtained was concentrated to dryness by evaporating the solvent. The percent yield was calculated. Extract was stored at room temperature and protected from direct sunlight. The prepared extract was subjected to preliminary phytochemical screening using standard chemical tests [17].

Animals

Swiss albino mice (20–30 g) of either sex were obtained from National Institute of Biosciences, Pune, India. Animals were maintained in our animal house under standard laboratory conditions. Animals were exposed to day-night light cycle and room temperature ($24 \pm 2^\circ\text{C}$). All animals are allowed free access to readymade food pellets and water. Animals were handled according to standard protocols for the use of laboratory animals [18]. The experimental protocol was approved by the Institutional Animal Ethics Committee (1214/ac/08/CPCSEA).

Acute toxicity study

Acute toxicity study was performed by oral route in mice as per OECD guidelines 423.

Clonidine-induced catalepsy in mice

A bar test was performed to study the effect of clonidine-induced catalepsy [19–21]. Clonidine (1 mg/kg, s.c.) was injected to mice ($n=6$). Before 1 h of clonidine treatment, Group I received dist. water (1 ml/kg i.p.), Group II received chlorpheniramine maleate (10 mg/kg body weight, i.p.), Group III received methanolic extract 250 mg/kg

body weight i.p. (MEPBL250), and Group IV received methanolic extract 500 mg/kg body weight i.p. (MEPBL500). The forepaws of mice were placed on a horizontal bar and the time required to remove the paws for each animal was noted and the duration of catalepsy was measured at 15, 30, 60, 90, and 120 min.

Milk-induced leukocytosis and eosinophilia in mice

Swiss albino mice of either sex weighing between 20 and 30 g were divided into six groups of five animals each. All animals received boiled (boiling temp 70°C and boiling time 20 min) and cooled milk in dose of 4 ml/kg subcutaneously. Animals belong to Group I treated as control and received distilled water 10 ml/kg. p.o., Group II received methanolic extract 250 mg/kg.p.o. (MEPBL250), Group III received methanolic extract 500 mg/kg.p.o. (MEPBL500), whereas Group IV received dexamethasone 50 mg/kg i.p. Extract and standard drug were administered 1 h before milk injection. Blood samples were collected before and 24 h after milk administration from the retro-orbital plexus, under light ether anesthesia. Difference in total leukocyte and eosinophil count before and after 24 h drug administration was calculated [22].

Statistical analysis

The mean \pm SEM values were calculated for each group. The statistical analysis was performed using one-way analysis of variance (ANOVA) followed by Dunnett's test for individual groups compared with control. $p < 0.05$ was considered as statistically significant.

RESULTS

Acute toxicity study

Treatment with methanolic extract up to 2000 mg/kg orally to mice did not induce mortality. Hence, LD_{50} was considered to be more than 2000 mg/kg. Based on acute toxicity results, 250 and 500 mg/kg doses were selected.

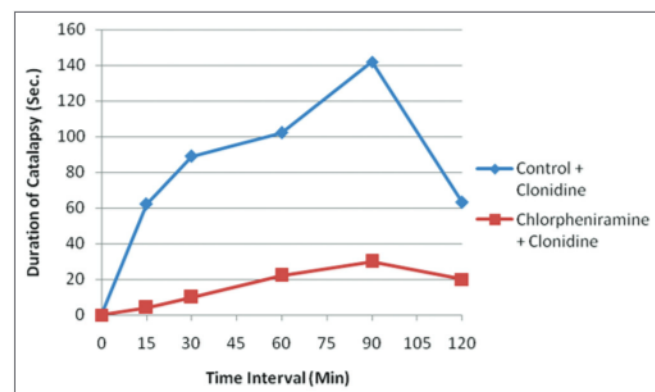


Fig. 1: Effect of chlorpheniramine maleate (10 mg/kg body weight, i.p.) on clonidine-induced catalepsy in mice

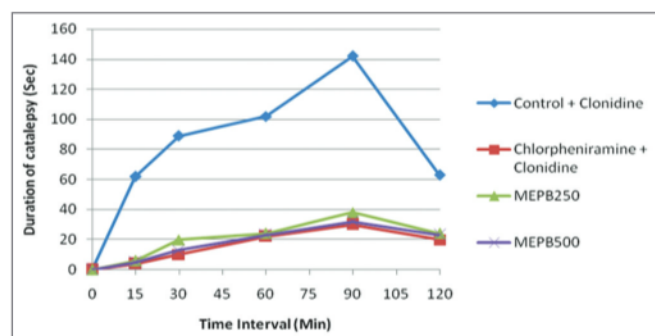


Fig. 2: Effect of *Piper betle* Linn. leaves extracts on clonidine-induced catalepsy in mice

Preliminary phytochemical screening

Preliminary phytochemical screening of the extract showed the presence of alkaloids, carbohydrates, proteins, flavonoids, phenolic compounds, and tannins.

Clonidine-induced catalepsy

All the groups showed a maximum duration of catalepsy at 90 min after the clonidine administration. There was a significant inhibition ($p < 0.05$) of clonidine-induced catalepsy in the animals pretreated with chlorpheniramine maleate (Fig. 1), MEPBL250, and MEPBL500 (Fig. 2 and Table 1).

Milk-induced leukocytosis and eosinophilia in mice

Subcutaneous administration of boiled and cooled milk at a dose of 4 ml/kg showed a significant increase in the leukocytes and eosinophils count after 24 h as compared to leukocyte count before milk administration.

DISCUSSION

Catalepsy is a condition in which the animal maintains imposed posture for a long time before regaining normal posture. Catalepsy is the sign of the extrapyramidal effect of drugs that inhibit dopaminergic transmission or increase histamine release in the brain. Clonidine, a α_2 -adrenoreceptor agonist induces dose-dependent catalepsy in mice, which is inhibited by H_1 receptor antagonist but not by H_2 receptor antagonist [23]. It is known that clonidine releases histamine from mast cells [24]. Clonidine-induced release of histamine from mast cells is inhibited by α_2 -adrenoceptor blocker. In the present investigation, all groups showed a maximum duration of catalepsy at 90 min after the clonidine administration. There was a significant inhibition ($p < 0.05$) of clonidine-induced catalepsy in the animals pretreated with *P. betle* leaves extract. This indicates the antihistaminic activity of *P. betle* leaves.

During asthmatic inflammation, leukocyte release cytokines, histamine, and major basic protein promote ongoing inflammation. An abnormal

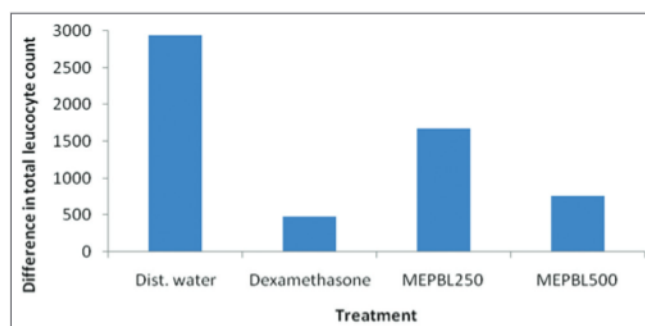


Fig. 3: Effect of *Piper betle* leaves extract on milk-induced leukocytosis in mice

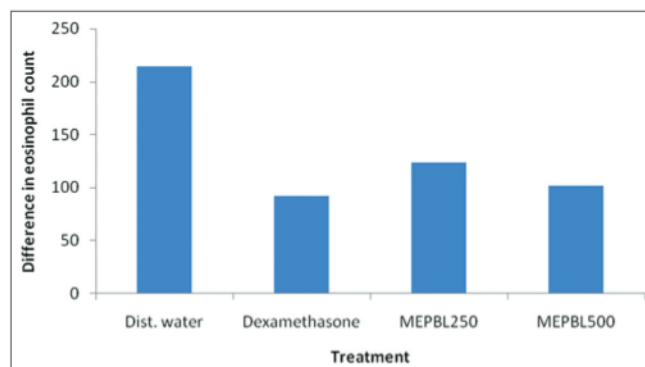


Fig. 4: Effect of *Piper betle* leaves extract on milk-induced eosinophilia in mice

Table 1: Effect of *Piper betle* leaves extracts on clonidine-induced catalepsy in mice

S. No.	Group	Duration of catalepsy (sec) at Mean±SEM				
		15 min	30 min	60 min	90 min	120 min
1	Control	62.00±4.46	89.33±4.82	102.50±3.81	142.33±12.38	63.00±5.19
2	Standard	04.33±0.66*	10.00±1.46*	22.00±3.36*	30.00±2.29*	20.00±2.38*
3	MEPBL 250	06.16±0.94*	19.83±1.88*	24.00±2.74*	38.00±6.19*	23.66±2.10*
4	MEPBL 500	05.00±0.73*	13.00±1.41*	23.00±2.39*	32.00±3.27*	23.50±4.65*

*p<0.05

Table 2: Effect of *Piper betle* leaves extract on milk-induced leukocytosis in mice

Group	Treatment	Difference in total leukocyte count (Per cu mm) (Mean±SEM)
I	Dist. water	2936.00±487.13
II	MEPBL250	1676±177.83*
III	MEPBL500	760.00±131.71**
VI	Dexamethasone (50 mg/kg i.p.)	476.00±110.40***

*p<0.04, **p<0.003, ***p<0.001

Table 3: Effect of *Piper betle* leaves extract on milk-induced eosinophilia in mice

Group	Treatment	Difference total eosinophil count (per cu mm) (Mean±SEM)
I	Dist. water	214.00±38.64
II	MEPBL250	124.00±28.57*
III	MEPBL500	102.00±10.54**
VI	Dexamethasone (50 mg/kg i.p.)	92.00±22.00***

*p<0.098, **p<0.023, ***p<0.025

increase in peripheral eosinophils count more than 4% of total leukocyte is termed as eosinophilia [25]. After the parental administration of milk, there is an increase in total leukocyte and eosinophil count, this stressful condition can be normalized by the administration of an antistress or adaptogenic drug. The involvement of eosinophil in bronchial mucosa, in which allergic inflammation occurs, is a critical contributor to the late asthmatic reaction of congestion and mucus hypersecretion. In the late phase, especially in the development of allergic asthma, eosinophil plays a role as an inflammatory cell. Eosinophil secretes mediators such as eosinophil cationic protein, tumor necrosis factor, eosinophil-derived neurotoxin, and prostaglandin results in epithelial shedding, bronchoconstriction, and promotion of inflammation in the respiratory tract often allergic. In the present study, it has been found that parenteral administration of milk at a dose of 4 ml/kg significantly induced the total leukocyte and eosinophil count (p<0.001) after 24 h. Animals of the group treated with MEPBL250 and MEPBL500 significantly inhibited an increase in the number of total leukocyte (Fig. 3 and Table 2) and eosinophil count. (Fig. 4 and Table 3).

CONCLUSION

The results of the present study revealed that *P. betle* Linn. leaves extract inhibits the clonidine-induced catalepsy and milk-induced leukocytosis and eosinophilia in mice, suggests its potential antihistaminic and antiallergic activities. However, we are screening *P. betle* leaves extract for other animal models of asthma to evaluate its efficacy in the management of asthma. We are also working on a phytochemical investigation of these extracts to pinpoint the chemical constituents responsible for the activity.

ACKNOWLEDGMENTS

We express our sincere thanks to Management and Principal of SVPM's College of Pharmacy, Malegaon Bk Tal., Baramati Dist., Pune,

for providing the necessary research facilities for this study. We also express our gratitude to Prof. R.B. Deshmukh, Head, Dept. of Botany, Agricultural Development Trust's Shirdabai Pawar Mahila Mahavidyalaya, Shirdanagar Tal-Baramati, for the authentication of the plant.

AUTHORS' CONTRIBUTIONS

Dr. Ravindra Y. Patil planned and designed the whole work and Ramdas N. Kale did the whole research work.

CONFLICTS OF INTEREST

The authors confirm that there were no conflicts of interest.

AUTHORS' FUNDING

This research did not receive any specific grant from funding agencies in the public, commercial, or not-for-profit sectors.

REFERENCES

- Warrier PK, Nambier VP, Ramanakutty C. Indian Medicinal Plants. Madras, India: Orient Longman Publishers Ltd.; 1996. p. 279.
- Kumar N, Misra P, Dube A, Bhattacharya S, Dikshit M, Ranade S. *Piper betle* Linn. a maligned Pan-Asiatic plant with an array of pharmacological activities and prospects for drug discovery. Curr Sci 2010;99:922-32.
- Bhattacharya S, Banerjee D, Bauri AK, Chattopadhyay S, Bandyopadhyay SK. Healing property of the *Piper betel* phenol, allylpyrocatechol against indomethacin-induced stomach ulceration and mechanism of action. World J Gastroenterol 2007;13:3705-13.
- Sapna S, Anju D, Sanju N. Pharmacognostical and phytochemical studies of *piper betle* Linn leaf. Int J Pharm Pharm Sci 2016;8:222-6.
- Gundala SR, Aneja R. *Piper betel* leaf: A reservoir of potential xenohormetic nutraceuticals with cancer-fighting properties. Cancer Prev Res (Phila) 2014;7:477-86.
- Arif B, Risris K, Tazyinul QA. Wound-healing test of piper betle leaf extract and *Aloe vera* in gel preparation. Int J Appl Pharm 2018;10:86-91.
- Marlia S, Sophi D, Natalia P. Antimicrobial activity of standardized *piper betel* extract and its mouthwash preparation. Int J Pharm Pharm Sci 2014;6:243-6.
- Agarwal T, Singh R, Shukla AD, Waris I, Gujrati A. Comparative analysis of antibacterial activity of four *Piper betel* varieties. Adv Appl Sci Res 2012;3:698-705.
- Jaiswal SG, Patel M, Saxena DK, Naik SN. Antioxidant properties of *Piper betel* (L) leaf extracts from six different geographical domain of India. J Bioresour Eng Technol 2014;2:12-20.
- Majumdar B, Chaudhuri SG, Ray A, Bandyopadhyay SK. Effect of ethanol extract of *Piper betle* Linn leaf on healing of NSAID-induced experimental ulcer—a novel role of free radical scavenging action. Indian J Exp Biol 2003;41:311-5.
- Chan EW, Wong SK. Phytochemistry and pharmacology of three *Piper* species: An update. Int J Pharmacogn 2014;1:534-44.
- Singh M, Shakya S, Soni VK, Dangi A, Kumar N, Bhattacharya SM. The n-hexane and chloroform fractions of *Piper betle* L. trigger different arms of immune responses in BALB/c mice and exhibit antifilarial activity against human lymphatic filarid *Brugia malayi*. Int Immunopharmacol 2009;9:716-28.
- Pal M, Chandrashekar K. Mosquito repellent activity of *Piper betel* Linn. Int J Pharm Life Sci 2010;1:313-5.
- Alam B, Akter F, Parvin N, Sharmin Pia R, Akter S, Chowdhury J, et al. Antioxidant, analgesic and anti-inflammatory activities of

- the methanolic extract of *Piper betle* leaves. Avicenna J Phytomed 2013;3:112-25.
15. Sarma C, Rasane P, Kaur S, Singh J, Singh J, Gat Y, et al. Antioxidant and antimicrobial potential of selected varieties of *Piper betle* L. (Betel leaf). An Acad Bras Cienc 2018;90:3871-8.
 16. Fathima Begam KM, Ravichandran P, Manimekalai V. Phytochemical analysis of some selected varieties of *piper betle* L. Int J Curr Pharm Res 2018;10:89-93.
 17. Khandelwal KR. Practical Pharmacognosy Technique and Experiments. 23rd ed. Pune: Nirali Prakashan; 2005. p. 15-29.
 18. National Research Council. Guide for the Care and Use of Laboratory Animals. Washington, DC: Institute for Laboratory Animal Research, National Academics Press; 2011. p. 11-40.
 19. Ferré S, Guix T, Prat G, Jane F, Casas M. Is experimental catalepsy properly measured? Pharmacol Biochem Behav 1990;35:753-7.
 20. Taur DJ, Nirmal SA, Patil RY. Effect of various extracts of *Ficus bengalensis* bark on clonidine and haloperidol-induced catalepsy in mice. Pharmacologyonline 2007;3:470-7.
 21. Ghaisas MM, Bulani VD, Suralkar AA, Limaye RP. Effect of *Calotropis gigantea* on clonidine and haloperidol induced catalepsy. Pharmacologyonline 2009;3:484-8.
 22. Bhargava KP, Singh N. Anti-stress activity of *Ocimum sanctum* Linn. Indian J Med Res 1981;73:443-51.
 23. Jadhav JH, Balsara JJ, Chandorkar AG. Involvement of histaminergic mechanisms in the cataleptogenic effect of clonidine in mice. J Pharm Pharmacol 1983;35:671-3.
 24. Lakdawala AD, Dadkar NK, Dohadwalla AN. Action of clonidine on the mast cells of rats. J Pharm Pharmacol 1980;32:790-1.
 25. Brekhman LI, Dardymov IV. New substances of plant origin which increase nonspecific resistance. Annu Rev Pharmacol 1969;9:419-28.

Compatibility Testing of Nateglinide with Different Grades of Cellulose Ethers and Excipients Used in Sustained Release Formulations

Amit J Kasabe¹, Ajit S Kulkarni², Vinod L Gaikwad³

¹Department of Pharmaceutical Chemistry, PDEA's Shankarrao Ursal College of Pharmaceutical Sciences and Research Centre, Kharadi, Pune-411014, Maharashtra, India.

²Department of Pharmaceutics, Satara College of Pharmacy, Satara - 415004, Maharashtra, India.

³Department of Pharmaceutics, BV DU Poona College of Pharmacy, Erandwane, Pune (411038), Maharashtra, India.

Received: 16th Nov, 18; Revised and Accepted: 14th Dec, 18; Available Online: 25th Dec, 2018

ABSTRACT

Compatibility testing was done to assess interaction between Nateglinide (NTG) and different pharmaceutical excipients and polymers, which are used in a sustained release formulation to manufacture tablet. To evaluate the compatibility between drug, excipients and polymers, different techniques such as Differential Scanning Calorimetry (DSC), Infrared Spectroscopic study (IR) and Isothermal stress testing (IST) study were employed. The results of DSC curves showed that, all excipients and polymers are compatible with the NTG. Except DSC curves of magnesium stearate, which shows certain interaction with the NTG, however, it overcome in the results of IR and IST studies, which showed that all the excipients, polymers used in this study are compatible with the NTG.

Keywords: Isothermal stress testing (IST), Nateglinide, Compatibility study.

INTRODUCTION

Nateglinide, a D-phenylalanine derivative is an anti-diabetic drug that is quick but short acting and controls postprandial blood glucose (PBG) effectively. Nateglinide belongs to the meglitinide class of anti-diabetic drugs used to treat type 2 diabetes by stimulation of pancreatic beta cells that results in the release of proinsulin. Nateglinide is rapidly and completely absorbed following oral administration. Chemically, it is (2R) -2-[trans-4-isopropyl-cyclohexanecarbonyl] - amino] -3-phenyl-propionic acid (Figure 1)^{1, 12,13,15,16}

Studies of drug-excipient compatibility represent an important phase in the preformulation stage of the development of all dosage forms. The potential physical and chemical interactions between drugs and excipients can affect the chemical, physical, therapeutic properties and stability of the dosage form. The excipients and polymers are generally used in dosage form to ease in administration of the drug, to facilitate the formulation of the drug product, to increase the stability of the formulation. Excipients or polymers may interact with drugs that gives rise to changes in the chemical nature, solubility, absorption and therapeutic response of drugs. Therefore, the stable and effective solid dosage form depends on the selection of the occupants which can be achieved through the study of the interaction between the drug and excipients in the solid state. Differential scanning calorimetry (DSC) is rapidly used as a tool for the

evaluation of the drug-excipient compatibility. However, caution needs to be exercised in the interpretation of DSC results.

This is because of the requirement of high temperature conditions and the lack of moisture in conducting these experiments. Hence, conclusions based on the DSC results alone may be misleading and to avoid this another methods such as IR spectroscopic study and Isothermal stress testing (IST) study is commonly employed for evaluating the drug-excipient compatibility^{1,2}.

IST involves storage of drug-excipient blends with or without moisture at a temperature (50°C) for a specific period of time (3weeks) to accelerate the ageing of drug and interaction with excipients. The IST has specific application in the pharmaceutical industry where the interaction between drug and excipients is visually observed and the drug content determined quantitatively. However, the disadvantage of this method is time consuming and laborious. Ideally, all the techniques, DSC, IR and IST should be used in combination during the compatibility studies for the selection of the excipients.

In this study, DSC, IR and IST study were used for evaluating the compatibility of NTG with selected excipients which are used in the sustained release formulation. In case where the DSC curve is suspected, infrared (IR) spectrum of pure drug was compared with that of drug-excipient mixture and pure excipient. Excipients found to be compatible with each other.

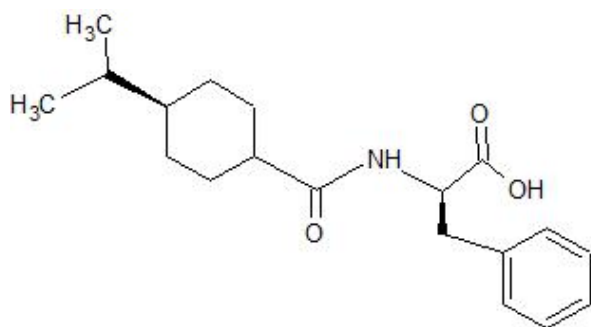


Figure 1: Structure of Nateglinide.

Excipients which were included in the prototype formula were tested using the technique of IST.

MATERIALS AND METHODS

Materials

Nateglinide USP, a gift sample from CIPLA Pharmaceuticals, Kurkumbh, Pune, India. HPMCK100M and HPMCK4M (Methocel) was a kind gift sample by Ashland Inc., USA. Microcrystalline Cellulose PH101, Microcrystalline Cellulose PH102 (Avicel), Talc, Lactose, Magnesium stearate was procured from commercial suppliers. Methanol and Water used throughout the study is of HPLC grade (Merck Inc.) and are procured from commercial suppliers.

Methods

Differential Scanning Calorimetry (DSC)

A differential scanning calorimeter (Mettler, Toledo) was used for thermal analysis of drug and mixtures of drug – excipients and drug- polymer. The selected excipients and polymers were mixed in an appropriate ratio. Individual samples of drug, excipients and polymers as well as mixtures of drug – excipients and drug- polymer were weighed directly in the DSC aluminium crucible and scanned in the temperature range of 40°C-350°C under an atmosphere of drug nitrogen. The heating rate was 2°C/min. and the curves obtained in the study were observed for any interaction^{4, 5, 8, 10,11,14}.

IR Spectroscopy

IR spectra of drug and mixture of drug – excipients and drug- polymer were recorded on in the range of 400nm-200nm using potassium bromide discs^{1,3}.

Isothermal Stress Testing (IST)

For Stressed Samples

The pure drug (NTG), selected polymer/s and occupant/s were weighed (1:1) in 4 ml glass vials (n = 3) and mixed on a vortex mixer for 2 min. for confirming homogenous mixing.

In each vial, 10 % of the distilled water was added and sealed using a Teflon-lined screw cap and stored at 50° C in hot air oven (Lab India, India).

For Control Samples

The pure drug (NTG), selected polymer/s and occupant/s were weighed (1:1) in 4 ml glass vials (n = 3) and mixed on a vortex mixer for 2 min. for confirming homogenous mixing.

The vials were sealed using a Teflon-lined screw cap and stored at 2-8° C in a refrigerator.

These sample/s were regularly examined for any change of colour. After 3 weeks (21 days) these samples were analysed quantitatively by using UV-visible spectrophotometer scanned between 400-200nm (Model UV-1800 Shimadzu)².

Linearity Range

Different aliquots of 5ppm to 50ppm were prepared and the solution is scanned in the range of 400nm to 200nm and absorbance is measured and graph is plotted concentration verses absorbance and linearity is calculated.

Preparation of Stock solution

10mg of pure Nateglinide was dissolved in 100ml of methanol (100ppm)

Preparation of Sample solution

0.5, 10, 15, 20, 25, 30, 35, 40, 45, 50 ml of stock solution was diluted to 10ml of methanol in 10ml volumetric flask to get respective ppm solutions.

RESULTS AND DISCUSSION

Compatibility Study

DSC

Selected DSC curves of drug and drug-excipients and drug-polymer mixtures are shown in Figure 2-30 for “0” days, “10” days, “20” days, “30” day’s intervals. The thermal behaviour of drug, respective excipients and the combinations are compared in the DSC curves. Peak transition temperature (T_{peak}), Onset Temperature for various mixtures is summarized in Table 2. The majority of DSC thermograms of drug alone and in combination with different polymers shows the onset temperature of peak (T_{onset}) [~130°C] and peak transition temperature (T_{peak}) [~132°C].

The thermogram of NTG showed a sharp endothermic peak at 131.94°C and peak onset 130.68°C. (Figure 2) In the majority of thermograms, the melting endotherm of NTG (T_{onset} and T_{peak}) was well preserved with light broadening shifting towards the lower temperature range. This change in shape and shifting of peak towards a lower temperature range could be due to mixing of the drug with accidents and my not necessarily indicate potential incompatibility^{6,7, 10,11,14}.

The DSC thermogram of NTG and K100M showed a sharp endothermic peak at 132.56°C and peak onset at 129.99°C. The endothermic peak of NTG was well preserved, this shows that the NTG is compatible with K100M. (Figure 3) The DSC thermogram of NTG and K4M showed a sharp endothermic peak at 132.27°C and peak onset at 130.05°C. The endothermic peak of NTG was well preserved, this shows that the NTG is compatible with K4M. (Figure 4) The DSC thermogram of NTG and Microcrystalline Cellulose AVICEL PH101 showed a sharp endothermic peak at 131.72°C and peak onset at 129.30°C. The endothermic peak of NTG was well preserved, this shows that the NTG is compatible with AVICEL PH101. (Figure 5)

The DSC thermogram of NTG and Microcrystalline Cellulose AVICEL PH102 showed a sharp endothermic peak at 132.30°C and peak onset at 130.30°C. The endothermic peak of NTG was well preserved, this shows

that the NTG is compatible with AVICEL PH102. (Figure 6)

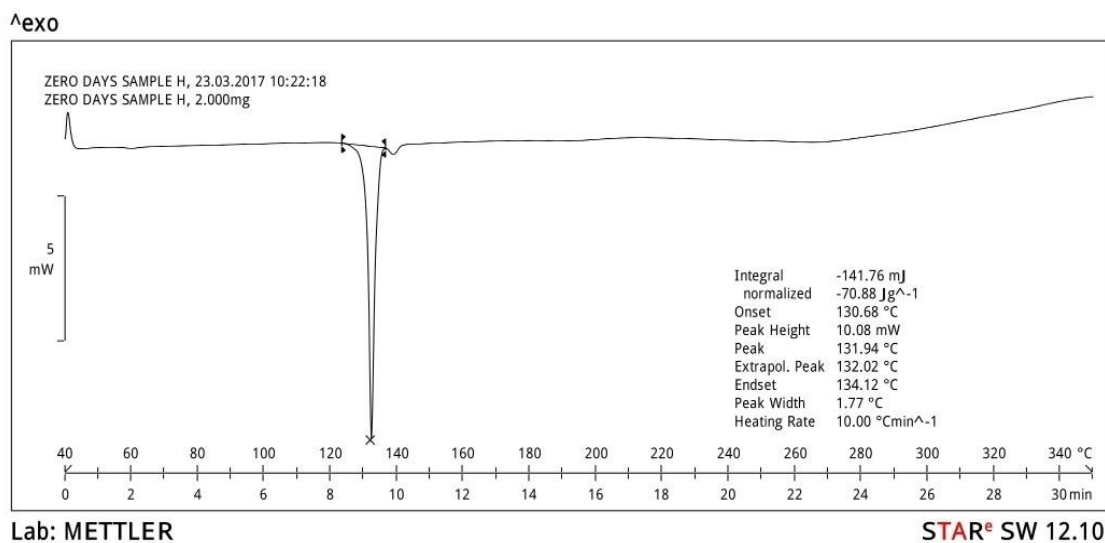


Figure 2: DSC thermogram of NTG ('0' days).

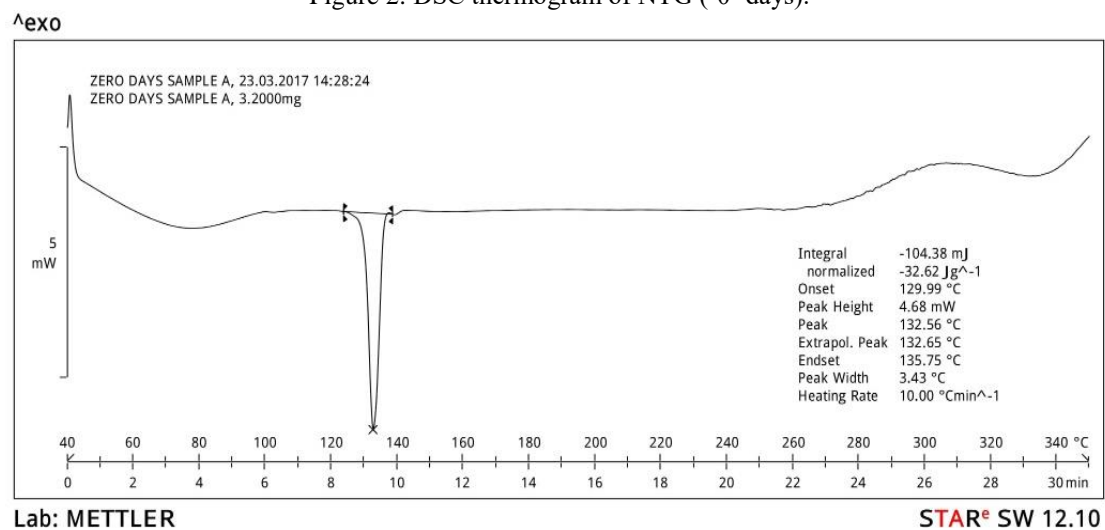


Figure 3: DSC thermogram of NTG + K100M ('0' days).

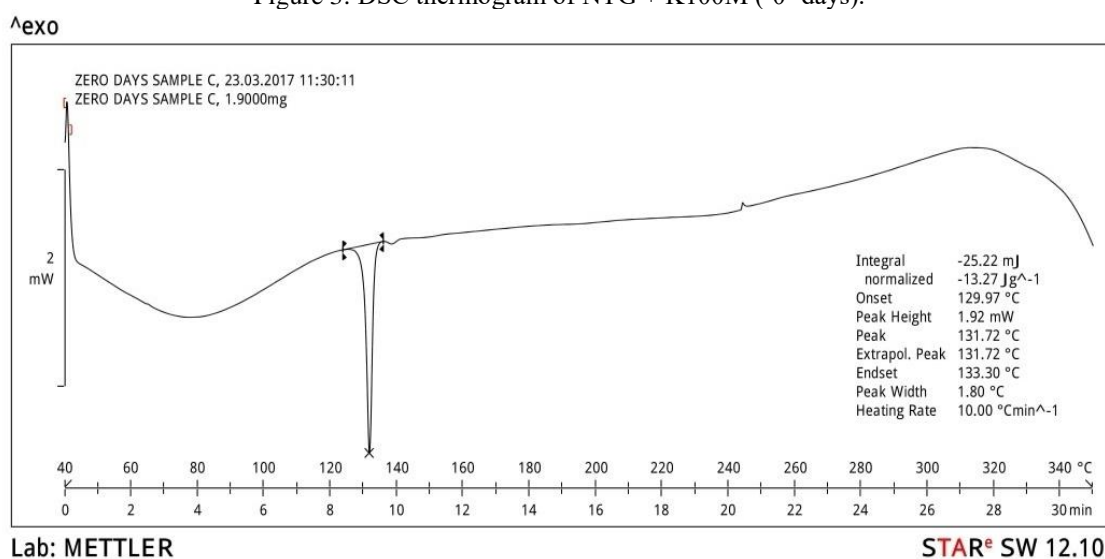


Figure 4: DSC thermogram of NTG + K4M ('0' days).

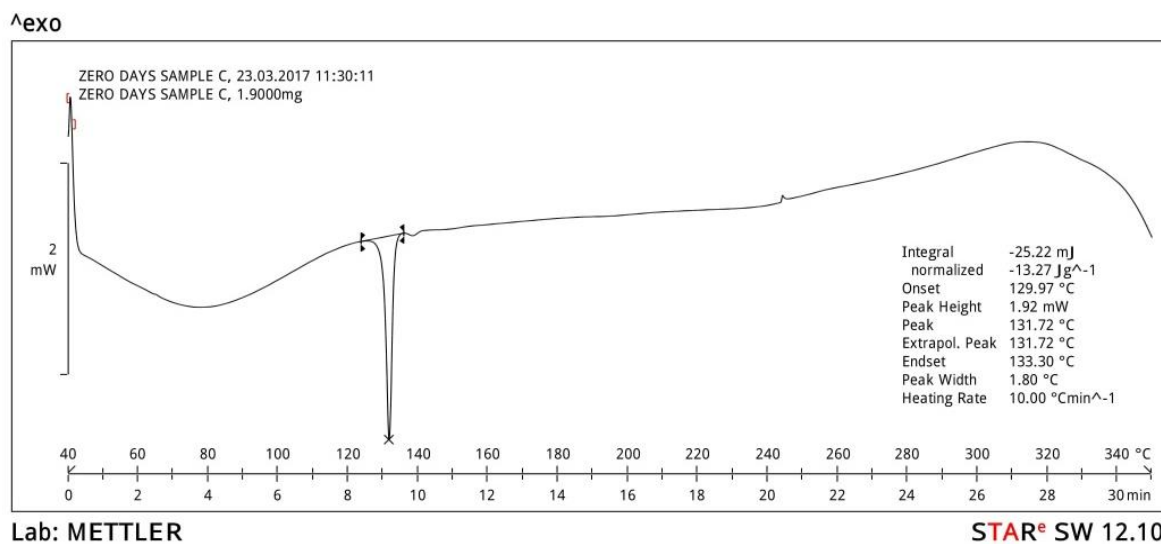


Figure 5: DSC thermogram of NTG + AVICEL PH101 ('0' days).

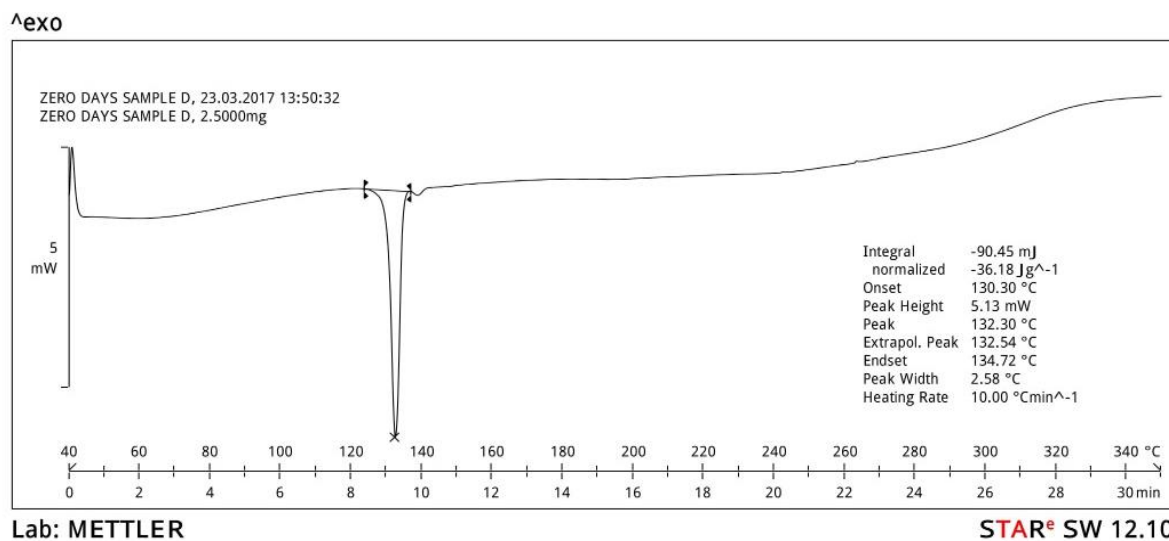


Figure 6: DSC thermogram of NTG + AVICEL PH102 ('0' days).

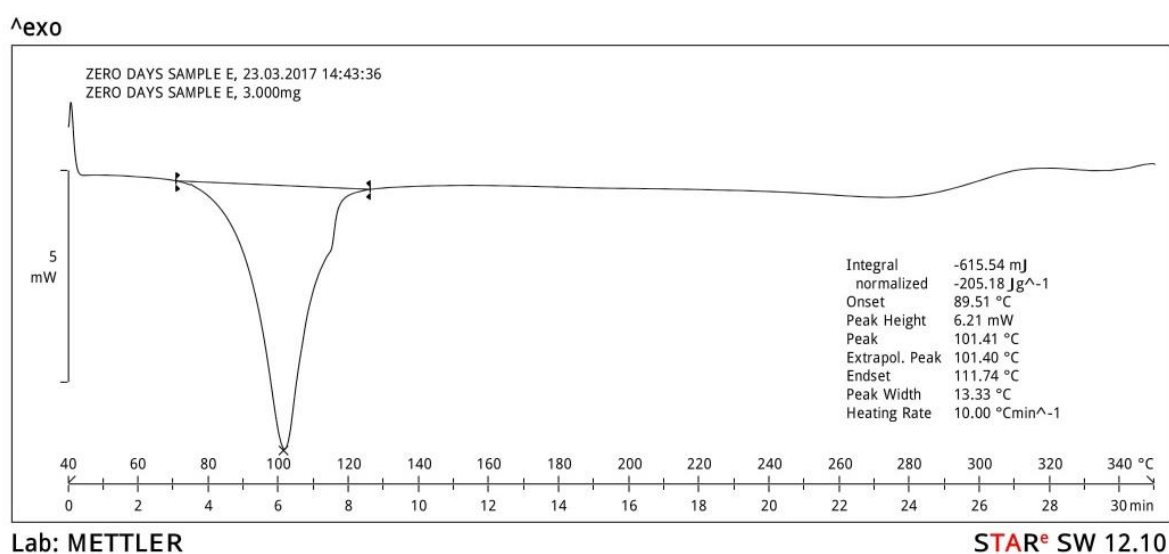


Figure 7: DSC thermogram of NTG + MG-S ('0' days).

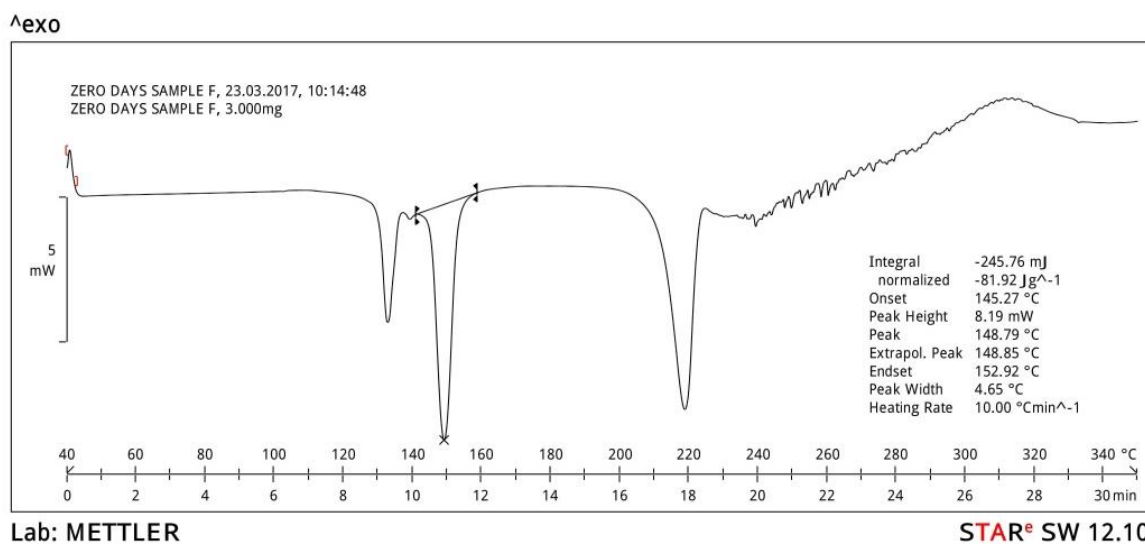


Figure 8: DSC thermogram of NTG + Lactose ('0' days).

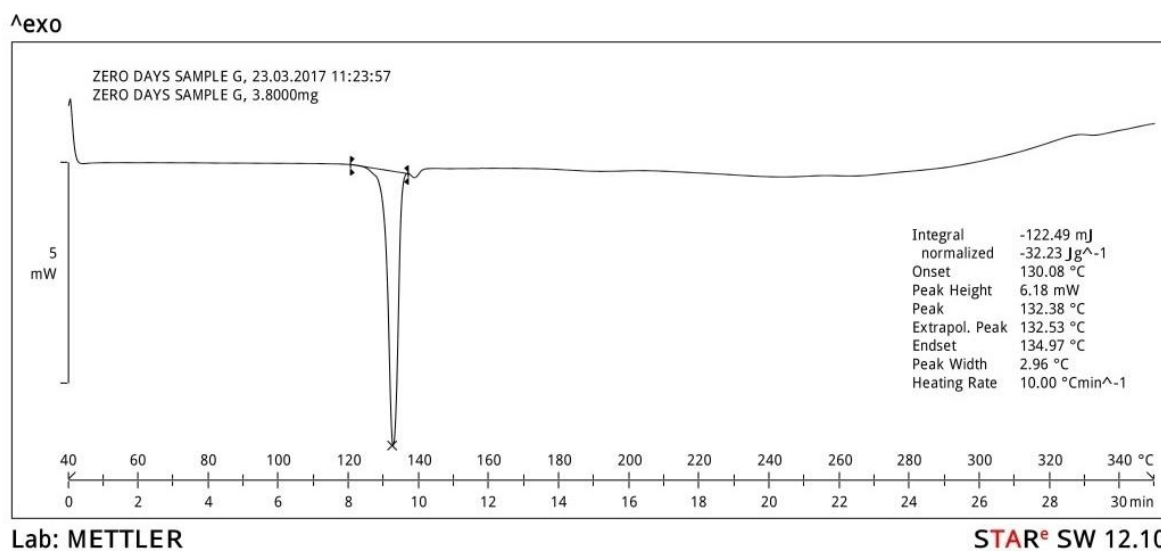


Figure 9: DSC thermogram of NTG + Talc ('0' days).

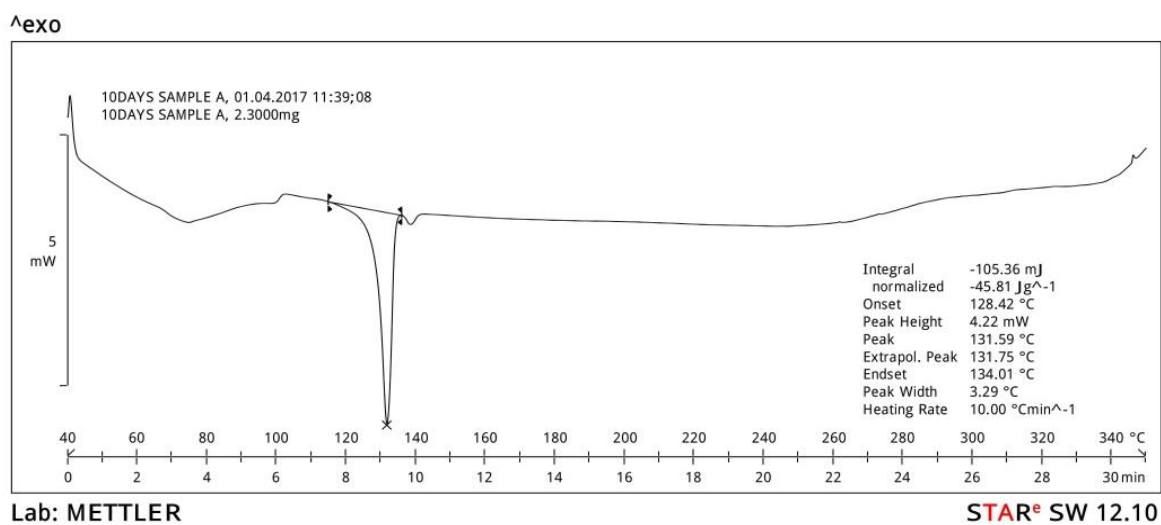


Figure 10: DSC thermogram of NTG + K100M ('10' days).

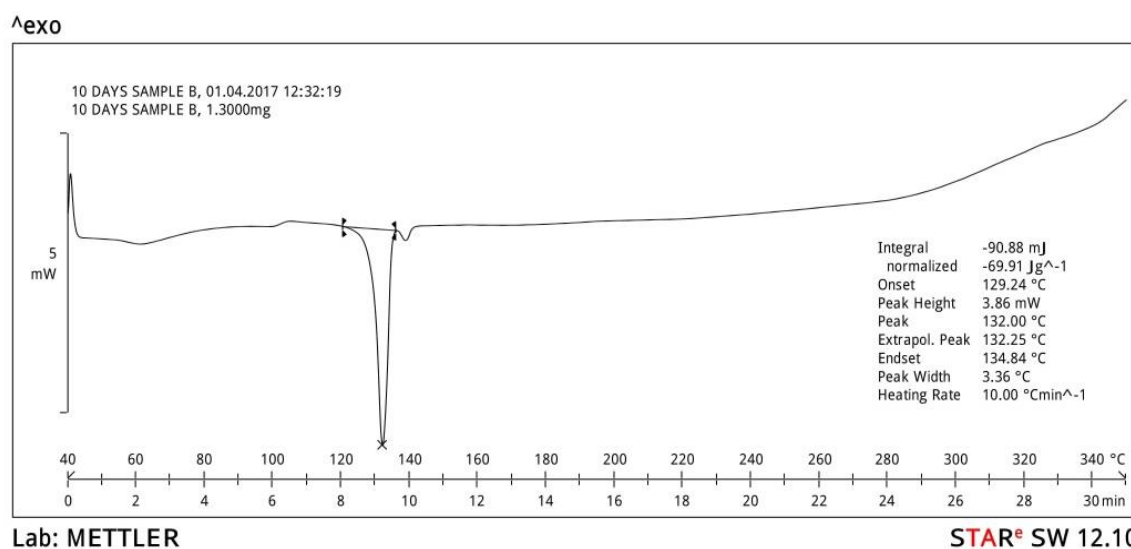


Figure 11: DSC thermogram of NTG + K4M ('10' days).

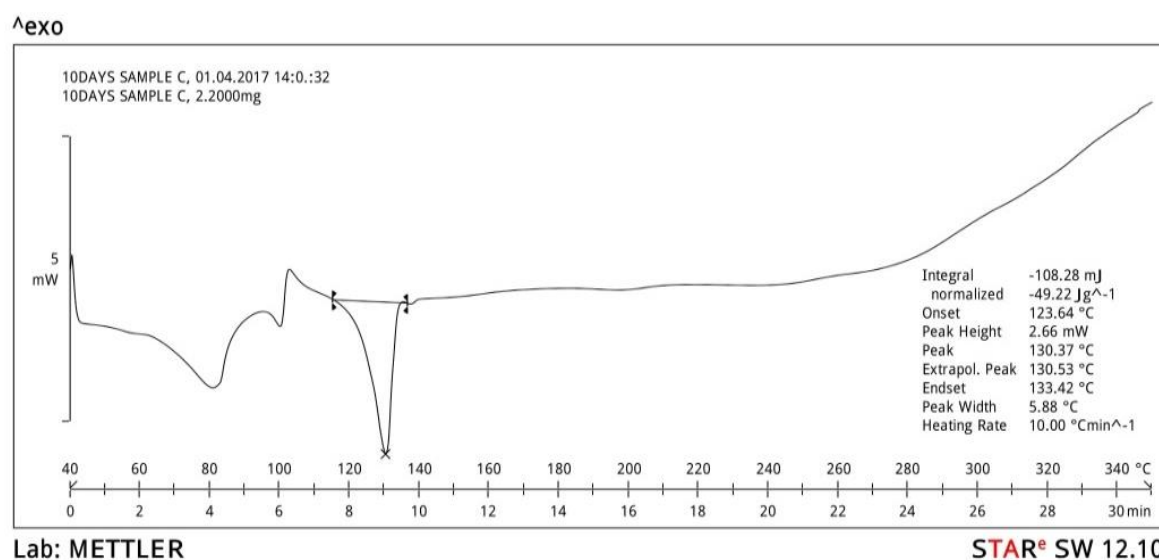


Figure 12: DSC thermogram of NTG + AVICEL PH101 ('10' days).

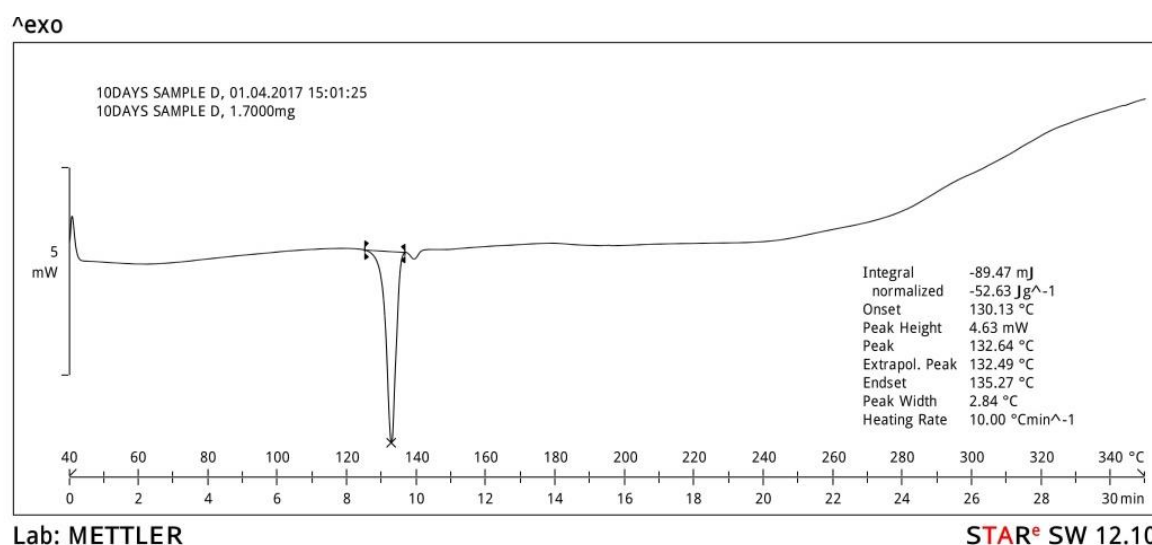


Figure 13: DSC thermogram of NTG + AVICEL PH102 ('10' days).

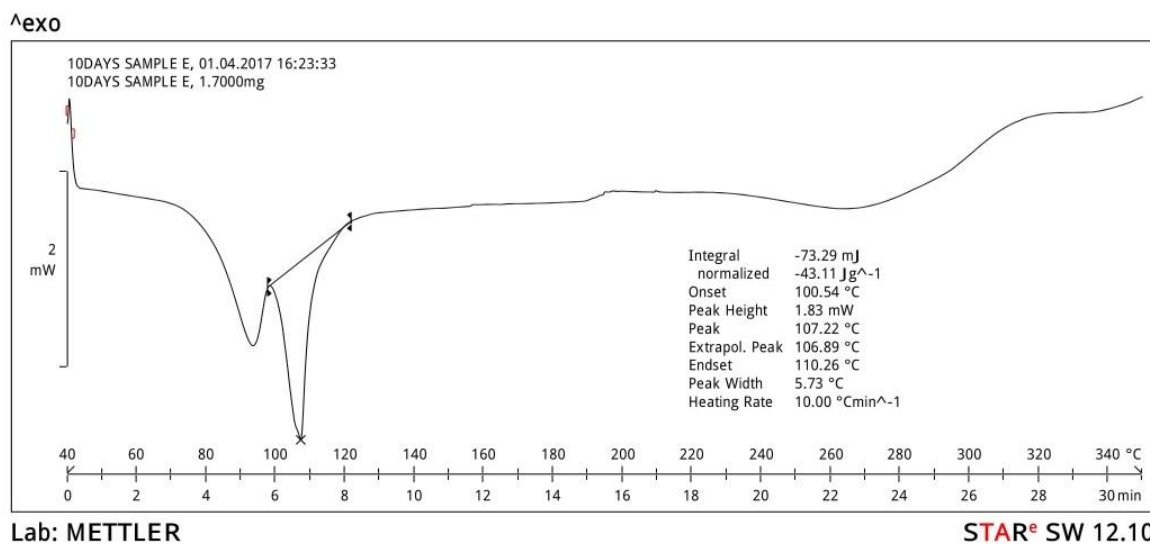


Figure 14: DSC thermogram of NTG + MG-S ('10' days).

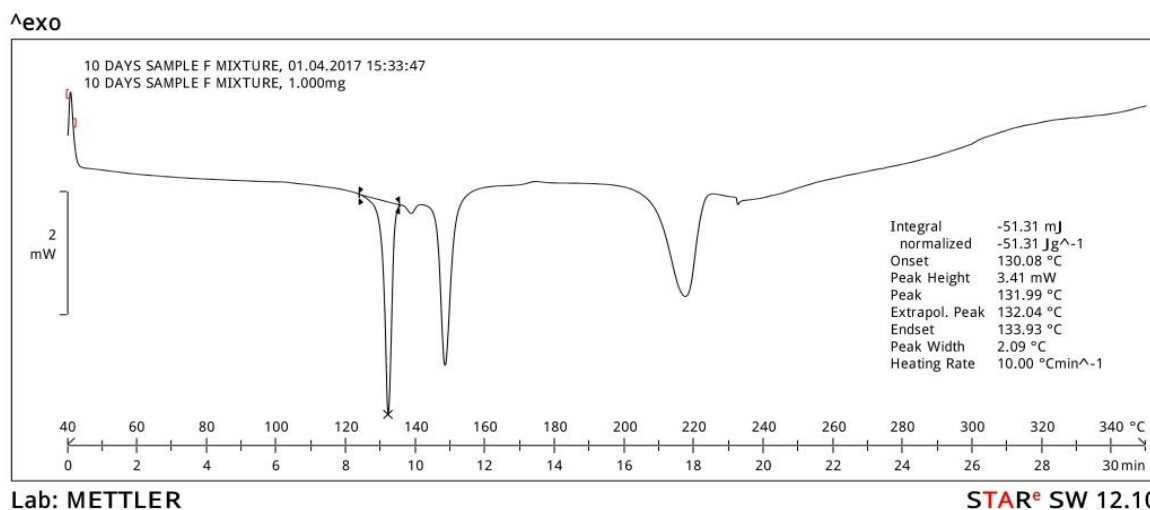


Figure 15: DSC thermogram of NTG + Lactose ('10' days).

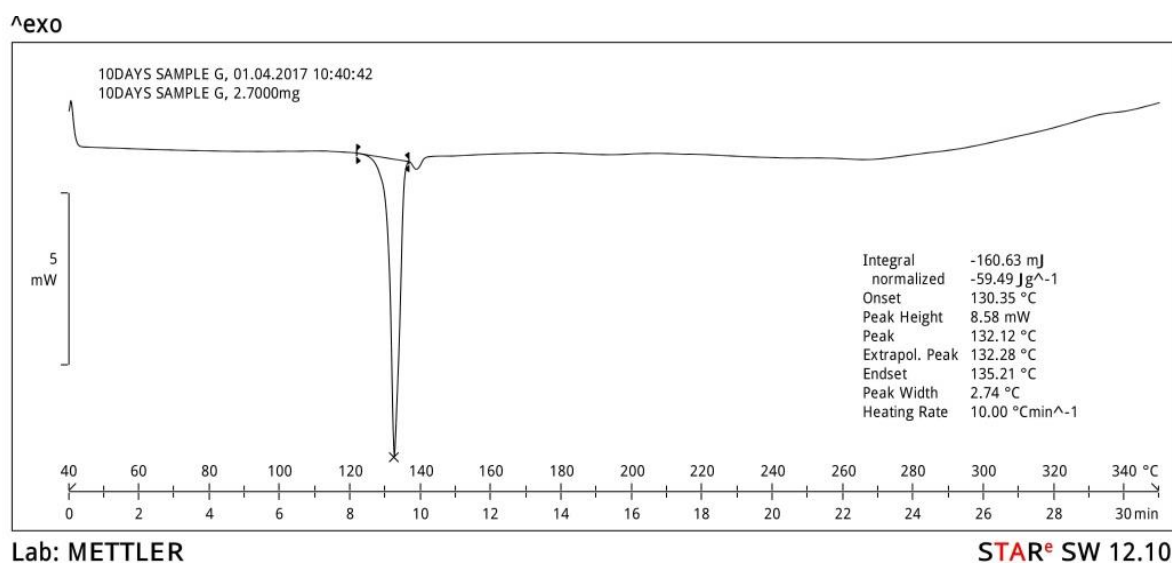
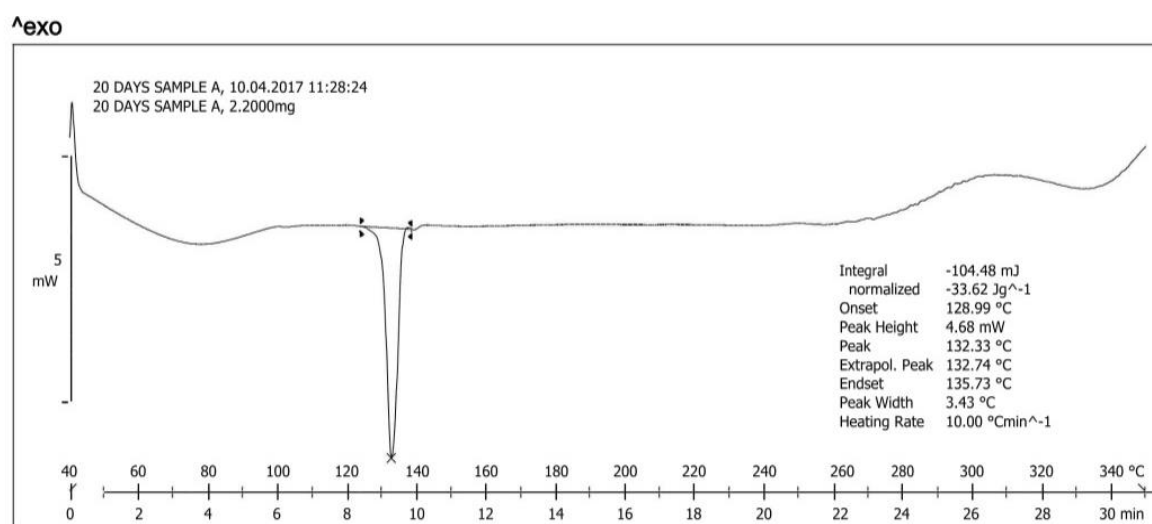


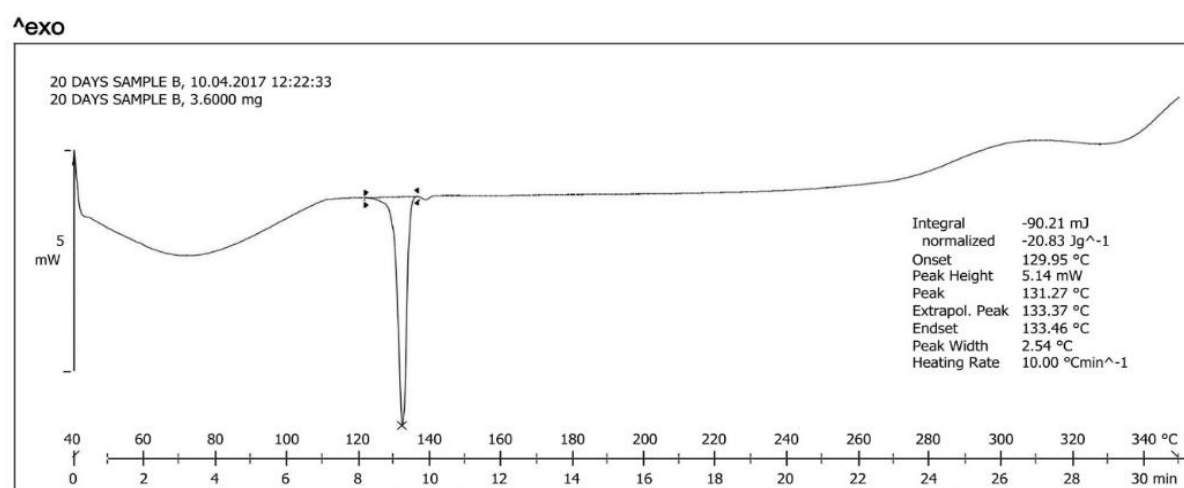
Figure 16: DSC thermogram of NTG +Talc ('10' days).



Lab: METTLER

STAR[®] SW 12.10

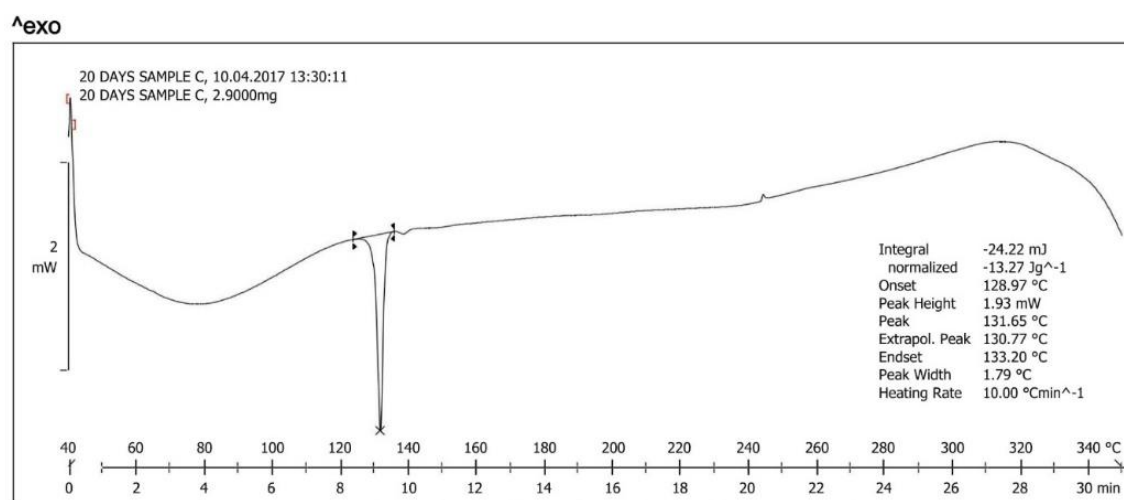
Figure 17: DSC thermogram of NTG + K100M ('20' days).



Lab: METTLER

STAR[®] SW 12.10

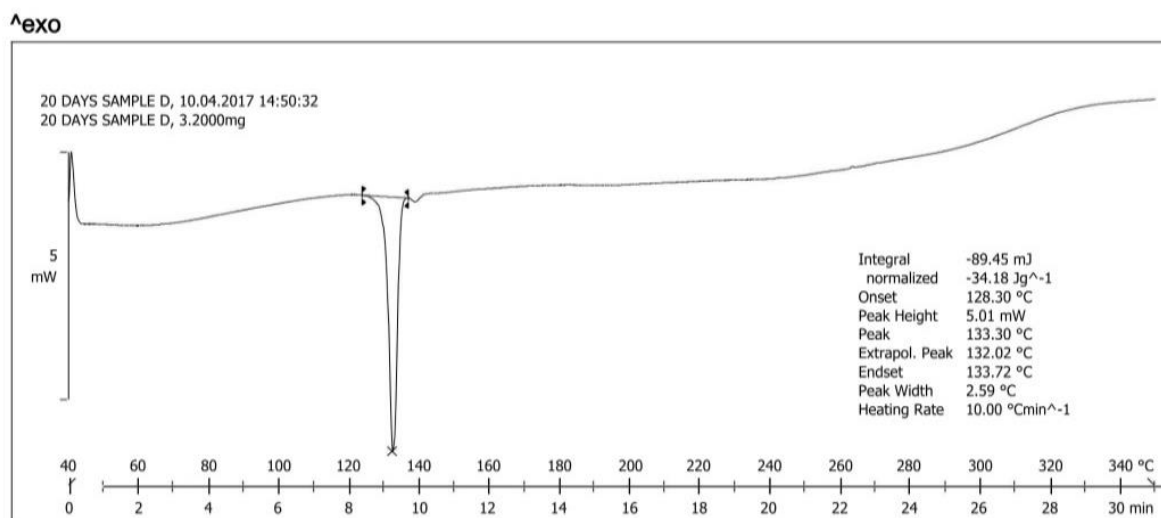
Figure 18: DSC thermogram of NTG + K4M ('20' days).



Lab: METTLER

STAR[®] SW 12.10

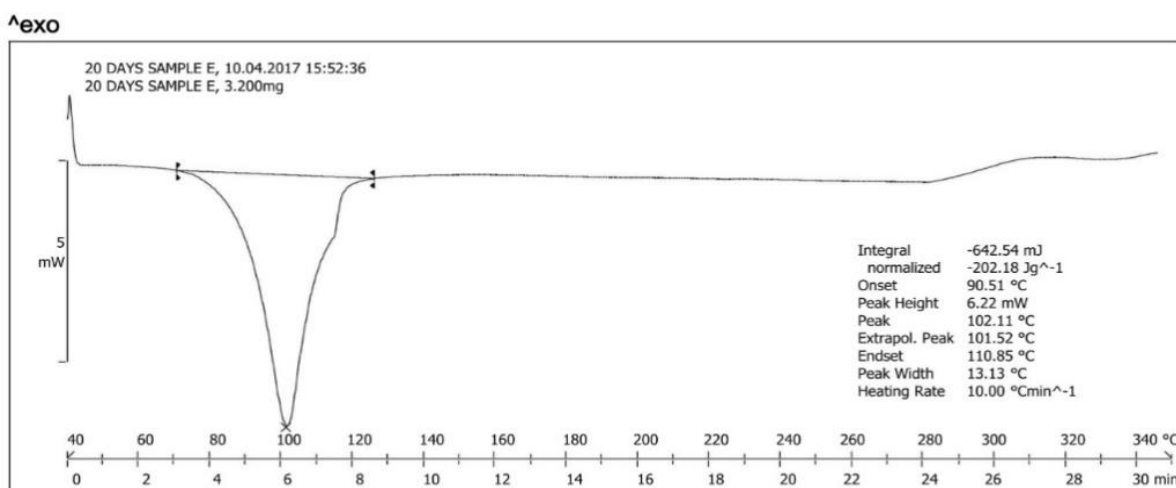
Figure 19: DSC thermogram of NTG + AVICEL PH101 ('20' days).



Lab: METTLER

STAR[®] SW 12.10

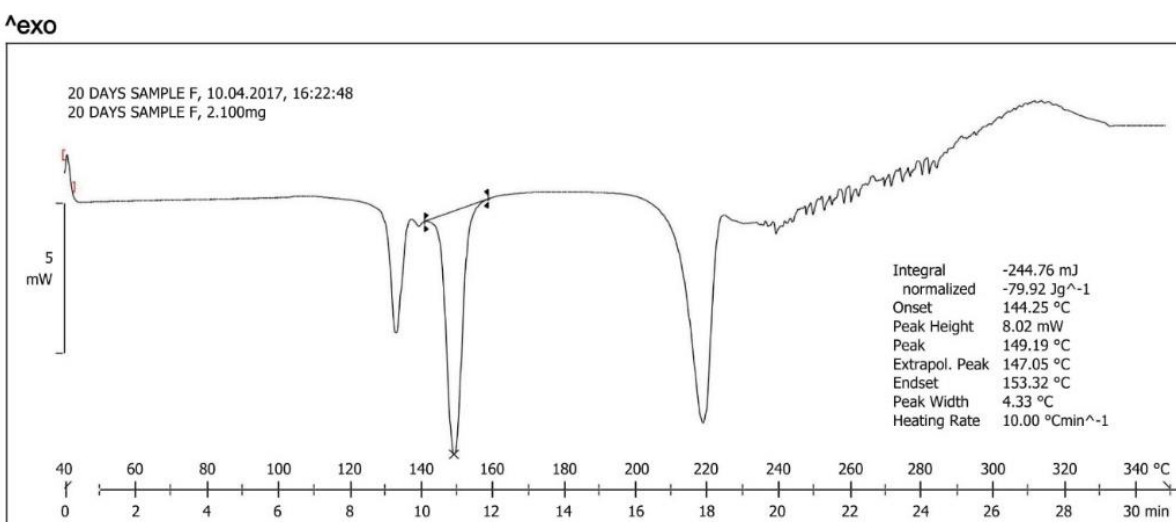
Figure 20: DSC thermogram of NTG + AVICEL PH102 ('20' days).



Lab: METTLER

STAR[®] SW 12.10

Figure 21: DSC thermogram of NTG + MG-S ('20' days).



Lab: METTLER

STAR[®] SW 12.10

Figure 22: DSC thermogram of NTG + Lactose ('20' days).

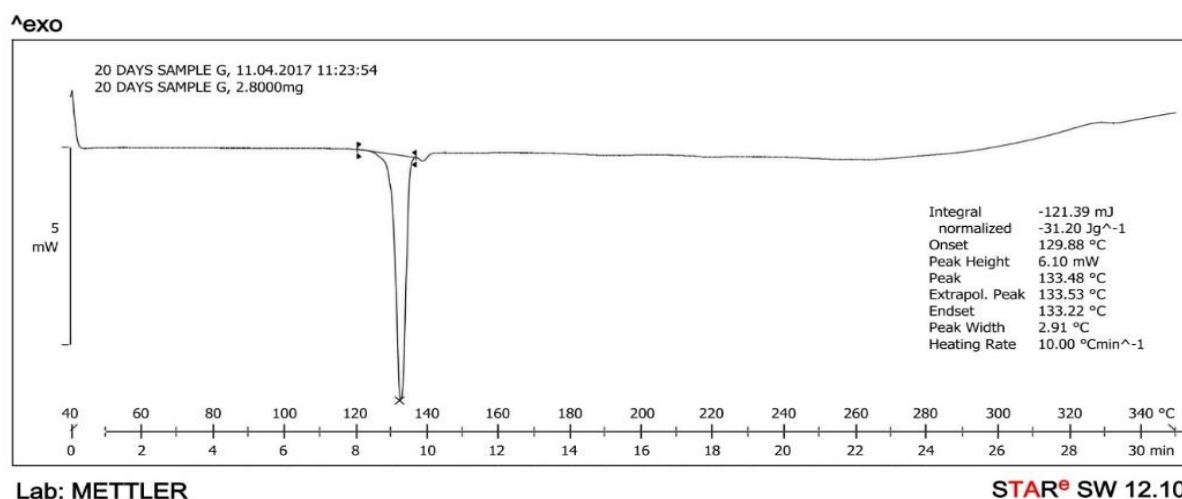


Figure 23: DSC thermogram of NTG +Talc ('20' days).

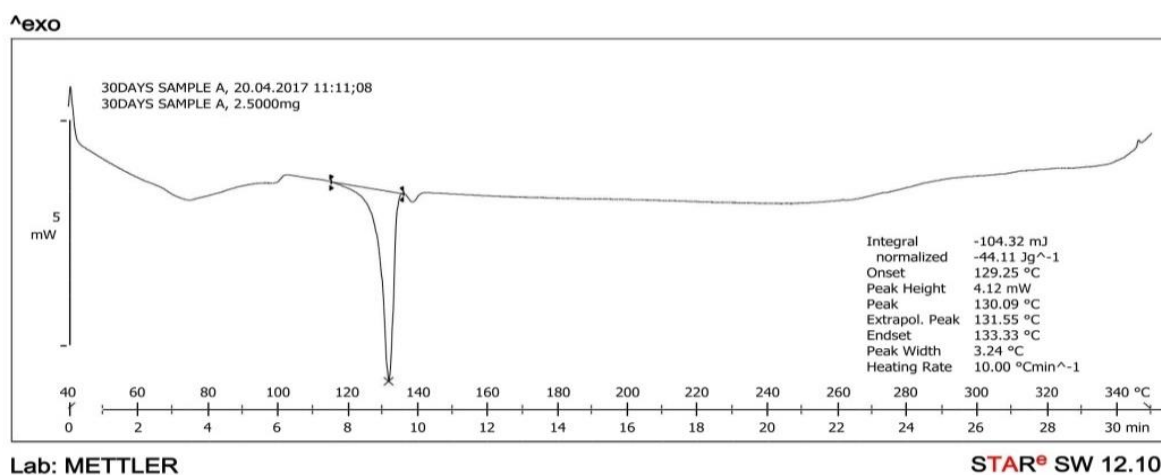


Figure 24: DSC thermogram of NTG + K100M ('30' days).

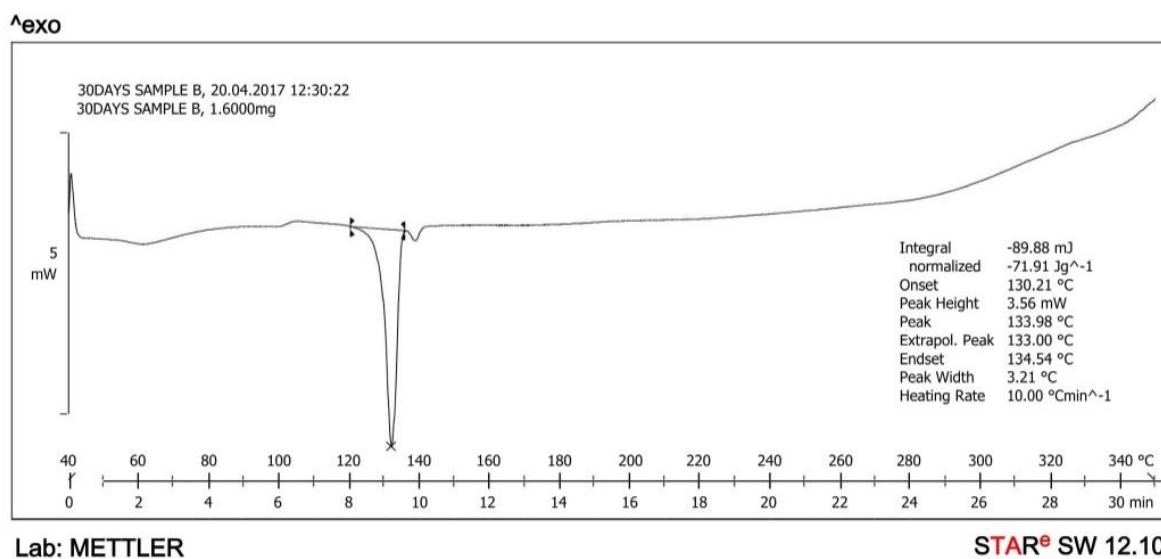


Figure 25: DSC thermogram of NTG + K4M ('30' days).

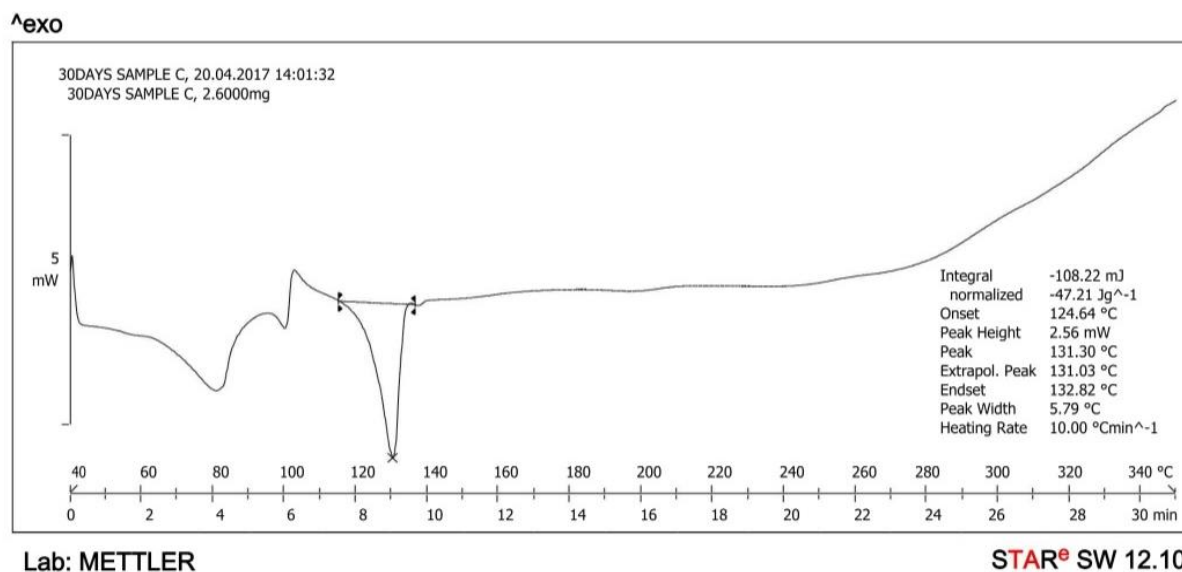


Figure 26: DSC thermogram of NTG + AVICEL PH101 ('30' days).

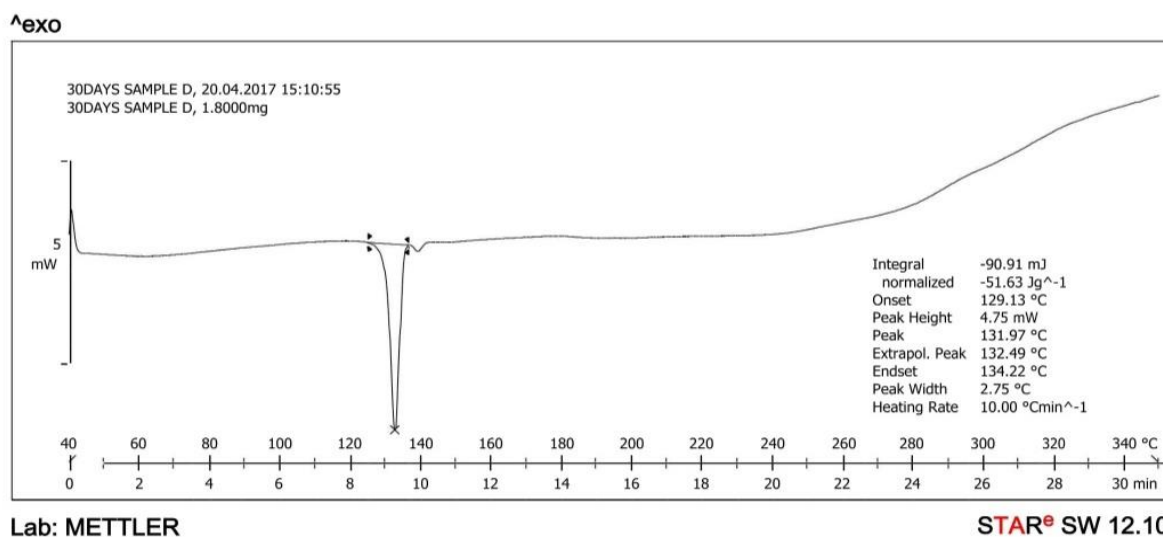


Figure 27: DSC thermogram of NTG + AVICEL PH102 ('30' days).

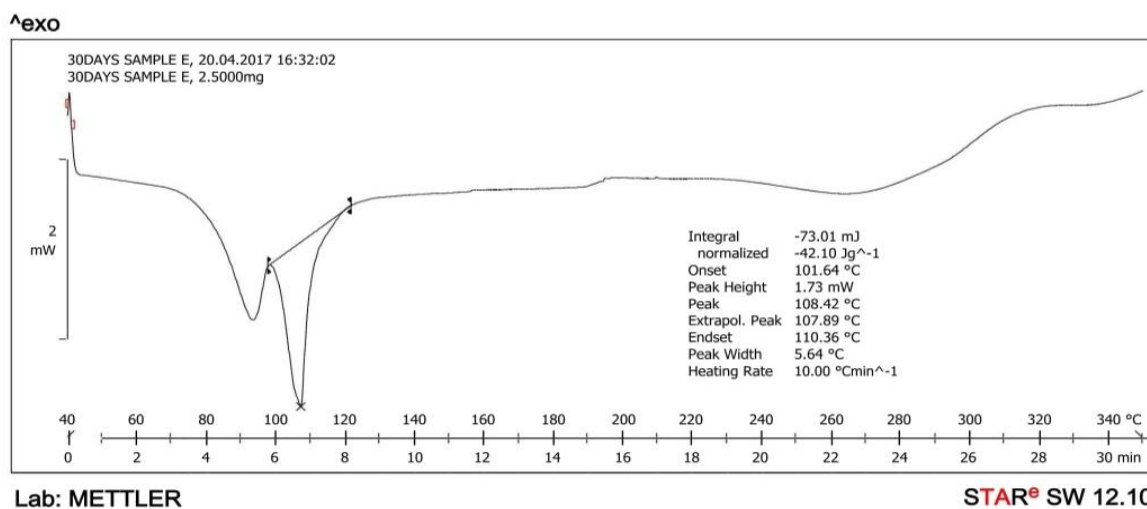


Figure 28: DSC thermogram of NTG + MG-S.

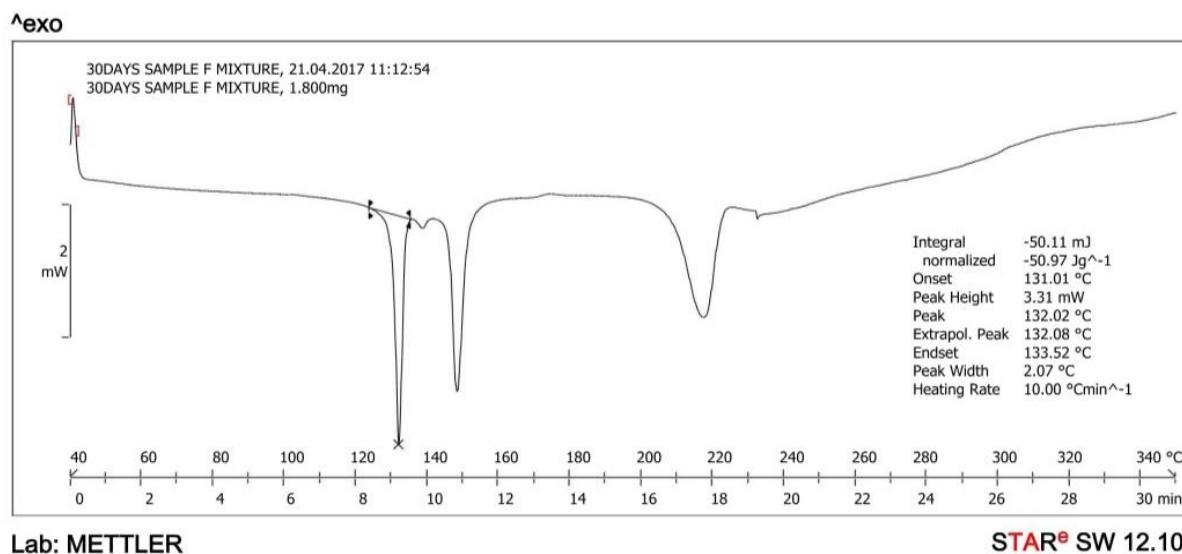


Figure 29: DSC thermogram of NTG + Lactose.

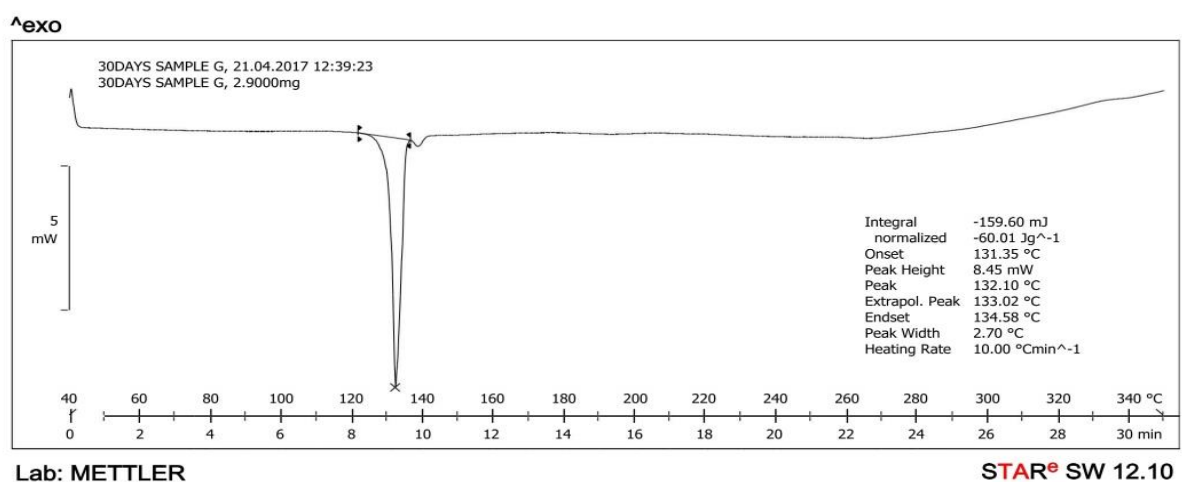


Figure 30: DSC thermogram of NTG +Talc.

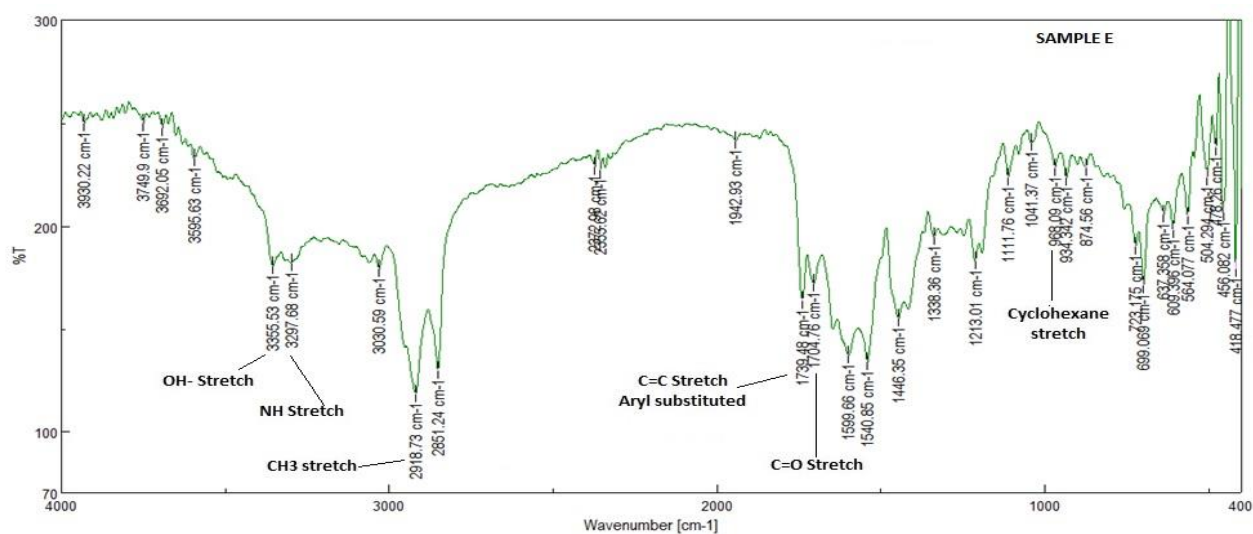


Figure 31: IR spectra of NTG +Magnesium Stearate.

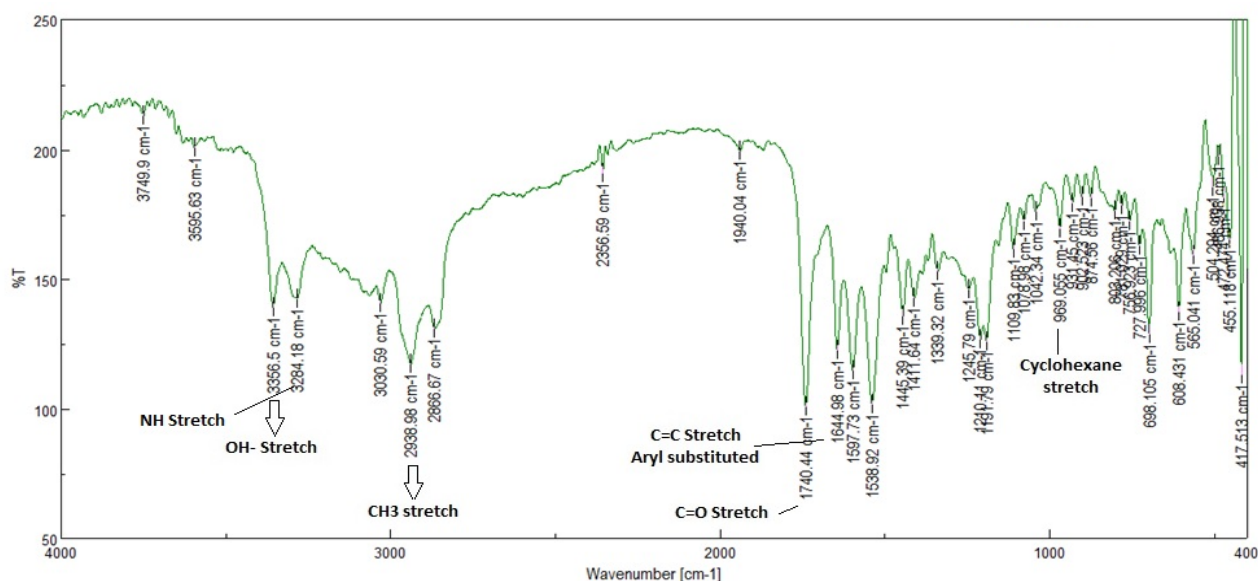


Figure 32: IR spectra of NTG.

The DSC thermogram of NTG and Magnesium Stearate (MG-S) showed a sharp endothermic peak at 101.41°C and peak onset at 89.91°C with irregular thermogram. There is disappearance of the peak of NTG indicates that, there may be physical interaction between NTG and MG-S. Therefore, the NTG - MG-S mixture was subjected to IR study and its spectrum was compared with IR spectra of NTG, which indicates that there is no any physical interaction between NTG and MG-S. (Figure 31, 32)

The DSC thermogram of NTG and Lactose showed a sharp endothermic peak at 148.79°C and peak onset at 145.27°C which indicates dehydration of bound water. The DSC thermogram also showed the melting point peak at 220°C. This indicates that there is no physical interaction between NTG and Lactose. (Figure 8)

The DSC thermogram of NTG and Talc showed a sharp endothermic peak at 132.38°C and peak onset at 130.08°C. The endothermic peak of NTG was well preserved, this shows that the NTG is compatible with Talc. (Figure 9)

The DSC thermogram of NTG and K100M showed a sharp endothermic peak at 131.59°C and peak onset at 128.42°C. The endothermic peak of NTG was well preserved, this shows that the NTG is compatible with K100M. (Figure 10)

The DSC thermogram of NTG and K4M showed a sharp endothermic peak at 132.00°C and peak onset at 129.24°C. The endothermic peak of NTG was well preserved, this shows that the NTG is compatible with K4M. (Figure 11)

The DSC thermogram of NTG and Microcrystalline Cellulose AVICEL PH101 showed a sharp endothermic peak at 130.37°C and peak onset at 123.64°C. The endothermic peak of NTG was well preserved, this shows that the NTG is compatible with AVICEL PH101. (Figure 12)

The DSC thermogram of NTG and Microcrystalline Cellulose AVICEL PH102 showed a sharp endothermic peak at 132.64°C and peak onset at 130.13°C. The endothermic peak of NTG was well preserved, this shows

that the NTG is compatible with AVICEL PH102. (Figure 13)

The DSC thermogram of NTG and Magnesium Stearate (MG-S) showed a sharp endothermic peak at 107.22°C and peak onset at 100.54°C with irregular thermogram. There is disappearance of the peak of NTG indicates that, there may be physical interaction between NTG and MG-S. Therefore, the NTG - MG-S mixture was subjected to IR study and its spectrum was compared with IR spectra of NTG, which indicates that there is no any physical interaction between NTG and MG-S. (Figure 31,32)

The DSC thermogram of NTG and Lactose showed a sharp endothermic peak at 131.99°C and peak onset at 130.08°C which indicates dehydration of bound water. The DSC thermogram also showed the melting point peak at 219°C. This indicates that there is no physical interaction between NTG and Lactose. (Figure 15)

The DSC thermogram of NTG and Talc showed a sharp endothermic peak at 132.12°C and peak onset at 130.35°C. The endothermic peak of NTG was well preserved, this shows that the NTG is compatible with Talc. (Figure 16)

The DSC thermogram of NTG and K100M showed a sharp endothermic peak at 132.33°C and peak onset at 128.99°C. The endothermic peak of NTG was well preserved, this shows that the NTG is compatible with K100M. (Figure 17)

The DSC thermogram of NTG and K4M showed a sharp endothermic peak at 131.27°C and peak onset at 129.95°C. The endothermic peak of NTG was well preserved, this shows that the NTG is compatible with K4M. (Figure 18)

The DSC thermogram of NTG and Microcrystalline Cellulose AVICEL PH101 showed a sharp endothermic peak at 131.65°C and peak onset at 128.97°C. The endothermic peak of NTG was well preserved, this shows that the NTG is compatible with AVICEL PH101. (Figure 19)

The DSC thermogram of NTG and Microcrystalline Cellulose AVICEL PH102 showed a sharp endothermic peak at 133.30°C and peak onset at 128.30°C. The

Table 1: Results of UV analysis of the samples under IST conditions after 3 weeks of storage.

Sr. No.	Sample	Ratio (Drug + Excipients / polymer)	% Drug Remaining	
			^B Control Sample (2-8°C)	^C Stressed Sample (50°C)
	A		101.64	99.6
	B		102.15	99.8
	C		101.25	99.48
	D		101.92	100.17
	E		101.96	99.56
	F		102.2	100.49
	G	1:1	101.44	99.67
	H		101.79	100.01

^A Values are expressed as standard deviation^B Drug excipients/polymers blend without water and stored in refrigerator (2-8°C)^C Drug excipients/polymers blend with 10% added water and stored at 50°C for 3 weeks.

endothermic peak of NTG was well preserved, this shows that the NTG is compatible with AVICEL PH102. (Figure 20)

The DSC thermogram of NTG and Magnesium Stearate (MG-S) showed a sharp endothermic peak at 102.11°C and peak onset at 90.51°C with irregular thermogram. There is disappearance of the peak of NTG indicates that, there may be physical interaction between NTG and MG-S. Therefore, the NTG - MG-S mixture was subjected to IR study and its spectrum was compared with IR spectra of NTG, which indicates that there is no any physical interaction between NTG and MG-S. (Figure 31, 32)

The DSC thermogram of NTG and Lactose showed a sharp endothermic peak at 149.19°C and peak onset at 144.25°C which indicates dehydration of bound water. The DSC thermogram also showed the melting point peak at 220°C. This indicates that there is no physical interaction between NTG and Lactose. (Figure 22)

The DSC thermogram of NTG and Talc showed a sharp endothermic peak at 133.48°C and peak onset at 129.88°C. The endothermic peak of NTG was well preserved, this shows that the NTG is compatible with Talc. (Figure 23)

The DSC thermogram of NTG and K100M showed a sharp endothermic peak at 130.09°C and peak onset at 129.25°C. The endothermic peak of NTG was well preserved, this shows that the NTG is compatible with K100M. (Figure 24)

The DSC thermogram of NTG and K4M showed a sharp endothermic peak at 133.98°C and peak onset at 130.21°C. The endothermic peak of NTG was well preserved, this shows that the NTG is compatible with K4M. (Figure 25)

The DSC thermogram of NTG and Microcrystalline Cellulose AVICEL PH101 showed a sharp endothermic peak at 131.30°C and peak onset at 124.64°C. The endothermic peak of NTG was well preserved, this shows that the NTG is compatible with AVICEL PH101. (Figure 26)

The DSC thermogram of NTG and Microcrystalline Cellulose AVICEL PH102 showed a sharp endothermic peak at 131.97°C and peak onset at 129.13°C. The endothermic peak of NTG was well preserved, this shows that the NTG is compatible with AVICEL PH102. (Figure 27)

The DSC thermogram of NTG and Magnesium Stearate (MG-S) showed a sharp endothermic peak at 108.42°C and peak onset at 101.64°C with irregular thermogram. There is disappearance of the peak of NTG indicates that, there may be physical interaction between NTG and MG-S. Therefore, the NTG - MG-S mixture was subjected to IR study and its spectrum was compared with IR spectra of NTG, which indicates that there is no any physical interaction between NTG and MG-S. (Figure 31,32)

The DSC thermogram of NTG and Lactose showed a sharp endothermic peak at 132.02.19°C and peak onset at 131.01°C which indicates dehydration of bound water. The DSC thermogram also showed the melting point peak at 220°C. This indicates that there is no physical interaction between NTG and Lactose. (Figure 29)

The DSC thermogram of NTG and Talc showed a sharp endothermic peak at 132.10°C and peak onset at 131.35°C. The endothermic peak of NTG was well preserved, this shows that the NTG is compatible with Talc. (Figure 30)

Isothermal Stress Testing (IST)

The drug-excipient mixtures were tested using the technique of IST and the quantitative results obtained after UV analysis are shown in Table 1. It has been observed from the Table 2 that there is a little change in the drug content of the samples after storage of drug-excipient blends under stressed conditions of IST studies after 3 weeks of storage at stressed conditions, also the from DSC and IR study it clearly indicates that NTG was not degraded in drug-excipients mixture. Therefore, it was considered that the NTG and the excipients used are compatible with each other.

In case of NTG-magnesium stearate mixture, a definite conclusion could not be drawn based on the DSC results alone. However, the results of IST studies showed that the residual drug concentration was within the limit and in the IR spectrum of NTG-magnesium stearate mixture, the characteristic bands of NTG were well preserved confirming the compatibility.

CONCLUSION

The results of the compatibility studies confirmed that DSC and IR could be used as the intensive methods to evaluate and ascertain the compatibility between NTG, polymers and excipients. However, the techniques of IST

after storage of the mixture of NTG and individual excipients under stressed conditions should also be adopted in conjunction with DSC and IR studies to confirm conclusion. In this study, the DSC study along with IR spectroscopy and UV analysis (for IST studies) were successfully employed to assess the compatibility of NTG with the excipients and polymers.

From overall results of the DSC studies an interaction was suspected between NTG and magnesium stearate. However, based on the results of IR spectroscopy and IST study, the possibility of incompatibility between NTG and magnesium stearate was completely ruled out. Thus, the methods of DSC, IR spectroscopy, and IST have been proved to be successful in the assessment of the compatibility of NTG, polymers and excipients which are used in the sustained release formulations.

REFERENCES

1. Pani N.R., Nath L.K. & Acharya S (2012). Application of DSC, IST, and FTIR study in the compatibility testing of nateglinide with different pharmaceutical excipients. *J Therm Anal Calorim.* 108, 219–226.
2. Pani N.R., Nath L.K. & Acharya S. (2011). Compatibility studies of nateglinide with excipients in immediate release tablets. *Acta Pharm.* 61 (2), 237-47. Doi: 10.2478/v10007-011-0016-4.
3. Govindasamy G., Krishnamoorthy K., Rajappan M (2013). Selection of Excipients for Nanoparticles Formulations of Nateglinide through Drug-Excipients Compatibility Study. *Int J Pharm PharmSci.*, 5, 2, 371-377.
4. R.A. Meyers (2012). Interpretation of Infrared Spectra: A Practical Approach by John Coates, *Encyclopedia of Analytical Chemistry*, John Wiley & Sons Ltd., 1-23p.
5. Sharma P.R., Lewis S.A. (2013) Design and in vitro/in vivo evaluation of extended release matrix tablets of nateglinide. *Journal of Young Pharmacists*, 5, 167-172.
6. Desu P.K. (2015) Formulation and evaluation of Nateglinide dispersible tablet by direct compression method. *International Journal of Advances in Scientific Research*, 1, 1, 51-56.
7. Verma R.K., Garg S. (2005) Selection of excipients for extended release formulation of glipizide through drug–excipient compatibility testing. *J Pharm Biomed Anal.* 38, 633-44.
8. Mura P, Manderioli A, Bramanti G, Furlanetto S, Pinzauti S. (1995) Utilization of differential scanning calorimetry as a screening technique to determine the compatibility of ketoprofen with excipients. *Int J Pharm.* 119, 71-9.
9. Mura P, Faucci MT, Manderioli A, Bramanti G, Ceccarelli L. (1998) Compatibility study between ibuprofen and pharmaceutical excipients using differential scanning calorimetry, hot-stage microscopy and scanning electron microscopy. *J Pharm Biomed Anal.* 18, 151-63.
10. Interpreting Unexpected Events and Transitions in DSC Results- TA Instruments. <http://www.tainstruments.com/pdf/literature/TA039.pdf>.
11. How to Interpret the Unexpected Transitions in DSC Results- TA Instruments. <https://www.azom.com/article.aspx?ArticleID=12101>.
12. G. Raveendra Babu1, A. Lakshmana Rao, Sri Lakshmi surekha P, T. Kalapaveen and P. Sambhasiva Rao. (2013). Spectrophotometric Methods for Estimation of Nateglinide in Bulk Drug and Its Dosage Form. *IJPCBS*, 3(4), 1160-1164.
13. ICH Harmonised Tripartite Guideline. Validation of Analytical Procedures: Text and Methodology Q2 (R1) (2005). pp1-11.
14. Interpreting DSC curves. http://www.masontechnology.ie/x/Usercom_11.pdf.
15. Mali R.R., Goel V. & Gupta S. (2015). Novel study in sustained release drug delivery system: A review. *Int. J. Pharm. Med. Res.* 3 (2), 204-215.
16. Patel K.B., Vyas J.R. & Upadhyay U.M. (2015). Formulation and evaluation of sustained release matrix tablets of nateglinide. *Journal of drug delivery & Therapeutics*, 5(5), 19-25.

Research Article

Formulation development and evaluation of sustained release tablet containing tamoxifen citrate and ibuprofen in treatment of metastatic breast cancer.

SHRUTI SONAWANE^{*1}, VINAYAK MADANE¹, AMIT KASABE¹, SANTOSH FATTEPUR², NAGARAJA SREEHARSHA^{3,4}

¹Department of Pharmaceutical Quality Assurance, PDEA'S Shankarrao Ursal College of Pharmaceutical Sciences and Research Centre, Kharadi, Pune, Maharashtra, India.

²School of Pharmacy, Management and Science University, Seksyen 13, 40100, Shah Alam, Selangor, Malaysia.

³Department of Pharmaceutical Sciences, College of Clinical Pharmacy, King Faisal University, Al-Ahsa-31982, Saudi Arabia.

⁴Department of Pharmaceutics, Vidya Siri College of Pharmacy, Off Sarjapura Road, Bengaluru - 560 035, Karnataka, India.

*Corresponding Author

Email ID: shrutisan99@gmail.com

Received: 28.08.20, Revised: 16.09.20, Accepted: 15.10.20

ABSTRACT

Cancer is a group of diseases which include an abnormal increase in cell count, which may invade or spread into other parts of the body. One of the hallmarks of cancer is metastasis, which separates it from benign tumours. In case of breast cancer it may metastasize anywhere in the body. In the metastasis of breast cancer, inflammation or swelling with cancer cell generation can occur. In the present research, sustained release tablet containing tamoxifen citrate and ibuprofen is formulated which can be used in the treatment of metastasis of breast cancer. Tamoxifen citrate is an estrogen-blocker with potent antiestrogenic properties and Ibuprofen is a NSAID with antipyretic and analgesic effects being an inhibitor of cyclooxygenase. The combination tablet of Tamoxifen citrate and Ibuprofen with different HPMC grade polymers such as K35 M, E4 M and E10 M were formulated. The pre-formulation studies such as rest angle, bulk density, tapped density; the Hausner ratio and the Carr index were found to be within the normal limit. The absence of possible chemical reactions between the drug and polymers was suggested by FTIR spectra. Powder mixtures were compressed into tablets for weight variation, thickness, stiffness, friability and drug content evaluation after compression. The in vitro release of medicines was investigated for 12 hours with USP Type-II dissolution apparatus. Results showed that the drug release was maintained over 12 hours by formulations containing various polymers.

Keywords: Tamoxifen citrate, ibuprofen, sustained release, metastatic breast cancer.

INTRODUCTION

Cancer is a group of diseases which include an abnormal increase in cell count, which may invade or spread into other parts of the body. Not all tumours or lumps are cancerous, and tumours that are benign are not labelled as cancer because they do not spread to other areas of the body. More than 100 different identified cancers affect humans. One of the hallmarks of cancer is metastasis, which separates it from benign tumours. But in varying degrees, most cancers can metastasize. Breast cancer may metastasize anywhere in the body but mostly metastasizes bone, lung, lymph nodes, liver and brain, the bone being the most common location. Metastatic breast cancer treatment depends on where the metastatic tumours occur and involves surgery, radiation, chemotherapy, biological and

hormonal treatment. In the metastasis of breast cancer, inflammation or swelling with cancer cell generation can occur. With this in mind, we decided to formulate the tablet containing tamoxifen citrate and ibuprofen for continuous release. [5,6,10-12] Tamoxifen citrate is an estrogen-blocker with potent antiestrogenic properties and also acts as estrogen receptor modulator having applicability in the treatment of breast cancer and infertility.[1-3]

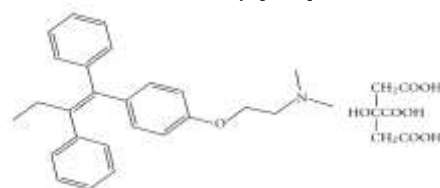


Fig.1: Structure of Tamoxifen citrate.

Ibuprofen is a non-steroidal antiinflammatory drug (NSAID) with antipyretic and analgesic effects being an inhibitor of cyclooxygenase, the enzyme responsible for the conversion of arachidonic acid to prostaglandins.

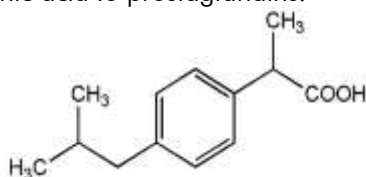


Fig.2: Structure of Ibuprofen.

The aim of the present research is to formulate and evaluate sustained release tablet containing tamoxifen citrate and ibuprofen in treatment of metastatic breast cancer.

MATERIALS AND METHODS

Materials

Tamoxifen citrate, a gift sample from Khandelwal laboratories, Mumbai, India. Polymers such as HPMC E4M, K35M and E10M were a gift sample by Ashland Inc., Netherland. Ibuprofen, talc, magnesium stearate and microcrystalline cellulose (PH102) were procured from commercial suppliers. Methanol and water used throughout the study is of HPLC grade and are procured from commercial suppliers.

Methods[4,13,14]

Preformulation evaluation

Identification of Pure drug (Tamoxifen Citrate)

Identification of pure drug (TAM) was carried out by Fourier Transform Infra-red Spectrophotometry (Shimadzu 8400s).

UV Spectroscopy: (Determination of λ maximum) [Shimadzu, uv1800]

Procedure-

1. Weigh and Transfer an accurately weighed quantity of the powder of pure TAM to 100ml volumetric flask.
2. Add little amount of methanol, and sonicate the solution for 30 min.
3. Then make up the volume up to mark by using methanol.
4. Filter the solution through the whatmann filter paper to get the clear solution. (100ppm solution of TAM- Standard Stock solution)
5. UV spectrum of stock solution was recorded in the wavelength range 200- 400nm and λ max of drug was determined by using methanol as blank.

Calibration curve

Preparation of standard stock solution

1. Weigh and Transfer an accurately weighed quantity of the powder of pure TAM to 100ml volumetric flask.
2. Add little amount of methanol, and sonicate the solution for 30 min.
3. Then make up the volume up to mark by using methanol.
4. Filter the solution through the whatmann filter paper to get the clear solution. (100ppm solution of TAM- Standard Stock solution)

Preparation of working stock solution

1. Then standard stock solution is diluted with methanol by withdrawing 0.8ml, 1.0ml and 1.2ml of the standard stock solution (100ppm solution of TAM) to prepare 8ppm, 10ppm and 12ppm solution respectively.
2. Measure the absorbance spectrophotometrically by scanning wavelength in the range 400nm to 200nm at λ max, using methanol as blank.
3. Note down the absorbance.
4. A standard plot of absorbance v/s concentration of drug in $\mu\text{g/ml}$ was plotted.

Drug-excipient compatibility study

A. IR spectroscopy

IR spectra of the drug and blend of drug and selected excipients were recorded on FTIR- 8400s spectrophotometer in the range of 4000-500 cm^{-1} using potassium bromide discs.

B. Differential scanning Calorimetry (DSC) [14]

Differential scanning calorimeter (DSC) is a thermal analysis technique which measures the temperature and heat flow associated with transitions in materials as a function of temperature and time.

C. Isothermal Stress Testing [13]

Isothermal stress testing (IST) study involves storing the drug excipient mixture with or without moisture at high temperature or at low temperature and determining the drug content.

- **Mixing ratio-** 1:1 (20mg TAM +200mg IBU + 80mg Excipient/s)
- **Storage condition-**
 - a. **For control sample-** 2-8°C
 - b. **For stressed sample-** 50°C
- **Study period (in days)-** 21 days
- **Sample withdrawn interval (in days)-** "21" days

Pre-compression evaluation[7-10]

The different parameters were evaluated such as angle of repose, bulk density, tapped density, Hauser's ratio and compressibility index.

1. Angle of Repose

A fixed funnel method was used to determine the angle of repose. The fixed funnel method uses a

funnel secured at a specified height (2 cm) over the graphic paper on a flat horizontal surface. Pellets or tablet blends have been thoroughly poured into the funnel until the apex of the conical pile touches the tip of the funnel. Thus, r is the conical pile's radius. The angle of rest has been calculated using the next equation.

$$\theta = \tan^{-1} (h/r) \dots\dots \text{Equation 1}$$

Where,

h = Height of pile

r = Radius of pile

θ = Angle of repose

2. Bulk Density

A powder (about 60gm) is transferred into the 100ml graduated cylinder through a standard sieve number 20. A weighted quantity (about 50gm). The volume of bulk is measured by dropping the cylinder (containing powder) three times above 1 inch at 2 s intervals on a hard wooden surface. Sometimes the container needs to be dropped or tapped 500 times in order to get an appropriate volume.

$$\text{Bulk density (p)} = (\text{Weight of the powder/ bulk volume}) \dots\dots \text{Formula 1}$$

3. Tapped Density

Tapped density is ratio of the mass of tablet blend to tapped volume of tablet blend. Accurately weighed amount of tablet blend poured in graduated cylinder and height is measured. Then cylinder was allowed to 100 tap under its own weight on to a hard surface. The tapping was continued until no further Change in height was noted.

$$\text{Tapped Density} = (\text{Weight of the powder/tapped volume}) \dots\dots \text{Formula 2}$$

4. Compressibility Index (Carr's Index)

Compressibility is the ability of powder to decrease in volume under pressure using bulk density and tapped density the percentage compressibility of powder were determined, which is given as Carr's compressibility index. It is indirectly related to the relative flow rate. Carr's compressibility index was determined by the given formula,

$$\text{Compressibility Index (\%)} = (\text{Tapped density - Bulk density}) \times 100 / \text{Tapped density}$$

..... **Formula 3**

5. Hauser's Ratio

Hauser's ratio indicates the flow properties of powder and measured by the ratio of tapped density to bulk density. Hauser's ratio was determined by the given formula,

$$\text{Hauser's ratio} = \text{Tapped Density / Bulk Density} \dots\dots \text{Formula 4}$$

Preparation of Tamoxifen Citrate 20mg sustained release tablet by direct compression method (Batches- F1 –F9)

Preparation of Tablet: Direct Compression Method

Procedure

1. All ingredients were weighed correctly and co sifted through the # 40 sieve (TAM+IBU+K35M+K4M+E10M+all excipients).
2. The above mixture was mixed for 5min in polybag.

3. The above blend was lubricated with magnesium stearate and talc, precisely weighed and passed through # 60 sheets.

The final mix was compressed into a tablet using 6 stations (Create, 08 station) with an average hardness of 4.0 to 6.0kg / cm², with a die of 9 mm.

Table 1: Preparation of Batches. (Pioglitazone layer)

Batches	Ingredients							
	TAM	IBU	HPMC			Talc	MCC	Magnesium Stearate
			K35M	K4M	E10M			
F1	20mg	200mg	10mg	-	-	5mg	q.s.	5mg
F2	20mg	200mg	20mg	-	-	5mg	q.s.	5mg
F3	20mg	200mg	30mg	-	-	5mg	q.s.	5mg
F4	20mg	200mg	-	10mg	-	5mg	q.s.	5mg
F5	20mg	200mg	-	20mg	-	5mg	q.s.	5mg
F6	20mg	200mg	-	30mg	-	5mg	q.s.	5mg
F7	20mg	200mg	-	-	10mg	5mg	q.s.	5mg
F8	20mg	200mg	-	-	20mg	5mg	q.s.	5mg
F9	20mg	200mg	-	-	30mg	5mg	q.s.	5mg

Total Weight of the tablet- 300mg

Post Compression evaluation

1. General appearance

In these the colour, odour, tasteless, solubility, are carried out.

2. Weight Variation

A tablet intended to contain a certain amount of medicine in a certain quantity of a tablet formula regularly tests the weight of the tablet to ensure that the tablet contains the right amount of medicine. In testing, 10 tablets were taken and measured on a digital weighing balance individually. The average weight of each tablet was calculated and the average weight was compared. If not more than 2 tablets are outside the percentage limit and no tablet is different by more than 2 times the percentage limit, the tablet passes the test.

$$\% \text{ Weight variation} = \frac{\text{Average weight} - \text{Weight of each tablet}}{\text{Average weight}} \times 100$$

..... **Formula 5**

3. Thickness

Thickness was measured using Vernier calliper. It was determined by checking three tablets from each formulation.

4. Hardness

Hardness is defined as 'the force to break a tablet in a diametric compression test.' Hardness is therefore often referred to as crushing strength. The strength before use depends on its hardness. Pfizer hardness tester measured the hardness of the tablet. A tablet has been placed in the hardness test and the load needed to crush the tablet has been measured.

5. Friability Test

This test assesses the ability of tablets to resist abrasion in packaging, handling and transportation. In general, friability indicates low cohesion of tablet ingredients. The initial weight of 10 comprises a friabilator consisting of a circular, plastic chamber divided into 2-3 compartments. The chamber rotates for 4 minutes at 25 rpm and drops the tablets for 15 cm and provides 100 revolutions. Afterwards, the tablets are again weighed. The weight difference is noted and shown as a percentage. It should be preferably below 1.0 %.

$$\% \text{ Friability} = (W1 - W2) / W1 \times 100 \quad \text{.....}$$

Formula 6

Where,

W1 = weight of tablets before test,

W2 = weight of Tablet after test

6. Assay of Tablet

Not less than 20 tablets weigh and finely powder. Transfer to 100 ml volumetric bottle an accurately weighed amount of powder equivalent to 10 mg

pioglitazone. Add little methanol and sauté the solution for 30 minutes. Then the volume is marked with methanol. Filter the solution via the philtre paper of Whatmans to obtain a clear solution. (Pioglitazone-Stock Solution 100ppm). Remove 0.8ml, 1.0ml and 1.2ml of stock solution (pioglitazone solution 100 ppm) respectively for preparation of 8ppm, 10ppm and 12ppm solution. Measure spectrophotometrical absorption by scanning the wavelength between 400 nm and 200 nm using blank methanol. Notice the absorption.

7. In Vitro Study Dissolution study for formulated batches F1-F18 was performed as per USP.

Procedure-

For acid stage

1. Hydrochloric acid with 0.5 percent Sodium lauryl sulphate was placed in the vessel and the USP-II (paddle method) appliance was assembled. 900 ml of 0.01N
2. The medium could be balanced at a temperature of $37 \pm 0.5^\circ \text{C}$.
3. A tablet of each batch was placed and covered in the ship; the device was operated at 50 rpm for up to 2 hours.
4. The 2ml sample was removed at 0, 0.5, 1 and 2 hours.
5. After extracting the sample, the fresh medium 2ml was substituted.
6. Using UV spectroscopy, absorption of the sample solution was measured at 206 nm.

Procedure-

For buffer stage

1. The vessel was fitted with 900 ml of phosphate buffer (PH- 6.8)
2. A tablet of each load was placed in a vessel which was removed and covered with acid vessel and the apparatus was operated at 50 rpm for up to 13 hours.
3. The sample 2ml was removed at 0, 1, 2, 4, 6, 8, 12, hours.
4. After extracting the sample, the fresh medium 2ml was substituted.
5. The absorption of the sample solution was measured by means of UV spectroscopy at 270 nm and 265 nm.

RESULTS AND DISCUSSION

Identification of Pure Drug (Tamoxifen citrate & Ibuprofen)

Identification of pure drug (TAM) was carried out by Fourier Transform Infra-red Spectrophotometry (Shimadzu 8400s). It showed characteristics peak of pure drug.

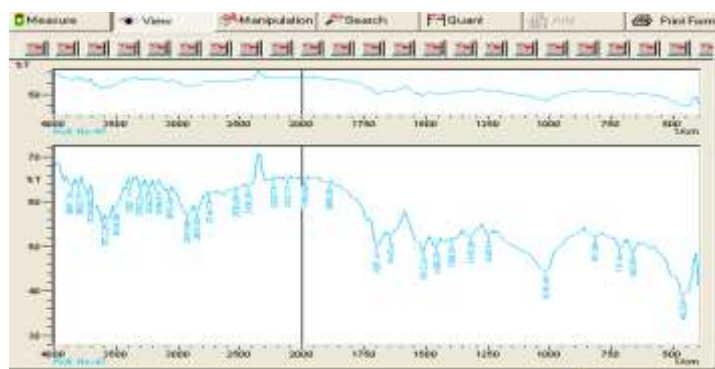


Fig.3: FTIR Spectra of Tamoxifen Citrate and Ibuprofen.

Table 2. Characteristic peak of Tamoxifen Citrate (TAM).

IR signals cm^{-1}	Functional groups
3363.89	-OH stretching
2960	-CH ₃ stretching
1629.85	-C=O stretching
1480	C=C stretching

Table 3: Characteristic peak of Ibuprofen (IBU).

IR signals cm^{-1}	Functional groups
3000	-OH stretching
2966.52	-CH ₃ stretching
1720	-C=O stretching
1500	C=C stretching

methanol was found to be 275nm which is in compliance with the reported value in literature. It obeys Beer Lambert's law over concentration range of 05 -50 $\mu\text{g/ml}$. It showed r^2 value of 0.992.

Drug-Excipient Compatibility Study

a) FTIR spectroscopy: FTIR spectrum of pure TAM, IBU physical mixture of drug and polymers were studied. It was observed that there were no major shifts in main peaks of drug. The IR spectra of the different mixture shows, the characteristic bands of TAM and IBU. Figure 4 shows the representative spectra of TAM+IBU+ K35. This indicates that there was no any compatibility problem of drug with polymers and excipients used in the formulation.

UV-Spectroscopy (Determination of λ maximum): The λ max of pure drug TAM in

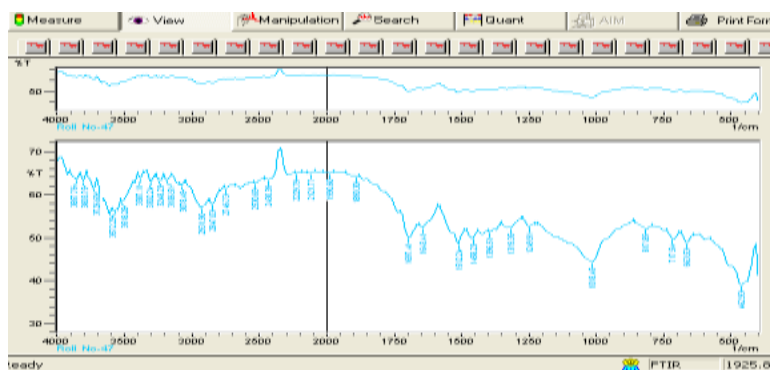


Fig.4: IR spectra of TAM+IBU+ K35.

IR spectra of mixture of TAM +IBU+ K35 shows characteristics bands of TAM at 3357.46cm^{-1} (-OH), 3295.75cm^{-1} (-NH=), 2939.95cm^{-1} (-CH₃), 1740.44cm^{-1} (C=O), 1644.95cm^{-1} (C=C), 1486cm^{-1} which indicates there is no any physical interaction between TAM +IBU+ K35. Similarly the IR spectrum for all other samples showed the characteristics peaks, which confirms no incompatibility.

Isothermal Stress Testing (IST)

Differential scanning Calorimetry (DSC)

DSC study- DSC study was performed to study drug-excipients compatibility. The majority of DSC thermograms of drug alone and in combination with different polymers shows onset temperature of peak (Tonset) [$\sim 71.48^\circ\text{C}$] and peak transition temperature (Tpeak) [$\sim 76.52^\circ\text{C}$]. The thermogram of TAM and IBU showed a sharp endothermic peak at $\sim 80.76^\circ\text{C}$ and peak onset $\sim 71.48^\circ\text{C}$. In majority of thermograms, the melting endotherm of TAM and IBU (T onset and T peak) was well preserved with light broadening

shifting towards the lower temperature range. This change in shape and shifting of peak towards lower temperature range could be due to mixing of the drug with excipients and may not necessarily indicate potential incompatibility.

The DSC thermogram of TAM, IBU and K35 showed a sharp endothermic peak at 80.76°C and peak onset at 76.52°C. The endothermic peak of TAM was well preserved; this shows that the TAM is compatible with K35. (Figure 5)

Assay

The drug and excipients mixtures of control sample and stressed samples were tested for assay by UV spectroscopy. % assay was found to be in between 95.00 to 105.00, which is complying as per the ICH guidelines.

Pre compression study

1. Angle of Repose- θ

The formulated batches were found to be complying as excellent in flow ability, bulk density, tapped density, Carr's index and Hausner's ratio as per USP guidelines. The results are tabulate in table 4.

Table 4: Pre-compression parameters evaluation.

Batch	Mean θ	S.D (+-)	Mean Db	S.D. \pm	Mean Dt	S.D. \pm	Carr's Index	Hausner Ratio
F1	28.21	± 0.513842	0.41	± 0.005774	0.42	± 0.005774	2.38	1.02
F2	31.10	± 0.484974	0.40	± 0.005774	0.42	± 0.005774	4.76	1.05
F3	27.01	± 0.785196	0.41	± 0.005774	0.42	± 0.005774	2.38	1.02
F4	28.80	± 0.880019	0.41	± 0.005774	0.42	± 0.005774	2.38	1.02
F5	30.24	± 0.981495	0.41	± 0.005774	0.43	± 0.005774	4.76	1.05
F6	28.21	± 0.513842	0.41	± 0.005774	0.42	± 0.005774	2.38	1.02
F7	28.80	± 0.880019	0.41	± 0.005774	0.42	± 0.005774	2.38	1.02
F8	30.81	± 0.981495	0.41	± 0.005774	0.42	± 0.005774	2.38	1.02
F9	29.09	± 1.016136	0.41	± 0.005774	0.42	± 0.005774	2.38	1.02

\pm S.D. n=3

Post compression evaluation

1. General appearance: The formulated tablets were assessed for its general appearance and observations were made for shape, color and texture and found to be complying.

2. Weight Variation test: All compressed tablets of batch F1-F9 were evaluated for % weight variation, which showed % weight variation between 0.25-1.0 % (n=3) from an average weight of tablet (300 \pm 5mg) complying as per standard.

3. Hardness

For all batches F1-F9, strength of tablet was found to be within limit as per standard record which lies in between 5.3 \pm 0.057 to 5.5 \pm 0.115 kg/cm² (n=3).

4. Friability test

For all batches F1-F9 friability was found to be lies between 0.26-0.55; which conform the standard limit (1%, n=3).

5. Assay of Tablet (Drug content)

The formulated tablets batches F1-F9 were tested for assay by UV spectroscopy. % assay was found to be in between 95.00 to 105.00, which is complying as per the standard record limit (95%-105%).

6. Stability Study (Accelerated)

Accelerated stability tests were carried out in compliance with ICH stability guidelines for F1 to

F9 formulations. Parameters such as hardness, drug content percentage and cumulative release were calculated. The shape, texture and colour of the formulated tablets of F1 to F9 were not affected. No noticeable hardness, percent drug content and cumulative % drug release were observed. The formulated F1- F9 batches tablets have thus been found to be stable during the analysis.

7. Dissolution Profile

The in vitro dissolution analysis was tested to better align various models. The statistics were presented in Table 5. Figure 7- Figure 12 identified in-vitro drug releases for F1 to F9.

Batch F1 to F9 is found to follow zero order models for the release of drugs. T1 to T3 formulations consisting of the polymer class K35 M at various concentrations i.e. 10 mg, 20 mg and 30 mg. In comparison, for formulations T4 to T6, K4 M and E10 M were composed of formulations T7 to T9. Similarly for the formulation of I1-I9 consist IBU. It was noted that for F1 to F9 formulations, a percentage of drug release decreases with increasing concentrations of polymers. The pattern is also followed for the majority of the lots. The percentage of drug release depends on the polymer used and concentration in the formula.

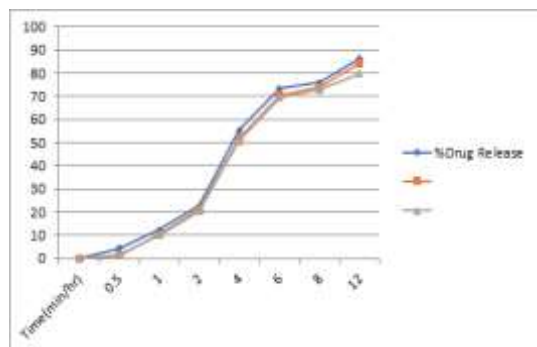


Fig.5: T1-T3 % Drug Release.

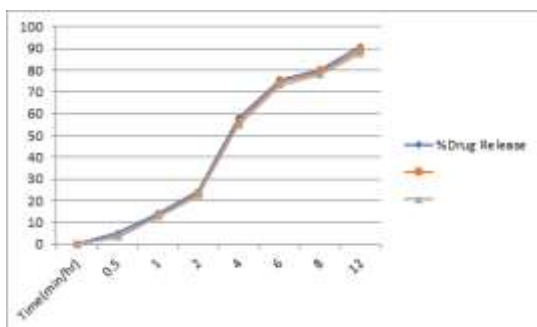


Fig.6: T4-T6 % Drug Release.

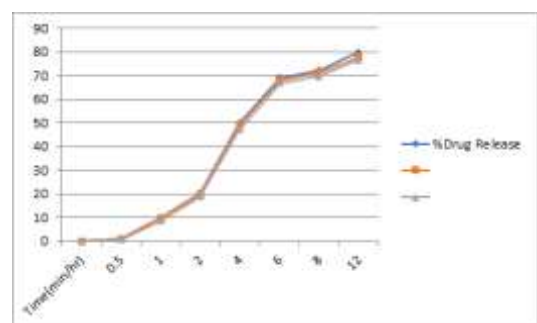


Fig.7: T7-T9 % Drug Release.

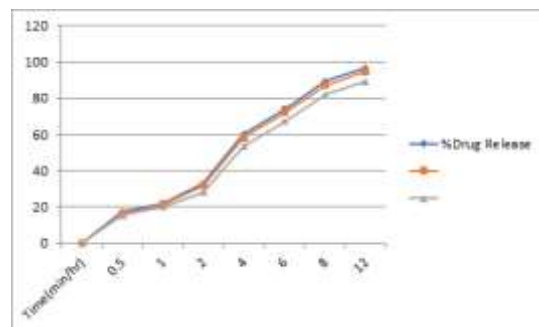


Fig.8: I1-I3 % Drug Release.

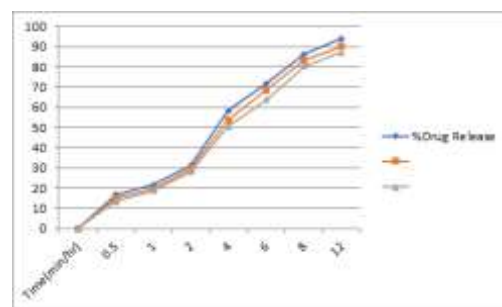


Fig.9: I4-I6 % Drug Release.

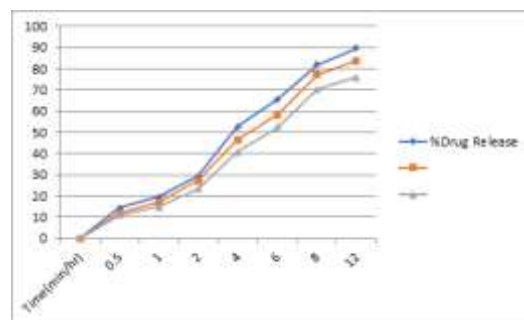


Fig.10: I7-I9 % Drug Release.

Table 5: Drug release kinetic study.

Formulation Code	Time		Best fit model
	in Min	Peppas	
T1	720	0.738	Zero Order
T2	720	0.851	Zero Order
T3	720	0.627	Zero Order
T4	720	0.79	Zero Order
T5	720	0.375	Zero Order
T6	720	0.986	Zero Order
T7	720	0.855	Zero Order
T8	720	0.986	Zero Order
T9	720	0.96	Zero Order
I1	720	0.991	Zero Order
I2	720	0.842	Zero Order
I3	720	0.725	Zero Order
I4	720	0.829	Zero Order
I5	720	0.898	Zero Order
I6	720	0.855	Zero Order
I7	720	0.991	Zero Order

18	720	0.842	Zero Order
19	720	0.725	Zero Order

CONCLUSION

The Tamoxifen citrate Sustained Release tablets were prepared using the direct compression process. Tamoxifen citrate tablets with different HPMC levels such as K35 M, E4 M and E10 M were formulated. Polymers used in formulation do not interfere with drugs that might be more helpful over a longer time to achieve the optimal SR. The pre-formulation studies such as rest angle, bulk density, tapped density, the Hausner ratio and the Carr index were found to be within the normal limit. The absence of possible chemical reactions between the drug and polymers was suggested by FTIR spectra.

Powder mixtures were compressed into tablets for weight variation, thickness, stiffness, friability and drug content evaluation after compression. Both tablet lots have shown satisfactory results. The in vitro release of medicines was investigated for 12 hours with USP Type-II dissolution apparatus. Results showed that the drug release was maintained over 12 hours by formulations containing various polymers. For F1 to F9 formulations, a percentage of drug release decreases with increasing levels of polymers. Thus, it was concluded that the polymers play a major role in formulating Tamoxifen citrate and ibuprofen continuous release tablets.

ACKNOWLEDGEMENT

The authors are greatly thankful to Ashland Inc. Ltd., Netherlands for providing gift samples of HPMC polymer different grades, Cipla Ltd. (Kurlumbh, Maharashtra, India) for the kind gift of Pioglitazone.

Conflict of interest: The authors declare no conflict of interest.

REFERENCES

1. "Metastasis", Merriam-Webster online, accessed 20 Aug 2017.
2. "Invasion and metastasis". Cancer Australia. 2014-12-16. Retrieved 2018-10-26.
3. World Health Organization (2019). World Health Organization model list of essential

medicines: 21st list 2019. Geneva: World Health Organization. hdl:10665/325771.

WHO/MVP/EMP/IAU/2019.06. License: CC BY-NC-SA 3.0 IGO.

4. Indian Pharmacopoeia, Government of India, Ministry of health and family welfare, 2010; (1): 193,559-560.
5. Ravi KN, Narayanaswamy VB, Senthil A, Mehul D, Tejas L, Mahalaxmi R. Formulation and evaluation of sustained release matrix tablets of Lornoxicam. Indo-Global Research Journal of Pharmaceutical Sciences 2011;1(3):92-99.
6. Uddin M. Development of sustained release tablet of Valsartan. World J Pharm Pharma Sci. 2015;3(5):1196-05.
7. Dokala GK, Pallavi C. Direct Compression - An Overview. International Journal of Research in Pharmaceutical and Biomedical Sciences, January- March 2013; Volume 4 (1): 155-158.
8. Mali R.R., Goel V. & Gupta S. (2015). Novel study in sustained release drug delivery system: A review. Int. J. Pharm. Med. Res. 3 (2), 204-215.
9. Patel K.B., Vyas J.R. & Upadhyay U.M. (2015). Formulation and evaluation of sustained release matrix tablets of nateglinide. Journal of drug delivery & Therapeutics, 5(5), 19-25.
10. Dusane A.R., Gaikwad P.D., Bankar V.H. & Pawar S.P. (2011). A review on sustained released technology. International Journal of Research in Ayurveda & Pharmacy, 2(6), 1701-1708.
11. Gupta M.M. & Ray B. (2012). A review on sustained release technology. International Journal of Therapeutic Applications, 8, 18-23.
12. Chugh I., Seth N., Rana A.C. & Gupta S. (2012). Oral sustained release drug delivery system: An overview. International research journal of Pharmacy, 3(5), 57-62.
13. Pani N.R., Nath L.K. & Acharya S. (2011). Compatibility studies of nateglinide with excipients in immediate release tablets. Acta Pharm. 61 (2), 237-47. Doi: 10.2478/v10007-011-0016-4.
14. Interpreting Unexpected Events and Transitions in DSC Results- TA Instruments. <http://www.tainstruments.com/pdf/literature/TA039.pdf>.

Research Article

Formulation development and evaluation of sustained release bilayer tablet containing pioglitazone and glucosum in management of hypoglycemic diabetes.

VINAYAK MADANE^{*1}, SHRUTI SONAWANE¹, AMIT KASABE¹, SANTOSH FATTEPUR², NAGARAJA SREEHARSHA^{3,4}

¹Department of Pharmaceutical Quality Assurance, PDEA'S Shankarrao Ursal College of Pharmaceutical Sciences and Research Centre, Kharadi, Pune, Maharashtra, India.

²School of Pharmacy, Management and Science University, Seksyen 13, 40100, Shah Alam, Selangor, Malaysia.

³Department of Pharmaceutical Sciences, College of Clinical Pharmacy, King Faisal University, Al-Ahsa-31982, Saudi Arabia.

⁴Department of Pharmaceutics, Vidya Siri College of Pharmacy, Off Sarjapura Road, Bengaluru - 560 035, Karnataka, India.

*Corresponding Author

Email ID: vinu2231@gmail.com

Received: 29.08.20, Revised: 18.09.20, Accepted: 15.10.20

ABSTRACT

Increasingly, pharmaceutical invention and research are focusing on delivery systems that improve desirable therapeutic objectives while minimising side effects. Nowadays there are very few medicines coming out of research and development and already existing drugs are facing resistance issues because of their irrational use of drugs such as antibiotics. Bilayered tablets for effective use in the treatment of hypoglycaemia, i.e. low blood glucose or low blood sugar, will be developed and tested in this study. Hypoglycaemia is one of the well-known drawbacks associated with most antidiabetic agents used in the administration of type 2 diabetes mellitus. So it needs to be overcome or handled quickly, if left untreated, may escalate and cause confusion, torment or fainting and may lead to convulsions, coma, and even death. So, to overcome above problem, bilayer tablet containing Pioglitazone and Glucosum is formulated. Pioglitazone is a hyperglycaemic ant used for the treatment of type II diabetes mellitus, whereas; Glucosum is one of a group of -carbohydrates called single sugars. The bilayer tablet includes pioglitazone and glucosum along with the use of various grade polymers, namely HPMC. K35 M, K4 M AND E10 M and other excipients have been found to be consistent with different concentrations of polymers. The results of the pre- and post-compression parameters were verified according to USP guidelines. In vitro drug release for F1 to F18 formulation were found to follow peppas model for drug release.

Keywords: Sustained release bilayer tablet, Pioglitazone, Glucosum, hypoglycaemia.

INTRODUCTION

Increasingly, pharmaceutical invention and research are focusing on delivery systems that improve desirable therapeutic objectives while minimising side effects. The method for the distribution of oral drugs is one of the frontier fields of controlled drug delivery. Such dosages provide a big benefit in accordance with the patient. The Sustained Release dosage forms are designed to release a drug at a default rate in order to maintain a steady concentration of drugs with minimal side effects for a certain period of time. Nowadays there are very few medicines coming out of research and development and already existing drugs are facing resistance issues because of their irrational use of drugs such as antibiotics.[11,12]

Bilayered tablets for effective use in the treatment of hypoglycaemia, i.e. low blood glucose or low blood sugar, will be developed and tested in this study. Hypoglycaemia can suddenly occur. It is normally mild and can be conveniently and rapidly handled with a small amount of glucose-rich food or consuming it. Hypoglycaemia, if left untreated, may escalate and cause confusion, torment or fainting. Serious hypoglycaemia can lead to convulsions, coma, and even death. By looking at this point, the tablet is formulated to resolve this certainly. [1-5]

By using the delaying polymers such as hydroxypropyl methyl cellulose (different grades / s) on both stages, the Bilayer tablet was formulated. The primary layer consisting of pioglitazone and the secondary layer consisted of a certain concentration of glucosum to release the

active drug and glucosum at the desired time, by maintaining a normal level of blood glucose and limiting it to a low margin.

Pioglitazone is a hyperglycaemic ant used for the treatment of type II diabetes mellitus available in conjunction with metformin, repaglinide, insulin or sulfonylurea that has been used on the market to boost both long and short periods of glycaemia control and serum lipid profiles. Hypoglycaemia is one of the well-known drawbacks associated with most antidiabetic agents used in the administration of type 2 diabetes mellitus. So it needs to be overcome or handled quickly.

Glucosum is one of a group of -carbohydrates called single sugars. It is present in fruit and sweetness and is the biggest free sugar in the blood of higher animals. [6-10]

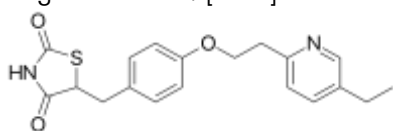


Fig.1: Structure of Pioglitazone.

MATERIALS AND METHODS

Materials: Pioglitazone USP (Pure) and Pioglitazone USP working standard was obtained as gift sample from Cipla Limited., Kurkumbh, Pune, India. HPMC K35, K4M, E10M cellulose were obtained as gift sample along with certificate of analysis (COA) from Ashland Inc., Netherland. The following excipients were purchased from commercial sources such as; Microcrystalline cellulose (MCC) Avicel PH102, Magnesium Stearate, Talc, Lactose. HPLC grade Water (Merck) was used.

Methods[13-18]

Identification of Pioglitazone: Identification of pure pioglitazone was carried out by Fourier Transform Infra-red Spectrophotometry (Shimadzu 8400s).

UV Spectroscopy: In the phosphate buffer pH 6.8, the stock solution of Pioglitazone was produced; the UV spectrum of 10 µg / ml was taken to determine its maximum absorption (µmax). Prepared normal and sample solutions and solution strength is 200 ppm per 50 ml to verify the sample absorption in UV spectrophotometry visible. After preparation and evaluation, with blank absorbance at 220 nm and blank solutions, the absorbance in 1 cm cell at the wavelength of the maximum absorbance is 220 nm. Calculate Pioglitazone HCL quantity (in mg) per tablet. By plotting the calibration curve, a typical plot of absorption v / s drug concentration at µg / ml was compiled.

Drug-excipients compatibility study: Compatibility studies of drug excipients are an important phase in the development of all dosage

forms during the preformulation. The potential physical and chemical interactions between medicines and excipients can influence the chemical, physical and treatment. The DSC graph and IR spectra were used to study compatibility of drug excipients.

IR Spectroscopy: IR spectra of drug and mixture of drug – excipients and drug- polymer were recorded on in the range of 400nm- 200nm using potassium bromide discs.

Methods-Mixing ratio- 1:1 (100mg Pioglitazone + 100mg Excipients/s)

Storage condition- At Room temperature

Sample withdrawn interval (in days)- “0” days, “10” days, “20” days, “30” days

DSC: For the thermal analysis of medicinal products and drug mixtures – excipients and drug polymers a differential scan calorimeter (Mettler / Toledo) was used. In an appropriate ratio the selected excipients and polymers were mixed. Individual samples of medicinal products, excipients and polymers as well as medicinal excipients and pharmaceutical polymers were directly weighed onto the DSC aluminium crusher and scanned under the drug nitrogen atmosphere at temperature ranges between 40 ° C and 350 ° C.

Mixing ratio- 1:1 (100mg Pioglitazone + 100mg Excipients/s)

Storage condition- At Room temperature

Sample withdrawn interval (in days)- “0” days, “10” days, “20” days, “30” days

Isothermal Stress Testing (IST)[17-18]

IST studies were performed in controlled and stressed temperature to study active and inactive compatibility. Following parameters were used for the study.

Mixing ratio- 1:1 (100mg Pioglitazone + 100mg Excipients/s)

Storage condition-

a. For control sample- 2-8°C

b. For stressed sample- 50°C

Study period (in days)- 21 days

Test- Assay by UV spectroscopy

Sample withdrawn interval (in days)- “21” days

Procedure-

a. For stressed sample-(50°C)

1. In 4 ml glass vials (n = 2), the drug with selected polymers and excipients in 1:1 proportions was weighed.

2. Glass vials then mixed for 2 min on a Remi mixer.

3. 10% distilled water was added to each labelled vial.

4. Screw cap is applied to the vials and stored in hot air ovens at 50 ° C (Technical, India).

5. These samples were checked regularly for any colour changes.

6. After three weeks, the UV-visible spectrophotometer (model UV-1601 Shimadzu) was used to analyse these samples quantitatively at 210 nm.

b. For control sample-(2-8°C)

1. In 4 ml glass vials (n = 2), the drug with selected polymers and excipients in 1:1 proportions was weighed.

2. Glass vials then mixed for 2 min on a Remi mixer.

3. The vials are screwed with a Teflon screw cap and stored in the refrigerator (Samsung, India) at 2-8 °C.

4. These samples were checked regularly for any colour changes.

5. These samples were quantitatively analysed at 210 nm after 3 weeks with a UV-visible spectrophotometer (model UV-1601 Shimadzu)

Pre-compression evaluation

The different parameters were evaluated such as angle of repose, bulk density, tapped density, Hauser's ratio and compressibility index.

1. Angle of Repose

A fixed funnel method was used to determine the angle of repose. The fixed funnel method uses a funnel secured at a specified height (2 cm) over the graphic paper on a flat horizontal surface. Pellets or tablet blends have been thoroughly poured into the funnel until the apex of the conical pile touches the tip of the funnel. Thus, r is the conical pile's radius. The angle of rest has been calculated using the next equation.

$$\theta = \tan^{-1} (h/r) \dots\dots \text{Equation 1}$$

Where,

h = Height of pile; r = Radius of pile; θ = Angle of repose

2. Bulk Density: A powder (about 60gm) is transferred into the 100ml graduated cylinder through a standard sieve number 20. A weighted quantity (about 50gm). The volume of bulk is measured by dropping the cylinder (containing powder) three times above 1 inch at 2 s intervals on a hard wooden surface. Sometimes the container needs to be dropped or tapped 500 times in order to get an appropriate volume.

Bulk density (ρ) = (Weight of the powder/ bulk volume) **Formula 1**

3. Tapped Density: Tapped density is ratio of the mass of tablet blend to tapped volume of tablet blend. Accurately weighed amount of tablet blend poured in graduated cylinder and height is measured. Then cylinder was allowed to 100 tap under its own weight on to a hard surface. The tapping was continued until no further Change in height was noted.

Tapped Density = (Weight of the powder/tapped volume) **Formula 2**

4. Compressibility Index (Carr's Index): Compressibility is the ability of powder to decrease in volume under pressure using bulk density and tapped density the percentage compressibility of powder were determined, which is given as Carr's compressibility index. It is indirectly related to the relative flow rate. Carr's compressibility index was determined by the given formula,

Compressibility Index (%) = (Tapped density- Bulk density) X 100/ Tapped density

..... **Formula 3**

5. Hauser's Ratio: Hauser's ratio indicates the flow properties of powder and measured by the ratio of tapped density to bulk density. Hauser's ratio was determined by the given formula,

Hauser's ratio = Tapped Density /Bulk Density

..... **Formula 4**

Preparation of Tablet: Direct Compression Method

Procedure

1. All ingredients were weighed correctly and co sifted through the # 40 sieve (Pioglitazone+Deextrose+K35M+K4M+E10M+a ll excipients).

2. The above mixture was mixed for 5min in polybag.

3. The above blend was lubricated with magnesium stearate and talc, precisely weighed and passed through # 60 sheets.

The final mix was compressed into a tablet using 6 stations (Create, 08 station) with an average hardness of 4.0 to 6.0kg / cm², with a die of 9 mm.

Table 1: Preparation of Batches. (Pioglitazone layer)

Batches	Ingredients						
	PIO	HPMC			Talc	MCC	Magnesium Stearate
		K35M	K4M	E10M			
F1	10mg	10mg	-	-	5mg	q.s.	5mg
F2	10mg	20mg	-	-	5mg	q.s.	5mg
F3	10mg	30mg	-	-	5mg	q.s.	5mg
F4	10mg	-	10mg	-	5mg	q.s.	5mg
F5	10mg	-	20mg	-	5mg	q.s.	5mg

F6	10mg	-	30mg	-	5mg	q.s.	5mg
F7	10mg	-	-	10mg	5mg	q.s.	5mg
F8	10mg	-	-	20mg	5mg	q.s.	5mg
F9	10mg	-	-	30mg	5mg	q.s.	5mg

Total Weight of the tablet- 200mg

Table 2: Preparation of Batches. (Glucosum layer)

Batches	Ingredients						
	GLUCOSUM	HPMC			Talc	MCC	Magnesium Stearate
		K35M	K4M	E10M			
F10	200mg	10mg	-	-	5mg	q.s.	5mg
F11	200mg	20mg	-	-	5mg	q.s.	5mg
F12	200mg	30mg	-	-	5mg	q.s.	5mg
F13	200mg	-	10mg	-	5mg	q.s.	5mg
F14	200mg	-	20mg	-	5mg	q.s.	5mg
F15	200mg	-	30mg	-	5mg	q.s.	5mg
F16	200mg	-	-	10mg	5mg	q.s.	5mg
F17	200mg	-	-	20mg	5mg	q.s.	5mg
F18	200mg	-	-	30mg	5mg	q.s.	5mg

Total Weight of the tablet- 300mg

Post Compression evaluation

1. **General appearance:** In these the colour, odour, tasteless, solubility, are carried out.

2. **Weight Variation:** A tablet intended to contain a certain amount of medicine in a certain quantity of a tablet formula regularly tests the weight of the tablet to ensure that the tablet contains the right amount of medicine. In testing, 10 tablets were taken and measured on a digital weighing balance individually. The average weight of each tablet was calculated and the average weight was compared. If not more than 2 tablets are outside the percentage limit and no tablet is different by more than 2 times the percentage limit, the tablet passes the test.

$$\% \text{ Weight variation} = \frac{\text{Average weight} - \text{Weight of each tablet}}{\text{Average weight}} \times 100$$

..... **Formula 5**

3. **Thickness:** Thickness was measured using Vernier calliper. It was determined by checking three tablets from each formulation.

4. **Hardness:** Hardness is defined as 'the force to break a tablet in a diametric compression test.' Hardness is therefore often referred to as crushing strength. The strength before use depends on its hardness. Pfizer hardness tester measured the hardness of the tablet. A tablet has been placed in the hardness test and the load needed to crush the tablet has been measured.

5. **Friability Test:** This test assesses the ability of tablets to resist abrasion in packaging, handling and transportation. In general, friability indicates low cohesion of tablet ingredients. The initial weight of 10 comprises a friabilator consisting of a circular, plastic chamber divided into 2-3

compartments. The chamber rotates for 4 minutes at 25 rpm and drops the tablets for 15 cm and provides 100 revolutions. Afterwards, the tablets are again weighed. The weight difference is noted and shown as a percentage. It should be preferably below 1.0 %.

$$\% \text{ Friability} = (W1-W2)/W1 \times 100 \quad \dots\dots$$

Formula 6

Where,

W1= weight of tablets before test, W2 = weight of Tablet after test

6. **Assay of Tablet:** Not less than 20 tablets weigh and finely powder. Transfer to 100 ml volumetric bottle an accurately weighed amount of powder equivalent to 10 mg pioglitazone. Add little methanol and sauté the solution for 30 minutes. Then the volume is marked with methanol. Filter the solution via the philtre paper of Whatmans to obtain a clear solution. (Pioglitazone-Stock Solution 100ppm). Remove 0.8ml, 1.0ml and 1.2ml of stock solution (pioglitazone solution 100 ppm) respectively for preparation of 8ppm, 10ppm and 12ppm solution. Measure spectrophotometrical absorption by scanning the wavelength between 400 nm and 200 nm using blank methanol. Notice the absorption.

7. **In Vitro Study Dissolution study for formulated batches F1-F18 was performed as per USP.**

Procedure-

For acid stage

1. Hydrochloric acid with 0.5 percent Sodium lauryl sulphate was placed in the vessel and the USP-II (paddle method) appliance was assembled. 900 ml of 0.01N

2. The medium could be balanced at a temperature of $37 \pm 0.5^\circ \text{C}$.
3. A tablet of each batch was placed and covered in the ship; the device was operated at 50 rpm for up to 2 hours.
4. The 2ml sample was removed at 0, 0.5, 1 and 2 hours.
5. After extracting the sample, the fresh medium 2ml was substituted.
6. Using UV spectroscopy, absorption of the sample solution was measured at 210 nm.

Procedure-

For buffer stage

1. The vessel was fitted with 900 ml of phosphate buffer (PH- 6.8)
2. A tablet of each load was placed in a vessel which was removed and covered with acid vessel and the apparatus was operated at 50 rpm for up to 13 hours.
3. The sample 2ml was removed at 0, 1, 2, 4, 6, 8, 12, hours.
4. After extracting the sample, the fresh medium 2ml was substituted.

5. The absorption of the sample solution was measured by means of UV spectroscopy at 270 nm and 265 nm.

9. Stability Study (Accelerated): Accelerated stability testing was carried out for 3 months in accordance with the ICH stability test guidelines. The temperature and relative humidity are regulated in accordance with the guidelines. The study was conducted using Photo Chamber Stability-Make-Labtop India. The parameters are listed below,

Study Period- 6 Months

Test Performed- Hardness, % drug content, dissolution study (% cumulative drug release)

RESULTS AND DISCUSSION

Identification of Pure drug

Identification of pure drug (Pioglitazone) was carried out by Fourier Transform Infra-red Spectrophotometry (Shimadzu 8400s). It showed characteristics peak of pure drug. (Figure 2, Table 3).

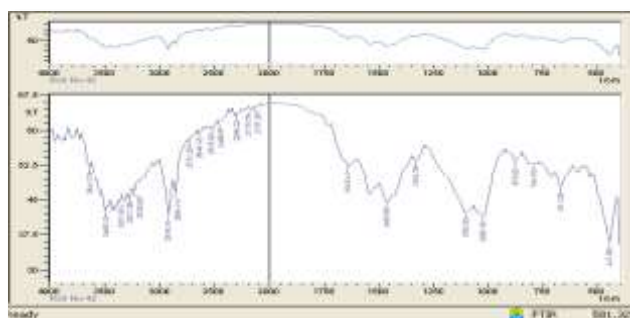


Fig.2: IR spectra of Pioglitazone.

Table 3: Characteristic peak of Pioglitazone.

IR signals cm^{-1}	Functional groups
3357.46	-OH stretching
2938.02	-CH ₃ stretching
1741.41	-C=O stretching
1644.98	C=C stretching

UV Spectroscopy: (Determination of λ maximum): The λ max of pure drug in methanol was found to be 210.0 nm which is in compliance with the reported value in literature. (Figure 3)

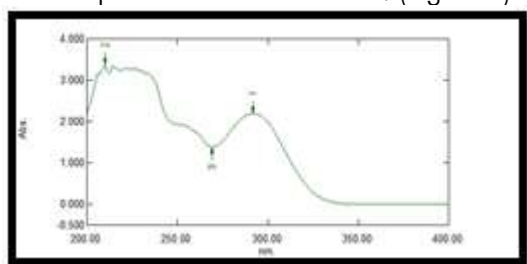


Fig.3: UV spectrum of Pioglitazone.

Calibration Curve: Calibration curve of pure Pioglitazone obeys Beer Lambert's law over concentration range of 10 -100 $\mu\text{g/ml}$. It showed r^2 value of 0.9978.

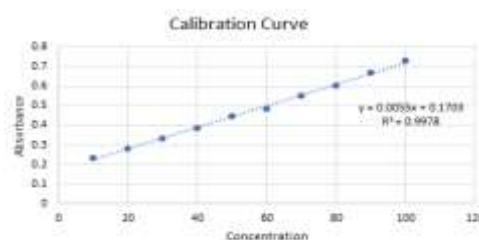


Fig.4: Calibration curve of Pioglitazone.

Drug Excipients Compatibility Study

FTIR: FTIR spectrum of pure pioglitazone and physical mixture of drug and polymers were studied. It was observed that there were no major shifts in main peaks of drug. This indicates that there was no any compatibility problem of drug with polymers and excipients used in the formulation.

IR Spectroscopy- '0' days

IR spectroscopic study was performed for all mixtures to find out interaction between drug and polymers. The IR spectra of the different mixture shows, the characteristic bands of pioglitazone.

The spectra of mixture of pioglitazone + polymers shows characteristics bands of pioglitazone at 3357.46cm⁻¹(-OH), 3295.75 cm⁻¹(-NH=), 2939.95 cm⁻¹(-CH₃), 1740.44 cm⁻¹(C=O), 1644.95 cm⁻¹(C=C), 968.09cm⁻¹(cycloalkane), 1238.23 cm⁻¹(C-O) which indicates there is no

any physical interaction between pioglitazone and polymer. (Figure 5). Similarly the spectra were studied for mixture of dextrose and polymer, which shows characteristics bands of dextrose at 3357.5 cm⁻¹(-OH), 2940.91 cm⁻¹(-CH₃), 1740.44 cm⁻¹(C=O), 1238.23 cm⁻¹(C-O), 1645.95 cm⁻¹(C=C), 968.09cm⁻¹(cycloalkane) which indicates there is no any physical interaction between dextrose and polymers. (Figure 6)

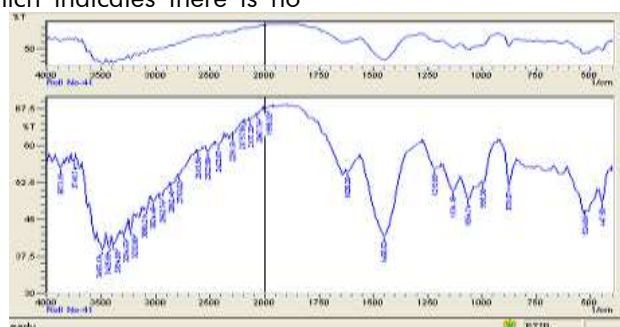


Fig.5: Representative IR spectra of Pioglitazone +K35M.

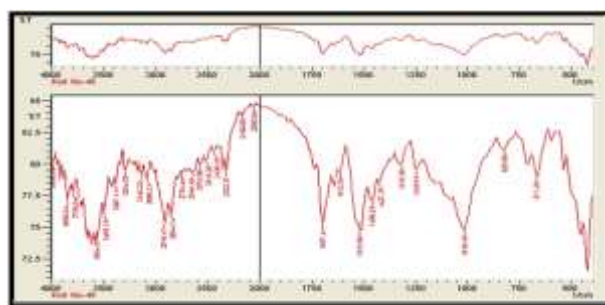


Fig.6: Representative IR spectra of Dextrose+ Metolose 90SH-10000.

Isothermal Stress Testing (IST)

Differential scanning Calorimetry

Selected DSC curves of medicinal drugs and drug excipients are shown in Figure 3-8 at "0" days, "10" days, "20" days, "30" day intervals. In the DSC curves, the thermal activity of the drug, its respective excipients and combinations are compared. (Table 2). The majority of the drug thermogram DSC alone in combination with various polymers displays the starting temperature of the peak (T onset) [$\sim 173^\circ\text{C}$] and the peak (T) transitions temperature [$\sim 178^\circ\text{C}$]. The Pioglitazone thermogram was sharp at 183°C and a peak at 173°C . (Figure 3) The melting endothermic of pioglitazone (T onset and T peak) has been maintained for the majority of thermographs, with light widening shifting

towards the lower temperature range. This shape and shift of the peak to lower temperature could be caused by mixing the drug with accidents and my incompatibility is not necessarily apparent.

Assay: The drug and excipients mixtures of control sample and stressed samples were tested for assay by UV spectroscopy. % assay was found to be in between 99.00 to 101.00, which is complying as per the ICH guidelines.

Pre compression study-

1. Angle of Repose- θ

The formulated batches were found to be complying as excellent in flow ability, bulk density, tapped density, Carr's index and Hausner's ratio as per USP guidelines. The results are tabulate in table 4.

Table 4: Pre-compression parameters evaluation.

Batch	Mean θ	S.D (+-)	Mean Db	S.D. \pm	Mean Dt	S.D. \pm	Carr's Index	Hausner Ratio
F1	28.19	0.53519	0.43	0.01155	0.41	0.00577	2.36	1.0
F2	29.33	0.73512	0.44	0.00577	0.41	0.00577	6.45	0.9

F3	27.01	0.78520	0.42	0.00577	0.41	0.00577	2.46	1.0
F4	28.80	0.88002	0.42	0.01000	0.41	0.00577	1.61	1.0
F5	29.77	0.22301	0.45	0.00577	0.41	0.01528	8.87	0.9
F6	28.22	0.51384	0.43	0.00577	0.41	0.00577	4.03	1.0
F7	28.80	0.88002	0.42	0.00577	0.41	0.00577	1.61	1.0
F8	30.36	0.90146	0.43	0.00577	0.41	0.00577	4.03	1.0
F9	29.09	1.01614	0.41	0.00577	0.41	0.00577	0.00	1.0
F10	27.17	0.69176	0.42	0.00577	0.41	0.00577	1.61	1.0
F11	28.22	0.51384	0.41	0.00577	0.40	0.00577	2.48	1.0
F12	29.49	0.32909	0.44	0.01155	0.42	0.00577	5.60	1.0
F13	28.80	0.88002	0.42	0.00577	0.41	0.00577	1.61	1.0
F14	28.22	0.51384	0.43	0.00577	0.42	0.00577	3.20	1.0
F15	29.89	0.42253	0.43	0.01155	0.42	0.00577	3.20	1.0
F16	29.56	0.20785	0.41	0.00577	0.41	0.01000	0.81	1.0
F17	28.90	0.73912	0.42	0.00577	0.41	0.00577	0.81	1.0
F18	29.79	0.19053	0.43	0.00577	0.41	0.00577	4.92	1.0

±S.D. n=3

Post compression evaluation

1. **General appearance:** The formulated tablets were assessed for its general appearance and observations were made for shape, color and texture and found to be complying.

2. **Weight Variation test:** All compressed tablets of batch F1-F18 were evaluated for % weight variation, which showed % weight variation between 0.25-1.0 % (n=3) from an average weight of tablet (400 ±5mg) complying as per standard (for 324mg ±5.0% deviation).

3. **Hardness:** For all batches F1-F18, strength of tablet was found to be within limit as per standard record which lies in between 5.3 ±0.057 to 5.5 ±0.115 kg/cm² (n=3).

4. **Friability test:** For all batches F1-F18 friability was found to be lies between 0.26-0.55; which conform the standard limit (1%, n=3).

5. **Assay of Tablet (Drug content):** The formulated tablets batches F1-F18 were tested for assay by UV spectroscopy. % assay was found to be in between 95.00 to 105.00, which is complying as per the standard record limit (95%-105%).

6. **Stability Study (Accelerated):** Accelerated stability tests were carried out in compliance with ICH stability guidelines for F1 to F18 formulations. Parameters such as hardness, drug content percentage and cumulative release were calculated. The shape, texture and colour of the formulated tablets of F1 to F18 were not affected. No noticeable hardness, percent drug content and cumulative% drug release were observed. The formulated F1- F18 batches tablets have thus been found to be stable during the analysis.

7. **Dissolution Profile:** The in vitro dissolution analysis was tested to better align various models. The statistics were presented in Table 5. Figure 7-

Figure 12 identified in vitro drug releases for F1 to F18. Batch F1 to F18 is found to follow peppas models for the release of drugs. P1 to P3 formulations consisting of the polymer class K35 M at various concentrations i.e. 10 mg , 20 mg and 30 mg. In comparison, for formulations P4 to P6, K4 M and E10 M were composed of formulations P7 to P9. Similarly for the formulation of D1-D9 glucosum layers. It was noted that for P1 to P3 formulations, a percentage of drug release decreases with increasing concentrations of polymers. The pattern is also followed for the majority of the lots. The percentage of drug release depends on the polymer used and concentration in the formula.

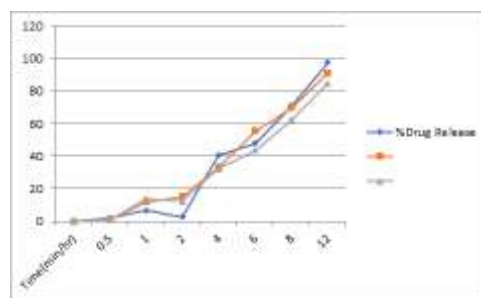


Fig.7: % drug Release of batches P1, P2, P3.

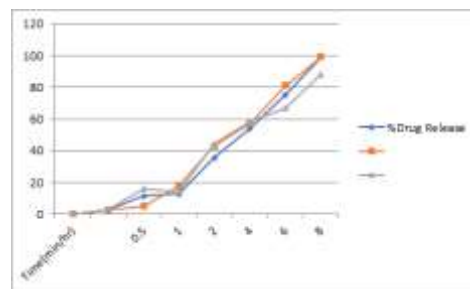


Fig.8: % drug Release of batches P4, P5, P6.

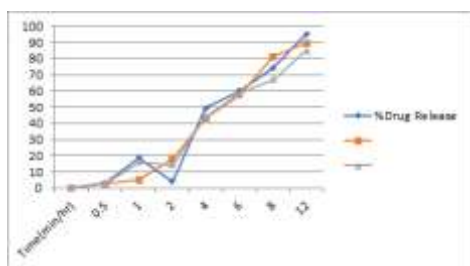


Fig.9: % drug Release of batches P7, P8, P9.

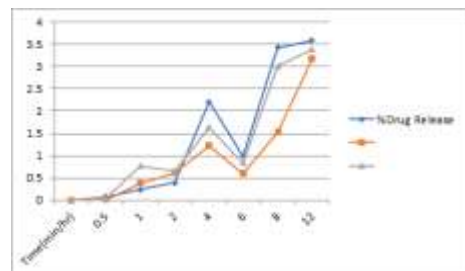


Fig.10: % drug Release of batches D1, D2, D3.

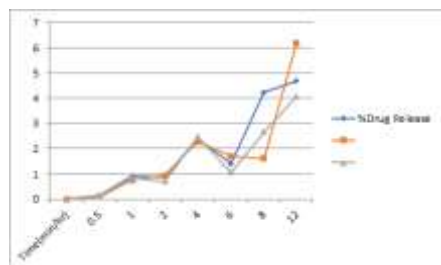


Fig.11: % drug Release of batches D4, D5, D6.

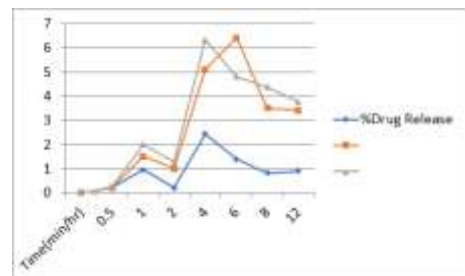


Fig.12: % drug Release of batches D7, D8, D9.

Table 5: Best Model Fitting for formulation F1-F18.

Formulation Code	Time in Min	Peppas	Best fit model
P1	720	0.96	Peppas
P2	720	0.991	Peppas
P3	720	0.842	Peppas
P4	720	0.725	Peppas
P5	720	0.829	Peppas
P6	720	0.738	Peppas
P7	720	0.851	Peppas
P8	720	0.627	Peppas
P9	720	0.79	Peppas
D10	720	0.375	Peppas
D11	720	0.435	Peppas

D12	720	0.931	Peppas
D13	720	0.998	Peppas
D14	720	0.898	Peppas
D15	720	0.855	Peppas
D16	720	0.986	Peppas
D17	720	0.855	Peppas
D18	720	0.986	Peppas

CONCLUSION

The bilayer tablet includes pioglitazone and glucosum along with the use of various grade polymers, namely HPMC. K35 M, K4 M AND E10 M and other excipients have been found to be consistent with different concentrations of polymers. The results of the pre- and post-compression parameters were verified according to USP guidelines. In vitro drug release for F1 to F18 formulation peppas were used for drug release models. P1 to P3 formulations consisting of the polymer class K35 M at various concentrations i.e. 10 mg , 20 mg and 30 mg. In comparison, for formulations P4 to P6, K4 M and E10 M were composed of formulations P7 to P9. Similarly for the formulation of D1-D9 glucosum layers. It was noted that for P1 to P3 formulations, a percentage of drug release decreases with increasing concentrations of polymers. The pattern is also followed for the majority of the lots. The percentage of drug release depends on the polymer used and concentration in the formula.

ACKNOWLEDGEMENT

The authors are greatly thankful to Ashland Inc. Ltd., Netherlands for providing gift samples of HPMC polymer different grades, Cipla Ltd. (Kurlumbh, Maharashtra, India) for the kind gift of Pioglitazone.

Conflict of interest: The authors declare no conflict of interest.

REFERENCES

1. Zimmet P: The burden of Type 2 diabetes: are we doing enough? Diabetes Metab. 29(4 Pt 2), 6S9–6S18 (2003).
2. Rathmann W, Haastert B, Icks A et al.: High prevalence of undiagnosed diabetes mellitus in Southern Germany: target populations for efficient screening. The KORA survey 2000. Diabetologia 46(2),182–189 (2003).
3. Wascher TC, Sourij H, Roth M, Dittrich P: Prevalence of pathological glucose metabolism in patients undergoing elective coronary angiography. Atherosclerosis 176(2),419–421 (2004).
4. Bartnik M, Ryden L, Ferrari R et al.: The prevalence of abnormal glucose regulation in patients with coronary artery disease across

- Europe. The Euro Heart Survey on diabetes and the heart. *Eur. Heart J.* 25(21),1880–1890 (2004).
5. Haffner SM, Lehto S, Ronnema T,Pyorala K, Laakso M: Mortality from coronary heart disease in subjects with Type 2 diabetes and in nondiabetic subjects with and without prior myocardial infarction. *N. Engl. J. Med.* 339(4),229–234 (1998).
6. Stratton IM, Adler AI, Neil HA et al.: Association of glycaemia with macrovascular and microvascular complications of Type 2diabetes (UKPDS 35): prospective observational study. *BMJ* 321(7258),405–412 (2000).
7. Nathan DM, Cleary PA, Backlund JY et al.: Intensive diabetes treatment and cardiovascular disease in patients with Type 1 diabetes. *N. Engl. J. Med.* 353(25), 2643–2653 (2005).
8. Turner RC, Cull CA, Frighi V, Holman RR: Glycemic control with diet, sulfonylurea, metformin, or insulin in patients withType 2 diabetes mellitus: progressive requirement for multiple therapies (UKPDS 49). UK Prospective Diabetes Study (UKPDS) Group. *JAMA* 281(21),2005–2012 (1999).
9. Tuomilehto J, Lindstrom J, Eriksson J Get al.: Prevention of Type 2 diabetes mellitusby changes in lifestyle among subjects with impaired glucose tolerance. *N. Engl. J. Med.*344(18), 1343–1350 (2001).
10. Knowler WC, Barrett-Connor E, Fowler S E et al.: Reduction in the incidence of Type 2diabetes with lifestyle intervention or metformin. *N. Engl. J. Med.* 346(6), 393–403 (2002).
11. Gerstein HC, Yusuf S, Bosch J et al.: Effect of rosiglitazone on the frequency of diabetes in patients with impaired glucose tolerance or impaired fasting glucose: a randomised controlled trial. *Lancet* 368(9541),1096–1105 (2006).
12. Mali R.R., Goel V. & Gupta S. (2015). Novel study in sustained release drug delivery system: A review. *Int. J. Pharm. Med. Res.* 3 (2), 204-215.
13. Patel K.B., Vyas J.R. & Upadhyay U.M. (2015). Formulation and evaluation of sustained release matrix tablets of nateglinide. *Journal of drug delivery & Therapeutics*, 5(5), 19-25.
14. Dusane A.R., Gaikwad P.D., Bankar V.H. & Pawar S.P. (2011). A review on sustained released technology. *International Journal of Research in Ayurveda & Pharmacy*, 2(6), 1701-1708.
15. Gupta M.M. & Ray B. (2012). A review on sustained release technology. *International Journal of Therapeutic Applications*, 8, 18-23.
16. Chugh I., Seth N., Rana A.C. & Gupta S. (2012). Oral sustained release drug delivery system: An overview. *International research journal of Pharmacy*, 3(5), 57-62.
17. Pani N.R., Nath L.K. & Acharya S. (2011). Compatibility studies of nateglinide with excipients in immediate release tablets. *Acta Pharm.* 61 (2), 237-47. Doi: 10.2478/v10007-011-0016-4.
18. Interpreting Unexpected Events and Transitions in DSC Results- TA Instruments. http://www.tainstruments.com/pdf/literature/TA_039.pdf.



Pune District Education Association's
**Shankarrao Ursal College of Pharmaceutical
Sciences & Research Centre, Kharadi, Pune-14.**



Academic Year 2018-19



Research Article

QSPR Modeling of Biopharmaceutical Properties of Hydroxypropyl Methylcellulose (Cellulose Ethers) Tablets Based on Its Degree of Polymerization

Amit J. Kasabe,¹ Ajit S. Kulkarni,^{2,4} and Vinod L. Gaikwad³

Received 4 April 2019; accepted 18 August 2019

Abstract. Quantitative structure-property relationship (QSPR) approach has been widely used in predicting physicochemical properties of compounds. However, its application in the estimation of formulation properties based on the polymer used in it to achieve desired formulation characteristics is an extremely challenging process. In the present research, predictive QSPR models were developed by correlating the physicochemical properties of varying grades of cellulose ethers (hydroxypropyl methylcellulose, HPMC) with those of nateglinide (NTG) containing tablets (*in vitro* and *in vivo* properties). Sustained release tablets of NTG were prepared by using different grades and concentrations of HPMC and subsequently characterized for *in vitro* as well as *in vivo* parameters. Further, QSPR models for individual formulation property were developed by correlating the polymeric physicochemical properties with the formulation characteristics. Subsequently, a true external validation method was used to validate the predictability of developed models. The dissolution study indicated Korsmeyer-Peppas as the best fit model following non-Fickian as drug transport mechanism extending the drug release up to 12 h. *In vivo* studies showed limited absorption of the NTG. Developed QSPR models showed promising validated predictability for formulation characteristics. The applicability of present work in formulation development could significantly reduce the time and cost expenditure on design trials without actually formulating a delivery system.

KEY WORDS: QSPR modeling; biopharmaceutical; degree of polymerization; HPMC; *in vivo*.

INTRODUCTION

Sustained drug delivery system offers several advantages over conventional one such as control over the rate of drug delivery as well as reduction of the interval between successive dosing. Different release-retarding agents such as cellulose ethers (HPMC) at varying concentrations were used in the sustained delivery system to modify the ADME and related physicochemical parameters of the drug (1–5). Moreover, the physicochemical properties of cellulose ethers certainly affect the dissolution parameters with modification of other physical characteristics of tablet formulation (strength or hardness). A prediction methodology like QSPR can be used to predict the properties of the compound or formulation in advance through the calculation of the molecular descriptors quantitatively from the structure. QSPR approach quantifies the structural information as well as develops a statistical relationship between the structure and the formulation property. Development of a QSPR model involves the representation of the polymeric structure, calculation, and selection of descriptors followed by model development and validation. The descriptor encodes structural information of the molecule that expresses molecular properties representing different physicochemical subclasses

¹ Department of Pharmaceutical Chemistry, PDEA's Shankarrao Ursal College of Pharmaceutical Sciences and Research Center, Kharadi, Pune, Maharashtra 411014, India.

² Department of Pharmaceutics, Satara College of Pharmacy, Satara, Maharashtra 415004, India.

³ Department of Pharmaceutics, BVDU Poona College of Pharmacy, Erandwane, Pune, Maharashtra 411038, India.

⁴ To whom correspondence should be addressed. (e-mail: dr.kulkarniajits@gmail.com)

Abbreviations: ADME, Absorption, Distribution, Metabolism, and Excretion; AUC, Area Under the Curve; BCS, Biopharmaceutical Classification System; DSC, Differential Scanning Calorimetry; ERC, Elimination Rate Constant; FTIR, Fourier Transform Infrared; GLZ, Gliclazide; HCl, Hydrochloric Acid; HPLC, High Performance Liquid Chromatography; HPMC, Hydroxypropyl Methylcellulose; ICH, International Conference on Harmonization; LOD, Limit of Detection; LOQ, Limit of Quantitation; MCC, Microcrystalline Cellulose; MDS, Molecular Design Suite; MRT, Maximum Retention Time; NTG, Nateglinide; QSPR, Quantitative Structure-Property Relationship; RMSE, Root Mean Square Error; RPM, Rotations Per Minute; $t_{1/2}$, Half-life; USP, United States Pharmacopeia; V_D , Volume of Distribution; vdW , van der Waals.

such as hydrophilicity/hydrophobicity, steric, electronic, electrostatic, constitutional, geometrical, topological, quantum-chemical, etc. The significant impact of these descriptors on desired formulation property can be identified by the implementation of different statistical techniques that will help to explore the relationship between the input variables (physicochemical descriptors) and the property of interest (6–13).

Integration of a QSPR approach in formulation development could help to find out the most significant physicochemical properties of a polymer system that affects the desired formulation property. Moreover, developing a formulation with desired characteristics through early prediction of the critical material parameters affecting the *in vitro/in vivo* performance of the formulation could also be possible (6–17). Moreover, the well-established QSPR model could be used to predict the properties of compounds that have been under development or even not known. Such developed QSPR models could be used to predict the formulation property from a given blend of polymers as well as to predict the formulation composition for the required characteristics well in advance (6–13). Hence, the QSPR expedites the process of development of a new molecule and/or new formulation. Previous researchers have successfully implemented the QSPR approach in formulation development of tablet formulations and liposomal drug delivery system (6–13). Therefore, QSPR modeling could serve as an emerging trend or tool to skip costly conventional formulation development process.

The purpose of the present study is to develop predictive QSPR models for different *in vitro* parameters (dissolution, drug content, swelling index, angle of repose, friability, hardness) as well as for *in vivo* parameters (C_{\max} , ERC, V_D , $t_{1/2}$, MRT, and clearance) of an NTG-containing tablet formulation based on the polymeric physicochemical descriptors.

MATERIALS AND METHODS

Materials

NTG USP was received as a gift sample from Cipla Ltd., Kurkumbh (Maharashtra, India). GLZ was kindly gifted by Glenmark Pharmaceuticals, Mumbai (Maharashtra, India). HPMC BENECCEL of different grades (K4M, K15M, K35M and K100M, and K250PH) was supplied as gift sample by Ashland Inc. Ltd., Netherlands. MCC (Avicel PH102), magnesium stearate, and talc were kindly gifted by Colorcon Asia Ltd., Goa (India). All other chemicals used were of HPLC or analytical grade.

Methods

Preformulation Study

Drug-Excipient Compatibility Study.

- FTIR Spectroscopy

The physical mixture of the pure drug (NTG) with different grades of polymers was stored for 1 month at room temperature. Further, the stored samples were scanned intermittently ('0', '10', '20', and '30' days), after mixing with previously dried KBr (105°C for 3 h) within range of $400\text{--}4000\text{ cm}^{-1}$ using FTIR spectrometer (Shimadzu 8400s, Japan) (18–20).

- DSC Study

DSC thermograms of pure drug, excipients, and physical mixture were recorded using differential scanning calorimeter (Mettler Toledo, India) at predetermined time intervals ('0', '10', '20', and '30' days). The sample was weighed directly into the DSC aluminum crucible (1:1, NTG/excipient ratio) and scanned within a temperature range of $50\text{--}400^\circ\text{C}$, at a heating rate of $10^\circ\text{C}/\text{min}$ under a dry nitrogen atmosphere (19–23).

Isothermal Stress Testing. Isothermal stress testing was performed on the drug-excipient mixture (1:1) stored at high (50°C for stressed sample) as well as low ($2\text{--}8^\circ\text{C}$ for control sample) temperature, with or without moisture for 21 days and the drug content was determined (19,20,23).

Preparation of NTG Tablets

NTG tablets (F1–F16) were prepared by direct compression method. Initially, all ingredients were sifted by passing through #40 sieve number and weighed accurately as per composition is given in Table 1. Further, all the powder ingredients were blended (Equitron Equipments Pvt. Ltd., India) for 5 min and lubricated with magnesium stearate and talc, previously passed through #40 sieve. The final blend was compressed into a tablet using eight-station tablet compression machine (Create, India) having a set of 9 mm die and punches to get the hardness within the range of $4\text{--}6\text{ kg}/\text{cm}^2$.

Evaluation of NTG Tablets (7–11,13,18,24,25)

Weight Variation. A total of 20 tablets were randomly selected from each batch (F1–F16) and weighed individually. The weight of individual tablet was compared with an average weight for calculation of the weight variation test.

Hardness. The hardness of the tablets (F1–F16) was determined using the Monsanto hardness tester ($n = 6$). The tablet was placed in between the lower and upper plunger, and an indicator scale was set to zero. The upper plunger was then forced against a spring by turning a threaded bolt until the tablet breaks and indicator scale was recorded as hardness or force required to break the tablet (kg/cm^2).

Friability. Friability was performed using the Roche Friabilator (Electrolab, Mumbai, India). A pre-weighed sample of 20 tablets (F1–F16) was placed in the drum which was allowed to rotate at 25 rpm for 4 min. Further, the tablets were removed, dedusted, and reweighed. The difference in the weight was determined and used to calculate the % friability (Eq. 1).

$$\% \text{Friability} = \frac{W_1 - W_2}{W_1} \times 100 \quad (1)$$

where W_1 and W_2 are the weights of tablets before and after the test.

Drug Content. A total of 20 tablets from all batches (F1–F16) were weighed and finely powdered. A quantity of powder equivalent to 10 mg of NTG was accurately weighed

Table 1. The Composition of NTG Tablets

Batch code	NTG	HPMC K4M	HPMC K15M	HPMC K35M	HPMC K100M	H P M C K250 PH	MCC PH102	Magnesium stearate	Talc	Total
F1	120	200	–	–	–	–	70	2	8	400
F2	120	150	–	–	–	–	120	2	8	400
F3	120	100	–	–	–	–	170	2	8	400
F4	120	50	–	–	–	–	220	2	8	400
F5	120	–	200	–	–	–	70	2	8	400
F6	120	–	150	–	–	–	120	2	8	400
F7	120	–	100	–	–	–	170	2	8	400
F8	120	–	50	–	–	–	220	2	8	400
F9	120	–	–	200	–	–	70	2	8	400
F10	120	–	–	150	–	–	120	2	8	400
F11	120	–	–	100	–	–	170	2	8	400
F12	120	–	–	50	–	–	220	2	8	400
F13	120	–	–	–	200	–	70	2	8	400
F14	120	–	–	–	150	–	120	2	8	400
F15	120	–	–	–	100	–	170	2	8	400
F16	120	–	–	–	50	–	220	2	8	400
VF1	120	–	–	–	–	200	70	2	8	400
VF2	120	–	–	–	–	100	170	2	8	400
VF3	120	–	–	–	–	50	220	2	8	400

All quantities are expressed in mg

and dissolved in 100 mL methanol with the aid of sonication for 30 min. The resultant solution was filtered through the Whatman filter paper no. 42, suitably diluted, and analyzed spectrophotometrically (UV-Visible spectrophotometer 1801, Shimadzu Corporation, Japan) at observed absorption maxima using methanol as a blank.

Swelling Index. Swelling index of tablets from each batch (F1–F16) was determined parallel to the dissolution study to correlate the phenomena of drug release with the type and content of the HPMC. The weight of the tablet was recorded before the dissolution study (S_1) and at time intervals of 2, 4, 8, 12, and 15 h (S_2). Further, the swelling index (% hydration) was calculated using Eq. 2.

$$\text{Swelling Index} = \frac{S_2 - S_1}{S_1} \times 100 \quad (2)$$

where S_1 and S_2 are the weights of dry and hydrated tablets, respectively.

In Vitro Dissolution Study. An *in vitro* dissolution study was performed for NTG tablets from all batches (F1–F16) in triplicate ($n=3$) using USP type II (paddle) dissolution test apparatus (Electrolab TDT06L, Mumbai, India). Dissolution medium used was 900 mL of 0.01 N HCl with 0.5% sodium lauryl sulfate for an initial 2 h followed by phosphate buffer pH 6.8 (900 mL) for remaining hours. The medium was maintained at $37 \pm 0.5^\circ\text{C}$ at a constant stirring rate of 50 rpm throughout the dissolution study. At specified time points, 5-mL aliquots were withdrawn and replaced with fresh dissolution medium. The withdrawn samples were filtered using Whatman filter paper no. 42 and analyzed by using UV-Visible spectrophotometer (1801, Shimadzu Corporation, Japan) using the respective dissolution medium as a blank.

In Vivo Study in White Albino Rabbits.

• Experimental Animals

The *in vivo* study was conducted as per the guidelines of Committee for the Purpose of Control and Supervision of Experiments on Animals (CPCSEA, Government of India) and approved by Institutional Animal Ethics Committee, PDEA's SGRS College of Pharmacy, Saswad, No. IAEC/SGRS/2018/5.

Based on the *in vitro* test results, tablet formulations containing a low content of each grade of HPMC (batch F4, F8, F12, and F16) were selected for *in vivo* study in white albino rabbits (1.5 to 2.0 kg of weight). Before initiation of the study, all the animals were kept in the animal house maintained at temperature 25°C . The rabbits were divided into 06 groups (group 1: control, group 2: standard, group 3 to group 6: F4, F8, F12, and F16 tablet formulations) composed of 04 rabbits in each group and hold in the restrainers. Tablets were ingested *via* gastric intubation (group 3 to group 6), and blood samples were collected from marginal ear veins at predetermined time intervals up to 12 h. The withdrawn blood samples were kept in heparinized tubes, and further plasma was obtained by centrifugation (Remi Motors, Mumbai, India) at 3500 rpm for 5 min at 4°C .

- Bioanalytical Method Development
- Mobile Phase Selection

The extraction study was carried out for the selection of best suitable mobile phase based on the maximum % recovery of NTG using different solvents (methanol, dichloromethane, and acetonitrile with phosphate buffer pH 6.8). The eluent was filtered through a $0.45\text{-}\mu\text{m}$ membrane filter, and content was determined using the UV detector at 210 nm with a flow rate of 1 mL/min and a sample size of 20 μL .

• Linearity Range Determination

Linearity was estimated from the calibration curve plotted between peak area ratio of NTG to GLZ (internal standard)

versus plasma NTG concentrations. The accuracy and precision of the method were estimated by intraday and interday analysis and are expressed as the % coefficient of variation. The LOD and LOQ were estimated from the standard deviation of the absorbances of blank and mean of the absorbances.

- Preparation of Standard Solution

Stock solutions of NTG (665.965 mg/mL) and GLZ (internal standard; 250 mg/mL) were prepared separately in methanol. The stock solution was suitably diluted using mobile phase to obtain the working stock solution. A calibration curve was prepared by spiking fresh working NTG stock solution into the control blank plasma to obtain the concentrations of 100.05, 166.51, 238.16, 339.02, 492.14, 698.96, 997.97, 1649.26, and 3301.12 ng/mL.

- Preparation of Sample Solution

About 180 mL of blood plasma spiked with 10 mL of the standard drug was centrifuged for 2 min. Further, 10 mL of internal standard solution (250 mg/mL) was added and again centrifuged for 2 min. This solution mixture was added to 1.5 mL of acetonitrile, and the resulting solution obtained was subsequently centrifuged at 10,000 rpm for 5 min at 4°C. Further, the organic layer was separated and dried using evaporator. The residue traces so obtained was mixed with 100 mL of the mobile phase.

- Instruments

HPLC (Jasco PU-2085, Japan) quaternary gradient pump inbuilt with UV-Visible detector and C18 column (Hypersil ODS C18—250 mm length, 4.6 mm diameter) was used for analysis.

- Procedure for Analysis

The resulting sample solutions were injected into the HPLC column and analyzed to calculate the AUC by linear trapezoidal rule for tablet batches F4, F8, F12, and F16. Further, different pharmacokinetic parameters (C_{max} , ERC, $t_{1/2}$, V_D , MRT, and clearance) were estimated by using PK Solver software (V2-Pharmpk.com).

QSPR Modeling

Polymeric Structure Representation and Energy Minimization. The structural similarity among the different grades of HPMC (K4M, K15M, K35M, K100M) imposed to consider some physicochemical property of HPMC such as the degree of polymerization to differentiate between different grades (Table II). The chemical structures of different

Table II. The Degree of Polymerization of Different Grades of HPMC (32,33)

HPMC grade	Degree of polymerization
K4M	460
K15M	650
K35M	950
K100M	1160
K250 PH	848

HPMC grades were drawn based on its degree of polymerization using a structure building tool of Vlife MDS 4.2 software. The drawn structures were subsequently processed for energy minimization.

Calculation and Selection of Descriptors. The energy-minimized HPMC structures were further processed for calculation of several physicochemical descriptors (total 87 descriptors) which likely to have expected a significant effect on formulation property of interest. These descriptors represent different physicochemical properties of the HPMC structure calculated based on its degree of polymerization. The descriptors with invariable correlation were subsequently removed, and the final dataset of 22 descriptors obtained (Table III) was used for further processing.

Development and Validation of QSPR Models. QSPR models were developed by using partial least square regression method where a calculated set of descriptors having a significant contribution and individual impact were correlated with the desired formulation property (Vlife MDS 4.2 software). A QSPR model with high coefficient of determination (r^2) and low standard error was finally selected for each of the formulation property (*in vitro* such as friability, hardness, angle of repose, drug content, and $t_{90\%}$ —time required for 90% of the total drug release and *in vivo* such as C_{max} , ERC, $t_{1/2}$, V_D , MRT, and clearance).

The predictability of the QSPR model developed for each formulation property of interest was subsequently validated by true external validation method using descriptor dataset calculated for another grade of HPMC (K250 PH). NTG tablet formulations (batches VF1, VF2, and VF3) containing HPMC K250 PH (Table I) were prepared by direct compression method and characterized for targeted

Table III. List of Selected Physicochemical Descriptors

Sr. No.	Name of descriptors
1.	BalabanIndexJ
2.	SAHydrophilicArea
3.	XAHydrophobicArea
4.	XAMostHydrophilic
5.	Mol.Wt.
6.	SAMostHydrophilic
7.	XAHydrophilicArea
8.	XAMostHydrophobic
9.	XKMostHydrophobic
10.	XKAverage
11.	SAMostHydrophobic
12.	XKHydrophilicArea
13.	XAAverage
14.	XKMostHydrophilic
15.	XKMostHydrophobicHydrophilicDistance
16.	SAMostHydrophobicHydrophilicDistance
17.	SAHydrophobicArea
18.	SKMostHydrophobicHydrophilicDistance
19.	H-AcceptorCount
20.	SKMostHydrophobic
21.	XAAverageHydrophilicity
22.	SKMostHydrophilic

in vitro and *in vivo* properties. Further, the observed results were compared with the predicted values for the validation of the developed QSPR models.

RESULTS AND DISCUSSION

Preformulation Study

Drug-Excipient Compatibility Study

FTIR Spectroscopy. FTIR spectra of pure NTG (Fig. 1) showed characteristics peaks at 3357.46 (–OH stretching, alcohol group), 2938.02 (–CH₃ stretching, methyl group), 1741.41 (–C=O stretching, ketonic group), 1644.98 (C=C stretching), and 968.09 (C=C stretching, unsaturated bonding). All these observed peaks were in agreement with previously reported results (26,27).

Compatibility between NTG and excipients (physical mixture) was studied at 0, 10, 20, and 30 days stored at ambient condition. The physical mixture of pure NTG with different grades of HPMC (K4M, K15M, K35M, and K100M) showed very little or no change in characteristics peaks of pure NTG when analyzed at different time points (Figs. 2, 3, 4, and 5 and Tables IV, V, VI, and VII). This is indicative of the compatibility between the pure NTG and polymers used in the tablet formulation.

DSC Study. DSC thermograms either of drug alone or in combination with different polymers stored at ambient condition for 0, 10, 20, and 30 days showed onset temperature of a peak (T_{onset}) and peak transition temperature (T_{peak}). DSC thermograms showed a sharp endothermic peak (T_{peak}) at ~132°C for both NTG (Fig. 6) and physical mixture (Figs. 7, 8, 9, and 10), whereas, peak onset (T_{onset}) was observed at ~130°C for NTG (Fig. 6) and ~129°C for physical mixture (Fig. 7, 8, 9, and 10).

The melting endotherm of NTG and physical mixture (T_{onset} and T_{peak}) was found to be well preserved with light broadening with a shift towards the low-temperature range. This change in shape and shifting of the peak could be attributed to the proper mixing of the drug with excipients, which may not necessarily indicate their potential incompatibility (Figs. 2, 3, 4 and 5).

Isothermal Stress Testing

The drug and excipient mixtures of control and stressed samples were tested for drug content by UV-Visible spectroscopy. The absorbance of NTG in methanol was recorded at 210 nm (λ_{max}) over a concentration range of 5–50 µg/mL. The drug content was observed within the range of 99.48 to 102.15% complying the limits prescribed as per the ICH guidelines Q2 [R1] (95–105%) (28).

Preparation and Evaluation of NTG Tablets

The tablets from all batches (F1–F16) were round in shape, white in color, and smooth in appearance.

Weight Variation

The weight variation for all batches (F1–F16) was observed between 0.65 ± 0.85 and $2.1 \pm 1.26\%$ ($n=20$) from an average weight of tablet (400 ± 5 mg) which was within the acceptable limits of 5% deviation (for more than 324 mg tablet weight) (29).

Hardness

Tablets from all batches (F1–F16) showed harness within desired limits (5.3 ± 0.11 to 5.5 ± 0.18 kg/cm², Table VIII) as measured in triplicate ($n=3$). This indicated enough strength of tablets to withstand the mechanical shocks commonly observed during the handling and the shipment.

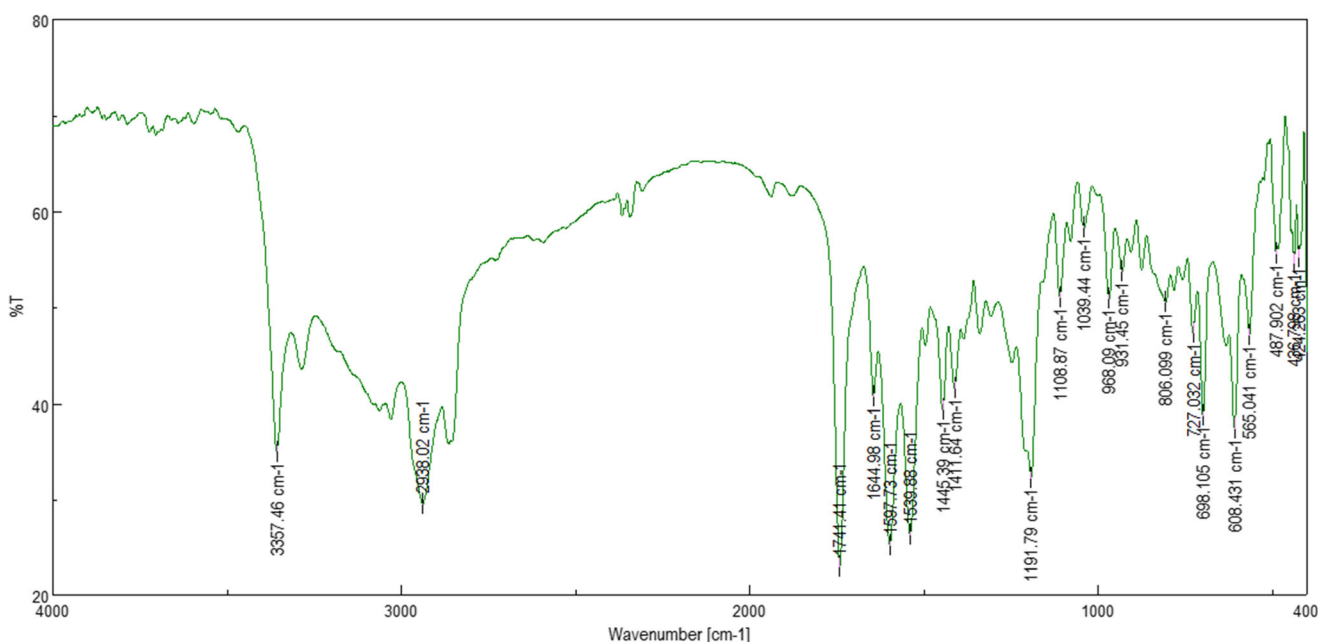


Fig. 1. FTIR spectrum of pure NTG

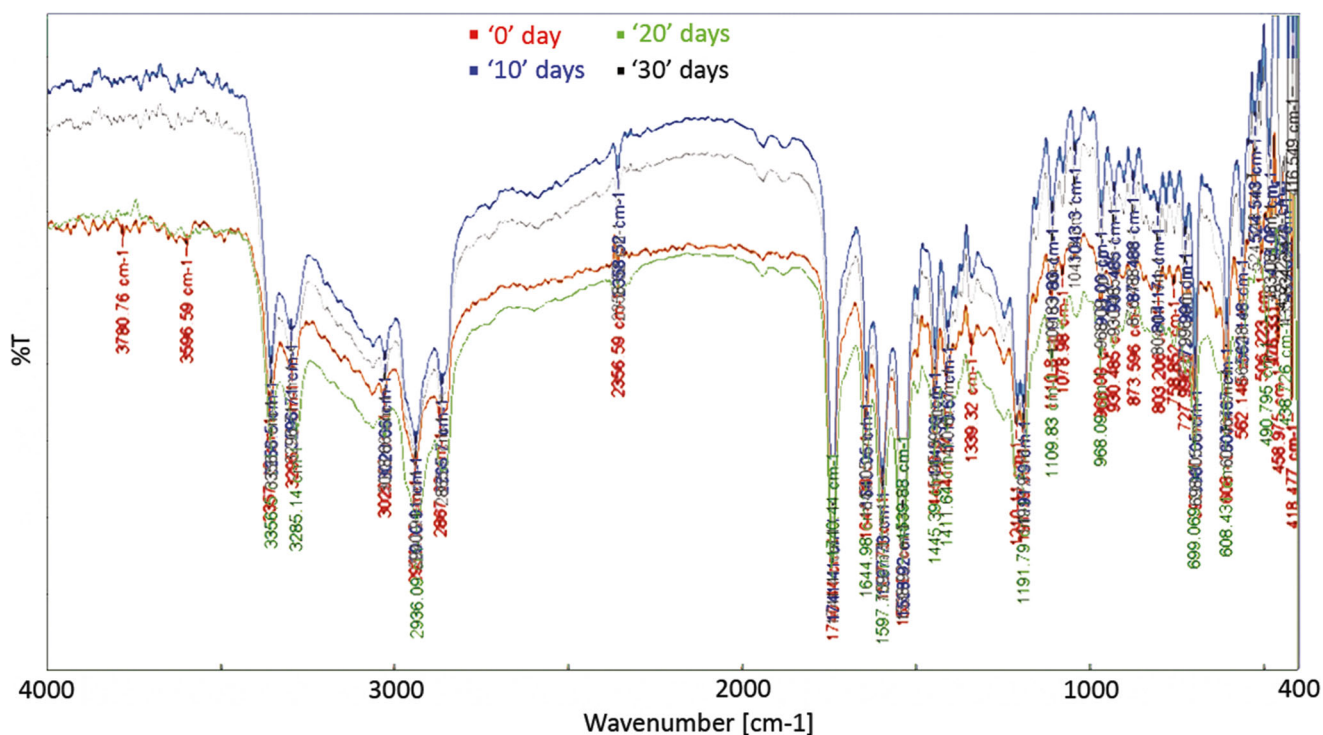


Fig. 2. FTIR spectrum of the physical mixture (pure NTG with K100M) at 0, 10, 20, and 30 days

Friability

Friability for tablets from all batches (F1–F16) was found in the range of 0.26 to 0.63 (Table VIII), which was within the prescribed limit (<1%).

Drug Content

The drug content of tablets from all batches (F1–F16) determined using UV-Visible spectrophotometer at 210 nm (λ_{max}) was observed within the range of 96.23 ± 2.22 to $102.07 \pm 0.32\%$ (Table VIII).

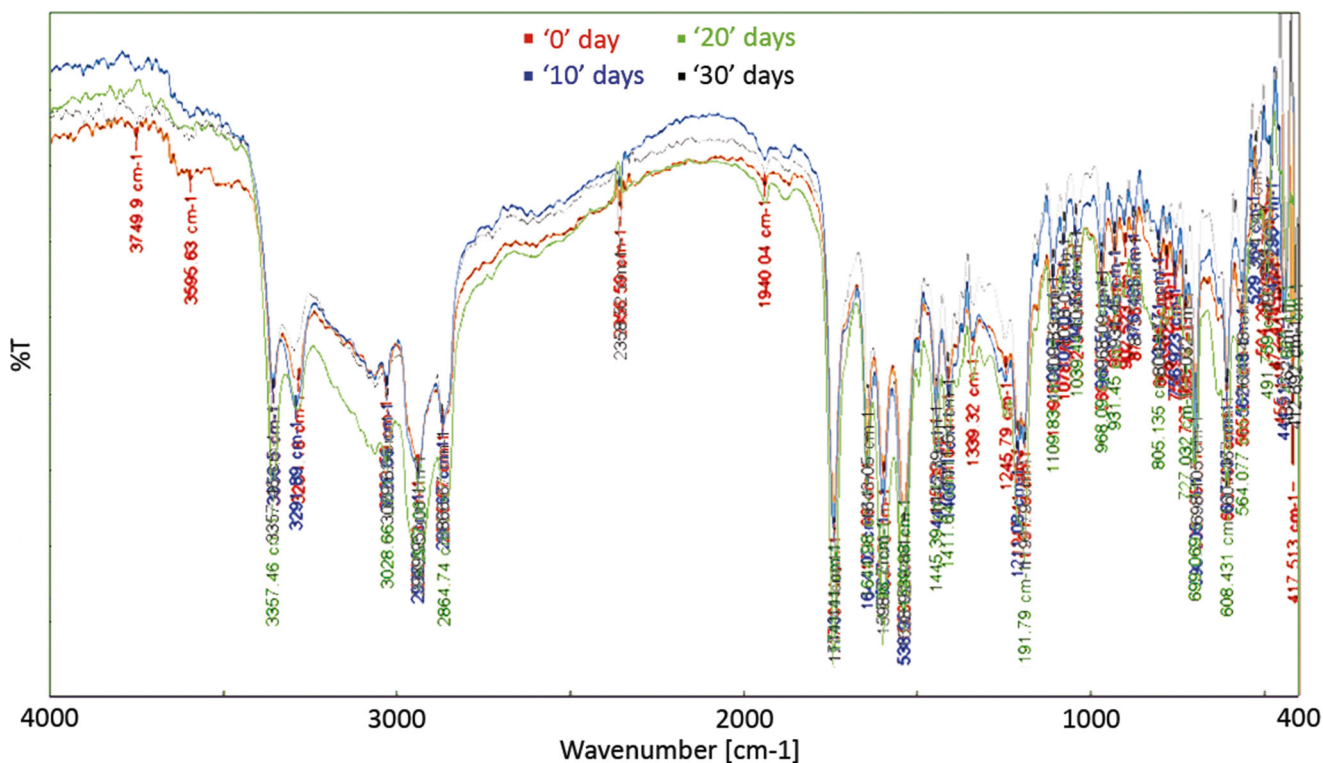


Fig. 3. FTIR spectrum of the physical mixture (pure NTG with K35M) at 0, 10, 20, and 30 days

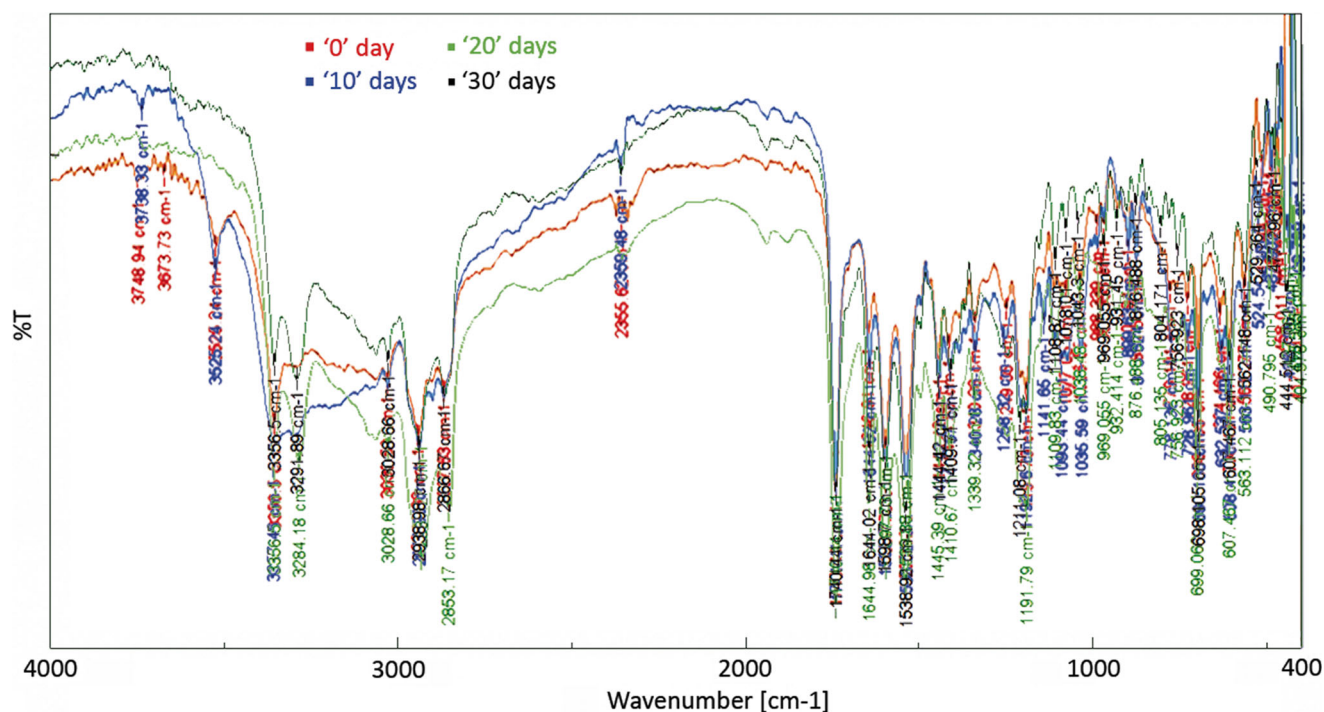


Fig. 4. FTIR spectrum of the physical mixture (pure NTG with K15M) at 0, 10, 20, and 30 days

Swelling Index

The type or grade and concentration of HPMC have shown an effect on the swelling index of tablets. The high content within the similar grade of HPMC showed high swelling index (batches F1 to F4 or F5 to F8 or F9 to F12 or F13 to F16). Likewise, the high grade with the same content of HPMC also showed high swelling index

(batches F1, F5, F9, and F13 or F2, F6, F10, and F14 or F3, F7, F11, and F15 or F4, F8, F12, and F16). Therefore, batch F13 containing HPMC K100M at high content exhibited the highest swelling index ($67.04 \pm 0.99\%$) among all the batches (Table IX). This was attributed to enhanced hydration as well as gel formation around the surface of the tablet.

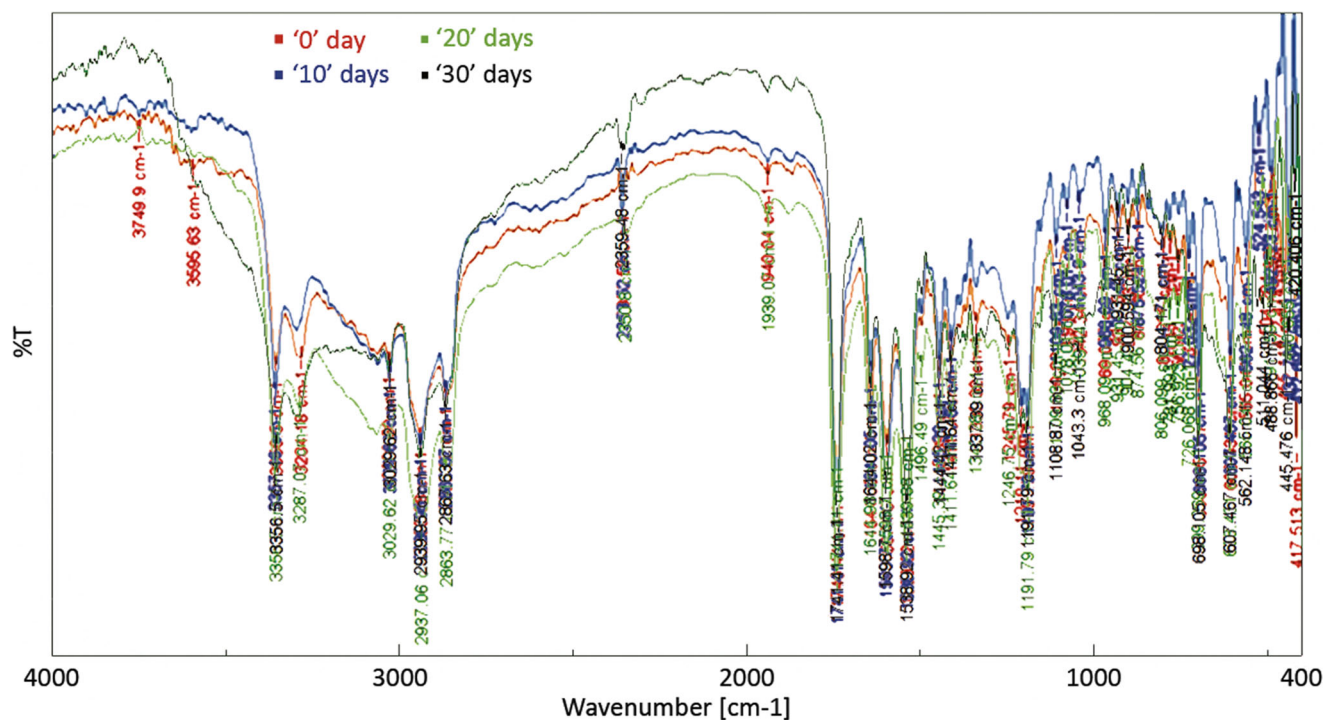


Fig. 5. FTIR spectrum of the physical mixture (pure NTG with K4M) at 0, 10, 20, and 30 days

Table IV. Characteristic Peaks for Pure NTG and Physical Mixture (NTG with K100M) at 0, 10, 20, and 30 days

Functional groups	IR peak (cm ⁻¹)				
	Pure NTG	Physical mixture (NTG with K100M)			
		0 day	10 days	20 days	30 days
–OH stretching (alcohol group)	3357.46	3357.46	3356.5	3356.5	3356.5
–CH ₃ stretching (methyl group)	2938.02	2939.95	2940.91	2936.09	2940.91
–C=O stretching (ketonic group)	1741.41	1741.41	1741.41	1740.44	1741.41
C=C stretching	1644.98	1643.05	1643.05	1644.98	1643.05
C=C stretching (unsaturated bonding)	968.09	968.09	968.09	968.09	968.09

In Vitro Dissolution Study

In vitro drug release kinetics from all batches (F1–F16) showed Korsmeyer-Peppas as best fit model following non-Fickian transport ($0.45 < n < 0.89$) as drug release mechanism (Table IX). Batches F1 to F4 (HPMC K4M), F5 to F8 (HPMC K15M), F9 to F12 (HPMC K35M), and F13 to F16 (HPMC K100M) showed concentration-dependent effect on $t_{90\%}$, where slow rate of drug release was attributed to the relatively high content (200 mg) of the HPMC polymer (Table IX, Figs. 11–12). Moreover, relative high degree of polymerization or grade (K100M) of HPMC polymer at equal content found to reduce the rate of drug release as observed in between batches F1, F5, F9, and F13 or F2, F6, F10, and F14 or F3, F7, F11 and F15 or F4, F8, F12, and F16 (Table IX, Figs. 11–12). Furthermore, a high degree of polymerization or grade of HPMC (batches F13 to F16) results in more hydration as well as the increased thickness of the gel layer (due to high swelling index) that ultimately reduces the inside penetration of the dissolution media. Consequently, the pathlength for drug diffusion increases with time that ultimately reduces the rate of drug release from the polymeric matrices (Table IX and Fig. 12). Moreover, HPMC with a high degree of polymerization and content (batch F13) can retain matrix integrity for maximum time with net effect as least erosion of the matrix and hence, the slowest rate of drug release among all the batches (Table IX and Fig. 12).

In Vivo Study in White Albino Rabbits

Bioanalytical Method Development.

- Mobile Phase Selection

Phosphate buffer (10 mM, pH 6.8) with acetonitrile (65:35) showed maximum extraction and hence selected as the mobile phase.

- Linearity Range Determination

The chromatographic response (ratio of NTG peak to internal standard vs. NTG concentration) was found to be linear over the range of 100.05–3301.12 ng/mL with a correlation coefficient (r), slope, and intercept as 0.999, 7089, and –1586.3, respectively. The % coefficient of variation suggested the high level of accuracy (% recovery-intraday: 96.90 to 99.47% and interday: 98.54 to 99.48%) and precision (% relative standard deviation-intraday: 1.09 to 2.13% and interday: 1.17 to 2.70%) of the developed method. The LOD and LOQ values for NTG were observed as 0.000653 µg/mL and 0.001979 µg/mL, respectively.

The values of coefficient of variance suggest high level of precision (% RSD-interday: 1.17–2.70; intraday: 1.09–2.13) and accuracy (% recovery-interday: 98.54–99.48; intraday: 96.90–99.47) of the method. The LOD and LOQ values for nateglinide were 0.000653 µg/mL and 0.001979 µg/mL.

Table V. Characteristic Peaks for Pure NTG and Physical Mixture (NTG with K35M) at 0, 10, 20, and 30 days

Functional groups	IR peak (cm ⁻¹)				
	Pure NTG	Physical mixture (NTG with K35M)			
		0 day	10 days	20 days	30 days
–OH stretching (alcohol group)	3357.46	3356.5	3356.5	3357.46	3356.5
–CH ₃ stretching (methyl group)	2938.02	2938.98	2938.98	2937.06	2938.98
–C=O stretching (ketonic group)	1741.41	1740.44	1740.44	1741.41	1740.44
C=C stretching	1644.98	1644.98	1644.02	1644.98	1644.02
C=C stretching (unsaturated bonding)	968.09	969.05	969.055	968.09	969.055

Table VI. Characteristic Peaks for Pure NTG and Physical Mixture (NTG with K15M) at 0, 10, 20, and 30 Days

Functional groups	IR peak (cm ⁻¹)				
	Pure NTG	Physical mixture (NTG with K15 M)			
		0 day	10 days	20 days	30 days
–OH stretching (alcohol group)	3357.46	3356.05	3357.46	3356.5	3357.46
–CH ₃ stretching (methyl group)	2938.02	2941.88	2938.98	2931.27	2938.98
–C=O stretching (ketonic group)	1741.41	1740.44	1741.41	1740.44	1741.41
C=C stretching	1644.98	1646.91	1644.02	1644.98	1644.02
C=C stretching (unsaturated bonding)	968.09	968.30	–	969.055	–

Table VII. Characteristic Peaks for Pure NTG and Physical Mixture (NTG with K4M) at 0, 10, 20, and 30 Days

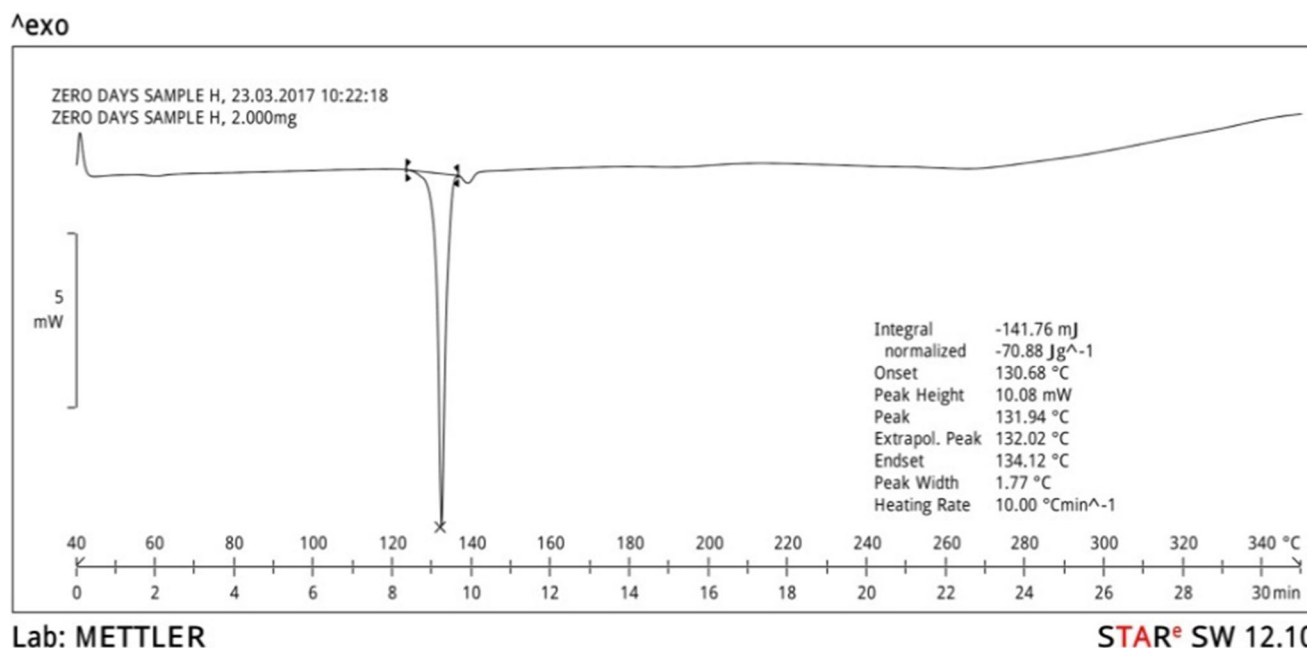
Functional groups	IR peak (cm ⁻¹)				
	Pure NTG	Physical mixture (NTG with K4M)			
		0 day	10 days	20 days	30 days
–OH stretching (alcohol group)	3357.46	3357.5	3357.46	3356.5	3357.46
–CH ₃ stretching (methyl group)	2938.02	2940.91	2939.95	2937.06	2939.95
–C=O stretching (ketonic group)	1741.41	1740.44	1741.41	1741.41	1741.41
C=C stretching	1644.98	1645.95	1643.05	1644.98	1643.05
C=C stretching (unsaturated bonding)	968.09	968.09	968.09	968.09	968.09

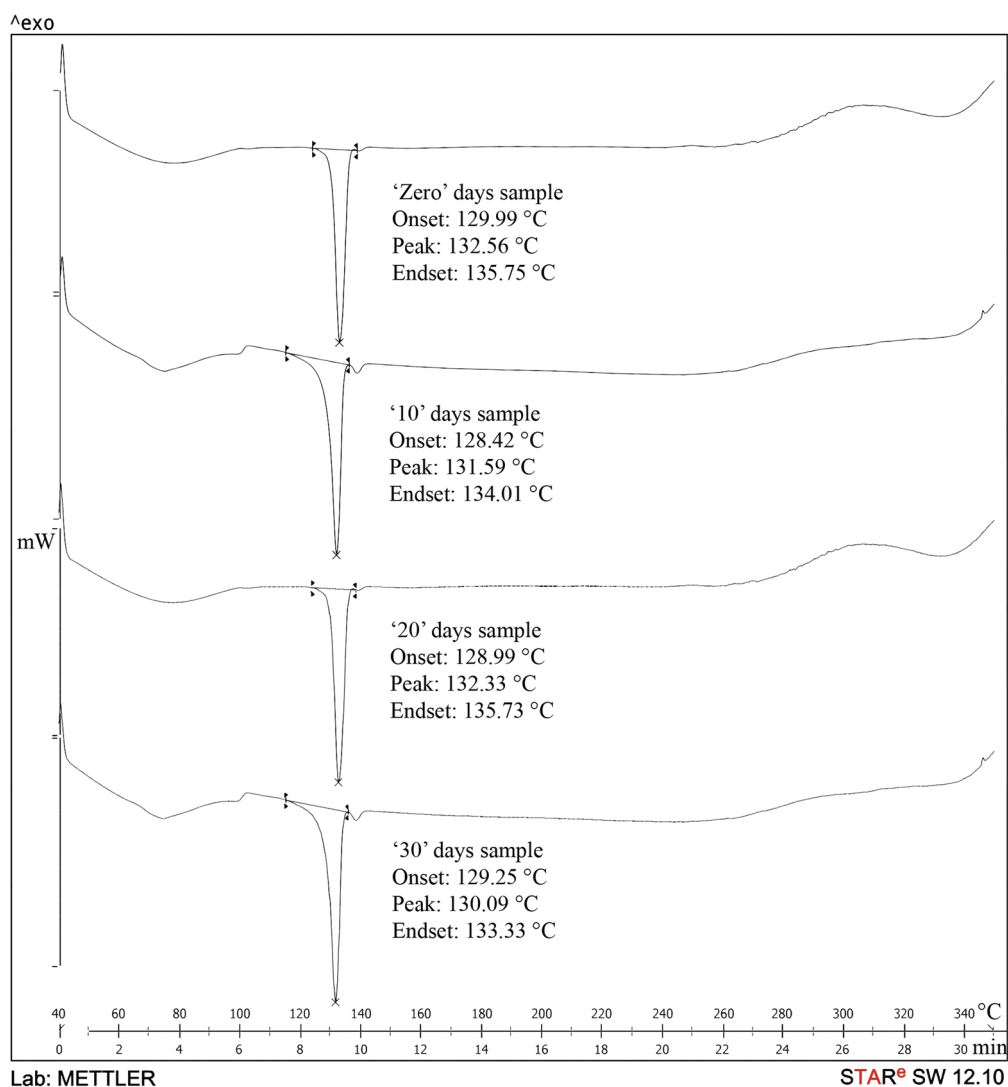
- Determination of Pharmacokinetic Parameters

Several *in vivo* pharmacokinetic parameters such as C_{max} , ERC, V_D , $t_{1/2}$, MRT, and clearance (Table X) were estimated from the dose-response curve (Figs. 13, 14, 15, and 16) for formulation batches (F4, F8, F12, and F16)

containing low content (50 mg) of HPMC selected on basis of *in vitro* test results.

C_{max} value is indicative of the rate of drug absorption after administration of the tablet. The high $t_{1/2}$ of the tablet formulations compared to the original (1.5 h) (30) is attributed to the delayed removal of the drug from the rabbit

**Fig. 6.** DSC thermogram of pure NTG



Lab: METTLER

STAR® SW 12.10

Fig. 7. DSC thermogram of the physical mixture (pure NTG with K100M) at 0, 10, 20, and 30 days

plasma. This was further supported by the low value of ERC than that for immediate release tablet (0.3) (31). Among the tested formulations (F4, F8, F12, and F16) containing 50 mg of different grades of HPMC, batch F12 (HPMC K35M) exhibited high $t_{1/2}$ and low ERC attributed to drug disposition and prolonged effect (Table X).

Low clearance value and high MRT for batch F12 are also indicative of delayed elimination with enhanced retention due to the inclusion of release rate-limiting polymer in the tablet formulation (Table X). This could have facilitated the complete absorption of NTG. Therefore, it can be concluded that the extended rate of drug release would not have induced unexpected or different *in vivo* pharmacokinetics.

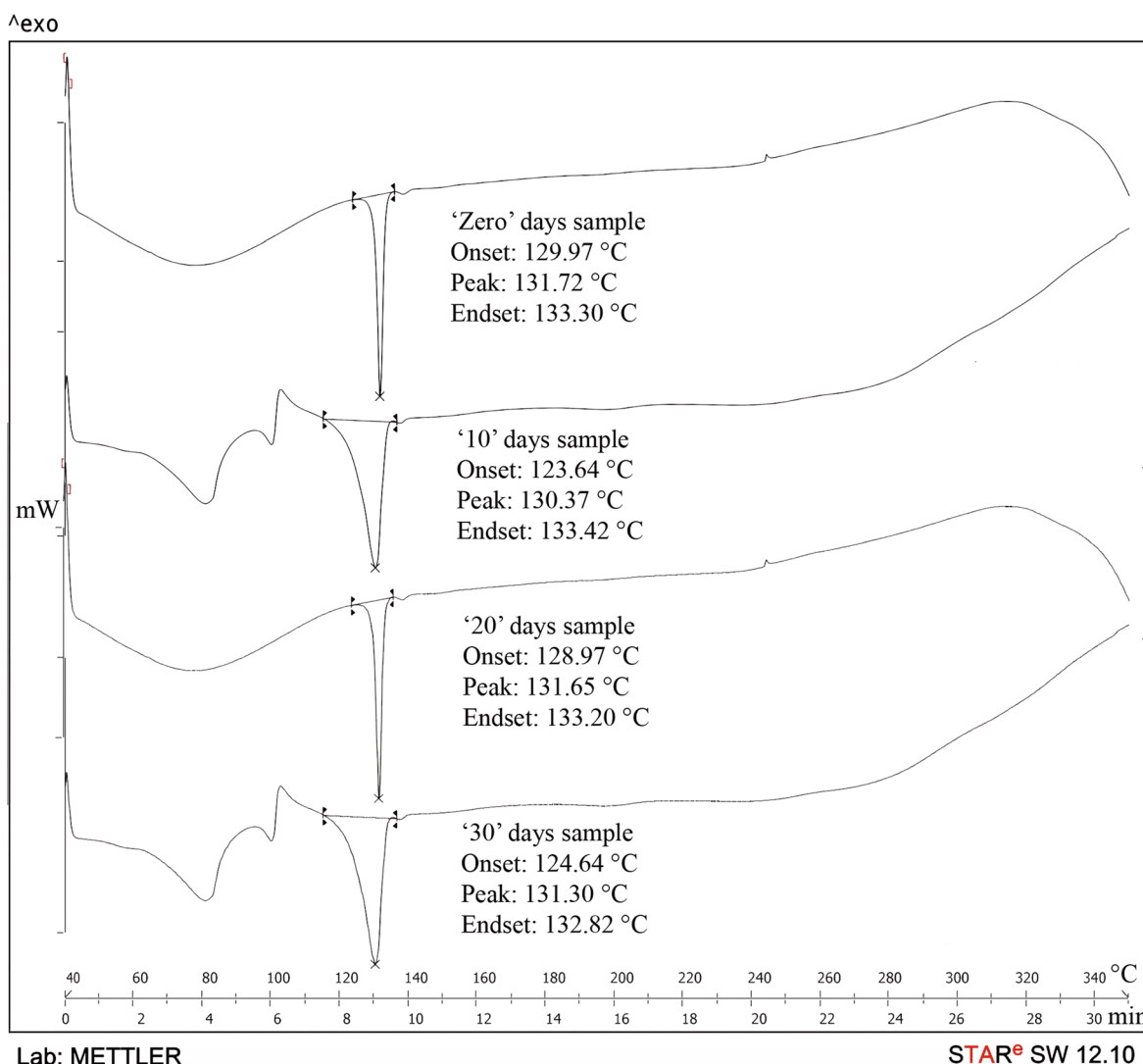
pool of calculated descriptors, a set of descriptors showing significant contribution and individual impact on formulation property was selected and subsequently correlated with the formulation property of interest ($t_{90\%}$, swelling index, drug content, friability, hardness, or angle of repose). This resulted in a generation of QSPR model each for four different polymeric concentrations (200, 150, 100, and 50 mg) as well as for individual *in vitro* property using Vlife MDS 4.2 software. From these models, a best QSPR model irrespective of polymeric content was selected for each formulation property (six QSPR models) by considering model quality parameters such as coefficient of determination (r^2), predicted correlation coefficient, RMSE, standard error, F-statistics, and P value (Table XI).

Development of a QSPR Model

QSPR Modeling (6–17)

The physicochemical descriptors ($n = 87$) for varying grades of HPMC (K4M, K15M, K35M, and K100M) were calculated based on its degree of polymerization. From the

Angle of Repose. XKMostHydrophobicHydrophilicDistance signifies the distance between a most hydrophobic and hydrophilic point on the vdW surface (By Kellog Method using Xlogp). This term is associated with the polarity of polymer on the



Lab: METTLER

STAR[®] SW 12.10

Fig. 8. DSC thermogram of the physical mixture (pure NTG with K35M) at 0, 10, 20, and 30 days

vdW surface. The positive impact (± 0.078) of this descriptor indicates a direct relationship with the angle of repose. Increased hydrophobic-hydrophilic distance is indicative of a decrease in net polarity and hence, high hydrophobicity. The hydrophobic character of polymer in powder blend does not allow to absorb the moisture with net effect as an increase in the angle of repose of the blend.

Additionally, SKMostHydrophobicHydrophilicDistance signifies the distance between a most hydrophobic and hydrophilic point on the vdW surface (By Kellogg Method using Slogp). The increased distance between these two points is related to the high non-polarity or hydrophobicity on the polymer surface. This does not allow powder blend to absorb moisture from the surroundings and hence, increases the angle of repose as indicated by the positive value of the descriptor (± 0.076).

$$\begin{aligned} \text{Angle of Repose} = & 25 + 0.078 \times \text{SKMostHydrophobicHydrophilicDistance} \\ & + 0.076 \times \text{SKMostHydrophobicHydrophilicDistance} \\ & + 0.002 \times \text{SAHydrophilicArea} \pm 0.058 \end{aligned}$$

(3)

QSPR model for the angle of repose (Eq. 3) showed a significant effect of all independent variables on the angle of repose as indicated by F-statistics, p value (< 0.05), and X-variance (≤ 1). Furthermore, high r^2 , low RMSE, and standard error are indicative of a good correlation between independent variables and response. Moreover, the developed model showed considerable predictability (predicted $r^2 = 0.905$) for the angle of repose (Table XI).

Hardness. SKMostHydrophobicHydrophilicDistance descriptor exhibited the least positive ($+0.00852$) but a significant effect on tablet hardness (F-value = 13.89). The positive impact of descriptor signifies the formation of the harder tablet with an increase in hydrophobic character or reduction in net polarity index on the polymer surface.

$$\text{Hardness} = 5.560 + 0.00852$$

$$\times \text{SKMostHydrophobicHydrophilicDistance}$$

$$\pm 0.001$$

(4)

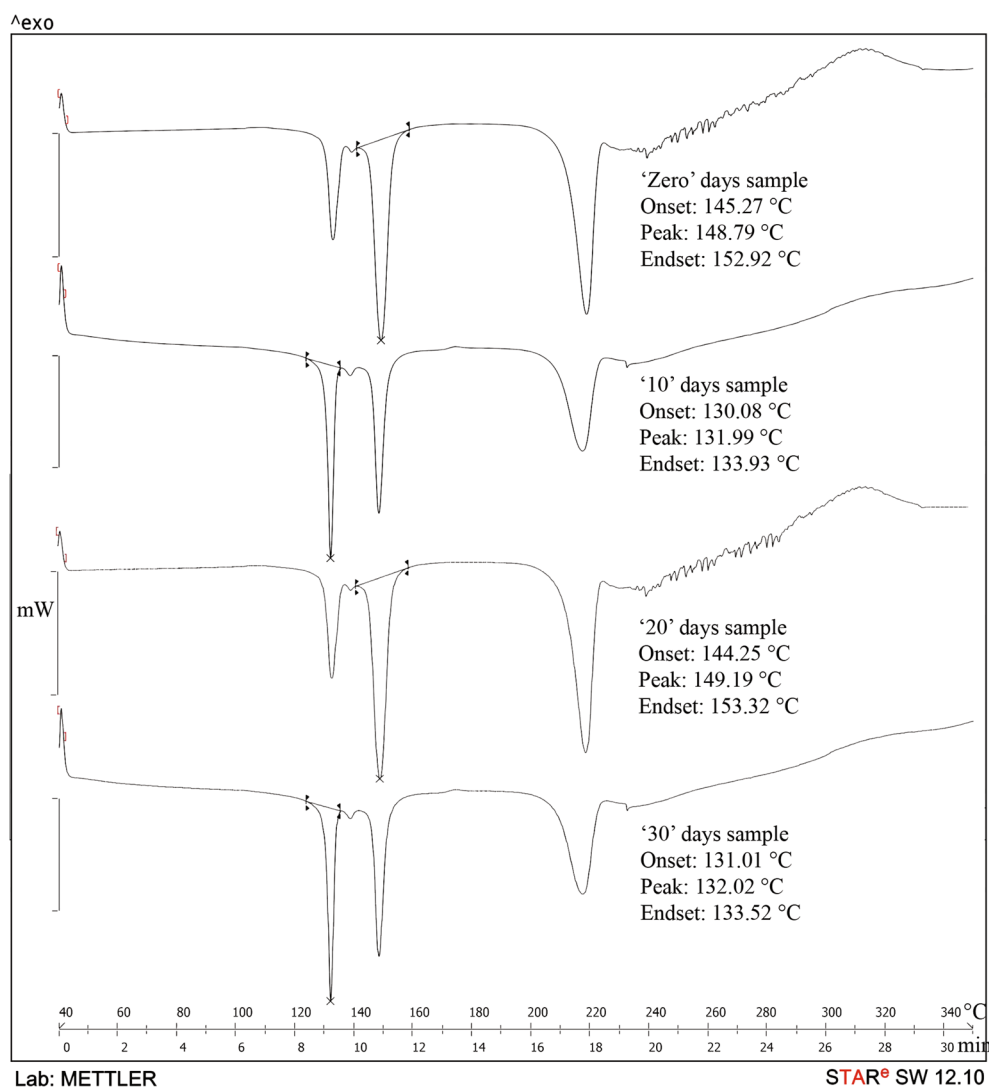


Fig. 9. DSC thermogram of the physical mixture (pure NTG with K15M) at 0, 10, 20, and 30 days

QSPR model for hardness (Eq. 4) indicated a significant effect of the independent variable on hardness (F-statistics, p value < 0.05 , and X-variance ≤ 1) and a good correlation between the variables (high r^2 , low RMSE, and standard error). However, the predictability of the developed model was too low for hardness (predicted $r^2 = 0.717$, Table XI).

Friability. 'XKMostHydrophobicHydrophilicDistance' relates to hydrophobicity over the polymer surface through the distance between most hydrophilic and hydrophobic points on the vdW surface (By Kellog Method using Xlogp). Negative (-2.798) but significant impact of this descriptor is indicative of reduced tablet friability in the presence of hydrophobic polymer, which is in accordance with the hardness results.

'XAHydrophobicArea' is a vdW surface descriptor that denotes hydrophobic surface area over the polymer surface showed a negative effect (-6.887) on friability. The hydrophobic character of both NTG and polymer could have resulted in improved physical bonding that leads to the formation of a tablet with reduced friability.

Another vdW surface descriptor 'SAHydrophilicArea' signifies hydrophilic surface area on the polymer surface (by Audry method using SlogP). The positive ($+6.787$), significant effect of this descriptor is in accordance with the negative effect of 'XAHydrophobicArea' which indicates increased friability in the presence of a polymer with high hydrophilic character.

Moreover, a distance-based topological descriptor, 'BalabanIndexJ', represents the three-dimensional (3D) volume of the polymeric structure and it is calculated by using Eq. 5,

$$J = (E/\mu + 1) \sum (ds_i, ds_j) \quad (5)$$

where ds_i and ds_j are the sum of the row 'i' and 'j' of the distance matrix; μ and E are the number of rings and edges in a molecule, respectively. The positive ($+0.063$) yet significant impact of this descriptor allowed its consideration in the QSPR model development. This was attributed to reduced drug-polymer interaction due to the high volume of the drug with net effect as increased friability.

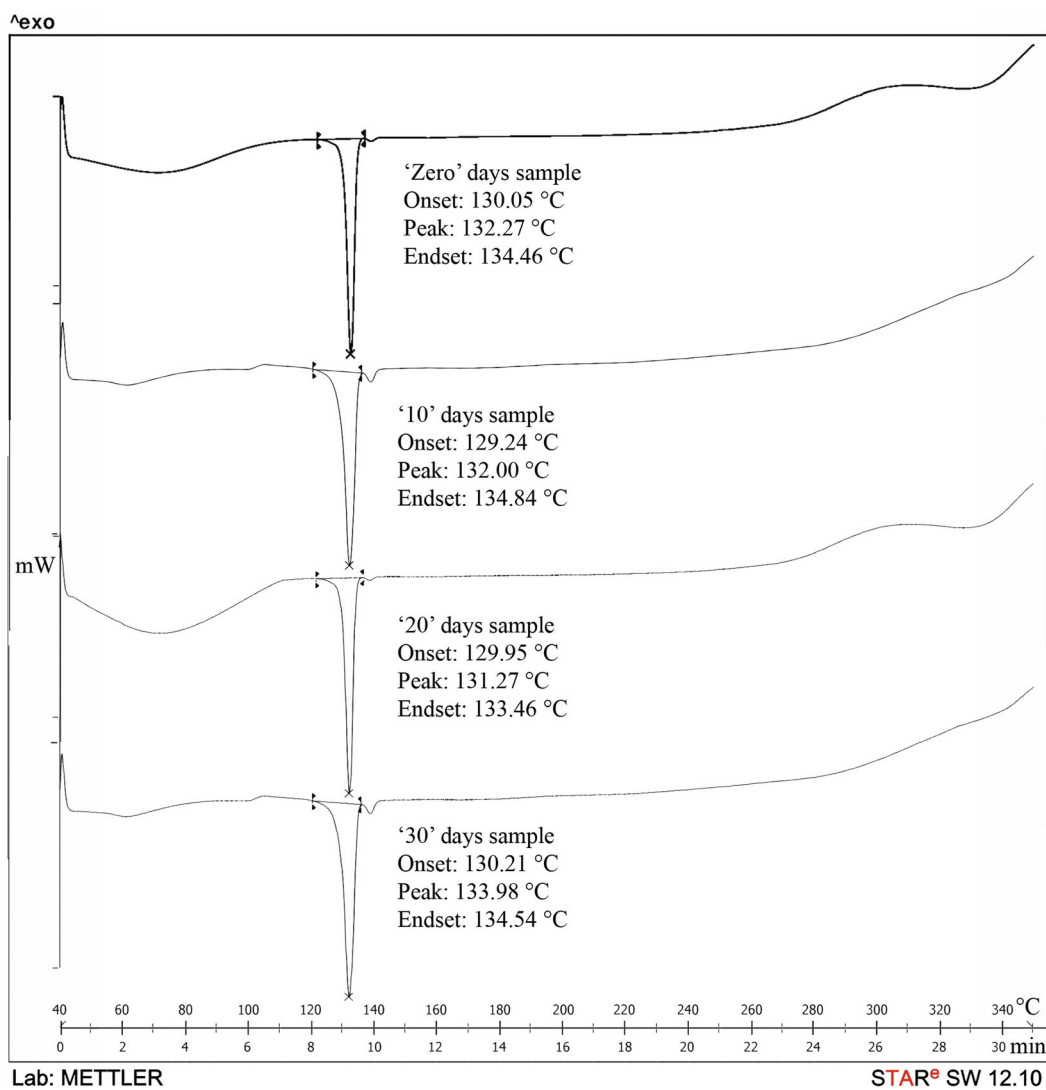


Fig. 10. DSC thermogram of the physical mixture (pure NTG with K4M) at 0, 10, 20, and 30 days

Table VIII. Characterization of NTG Tablet Formulations

Batch code	Angle of repose (°)	Weight variation (%)	Hardness (kg/cm ²)	Friability	Drug content (%)
F1	28.21 ± 2.1	0.75 ± 0.58	5.5 ± 0.18	0.26	98.1 ± 3.20
F2	31.1 ± 1.7	1.25 ± 1.06	5.3 ± 0.11	0.26	99.65 ± 1.8
F3	27.01 ± 1.8	0.89 ± 1.05	5.5 ± 0.18	0.48	99.33 ± 0.5
F4	28.8 ± 2.2	1.26 ± 0.98	5.3 ± 0.13	0.53	100.6 ± 0.98
F5	30.24 ± 0.98	0.65 ± 0.85	5.4 ± 0.18	0.37	99.3 ± 2.38
F6	28.21 ± 1.4	1.02 ± 1.02	5.4 ± 0.11	0.45	102.07 ± 0.32
F7	28.8 ± 2.1	1.26 ± 1.26	5.4 ± 0.18	0.48	101.69 ± 1.89
F8	30.81 ± 1.8	0.98 ± 1.01	5.4 ± 0.19	0.51	96.23 ± 2.22
F9	29.09 ± 1.4	1.69 ± 0.98	5.4 ± 0.12	0.55	98.24 ± 3.56
F10	27.16 ± 1.2	2.01 ± 1.06	5.5 ± 0.09	0.63	98.53 ± 0.36
F11	28.21 ± 2.2	1.06 ± 1.02	5.5 ± 0.15	0.32	98.9 ± 1.12
F12	30.24 ± 2.1	0.74 ± 0.88	5.5 ± 0.18	0.48	98.55 ± 0.97
F13	28.8 ± 1.9	0.65 ± 0.94	5.5 ± 0.13	0.48	98.05 ± 1.26
F14	28.21 ± 2.2	0.78 ± 1.08	5.4 ± 0.11	0.48	96.72 ± 0.62
F15	30.24 ± 1.7	2.1 ± 1.26	5.4 ± 0.18	0.36	96.3 ± 3.22
F16	29.39 ± 1.4	1.03 ± 0.88	5.4 ± 0.09	0.38	98.15 ± 2.56

Average ± standard deviation

Table IX. *In Vitro* Dissolution Study from NTG-HPMC Tablet Formulations

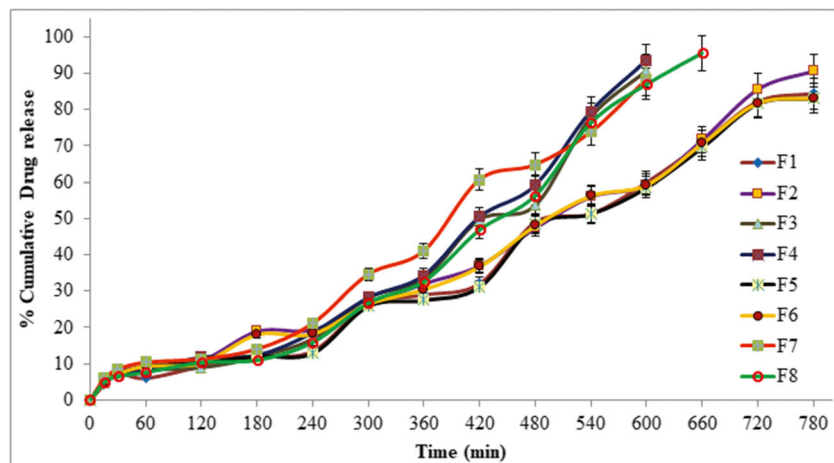
Batch code	Swelling Index (%)	Zero order (r^2)*	First order (r^2)*	Higuchi (r^2)*	Matrix (r^2)*	Hixon (r^2)*	Crowell	Korsmeyer-Peppas		Best fit model	t ₉₀ % (min)
								(r^2)*	(n)*		
F1	55.56 ± 1.23	0.682	0.676	0.022		0.029		0.960	0.6067	Korsmeyer-Peppas	864
F2	49.11 ± 1.15	0.059	–	0.230		0.082		0.991	0.5955	Korsmeyer-Peppas	852
F3	40.11 ± 2.01	0.319	–	0.354		0.582		0.842	0.6610	Korsmeyer-Peppas	720
F4	25.74 ± 1.98	0.033	–	0.305		0.244		0.725	0.6715	Korsmeyer-Peppas	648
F5	59.79 ± 1.56	0.203	–	0.939		0.440		0.829	0.6569	Korsmeyer-Peppas	868
F6	49.55 ± 2.02	0.023	–	0.150		0.150		0.738	0.6437	Korsmeyer-Peppas	858
F7	42.79 ± 2.59	0.988	–	0.016		0.846		0.851	0.6634	Korsmeyer-Peppas	726
F8	32.54 ± 1.87	0.021	–	0.371		0.135		0.627	0.6702	Korsmeyer-Peppas	660
F9	63.78 ± 1.02	0.813	–	0.558		0.471		0.790	0.6579	Korsmeyer-Peppas	876
F10	50.55 ± 1.25	0.041	–	0.037		0.136		0.375	0.6519	Korsmeyer-Peppas	858
F11	43.49 ± 2.06	0.688	–	0.129		0.313		0.435	0.6659	Korsmeyer-Peppas	798
F12	32.71 ± 2.16	0.093	–	0.271		0.848		0.931	0.6542	Korsmeyer-Peppas	665
F13	67.04 ± 0.99	0.436	0.067	0.259		0.058		0.998	0.6184	Korsmeyer-Peppas	886
F14	51.07 ± 1.06	0.436	0.067	0.259		0.058		0.898	0.5995	Korsmeyer-Peppas	862
F15	47.23 ± 1.98	0.580	0.034	0.092		0.101		0.855	0.6013	Korsmeyer-Peppas	840
F16	38.29 ± 2.05	0.027	0.145	0.262		0.394		0.986	0.6027	Korsmeyer-Peppas	684

Where (r^2) is the correlation coefficient and (n) is release exponent

$$\text{Friability} = 0.5298 - 2.798 \times \text{XKMostHydrophobicHydrophilicDistance} - 6.887 \times \text{XAHydrophobicArea} + 0.063 \times \text{BalabanIndexJ} + 6.787 \times \text{SAHydrophilicArea} \pm 0.00$$

(6)

QSPR model (Eq. 6) indicated a significant effect of all independent variables on tablet friability (F-statistics, p value < 0.05 , and X-variance ≤ 1). Moreover, a good correlation between the variables (high r^2 , low RMSE, and standard

**Fig. 11.** *In vitro* dissolution study of F1 to F8 tablet formulations

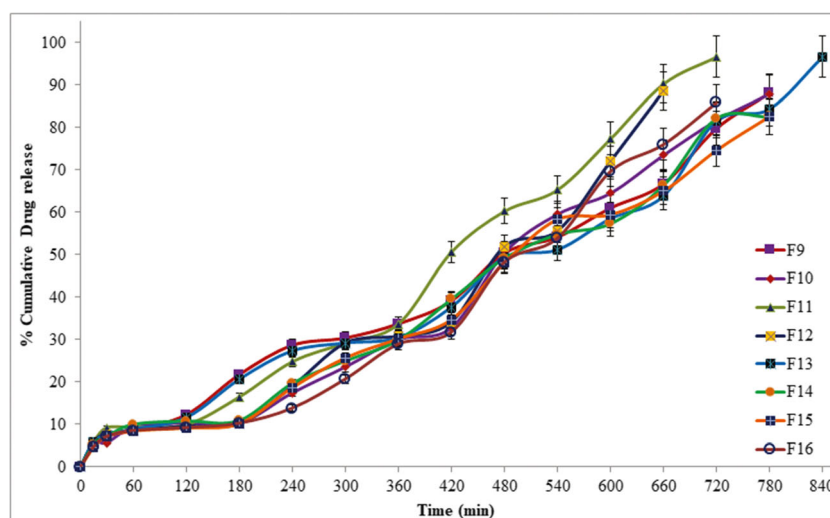


Fig. 12. *In vitro* dissolution study of F9 to F16 tablet formulations

error) and considerable predictability of the developed model for friability (predicted $r^2 = 0.815$) was observed (Table XI).

Drug Content. The positive effect (+0.189) of ‘SAMostHydrophobicHydrophilicDistance’ (By Audry Method using Slogp) is indicative of the increased drug content in the presence of the hydrophobic character of the polymer. Moreover, reduced net polarity index due to the increased distance between hydrophilic-hydrophobic points (hydrophobic character) on the polymer surface could result into improved interaction as well as bonding with the hydrophobic drug and hence, drug content of the tablet. However, lower and similar (+0.097) yet the significant effect was exhibited by the ‘XAMostHydrophobicHydrophilicDistance’ descriptor (by Audry Method using Xlogp).

$$\text{Drug Content} = 97.936 + 0.189 \times \text{SAMostHydrophobicHydrophilicDistance} + 0.097 \times \text{XAMostHydrophobicHydrophilicDistance} \pm 0.048 \quad (7)$$

QSPR model developed for drug content (Eq. 7) exhibited a significant effect of all explanatory variables in the model on the drug content (F-statistics, p value < 0.05, and X-variance ≤ 1). Moreover, an excellent correlation was observed between the independent variables and the response (high r^2 , low standard error, and RMSE). Furthermore, the developed model showed good predictability (predicted $r^2 = 0.969$) for the drug content (Table XI).

Swelling Index. ‘BalabanIndexJ’, a distance-based topological descriptor (Eq. 5), represents the three-dimensional volume of the polymer. The positive effect of this descriptor (+8.597) is indicative of an improved swelling index of high volume HPMC with entrapment of the maximum volume of dissolution media. This could have resulted in increased pathlength for drug diffusion and hence sustained the drug release. Moreover, similar (+0.008) yet the significant effect of ‘SAHydrophilicArea’ is indicative of enhanced swelling index in the presence of hydrophilic HPMC. However, the negative impact of both the hydrophobic descriptors, ‘SAHydrophobicArea’ (−0.010) and ‘XAMostHydrophobicHydrophilicDistance’ (−0.213), indicated a decrease in swelling index, which is in accordance with previously discussed results.

$$\text{Swelling Index} = 62.212 - 0.213 \times \text{XAMostHydrophobicHydrophilicDistance} - 0.010 \times \text{SAHydrophobicArea} + 8.597 \times \text{BalabanIndexJ} + 0.008 \times \text{SAHydrophilicArea} \pm 0.548 \quad (8)$$

Developed QSPR model (Eq. 8) shows a significant effect of all independent descriptors on swelling index as depicted from F-statistics (191.22), p value (< 0.05), and X-variance (≤ 1). All the independent variables exhibited a good correlation with the dependent variable as indicated by high r^2 , low RMSE, and standard error. Moreover, the developed model can significantly predict the swelling index well in advance for other grades of polymer (predicted $r^2 = 0.981$, Table XI).

Table X. *In Vivo* Characterization of Tablet Formulations

Batch code	C_{\max} (μg/mL)	ERC (min ^{−1})	V_D (mL)	$t_{1/2}$ (h)	MRT (min)	Clearance (L/h)
F4	121.348	0.265	19.571	2.612	522.817	5.191
F8	130.085	0.286	21.776	2.414	428.212	6.249
F12	105.042	0.236	18.379	2.929	617.550	4.347
F16	126.503	0.248	22.649	2.783	516.372	5.639

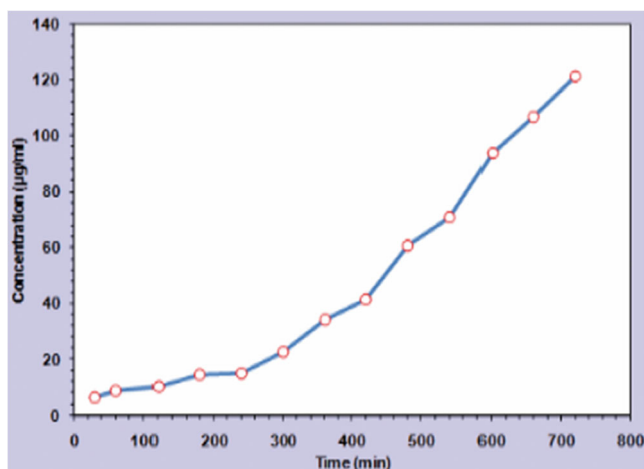


Fig. 13. Plasma drug concentration vs. time profile (dose-response curve) of F4 batch

In Vitro Dissolution Study ($t_{90\%}$). The vdW surface descriptors representing hydrophilicity viz. ‘XAMostHydrophilic’ (−1407.133), ‘SAHydrophilicArea’ by Audry method using Slogp (−0.081), and ‘XKHydrophilicArea’ by Kellog method using Xlogp (−0.043) showed a negative impact on $t_{90\%}$ (Table XI). This is indicative of fast drug release in the presence of hydrophilic HPMC attributed to increased wetting of polymer.

However, the positive impact of hydrophobicity, indicating descriptors such as ‘XKMostHydrophobic’ (+142.970) and ‘XKAverageHydrophobicity’ (+266.417), is indicative of increased $t_{90\%}$ and hence slow drug release. This was attributed to the improved interaction between hydrophobic drug and polymer that lead to reduced availability of the drug to the dissolution media. Moreover, reduced wetting restricts the further entry of dissolution media into the core of tablet that results in a reduced rate of drug release.

$$t_{90\%} = -170.318 - 0.081 \times \text{SAHydrophilicArea} - 1407.133 \times \text{XAMostHydrophilic} - 0.043 \times \text{XKHydrophilicArea} + 266.417 \times \text{XKAverageHydrophobicity} + 142.970 \times \text{XKMostHydrophobic} \pm 0.30$$

(9)

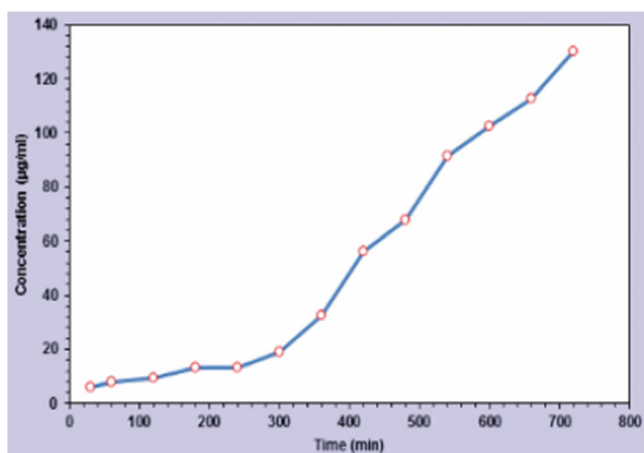


Fig. 14. Plasma drug concentration vs. time profile (dose-response curve) of F8 batch

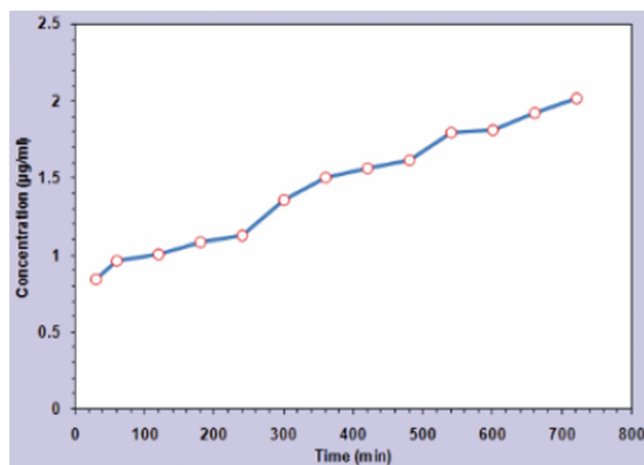


Fig. 15. Plasma drug concentration vs. time profile (dose-response curve) of F12 batch

QSPR model developed (Eq. 9) exhibited the significant effect of all descriptors included in the model on $t_{90\%}$ (F-statistics, p value (<0.05), and X-variance (≤ 1). A good correlation between descriptors and response was observed from high r^2 , low standard error, and RMSE. The developed model showed considerable predictability for predicting $t_{90\%}$ from other grades of polymer well in advance (predicted $r^2 = 0.887$).

In Vivo Study. Various *in vivo* parameters tested for tablet formulations were processed for development of QSPR models (Table XII). Similar to *in vitro* studies, a set of significant descriptors was correlated with *in vivo* properties of tablet formulations (C_{\max} , ERC, V_D , $t_{1/2}$, MRT, and clearance). This resulted in the generation of several QSPR models for selected polymer concentration (50 mg) for each *in vivo* property (Vlife MDS 4.2 software). From these models, a best QSPR model was selected for each formulation *in vivo* property (six QSPR models) by considering model quality parameters such as coefficient of determination (r^2), predicted correlation coefficient, RMSE, standard error, F-statistics, and P value (Table XII).

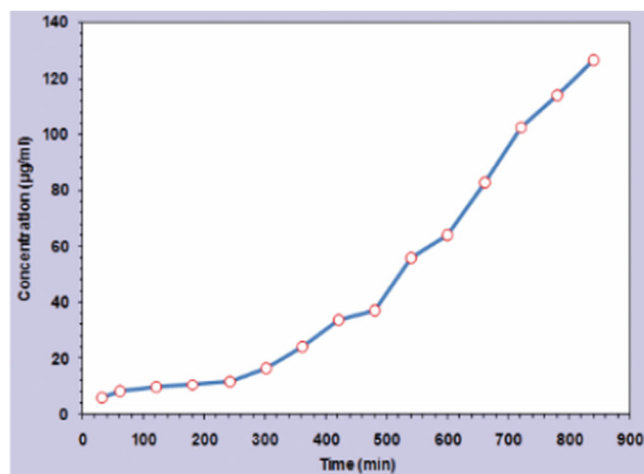


Fig. 16. Plasma drug concentration vs. time profile (dose-response curve) of F16 batch

Table XI. QSPR Model Parameters for the *In Vitro* Study of Tablet Formulations

Parameter	Angle of repose (100 mg)	Hardness (100 mg)	Friability (50 mg)	Drug content (200 mg)	Swelling Index (200 mg)	$t_{90\%}$ (50 mg)
r^2	0.957	0.874	0.930	0.982	0.990	0.999
Predicted r^2	0.905	0.717	0.815	0.969	0.981	0.887
RMSE	0.240	0.0	0.015	0.218	0.740	1.809
Standard error	0.058	0.001	0.000	0.048	0.548	0.30
F-statistics	44.95	13.89	30.64	106.58	191.22	17,872
P value	0.022	0.045	0.031	0.009	0.005	0.005
X-variance	0.87	1.0	0.86	0.88	0.93	0.6
Intercept	25	5.560	0.5298	97.936	62.212	-170.318
SAHydrophilicArea	0.002	-	6.787	-	0.008	-0.081
XAMostHydrophilic	-	-	-	-	-	-1407.133
XKAverageHydrophobicity	-	-	-	-	-	266.417
XKHydrophilicArea	-	-	-	-	-	-0.043
XKMostHydrophobic	-	-	-	-	-	142.970
BalabanIndexJ	-	-	0.063	-	8.597	-
SAHydrophobicArea	-	-	-	-	-0.010	-
XAMostHydrophobicHydrophilicDistance	-	-	-	0.097	-0.213	-
SKMostHydrophobicHydrophilicDistance	0.076	0.00852	-	-	-	-
XKMostHydrophobicHydrophilicDistance	0.078	-	-2.798	-	-	-
XAHydrophobicArea	-	-	-6.887	-	-	-
SAMostHydrophobicHydrophilicDistance	-	-	-	0.189	-	-

QSPR models developed individually for all *in vivo* parameters viz. C_{max} , ERC, V_D , $t_{1/2}$, MRT, and clearance exhibited the positive effect of 'SAMostHydrophobicHydrophilicDistance', 'SKMostHydrophobicHydrophilicDistance', 'XAMostHydrophobicHydrophilicDistance', 'XKMostHydrophobicHydrophilicDistance', and 'XAHydrophobicArea' descriptors (Table XII). All these

descriptors signify reduced net polarity or hydrophobicity on the polymer surface, which results in strong physical interaction with the lipophilic drug. This strong interaction of NTG with highly hydrophilic HPMC enhances its solubilization in dissolution media and ultimately *in vivo* parameters (C_{max} , ERC, V_D , $t_{1/2}$, MRT, and clearance) of highly permeable NTG (BCS Class-II drug). QSPR models developed for all *in vivo* parameters are given in Eqs. 10–15.

Table XII. QSPR Model Parameters for *In Vivo* Study

Parameters	Pharmacokinetic parameters (50 mg)					
	C_{max}	ERC	V_D	$t_{1/2}$	MRT	Clearance
r^2	0.994	0.886	0.922	0.912	0.893	0.879
Predicted r^2	0.876	0.589	0.516	0.589	0.325	0.546
RMSE	0.105	0.006	0.168	0.057	23.005	0.241
Standard error	0.045	0.0002	0.9027	0.0132	529.241	0.2326
F-statistics	4126.26	15.54	50.72	20.41	16.76	14.53
p value	0.011	0.054	0.041	0.046	0.054	0.052
X Variance	0.5	0.6	0.6	0.6	0.4	0.5
Intercept	103.26	0.25	15.82	2.78	417.404	4.28
SAMostHydrophobicHydrophilicDistance	+ 0.981	+ 0.002	+ 0.122	+ 0.010	-	+ 0.0088
SKMostHydrophobicHydrophilicDistance	+ 0.562	-	+ 0.254	-	+ 11.129	-
XAMostHydrophobicHydrophilicDistance	+ 0.423	+ 0.001	+ 0.0044	-	+ 3.64	+ 0.0029
XKMostHydrophobicHydrophilicDistance	-	-	-	+ 0.02	-	+ 0.0036
XAHydrophobicArea	-	-	-	-	+ 0.0037	-

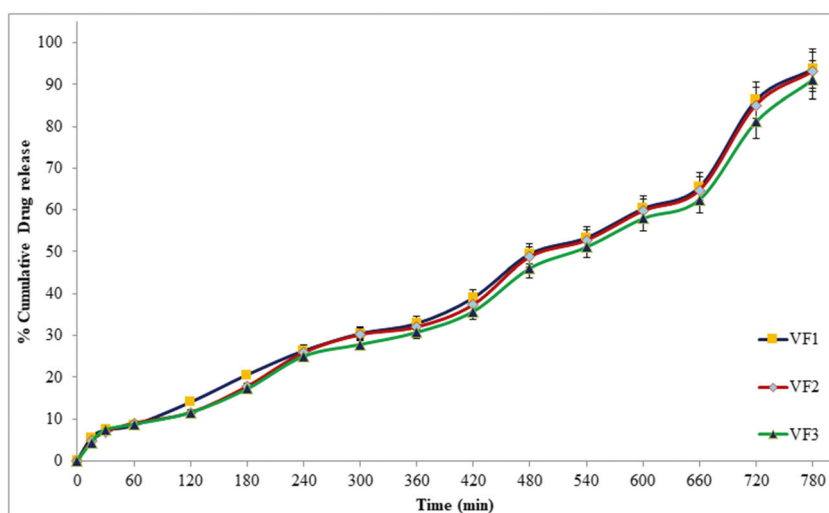


Fig. 17. *In vitro* dissolution study from validation batches (VF1 to VF3)

$$C_{\max} = 103.26 + 0.981 \times \text{SAMostHydrophobicHydrophilicDistance} \\ + 0.562 \times \text{SKMostHydrophobicHydrophilicDistance} + \\ 0.423 \times \text{XAMostHydrophobicHydrophilicDistance} \pm 0.045$$

(10)

$$t_{1/2} = 2.78 + 0.010 \times \text{SAMostHydrophobicHydrophilicDistance} \\ + 0.02 \times \text{XKMostHydrophobicHydrophilicDistance} \pm 0.0132$$

(13)

$$\text{ERC} = 0.25 + 0.002 \times \text{SAMostHydrophobicHydrophilicDistance} \\ + 0.001 \times \text{XAMostHydrophobicHydrophilicDistance} \pm 0.0002$$

(11)

$$\text{MRT} = 417.404 + 11.129 \times \text{SKMostHydrophobicHydrophilicDistance} \\ + 3.64 \times \text{XAMostHydrophobicHydrophilicDistance} \\ + 0.0037 \times \text{XAHydrophobicArea} \pm 529.241$$

(14)

$$V_D = 15.82 + 0.254 \times \text{SKMostHydrophobicHydrophilicDistance} \\ + 0.0044 \times \text{XAMostHydrophobicHydrophilicDistance} \\ + 0.122 \times \text{SAMostHydrophobicHydrophilicDistance} \pm 0.9027$$

(12)

$$\text{Clearance} = 4.28 + 0.0088 \times \text{SAMostHydrophobicHydrophilicDistance} \\ + 0.0036 \times \text{XKMostHydrophobicHydrophilicDistance} \\ + 0.0029 \times \text{XAMostHydrophobicHydrophilicDistance} \pm 0.2326$$

(15)

All QSPR models developed (Eqs. 10–15) showed a significant effect of all the descriptors included in the model on the respective *in vivo* property as depicted from F-statistics, *p* value (<0.05), and X-variance (≤ 1). Developed models indicated a good correlation between independent variables (descriptors) and response property under investigation (high r^2 , low standard error, and RMSE). Therefore, these predictive QSPR models can be used to predict *in vivo* parameters for NTG from other grades of HPMC with considerable predictability (predicted $r^2 = 0.325$ to 0.876).

Validation of Developed QSPR Models (6,9)

External and internal validation methods were used for the validation of QSPR models. In the internal validation method, Leave-One-Out approach was used during model development wherein cross-validation was performed between the training and test set molecules. In true external

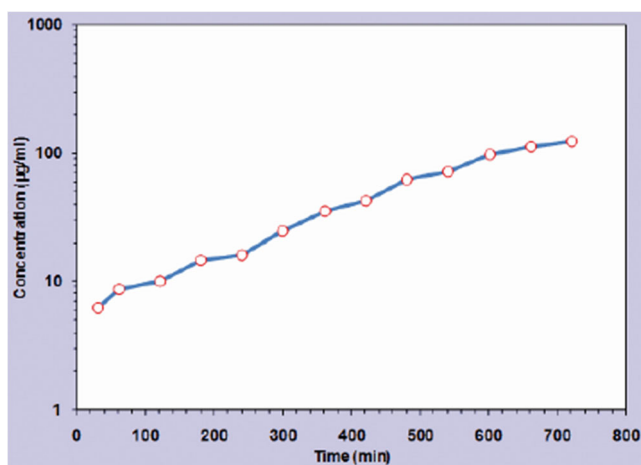


Fig. 18. Plasma drug concentration vs. time profile (dose-response curve) of VF3 batch

Table XIII. Predicted and Observed Values for *In Vitro* and *In Vivo* Parameters

Formulation property		Validation batch code	Predicted value	Observed value
<i>In-vitro</i>	Angle of repose (°)	VF1	33.22	30.11 ± 1.9
		VF2	28.67	30.67 ± 1.82
		VF3	30.5	29.53 ± 2.3
	Hardness (kg/cm ²)	VF1	5.4	5.5 ± 0.18
		VF2	5.7	4.3 ± 0.12
		VF3	5.5	5.6 ± 0.19
	Friability	VF1	0.46	0.62
		VF2	0.44	0.54
		VF3	0.36	0.43
	Drug content (%)	VF1	100	98.5 ± 1.25
		VF2	100	101.7 ± 2.02
		VF3	101	99.99 ± 1.85
	Swelling index	VF1	33	32.1 ± 1.98
		VF2	40	30.6 ± 1.17
		VF3	55	13.4 ± 2.06
<i>In vivo</i>	<i>t</i> _{90%} (min)	VF1	805	828
		VF2	858	840
		VF3	875	781
	<i>C</i> _{max} (µg/mL)	VF3	130.51	146.693
	ERC (min ⁻¹)		0.279	0.171
	<i>V</i> _D (mL)		21.66	11.84
	<i>t</i> _{1/2} (h)		2.46	1.47
	MRT (min)		492.63	189.15
	Clearance (L/h)		6.33	10.82

validation method, a different grade of HPMC (K250 PH) was used to validate the predictability of QSPR models developed based on the degree of polymerization of HPMC. Tablet formulations prepared (VF1, VF2, and VF3, Table I) using different concentrations of HPMC K250 PH were characterized as discussed before for *in vitro* as well as *in vivo* parameters. The results obtained were then correlated with the values predicted by the QSPR models. The closeness between the predicted and experimental values of all tested concentrations (VF1, VF2, and VF3) for *in vitro* and *in vivo* parameters validated the developed QSPR models (Figs. 17 and 18 and Table XIII).

Therefore, developed models could be successfully applied for prediction of the *in vitro* as well as *in vivo* characteristics of a formulation containing different (K) grades of HPMC for varying concentrations well in advance by considering polymeric properties (degree of polymerization). Moreover, developed QSPR models could also assist in the prediction of formulation composition for the desired property.

CONCLUSION

The sustained release tablets of NTG prepared using varying concentrations as well as different grades of HPMC showed results within an acceptable range for all *in vitro* parameters, including drug release up to 12 h. The QSPR models developed by considering the degree of polymerization of HPMC were subsequently validated by true external validation method, which showed good predictability for all *in vitro* and *in vivo* parameters. Therefore, developed QSPR models could be successfully used to predict the characteristics of the formulation containing other grades of HPMC at

different concentrations as well as to predict the composition of formulation for the desired property. This could have a positive pharmacoeconomic impact through the saving of repetitive experimentation and hence, cost expenditure on formulation development trials.

ACKNOWLEDGMENTS

The authors are grateful to Ashland Inc. Ltd., Netherlands for providing gift samples of different grades of HPMC (K4M, K15M, K35M, K100M, and K250 PH); Cipla Ltd. (Kurkumbh, Maharashtra, India) for kind gift sample of Nateglinide, Glenmark Pharmaceuticals (Mumbai, Maharashtra, India) for supplying gift sample of Gliclazide; and Colorcon Asia Ltd. (Goa, India) for providing gift samples of microcrystalline cellulose (Avicel PH102), magnesium stearate, and talc.

COMPLIANCE WITH ETHICAL STANDARDS

Authors declare that the experiments are in compliance with the current laws of India.

Conflict of Interest The authors declare that they have no conflict of interest.

Ethical Standards Authors declare that the experiments comply with the current laws of India.

Statement of Human and Animal Rights This article contained studies with animal subjects performed by the first author and was duly approved by the Institutional Animal Ethics Committee.

REFERENCES

- Mali RR, Goel V, Gupta S. Novel study in sustained release drug delivery system: a review. *Int J Pharm Med Res*. 2015;3:204–15.
- Patel KB, Vyas JR, Upadhyay UM. Formulation and evaluation of sustained release matrix tablets of Nateglinide. *J Drug Deliv Ther*. 2015;5:19–25.
- Dusane AR, Gaikwad PD, Bankar VH, Pawar SP. A review on: sustained released technology. *Int J Res Ayurveda Pharm*. 2011;2:1701–8.
- Gupta MM, Brijesh R. A review on: sustained release technology. *Int J Ther Appl* [Internet]. 2012 [cited 2019 Mar 2];8:18–23. Available from: http://journal.npaa.in/admin/ufile/1372744692IJTA_8_18-23.pdf
- Chugh I, Seth N, Rana AC, Gupta S. Oral sustained release drug delivery system: an overview. *Int Res J Pharm*. 2012;3:57–62.
- Bhatia NM, Gaikwad VL, Mane RV, Dhavale RP, Bhatia MS. Quantitative structure-property relationship modeling for prediction of hydrophilic drug entrapment in liposomes for lung targeted delivery. *New J Chem*. 2018;42:4384–93.
- Gaikwad VL, Bhatia NM, Singhvi I, Mahadik KR, Bhatia MS. Computational modeling of polymeric physicochemical properties for formulation development of a drug containing basic functionality. *J Pharm Sci*. 2017;106:3337–45.
- Gaikwad VL, Bhatia MS, Singhvi I. Statistical significance of polymeric physicochemical properties in the development of formulations containing a drug from neutral class. *Arab J Chem*. 2016;9:S1915–27.
- Gaikwad VL, Bhatia NM, Desai SA, Bhatia MS. Quantitative structure-property relationship modeling of excipient properties for prediction of formulation characteristics. *Carbohydr Polym*. 2016;151:593–9.
- Gaikwad VL, Bhatia MS, Singhvi I. Experimental and chemoinformatics evaluation of some physicochemical properties of excipients influencing release kinetics of the acidic drug ibuprofen. *Chemosphere*. 2015;138:494–502.
- Gaikwad VL, Bhatia MS, Singhvi I. Statistical modeling of physical characteristics of fast disintegrating glipizide tablets using polymeric properties. *Int J Pharm Technol*. 2013;5:5586–601.
- Gaikwad VL, Bhatia MS. Polymers influencing transportability profile of drug. *Saudi Pharm J*. 2013;21:327–35.
- Gaikwad VL, Bhatia MS, Singhvi I. Effect of polymeric properties on physical characteristics of fast disintegrating ibuprofen tablets: a statistical approach. *Der Pharm Lett*. 2013;5:140–7.
- Fayet G, Rotureau P, Prana V, Adamo C. Prediction of physico-chemical properties for REACH based on QSPR models. In: De Rademaeker E, Fabiano B, Senni Buratti S, editors. *Proc. 14th Int. Symp. Loss Prev. Saf. Promot. Process Ind.* [Internet]. Florence; 2013 [cited 2019 Mar 2]. p. 925–30. Available from: <https://hal-ineris.archives-ouvertes.fr/ineris-00976244>
- Siepmann J, Peppas NA. Modeling of drug release from delivery systems based on hydroxypropyl methylcellulose (HPMC). *Adv Drug Deliv Rev Elsevier*. 2001;48:139–57.
- Brauner N, Stateva RP, Cholakov GS, Mordechai S. Structurally “targeted” quantitative structure-property relationship method for property prediction. *Ind Eng Chem Res American Chemical Society*. 2006;45:8430–7.
- Gafourian T, Safari A, Adibkia K, Parviz F, Nokhodchi A. A drug release study from hydroxypropylmethylcellulose (HPMC) matrices using QSPR modeling. *J Pharm Sci*. 2007;96:3334–51.
- Jain S, Bhandari A, Purohit S. Spectrophotometric determination of nateglinide in bulk and tablet dosage forms. *Asian J Pharm*. 2009;3:218–21.
- Pani NR, Nath LK, Acharya S. Compatibility studies of nateglinide with excipients in immediate release tablets. *Acta Pharma*. 2011;61:237–47.
- ICH. Stability testing: Photostability testing of new drug substances and products Q1B [Internet]. ICH. 1996 [cited 2019 Mar 2]. p. 1–12. Available from: https://www.ich.org/fileadmin/Public_Web_Site/ICH_Products/Guidelines/Quality/Q1B/Step4/Q1B_Guideline.pdf.
- TA Instruments. Interpreting unexpected events and transitions in DSC results [Internet]. 2016. Available from: <http://www.tainstruments.com/pdf/literature/TA039.pdf>. Accessed 01 Mar 2019.
- TA Instruments. How to interpret the unexpected transitions in DSC results [Internet]. AZOM. 2015 [cited 2019 Mar 2]. p. 1–10. Available from: <https://www.azom.com/article.aspx?ArticleID=12101>.
- Mettler Toledo. Interpreting DSC curves Part 1: Dynamic measurements [Internet]. Mettler Toledo. 2000 [cited 2019 Mar 2]. p. 1–28. Available from: http://www.masontechnology.ie/x/Usercom_11.pdf.
- Hacıoğlu A, Çitlak A, Karakuş S. Development and validation of an HPLC method for determination of nateglinide in drug substances. *Marmara Pharm J*. 2015;2(19):103–8.
- Raveendra Babu G, Rao AL, Sri Lakshmi SP, Kalapraeven T, Rao PS. Spectrophotometric methods for estimation of nateglinide in bulk drug and its dosage form. *Int J Pharm Chem Biol Sci*. 2013;3:1160–4.
- USPNF. United States Pharmacopeia [USP] 22 – National Formulary [NF] 17. Rockville, MD: United States Pharmacopeial Convention, Inc.; 1995.
- IPCommission. Indian Pharmacopeia. Ghaziabad: Indian Pharmacopoeia Commission, Govt. of India, Ministry of Health and Family Welfare; 1996.
- ICH. Validation of analytical procedures: Text and methodology Q2(R1) [Internet]. ICH. 2005 [cited 2019 Mar 2]. p. 1–17. Available from: https://www.ich.org/fileadmin/Public_Web_Site/ICH_Products/Guidelines/Quality/Q2_R1/Step4/Q2_R1_Guideline.pdf.
- USPNF. United States Pharmacopeia [USP] 38 – National Formulary [NF] 33. Rockville, MD: United States Pharmacopeial Convention, Inc.; 2015.
- FDA. Nateglinide Tablets [Internet]. U.S. Food Drug Adm. 2009 [cited 2019 Apr 1]. p. 1–2. Available from: https://www.accessdata.fda.gov/drugsatfda_docs/label/2009/077467s000lbl.pdf
- Novartis Pharmaceuticals Canada Inc. PrStarlix* (Nateglinide): Product Monograph [Internet]. Novartis Pharm. Canada Inc. 2011 [cited 2019 Apr 1]. p. 1–34. Available from: https://www.novartis.ca/sites/www.novartis.ca/files/starlix_scrip_e.pdf.
- DOW. Chemistry of METHOCEL™. Cellulose Ethers - a technical review [Internet]. Dow Chem. Co. 2013 [cited 2019 Apr 2]. p. 1–16. Available from: http://msdssearch.dow.com/PublishedLiteratureDOWCOM/dh_08e5/0901b803808e5f58.pdf?filepath=dowwolff/pdfs/noreg/198-02289.pdf&fromPage=GetDoc.
- DOW. METHOCEL Cellulose Ethers. Technical Handbook [Internet]. Dow Chem. Co. 2002 [cited 2019 Apr 2]. p. 1–32. Available from: http://msdssearch.dow.com/PublishedLiteratureDOWCOM/dh_096d/0901b8038096d9ff.pdf?filepath=/pdfs/noreg/192-01062.pdf&fromPage=GetDoc.



ANTI STRESS, ADAPTOGENIC ACTIVITY OF STANDARDIZED DRIED FRUIT EXTRACT OF AEGLE MARMELOS AGAINST DIVERSE STRESSORS

R. DURAISAMI¹, VIJAY A. MOHITE^{2*} AND AMIT J KASBE³

Department of Pharmacognosy, ²Department of Pharmacology, ³Department of Pharmaceutical Chemistry, Nandha College of Pharmacy and Research Institute, Erode-638052, Tamilnadu, India Email: vijay1318@gmail.com

ABSTRACT

The Standardized dried aqueous extracts of Aegle marmelos (SDEAM) were evaluated for anti stress and adaptogenic activities using Swimming endurance and post-swimming motor function test, Cold swimming endurance test and forced swim test in rats. The extracts showed the presence of phenolics, flavonoids, carbohydrates and volatile oils in preliminary phytochemical screening. In present study the test extracts when subjected to forced swim model for adaptogenic activity in rats does not showed an increase in serum cholesterol and serum triglyceride level, but the increase was not sustained on subsequent groups. It also increases the swimming endurance time significantly along with the post motor function like Rota rod falling time and spontaneous motor activity. The test extract also increases the cold swimming endurance time significantly. The test extracts could restrict the increase in the level of these markers during stress.

Keywords: Aegle marmelos, Anti stress, Adaptogenic, Serum cholesterol, Serum triglyceride.

INTRODUCTION

The definition¹ of an adaptogen first proposed by Soviet scientists in the late 1950s, namely that an adaptogen is any substance that exerts effects on both sick and healthy individuals by 'correcting' any dysfunction(s) without producing unwanted side effects, was used as a point of departure. Traditional medicines are rich in non-specific anti-stress agents which are of increasing clinical significance. The action of an adaptogen has to be non-specific, that is to say, resistance to a wide variety of action of harmful factors, whether of a physical, chemical or a biological nature, has to increase. In other words, the action of an adaptogen has to be more intense as unfavorable changes occur in an organism, whereas the stressors external or environmental demands that placed on us is reverted by anti stress agents. Aegle marmelos² is a fruit-bearing tree indigenous to dry forest on hills and plains of central and southern India, Sri Lanka, Myanmar, Pakistan, Bangladesh, Nepal, Vietnam, Laos, Cambodia and Thailand. It belongs to the family Rutaceae, related to citrus. Plants were employed largely as analgesic, anti-inflammatory, antiviral, antimicrobial. The unripe dried fruit is astringent, digestive, stomachic and used to cure diarrhea and dysentery. The ripe fruit is a good and simple cure for dyspepsia. Aqueous leaf extract of Aegle marmelos has preventive effect on isoprenaline (isoproterenol) induced myocardial infarction. The effect of constituents isolated from methanolic extract of root bark of Bael on spontaneous beating of cultured mouse myocardial cells was examined. The extract at a concentration of 100Hg/ml inhibited the beating rate by approximately 50%.

With the view to study the test drug for nonspecific anti-stress activity, tests involving diverse stressors were employed viz. swimming endurance and post-swimming motor function test, cold swimming endurance test, anoxia tolerance test.

MATERIALS AND METHODS

Plant Material

The standardized dried extract of Aegle marmelos was obtained from Amruta Herbal Pvt. Ltd., Indore, along with certificate of analysis.

Experimental animals

Wistar albino rats of either sex weighing 125- 150 g, and albino mice of either sex weighing 25-35 g, were used. They were fed standard diet and water ad libitum and housed in cages at room temperature (30±2°C) with a 12 h light and dark cycle. Animal experiments were approved by the Institutional Animal Ethical Committee for the Purpose of Control and Supervision of

experiments on animals (CPCSEA), constituted under the directives of Ministry of Social Justice and Empowerment, Government of India.

Dosage schedule

The animals were divided into three groups of six animals each, for each test except for test 1 (swimming endurance and post-swimming motor function test) which was carried out with four such groups. In case of swimming endurance and post swimming motor function test Group I was administered with distilled water and was not subjected to stress daily for 7 days. Group II served as stress control and received the vehicle only (distilled water) in the same volume (5 ml/kg) and subjected to stress. In group III and group IV mice were administered with SDEAM 200 mg/kg and 400 mg/kg respectively. Whereas in case of cold swimming endurance test and adaptogenic activity (Forced swim model) Group I was administered with distilled water, Group II was administered with SDEAM I 200mg/kg and Group III was administered with SDEAM II 400 mg/kg.

EXPERIMENT

Swimming endurance and post-swimming motor function test³⁻⁵

The animals treated with SDEAM 100 mg/kg and 200 mg/kg were made to swim in a water tank (140x60x45 cm) maintained at room temperature (30±2°C) until they sank. This was recorded as the swimming time. The animals were removed and allowed to recover and dry for about 5 min. The animals were subsequently tested for muscle coordination on a Rota rod rotating at 15 rpm and the duration of stay on the rod was recorded. Immediately after that they were for spontaneous motor activity in a photoactometer for 10 min.

Cold swimming endurance test⁶

The animals treated with SDEAM 100 mg/kg and 200 mg/kg were made to swim in a water tank at 20±2°C until they sank (Bhattacharya, 1992).

Adaptogenic activity (Forced swim model)⁷

Albino rats of either sex (100-150 g) were divided in seven groups and administered the test extracts in similar manner as stated above. Stress was exerted by keeping rats in cylindrical vessels (length 48 cm and diameter 30 cm) filled with water to a height of 25 cm over period for two hours daily for seven days. Blood was collected from retro orbital plexus of each animal and the biochemical parameters such as SGPT, SGOT, serum glucose, cholesterol and triglycerides were determined.

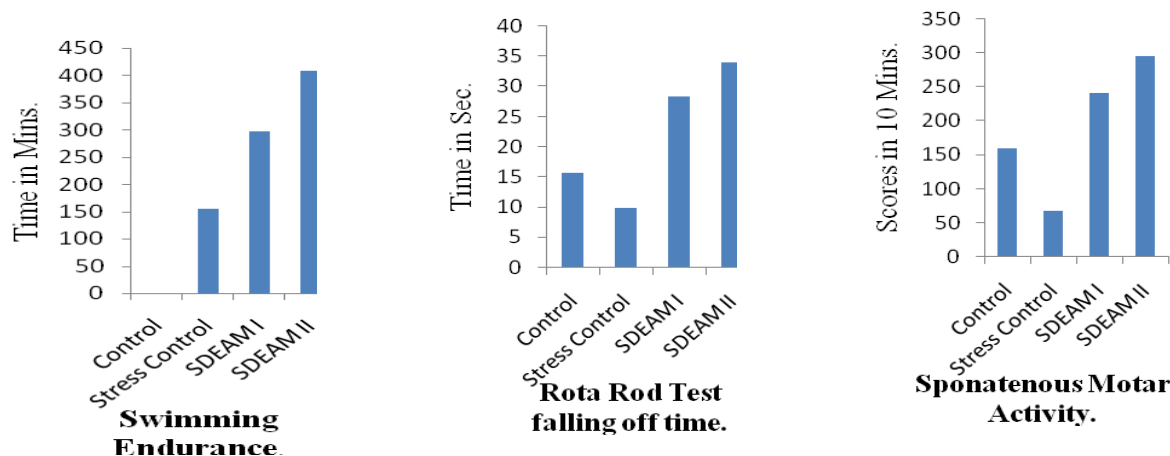


Fig. 1: Effect of Aegle marmelos on Swimming endurance and post-swimming motor function test

Table 1: Effect of Aegle marmelos on Swimming endurance and postswimming motor function test

Groups	Treatment	Dose Mg/Kg	Swimming Time In Mins	Rota-Rod Test Falling Off Time (Sec.)	Spontaneous Motor Activity
I	Control	-	-	15.66± 0.71	159.50±4.53
II	Stress Control	-	155.16±16.81	10.00±0.81*	67.66± 8.81**
III	SDEAM I	200	297.00±21.18**	28.33± 1.783**	241.00± 10.07**
IV	SDEAM II	400	408.83±11.70**	34.00±1.63**	295.83± 7.96**

n = 6, Values are mean±SEM, In case of Swimming endurance time *p<0.01 v/s Stress Control, While in case of Rota rod falling off time and spontaneous motor activity **p<0.01 v/s Control.

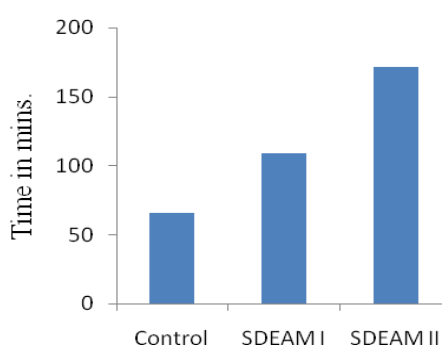


Fig. 2: Effect of Aegle marmelos on Cold swimming endurance test.

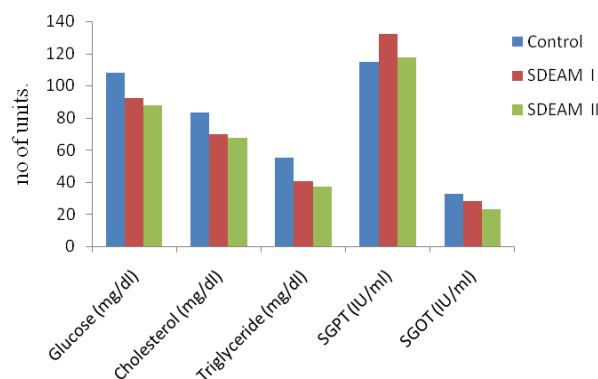


Fig. 3: Effect of Aegle marmelos on biochemical parameters in Adaptogenic activity. (Forced swim model).

Table 2: Effect of test extracts SDEAM on biochemical parameters in Adaptogenic activity

Group	Treatment	Dose mg/kg	Glucose (mg/dl)	Cholesterol (mg/dl)	Triglyceride (mg/dl)	SGPT (IU/ml)	SGOT (IU/ml)
I	Control	-	108.02±3.06	83.25±3.06	55.07±1.169	114.75±1.65	32.80±1.11
II	SDEAM I	200	91.95±0.74**	69.50±2.63*	40.24±0.77*	132.25±2.05**	27.97±1.62 ^{ns}
III	SDEAM II	400	87.62±0.29**	67.25±1.65**	37.12±1.54**	117.25±0.47 ^{ns}	22.80±0.30*

n=6 per group, Values are mean±SEM, comparison of I with II, III is done using Dunnet test. n.s., Not significant, * p < 0.05, ** p < 0.01, *** p < 0.001

Statistical Analysis

All the results were expressed as mean ± standard error mean (S.E.M.). Data were analyzed using one-way ANOVA followed by Dunnett's t-test. p<0.05 was considered as statistically significant. The analysis was carried out using Graph pad software of version 4.

RESULTS

Swimming endurance and post-swimming motor function test

It was observed that SDEAM I and SDEAM II induced a striking increase in the swimming endurance and post-swimming motor

function, however, the improvement by SDEAM I was less than by SDEAM II. SDEAM I and SDEAM II significantly increased the swimming time (P<0.01) over stress control animals. The duration of stay on rota rod was significantly increased from 15.667±0.7149 in control group to 28.333±1.783 by SDEAM I (P<0.001) and to 34.000±1.633 by SDEAM II (P<0.01) as compared to stress control 10.00±0.8165 (P<0.01). The photoactometer reading for spontaneous motor activity was 159.50±4.537 in control group and 67.66± 8.819 in stress control group while it was significantly increased to 241.00± 10.073 (P<0.001) and 295.83±7.960 (P<0.05) in SDEAM I and SDEAM II treated groups, respectively (Table 1).

Cold swimming endurance test

SDEAM I and SDEAM II markedly increased the cold water swimming time of the test group by 108.67 ± 5.77 and 171.50 ± 5.88 over the control group 65.50 ± 4.639 ($P < 0.01$).

Adaptogenic activity (forced swim model).

In the present study, on stress induced forced swimming model for Adaptogenic activity the values of biochemical parameters like glucose, cholesterol, triglycerides in the serum were found lower when compared with that of the values of control group.

DISCUSSION

Mice when forced to swim in a restricted space from which they cannot escape, become immobile after an initial period of vigorous activity, indicating the stress. The pretreatment with adaptogen increase swimming endurance in mice. Mice pretreated with SDEAM I 200 mg/kg and SDEAM II 400 mg/kg show significant improvement in the swimming time.

An increase in glucose level was observed, but the increase was not sustained on subsequent days. It may be due to suppression of glycogenesis, lipogenesis, increased glycogenolysis, lipolysis, and insulin resistant, which regulates blood glucose level⁸.

The mechanism by which stress raises serum cholesterol is likely to be due to enhanced activity of hypothalamus- hypophyseal axis resulting in increased liberation of catecholamines and corticosteroids⁹. The change in serum triglyceride is possibly mediated via adrenal medullary secretions and through activation of sympathetic nervous system. In present study the test extracts when subjected to forced swim model for adaptogenic activity in rats showed an increase in serum cholesterol and serum triglyceride level in control group was observed, but the increase was not sustained on subsequent treated groups.

CONCLUSION

The studies indicate that the standardized dried extracts of Aegle marmelos possess a potential of significant antistress and adaptogenic activity, hence can be categorized as plant adaptogen. The results are encouraging to pursue further studies on the other

bioactivity guided fractionation of these extracts to isolate and characterize probable bio active molecules.

REFERENCES

1. Marina Davydov, A.D. Krikorian. *Eleutherococcus senticosus* (Rupr. & Maxim.) Maxim. (Araliaceae) as an adaptogen: a closer look. *Journal of Ethnopharmacology* 2000, 72: 345–393.
2. Priyabrata Pattanayak, Prithwiraj Mohapatra. *Phytopharmacology of Aegle marmelos* (L.) CORREA. *Pharmacognosy Reviews Supplement* 2008, 2(4): 50-56.
3. Ghufraan Ahmad, K.M. Yusuf Amin, Naeem A. Khan, Tajuddin. The anti-stress activity of a gem-containing Unani formulation against diverse stressors. *Journal of Ethnopharmacology* 1998, 59: 187–193.
4. Takagi, K., Saito, H., Tsuchiya, M. Effect of Panax ginseng root on spontaneous movement and exercise in mice. *Japanese Journal of Pharmacology* 1974, 24: 41–48.
5. Janseen, P.A.J., Jagenau, A., Niemegeers, C.J.E. *Journal of Pharmacology and Experimental Therapeutics* 1960, 129: 471–480.
6. Bhattacharya, S.K. Evaluation of adaptogenic activity of Trasina, an Ayurvedic formulation. In: *Proceeding of an International Seminar on Traditional Medicine* (7–9 November, Calcutta). Oxford and IBH Publishing, Calcutta, 1992, 320–326.
7. Joshi Uttara P. and Mishra S. H. Evaluation of aqueous and methanol extracts of Pistacia integerrima galls as potential immunomodulator. *Phcog Mag.* 2008, 4(14): 126-131.
8. G. Kaur, S.K. Kulkarni. Reversal of forced swimming-induced chronic fatigue in mice by antidepressant and herbal psychotropic drugs. *Indian Drugs.* 1998 35(12): 771-777.
9. A.Panossian, G. Wikman, H. Wagner. Plant adaptogen III. Earlier and more recent aspects of their mode of action. *Phytomedicine.* 1999, 6(4): 287-300.